



# ISAC

INTERNATIONAL SOCIETY FOR  
ADVANCEMENT OF CYTOMETRY

# MOVING FORWARD

*Empowering Scientists.  
Advancing Cytometry.*

---

**JUNE 3-7 // PHILADELPHIA, PA**

**CYTO 2022 PROGRAM BOOK**



ThermoFisher  
SCIENTIFIC

# See your cells in a whole new light

Run larger, multicolor experiments and get complete, precise immune cell data faster and easier

Introducing a combination of next-level spectral flow cytometry technologies that delivers an unmatched level of elegance and empowerment. With Invitrogen™ instruments and fluorophores together, you can run complex panels and get rich, reproducible results 10 to 100 times faster than with any other technology available.

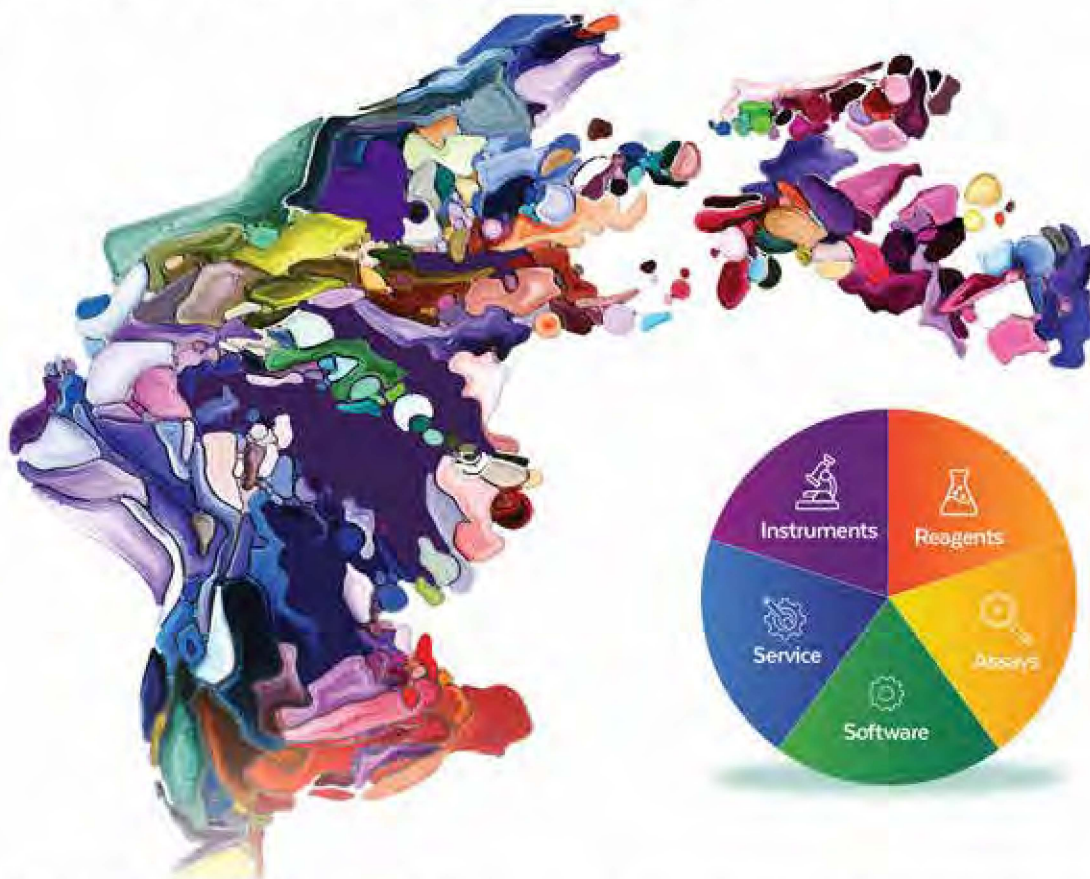
 Learn more at [thermofisher.com/flow](https://thermofisher.com/flow)

invitrogen

For Research Use Only. Not for use in diagnostic procedures. © 2022 Thermo Fisher Scientific Inc. All rights reserved. All trademarks are the property of Thermo Fisher Scientific and its subsidiaries unless otherwise specified. COL019959 0522

# A FULL SPECTRUM OF POSSIBILITIES

MORE DATA. MORE ANSWERS.



## A Full Spectrum of Single-Cell Analysis Solutions for Today's Most Challenging Biological Questions

- **High-parameter analysis** using 5-lasers and 64 fluorescent detectors on the Cytek® Aurora system
- **Cell sorting** with all the advantages of full spectrum flow cytometry with the Aurora CS system
- **Simple, powerful, and flexible** workflows on the Northern Lights™ system
- **Empower your assays** with cFluor® and Tonbo™ reagents

Cytek's Full Spectrum Profiling™ (FSP™) technology provides excellent resolution, intuitive workflows, and high multiplexing capabilities to reveal hidden populations and give you a new perspective to your biological questions.

**Come join us at CYTO 2022 - we're excited to see you in person!**  
**Booth #101**

**Don't miss our commercial tutorials**

Sunday, June 5, 2022 | 12:30 p.m. - 1:30 p.m.

Monday, June 6, 2022 | 12:30 p.m. - 1:30 p.m.



# TABLE OF CONTENTS

|                                                      |    |                                   |     |
|------------------------------------------------------|----|-----------------------------------|-----|
| Sponsors and Supporters.....                         | 5  | Program Schedule .....            | 25  |
| Welcome Letter .....                                 | 6  | Friday, June 3 .....              | 25  |
| ISAC 2020-22 Executive Committee and Councilors..... | 7  | Saturday, June 4.....             | 27  |
| Congress Organizers.....                             | 8  | Sunday, June 5.....               | 31  |
| ISAC Special Committees & Task Forces .....          | 9  | Monday, June 6 .....              | 34  |
| General Information .....                            | 15 | Tuesday, June 7.....              | 38  |
| Service Locations and Phone Numbers .....            | 16 | Poster Sessions .....             | 39  |
| City Map.....                                        | 17 | Exhibitor Agenda.....             | 57  |
| Convention Center Floor Plan .....                   | 18 | Exhibiting Companies .....        | 57  |
| Exhibitor Map .....                                  | 19 | Commercial Tutorials .....        | 65  |
| Schedule at a Glance .....                           | 20 | ISAC Marylou Ingram Scholars..... | 68  |
| Committee Meetings.....                              | 23 | SRL Emerging Leaders.....         | 71  |
| Special Lectures .....                               | 24 | Innovators.....                   | 74  |
|                                                      |    | Abstracts .....                   | 76  |
|                                                      |    | Poster Presentations.....         | 138 |
|                                                      |    | Author Index .....                | 263 |

# THANKS TO OUR SPONSORS

ISAC Gratefully acknowledges the following outstanding sponsors for their generous support of CYTO 2022!

## Platinum Sponsorship



Booth #325



Booth #101



Booth #415

## Gold Level Sponsors



Booth #338



Booth #437

## Silver Level Sponsors



Booth #107



Booth #309

## Mobile App

**Sony Biotechnology Inc.**

Booth #415

## Shared Interest Lounge

**Cytek Biosciences, Inc.**

Booth #101

## Shared Resource Lab Forum Event

**Cytek Biosciences, Inc.**

Booth #101

**Sony Biotechnology Inc.**

Booth #415

## CYTO Women

**BD Biosciences**

Booth #325

# WELCOME!



## **Dear Colleagues,**

On behalf of the CYTO 2022 Program Committee, ISAC Council, and the Co-Chair for CYTO 2022, Joel Sederstrom, it is my pleasure to welcome you to CYTO 2022, the 33rd Congress of the International Society for Advancement of Cytometry in Philadelphia, PA USA.

CYTO 2022 offers the opportunity for cytometrists at all levels and the commercial community to gather to share the most cutting edge science and technology in the single cell analysis domain. The meeting is in my hometown, Philadelphia, Pennsylvania, USA. Philly is the home of so many firsts, including the first medical school in the US, and it has recently been dubbed Cellicon Valley to reflect all the advances in cell therapy that have begun here. It is indeed appropriate that we celebrate our first back to live Congress in 3 years here in the City that Loves You Back!

We want to express our sincere thanks to the members of the ISAC Meetings Committee, CYTO Program Committee, the CYTO 2022 Hybrid Meeting Taskforce, as well as to the ISAC Scholars and Shared Resource Lab Emerging Leaders, who proposed themes and speakers, and assisted with abstract review and served as session chairs. Thanks go also to our Course and Tutorial faculty, Workshop leaders, and Session Chairs for contributing their time and talents. We could not have put on this meeting without the tireless effort of our ISAC office staff, Courtney Brooks Kamin, Executive Director and her team, Liz Bailey, Lanie Lesko, Casey Reiland, and Wendy Sahil. Our appreciation also goes out to the professional staff at Maritz Global Events for all they did to make our meeting a success!

We welcome you to Philadelphia and most of all, we celebrate being Back to Live!

### ***Jonni Moore***

ISAC President and Co-Chair of CYTO 2022

### ***Joel Sederstrom***

Co-Chair of CYTO 2022

# 2020-2022 EXECUTIVE COMMITTEE AND COUNCILORS



**Jonni Moore**  
President  
University of  
Pennsylvania



**Rachel Errington**  
President-Elect  
Cardiff University



**Andrea Cossarizza**  
Past President  
University of Modena  
and Reggio Emilia



**Kylie Price**  
Secretary  
Malaghan Institute of  
Medical Research



**Jessica Houston**  
Treasurer  
New Mexico State  
University



**Sara De Biasi**  
Councilor  
University of Modena  
and Reggio Emilia



**Paul Hutchinson**  
Councilor  
National University of  
Singapore



**Bill Telford**  
Councilor  
National Cancer  
Institute



**Rob Salomon**  
Councilor  
University of  
Technology, Sydney/  
Childrens Cancer  
Institute



**Aja Rieger**  
Councilor  
University of Alberta  
Edmonton



**Anna Belkina**  
Councilor  
Boston University



**Nicole Poulton**  
Councilor  
Bigelow Laboratory for  
Ocean Sciences



**Andrew Filby**  
Technology  
Development Councilor  
New Castle University



**Jonathan Irish**  
Biomedical Research  
Councilor  
Vanderbilt University



**Jessica Back**  
SRL Councilor  
Wayne State University

# CYTO 2022 CONGRESS ORGANIZERS

## ISAC STAFF

**Courtney Brooks-Kamin**  
Executive Director

**Liz Bailey**  
Assistant Director of Operations

**Casey Reiland**  
Education Manager

**Lanie Lesko**  
Senior Meetings Coordinator

700 Pennsylvania Ave. SE  
Washington, DC 20003  
(703) 537-7948  
Membership@isac-net.org

## CYTO CONGRESS MANAGEMENT

**Michael Gray, PMP, CMP**  
Project Manager

**Amy Alderman, CMP**  
Operations Manager, Event Management

**Kelly Hurt**  
Senior Registration Specialist

**Jennifer Hoffman**  
Meeting Events Housing Specialist

**Shaun Pirrera**  
Strategic Account Director

**Maritz Global Events**  
1395 North Highway Drive  
St. Louis, MO 63099 USA  
+1 636.827.1000  
CYTO@maritz.com

## CYTO 2022 MEETINGS COMMITTEE

Joel Sederstrom, Chair  
Joanne Lannigan, Co-chair  
Andy Filby, Council liaison  
Derek Davies  
Raluca Niesner  
Svetlana Mazel  
Pratip K. Chattopadhyay  
Andria Doty  
Gelo de la Cruz

Rui Gardner  
Alfonso Blanco  
Elena Holden  
Jack Dunne  
Han Wei  
Jonni Moore (Ex officio)  
Rachel Errington (Ex officio)  
Courtney Brooks Kamin (Ex officio)

---

## 2022 PROGRAM COMMITTEE

Nima Aghaeepour  
Kewal Asosingh  
Jessica Back  
Anna Belkina  
Alfonso Blanco  
Mariela Bollati  
Uttara Chakraborty  
Pratip K. Chattopadhyay  
Andrea Cossarizza  
Derek Davies  
Gelo de la Cruz  
Genny Del Zotto  
Andria Doty  
Jack Dunne  
Rachel Errington  
Diana Escobar  
Andy Filby  
David Galbraith  
Juan Garcia Vallejo  
Rui Gardner  
Keisuke Goda  
Hou Han Wei  
Julie Hill

Jessica Houston  
Jonathan Irish  
Derek Jones  
Joanne Lannigan  
Virginia Litwin  
Zosia Maciorowski  
Svetlana Mazel  
Helen McGuire  
Elisa Nemes  
Raluca Niesner  
John Nolan  
Betsy Ohlsson-Wilhem  
Ziv Porat  
Nicole Poulton  
Kylie Price  
Mario Roederer  
Joel Sederstrom  
Adrian Smith  
Paul Smith  
Vera Tang  
Sherry Thornton  
Rachel Walker



# ISAC SPECIAL COMMITTEES & TASK FORCES

## EDUCATION COMMITTEE

Sherry Thornton, Chair  
Bill Telford, Council Liaison  
Kewal Asosingh  
Evan Jellison  
Gelo Dela Cruz  
Zosia Maciorowski  
Awtar Krishan

Alexis Conway  
Julie Hill  
Steve Perfetto  
Kristen Reifel  
Florian Mair  
Kathy Daniels  
Kathleen Brundage

Silas Leavesly  
Heather Paich  
Iyadh Douagi  
Jonni Moore (Ex officio)  
Rachel Errington (Ex officio)  
Courtney Brooks Kamin (Ex officio)

---

## FINANCE COMMITTEE

Jessica Houston, Chair (Treasurer)  
Jessica Back, Council Liaison  
Ben Daniel  
Yolanda D Mahnke  
Rachael Walker

Tim Bushnell  
Radhika Rayanki  
David Haviland  
Stefano Papa  
Sok Lin Foo

Jonni Moore, (Ex officio)  
Rachel Errington, (Ex officio)  
Courtney Brooks Kamin (Ex officio)

---

## MEMBERSHIP SERVICES COMMITTEE

Alfonso Blanco, Chair  
Matt Niner, Co-chair  
Lourdes A. Arriaga-Pizano  
Mariela Bollati

Andria Doty  
Paul Hutchinson, Council Liaison  
Qianjun Zhang  
Jonni Moore (Ex officio)

Rachel Errington (Ex officio)  
Liz Bailey (Ex officio)  
Courtney Brooks Kamin (Ex officio)

---

## SCIENTIFIC COMMUNICATIONS COMMITTEE

Paul Wallace, Chair  
Sara De Biasi  
Xuanta Su  
Atilla Tarnok  
Paul Smith

Robert Zucker  
Nima Aghaeepour  
Pia Kvistborg  
Keisuke Goda  
Kewal Asosingh

Jessica Houston  
Rachael Sheridan  
Jonni Moore (Ex officio)  
Rachel Errington (Ex officio)  
Courtney Brooks Kamin (Ex officio)

---

## EQUITY, DIVERSITY, INCLUSION TASK FORCE

Kewal Asosingh  
Grace Chojnowski

Jonathan Irish  
Nima Aghaeepour

Benjamin Daniel  
Betsy Ohlsson-Wilhelm

# ISAC SPECIAL COMMITTEES & TASK FORCES

## ASSOCIATED SOCIETIES TASK FORCE

Lourdes Arriaga, Chair  
Alfonso Blanco  
Christine Childs  
Gelo dela Cruz  
Paula Fernandez

Lidia Gackowska  
Helen McGuire  
Katherina Psarra  
Joel Sederstrom  
Jose Carlos Segovia

Raif Yuecel  
Jonni Moore (Ex officio)  
Rachel Errington (Ex officio)  
Liz Bailey (Ex officio)  
Courtney Brooks Kamin (Ex officio)

---

## AWARDS AND NOMINATING COMMITTEE

Andrea Cossarizza, Chair  
Nima Aghaeepour  
Christine Childs  
Gelo dela Cruz  
Paula Fernandez  
Lidia Gackowska

Jessica Houston  
John Nolan  
Katherine Psarra  
Andreas Radbruch  
Joel Sedestrom  
Jose Carlos Segovia

Raif Yuecel  
Jonni Moore (Ex officio)  
Rachel Errington (Ex officio)  
Lanie Lesko (Ex officio)  
Courtney Brooks Kamin (Ex officio)

---

## BIOSAFETY COMMITTEE

Stephen Perfetto, Chair  
Kristen Reifel, Co-Chair  
Ben Fontes  
Brandon Swan  
Simon Monard

Geoffrey Lyon  
Jan Baijer  
Evan Jellison  
Dominic Jenner  
Elisa Nemes

Iyadh Douagi  
Avrill Aspland  
Jonni Moore (Ex officio)  
Rachel Errington (Ex officio)  
Courtney Brooks Kamin (Ex officio)

---

## CYTO INNOVATION COMMITTEE

Betsy Ohlsson-Wilhelm, Chair  
Andrew Filby  
Bill Hyun  
Craig LaBoda  
Diether Recktenwalkd  
Elena Holden  
Henning Ulrich  
Jakub Nedbal  
John Nolan

Kah Teong Soh  
Kirk Mutafooulos  
Nao Nitta  
Paul Smith  
Robert Salomon  
Benjamin Spurgeon  
Bin Fu  
Han Wei Hou  
Jingjing Zhao

Melanie Jimenez  
Sheng Ting Hung  
Takeaki Sugimura  
Jonni Moore (Ex officio)  
Rachel Errington (Ex officio)  
Casey Reiland (Ex officio)  
Courtney Brooks Kamin (Ex officio)

# ISAC SPECIAL COMMITTEES & TASK FORCES

## CYTO WOMEN TASK FORCE

Mariela Bollati, Chair  
Andrea Bedoya-López  
Diana Bonilla Escobar  
Grace Chojnowski  
Jessica Houston  
Kanutte Huse

Nicole Poulton  
Cynthia Morgan  
Erica Smit  
Allison Irvine  
Miho Suzuki  
Kiley Simmons

Mara Swaim  
Melanie O'Donahue  
Jonni Moore (Ex officio)  
Rachel Errington (Ex officio)  
Courtney Brooks Kamin (Ex officio)

---

## DATA COMMITTEE

Jonathan Irish, Chair  
Nima Aghaeepour, Co-chair  
Greg Finak  
Sierra Barone  
Anna Belkina

Laura Ferrer Font  
Vera Tang  
Josef Spidlen  
Gregory Veltri  
Joshua Welsh

Jonni Moore (Ex officio)  
Rachel Errington (Ex officio)  
Courtney Brooks Kamin (Ex officio)

---

## CYTO YOUTH

Alexis Conway, Chair  
Julie Hill, Co-Chair  
Dan Callen  
Roxana Del Rio Guerra  
Haley Pugsley  
Sherree Friend

Jennifer Wilshire  
Tim Crawford  
Emilie Jalbert  
Michele Black  
Derek Jones  
Luellen Fletcher

Tom Williams  
Aja Rieger  
Jonni Moore (Ex officio)  
Rachel Errington (Ex officio)  
Courtney Brooks Kamin (Ex officio)

---

## EXHIBIT ADVISORY TASK FORCE

Joel Sederstrom Chair  
Bob Balderas  
Monica DeLay  
Jan Fiser

Calvin Waller  
Michelle Malloy  
Martin English  
Jonni Moore (Ex officio)

Rachel Errington (Ex officio)  
Courtney Brooks Kamin (Ex officio)

---

## FLOW CYTOMETRY CONTENT TASK FORCE

Kewal Asosingh, Chair  
Evan Jellison, Co-Chair  
Steve McClellan  
Rachael Sheridan  
Lauren Nettenstrom  
Florian Mair

Tina DeCoste  
Roxana Del Rio Guerra  
Anna Belkina  
Jakob Zimmermann  
Paula Niewold  
Celine Silva Lages

Ermelinda Poriglia  
Matt Goff  
Meredith Weglarz  
Jonni Moore (Ex officio)  
Rachel Errington (Ex officio)  
Courtney Brooks Kamin (Ex officio)

# ISAC SPECIAL COMMITTEES & TASK FORCES

## FUNDRAISING TASK FORCE

David Galbraith, Chair  
Alfonso Blanco  
Jessica Houston  
Xu Huang  
John Nolan

Nicole Poulton  
J Paul Robinson  
Mario Roederer  
Paul Smith  
Qianjun Zhang

Jonni Moore (Ex officio)  
Rachel Errington (Ex officio)  
Courtney Brooks Kamin (Ex officio)

---

## GOVERNANCE COMMITTEE

Kylie Price, Chair  
Jonathan Irish  
David Galbraith  
Kathy Muirhead

Christian Kukat  
Roxana Del Rio Guerra  
Joe Tario  
Paul Wallace

Jonni Moore (Ex officio)  
Rachel Errington (Ex officio)  
Courtney Brooks Kamin (Ex officio)

---

## IMAGE CYTOMETRY CONTENT TASK FORCE

Silas Leavesley, Chair  
Andrew Filby, Council Liaison  
Mike Halter  
Jakub Nedbal  
Stephen Lockett

Gyorgy Vereb  
Bob Zucker  
Nao Nitta  
Joshua Deal  
Dominic Jenner

Andria Doty  
Jonni Moore (Ex officio)  
Rachel Errington (Ex officio)  
Courtney Brooks Kamin (Ex officio)

---

## INSTRUMENTS FOR SCIENCE (I4S) TASK FORCE

Alfonso Blanco, Chair  
Hemant Agrawal  
Bill Telford  
Iyadh Douagi  
Claud Lambert  
Anis Larbi  
Karen Hogg

Raif Yuecel  
Julie Nelson  
John Tigges  
Denis Polancec  
Andrea Bedoya  
Mariella Bollatti  
Gelo de la Cruz

Eman Abass  
Daniel Bituon  
Jonni Moore (Ex officio)  
Rachel Errington (Ex officio)  
Courtney Brooks Kamin (Ex officio)

---

## LEADERSHIP DEVELOPMENT COMMITTEE

Pratip Chattopadhyay, Chair  
Jessica Houston  
Matthew Linden

Betsy Ohlsson-Wilhelm  
J Paul Robinson  
Rachel Walker

Jonni Moore (Ex officio)  
Rachel Errington (Ex officio)  
Courtney Brooks Kamin (Ex officio)

# ISAC SPECIAL COMMITTEES & TASK FORCES

## LEARNING MANAGEMENT SYSTEM TASK FORCE

Florian Mair, Chair

Kathleen Daniels, Co-Chair

Heather Paich

Sofie Van Gassen

Dominic Jenner

Alice Wiedemann

Celine Silva-Lages

Jakob Zimmermann

Jonni Moore (Ex officio)

Rachel Errington (Ex officio)

Casey Reiland (Ex officio)

Courtney Brooks Kamin (Ex officio)

---

## LIVE EDUCATION DELIVERY TASK FORCE

Zosia Maciorowski, Chair

Awtar Krishan, co-chair

Qianjun Zhang

Paul Edward Hutchinson

Tomas Kalina

Kylie Price

William Telford

Katarzyna Piwocka

Sara De Biasi

Jonathan Irish

Gunner Deniz

Ziv Porat

Vivek Tanavde

Sumeet Gujral

Krishna Mandahar

Lyana Setiawan

Lize Engelbrecht

Elisa Nemes

Lydia Tesfa

Lourdes Arriago

Sindhu Cherian

Rui Gardner

Jonni Moore (Ex officio)

Rachel Errington (Ex officio)

Casey Reiland (Ex officio)

Courtney Brooks Kamin (Ex officio)

---

## MEETINGS COMMITTEE

Joel Sederstrom, Chair

Joanne Lannigan, Co-chair

Andy Filby, Council liaison

Derek Davies

Raluca Niesner

Svetlana Mazel

Pratip K. Chattopadhyay

Andria Doty

Gelo de la Cruz

Rui Gardner

Alfonso Blanco

Elena Holden

Jack Dunne

Han Wei

Jonni Moore (Ex officio)

Rachel Errington (Ex officio)

Courtney Brooks Kamin (Ex officio)

---

## MISSION CONTINUITY COMMITTEE

Paul Wallace, Chair

Courtney Brooks Kamin, Co-Chair

Nima Aghaeepour

Mariela Bollati

Jessica Houston

Tomáš Kalina

Joanne Lannigan

Kylie Price

Adrian Smith

Jonni Moore (Ex officio)

Rachel Errington (Ex officio)

# ISAC SPECIAL COMMITTEES & TASK FORCES

## SHARED RESOURCE LAB CONTENT TASK FORCE

Gelo Dela Cruz, Chair  
David Haviland  
Matt Bernard  
Lola Martinez

Dagna Sheerar  
Matt Cochran  
Isabella Pesce  
Claudia Bispo

Jonni Moore (Ex officio)  
Rachel Errington (Ex officio)  
Courtney Brooks Kamin (Ex officio)

---

## SHARED RESOURCE LAB SERVICES COMMITTEE

Michael Gregory, Chair  
Aja Rieger, Council Liaison  
Eva Orłowski  
Charlotte Christie Petersen

Derek Jones  
Timothy Bushnell  
Juan Garcia Vallejo  
Kathleen Brundage

Rachael Walker  
Jonni Moore (Ex officio)  
Rachel Errington (Ex officio)  
Courtney Brooks Kamin (Ex officio)

---

## SRL EMERGING LEADERS COMMITTEE

Rachael Walker, Chair  
Andrew Filby  
Juan Garcia Vallejo  
Dave Haviland  
Karen Helm

Charlotte Christie Petersen  
Radhika Rayanki  
Patricia Rogers  
Robert Salomon  
Adrian Smith

Anne Wilson  
Jonni Moore (Ex officio)  
Rachel Errington (Ex officio)  
Courtney Brooks Kamin (Ex officio)

# GENERAL INFORMATION

All Congress activities will be held at Pennsylvania Convention Center located at 1101 Arch St, Philadelphia, PA 19107 unless otherwise noted.

## CYTO Logistics and Services

Participation in CYTO 2022 is limited to registered delegates. Full Congress registration includes admission to all CYTO sessions such as workshops, parallel sessions, plenaries, Hooke Lecture, CYTO Innovation, scientific tutorials, commercial exhibits, poster sessions, commercial tutorials, refreshment breaks, happy hour, opening reception, and the closing reception. All attendees must wear the official CYTO badge to be admitted to all sessions, social activities, and the exhibit hall. Congress Management Staff will be located at Registration in the Broad Street Atrium.

## Companion/Guest Registration

Registered attendees of CYTO 2022 may sign up a spouse/guest as a Companion for 350. Companion registration allows entrance to the Opening Reception, Exhibit Hall, and the Closing Reception only. Companion registrants are not permitted in the session rooms at any time.

## Cell Phones

Please turn your phone to silent (not vibrate) mode prior to the start of a session.

## CMLE

This continuing medical laboratory education activity is recognized by the American Society for Clinical Pathology as meeting the criteria for up to 50 hours of CMLE credit. ASCP CMLE credit hours are acceptable to meet the continuing education requirement for the ASCP Board of Registry Certification Maintenance Program. If you're interested in earning CMLE credits, please follow these easy steps:

1. Be sure you get the QR code on your badge scanned at the door.
2. Complete an evaluation form for each session you attend using the mobile app.

CMLE certificates will be issued by the ISAC Executive Office following the meeting.

## Disabilities and Special Needs

If you have a disability or special need that may impact your participation in the meeting, please contact the Congress Management Staff at the Registration Desk. ISAC cannot ensure the availability of appropriate accommodations without prior notification of need.

## First Aid

If you need first aid, please contact the registration desk.

## Internet/Wireless Access

Wi-Fi Internet Service is available throughout the Pennsylvania Convention Center meeting rooms.

**Network: CYTO2022**

**Password: Philly2022**



## Mobile APP

The CYTO 2022 mobile app is available for download for iPhones/iPads, Androids, and desktops.

### Step 1: Download the MyEventHQ mobile app

Using the device you plan to bring to CYTO 2022, download MyEventHQ from your app store.

Don't have iOS or Android? Use the web version of the app found at <https://event.crowdcompass.com/cyto22app>. Enter CYTO22 and proceed to Step 3.

### Step 2: Add your event

After you've completed the download, open the app. Enter CYTO22 into the Find your event field and search for the event. Select the event.

### Step 3: Log in to the CYTO 2022 Event

Tap on Log In. Enter your First and Last Name and the Email Address you used to register, then tap Next. You will then receive an email and/or a text message with a 6-digit verification code; enter the code and tap Verify to complete your log in.

### Notes:

- Once logged in you will go through the profile set up wizard and be sure to mark your profile visible. At this point we encourage you to upload a profile picture.
- Make sure that your Notification Settings for the MyEventHQ app is turned on for you to receive notifications throughout the event.

## Recording

Recording any presentation or session (oral or poster) by any means, including audio taping or videotaping, is prohibited, except by an ISAC authorized agent for official purposes or by first authors who want to record their own poster presentations.

# SERVICE LOCATIONS

## CONGRESS/EXHIBITOR REGISTRATION & MANAGEMENT

### Broad Street Atrium

Friday, June 3, 0700-19:00

Saturday, June 4, 0730-19:00

Sunday, June 5, 0730-1830

Monday, June 6, 0730-1800

Tuesday, June 7, 0730-1400

---

## COMMERCIAL EXHIBITS

### Hall E

Saturday, June 4, 1745-1900

Sunday, June 5, 1000-1830

Monday, June 6, 1000-1800

Tuesday, June 7, 1000-1400

## POSTER PRESENTATIONS

### Hall E

Saturday, June 4, 1745-1900

Sunday, June 5, 1700-1830

Monday, June 6, 1700-1800

Tuesday, June 7, 1000-1400

---

## SPEAKER READY ROOM

### Room 126B, 100 Meeting Rooms Level

Presenters must test their presentations in the speaker ready room at least 4 hours prior to the start of their session. Morning presentations should come in the day before. Presenters will need to arrive 45 minutes before their session begins. Technicians will be checking the rooms to assist with set up. Laptops will be provided. However, if speakers decide to bring their own, they should also bring their own power and video adapters.

Thursday, June 2, 1300-1700

Friday, June 3, 0700-1700

Saturday, June 4, 0800-1700

Sunday, June 5, 0730-1700

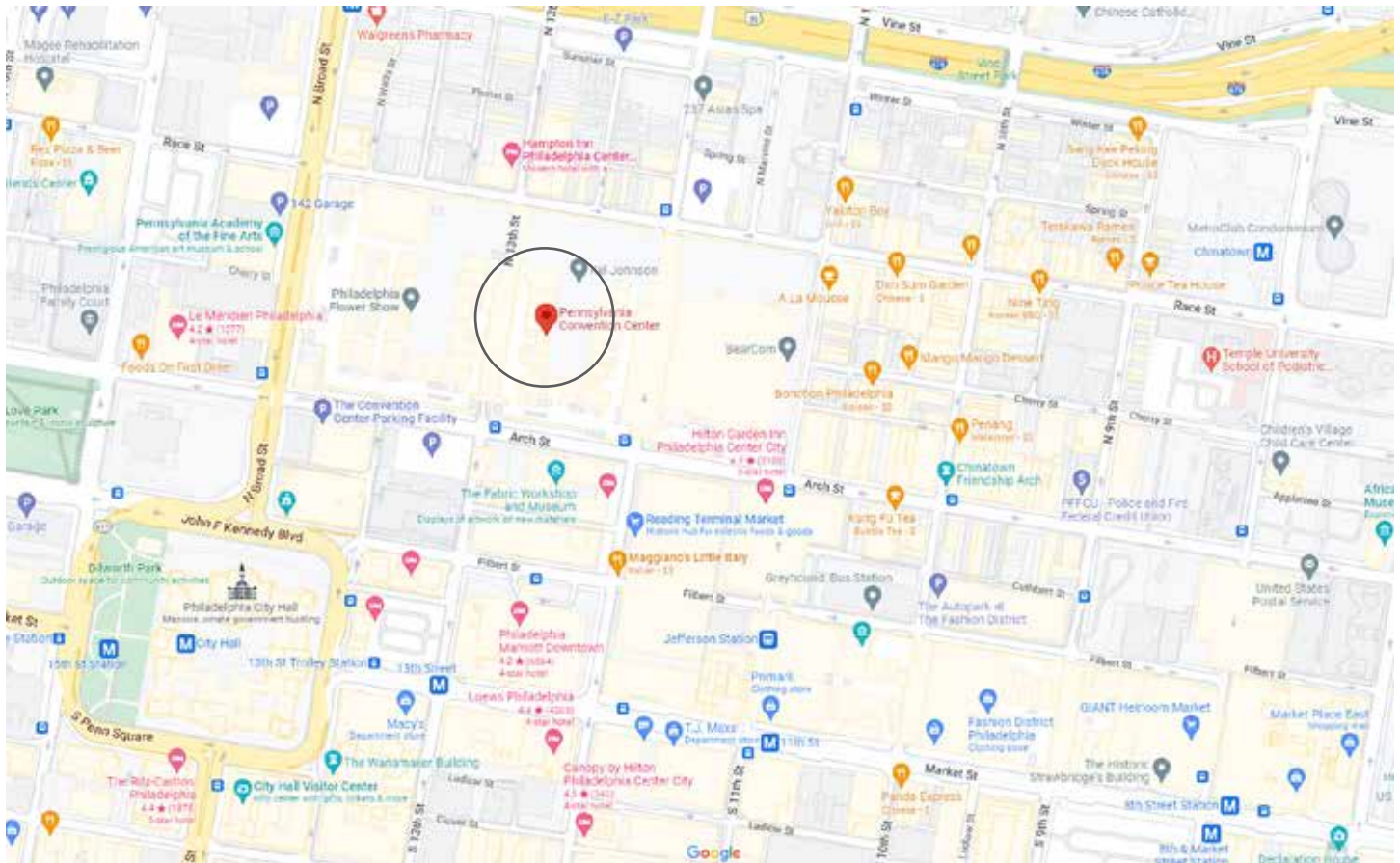
Monday, June 6, 0730-1700

Tuesday, June 7, 0730-1200



# MAPS

## PHILADELPHIA CITY MAP



## PHILADELPHIA INFO

### Dining Options

With over 1000 food establishments and 400 outdoor cafes, all within walking distance of the Pennsylvania Convention Center, Philadelphia has a range of dining options for everyone.

More information on where to eat while in Philadelphia can be found [here](#).

### Getting Around in Philadelphia

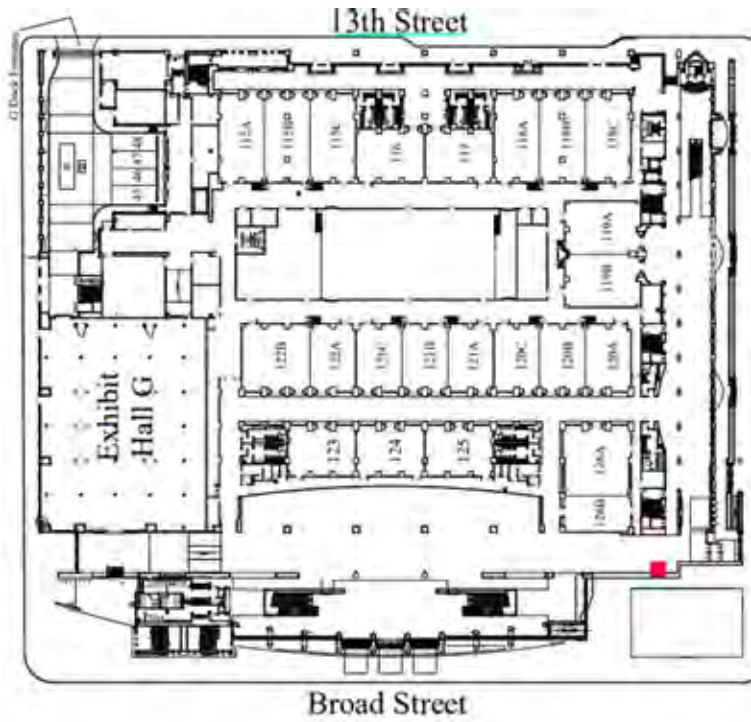
The Pennsylvania Convention Center is located in the heart of Center City Philadelphia within a major East Coast hub. The facility spans more than six blocks and is easily accessible by car, train, taxi, regional rail at Jefferson Station, and bus.

More information on Directions, Public Transit and Parking in Philadelphia can be found [here](#).

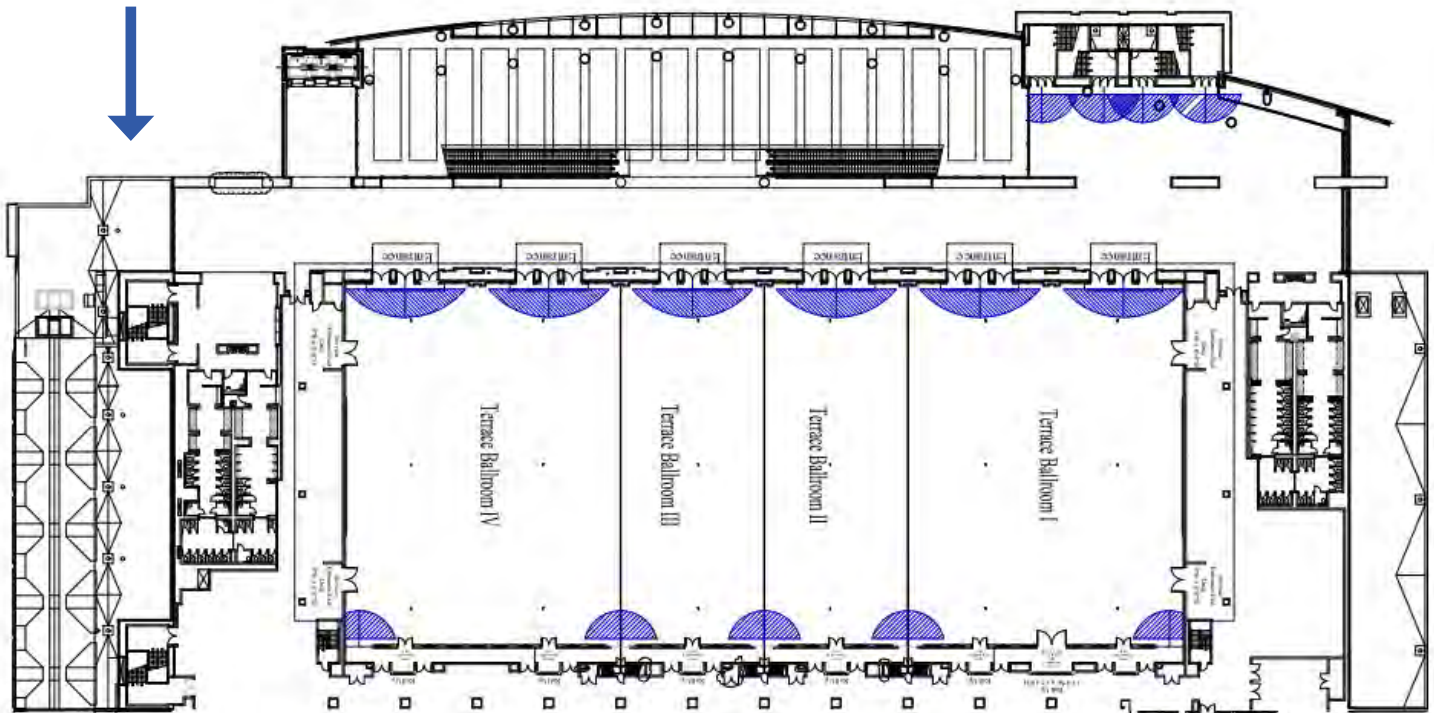
# MAPS

## PHILADELPHIA CONVENTION CENTER

Level 100  
Meeting Rooms

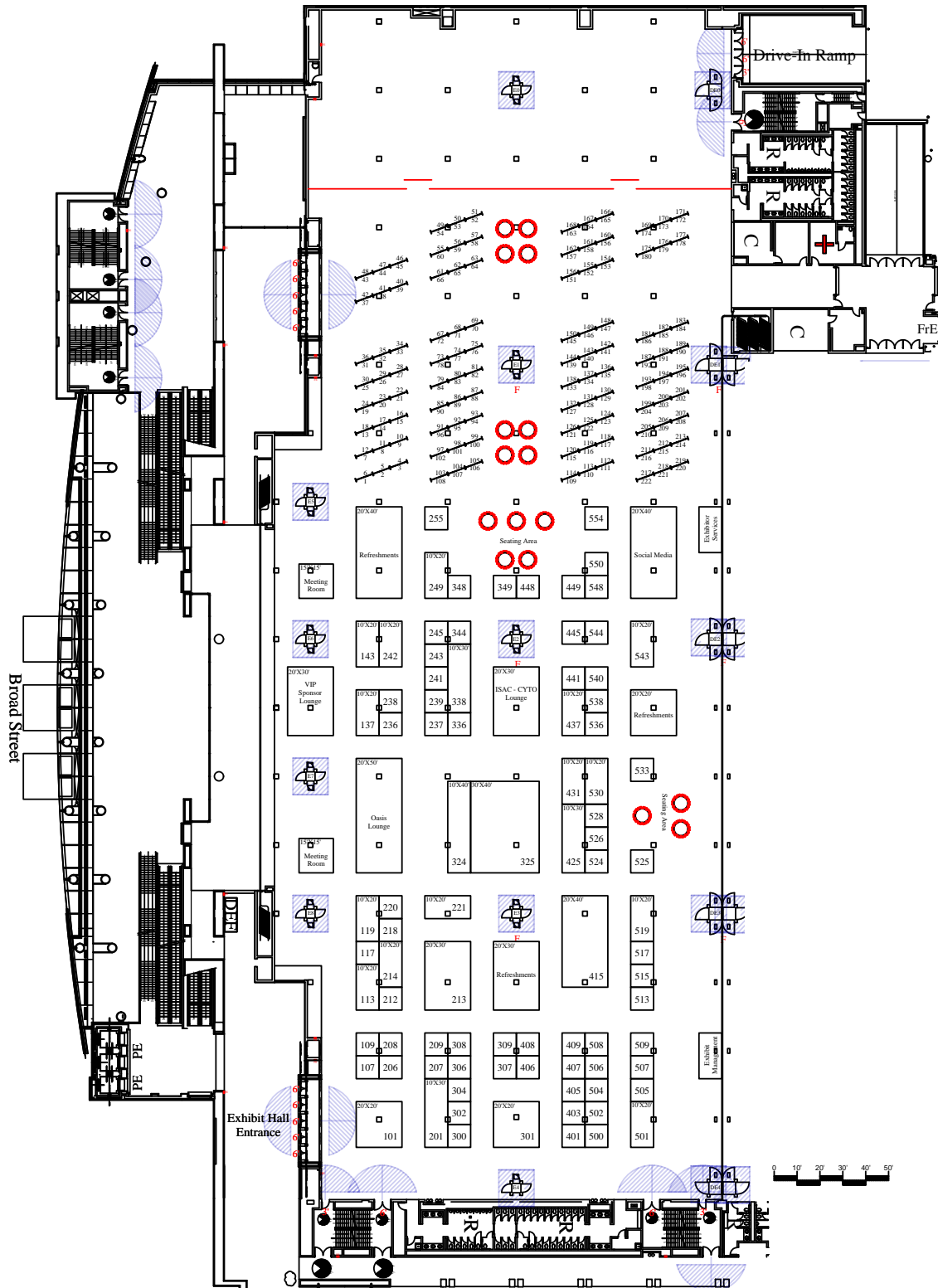


Terrace Ballroom



# MAPS

## EXHIBITOR MAP



# CONGRESS OVERVIEW

All Congress activities will be held at the Pennsylvania Convention Center unless noted otherwise.

## FRIDAY, JUNE 3

|           |                            |                                            |
|-----------|----------------------------|--------------------------------------------|
| 0700-1900 | Scientific Registration    | Broad Street Atrium                        |
| 0700-1900 | Exhibitor Registration     | Broad Street Atrium                        |
| 0730-0830 | Leadership Breakfast       | Room 125                                   |
| 0830-1000 | Scientific Tutorials 1-5   | Rooms 120AB, 120C, 121A, 121BC, 122B       |
| 1000-1030 | Coffee Break               | 100 Level Meeting Rooms Foyer              |
| 1030-1200 | Scientific Tutorials 7-12  | Rooms 120AB, 120C, 121A, 121BC, 122A, 122B |
| 1300-1430 | Scientific Tutorials 13-18 | Rooms 120AB, 120C, 121A, 121BC, 122A, 122B |
| 1445-1645 | CYTO Innovation            | Terrace Ballroom 1-2                       |
| 1700-1900 | SRL Networking             | Terrace Ballroom 3                         |

## SATURDAY, JUNE 4

|           |                                                        |                                            |
|-----------|--------------------------------------------------------|--------------------------------------------|
| 0730-1900 | Exhibitor Registration                                 | Broad Street Atrium                        |
| 0730-0830 | First Time Attendee And New Member Welcome Orientation | Room 120AB                                 |
| 0830-0850 | Welcome and Award Presentation                         | Terrace Ballroom 1-2                       |
| 0850-0920 | Howard Shapiro Tribute                                 | Terrace Ballroom 1-2                       |
| 0920-1045 | SRL Plenary                                            | Terrace Ballroom 1-2                       |
| 1045-1100 | Coffee Break                                           | Hall E                                     |
| 1100-1200 | Parallel Sessions                                      | Rooms 120AB, 120C, 121A, 121BC, 122A, 122B |
| 1215-1315 | Commercial Tutorials                                   | Rooms 120AB, 120C, 121A, 121BC, 122A, 122B |
| 1330-1500 | Plenary Session                                        | Terrace Ballroom 1-2                       |
| 1500-1515 | Coffee Break                                           | Hall E                                     |
| 1515-1630 | Workshops                                              | Rooms 120AB, 120C, 121A, 121BC, 122A, 122B |
| 1640-1745 | CYTO Women                                             | Terrace Ballroom 1-2                       |
| 1745-1900 | Exhibit Hall Opening Reception                         | Hall E                                     |

# CONGRESS OVERVIEW

All Congress activities will be held at the Pennsylvania Convention Center unless noted otherwise.

## SUNDAY, JUNE 5

|           |                         |                                            |
|-----------|-------------------------|--------------------------------------------|
| 0730-1830 | Scientific Registration | Broad Street Atrium                        |
| 0730-1830 | Exhibitor Registration  | Broad Street Atrium                        |
| 0830-0930 | Parallel Sessions       | Rooms 120AB, 120C, 121A, 121BC, 122A, 122B |
| 0930-1130 | Leadership Development  | Room 124                                   |
| 1000-1030 | Coffee Break            | Hall E                                     |
| 1000-1830 | Exhibit Hall Open       | Hall E                                     |
| 1130-1230 | Hooke Lecture           | Terrace Ballroom 1-2                       |
| 1245-1345 | Commercial Tutorials    | Rooms 120AB, 120C, 121A, 121BC, 122A, 122B |
| 1245-1345 | Societies Networking    | Room 123                                   |
| 1400-1600 | Plenary Session         | Terrace Ballroom 1-2                       |
| 1600-1630 | Coffee Break            | Hall E                                     |
| 1615-1730 | Workshops               | Rooms 120AB, 120C, 121A, 121BC, 122A, 122B |
| 1700-1830 | Poster Session          | Hall E                                     |
| 1745-1845 | Commercial Tutorials    | Room 120AB                                 |

# CONGRESS OVERVIEW

All Congress activities will be held at the Pennsylvania Convention Center unless noted otherwise.

## MONDAY, JUNE 6

|           |                          |                                            |
|-----------|--------------------------|--------------------------------------------|
| 0730-1830 | Scientific Registration  | Broad Street Atrium                        |
| 0730-1830 | Exhibitor Registration   | Broad Street Atrium                        |
| 0830-0930 | Parallel Sessions        | Rooms 120AB, 120C, 121A, 121BC, 122A, 122B |
| 1000-1100 | Coffee Break             | Hall E                                     |
| 1000-1800 | Exhibit Hall Open        | Hall E                                     |
| 1100-1230 | Weismann Keynote Lecture | Terrace Ballroom 1-2                       |
| 1230-1330 | Commercial Tutorials     | Rooms 120AB, 120C, 121A, 121BC, 122A, 122B |
| 1345-1515 | Plenary Session          | Terrace Ballroom 1-2                       |
| 1515-1545 | Coffee Break             | Hall E                                     |
| 1530-1700 | Plenary Session          | Terrace Ballroom 1-2                       |
| 1700-1800 | Poster Session           | Hall E                                     |
| 1715-1815 | Commercial Tutorials     | Rooms 120AB, 120C                          |

## TUESDAY, JUNE 7

|           |                         |                                            |
|-----------|-------------------------|--------------------------------------------|
| 0730-1400 | Scientific Registration | Broad Street Atrium                        |
| 0730-1400 | Exhibitor Registration  | Broad Street Atrium                        |
| 0800-0830 | ISAC Business Meeting   | Terrace Ballroom 1-2                       |
| 0830-1000 | Plenary Session         | Terrace Ballroom 1-2                       |
| 1000-1030 | Coffee Break            | Hall E                                     |
| 1000-1800 | Exhibit Hall Open       | Hall E                                     |
| 1015-1145 | Plenary Session         | Terrace Ballroom 1-2                       |
| 1200-1300 | Commercial Tutorials    | Rooms 120AB, 120C, 121A, 121BC, 122A, 122B |
| 1330-1500 | Plenary Session         | Terrace Ballroom 1-2                       |
| 1500-1530 | Awards Ceremony         | Terrace Ballroom 1-2                       |
| 1530-1730 | Closing Reception       | Terrace 3-4                                |

# ISAC COMMITTEE & TASK FORCE MEETINGS

## FRIDAY, JUNE 3

|           |                                      |          |
|-----------|--------------------------------------|----------|
| 0730-0830 | Finance Committee Meeting            | Room 123 |
| 0730-0830 | Mission Continuity Committee Meeting | Room 124 |

## SATURDAY, JUNE 4

|           |                                       |          |
|-----------|---------------------------------------|----------|
| 0730-0830 | Education Committee Meeting           | Room 123 |
| 0730-0830 | CYTO Innovation Committee Meeting     | Room 124 |
| 0730-0830 | Governance Committee Meeting          | Room 125 |
| 1215-1315 | Membership Services Committee Meeting | Room 123 |
| 1215-1315 | Cytometry A Editorial Board Meeting   | Room 124 |
| 1215-1315 | Biosafety Committee Meeting           | Room 125 |

## SUNDAY, JUNE 5

|           |                        |          |
|-----------|------------------------|----------|
| 0930-1130 | Leadership Development | Room 124 |
| 1245-1345 | Societies Networking   | Room 123 |

## MONDAY, JUNE 6

|           |                                          |          |
|-----------|------------------------------------------|----------|
| 0730-0830 | SRL Committee Meeting                    | Room 123 |
| 0730-0830 | Leadership Development Committee Meeting | Room 124 |
| 0730-0830 | Meetings Committee Meeting               | Room 125 |
| 1230-1330 | SRL Recognition Program Sub-Committee    | Room 124 |
| 1245-1345 | Flow Content Committee Meeting           | Room 123 |

# SPECIAL LECTURES

## INNOVATION OPENING SPEECH

Friday, June 3

The advancement of cytometry depends on the translation of innovative research into useful, accessible tools that can catalyze new biological understanding. CYTO Innovation is the forum within ISAC that explores the challenges and opportunities for translation of new cell analysis technologies into commercially viable products and services.

**14:45–15:45**

### **Cytometry Markets: Cytometry as a Service**

The fifth in a series of discussions about different aspects of the cytometry commercial ecosystem, the program will focus on the cytometry service markets, including on larger CROs serving the pharmaceutical and biotech industries, and well as smaller technology-focused start-ups using services to bring their products to market.

**15:45–16:45**

### **Technology Showcase 2022**

Three finalists will make their pitches to our panel of experienced cytometry business professionals to convince them and the audience of the commercial potential of their business plan.

## ROBERT HOOKE LECTURE

Sunday, June 5

Presented by Dr. E. John Wherry

Dr. E. John Wherry is the Barbara and Richard Schiffrin President's Distinguished Professor, Chair of the Department of Systems Pharmacology and Translational Therapeutics in the Perelman School of Medicine and Director of the UPenn Institute for Immunology.

Dr. Wherry received his Ph.D. at Thomas Jefferson University in 2000 and performed postdoctoral research at Emory University from 2000-2004. Dr. Wherry has received numerous honors including the Distinguished Alumni award from the Thomas Jefferson University, the Cancer Research Institute's Frederick W. Alt Award for New Discoveries in Immunology, the Stanley N. Cohen Biomedical Research Award from the University of Pennsylvania Perelman School of Medicine and was inducted as an AAAS Fellow in 2021. As of November 2021, Dr. Wherry has over 275 publications, an H-Index of 117, and his publications have been cited over 70,000 times.

He helped pioneer the field of T cell exhaustion, the mechanisms by which T cell responses are attenuated during chronic infections and cancer. Dr. Wherry's work has defined the underlying molecular and epigenetic mechanisms of exhausted T cells. He helped identify the role of the "checkpoint" molecule PD-1 and others for reinvigoration of exhausted T cells in cancer. These studies have led to new paradigms in immunotherapy for cancer and autoimmune diseases. In 2020-2021, Dr. Wherry's lab focused considerable effort on the immunology of COVID-19 and SARS-CoV-2 vaccination including establishing a new Immune Health Initiative at Penn to interrogate and identify these immune features to identify new treatment opportunities.



# PROGRAM SCHEDULE

The number listed before the abstract title references the abstract located in the back of the program book. Scientific Tutorials with an asterisk after the number may be recorded for CYTOU.

## FRIDAY, JUNE 3

### 0830–1000

#### Scientific Tutorial 01\*

Room 120AB, 100 Meeting Rooms Level

##### **Analysis I: Getting Started with Cytometry Data Science**

Jonathan Irish, Josef Spiden, Cass Mayeda, Nicolas Loof

Vanderbilt University, BD Biosciences

#### Scientific Tutorial 02

Room 121A, 100 Meeting Rooms Level

##### **What Are We Sorting? Basic Cellular Immunology for Flow Cytometrists**

Evan Jellison, Ph.D., Uconn Health, United States

#### Scientific Tutorial 03\*

Room 121BC, 100 Meeting Rooms Level

##### **Effective Use of Full Spectrum Cytometry**

Laura Ferre Font, Rui Gardner and Ana Longhini

Malaghan Institute of Medical Research, New Zealand and Memorial Sloan Kettering Cancer Center, United States

#### Scientific Tutorial 04

Room 120C, 100 Meeting Rooms Level

##### **Attaining ISAC SRL Recognition: Insights from the First Year**

Michael Gregory, Cleveland Clinic Florida Research and Innovation Center, United States; Kathleen Daniels, Sana Biotechnology

#### Scientific Tutorial 05

Room 122B, 100 Meeting Rooms Level

##### **When Flow Is Not The Way To Go: Multiplexed Imaging For Mapping Tissue at the Single Cell Level**

Andy Filby, Newcastle University

### 1000–1030

#### Coffee Break

100 Meeting Rooms Level Foyer

### 1030–1200

#### Scientific Tutorial 07\*

Room 120AB, 100 Meeting Rooms Level

##### **Analysis II: Tailoring Cytometry Data Science Workflows**

Jonathan Irish, Josef Spiden, Cass Mayeda, Nicolas Loof

Vanderbilt University, BD Biosciences

#### Scientific Tutorial 08\*

Room 121BC, 100 Meeting Rooms Level

##### **What Are We Sorting? Intermediate-genetic Manipulation and Molecular Biology for Slow Cytometrists**

David Galbraith, University of Arizona

#### Scientific Tutorial 09

Room 120C, 100 Meeting Rooms Level

##### **Writing, Publishing, and Reviewing: Advice, Tips and News from Cytometry Part A - The Journal of Quantitative Cell Science**

Attila Tarnok, China; Henning Ulrich and Melissa Asaro

University Leipzig, Germany; University of Sao Paulo and Wiley, United States

#### Scientific Tutorial 10

Room 121A, 100 Meeting Rooms Level

##### **Multiplexed Methods for Fluorescence Imaging, Also Multiplexed Tissue Imaging**

Andrea Radtke, Ph.D., National Institute of Allergy and Infectious Diseases (NIAID), United States

#### Scientific Tutorial 11

Room 122B, 100 Meeting Rooms Level

##### **How to Make Your Invention Commercializable**

Bill Hyun, University of California San Francisco, United States

#### Scientific Tutorial 12

Room 122A, 100 Meeting Rooms Level

##### **Single Cell Metabolism: Functional and Phenotypic Approaches For Cytometrists**

Rafael Argüello, Ph.D., CNRS, United States

# PROGRAM SCHEDULE

The number listed before the abstract title references the abstract located in the back of the program book. Scientific Tutorials with an asterisk after the number may be recorded for CYTOU.

## 1300–1430

### Scientific Tutorial 13

Room 122B, 100 Meeting Rooms Level

#### **Cytometry and The Scientific Method: How Can We Improve the Path from Laboratory to Literature and Back?**

David Galbraith, Ph.D., Virginia Litwin, Ph.D. and Peter Lopez

Arizona Cancer Center, Charles River Laboratories, and NYU Langone Health, United States

### Scientific Tutorial 14

Room 121A, 100 Meeting Rooms Level

#### **Emerging Trends in Cytometry**

Iyadh Douagi, Ph.D., NIAID, United States

### Scientific Tutorial 15

Room 120C, 100 Meeting Rooms Level

#### **RNA Imaging Techniques**

Ian Dardani, University of Pennsylvania, United States

### Scientific Tutorial 16\*

Room 121BC, 100 Meeting Rooms Level

#### **How to Assess the Biosafety Aspects of New and Atypical Flow Cytometers**

Dominic Jenner, Dstl; Evan Jellison, Ph.D., Uconn Health; Stephen Perfetto, NIAID

### Scientific Tutorial 17\*

Room 120AB, 100 Meeting Rooms Level

#### **Best Practices in Sorting, Including Bacteria and Viruses**

Jakob Zimmerman, Ph.D., Rachel Sheridan, Ph.D., Vera Tang, Ph.D. and Nicole Poulton, Ph.D.

Van Andel Institute, United States; University of Ottawa, Canada; Bigelow Laboratory for Ocean Sciences, United States

## 1445–1645

### **CYTOInnovation 2022**

#### **1445–1545**

#### **18 Main session: Technology Translation: Cytometry as a Service**

Speakers and topics are tentative

#### **19 View from the Top: The Role of Big and Small CROs in the Cytometry Ecosystem**

Virginia Litwin, Caprion/Covance; Reynold Capocasale, FlowMetric; Lynette Brown and/or Jennifer Stewart, Flow Contract Site Laboratory, LLC

#### **20 The Specialty CRO:**

#### **Making the Inaccessible Accessible**

Ryan Brinkman, CytoPex; Pratip Chattopadhyay, Talon Biomarkers; John Nolan, Cellarcus Biosciences

## 1545–1645

### **CYTOInnovation Technology Showcase 2022**

1545 - Welcome and Panel Introduction

1555 - Finalist 1

1610 - Finalist 2

1625 - Finalist 3

1640 - Closing Remarks

# PROGRAM SCHEDULE

## 1700–1900

### SRL Networking Event

Terrace Ballroom 3

Come meet others who know and share your world in a SRL/core facility environment. This event will provide opportunities to network with colleagues at all career stages who share your visions and challenges working in a SRL. Find out about core oriented ISAC programs and educational sessions at CYTO 2019. Learn how we can work together to achieve success and promote our mission in a shared environment. This is your opportunity to provide feedback on the Shared Resources Laboratories Committee plans for the coming year. Attendees will be admitted on a first come, first served basis until room capacity is reached.

## 1900–2100

### President's Reception

By Invitation Only

## SATURDAY, JUNE 4

### 0730–0830

#### CYTO 22 First Time Attendee and New Member Welcome Orientation

Room 120AB, 100 Meeting Rooms Level

The Welcome Orientation invites first time attendees as well as new member registrants to an opportunity to meet with old timers of the CYTO conferences as well as other first-time attendees. During the event, you will be introduced to ISAC Council members, the Membership Services Committee (MSC) members, and other leaders of ISAC.

### 0830–0850

#### Welcome and Award Presentation\*

Terrace Ballroom 1–2

### 0850–0920

#### Howard Shapiro Tribute\*

Terrace Ballroom 1–2

### 0920–1045

<sup>21</sup>

#### SRL Plenary - Delivering Technology to Investigators: The Shared Resource Lab\*

Chair: Rachel Walker, Co-Chair: Jessica Back

#### Delivering Technology to Investigators: The Shared Resource Lab

Jonni S. Moore, University of Philadelphia

#### The Innovation, Methodology and Application Research Theme @Newcastle University: A blueprint for delivering cutting-edge technologies to enable discovery

Andy Filby, Newcastle University

### 1045–1100

#### Coffee Break

100 Level Meeting Rooms Foyer

### 1100–1200

#### Parallel Session 01: Cytometry Assays #1

Room 120C, 100 Meeting Rooms Level

<sup>22</sup>

893900

#### Development of An Image-Based HCS Compatible Method for Endothelial Barrier Function Assessment

Leo Chan, Nexcelom Bioscience

# PROGRAM SCHEDULE

The number listed before the abstract title references the abstract located in the back of the program book. Scientific Tutorials with an asterisk after the number may be recorded for CYTOU.

23  
898241

## **Spectral Flow Cytometry and Imaging Studies on Cyanobacteria and Microplastics Using 64 Narrow Bandpass Filters And A Widefield Fluorescence Research Microscope**

Robert Zucker, Duke University

24  
898408

## **Functional Profiling Metabolism with A Fixation-Compatible System Analysing Micro-Samples of Blood**

Rafael Argüello, CNRS

### **1100-1200**

#### **Parallel Session 02: Cytometric Technologies #1-Cell Sorting\***

Room 120AB, 100 Meeting Rooms Level

26  
896958

## **High-Speed Image-Based Cell Sorting**

Eric Diebold, BD CellView Team

27  
898013

## **Light Scattering Pulse Shape Analysis With Multiple Forward Scatter Detectors In Flow Cytometry**

Toralk Kaiser, Jonas Gienger (Physikalisch-Technische Bundesanstalt), Konrad v. Volkmann (APE), Daniel Kage & K. Heinrich & J. Kirsch (German Rheumatism Research Centre Berlin (DRFZ) - Flow Cytometry Core Facility, Charitéplatz (Virchowweg 12), 10117 Berlin, Germany K. Feher (EMBL Australia Node in Single Molecule Science, School of Medical Sciences, University of New South Wales, Sydney, Australia) C. Giesecke-Thiel (Max Planck Institute for Molecular Genetics (MPIMG) - Flow Cytometry Facility, Ihnestraße 63-73, 14195 Berlin, Germany

28  
898460

## **Broadband Fingerprint-region Raman-activated Cell Sorting at 50 cells/s**

Matthew Lindley, Osaka University Graduate School of Engineering

29  
898551

## **Serial Flow Cytometry: Per-Particle Uncertainty Estimation From Repeated Measurements In Microfluidic Cytometer With Integrated Optical Waveguides**

Greg Cooksey, NIST

### **1100-1200**

#### **Parallel Session 03: Immunology**

Room 121A, 100 Meeting Rooms Level

30  
894440

## **4-1BBL-Containing Leukemic Extracellular Vesicles Promote Immunosuppressive Tregs And Dysfunction Of Effector T Cells, to Facilitate Progression of Myeloid Leukemia**

Julian Swatler, Nencki Institute of Experimental Biology

32  
898449

## **Preterm Birth (PTB) Detection: A Series of Immuno-Phenotypic Changes That May Serve As A Biomarker For Warning Signs.**

Nicolas Loof, BD Biosciences

33  
898497

## **Deep phenotyping of T cells in autoimmune Addison's disease by mass cytometry (Cytof)**

Shahinul Islam, University of Bergen

### **1100-1200**

#### **Parallel Session 04: SRL, Education and New Areas**

Room 122A, 100 Meeting Rooms Level

34  
892978

## **Cartography of The Human And Murine Immune System On A 30 Parameter Cytometer: Implementation Of Optimized, 'Ready-To-Use' And Shared Antibody Panels**

Anne-Laure Iscache, Inserm

35  
893901

## **Practical Cell Counting Method Selection To Increase The Quality Of Cell Counting Results**

Jordan Bell, Nexcelom Bioscience

36  
893672

## **Building an Industry Standard: Semantic Information Model For Flow Cytometry Discovery Biomarkers**

Goce Bogdanoski, Bristol Myers Squibb

# PROGRAM SCHEDULE

37  
894955

**The Ecology Of Microbial Communities –  
How They Can Be Synchronized And Stabilized**  
Susann Mueller, Helmholtz Center for Environmental Research

## 1100–1200

### Parallel Session 05: Image Cytometry\*

Room 121BC, 100 Meeting Rooms Level

39  
894940

**High-Throughput Image-Activated Cell Sorting  
by Mitochondrial Relocation**

Maik Herbig, The University of Tokyo

40  
894941

**Resolution-Enhanced Imaging Flow Cytometry  
by Deep Learning**

Maik Herbig, The University of Tokyo

41  
898119

**The Use of Deep Learning to Score the Imaging Flow  
Cytometry-Based In Vitro Micronucleus Assay**

Matthew Rodrigues, Luminex Corporation,

## 1100–1200

### Parallel Session 06: COVID-19 #1

Room 122B, 100 Meeting Rooms Level

42  
897017

**Uncovering the Pathogenesis Of Microvascular  
Thrombosis In COVID-19 Via High-Throughput  
Microscopy On A Chip**

Yuqi Zhou, The University of Tokyo

43  
898422

**Comprehensive Flow Cytometry Based Assessment  
of Anti-SARS-CoV-2 Antibody Isotypes in Vaccinated  
Control and Cancer Samples**

Kamala Tyagarajan, Luminex Corporation

44  
898474

**Spike-Specific Cellular and Humoral Immunity  
After BNT162b2 Mrna Vaccination in Older Adults:  
Benefits and Constrains Of “Booster” Vaccinations**

Axel Schulz, German Rheumatism Research Center

45  
898542

**An Optimized Flow Cytometry Protocol for Simultaneous  
Detection of T Cell Activation Induced Markers and  
Intracellular Cytokines: Application To SARS-CoV2  
Vaccinated Individuals**

Gianluca Rotta, BD Biosciences

## 1215–1315

### Commercial Tutorials

10X Genomics B.V: Room 121A

Akoya Biosciences: Room 122B

Cell Microsystems: Room 122A

Standard BioTools: Room 120C

Sony Biotechnology Inc: Room 120AB

Thermo Fisher Scientific: Room 121BC

## 1330–1500

### Plenary Session: Flow Cytometry Enabling Immunotherapy and Vaccine Clinical Trials

Terrace Ballroom 1–2

Chair: Thomas Lietchi, Co-Chair: Erica Smith

46

**High-parameter flow cytometric analysis of immune  
responses to SARS-CoV-2 mRNA vaccines in human  
lymph nodes**

Michela Locci, Ph.D. - Assistant Professor of Microbiology,  
Department of Microbiology, Perelman School of Medicine,  
University of Pennsylvania

47

**Evaluating Correlates and Mechanisms of Protection  
against Tuberculosis following Intravenous BCG  
Immunization in Nonhuman Primates**

Patricia Darrah, Ph.D. - Staff Scientist, National Institutes of  
Health

# PROGRAM SCHEDULE

The number listed before the abstract title references the abstract located in the back of the program book. Scientific Tutorials with an asterisk after the number may be recorded for CYTOU.

48

## **Flow Cytometry Enabling Immunotherapy and Vaccine Clinical Trials**

Steven De Rosa, MD - Research Associate Professor, Laboratory Medicine, University of Washington, Associate Member, Vaccine & Infectious Disease Division, Fred Hutch

**1500-1530**

### **Coffee Break**

100 Meeting Rooms Level Foyer

**1515-1630**

### **Workshop 01\***

Room 120AB, 100 Meeting Rooms Level

49

893673

### **Considerations for A Smooth Flow from Cell Sorting Into Genomics**

Claudia Bispo Gelo de la Cruz<sup>1</sup>, Lola Martinez<sup>2</sup>, Matthew Cochran<sup>3</sup>

<sup>1</sup>UCSF, <sup>2</sup>Spanish National Cancer Research Center,

<sup>3</sup>University of Rochester

### **Workshop 02**

Room 121A, 100 Meeting Rooms Level

50

893601

### **Can and If So How, Automation And Machine Learning Assist Timely Diagnosis And Prognosis In Everyday Clinical Routine?**

Attila Tarnok<sup>1</sup>, Kamila Czechowska<sup>2</sup>, Ryan Brinkman<sup>3</sup>, Wolfgang Kern<sup>4</sup>

<sup>1</sup>University of Leipzig, <sup>2</sup>Metafora Biosystems, <sup>3</sup>University of British Columbia, <sup>4</sup>Munich Leukemia Laboratory (MLL)

### **Workshop 03**

Room 120C, 100 Meeting Rooms Level

51

893614

### **Establishing a Biosafety Plan in an SRL**

Avrill Aspland<sup>1</sup>, Jessica Back<sup>2</sup>, Lauren Nettenstrom<sup>3</sup>, Lola Martinez<sup>4</sup>, Kristen M. Reifel

<sup>1</sup>University of Sydney and Centenary Institute, <sup>2</sup>Beth Israel Deaconess Medical Center, <sup>3</sup>Fluidigm Canada Inc., <sup>4</sup>Spanish National Cancer Research Center

### **Workshop 04\***

Room 121BC, 100 Meeting Rooms Level

52

892268

### **Consensus Best Practices for User Consultations in an SRL**

Amy Graham<sup>1</sup>, Kewal Asosingh<sup>1</sup>, Michael Gregory<sup>2</sup>

<sup>1</sup>Cleveland Clinic, <sup>2</sup>Cleveland Clinic Florida

### **Workshop 05**

Room 122B, 100 Meeting Rooms Level

53

893665

### **Extracellular Vesicle Measurement By Flow Cytometry: Practical Examples of MIFlowCyt-EV**

Edwin van der Pol<sup>1</sup>, Estefanía Lozano-Andrés<sup>2</sup>, John Nolan<sup>3</sup>, Vera Tang

<sup>1</sup>Amsterdam University Medical Centers, <sup>2</sup>Utrecht University,

<sup>3</sup>Cellarcus Biosciences

**1640-1745**

### **CYTO Women**

Terrace Ballroom 1-2

Chair: Mariela Bollati, Co-Chair: Kanutte Huse

Sponsored by BD Biosciences

55

### **Stress Management for Scientists**

Heather Hersh, PsyD - Founder and Principal, Thrive Well-being

56

Mónica Guzmán, Ph.D. - Associate Professor of Pharmacology in Medicine, Weill Cornell Medical College

**1745-1900**

### **Exhibit Hall Opening Reception**

Hall E

**1745-1900**

Exhibit Open

# PROGRAM SCHEDULE

## SUNDAY, JUNE 5

**0830-0930**

### Parallel Session 07: Data Analysis#1 Pipeline and Frameworks\*

Room 120AB, 100 Meeting Rooms Level

58  
894749

#### A Novel Cytometry Analysis Framework in Python: Application To Real-World Immunophenotyping Of Patients With Severe Sepsis

Ross Burton, Cardiff University

59  
898478

#### How To Build An Explainable Computational Pipeline To Diagnose And Subtype Patients With Lymphoid Primary Immunodeficiencies

Annelies Emmaneel, VIB-UGent Center for Inflammation Research

60  
898471

#### A Flow Cytometry-Based Computational Pipeline To Predict Outcome In Acute Myeloid Leukemia

Sarah Bonte, VIB-Ugent Center for Inflammation Research

**0830-0930**

### Parallel Session 08: Cell and Immune Therapy

Room 120C, 100 Meeting Rooms Level

61  
893738

#### Large-Batch Evaluation of Cell Counter Instrument-To-Instrument Consistency for Cell Therapy Applications

Jordan Bell, Nexcelom Bioscience,

62  
898429

#### Applications of Machine Vision-Based Cell Sorting For Clinical Diagnosis And Cell Therapy

Kazuki Teranishi, THINKCYTE INC

63  
901601

#### A 24-Color CAR T Cell Phenotyping Panel to Discern Effects Of Tumor Microenvironment

Martin Gomez, Kite Pharma a Gilead Company

64  
901954

#### Exhausting T Cell Exhaustion: Characterization of CD8 T Cells Chronically Stimulated In Vitro

Florence Perrin Patel, GlaxoSmithKline

**0830-0930**

### Parallel Session 09: Quality Assurance

Room 121A, 100 Meeting Rooms Level

65  
894086

#### Ensuring Full Spectrum Flow Cytometry Data Quality for High-Dimensional Analysis

Laura Ferrer Font, Cytek Biosciences

66  
894436

#### Synthetic Cell Mimics for Next-Generation Flow Cytometry-Based Assays

Ling Zhang, Slingshot Biosciences,

67  
894939

#### A Standardized Metric for Throughput For Cytometry

Maik Herbig, The University of Tokyo

68  
898442

#### Cell Spike-ins Add Assurance to Flow Cytometry Measurements of Complex Microbial Communities

Kirsten Parratt, National Institute of Standards and Technology

**0830-0930**

### Parallel Session 10:

#### High Dimensional Cytometry #1

Room 122A, 100 Meeting Rooms Level

69  
894802

#### High-dimensional immune cell profiling to understand how the immune system changes throughout life: implications for human disease.

Sedi Jalali, Murdoch Children's Research Institute

# PROGRAM SCHEDULE

The number listed before the abstract title references the abstract located in the back of the program book. Scientific Tutorials with an asterisk after the number may be recorded for CYTOU.

70  
898477

## **Unraveling Immunotherapy Response in Lung Cancer by Computational Cytometry**

Katrien Quintelier, VIB-UGent Center for Inflammation Research

71  
898500

## **Methods Used to Validate Cluster and Multidimensional Reduction Programs using data from a SARS-CoV-2 NHP challenge study and NHP BAL samples infected with SARS-CoV-2**

Stephen Perfetto, NIAID

72  
898538

## **Using Full Spectrum Cytometry to Expand and Enhance High Parameter Immune Fingerprints in Health and Disease**

Derek Jones, University of Pennsylvania

### **0830-930**

#### **Parallel Session 11: Diagnosis, Drug Development, Translation #1\***

Room 121BC, 100 Meeting Rooms Level

74  
896516

## **Uncovering the Pathogenesis and Treatment Of Atherosclerosis By High-Throughput Microscopy**

Ryo Nishiyama, University of Tokyo

75  
896622

## **Detection And Characterization Of Circulating Tumor Cell Clusters By High-Throughput Optomechanical Imaging Flow Cytometry**

Hiroki Matsumura, The University of Tokyo

76  
898552

## **To PCR Or Not To PCR: Early Flow Cytometry-Based Measures of HIV infection for Clinical Studies**

Veronica Obregon-Perko, BD Biosciences

### **0830-0930**

#### **Parallel Session 12: Submicron Cytometry**

Room 122B, 100 Meeting Rooms Level

77  
896956

## **Selective Nanovial Capture and Single-Cell Sorting of Live Antigen-Specific T Cells Based on Cytokine Secretion**

Doyeon Koo, University of California Los Angeles

78  
896936

## **Practical Procedure To Prevent Swarm Detection Of Extracellular Vesicles By Flow Cytometry**

Naomi Buntsma, Amsterdam University Medical Centers

79  
897384

## **An Imaging Flow Cytometry-based Methodology for the Analysis of Single Extracellular Vesicles in Unprocessed Human Plasma**

Edwin van der Pol

80  
898803

## **Quantitative Analysis of Molecular Cargo Transfer From Cells To EVs**

John Nolan, Stanford University School of Medicine

### **0930-1130**

#### **Leadership Development Session**

Room 124, 100 Meeting Rooms Level

### **1000-1030**

#### **Coffee Break**

Hall E

### **1000-1830**

#### **Poster Viewing Hours**

Exhibits Open

### **1000-1830**

#### **Exhibit Hall Open**

Hall E



# PROGRAM SCHEDULE

## 1130–1230

### Robert Hooke Lecture

Terrace Ballroom 1–2

Chair: Jonni Moore

81

Dr. E. John Wherry, UPenn Institute for Immunology

## 1245–1345

### Commercial Tutorials

BD Biosciences: Room 120AB

Cytex Biosciences, Inc: Room 122A

Luminex Corporation: Room 121A

Miltenyi Biotech B.V. & Co. KG: Room 121BC

Slingshot Biosciences: Room 122B

Thermo Fisher Scientific: Room 120C

## 1245–1345

### Societies Networking

Terrace Ballroom 3

## 1400–1600

### Plenary Session:

#### A New Era of Cell and Immune Therapy

Terrace Ballroom 1–2

Chair: Jonni Moore, Co-Chair: Diana Bonilla

82

#### Performance Enhancement of Immunity: Pushing the Design and Engineering Envelope in T Cell Manufacturing

Bruce Levine Ph.D., University of Pennsylvania

83

#### Understanding Multiple Myeloma Resistance to CAR T cell Therapy through Single Cell Analysis

Michael Milone, MD, PhD, University of Pennsylvania

84

#### Mechanisms behind CAR T cells

Marcela Maus, VMD, PhD, Massachusetts General Hospital

85

#### Unleashing Immune Cells to Cure Multiple Myeloma

Krina Patel, MD

## 1600–1630

### Coffee Break

Hall E

## 1630–1745

### Workshop 07\*

Room 120AB, 100 Meeting Rooms Level

86

893667

#### Engaging the un-Engaged and How to Keep Them

Gelo de la Cruz<sup>1</sup>, Alfonso Blanco<sup>1</sup>, Lourdes Arriaga-Pizano<sup>2</sup>

<sup>1</sup> Novo Nordisk Foundation Center for Stem Cell Medicine (reNEW), <sup>2</sup> IMSS Mexican Institute of Social Security

### Workshop 08

Room 121A, 100 Meeting Rooms Level

87

893601

#### Can and If So How, Automation and Machine Learning Assist Timely Diagnosis and Prognosis in Everyday Clinical Routine?

Attila Tarnok<sup>1</sup>, Kamila Czechowska<sup>2</sup>, Ryan Brinkman<sup>3</sup>, Wolfgang Kern<sup>4</sup>

<sup>1</sup> University of Leipzig, <sup>2</sup> Metafora Biosystems, <sup>3</sup> University of British Columbia, <sup>4</sup> Munich Leukemia Laboratory (MLL)

### Workshop 09

Room 120C, 100 Meeting Rooms Level

88

892952

#### How Can SRLs Best Support High-Dimensional Data Analysis?

Laura Ferrer Font<sup>1</sup>, David Gravano<sup>2</sup>, Lauren Nettenstrom<sup>3</sup>

<sup>1</sup> Cytex Biosciences <sup>2</sup> University of California Merced, <sup>3</sup> Fluidigm Canada Inc.

### Workshop 10\*

Room 121BC, 100 Meeting Rooms Level

89

892170

#### Tools for Implementing Measurement Assurance in Every Laboratory Setting: Recent Advances

John Nolan<sup>1</sup>, Lili Wang<sup>2</sup>, Virginia Litwin<sup>3</sup>

<sup>1</sup> Cellarcus Biosciences, <sup>2</sup> NIST, <sup>3</sup> Charles River Laboratories

# PROGRAM SCHEDULE

The number listed before the abstract title references the abstract located in the back of the program book. Scientific Tutorials with an asterisk after the number may be recorded for CYTOU.

## Workshop 11

Room 122B, 100 Meeting Rooms Level

90  
893221

### How Will Technical Innovations Shape the Future Of Cytometry?

Betsy Ohlsson-Wilhem, SciGro

## Workshop 12

Room 122A, 100 Meeting Rooms Level

91  
892909

### Online Tools for Panel Design! Useful Resources or a Waste Of Time?

Marcus Eich<sup>1</sup> and Steffen Schmitt<sup>2</sup>

<sup>1</sup> HI-STEM gGmbH, <sup>2</sup> German Cancer Research Center (DKFZ)

## 1700–1830

### Poster Session 1

Hall E

## 1745–1845

### Commercial Tutorial

CellCarta: Room 120AB

## MONDAY, JUNE 6

### 0830–0930

#### Parallel Session 13: Diagnostics, Drug Development, Translation #2

Room 120C, 100 Meeting Rooms Level

92  
898217

#### Distinct Intestinal Microbiota Phenotypes Identify Chronic Inflammatory Diseases

Lisa Budzinski, German Rheumatism Research Center

93  
898440

#### Trust the Process: Bringing High-Dimensional Data Analysis Tools To A Modern CLL Diagnostic Workflow

John Quinn, BD Biosciences

94  
895403

#### Changes In The Ovarian Cancer Microenvironment Associated With Tumor Progression And Chemoresistance

Alexander Xu, Cedars Sinai Medical Center

### 0830–0930

#### Parallel Session 14: Cytometry Assays #2

Room 121A, 100 Meeting Rooms Level

96  
898258

#### Assessment Of Live-Cell Imaging And Flow Cytometry Methods For SARS-CoV-2 Pseudovirus Neutralization Assays Compared To A Surrogate Bead-Based Neutralization Assay

John O'Rourke, BennuBio Inc

97  
898430

#### Measuring Apoptosis In Intact Multicellular Spheroids Using The Velocyt™ Large Particle, Multi-Stream Flow Cytometer

Matthew Saunders, BennuBio Inc

# PROGRAM SCHEDULE

98  
898462

## **Flow Cytometry Analysis Of Protein Expression Using Antibody-Oligonucleotide Conjugates Followed By Single-Cell CITE-Seq**

Xiaoshan Shi, BD Biosciences

99  
898524

## **Identification Of Human Mesenchymal Stem Cell Biomarkers By Aptamer Cytometry**

Henning Ulrich, University of Sao Paulo

### **0830-0930**

#### **Parallel Session 15:**

#### **Cytometric Technologies #2-Multiplexing+**

Room 122A, 100 Meeting Rooms Level

100  
893151

## **Multiplexed Analysis Of Living Cells With SAFE Bioorthogonal Cycling**

Jina Ko, University of Pennsylvania

101  
898399

## **Multiplex flow cytometry with Raman tags**

Ryo Nishiyama, The University of Tokyo

102  
898435

## **Time-Lapse Flow Cytometry Using Laser Particle Barcoding Of Individual Cells**

Sheldon Kwok, LASE Innovation Inc.

103  
898505

## **Analysis of a 12-Color Panel using a Compensation-Free Flow Cytometer with 6 Fluorescence Detectors**

Alan Chin, Kinetic River Corp

### **0830-0930**

#### **Parallel Session 16: COVID-19 #2\***

Room 122B, 100 Meeting Rooms Level

104  
894930

## **mRNA Vaccine-Induced T Cells Transition To A Resting Memory State Capable Of Rapid Proliferation And Differentiation To Effector Lineages Upon Antigen Re-Exposure**

Mark Painter, University of Pennsylvania

105  
898178

## **Validation and FDA approval of a high parameter intracellular flow cytometry panel for the detection of Th1 and Th2 responses for characterizing antigen specific T cell responses to SARS-CoV-2 infection and vaccine candidates**

Katharine Schwedhelm, Fred Hutchinson Cancer Research Center

106  
898506

## **Remodeling of T cell dynamics during long COVID is dependent on severity of SARS-CoV-2 infection**

Julian Swatler, Nencki Institute of Experimental Biology

107  
898555

## **Baseline immune signatures determine COVID-19 severity**

Thomas Liechti, NIH

# PROGRAM SCHEDULE

The number listed before the abstract title references the abstract located in the back of the program book. Scientific Tutorials with an asterisk after the number may be recorded for CYTOU.

## 0830-0930

### Parallel Session 17: High Dimensional Cytometry #2\*

Room 121BC, 100 Meeting Rooms Level

108  
894659

#### Functional single-cell Proteomics of Glioblastoma Defines Extensive Drug Response Heterogeneity and Therapy-Induced Cellular Plasticity

Dena Panovska, KULeuven

109  
898424

#### Toward Ultra-High Parameter Spectral Flow: Probing and Overcoming The Limits Of Spread

Peter Mage, BD Biosciences

110  
898556

#### Quantifying neural cell identity with mass cytometry in ex vivo cultures of primary human glioblastoma

Stephanie Medina, Vanderbilt University

111  
898409

#### Developing an Imaging Mass Cytometry Immunophenotyping Panel for Non-Human Primate Tissues

Paula Niewold, Leiden University Medical Centre

## 0830-0930

### Parallel Session 18: Data Analysis#2 - Alignment and Reproducibility

Room 122B, 100 Meeting Rooms Level

112  
898470

#### A Side-By-Side Comparison of CITE-seq and Flow Cytometry Data of the COVID-19 SARPAC Study

Artuur Couckuyt, VIB-UGent Center for Inflammation Research

113  
898519

#### BACCHUS: Batch Alignment using Canonical Correlation in a High-dimensional Unsupervised Setting

Matei Ionita, University of Pennsylvania

114  
898537

#### Reproducibility in Cytometry: Signals Analysis, Uncertainty Quantification, and Implications for Doublet Deconvolution

Paul Patrone, NIST

115  
898560

#### Alignment, Segmentation and Neighborhood Analysis in Cyclic Immunohistochemistry Data Using CASSATT

Asa Brockman, Vanderbilt University

## 1000-1800

### Poster Viewing Hours Exhibits Open

Hall E

## 1000-1100

### Coffee Break

Hall E

## 1000-1830

### Exhibit Hall Open

Hall E

## 1100-1230

### Keynote Lecture

Terrace Ballroom 1-2

Chair: Jonni Moore

116

#### Nucleoside-modified mRNA-LNP therapeutics

Drew Weismann, University of Pennsylvania

# PROGRAM SCHEDULE

## 1230–1330

### Commercial Tutorials

BD Biosciences: Room 120AB

Bio-Rad Laboratories: Room 120C

Cytek Biosciences, Inc.: Room 121BC

Luminex Corporation: Room 120AB

Tercen Data Analytics Ltd.: Room 121A

Thermo Fisher Scientific: Room 122A

## 1345–1515

### Plenary Session: Novel Clinical Trial Designs for Advanced Therapies

Terrace Ballroom 1–2

Chair: Virginia Litwin, Co-Chair: Jack Dunne

117

#### Advancing novel therapies through cytometry biomarker-driven clinical trial design

Cherie Green, Ozette Technologies

118

#### Application of flow cytometry in clinical development of vaccines against infectious diseases: Benefits and challenges

Stéphane Pillet, Medicago

119

#### Flow cytometry is a powerful tool for informing on dosing decisions in early drug development.

Michelle Graham

## 1515–1545

### Coffee Break

Hall E

## 1530–1700

### Plenary Session: Game Changing Tech and Imaging Cytometry

Terrace Ballroom 1–2

Chair: Genny Del Zotto, Co-Chair: Keisuke Goda

120

#### Single-cell multi-omics analysis reveals novel inflammatory associations in cardiovascular disease

Helen McGuire, University of Sydney

121

#### Unraveling the immune involvement of draining sentinel lymph nodes in melanoma metastasis by multiplexed imaging

Idan Milo, Weizmann Institute of Science

122

Wolfgang Kern, Munich Leukemia Laboratory (MLL)

## 1700–1800

### Poster Session 2

## 1715–1815

### Commercial Tutorials

Standard BioTools: Room 120C

Curiox Biosystems: Room 120AB

# PROGRAM SCHEDULE

The number listed before the abstract title references the abstract located in the back of the program book. Scientific Tutorials with an asterisk after the number may be recorded for CYTOU.

## TUESDAY, JUNE 7

### 800–830

#### ISAC Business Meeting

Terrace Ballroom 1–2

Everyone is welcome!

### 830–1000

#### Plenary Session: Cytometry Data Science, Standards, and Integration

Terrace Ballroom 1–2

Chair: Nima Aghaeepour

124

#### Towards Quantitative and Standardized Flow Cytometric Assays

Lili Wang, NIST

125

#### Deep Geometric and Topological Representations for Extracting Insights from Biomedical Data

Smita Krishnaswamy, Yale University

### 1000–1030

#### Coffee Break

Hall E

### 1000–1830

#### Exhibit Hall Open

Hall E

### 1015–1145

#### Plenary Session: Nanocytometry: Vesicle-mediated Intercellular Communication

Terrace Ballroom 1–2

126

#### Digital Flow Cytometry for Single-Ev Analysis

Daniel Chiu

127

#### Acoustofluidic Technologies for the Manipulation of Cells And Extracellular Vesicles

Tony Jun Huang

### 1200–1300

#### Commercial Tutorials

10x Genomics B.V: Room 121A

Agilent Technologies: Room 120C

Dotmatics, Inc.: Room 120AB

FlowJo, LLC: Room 122A

NanoCollect Biomedical, Inc.: Room 122A

Sony Biotechnology Inc.: Room 121BC

### 1330–1500

#### Plenary Session: Environmental Cytometry

Terrace Ballroom 1–2

Chair: Nicole Poulton, Co-Chair: Gert Van Isterdael

129

#### Tales of Life and Death in the Ocean From Automated Flow Cytometry and Imaging

Heidi Sosik, Woods Hole Oceanographic Institution

130

#### Cytometric Dissection of Cell Functions and Development in Complex Organs and Tissues

David Galbraith, University of Arizona

### 1500–1530

#### Awards Ceremony and Closing

Terrace Ballroom 1–2

### 1530–1730

#### Closing Reception

Terrace Ballroom 3–4

# POSTER SESSIONS

**SUNDAY, JUNE 5, 2022**

## **Poster Session 1**

Hall E

### **Biosafety**

897148

P1

#### **Adaptation of Standard Aerosol Containment Evaluation Procedure for use in BD FACSAria™ Fusion**

Paul Hallberg, University of Pennsylvania

### **COVID-19 research**

901356

P3

#### **Cognitive Symptoms Of Long COVID After Severe SARS-COV-2 Infection Correlate With Prolonged Production of IL-2 and TNF- $\alpha$ Proinflammatory Cytokines by CD8+ T Cells**

Milena Wiech, Nenckie Institute of Experimental Biology PAS, Warsaw

898466

P9

#### **ABSTRACT SUBMISSION FOR TALK: Comprehensive Mapping of Innate And Adaptive Immune Response Dynamics Across The Blood and Respiratory Tract in COVID-19**

Thomas Ashhurst, The University of Sydney

### **CYTO Innovation**

899761

P11

#### **Polymer-Based Synthetic Cells For Next-Generation, Multi-Modal Viability Staining And Analysis**

Martina de Geus, Slingshot Biosciences

901291

P13

#### **Expand Your Dry, Multicolor Panels With Supernova Polymer Dyes**

Mehul Jivrajani, Beckman Coulter

901951

P15

#### **Using 3D Printing and Fabrication to Improve Cytometry Instrumentation**

William Schott, The Jackson Laboratory

901996

P17

#### **Comparison of Immunomagnetic Bead Types: Cell Yield, Losses, And Time Efficiencies For Cell Therapeutics Manufacturing**

Caroline Hoedemaker, Raven Biomaterials LLC

### **Cytometric Technologies**

901483

P19

#### **Optimized Cell Isolation For Mammalian and Plant Cells Using a Gentle Microfluidic Cell Sorter**

Dorinda Moellering, NanoCollect Biomedical

901547

P21

#### **Imaging Second Messenger Responses Of Multi-Labeled Cells Using A Prototype LED-based Excitation-Scanning Spectral Microscope Platform**

Craig Browning, University of South Alabama

901580

P23

#### **Automating Antibody Titration Using a CytoFLEX LX Flow Cytometer Integrated with a Biomek i7 Multichannel Workstation and Cytobank Streamlined Data Analysis**

Rita Bowers, Beckman Coulter, Inc.

901593

P25

#### **Use Dual Wavelength Side Scatter Light for Detecting Nanometer Size Particles and Large Particles in Flow Cytometry**

Nan Li, Agilent Technologies

# POSTER SESSIONS

The number listed before the abstract title references the abstract located in the back of the program book.

901625  
P27

## **Designing Spectrally Clean Fluorescent Dyes For High Dimensional Biological Analysis**

Sean Burrows, Thermo Fisher Scientific

901933  
P29

## **Concurrent and Full Intensity Detection Of Fluorescent Proteins, DNA, and Intranuclear Markers By Cyclic Flow Cytometry**

Marissa Fahlberg, LASE Innovation

901988  
P31

## **Addressing the Need For Workflow Efficiency In Multi-User Laboratories – Optimizing the MA900 Cell Sorter to Ensure Robustness And Operational Performance.**

Toshiyuki Kaimi, Sony corporation

902025  
P33

## **Frequency Encoded Multiplexing in Multiple Region Flow Cytometry**

Frederick Esch, NIST

902041  
P35

## **Ultra-High Event Rate Detection & Microfluidic Cell Sorting Utilizing Inertial Focusing on the MACSQuant® Tyto® Sorter**

Daryl Grummitt, Miltenyi Biotec

898173  
P39

## **CellMek SPS Instrument Performance: Percent Gated Populations From Automated Versus Manual Sample Preparations Using A Wash/Stain/Lyse & Fix/Wash Workflow with a 10-color Antibody Panel In Liquid Or Dry Format**

Kelly Andrews, Beckman Coulter

898432  
P41

## **Are My Purified Cells Performing Optimally After Sorting Using Conventional Droplet Cell Sorting?**

Peter Lopez, NYU Grossman School of Medicine

898509  
P43

## **Automated Autofluorescence Removal in Flow Cytometry**

Alan Chin, Kinetic River

## **Cytometry Assays**

897457  
P45

## **Characterization of UKNEQAS B-ALL Samples Using an RUO One-tube 12-color Antibody Panel on the RUO 12-color BD FACSLyric™ Flow Cytometer**

Yang Zeng, BD Biosciences

900929  
P47

## **Interference Evaluation of the BD® Stem Cell Enumeration Kit on BD FACSLyric™ Flow Cytometer**

Diem Le, BD Biosciences

900959  
P49

## **Precision Performance of Cytex® cFluor® 6-Color TBNK-SL Assay on Northern Light™ (NL) CLC Cytometer Systems**

Jennifer Liu, Cytex Biosciences Inc.

901561  
P53

## **Development of a Flow Cytometric Assay For Differentiating T Cell Memory Phenotypes in CAR-T Process Development**

Susan Foster, Beam Therapeutics

901636  
P55

## **Assessing Viability Dyes For Use on Full Spectral Flow Cytometers**

Sam Thompson, Babraham Institute



# POSTER SESSIONS

901821  
P57

## **Tracking Novel HLA Design Features in Engineered Cells Using PrimeFlow™ RNA Assay**

Marjorie Ison-Dugenny, Kite Pharma

901853  
P58

## **Cryopreservation of Live-Cell Barcodes: A Time-course Study Examining The Stability of CD45 Cadmium Barcodes After Freezing at -80°C for 1 Week to 3 Months**

Martha Brainard, 2seventybio

901898  
P59

## **High-throughput Screening of Antigen-specific IgG Secreting Cells And Linked Single-cell Sequencing Using Nanovial Technology**

Lucie Bosler, Partillion

901942  
P61

## **Accurate Enumeration of Probiotic Bacteria by Flow Cytometry Depends on the Strain and Storage Conditions**

Kevin Galles, IFF

901966  
P63

## **Development of a Novel Flow Cytometry-Based Receptor Occupancy Assay For Assessing Target Engagement of Anti-CCR8 Antibody in FIH Clinical Trial**

Isha Pradhan, Bristol Myers Squibb

901992  
P65

## **Assessing Cytometers For Detection Of Small Particles.**

Rachael Walker, Babraham Institute

902002  
P67

## **Cellular Barcoding Method Using HPMA Polymer Coupled Spectral Probes**

Tomáš Kalina, Charles University, 2nd Faculty of Medicine

902016  
P69

## **Cytokine Multiplexing on a Full Spectral Cytometer**

Michael Solga, University of Virginia Flow Core

902030  
P71

## **Development of a CD137 Receptor Occupancy Assay To Support The Phase I/II Study of BT7480, a Bicycle Tumor-Targeted Immune Cell Agonist™ (Bicycle TICA™)**

Chintan Jobaliya, FlowMetric, a KCAS company

904059  
P73

## **Development of a Flow Cytometry Assay To Monitor Human PBMC Engraftment and PD Response in Humanized NSG Mice**

Janina Schwarte

904672  
P75

## **Barcoding Developed for Cell Cycle Analysis: A Rigorous, Efficient Method Of Simplifying Compound Screening**

Laura Prickett, AstraZeneca

898428  
P77

## **Imaging Flow Cytometry As A New Route For High-Throughput Characterisation Of Pattern Recognition Receptors Binding Capabilities For Point-of-Care Device Development**

Andrew Farthing, University of Glasgow

## **Data Analysis**

901658  
P81

## **Automatic Identification Of Diagnostic Biomarkers For Rheumatic Diseases: Lessons Learned Building and End-To-End Machine Learning Workflow**

Pablo López-García, CBmed GmbH - Center for Biomarker Research

901908  
P83

## **How to Make Your Flow Cytometry Life Easier: Finding Differences In B Cell Subsets Between Autoimmune Diseases And Healthy Controls Using CITRUS**

Verena Pfeifer, CBmed

901912  
P84

## **A Machine Learning Workflow for Automatic Immune Phenotyping of Type 1 Diabetes Samples**

Jose Vera-Ramos, CBmed

# POSTER SESSIONS

The number listed before the abstract title references the abstract located in the back of the program book.

901939  
P85

## **Benefits of an Open Source Similarity Score For Multiparametric Flow Cytometry Controls.**

Sara Garcia, CNIO

902022  
P86

## **MetaFlow: Innovative Cloud Based Topological Analysis Platform for High-Dimensional Flow Cytometry Data**

Kamila Czechowska, Metafora Biosystems

902027  
P87

## **Quantitative Digital Image Analysis Of Ultra-High Plex Immunofluorescence Imaging**

Bassem Ben Cheikh, Akoya Biosciences

902042  
P88

## **Automated Data Analysis of a 24-Color Nonhuman Primate Leukocyte Immunophenotyping Panel**

James Thomas, Leidos Biomedical Research, Inc.

902312  
P89

## **Implementation and Validation Of An Automated Spectral Flow Cytometry Analysis Pipeline In Large Scale Human Immune Profiling.**

Ekambaram Ganapathy

898154  
P91

## **Fully Automated Large-Scale Integration Of Mass Cytometry Datasets Using Deep Learning Reveals Insights into the COVID-19 T-cell Landscape**

Hajar Saihi, QMUL

898423  
P93

## **PhenoComb: A Discovery Tool To Assess Complex Phenotypes In High-Dimension, Single-Cell Datasets.**

David Woods, CU Anschutz

898517  
P95

## **Robust Identification of Biomarkers Through A Clustering Approach Guided By Patient Outcomes: Application In B-cell ALL, Melanoma And Rheumatoid Arthritis**

Julien Nourikyan, AltraBio SAS

898554  
P97

## **A Simple Guide For Selecting A Cytometry Data Analysis Strategy**

Alice Wiedeman, Benaroya Research Institute

## **Diagnostics**

906041  
P99

## **Novel 355nm (and Lower) Excitable and Tuneable Emission (Blue through Red) Fluorophores Utilised in Flow Cytometry**

Sareena Sund, High Dimensional Cytometry

897392  
P101

## **From Automated Antibody Mixing to Reliable Analysis**

Victor Bosteels, VIB-UGent Center for Inflammation Research

901054  
P103

## **Determination of Optimal Settings For Detector Voltages For Resolution Of A 14-Color Panel On The Bigfoot Cell Sorter**

Kenneth Quayle, CCHMC

901481  
P105

## **Expanding the Maxpar Direct Immune Profiling Assay to enable Comprehensive Antigen-Specific Immune Analysis**

Michael Cohen, Fluidigm Canada

901599  
P107

## **Identifying Relapse Associated Proteins by Human Surfaceome Screening in B-ALL**

Dorra Jedoui, Stanford university

901810  
P109

## **Time to Meet The Moment: High-Speed Cell Sorting Using Real-Time Full Spectral Unmixing**

Iyadh Douagi, NIH

901827  
P111

## **Expanding Panel Size In Spectral Flow Cytometry With Starbright Dyes Excitable By The Ultraviolet, Violet, Blue And Yellow Lasers.**

Michael Blundell, Bio-Rad

# POSTER SESSIONS

901909  
P113

**Seeing More with the 320nm Laser – How the ID7000 Spectral Cell Analyzer can distinguish Fluorochromes with adjacent and overlapping spectra**

Koji Futamura, Sony Corporation

901998  
P115

**A 50+ Color Full Spectrum Panel To Assess The Immune Landscape In Finite Quantities Of Human Blood And Tissue**

Andrew Konecny, Fred Hutchinson Cancer Research Center

## Image Cytometry

896847  
P117

**Imaging Flow Cytometry Analysis Of Climate Change Scenarios In Freshwater Aquatic Systems: A Case Of Microcystis spp. Blooms**

Adina Zhumakhanova, Nazarbayev University

898669  
P119

**From Image To Flow: An Example Work Flow For Single Cell Image Analysis From Transmitted Light Confocal Images**

Dominic Jenner, Dstl

901385  
P121

**Imaging Mass Cytometry Identifies Structural and Cellular Composition of the Mouse Tissue Microenvironment**

Clinton Hupple, Fluidigm

901629  
P123

**Combining machine learning and imaging flow cytometry to reduce the need for functional staining in monitoring of infection in algal blooms**

**Maxim Lippeveld, Flora Vincent, Daniel Peralta, Assaf Vardi, Yvan Saeys**

Maxim Lippeveld, Ghent University

901847  
P125

**Improving Plant Protoplast Cell Sorting Outcomes With High-Speed Fluorescence Image-Enabled Cell Sorting.**

Gert Van Isterdael, VIB-Ghent University

901921  
P127

**Ultrahigh-Content Imaging Helps To Identify CAR Target Candidates Against Pancreatic Adenocarcinoma**

Nathan Brady, Miltenyi Biotec B.V. & Co. KG

901980  
P129

**Altering Gating and Analysis through Integration of High Speed, High Resolution Imaging with Flow Cytometry Data**

Heaven Roberts, Thermo Fisher Scientific

898476  
P135

**Let's take a Cell-fie: A High-Dimensional Learning Workflow Trained On Cell Morphologies Accurately Predicts Cell Subset Heterogeneity Within Imaging Cytometry Data**

Ioannis Panetas, BD

898510  
P137

**Integration and Control of Low-Cost Industrial Cameras in a Home-Built Flow Cytometer**

Martin Hussels, Physikalisch-Technische Bundesanstalt

898518  
P139

**Let's take a Cell-fie: A High-Dimensional Learning Workflow Trained On Cell Morphologies Accurately Predicts Cell Subset Heterogeneity Within Imaging Cytometry Data**

Ioannis Panetas, BD

898563  
P141

**Studying Bacterial-Environmental Effects By Imaging Flow Cytometry**

Ziv Porat, Weizmann Institute of Science

# POSTER SESSIONS

The number listed before the abstract title references the abstract located in the back of the program book.

## Immunology

897502  
P143

### **Th17 is the Main Phenotype Displayed by CD4+ CD28null Cells From Patients With Rheumatoid Arthritis**

Mariana Patlan, Instituto Nacional de Cardiologia

899335  
P145

### **NIST Measurements of NanoParticle Intensity and Number Concentration for Characterization of Viruses and EVs using Flow Cytometry**

Paul DeRose, NIST

901059  
P147

### **Contributions of Extracellular Vesicles In The Pathophysiology Of Human Cutaneous Leishmaniasis**

Vanessa Costa, Fiocruz

901280  
P149

### **A 26-color Panel For Comprehensive Immunophenotyping Of Leukocyte Subsets Across Different Murine Tissues Using the Agilent NovoCyte Penteon Flow Cytometer**

Ming Lei, Agilent

901284  
P151

### **Frozen Murine Monocytes Isolated From Bone Marrow Are Not Able To Efficiently Differentiate And Present Exogenous Nanoparticle Bound Hiv-1 P24 Antigen Due To Failure Of Early Endosome Formation**

Katerina Zachova, Palacky University Olomouc, Czech Republic

901299  
P153

### **Diversity of Intratumoral Regulatory T Cells In Non-Hodgkin lymphoma**

Kanutte Huse, Oslo University Hospital

901564  
P155

### **TNFAIP3 Expression in RAG Mice Drive Colitis in TNF $\alpha$ Dependent Way**

Alvaro Torres Huerta, IUSM

901849  
P156

### **PD-L1 Expression in NSCLC MDSCs and its Potential Use As A Biomarker To Determine Treatment Response Through Dimensionality Reduction Of Flow Cytometric Data**

Roser Salvia-Cerdà, Germans Trias i Pujol Research Institute (IGTP)

901926  
P157

### **Studying the Immune-Profile In Patients With Paraneoplastic Cerebellar Degeneration Using Imaging Mass Cytometry**

Ida Viktoria Herdlevær, Haukeland Univeristy Hospital

901987  
P158

### **CD8+ Regulatory T-cell Subset Distribution In Adolescents With Primary Hypertension Is Associated With Hypertension Severity And Hypertensive Target Organ Damage**

Lidia Gackowska, Izabela Kubiszewska, Anna Helmin-Basa, J.Michalkiewicz, M.Wiese-Szadkowska, A.Wierzbicka-Rucinska, L.Obrycki, Mieczyslaw Litwin

901995  
P159

### **T cell Subsets Correlating With The Onset of GvHD**

Petra Hadlová, Charles University

902009  
P161

### **Suppressive Eosinophils in Patients with Type 1 Diabetes – What Is Its Role In Immunoregulation And Autoimmunity?**

Christine Lingblom, Sahlgrenska University Hospital

902038  
P163

### **Enhanced Expansion And Effector Function Assessment of Natural Killer (NK) Cell Activity for Immunotherapy**

Jody Bonnevier, Bio-Techne

898485  
P165

### **T Cell Subset Analysis in Autoimmune Addison's Disease (AAD) Using Mass Cytometry in Suspension (CyTOF)**

Shahinul Islam, University of Bergen

# POSTER SESSIONS

## Optimized Multicolor Immunofluorescence Panel (OMIP)

901505  
P167

### Optimization of a 24-Color Flow Cytometry Panel for Natural Killer Cell Phenotypic Profiles Analysis

Matthew Creegan, Henry M Jackson Foundation for the Advancement of Military Medicine

901532  
P169

### Leveraging DNA in Fluorescent Reporter Technology To Enable Higher Plex Flow Cytometry

Brandon Trent, ThermoFisher Scientific

901917  
P171

### Development and Validation Of A 30-Colour Spectral Flow Cytometry Immunophenotyping Panel Designed For Determination Of Antigen-Specific B cells, T cell subsets, MAIT, and NK cells, Plus A Variety Of Activation Markers In Human Cryopreserved PBMC

Esther Perez Garcia, GlaxoSmithKline

## Other cytometry Applications

901487  
P173

### Groundwater-borne Microbes Affect The Distribution Of Highly Auto-Fluorescent Cyanobacterial Populations In Coastal Seawater

Ekaterina Kopitman, Weizmann Institute of Science

901961  
P175

### Per-cell Uncertainty Estimates In A Serial Microcytometer.

Megan Catterton, NIST

901983  
P177

### Correlating NAD(P)H Lifetime Shifts To Treatment Of Breast Cancer Cells: A Metabolic Screening Study With Time-Resolved Flow Cytometry

Samantha Valentino, New Mexico State University

## Quality Assurance/Standardization

898804  
P179

### MIFlowCyt-EV Reporting Of Single Vesicle Flow Cytometry Methods And Results

John Nolan, Scintillon Institute

901438  
P181

### Polymer-based Synthetic Cells For Next-Generation Compensation And Spectral Unmixing

Anh-Tuan Nguyen, Slingshot Biosciences

901528  
P183

### Antibody Quality - How Antibody Validation Contributes To Optimal Research Conditions

Stefanie Ginster, Miltenyi Biotec

901546  
P184

### Monitor Critical Parameters in Advanced Flow Cytometers

Daniela Ischiu Gutierrez, NIAID

901566  
P185

### PBMC Processing Conditions To Optimize Isolation of Immune Cell Subsets

Ajinkya Pattekar, University of Pennsylvania

894956  
P186

### Bacterial Mock Communities As Standards For Reproducible Cytometric Microbiome Analysis

Susann Mueller, Helmholtz Centre for Environmental Research – UFZ

# POSTER SESSIONS

The number listed before the abstract title references the abstract located in the back of the program book.

## Shared Resource Laboratories

901296  
P187

### Step by Step Approach for Training and Education of Flow Cytometry Users Including Roadblocks and Cross Platform Considerations: An SRL Perspective

Kathleen Daniels, Sana Biotechnology

901381  
P188

### Optimizing User-Staff Communication in a Large Multi-Site Shared Resource Laboratory

William Murphy, University of Pennsylvania

901404  
P189

### Flow Cores in the Time of COVID

John Tigges, Beth Israel Lahey Health

901928  
P190

### SRL Technicians Exchange: How Knowledge Sharing Increases Versatility and Offers Fresh Insight in Facility Operations.

Sam Thompson, Babraham Institute

902028  
P191

### TROUBLESHOOTERS WANTED: FlowRemedy Diagnostic Chart for Cytometer Users in the Shared Resource Laboratory

Jennifer Jakubowski, University of Pennsylvania

## Single Cell “-omics”

898809  
P193

### Flow Cytometry Based Single Cell Isolation and RNA Sequencing Of Primary Tumor, Rare Circulating Tumor Cells And Metastases Characterizes The Poorly Defined Metastatic Cascade In Pancreatic Cancer

Moen Sen, University of Pennsylvania

901028  
P195

### “Single-cell Immune Profiling of the SARS-CoV-2 Immune Response

Kivin Jacobsen<sup>1</sup>, Amir Ameri<sup>1</sup>, Dilek Inekci<sup>1</sup>, Charlotte Halgreen<sup>1</sup> and Liselotte Brix<sup>1</sup>

<sup>1</sup> Immudex, Bredevej 2A, DK-2100 Virum”

## Immudex Aps

901251  
P197

### Single Cell Proteomics Complements Transcriptomic Read Outs Enabling Detailed Cell Type Classification On Multiple Sample Types

Rea Dabelic, 10x Genomics

901813  
P199

### CostaL: An Accurate And Scalable Graph-Based Clustering Algorithm For High-Dimensional Single-Cell Data Analysis

Yijia Li, University Of Minnesota

901981  
P201

### An Automation-Based Workflow For Gentle Dissociation And High-Speed Nuclei Sorting Upstream Of Single Nuclei RNA Sequencing.

Evelyn Rodriguez-Mesa, Owlbiomedical

902036  
P203

### Morphological Characterization And Sorting Of Viable And Label-Free Malignant Cells From NSCLC Tissue Using Deep Learning

Chassidy Johnson, Deepcell

898531  
P205

### Parallelization of Single-Cell Multi-Omics Assays by Designing Smart Consumables

Ricarda Wallinger, STRATEC Consumables GmbH

## Submicron Cytometry

899721  
P207

### Conjugated Oligoelectrolytes (Coe): A Novel Class of Fluorogenic Membrane Dyes That Do Not Form Micelles Of The Same Size As Extracellular Vesicles

Wan Ni Geraldine Chia, National University of Singapore

901416  
P209

### “Optimization and Quantification Of Small Particle Sensitivity On The Cytek Aurora Platform Using FCMPASS Software.

Authors: Joshua A. Welsh, Vera A. Tang, Claudia Bispo, Jennifer C. Jones, Maria Jaimes, and Joanne Lannigan  
Vera Tang, University of Ottawa

# POSTER SESSIONS

901850  
P211

## **A Rapid Method For Assessing The Accumulation Of Nanoplastics In Human Peripheral Blood**

Roser Salvia-Cerdà, Germans Trias i Pujol Research Institute (IGTP)

901994  
P213

## **Sized Based Separation of Extracellular Vesicles Using an Elasto-Inertial Approach**

Hassan Pouraria, New Mexico state university

902034  
P215

## **Lectin-based Multi-Parametric Flow Cytometry Analysis Of Glycosignatures In Prostate Cancer Patient Extracellular Vesicles.**

Michelle Gomes, OHSU

902047  
P216

## **The Delaware: A Flow NanoCytometer for Nanoparticle Analysis**

Giacomo Vacca, Kinetic River Corp.

896787  
P217

## **Next Generation nanoFACS with High Resolution Imaging And Custom 50um Nozzle**

Terry Morgan, OHSU

898467  
P218

## **Small Particle Flow Cytometry Using 3D Light Scatter Detection Enhances Extracellular Vesicle Analysis In Liquid Biopsies Highlighting The Potential To Segregate EVs by Refractive Index.**

Desmond PINK, Nanostics

898521  
P219

## **Proteomic Characterisation of CD81-tdTomato Prostate Cancer-derived sEVs and Their Distribution in Two-Dimensional Dynamic Cell Systems**

Rachel Errington, Cardiff University

898527  
P220

## **Physical Association Of Lipoprotein Particles and Extracellular Vesicles Unveiled By Single Particle Flow Cytometry**

Estefania Lozano-Andres, Utrecht University

898529  
P221

## **Small Particle Flow Cytometry Using 3D Light Scatter Detection Enhances Extracellular Vesicle Analysis In Liquid Biopsies Highlighting The Potential To Segregate EVs by Refractive Index.**

Additional author: Robert Paproski, John D Lewis, Desmond PINK Nanostics

## **Therapeutics**

897407  
P222

## **Design of “Smart” Nanoparticles For Combined In-Vivo Imaging And Advanced Drug Delivery Therapeutics For Single-Cell Nanomedicine**

James Leary, Aurora Life Technologies LLC

901367  
P223

## **Evaluation of Dry DURAClone Antibody Panels For The Characterization Of Human PBMCs, Enriched T cell Fractions and anti-BCMA CAR-T cells**

Rita Bowers, Beckman Coulter, Inc.

901841  
P224

## **Delivery of Oligonucleotides Into Tumor Cells Via Monoclonal Antibodies: Targeting of mRNA Following Release Of Antisense Oligonucleotides Through Cell Surface Protease Activities Using Antibody Substrate Oligonucleotide Conjugates (ASOCs)**

Beverly Packard, Oncolmmunin, Inc.

# POSTER SESSIONS

The number listed before the abstract title references the abstract located in the back of the program book.

## MONDAY, JUNE 6, 2022

1700–1800

### Poster Session 2

Hall E

#### COVID-19 research

901582

P4

**Evaluation of absolute and percentage counts of the total, B, NK, T lymphocytes, and TCD4 and TCD8 subpopulations in patients with COVID-19 during the hospitalization and after hospital discharge**

Gabriela Eburneo, UNIFESP

901596

P6

**SARS-CoV-2 vaccine Humoral and Cellular responses in B cell immunocompetence and immunodeficiency**

Berenice Cabrera-Martinez, University of Colorado Anschutz Medical Campus

896789

P8

**Physical phenotype of blood cells is altered in COVID-19 an beyond: causal relation for long-term imprint?**

Martin Kräter, Max Planck Institute for the Science of Light

898540

P10

**Comprehensive mapping of innate and adaptive immune response dynamics across the blood and respiratory tract in COVID-19**

Thomas Ashhurst, The University of Sydney

#### CYTO Innovation

901203

P12

**High-density glass-bottom nanowell-in-microwell arrays for cell tracking image cytometry**

Jeonghyun Lee, University of British Columbia

901295

P14

**A UV-C LED-based reactor for continuous decontamination of the sheath fluid in a flow-cytometric cell sorter**

Toralf Kaiser, DRFZ

901985

P16

**Novel live-cell and fixable mitochondrial probes for cytometry and imaging.**

Hannah Maple, Bio-Techne

901203

P12

**High-density glass-bottom nanowell-in-microwell arrays for cell tracking image cytometry**

Jeonghyun Lee, University of British Columbia

901295

P14

**A UV-C LED-based reactor for continuous decontamination of the sheath fluid in a flow-cytometric cell sorter**

Toralf Kaiser, DRFZ

901985

P16

**Novel live-cell and fixable mitochondrial probes for cytometry and imaging.**

Hannah Maple, Bio-Techne

#### Cytometric Technologies

898418

P18

**CellMek SPS Instrument Performance: Cellular and Reagent Carryover when using the Cell Wash Module**

Brittany Kuhl, Beckman Coulter Inc

901523

P20

**Internally stained multiple fluorescent microsphere intensity reference with assigned ERF-values for quantitative flow cytometry analysis**

Yu-Zhong Zhang, Thermo Fisher Scientific

901556

P22

**Semi and fully automated sample preparation platforms improve washing efficiency, reproducibility, and recovery of live leukocytes in fresh and freeze-thawed specimens**

Geoffrey Feld, Curiox Biosystems



# POSTER SESSIONS

901583  
P24

## **Performance of SiPM for Dim Fluorescence Signal Detection in Flow Cytometry**

Nan Li, Agilent Technologies

901598  
P26

## **Time-resolved measurements of MCF-7 breast cancer cells using CD29-Alexa Fluor 488 and CD29-FITC as discriminants with acoustofluidic flow cytometry**

Jesus Sambrano, New Mexico State University

901896  
P28

## **Optimization and set-up of the BD Spectral Enabled Prototype Analyzer**

Erica Smit, Vaccine Research Center, NIH

901955  
P30

## **High Marker T Cell Characterization with Reduced Spillover using Cyclic Flow Cytometry**

Sean Cosgriff, LASE Innovation

902018  
P32

## **Uniform Light-Sheet Excitation Beam Formed by Integrated Optics for Sensitive Optofluidic Cytometry**

Matthew DiSalvo, National Institute of Standards and Technology

902040  
P34

## **Fluorescence and Transmission Intensity-Over-Time Measurement Simulation in an Optofluidic Cytometer**

Nikita Podobedov, National Institute of Standards and Technology

902044  
P36

## **Sorting large and fragile cells - A model cell line and novel microfluidic device**

Benjamin Fynn, Owl Biomedical

894183  
P38

## **“Linking Blood Analyzer and Flow Cytometry Capabilities Creates a Powerful Method for Monitoring Tumor Cell Engraftment and Aiding Drug Development Decisions in Mouse Models**

Antony Chadderton, Melody Diamond, and Matthew Stubbs, Incyte Research Institute, Wilmington, DE; Tony Chadderton, Incyte

898201  
P40

## **CellMek SPS Instrument Performance: Repeatability and reproducibility of a wash/stain/lyse & fix/wash workflow with a 10-color antibody panel in DURACartridge custom dry reagent format**

Xizi Dai, Beckman Coulter

898436  
P42

## **Multiphysics innovation for high speed, high recovery, and high viability automated cell separation**

Liping Yu, Applied Cells, Inc

898545  
P44

## **Utilization of Distinct Autofluorescent Spectra From Different Subsets Provides Best Fluorescent Signal Resolution in High Parameter Spectral Flow Cytometry**

Nicholas Wanner, Cleveland Clinic

## **Cytometry Assays**

898448  
P46

## **Performance evaluation of the BD Leucocount™ Assay on the BD FACSLyric™ and BD FACSCalibur™ Flow Cytometers using UK NEQAS leukoreduced RBC and PLT samples**

Angela Chen, BD

898661  
P48

## **Multi-site evaluation of the BD® Stem Cell Enumeration Kit for CD34 cell enumeration on BD FACSLyric™ and BD FACSCanto™ II Flow Cytometers**

Yang Zeng, BD Biosciences

901025  
P50

## **Development of a 10-color flow cytometric assay to assess binding of a monoclonal antibody (VB421) against IGF-1R in Peripheral Blood Mononuclear Cells (PBMCs) from patients with Thyroid Eye Disease.**

Michael Podolsky, BioAgilytix

901545  
P52

## **Visualization of calcium flux in bone marrow using leukaemia initiating cells transduced with Salsa6f**

Pathik Sen, Massachusetts General Hospital

# POSTER SESSIONS

The number listed before the abstract title references the abstract located in the back of the program book.

901591  
P54

## **Novel Whole Blood Depletion Assay to Assess Fc Effector Function of Therapeutic Antibodies**

Benjamin Ordonia, Genentech, Inc.

901809  
P56

## **Effects of fixation And Photobleaching On Fluorochrome Stability Revealed By Full Spectral Flow Cytometry Analysis**

Iyadh Douagi, NIH

901853  
P58

## **Cryopreservation of Live-Cell Barcodes: A Time-Course Study Examining The Stability of CD45 Cadmium Barcodes After Freezing at -80°C for 1 week to 3 months**

Martha Brainard, 2seventybio

901911  
P60

## **A Quantitative, Lyse No-Wash Blood Flow Cytometric Assay To Monitor Immune Subpopulation Changes In Inflammatory Disease Mouse Models.**

Sofia Grammenoudi, Bsrc Alexander Fleming

901958  
P62

## **Flow Cytometric Analysis of mTORC1 and mTORC2 Signaling Pathway Markers in Human Smart Tube Samples**

Heather Evans-Marin, FlowMetric

901974  
P64

## **Detecting Human Eosinophils in Peripheral Blood by Adding a Heterogeneous Auto-Fluorescent Parameter as a Fluorescent Tag in Cytex Aurora**

Jiangfang Wang, GlaxoSmithKline

901997  
P66

## **Fast and Simple Assay Of Cell Cycle Analysis Via Direct Labeling Of Newly Synthesized DNA**

Erika Kuzmova, Institute of Organic Chemistry and Biochemistry of the Czech Academy of Sciences

902015  
P68

## **Steric Hindrance of HIV Envelope for Binding to Streptavidin Results in Reduced Valency of B Cell Tetramers**

Evan Trudeau, Duke Human Vaccine Institute

902026  
P70

## **Cell Sorting, FLIM and Imaging Analysis of Plasmodium falciparum Exposed to Artemisinin**

Ludmila Krymskaya, NIH

902032  
P72

## **New Fixable Viability Dyes And Applications For Flow Cytometry**

Brandon Trent, ThermoFisher Scientific

904062  
P74

## **Identifying Unconventional T Cell Populations in Non-Human Primates in Mycobacterium tuberculosis Vaccines Studies using Flow Cytometry**

Samantha Provost

898406  
P76

## **Quantitative Expression Profiling of Surface Antigens on Peripheral Blood Leukocyte subsets and Childhood T-cell Acute Lymphoblastic Leukemia (T-ALL) [MvZ1]Cells using a Standardized Flow Cytometry Workflow: A HCDM CDMaps Initiative**

Tomáš Kalina, Charles University, 2nd Faculty of Medicine

# POSTER SESSIONS

## Cytometry Education

902029  
P78

### Expanding Practical Education in a Core Facility with the Attune CytPix Brightfield Imaging Capable Flow Cytometer

Cora Chadick, Amsterdam UMC

## Data Analysis

901495  
P80

### Automated Analysis of 14-Color Immunophenotyping Data

Benjamin Hunsberger, Verity Software House

901823  
P82

### Identification of immunologic Similarities Between Autoimmune Diseases Using Flow Cytometry And Disease Sub-Clustering

Laurin Herbsthofer, CBmed GmbH

901912  
P84

### A Machine Learning Workflow for Automatic Immune Phenotyping of Type 1 Diabetes Samples

José Antonio Vera-Ramos, CBmed

902022  
P86

### MetaFlow: Innovative Cloud Based Topological Analysis Platform for High-Dimensional Flow Cytometry Data

Kamila Czechowska, Metafora Biosystems

902042  
P88

### Automated Data Analysis of a 24-Color Nonhuman Primate Leukocyte Immunophenotyping Panel

James Thomas, Leidos Biomedical Research, Inc.

904674  
P90

### Separating Flow Cytometry Populations Based on Probabilistic Analysis

Danielle Middlebrooks

898212  
P92

### flowSim: Improving The Quality Of Training Sets And Machine Learning Models Applied to FCM Data Analysis

Sebastiano Montante, BC Cancer Research Center

898475  
P94

### Projection of High-Dimensional Cytometry Data Using Regularised Autoencoders

David Novak, IRC-VIB UGent

898548  
P96

### Analysis Paralysis: How to Choose The Optimal Algorithm For Compensation When Highly Autofluorescent Cells Are Present

Jack Panopoulos, BD

## Diagnostics

901376  
P98

### MACSima Imaging Cyclic Staining (MICS) Technology Reveals Combinatorial Target Pairs for CAR T cell Treatment Of Solid Tumors

Travis Jennings, Miltenyi Biotec

902007  
P100

### Evaluation of a Complex Antigen To Stimulate Cellular Responses To Coccidioides And Advance Diagnostics.

Mrinalini Kala, University of Arizona

## High Dimensional Cytometry

901032  
P102

### Advancements in Single Cell Multiomic Profiling Of Antigen-Specific T cells with dCODE Dextramer® (RiO) and BD® AbSeq Reagents on the BD Rhapsody™ Single-Cell Analysis System

Kivin Jacobsen, Immudex aps

901397  
P104

### CyTOF XT allows For Automated And Streamlined High-Plex Cytometric Immunophenotyping

Lauren Tracey, Fluidigm

901590  
P106

### Extending the Capabilities Of A High-Parameter Immunophenotyping Assay With Cytoplasmic Staining Applications For Mass Cytometry

Huihui Yao, Fluidigm Canada Inc

# POSTER SESSIONS

The number listed before the abstract title references the abstract located in the back of the program book.

901796  
P108

## **DNA-Based Dye Nanostructures Enable New Directions in Spectral Flow Cytometry**

Nick Pinkin, Thermo Fisher Scientific

901826  
P110

## **Build Bigger Better Panels With Superior Dyes Excitable By The Ultraviolet, Violet, Blue And Yellow Lasers.**

Michael Blundell, Bio-Rad

901859  
P112

## **22-color Spectral Flow Cytometry Panel Development for Exploring Circulating Gut-homing T cells in CeD Patients after Dietary Gluten Challenges**

Taryn Mockus, GSK

901925  
P114

## **Characterization of Autologous Hematopoietic Stem Cell Transplantation in Multiple Sclerosis**

Jonas Bull Haugsøen, University of Bergen

## **Image Cytometry**

896542  
P116

## **Hyperspectral Imaging, Region Analysis, and Filtering To Identify Second Messenger Signals in Signal-Limited Images**

Silas Leavesley, University of South Alabama

901041  
P120

## **A Rapid and Fully Automated in Vitro Micronucleus Assay Using Imaging Flow Cytometry and Convolutional Neural Network Analysis**

Raymond Kong, Luminex Corporation

901488  
P122

## **Multi-Dimensional Imaging Flow Cytometer for Improved Cell Counting Accuracy**

Christian Goerke, Physikalisch-Technische Bundesanstalt

90191

## **Bright Fluorescent Conjugates For Imaging Applications With Erasable Signal Via Dual-Release Mechanism**

Thorge Reiber, Miltenyi Biotec

901952  
P128

## **Exploring Imaging Flow Cytometry and Morphometrics for Characterization of Leukemic Stem Cells in Acute Myeloid Leukemia**

Trine Engelbrecht Hybel, Aarhus University Hospital & Aarhus University

893902  
P130

## **High-Throughput Chemotherapeutic Drug Screening Of Tumor Spheroids With Individual Spheroid Results Using Image Cytometry**

Leo Chan, Nexcelom Bioscience

896493  
P132

## **Imaging Flow Cytometer Based On Linear Array Spot Illumination Generated By Diffractive Optical Elements**

Yong Han, Tsinghua University

898251  
P134

## **High Dimensional Imaging Of Human Cutaneous Squamous Cell Carcinoma Reveals A Specific Signature Associated With Relapse**

Aïda Meghraoui, AMKbiotech

898504  
P136

## **Imaging Flow Cytometry-Based Analysis of Leishmania's Cell Cycle**

Jessie Howell, University of Glasgow

898516  
P138

## **Exploring Cell-Cell Interactions Through Simultaneous Imaging Cytometry and Multi-Color Immunophenotyping**

Authors: Aaron J Middlebrook, Peter Mage, Keegan Owsley, Tri Le, Patricia Lovelace and Eric Diebold  
Aaron Middlebrook

# POSTER SESSIONS

## BD Biosciences

898534

P140

### **Using Integrated Multidimensional Mass Cytometry and Multiplex Immunohistochemistry to Infer Spatial Relationships Between Phenotypically Distinct Glioblastoma Infiltrating Immune Cells**

Todd Bartkowiak, Vanderbilt University

898564

P142

### **Imaging Flow Cytometry as a Tool To Study Distribution Dynamics Of Extra-Cellular Vesicles RNA Cargo Within Immune Cells**

Ziv Porat, Weizmann Institute of Science

## Immunology

898433

P144

### **The Critical Role of IL-23 Receptor Positive T cells in the Pathogenesis of Anterior Uveitis Associated with Spondyloarthritis**

Robert Hedley, University of Oxford

899722

P146

### **High-risk Neuroblastoma Survivors Show Signs Of Immunosenescence Early After Therapy And Retain Increased Myeloid Cell Activation Status**

Petra Laznickova, Fnusa-Icrc

901279

P148

### **Phenotypic Analysis Of Mouse Hematopoietic Stem And Progenitor Cells Using A 14-Color Panel With The Agilent Novocyte Penton Flow Cytometer**

Ming Lei, Agilent

901281

P150

### **What Is Responsible For Abnormal Galactose-Deficient IgA Production In IgA Nephropathy? Looking For The Source**

Petr Kosztyu, Palacky University in Olomouc

901285

P152

### **Influence of IL-6 on B Regulatory Lymphocytes and $\lambda$ Light Chain Expression in IgA Nephropathy**

Jana Jemelková, Palacky University

901502

P154

### **Exploring the Association of Preexisting Mycobacterial T Cell Responses With Mtb Challenge Outcome in Unvaccinated and Vaccinated NHP**

Evan Lamb, Samantha Provost, Mitzi Donaldson, Patricia A. Darrah, Kathryn Foulds, Mario Roederer, Vaccine Research Center, NIAID, NIH, Bethesda, MD

Evan Lamb, NIH

901849

P156

### **PD-L1 Expression in NSCLC MDSCs and its Potential Use as a Biomarker to Determine Treatment Response Through Dimensionality Reduction of Flow Cytometric Data**

Roser Salvia-Cerdà, Germans Trias i Pujol Research Institute (IGTP)

901987

P158

### **CD8+ Regulatory T-cell Subset Distribution in Adolescents With Primary Hypertension is Associated With Hypertension Severity And Hypertensive Target Organ Damage**

Lidia Gackowska, Nicolaus Copernicus University in Torun, Collegium Medicum in Bydgoszcz

902003

P160

### **The Distribution of CD4+ T cell Subpopulations in Adolescents With Non-Alcoholic Fatty Liver Disease.**

Izabela Kubiszewska, Lidia Gackowska, Anna Helmin-Basa, Jacek Michalkiewicz, Malgorzata Wiese-Szadkowska, Sara Balcerowska, Aleksandra Wasilow, Aldona Wierzbicka-Rucinska, Wojciech Janczyk, Piotr Socha

902014

P162

### **Regulatory B Cells In The Development And Control Of Nonalcoholic Fatty Liver Disease In Adolescents**

Anna Helmin-Basa, Nicolaus Copernicus University in Torun, Collegium Medicum in Bydgoszcz

898434

P164

### **The Critical Role of IL-23 Receptor Positive T cells in the Pathogenesis of Anterior Uveitis Associated with Spondyloarthritis**

Robert Hedley, University of Oxford

# POSTER SESSIONS

The number listed before the abstract title references the abstract located in the back of the program book.

## Optimized Multicolor Immunofluorescence Panel (OMIP)

901366  
P166

**Use of Vio® and Vio® Bright Dyes with REAfinity™ Recombinant Antibodies for Phenotypic Characterization of Human  $\gamma\delta$  T-cells by Multicolor Flow Cytometry**

Dirk Meineke, Miltenyi Biotec B.V. & Co. KG

901506  
P168

**Comprehensive Immunomonitoring Of Patients After Hematopoietic Stem Cell Transplantation Using OMIP-080**

Sarka Vanikova, Institute of Hematology and Blood Transfusion

901915  
P170

**Development and Validation of a 23-Colour Spectral Flow Cytometry Immunophenotyping Panel Designed for Determination of Activated Dendritic Cell, Monocyte and B Cell Populations in Human Cryopreserved PBMC**

Irene del Molino del Barrio, GSK

## Other cytometry applications

898256  
P172

**CellMek SPS Instrument Performance: WBC and Subpopulation Recoveries Using Specimen Wash and Sample Wash Workflows**

Casey Roberts, Beckman Coulter

901489  
P174

**Method for Low Cell Number Sample Preparation – Automated Up-Concentration, Washing And Staining Using Acoustic Trapping**

Jessica Congiu, AcouSort AB

901979  
P176

**Hot Flow: Attune Plumbing for Radioactive Samples**

Kathryn Fox, UW-Madison

902004  
P178

**Innate Immune Response In Alzheimer's Disease Mediated By Bradykinin**

Micheli Pillat, Federal University of Santa Maria

## Quality Assurance/Standardization

901427  
P180

**Impact of Fixation on Autofluorescence, Fluorescence, Spectral signature, and Data Quality**

Giri Buruzula, NIBR

901468  
P182

**Flow Cytometry Optimization Protocol Improves Detection of Fluorescent EV Populations**

Joshua Welsh, NIH

901546  
P184

**Monitor Critical Parameters in Advanced Flow Cytometers**

Daniela Ischiu Gutierrez, NIAID

894956  
P186

**Bacterial Mock Communities As Standards For Reproducible Cytometric Microbiome Analysis**

Susann Mueller, Helmholtz Centre for Environmental Research – UFZ

## Shared Resource Laboratories

901381  
P188

**Optimizing User-Staff Communication in a Large Multi-Site Shared Resource Laboratory**

William Murphy, University of Pennsylvania

901928  
P190

**SRL Technicians Exchange: How Knowledge Sharing Increases Versatility and Offers Fresh Insight in Facility Operations.**

Sam Thompson, Babraham Institute

902031  
P192

**Quality Control Testing of Biobank Cryopreserved PBMCs**

Karen Millerchip, MD Anderson Cancer Center

# POSTER SESSIONS

## Single cell “-omics”

900938  
P194

**An Integrated Single-Cell Multiomics Approach To Characterize mRNA, Intracellular, And Surface Proteins Using Intracellular AbSeq and BD® AbSeq Immune Discovery Panel**

Adam Wright, BD Biosciences

901130  
P196

**High-Parameter Protein Profiling on the BD Rhapsody™ Single-Cell Analysis System**

Manish Thakran, Texas A&M University

901539  
P198

**Single-Cell Interactive Cytometry Using Made-To-Order Droplet Ensembles**

Russell Colem, Scribe Biosciences, Inc.

901902  
P200

**Accelerating Generation Of Single Cell Clones by Using CellRaft™ AIR System Coupled With Fluorescence Activated Cell Sorting**

Sobha Thamminana, Kite Pharma

902035  
P202

**Realtime Enrichment And High-Dimensional Morphology Analysis Of Malignant Cells from Effusion Samples Using Deep Learning**

Chassidy Johnson, Deepcell

898319  
P204

**See-N-Seq: RNA Sequencing of Target Single Cells Identified by Microscopy**

Jeonghyun Lee, University of British Columbia

898549  
P206

**A Virus, A Stim And A Control Enter A Room: Novel Phenotypic Differences Discovered From Sort To Sequence Experiments**

Jack Panopoulos, BD

## Submicron Cytometry

901042  
P208

**Enrichment of microRNA and Virus-Like Particles Using a Novel Avalanche Photodiode-Based Benchtop Cell Sorter**

John Tigges, Beth Israel Lahey Health

901685  
P210

**Fluorescent Nanoparticle Flow Cytometry Calibrators with NIST-assigned ERF and Concentration Values for Viral and EV Analysis**

Adam York, Thermo Fisher Scientific

901984  
P212

**Detection of Extracellular Vesicles Using the BD FACSymphony™ A1 Cell Analyzer**

Tina Van Den Broeck, Becton Dickinson

902008  
P214

**Good Practice For Analyzing Extracellular Vesicles Using the BD FACSymphony™ A1 Cell Analyzer**

Stephanie Widmann, BD

902047  
P216

**The Delaware: A Flow NanoCytometer for Nanoparticle Analysis**

Giacomo Vacca, Kinetic River Corp.

898467  
P218

**Small Particle Flow Cytometry Using 3D Light Scatter Detection Enhances Extracellular Vesicle Analysis in Liquid Biopsies Highlighting the Potential to Segregate EVs by Refractive Index**

Desmond PINK, Nanostics

898527  
P220

**Physical Association Of Lipoprotein Particles and Extracellular Vesicles Unveiled by Single Particle Flow Cytometry**

Estefania Lozano-Andres, Utrecht University

# POSTER SESSIONS

The number listed before the abstract title references the abstract located in the back of the program book.

## Therapeutics

897407  
P222

### **Design of “Smart” Nanoparticles for Combined In-vivo Imaging and Advanced Drug Delivery Therapeutics for Single-Cell Nanomedicine**

James Leary, Aurora Life Technologies LLC

901841  
P224

### **Delivery of Oligonucleotides Into Tumor Cells via Monoclonal Antibodies: Targeting of mRNA Following Release of Antisense Oligonucleotides Through Cell Surface Protease Activities Using Antibody Substrate Oligonucleotide Conjugates (ASOCs)**

Beverly Packard, Oncolmmunin, Inc.



biotechne®

**Find the right antibody  
to solve your research  
question with confidence.**

Join Us at Booth # 513





# EXHIBITOR LISTING

Visit the Exhibits & Posters in Hall E

## SATURDAY, JUNE 4

1775-1900 Commercial Exhibits and Posters Open/Opening Reception

## SUNDAY, JUNE 5

1000-1830 Poster Viewing Commercial Exhibits

1000-1100 Coffee Break

1600-1630 Coffee Break

1700-1830 Poster Session 1

## MONDAY, JUNE 6

1000-1800 Poster Viewing Commercial Exhibits

1000-1100 Coffee Break

1515-1545 Coffee Break

1700-1800 Poster Session 2

## TUESDAY, JUNE 7

1000-1400 Poster Viewing Commercial Exhibits

1000-1030 Coffee Break

| COMPANY                                         | BOOTH |
|-------------------------------------------------|-------|
| 10x Genomics B.V.....                           | 107   |
| AcouSort AB.....                                | 536   |
| Agilent Technologies .....                      | 338   |
| Akoya Biosciences.....                          | 508   |
| APE Angewandte Physik- und Elektronik GmbH..... | 515   |
| Apogee Flow Systems.....                        | 349   |
| Applied Cells.....                              | 519   |
| Applied Cytometry .....                         | 448   |
| Bangs Laboratories.....                         | 309   |
| BD Biosciences.....                             | 325   |
| Beckman Coulter Life Sciences.....              | 221   |
| BenchSci .....                                  | 554   |
| BennuBio Inc. ....                              | 238   |
| bioBUBBLE, Inc. ....                            | 406   |
| BioLegend, Inc.....                             | 137   |
| Bio-Rad Laboratories .....                      | 437   |
| Biostat Limited .....                           | 207   |
| Bio-Techne .....                                | 513   |
| BlueCatBio.....                                 | 239   |
| Canopy Biosciences.....                         | 401   |
| Caprico Biotechnologies, Inc. ....              | 509   |
| Cell Microsystems .....                         | 236   |
| Cellarcus Biosciences .....                     | 117   |
| CellCarta.....                                  | 348   |
| Cellenion .....                                 | 431   |
| Cellsonics Inc .....                            | 526   |
| Cellular Highways .....                         | 405   |

# EXHIBITOR LISTING

| <b>COMPANY</b>                     | <b>BOOTH</b> | <b>COMPANY</b>                         | <b>BOOTH</b> |
|------------------------------------|--------------|----------------------------------------|--------------|
| Certified Genetool .....           | 502          | Nodexus Inc.....                       | 242          |
| Chroma Technology .....            | 500          | Omega Optical .....                    | 507          |
| Coherent.....                      | 501          | On-chip Biotechnologies Co, Ltd. ....  | 218          |
| Countstar.....                     | 505          | opto biolabs.....                      | 306          |
| Curiox Biosystems .....            | 214          | OptoSigma.....                         | 445          |
| Cytek Biosciences, Inc. ....       | 101          | Osela Inc.....                         | 403          |
| Dotmatics, Inc.....                | 425          | Particle Metrix, Inc. ....             | 212          |
| EasyPanel.....                     | 441          | Partillion Bioscience.....             | 517          |
| EXBIO Praha, a.s. ....             | 407          | Pavilion Integration Corporation ..... | 109          |
| FISBA AG .....                     | 524          | RPMC Lasers .....                      | 255          |
| FlowJo, LLC.....                   | 324          | Sartorius.....                         | 208          |
| FlowMetric.....                    | 544          | Slingshot Biosciences .....            | 237          |
| Fluidigm Corporation .....         | 113          | Sony Biotechnology Inc.....            | 415          |
| FluoroFinder .....                 | 408          | Spherotech, Inc.....                   | 209          |
| Hamamatsu Corporation .....        | 249          | STRATEC Consumables GmbH .....         | 336          |
| Hitronics Technologies Inc.....    | 504          | Stratedigm, Inc. ....                  | 530          |
| Immudex .....                      | 300          | Stratocore.....                        | 206          |
| Kinetic River Corp. ....           | 143          | Teledyne Photometrics.....             | 307          |
| Leinco Technologies.....           | 220          | Tercen Data Analytics Ltd.....         | 245          |
| Luminex Corporation.....           | 201          | The Lee Company.....                   | 449          |
| Metafora Biosystems .....          | 344          | Thermo Fisher Scientific .....         | 302          |
| Miltenyi Biotec B.V. & Co. KG..... | 213          | Thermo Fisher Scientific .....         | 301          |
| Mission Bio.....                   | 525          | ThinkCyte .....                        | Booth 243    |
| Namocell Inc.....                  | 533          | TissueGnostics USA .....               | 543          |
| NanoCollect Biomedical, Inc.....   | 304          | Union Biometrica, Inc. ....            | 119          |
| NanoFCM Inc. ....                  | 308          | Verity Software House.....             | 409          |
| Nexcelom by PerkinElmer .....      | 548          |                                        |              |

# EXHIBITING COMPANIES

## **10x Genomics B.V, Booth 107**

6230 Stoneridge Mall Rd  
Pleasanton, CA 94599  
925-548-7307  
<http://www.10xgenomics.com>

## **AcouSort AB, Booth 536**

406, Medicon Village  
Lund, Sweden 22381  
456-059-0993  
<https://acousort.com/>

## **Agilent Technologies, Booth 338**

5301 Stevens Creek Blvd  
Santa Clara, CA 95051  
800-227-9770  
<https://www.agilent.com/>

## **Akoya Biosciences, Booth 508**

1080 O'Brien Drive  
Menlo Park, CA 94025  
510-432-2622  
<https://www.akoyabio.com/>

## **APE Angewandte Physik- und Elektronik GmbH, Booth 515**

Plauener Strasse 163-165, Haus N  
Berlin, Germany 13053  
<https://www.ape-berlin.de>

## **Apogee Flow Systems, Booth 349**

Unit 7 Grovelands, Boundary Way  
Hemel Hempstead,  
United Kingdom HP2 7TE  
+44 208 123 6831  
<https://www.apogeefflow.com>

## **Applied Cells, Booth 519**

3350 Scott Blvd, Building 6  
Santa Clara, CA 95054-3111  
512-589-3872  
<https://appliedcells.com/>

## **Applied Cytometry, Booth 448**

Matrix Business Centre, Nobel Way, Dinnington  
Sheffield, United Kingdom S25 3QB  
+44 (0) 1909 547 210  
<http://www.appliedcytometry.com>

## **Bangs Laboratories, Booth 309**

9025 Technology Drive  
Fishers, IN 46038  
317-570-7020  
<http://www.bangslabs.com>

## **BD Biosciences, Booth 325**

2350 Qume Dr.  
San Jose, CA 95131  
877-232-8995  
<http://www.bdbiosciences.com>

## **Beckman Coulter Life Sciences, Booth 221**

5350 Lakeview Parkway  
Indianapolis, IN 46268  
714-342-9074  
<http://www.beckmancoulter.com>

## **BenchSci, Booth 554**

25 York St Suite 1100  
Toronto, ON  
Canada M5J 2V5  
647-570-3786  
<https://www.benchsci.com/>

## **BennuBio Inc., Booth 238**

6610 Gulton Ct NE  
Albuquerque, NM 87109  
415-933-0150  
<http://www.bennubio.com>

## **bioBUBBLE, Inc., Booth 406**

1411 E. Magnolia St.  
Fort Collins, CO 80524  
970-224-4262  
<http://www.biobubble.com>

## **BioLegend, Inc., Booth 137**

8999 BioLegend Way  
San Diego, CA 92121  
858-455-9588  
<http://www.biolegend.com>

## **Bio-Rad Laboratories, Booth 437**

255 Linus Pauling Drive  
HERCULES, CA 94547  
510-408-2158  
<http://www.bio-rad.com>

# EXHIBITING COMPANIES

## **Biostat Limited, Booth 207**

56A Charnwood Road, Shepshed  
Loughborough, LEICS  
United Kingdom LE12 9NP  
44 1509 651063  
<http://www.biostat.com>

## **Bio-Techne, Booth 513**

614 McKinley Place NE  
Minneapolis, MN 55413  
612-379-2956  
<http://www.bio-techne.com>

## **BlueCatBio, Booth 239**

58 ELSINORE ST  
Concord, MA 01742  
978-405-2533  
[www.bluecatbio.com](http://www.bluecatbio.com)

## **Canopy Biosciences, Booth 401**

4340 Duncan Ave, Suite 220  
St. Louis, MO 63110  
314-640-0966  
[canopybiosciences.com](http://www.canopybiosciences.com)

## **Caprico Biotechnologies, Inc., Booth 509**

400 Pinnacle Way, STE 430  
Norcross, GA 30071  
678-691-2143  
<https://www.capricobio.com/>

## **Cell Microsystems, Booth 236**

801 Capitola Drive, Ste 10  
Durham, NC 27713  
[www.cellmicrosystems.com](http://www.cellmicrosystems.com)

## **Cellarcus Biosciences, Booth 117**

505 Coast Blvd S Ste 409  
La Jolla, CA 92037  
858-239-2100  
<http://www.cellarcus.com>

## **CellCarta, Booth 348**

201 President Kennedy Ave, Suite 3900  
Montreal, QC  
Canada H2X 3Y7  
418-370-9301  
[cellcarta.com](http://www.cellcarta.com)

## **Cellenion, Booth 431**

4405 E. Baseline Road #123  
Phoenix, AZ 85042  
714-325-9153  
[www.cellenion.com](http://www.cellenion.com)

## **Cellsonics Inc, Booth 526**

76 Bonaventura Drive  
San Jose, CA 95134  
408-821-4222  
[www.cellsonics.com](http://www.cellsonics.com)

## **Cellular Highways, Booth 405**

Melbourn Science Park  
Melbourn, Royston, Hertfordshire  
United Kingdom SG8 6EE  
441763262626  
[www.cellularhighways.com](http://www.cellularhighways.com)

## **Certified Genetool, Booth 502**

7074 Commerce Circle, Suite A  
Pleasanton, CA 94588  
925-737-0800  
<http://www.cgenetool.com>

## **Chroma Technology, Booth 500**

10 Imtec Lane  
Bellows Falls, VT 05101  
802-428-2500  
[www.chroma.com](http://www.chroma.com)

## **Coherent, Booth 501**

5100 Patrick Henry Dr.  
Santa Clara, CA 95054  
408-764-4000  
<http://www.coherent.com>

## **Countstar, Booth 505**

8206 Rockville Rd., 248  
INDIANAPOLIS, IN 46214-3113  
682-465-5856  
[www.countstar.com](http://www.countstar.com)

## **Curiox Biosystems, Booth 214**

400 West Cummings Park, Ste 4350  
Woburn, MA 01801  
<https://www.curiox.com/>

# EXHIBITING COMPANIES

## **Cytek Biosciences, Inc., Booth 101**

47215 Lakeview Blvd  
Fremont, CA 94538  
408-674-2409  
<https://cytekbio.com/>

## **Dotmatics, Inc., Booth 425**

6050 Santo Road, Suite 270  
San Diego, CA 92124  
760-717-2989  
[www.dotmatics.com](http://www.dotmatics.com)

## **EasyPanel, Booth 441**

54 rue Dunois  
Paris, France 75013  
066-602-9523  
<https://flow-cytometry.net/>

## **EXBIO Praha, a.s., Booth 407**

Nad Safinou II 341  
Vestec, Czech Republic 252 50  
+420 261 090 595  
[www.exbio.cz](http://www.exbio.cz)

## **FISBA AG, Booth 524**

Rorschacher Strasse 268  
St. Gallen, Switzerland 9016  
071-282-3131  
[www.fisba.com](http://www.fisba.com)

## **FlowJo, LLC, Booth 324**

385 Williamson Way  
Ashland, OR 97520  
541-201-0022  
<http://www.flowjo.com>

## **FlowMetric, Booth 544**

3805 Old Easton Rd.  
Doylestown, PA 18902  
267-893-6630  
[www.flowmetric.com](http://www.flowmetric.com)

## **Fluidigm Corporation, Booth 113**

2 Tower Place, Suite 2000  
South San Francisco, CA 94080  
650-452-4388  
<http://www.fluidigm.com>

## **FluoroFinder, Booth 408**

329 Interlocken Pkwy  
Broomfield, CO 80021  
541-350-2729  
<https://fluorofinder.com/>

## **Hamamatsu Corporation, Booth 249**

360 Foothill Rd  
Bridgewater, NJ 08807  
908-231-0960  
<http://www.hamamatsu.com>

## **Hitronics Technologies Inc, Booth 504**

1551 McCarthy Blvd., #116  
Milpitas, CA 95035  
408-791-6352  
[www.hi-tronics.com](http://www.hi-tronics.com)

## **Immudex, Booth 300**

4031 University Drive, Suite 100  
Fairfax, VA 22030  
703-766-4688  
<http://www.immudex.com>

## **Kinetic River Corp., Booth 143**

897 Independence Avenue, Suite 4A  
Mountain View, CA 94043-2357  
650-269-0726  
<http://www.kineticriver.com>

## **Leinco Technologies, Booth 220**

410 Axminister Drive  
Fenton, MO 63026  
636-230-9477  
<http://www.leinco.com>

## **Luminex Corporation, Booth 201**

12212 Technology Boulevard  
Austin, TX 78727  
512-569-3548  
<http://www.luminexcorp.com>

## **Metafora Biosystems, Booth 344**

29 rue du Faubourg Saint Jacques  
Paris, France 75014  
+33 9 61 63 65 17  
<https://www.metafora-biosystems.com/>

# EXHIBITING COMPANIES

## **Miltenyi Biotec B.V. & Co. KG, Booth 213**

Friedrich-Ebert-Str. 68  
Bergisch-Gladbach, Germany 51429  
+49 2204 83063190  
<http://www.miltenyibiotec.com>

## **Mission Bio, Booth 525**

400 E. Jamie Ct.  
South San Francisco, CA 94080  
415-854-0058  
[www.missionbio.com](http://www.missionbio.com)

## **Namocell Inc., Booth 533**

2485 Old Middlefield Way, Suite 30  
Mountain View, CA 94043  
650-576-3851  
[www.namocell.com](http://www.namocell.com)

## **NanoCollect Biomedical, Inc, Booth 304**

9525 Towne Centre Dr, Suite 150  
San Diego, CA 92121  
877-745-7678  
<http://www.nanocollect.com>

## **NanoFCM Inc., Booth 308**

D6 Thane Road  
Nottingham, United Kingdom NG90 6BH  
<http://www.nanofcm.com>

## **Nexcelom by PerkinElmer, Booth 548**

360 Merrimack Street  
Lawrence, MA 01843  
978-327-5340  
<https://www.nexcelom.com/>

## **Nodexus Inc, Booth 242**

22693 Hesperian Blvd. Suite 175  
Hayward, CA 94541  
<http://www.nodexus.com>

## **Omega Optical, Booth 507**

21 Omega Dr.  
Brattleboro, VT 05301  
<http://www.omegafilters.com>

## **On-chip Biotechnologies Co., Ltd., Booth 218**

2-16-17 Naka-cho  
Koganei, Tokyo, Japan 1840012  
+81-42 385 0461  
<https://on-chipbio.com/>

## **opto biolabs, Booth 306**

Schänzlestr. 1  
Freiburg, BW  
Germany 79104  
-2033568  
[www.optobiolabs.com](http://www.optobiolabs.com)

## **OptoSigma, Booth 445**

3210 S Croddy Way  
Santa Ana, CA 92704  
[www.optosigma.com](http://www.optosigma.com)

## **Osela Inc., Booth 403**

1869 32nd Avenue  
Lachine, QC  
Canada H8T 3J1  
514-631-2227  
<http://www.osela.com>

## **Particle Metrix, Inc., Booth 212**

1514 Saddle Club Road  
Mebane, NC 27302  
919-667-6960  
<https://www.particle-metrix.de/en/products/zetaview-nanoparticle-tracking.html>

## **Partillion Bioscience, Booth 517**

570 Westwood Plaza, Bldg. 114  
Los Angeles, CA 90095  
<https://www.partillion.com/>

## **Pavilion Integration Corporation, Booth 109**

2528 Qume Dr. Ste 1  
San Jose, CA 95131  
408-453-8801  
<http://www.pavilionintegration.com>

## **RPMC Lasers, Booth 255**

8495 Veterans Memorial Pkwy  
Ofallon, MO 63366  
636-272-7227-221  
<https://www.rpmclasers.com/>

# EXHIBITING COMPANIES

## **Sartorius, Booth 208**

565 Johnson Ave.  
Bohemia, NY 11716  
<https://www.sartorius.com/en>

## **Slingshot Biosciences, Booth 237**

1250 45th Street, Suite 330  
Emeryville, CA 94608  
408-396-3704  
[www.slingshotbio.com](http://www.slingshotbio.com)

## **Sony Biotechnology Inc., Booth 415**

1730 North First St.  
San Jose, CA 95112  
800-275-5963  
<http://www.sonybiotechnology.com>

## **Spherotech, Inc., Booth 209**

27845 Irma Lee Circle, Unit 101  
Lake Forest, IL 60045  
847-680-8922  
<http://www.spherotech.com>

## **STRATEC Consumables GmbH, Booth 336**

Sonystrasse 20  
Anif, Salzburg  
Austria 5081  
+436246 21250  
[www.stratec.com](http://www.stratec.com)

## **Stratedigm, Inc., Booth 530**

911 Bern Ct., Suite 100  
San Jose, CA 95112  
408-785-6838  
<http://www.stratedigm.com>

## **Stratocore, Booth 206**

33 avenue Maine, 26th floor  
Paris, ILE DE FRANCE  
France 75015  
33 1 84 16 10 92  
<http://www.stratocore.com>

## **Teledyne Photometrics, Booth 307**

3440 E. Britannia Drive  
Tucson, AZ 85706  
[www.photometrics.com](http://www.photometrics.com)

## **Tercen Data Analytics Ltd., Booth 245**

Unit 3, Wallace House, Maritana Gate  
Canada Street, Waterford  
Ireland X91CR9X  
+353 1 582 0084  
[www.tercen.com](http://www.tercen.com)

## **The Lee Company, Booth 449**

2 Pettipaug Rd  
Westbrook, CT 06498  
860-399-6281 x2364  
[www.theleeco.com](http://www.theleeco.com)

## **Thermo Fisher Scientific, Booth 302**

5791 Van Allen Way  
Carlsbad, CA 92008  
608-273-6822  
<http://www.thermoscientific.com/nanodrop>

## **Thermo Fisher Scientific, Booth 301**

5791 Van Allen Way  
Carlsbad, CA 92008  
608-273-6822  
<http://www.thermoscientific.com/nanodrop>

## **ThinkCyte, Booth 243**

733 Industrial Road  
San Carlos, CA 94070  
512-589-3872  
<https://thinkcyte.com/>

## **TissueGnostics USA, Booth 543**

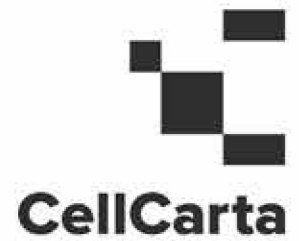
12522 Moorpark Street Suite #106  
Los Angeles, CA 91604  
818-856-8056  
<https://tissuegnostics.com/>

## **Union Biometrika, Inc., Booth 119**

84 October Hill Rd  
Holliston, MA 01746  
508-893-3115  
<http://www.unionbio.com>

## **Verity Software House, Booth 409**

45A Augusta Road  
Topsham, ME 04086  
207-729-6767  
<http://www.vsh.com>



**VISIT US AT  
BOOTH 348!**

Discover CellCarta – A global CRO laboratory offering immune monitoring services using **flow and mass cytometry**, and data analysis with **CellEngine™** software.

[cellcarta.com](http://cellcarta.com)



# COMMERCIAL TUTORIALS

## SATURDAY, JUNE 4

12:15–13:15

### 10x Genomics B.V

Room 121A  
6230 Stoneridge Mall Rd  
Pleasanton, CA 94599  
925-548-7307  
<http://www.10xgenomics.com>

### Akoya Biosciences

Room 122B  
1080 O'Brien Drive  
Menlo Park, CA 94025  
510-432-2622  
<https://www.akoyabio.com/>

### Cell Microsystems

Room 122A  
801 Capitola Drive, Ste 10  
Durham, NC 27713  
[www.cellmicrosystems.com](http://www.cellmicrosystems.com)

### Standard BioTools

Room 120C  
2 Tower Place, Suite 2000  
South San Francisco, CA 94080  
[www.standardbiotools.com](http://www.standardbiotools.com)

### Sony Biotechnology Inc.

Room 120AB  
1730 North First St.  
San Jose, CA 95112  
800-275-5963

### Thermo Fisher Scientific

Room 121BC  
5791 Van Allen Way  
Carlsbad, CA 92008  
608-273-6822

## SUNDAY, JUNE 5

12:45–13:45

### BD Biosciences

Room 120AB  
2350 Qume Dr.  
San Jose, CA 95131  
877-232-8995  
<http://www.bdbiosciences.com>

### Cytek Biosciences, Inc.

Room 122A  
47215 Lakeview Blvd  
Fremont, CA 94538  
408-674-2409  
<https://cytekbio.com/>

### Luminex Corporation

Room 121A  
12212 Technology Boulevard  
Austin, TX 78727  
512-569-3548  
<http://www.luminexcorp.com>

### Miltenyi Biotec B.V. & Co. KG

Room 121BC  
Friedrich-Ebert-Str. 68  
Bergisch-Gladbach,  
Germany 51429  
+49 2204 83063190  
<http://www.miltenyibiotec.com>

### Slingshot Biosciences

Room 122B  
1250 45th Street, Suite 330  
Emeryville, CA 94608  
408-396-3704  
[www.slingshotbio.com](http://www.slingshotbio.com)

### Thermo Fisher Scientific

Room 120C  
5791 Van Allen Way  
Carlsbad, CA 92008  
608-273-6822

# COMMERCIAL TUTORIALS

**17:45–18:45**

## **CellCarta**

**Room 120AB**

201 President Kennedy Ave, Suite 3900

Montreal, QC

Canada H2X 3Y7

418-370-9301

<https://cellcarta.com/>

**MONDAY, JUNE 6**

**12:30–13:30**

## **BD Biosciences**

**Room 122B**

2350 Qume Dr.

San Jose, CA 95131

877-232-8995

<http://www.bdbiosciences.com>

## **Bio-Rad Laboratories**

**Room 120C**

255 Linus Pauling Drive

HERCULES, CA 94547

510-408-2158

<http://www.bio-rad.com>

## **Cytek Biosciences, Inc.**

**Room 121BC**

47215 Lakeview Blvd

Fremont, CA 94538

408-674-2409

<https://cytekbio.com/>

## **Luminex Corporation**

**Room 120AB**

12212 Technology Boulevard

Austin, TX 78727

512-569-3548

<http://www.luminexcorp.com>

## **Tercen Data Analytics Ltd.**

**Room 121A**

Unit 3, Wallace House, Maritana Gate

Canada Street, Waterford

Ireland X91CR9X

+353 1 582 0084

## **Thermo Fisher Scientific**

**Room 122A**

5791 Van Allen Way

Carlsbad, CA 92008

608-273-6822

**17:15–18:15**

## **Curiox Biosystems**

**Room 120C**

400 West Cummings Park, Ste 4350

Woburn, MA 01801

<https://www.curiox.com/>

## **Standard BioTools**

**120AB**

2 Tower Place, Suite 2000

South San Francisco, CA 94080

[www.standardbiotools.com](http://www.standardbiotools.com)

# COMMERCIAL TUTORIALS

**TUESDAY, JUNE 7**  
**12:00-13:00**

## **10x Genomics B.V**

Room 121A  
6230 Stoneridge Mall Rd  
Pleasanton, CA 94599  
925-548-7307  
<http://www.10xgenomics.com>

## **Agilent Technologies**

Room 120C  
5301 Stevens Creek Blvd  
Santa Clara, CA 95051  
800-227-9770  
<https://www.agilent.com/>

## **Dotmatics, Inc.**

Room 120AB  
6050 Santo Road, Suite 270  
San Diego, CA 92124  
760-717-2989  
[www.dotmatics.com](http://www.dotmatics.com)

## **FlowJo, LLC**

Room 122A  
385 Williamson Way  
Ashland, OR 97520  
541-201-0022  
<http://www.flowjo.com>

## **NanoCollect Biomedical, Inc**

Room 122B  
9525 Towne Centre Dr, Suite 150  
San Diego, CA 92121  
877-745-7678  
<http://www.nanocollect.com>

## **Sony Biotechnology Inc.**

Room 120AB  
1730 North First St.  
San Jose, CA 95112  
800-275-5963



### ANALYZING EXTRACELLULAR VESICLES?

Get set with a Nanobead Calibration Kit, (50nm, 100nm) & Submicron Kit (0.2µm, 0.5µm, 0.8µm) (cat. code 834 & 832) comprised of highly defined microspheres with an internalized fluorescent dye to allow users to determine the capabilities of their cytometer and appropriate instrument settings for small particle analysis.

The figure shows two flow cytometry plots. The left plot is a scatter plot with axes labeled '100 nm' and '500 nm'. The right plot is a histogram with four peaks labeled '100 nm', '200 nm', '500 nm', and '800 nm'. The x-axis is labeled 'SSC-A' and the y-axis is 'COUNT'. Below the plots is the text 'Nanobead Kit & Submicron Kit'.

BangsLabs.com

# MARYLOU INGRAM SCHOLARS

The ISAC Marylou Ingram Scholars Program (IMISP) is designed to enhance the scientific and leadership experiences of research leaders specializing in state-of-the-art biomedicine, technology, and other areas of emerging sciences relevant to cytometry. Designed as a leadership development initiative for those under the age of 40, the program provides opportunities for mentorship training with another Society member, presentation opportunities, and other valuable professional development activities.

ISAC Marylou Ingram Scholars become integral parts of the Society through committee memberships, advisory boards and various taskforces, reviewing manuscripts submitted to Cytometry Part A (the official journal of ISAC), and creating educational material to further support the goals of ISAC. Being named an ISAC Marylou Ingram Scholar is an indication that you are recognized for your scientific skills, research accomplishments, leadership potential, and ability to achieve your career goals.

Marylou Ingram's contribution to the field of cytometry spanned nearly 70 years. Her distinguished career in academic medicine and research included time as faculty at the University of Rochester, Caltech and the University of Miami; at Los Alamos National Laboratory; and as a consultant to the National Cancer Institute, the FDA, Brookhaven National Laboratory, NASA, and other organizations. She was a pioneer in automated cell analysis, played a key role in developing automated cell analysis systems, and was founding director of the Institute for Cell Analysis at the University of Miami. Dr. Ingram spent two of her sabbaticals working directly with Wallace Coulter in the very early days of automated cell analysis, and she regularly interacted with him as he developed new technologies for analysis. From 1982 to 2013, she was a Senior Research Scientist at the Huntington Medical Research Institute in Pasadena, California. She headed the Tissue Engineering & In Vitro Systems program and led a research program on tumor spheroids with the aim of creating better models for studying tumor growth and drug responsiveness.

ISAC Marylou Ingram Scholars are awarded a five-year complimentary membership in the Society, a subscription to Cytometry Part A, and free registration and travel funding to attend the annual CYTO conferences.



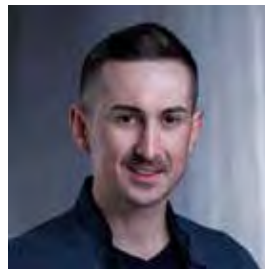
**Rafael J. Argüello** - Tenured Assistant Researcher, CRNS, Centre d'Immunologie de Marseille-Luminy, Marseille, France



**Micheli Pillat** - Assistant Professor, Federal University of Santa Maria, Santa Maria, Brazil



**Henry Hui** - Research Associate, Translational Cancer Pathology Laboratory, University of Western Australia, Perth, Australia



**Benjamin Spurgeon** - Postdoctoral Fellow, Boston Children's Hospital, Boston, MA, USA



**Gungun Lin** - Research Fellow, University of Technology Sydney, Sydney, Australia



**Lara Gibellini** - Assistant Professor, University of Modena and Reggio Emilia, Modena, Italy

# MARYLOU INGRAM SCHOLARS



**Felix Marsh**-Wakefield Research Associate, University Of Sydney, Sydney, Australia



**Paula Niewold** - Postdoctoral Researcher, Leiden University Medical Centre, Leiden, Netherlands



**David Woods** - Assistant Professor, University of Colorado Anschutz Medical Campus, Aurora, CO, USA



**Jakob Zimmermann** – Postdoc, Gastroenterology and Mucosal Immunology Group, Dept. for Biomedical Research, University of Bern, Bern, Switzerland



**Andre Görgens** - Postdoctoral Research Fellow, Karolinska Institutet, Department of Laboratory Medicine, Unit for Cell and Gene Therapy Research, Stockholm, Sweden



**Thomas Lechti** - Postdoctoral Researcher, Immunotechnology Section, Vaccine Research Center, National Institutes of Health, Bethesda, MD, USA



**Fabienne Lucas** - Clinical Pathology Resident, Brigham & Women's Hospital, Boston, MA, USA



**Helen McGuire** - Research Fellow, University of Sydney, Sydney, Australia



**Joshua Welsh** - Visiting Postdoctoral Fellow, Translational Nanobiology Lab, Laboratory of Pathology, National Cancer Institute, Bethesda, MD, USA



**Dominic Jenner** - Senior Scientist, Defence Science & Technology Laboratory, Salisbury, UK



**Ori Maguire** - Senior Flow Cytometry Specialist, Dept. of Flow and Image Cytometry, Roswell Park Comprehensive Cancer Center, Buffalo, NY, USA



**Peng Qiu** - Associate Professor, Georgia Institute of Technology and Emory University, Atlanta, GA, USA

# MARYLOU INGRAM SCHOLARS



**Aaron Tyznik** - Staff Scientist, BD Sciences, San Diego, CA, USA



**Sofie Van Gassen** - Postdoctoral Researcher, VIB-UGent Center for Inflammation Research, Ghent, Belgium



**Thomas Myles Ashhurst** - High-Dimensional Cytometry Specialist, Sydney Cytometry Core Facility and Discipline of Pathology, Sydney, Australia



**Kanutte Huse** - Research Scientist, Oslo University Hospital, Oslo, Norway



**Nao Nitta** - Founder & President, CYBO, Tokyo, Japan



**Kirstie Bertram** - Research Scientist, Centre for Virus Research, Westmead Institute for Medical Research

Kirstie has specialized since 2015 in interrogating immune cells from

human skin, type I and type II mucosa. With a particular interest in dendritic cells, macrophages, T cells and innate lymphocytes, she has refined cell isolation techniques to isolate cells from human skin, anogenital tissue, and intestine and interrogate them both phenotypically, with high-parameter flow cytometry and sorting for functional immunoassays. Kirstie has studied these cells and how they interact with viruses, particularly HIV and Herpes Simplex Virus. As well as the role they play in inflammatory bowel disease. Her expertise in investigating cells from human tissue, has been continuously expanded, with tissues as diverse as the human cornea, and a keen interest in immune cell phenotypes in inflamed mucosal tissues.



**Fan Xiong** - Senior Electrical Engineer Manager at KLA, Milpitas, CA, USA

Fan is a senior electrical engineer manager at KLA working on cutting-edge mask inspection tools. Previously, she worked as a senior staff electrical engineer and group leader at Bio-Rad Laboratories focusing on the R&D of flow cytometry instruments and real-time PCR instruments. She has been the acting secretary and next generation leader of Society for Design and Process Science (SDPS) for many years. She also actively serves as a technical committee member for various international journals and conferences and is interested in STEM outreach activities.



**Oliver Burton** - Staff Scientist, Babraham Institute, Laboratory of Adrian Liston, Cambridge, England

After receiving his PhD at the University of Cambridge, Oliver did his postdoctoral training at Boston Children's Hospital where he became a member of the Harvard Medical School faculty. Oliver now works as a staff scientist at the Babraham Institute in Cambridge, England in the laboratory of Adrian Liston. He is an immunologist with interests in regulatory T cells, tissue immunity and cellular migration.

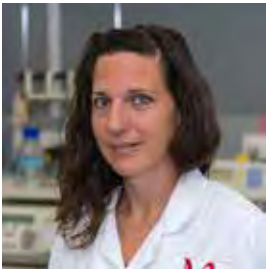
# SRL EMERGING LEADERS



**Arvill Aspland** - Operations Coordinator, Sydney Cytometry Core Research Facility, University of Sydney Centenary Institute, Sydney, Australia



**Caroline Roe** - Managing Director, Mass Cytometry Center of Excellence, Vanderbilt University, Nashville, TN, USA



**Laura Ferrer** - Deputy Manager & High-dimensional Spectral Flow Cytometry Specialist, Malaghan Institute of Medical Research, Wellington, New Zealand



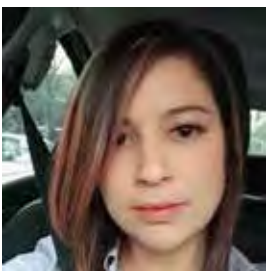
**Rachael Sheridan** - Manager, Flow Cytometry Core, Van Andel Institute, Grand Rapids, MI, USA



**Wei Wang** - Director of FACS Facility, The Palo Alto Veterans Institute for Research (PAVIR), Palo Alto, CA, USA



**Kathleen Daniels** - Associate Director, Flow Cytometry Core, Sana Biotechnology, Cambridge, MA, USA



**Andrea Bedoya López** - Administrative and Quality System Manager, National Flow Cytometry Laboratory, National Autonomous University of Mexico



**David Gravano** - Technical Director of Cytometry, Stem Cell Instrumentation Foundry, Merced, CA, USA



**Alexis Conway** - Flow Cytometry Specialist & Graduate Course Coordinator, Roswell Park Comprehensive Cancer Center, Buffalo, NY, USA



**Christopher Hall** - Senior Research Assistant, Babraham Institute, Cambridge, UK



**Lauren Nettenstrom** - Instrumentation Technologist, Carbone Cancer Center Flow Cytometry Laboratory, Univ. of Wisconsin-Madison, Madison, WI, USA



**Derek Jones** - Technical Director for Research and Development, University of Pennsylvania Flow Cytometry SRL, Philadelphia, PA, USA

# SRL EMERGING LEADERS



**Ziv Porat** - Associate Staff Scientist, Head of Flow Cytometry Unit, Weizmann Institute of Science, Rehovot, Israel



**Isabella Pesce** - Cell Analysis and Separation Core Facility Manager, Trento University, Trento, Italy



**Uttara Chakraborty** - Assistant Professor and In-charge Flow Cytometry & Microscopy, School of Regenerative Medicine, Manipal Academy of Higher Education, Karnataka, India



**Nicole Poulton** - Director for J.J. MacIsaac Facility for Aquatic Cytometry, Bigelow Laboratory for Ocean Sciences, East Boothbay, ME, USA



**Eva Orlowski-Oliver** - Flow Cytometry Scientist and Co-Manager, Burnet Institute, Melbourne, Australia



**Aja Rieger** - Faculty Service Officer/ Flow Core Manager, University of Alberta, Edmonton, Canada



**Kristen Reifel** - Principal Investigator in Genomics, Battelle National Biodefense Institute, Bethesda, MD, USA



**Suat Dervish** - Westmead Institute for Medical Research, Sydney, Australia



**Vera Tang** - Operations Manager and Adjunct Professor, Flow Cytometry and Virometry Core Facility, Ottawa, Canada



**Christian Kukat** - Max Planck Institute for Biology of Ageing, Cologne, Germany



**Cláudia Bispo** - Flow Cytometry Manager, University of California, San Francisco, CA, USA



**Radhika Rayanki** - AstraZeneca



# SRL EMERGING LEADERS



**Erica Smit** - Flow Cytometry Technical Specialist, Cape Town HVTN Immunology Laboratory/ Hutchinson Center Research Institute South Africa



**Diana Ordenez** - Head of the Flow Cytometry Core Facility, European Molecular Biology Laboratory (EMBL), Heidelberg, Germany

I am interested in the implementation of best practices to isolate cells for downstream

applications such as single-cell sequencing and metabolic assays. Recently, I have been exploring image-enabled cell sorting (ICS) for the rapid identification and isolation of cells with unique (sub)cellular phenotypes. I am amazed by this technology and would like to use it to characterize environmental samples. I am highly engaged in training activities covering flow cytometry and cell sorting principles. I want to develop training programs covering more recent techniques, including spectral cytometry and image-enabled cell sorting.



**Gert Van Isterdael** - VIB, Ghent



**André Mozes** – Head, Flow Cytometry Platform, Champalimaud Foundation, Lisbon, Portugal

My passion for flow cytometry started when I was finishing my graduation at the School of Health, Porto and since then I've been

exclusively dedicated to this exciting technology. For the last 12 years I've had the privilege to work in three different shared resource labs in both Portugal and Switzerland. As an active member of several scientific societies, I have had the opportunity to present my work in a multitude of countries (Switzerland, France, Spain, Portugal and USA). I'm very passionate about working with unusual sample types, so I'm always open to discuss new projects with other colleagues, private companies and startups. Recently I was invited to lead the Flow Cytometry Platform at the Champalimaud Foundation in Lisbon. Here I'm committed not only to improve the overall quality of our services but also to give my contribution to the entire Portuguese Flow Cytometry community.

**What if rethinking your antibodies ...**  
... could revolutionize your flow cytometry?

► [miltenyibiotec.com/think-again](https://www.miltenyibiotec.com/think-again)

Miltenyi Biotec provides products and services worldwide. Visit [www.miltenyibiotec.com/local](https://www.miltenyibiotec.com/local) to find your nearest Miltenyi Biotec contact.

Unless otherwise specifically indicated, Miltenyi Biotec products and services are for research use only and not for therapeutic or diagnostic use. The Miltenyi Biotec logo is a registered trademark or trademarks of Miltenyi Biotec and/or its affiliates in various countries worldwide.  
Copyright © 2022 Miltenyi Biotec and/or its affiliates. All rights reserved.

# INNOVATORS



**Bin Fu** - Master's Degree Candidate, University of Cambridge, Cambridge, UK



**Craig LaBoda** - CTO and Co-Founder, Phitonex, Inc., North Carolina, USA



**Han Wei Hou** - Assistant Professor, School of Mechanical and Aerospace Engineering, Nanyang Technological University, Singapore



**Kirk Mutafooulos** - R&D Director: Microfluidics Dept., Cytonome/ST, Massachusetts, USA



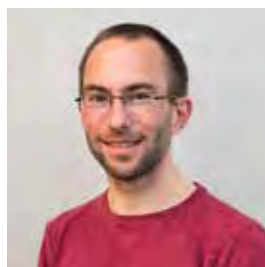
**Sheng-Ting Hung** - Postdoctoral Research Associate, National Tsing Hua University, Hsinchu, Taiwan



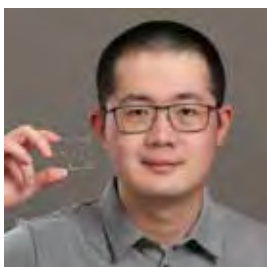
**Takeaki Sugimura** - Vice President of Engineering, CYBO, Tokyo, Japan



**Melanie Jimenez** - Research Fellow, University of Glasgow, Glasgow, Scotland



**Daniel Kage** - Post-doc at the Flow Cytometry Core Facility of the German Rheumatism Research Centre (DRFZ)



**Jingjing Zhao** - Postdoctoral Fellow, Stanford University, California, USA

Education: BSc, MSc, and PhD in Physics [Humboldt University Berlin, Paul Drude Institute (PDI), Federal Institute for Materials Research and Testing (BAM)]

Originally coming from semiconductors physics, Daniel transitioned via molecular physics and fluorescence spectroscopy to flow cytometry. Currently, he is working on improvements to the optics, signal processing, and data analysis for flow cytometers. In his lab, they combine pulse shape measurements, i.e. temporal resolution during cell transit through the laser beam, with angular resolution for scattered light.

# INNOVATORS



**Peter Mage, PhD** – Peter is a Senior Staff Engineer in the Advanced Technology Group at BD Biosciences, where he is responsible for inventing and commercializing new instrumentation and bioinformatics tools for understanding the immune

system at the single-cell level. Prior to joining BD in 2018, he developed technologies for in-vivo biosensing and drug delivery as a postdoc at Stanford University in the departments of Electrical Engineering and Radiology. Peter earned his PhD in Materials from UC Santa Barbara and holds bachelor's degrees in physics and math.



**Sajad Razavi Bazaz** - Sajad studied Biomedical Engineering at University of Technology Sydney, Sydney, Australia. He mainly investigated rigid (3D printed) microfluidic devices, where he was able to develop a new patented additive

manufacturing method for the fabrication of microfluidic devices and validated it through multiple microfluidic applications, ranging from sample processing and fluid washing to particles/cell sorting and cytometry applications. Upon the knowledge he has gained so far, Sajad is investigating miniaturization of current cytometry platforms and is working on developing microfluidic-based flow cytometry devices. In cytometry, liquid handling techniques play a crucial role; thus, Sajad is keen to collaborate with those with experience and knowledge through either numerical studies or experimental practices.

Build the *best* flow cytometry panels.

**World leading reagents and instruments**

StarBright Dyes are unique fluorescent nanoparticles conjugated to Bio-Rad's highly validated immunology antibodies. Developed specifically for flow cytometry, they have narrow excitation and emission spectra and give you exceptional brightness without the need for a special buffer. Combine StarBright Dyes with the fast and powerful ZE5 Cell Analyzer, an innovative instrument with flexible configurations to meet a broad range of experimental complexities and throughput, for the perfect synergy of reagents and instrument.

Explore flow cytometry at [bio-rad-antibodies.com/flow](https://bio-rad-antibodies.com/flow)

#ScienceForward

# CYTO 2022 ABSTRACTS

## FRIDAY, JUNE 3

### 02

#### **What Are We Sorting? Basic Cellular Immunology for Flow Cytometrists**

Evan Jellison, Ph.D., Uconn Health

This tutorial will focus on the major cell types that make up the mammalian immune system. As a general overview, it will focus on identification of major human and murine immune cell phenotypes incorporating cellular function, markers of differentiation, activation, location, and development. Example flow cytometry immunophenotyping studies will be used throughout and methods for using flow cytometry to study immune cell function will be incorporated wherever possible.

### 03

#### **Effective Use of Full Spectrum Cytometry**

Laura Ferre Font, Rui Gardner and Ana Longhini

Malaghan Institute of Medical Research, New Zealand and Memorial Sloan Kettering Cancer Center, United States

Technological advancements in fluorescence flow cytometry and an ever-expanding understanding of the complexity of the immune system have led to the development of large flow cytometry panels, moving beyond 40+ markers at the single-cell level. In contrast to conventional flow cytometers, full spectrum flow cytometers measure the entire emission spectrum of each fluorophore across all lasers. This allows for fluorophores with very similar emission maxima but unique overall spectral fingerprints to be used in conjunction, facilitating the design of larger panels. However, as panel size and complexity increase, so does the detail involved in designing and optimizing successful high-quality panels fit for downstream high-dimensional data analysis. In our tutorial we will exhaustively introduce full spectrum flow cytometry and we will aim to guide the audience through the journey of designing and optimizing a full spectrum flow cytometry panel. Additionally, several applications of full spectrum flow cytometry will be discussed providing the audience with a broad overview of the effective use of full spectrum flow cytometry.

### 04

#### **Attaining ISAC SRL Recognition: Insights from the First Year**

Michael Gregory, Cleveland Clinic Florida Research and Innovation Center, United States; Kathleen Daniels, Sana Biotechnology

In an ideal world, all Shared Resource Laboratories (SRLs) would adhere to the ISAC flow cytometry SRL best practices as outlined in the Barsky et al. 2016 Cytometry Part A paper\*. However, in practice adhering to Best Practices requires a lot of work and dedication by the SRL staff. ISAC's SRL Recognition Program launched last year in order to recognize and reward member-SRLs that adhere to these SRL Best Practices. Ten SRLs completed the very thorough application and review process in the inaugural year. This wealth of application data will allow this tutorial to discuss areas where there are common gaps between the ideal best practices and actual reported practices from the program. The tutorial will also address innovative areas where best practices may need to be expanded in the future.

\*Barsky, L et al. (2016) International Society for Advancement of Cytometry (ISAC) flow cytometry shared resource laboratory (SRL) best practices. Cytometry A. 2016 Nov;89(11):1017-1030.

### 05

#### **When Flow Is Not The Way To Go: Multiplexed Imaging For Mapping Tissue At The Single Cell Level**

Andy Filby, Newcastle University

Next-generation tools for multiplexed imaging have driven a new wave of innovation in understanding how single-cell function and tissue structure are interrelated. In previous work, we developed multiplexed ion beam imaging by time of flight, a highly multiplexed platform that uses secondary ion mass spectrometry to image dozens of antibodies tagged with metal reporters. As instrument throughput has increased, the breadth and depth of imaging data have increased as well. To extract meaningful information from these data, we have developed tools for cell identification, cell classification, and spatial analysis. During this workshop, these approaches will be discussed in the context of example applications in various contexts, including triple negative breast cancer, ductal carcinoma in situ, decidual remodeling during human pregnancy, and pulmonary tuberculosis.

# CYTO 2022 ABSTRACTS

08

## **What Are We Sorting? Intermediate-genetic Manipulation and Molecular Biology for Slow Cytometrists**

David Galbraith, University of Arizona

Flow cytometry has allowed for the evaluation of single cells based on their features, such as morphology, size, and expression of intracellular or extracellular proteins. Thus, using flow cytometry cells can be isolated based on one or many features. This tutorial will focus on discussing molecular biology techniques that harness flow cytometry to separate and identify genetically modified cells. Approaches such as CRISPR-Cas9 genome editing, chimeric antigen receptor technologies and cell transduction techniques will be discussed in the context of their utilization of flow cytometry and cell sorting.

09

## **Writing, Publishing, and Reviewing: Advice, Tips and News from Cytometry Part A – The Journal of Quantitative Cell Science**

Attila Tarnok, China; Henning Ulrich and Melissa Asaro

University of Leipzig, Germany; University of Sao Paulo and Wiley, United States

Course Objectives: Scientific journals require certain quality standards from manuscripts to be acceptable for further reviewing and publication. There are some very common reasons why a paper gets reviewed and accepted or rejected. This tutorial aims to highlight all major aspects of manuscript writing, submission and communication with the reviewers, points out what can (and very often does) go wrong and how to do it right in order to improve your chances to get your paper published. Special emphasis will be taken to focus on the needs for publishing cytometry data in biomedical and technical oriented journals such as Cytometry Part A. The process will be shown from the Editors and the publishers' point-of-view.

Course Details: How to write a good manuscript: Here the most important aspects of writing a good manuscript and the most common mistakes made in writing a manuscript will be explained and discussed.

Manuscript processing and reviewing process: The processing of manuscript within the journal will be presented and discussed from the editors, reviewers and publishers' perspective.

10

## **Multiplexed Methods for Fluorescence Imaging, Also Multiplexed Tissue Imaging**

Andrea Radtke, Ph.D., National Institute of Allergy and Infectious Diseases (NIAID), United States

Multiplexed antibody-based imaging empowers the study of complex cellular phenotypes in situ by providing a means to evaluate dozens of protein biomarkers in a single tissue section. One such method, Iterative Bleaching Extends multi-plexity (IBEX), is an iterative staining and chemical bleaching technique that enables comprehensive profiling (>65 parameters) of diverse tissues. IBEX is compatible with over 250 commercially available antibodies, 16 unique fluorophores, and can be easily adopted to different imaging platforms using slides and non-proprietary imaging chambers. The overall protocol consists of iterative cycles of antibody labelling, imaging, and chemical bleaching that can be completed at relatively low cost in 2-5 days by biologists with basic laboratory skills. This workshop will provide guidelines for successful adoption of IBEX and present several applications of the method to study normal and diseased tissues. Additionally, a significant amount of time will be devoted to the following topics related to image cytometry: optimal tissue processing, overcoming autofluorescence, and the construction of organ mapping antibody panels (OMAPs).

# CYTO 2022 ABSTRACTS

12

## Single Cell Metabolism: Functional And Phenotypic Approaches For Cytometrists

Rafael Argüello, Ph.D., CNRS, United States

Tutorial summary: Interest in immunometabolism is growing exponentially due to its implication in infection, autoimmunity, cancer and immunotherapies. However, studying immunometabolism ex-vivo has been technically challenging for the last decades. In the last two years, efforts from many different labs have generated a toolbox of functional and phenotypic markers that allow to characterize the metabolic profile of immune cells by flow cytometry. In this webinar we will overview update and compare the different tools available and guide you to perform your first immunometabolic studies by flow cytometry.

Learning Objectives: In this Webinar you will learn the latest advances in single cell technologies to study immunometabolism. I will NOT speak about the Krebs cycle, and you will learn about functional and phenotypic tools to study metabolism by flow cytometry. In particular, you will learn to interpret experiments and results from SCENITH and other methods.

Who Should Attend: Master, PhD, Postdocs and PIs interested to explore the immunometabolism field by flow cytometry.

13

## Cytometry and The Scientific Method: How Can We Improve the Path from Laboratory to Literature and Back?

David Galbraith, Ph.D., Virginia Litwin, Ph.D. and Peter Lopez

Arizona Cancer Center, Charles River Laboratories, and NYU Langone Health, United States

Rigor and reproducibility are key elements of science, and an article of faith has been that, as our understanding of science has increased in sophistication, this should be accompanied by a natural improvement in rigor and reproducibility. Various published metrics indicate this has not been the case, exemplified by commercial difficulties experienced in bringing new drugs to market, to the surprisingly poor ability to simply reproduce key specific discoveries through direct measurement. ISAC, given its grounding as a measurement-based society, has a longstanding history and interest in promoting rigor and reproducibility. This tutorial will build on previous ISAC initiatives in this important area. The information will be presented from the unique perspective of the Scientific Method, which describes a framework for conducting scientific research. Given that the Scientific Method was first conceived of circa the 17th century, it can be considered one of the first “best practices” guidelines.

The tutorial will begin with a review of the Scientific Method: Observation, research, hypothesis, discovery and testing, data analysis, publishing the conclusions, and formulating new questions. This will be followed by a discussion regarding how the Scientific Method has changed over time and how this structured process helps to ensure rigor and reproducibility.

The body of the tutorial will focus on practical information as to how to align the Scientific Method with what we do in flow cytometry laboratories to ensure rigor and reproducibility. Beginning with the instrument, the essentials for equipping a flow laboratory, and maintaining/validating instrument performance will be reviewed. Moving on to the assays, practices for designing, transferring and implementing standardized assays will be discussed. Methods to identify unsuspected variables, and to appropriately handle their contributions will be described. The problem of conscious and unconscious bias will be discussed, along with means to detect it, and eliminate its contribution. The importance of appropriate incorporation of statistical methods into the experimental

# CYTO 2022 ABSTRACTS

design will be emphasized. Ending with publication, information regarding tricks and recommendations for creating a clear, concise, and accurate manuscript and how to provide a meaningful and timely peer review will be presented. Given the increasing availability of data repositories, their routine deployment in the publication process will be discussed, along with that of check-lists to ensure accurate and comprehensive descriptions of how the various experimental methods were employed.

---

## 14

### Emerging Trends in Cytometry

Iyadh Douagi, Ph.D., NIAID, United States

The ability to extract quantitative information from single cells continues to be fundamental approach to propel discoveries in biology and medicine. Today, precise identification and fast enumeration of cells are routine methods for clinical and research laboratories. This tutorial will provide an overview of the recent technical advances and applications of flow and imaging cytometry. Through selected examples, we will outline how single-cell multiomics approaches can contribute to unravel layers of cell complexity and to gain new insights into the dynamics of cellular trajectories. Finally, we will discuss current limitations in coupling data sets originating from diverse single-cell technologies and analytics, and how data generated are increasingly challenged with demands for standardization, data annotation and sharing.

---

## 16

### How to Assess the Biosafety Aspects of New and Atypical Flow Cytometers

Dominic Jenner, Dstl; Evan Jellison, Ph.D., Uconn Health; Stephen Perfetto, NIAID

This tutorial will provide a framework for assessing the biosafety aspects of new and/or atypical instruments. Many newer flow cytometers differ from the traditional jet-in-air models that provided the basis for the ISAC Biosafety Committee guidelines. Manufacturers have redesigned various safety features and, in some cases such as microfluidic-based flow cytometers, are using new technologies in their instruments. We will discuss how to assess the biosafety aspects of these types of flow cytometers, including strategies to perform aerosol containment testing. After participation in this tutorial, the attendee will be able to formulate a plan to assess their instruments, determine any risks associated with procedures using these instruments, properly assess aerosol containment, and determine appropriate safety mitigation measures.

# CYTO 2022 ABSTRACTS

17

## Best Practices in Sorting, Including Bacteria and Viruses

Jakob Zimmerman, Ph.D., Rachel Sheridan, Ph.D., Vera Tang, Ph.D. and Nicole Poulton, Ph.D.

Van Andel Institute, United States; University of Ottawa, Canada; Bigelow Laboratory for Ocean Sciences, United States

Let's face it, the majority of samples that come through our cell sorters are probably going to be cell lines and lymphocytes. However, every now and then you will come across something different. In this tutorial we will focus on the best practices and recommendations for sorting samples that contain particles smaller than a cell (< 2 µm) such as nuclei, bacteria, phytoplankton, chromosomes, viruses, and extracellular vesicles. Some of these samples will be at the limit of detection for many commercial sorters and having the appropriate controls and best practices becomes important for interpretation and validation of both the data and the sorted sample. We will focus our initial discussion on instrument set up, controls, data interpretation, validation and provide additional resources.

In addition, we will provide examples of downstream applications of sorted small particles and how they can be used to answer questions pertaining to the human gut microbiota and marine ecology. The intestinal microbiota has been implicated in all aspects of human health and cell sorting of gut microbes for downstream applications can complement the classical sequencing-based approaches to better understand host-microbial mutualism. Gut microbiota samples are challenging given the abundance of diet- and host-derived particles thus requiring special precautions and adequate controls. In the aquatic environment, identification and sorting of marine phytoplankton, bacteria and viruses, are challenging due to the density of small particles in the natural environment. We will discuss sample preparation, optimization, sorting and validation for optimal data interpretation.

SATURDAY, JUNE 4

21

## The Innovation, Methodology and Application Research Theme @Newcastle University: A blueprint for delivering cutting-edge technologies to enable discovery

Andy Filby<sup>1</sup>

<sup>1</sup> Newcastle University

The shared resource lab (SRL) model is a highly effective way to ensure that cutting-edge, enabling technologies are widely available across numerous different fields of research. SRLs normally include and encompass a range of enabling technologies and methodologies for biomedical and life sciences research including genomics, proteomics, imaging modalities, single cell analysis (cytometry) and informatics. In many cases, a single project will involve several different technologies and methodologies as well as associated expertise. In all cases, these technologies and methodologies will be fast moving and constantly evolving. It is therefore essential that the right environment exists to both horizon scan for, evaluate and if successful, implement new solutions in this space. Since 2019, the crosscutting "Innovation, Methodology and Application (IMA) research theme within the Newcastle University Faculty of medical sciences (NU-FMS) has been a home and "rally point" for methodologists and technologists, regardless of job family. It has led in the creation of "Special Interest Groups" (SIGs) in technologies and methodologies that encompass all major areas of expertise and are led, where possible, by members of the relevant SRLs. In this talk, Dr Filby will discuss the IMA Theme and how it has become the embodiment of team science and a healthy, inclusive research culture. He will also discuss how it has also given birth to a strategic horizon-scanning community called "NU Tech-Scan"; that works right across the spectrum from discovery science to clinical/translational studies and beyond to identify, evaluate and if successful, implement new technologies in the SRL structure.



22

893900

## Development of An Image-Based HCS Compatible Method for Endothelial Barrier Function Assessment

Leo Chan<sup>1</sup>, Oleksii Dubrovskiy, Erica Hasten<sup>1</sup>, Steven Dudek<sup>2</sup>

<sup>1</sup> Nexcelom Bioscience, <sup>2</sup> University of Illinois in Chicago

Acute respiratory distress syndrome (ARDS) is a serious condition with high mortality rate that has increased in the recent years due to the COVID-19 pandemic. Currently, effective pharmacological therapies have yet been discovered for ARDS, despite decades of laboratory and clinical studies. ARDS onset typically generates an increase in the endothelial permeability causing the development of pulmonary edema that leads to respiratory failure during the primary event. In this work, we propose the use of phenotypic drug discovery (PDD) approach in the search for effective ARDS treatment due to its ability to identify first-in-class drugs and deliver results when the exact molecular mechanism is partially obscure. However, the PDD approach requires novel cell-based assays compatible with high-throughput and high-content screening (HTS/HCS) capability. Here we demonstrate a novel fluorescence-based image cytometry method for directly determining endothelial barrier function. The image cytometry method simultaneously allows for rapid measurement of cell monolayer permeability and cell-based analysis. The time-dependent cell permeability showed an increase in human pulmonary artery endothelial cells (HPAEC) in response to the thrombin and TNF- $\alpha$  treatment, which correlates with previously published data obtained by trans-endothelial resistance measurements (TER). The incorporation of image cytometry in combination with digital image analysis can substantially reduce assay variability and improves the signal window. Furthermore, the proposed image cytometry method can be easily adapted for HTS/HCS applications, which may be extended to assay permeability of brain endothelium, gut epithelium, and other cell barriers for potential therapeutic discovery.

23

898241

## Spectral Flow Cytometry and Imaging Studies on Cyanobacteria and Microplastics Using 64 Narrow Bandpass Filters And A Widefield Fluorescence Research Microscope

Robert Zucker<sup>1</sup>, Emma Brentjens<sup>2</sup>

<sup>1</sup> Duke University, <sup>2</sup> Oak Ridge Institute for Science and Education (ORISE)

Spectral flow cytometers yield increased resolution due in part to the 64 narrow bandpass detectors and unmixing software that are used to remove autofluorescence derived from metabolic fluorescence molecules. We have applied this flow technology to study the following applications without unmixing: 1) cyanobacteria metabolism, 2) effects of nutrient deficiency or chemical exposure on cyanobacteria, and 3) microplastic detection in cells and solution by spectral scatter. A research Nikon Ti2 microscope was used to confirm and add to the data derived from a Cytex Aurora spectral flow cytometer. Time measurements on cyanobacteria were made during specific wavelength illumination to monitor photosynthesis and metabolism. 3D localization of fluorescent polystyrene beads in mammalian cells was made using widefield confocal microscopy. *Microcystis aeruginosa* is a species of cyanobacteria present in inland lakes, streams, and water supplies. These bacteria can form harmful algal blooms, contaminating water with toxic compounds. The relationship between cyanobacteria, nutrient availability, growth, and death was investigated using an in vitro *Microcystis aeruginosa* cell line. Changes in cell metabolism were measured in the green (542 nm mean) and red (660 nm mean) fluorescent ranges. There was an increase in green fluorescence (potentially due to a buildup of metabolic proteins) followed by a decrease in red fluorescence from photosynthetic pigments. A decrease in cell size measured by light scatter was also detected. Different wavelengths of light and chemicals hydrogen peroxide (H<sub>2</sub>O<sub>2</sub>) and potassium permanganate (KMnO<sub>4</sub>), which are commonly used to treat water contaminated with cyanobacteria, affect cyanobacteria's physiology. An initial increase in red fluorescence (660 nm) followed by a decrease was shown after prolonged exposure to different wavelengths of light, indicating decreased photosynthesis. H<sub>2</sub>O<sub>2</sub> and KMnO<sub>4</sub> similarly induced as much as a fivefold increase in green fluorescence emission (542 nm) and an increase in red fluorescence within 24 hours before a decrease over longer periods of time. Microscope

# CYTO 2022 ABSTRACTS

observations of *Microcystis* were correlated to flow cytometry data showing decreased photosynthesis fluorescence, viability, and size after chemical treatment. This measurement approach detects a sensitive and early change in cyanobacteria functioning. Fluorescent particles were accumulated into cells using an in vitro cellular model system. The 200 nm fluorescence polystyrene beads were detected by measuring cellular fluorescence intensity. Particles were incorporated into several mammalian cell lines in a dose dependent manner and confirmed by microscopy. Using widefield confocal microscopy with deconvolution, the particles were found to concentrate in the endoplasmic reticulum surrounding the nuclei and near the mitochondria. Mitochondria morphology was studied using transfection. This abstract does not represent USEPA policy.

**24**  
898408

## Functional Profiling Metabolism with A Fixation-Compatible System Analysing Micro-Samples Of Blood

Rafael Argüello<sup>1</sup>, Julien P. Gigan<sup>3</sup>, Ania BAAZIZ<sup>2</sup>

<sup>1</sup> CNRS, <sup>2</sup> CIML, <sup>3</sup> AltraBio SAS

Development of personalized medicine requires methods that are able to capture a large array of biological markers that can predict cell function and response to treatment. There is compelling evidence that the response to treatments in the context of cancer and infection correlate with the metabolic state of different cells. Indeed, the metabolic profile of immune cells, infected cells and cancer cell subsets is a universal hallmark of their functional state. Current methods to profile energy metabolism require large number of cells, cell culture media and are not adapted to analyse patient samples. We have recently developed SCENITH, a method to functionally profile energetic metabolism with single cell resolution. Here, we present a SCENITH based approach that allows to functionally determine the metabolic profile in micro-samples of whole blood (i.e. <500 ul) compatible with non-invasive blood extraction systems. Our approach is fixation and shipping compatible; and can be revealed by Flow cytometry, CyTOF and also by Cite-seq and compatible with epigenetic analysis using CUT&RUN and CUT&TAG. We present here a very robust, 25 colors spectral flow cytometry panel that allows to determine the metabolic profile of virtually all immune cells in the blood. This revolutionary approach has the potential to be used at home by end users to link their health status and response to treatment with their

immune phenotype and functional immunometabolic profile. We envision that by using our SCENITH-based functional single-cell based approaches we will contribute to the identification of functional metabolic profiles that can predict disease development and response to treatment.

**26**  
896958

## High-Speed Image-Based Cell Sorting

Eric Diebold<sup>1</sup>

<sup>1</sup> BD Biosciences

Sorting cells at high speed (>10,000 events per second) using flow cytometry requires a complex technical integration of multiple optical, fluidic, and electronic subsystems, to separate single cells based upon a multiplexed evaluation of their protein expression. While flow cytometry has become ubiquitous in biomedical research over the past 50 years, conventional flow cytometers fundamentally cannot resolve spatial phenotypic characteristics at the subcellular level. This limitation renders flow cytometers unable to address certain biological questions that are typically interrogated with technologies such as fluorescence microscopy or laser-capture microdissection. Here, we present the demonstration of a cell sorter that resolves subcellular detail using multi-color fluorescence, brightfield, and darkfield imaging and sorts cells using real-time image-derived parameters at speeds up to 15,000 events per second. This sorter is enabled by the integration of a novel high-speed camera-less fluorescence imaging approach, custom-designed low-latency signal processing electronics, and a droplet-based sorter fluidics system. We describe the operational principles of this image-based sorter (ref. Schraivogel et al., Science 2022), and present results from several applications of this technology in areas that uniquely benefit from this new capability.

27

898013

## Light Scattering Pulse Shape Analysis With Multiple Forward Scatter Detectors In Flow Cytometry

Daniel Kage, K. Heinrich & J. Kirsch (German Rheumatism Research Centre Berlin (DRFZ) - Flow Cytometry Core Facility, Charitéplatz <sup>1</sup> (Virchowweg 12), 10117 Berlin, Germany K. Feher (EMBL Australia Node in Single Molecule Science, School of Medical Sciences, University of New South Wales, Sydney, Australia) C. Giesecke-Thiel (Max Planck Institute for Molecular Genetics (MPIMG) - Flow Cytometry Facility, Ihnestraße 63-73, 14195 Berlin, Germany

In a flow cytometer, particles of interest (e.g. cells, bacteria, extracellular vesicles) passing the laser spot create a time-dependent scattering intensity signal, resulting in a signal pulse. In standard instruments, this pulse shape is characterized by three read-out values: height, area, and width. However, additional information about the particles can be obtained by capturing the entire pulse shape of the scattered light. Furthermore, the angular distribution of the scattered light varies with particle size, shape, and internal structure. Thus, angle-resolved detection of the scattered light is another possibility to acquire particle-specific properties, which is not available in standard instruments. We equipped a flow cytometer with custom-made signal acquisition electronics, modified optics, and a fiber array to combine the angle- and time-resolved forward scatter detection for cells in multi-angle pulse shape flow cytometry (MAPS-FC). For a general assessment of this setup and a deeper understanding of the observed phenomena, measured data from polymer beads were compared to simulations based on Generalized Lorenz-Mie Theory (GLMT). As a proof-of-principle application, we also performed cell cycle analysis of different cell lines. The resulting measurements were validated by DNA staining. Using time- and angle-resolved measurements, we were able to define subgroups specific for the cell cycle phases G1, S, and G2/M. In-depth angle- and time-resolved data analysis by tailored clustering enables the scatter-based analysis of cells and could help in increasing the number of accessible parameters. Ongoing and future work aims at discovering further applications and the implementation of the proposed approach for label-free cell sorting.

28

898460

## Broadband fingerprint-region Raman-activated cell sorting at 50 cells/s

Kotaro Hiramatsu<sup>1</sup>, Keisuke Goda<sup>2</sup>, Matthew Lindley<sup>2</sup>, Julia Gala de Pablo<sup>3</sup>

<sup>1</sup> The University of Tokyo, <sup>2</sup> Osaka University Graduate School of Engineering, <sup>3</sup> University of Leeds

Raman-activated cell sorting promises label-free cell selection for applications such as genotype-phenotype linking, directed evolution, and human-targeted cell therapies. However, the typically long acquisition times of Raman measurement presents a challenge for large-scale sorting, particularly as measurement bandwidth increases. Here we demonstrate broadband (300 – 1,300 cm<sup>-1</sup>) coherent Raman-activated cell sorting at throughputs up to 50 cells/s, which is an ~25x increase over previous demonstrations at similar bandwidths. Our sorter combines a Fourier-transform coherent anti-Stokes Raman spectrometer for cell measurement, a microfluidic on-chip push-pull cell sorter for sample control, and a field-programmable gate array for real-time spectral analysis and decision making. We typify the performance of our flow-through cell sorter using polymer microbeads, then demonstrate sorting of three microalgal species based on analysis of their carotenoid or polysaccharide content. Sorting mixtures of analyte-rich and analyte-poor cells resulted in purities up to 93% and yields up to 51% for samples ranging from 4,500 to 12,000 cells. (Please note, there are two additional co-authors who could not be added due to space in the web form. I have been instructed they can be added later by CYTO staff if this manuscript is accepted. I will include their names as directed by email from CYTO staff: Jorgen Walker Peterson and Akihiro Isozaki.)

29

898551

## **Serial Flow Cytometry: Per-Particle Uncertainty Estimation From Repeated Measurements In Microfluidic Cytometer With Integrated Optical Waveguides**

Paul Patrone<sup>1</sup>, Matthew DiSalvo<sup>1</sup>, Gregory Cooksey<sup>1</sup>, Megan Catterton<sup>1</sup>

<sup>1</sup> NIST

Flow cytometers are highly utilized in biomedical research and clinical diagnostics because they are capable of quickly characterizing thousands of single cells. However, full utilization of this data is limited by lack of methods for uncertainty quantification (UQ). Fluorescent microspheres are traditionally used for UQ in cytometry, but per-cell UQ is impractical to estimate due to convolution between ideal measurement repeatability, the inherent distribution of the microspheres, and flow/device-induced variations. Thus, fundamental questions remain with respect to the impact of effects such as instrument configuration and operating parameters on measurement uncertainties. Such issues are critical for addressing important measurement challenges, i.e., separating true population heterogeneity from measurement repeatability, quantitative classification of sample components (including rare-event detection), and comparing measurements from different instruments. To address these problems, we have developed a new kind of cytometer that repeats measurements of objects at multiple points along a flow path to directly assess uncertainty of fluorescence and scatter intensities. Critically, the independent but practically identical measurement regions enable direct quantification of uncertainties associated with effects arising from operating conditions. For example, we use the system to characterize how flow focusing affects uncertainty. In contrast to conventional approaches that focus particles to the center of the stream, we direct them to stable inertial nodes that are not in the middle of the channel, which results in tighter control of particle positions and velocities. The instrument was automated to enable real-time quantification of measurement uncertainty and operated with particle velocities exceeding 1 m/s (< 0.2 % coefficient of variation), throughputs above 100 events per second, and tracking yields better than 99.9%. We report per-particle uncertainties in flow cytometry for the first time, with achievement of less than 2% variation across multiple interrogation regions for microspheres and cells. The system also captures an intensity profile as objects pass through the

measurement region. This permits, for example, identifying the singlets that comprise a doublet, which can't be done using conventional instruments. Sensitivity and background characterization of the microfluidic cytometer have also been optimized to achieve results similar to commercial systems. Overall, we show how per-particle uncertainty estimation permits real-time optimization of the flow control strategy along with evaluation of measurement precision across the instrument's dynamic range.

Gregory A. Cooksey<sup>1</sup>, Paul N. Patrone<sup>2</sup>, Matthew DiSalvo<sup>1</sup>, Megan A. Catterton<sup>1,3</sup>, Nikita Podobedov<sup>1,3</sup>, Jalal Sadeghi<sup>1,4</sup>, Eric W. Esch<sup>1,5</sup>, Anthony J. Kearsley<sup>2</sup>

<sup>1</sup> National Institute of Standards and Technology, Microsystems and Nanotechnology Division, Gaithersburg, MD, USA,

<sup>2</sup> National Institute of Standards and Technology, Applied and Computational Mathematics Division, Gaithersburg, MD, USA, <sup>3</sup> Johns Hopkins University, Department of Mechanical Engineering, Baltimore, MD, USA, <sup>4</sup> University of Maryland College Park, Institute for Research in Electronics and Applied Physics, College Park, MD, USA, <sup>5</sup> University of Maryland College Park, Department of Bioengineering, College Park, MD, USA

30

894440

## **4-<sup>1</sup>BBL-Containing Leukemic Extracellular Vesicles Promote Immunosuppressive Tregs And Dysfunction Of Effector T Cells, To Facilitate Progression Of Myeloid Leukemia**

Julian Swatler<sup>1</sup>, Laura Turos-Korgul<sup>1</sup>, Marta Brewinska-Olchowik<sup>1</sup>, Katarzyna Piwocka<sup>1</sup>

<sup>1</sup> Nencki Institute of Experimental Biology

Tumor extracellular vesicles (EVs) have been implicated as drivers of immunosuppression in cancer. However, influence of tumor EVs on functional, molecular and phenotypic properties of regulatory T cells (Tregs) and effector CD4+/CD8+ T cells has been poorly explored. This is also the case in chronic and acute myeloid leukemia (CML/AML), where few immunosuppression-promoting factors have been described. We aimed to precisely study the biology of different T cell subsets in response to CML- and AML-derived EVs and to assess relevance of this interaction for leukemia progression. We used ex vivo models with human sorted T cells and EVs from plasma of leukemic patients or released by CML/AML cells. EVs were characterized by electron

microscopy, western blotting and nanoparticle tracking analysis, according to MISEV guidelines. Lymphocytes were analyzed using classical and spectral flow cytometry (including 23-color Treg phenotyping panel), phospho-flow and RNA sequencing. For in vivo studies, an immunocompetent mouse model of CML-like disease was developed, induced by either wild-type or Rab27a-deficient (with attenuated secretion of EVs) leukemic cells. Leukemic EVs induced Foxp3+ iTregs from CD25- T cells and amplified suppressive activity of mature Tregs. Leukemic EVs led to significant remodeling of the transcriptome and upregulation of tumor Treg genes. By spectral flow cytometry and FlowSOM clustering, we detected two distinct, effector Treg (eTreg) subsets, upregulated by leukemic EVs - CD30+CCR8hiTNFR2hi eTreg1 and CD39+TIGIThi eTreg2. Leukemic EVs also influenced effector CD4+ and CD8+ T cells, by inducing expression of dysfunction markers PD-1, LAG-3 and CD39, downregulating secretion of anti-tumor cytokines (IFN- $\lambda$ , TNF- $\alpha$ , IL-6) and modulating glycolytic and mitochondrial metabolism. Both Treg and non-Treg T cells were modulated via upregulated phosphorylation of STAT5 and downregulation of mTOR-S6 signaling. In vivo, leukemic EVs contributed to elevated Treg numbers and activated CD44+CD62L- phenotype. Amongst effector CD4+ and CD8+ T cells, leukemic EVs secretion in vivo led to expansion of dysfunctional, CD39+ cells. These changes occurred in parallel with stronger engraftment of leukemic cells in vivo, pinpointing relevance of EVs and EVs-Treg/T cell interactions in leukemia progression. Finally, mass spectrometric profiling revealed that leukemic EVs shuttled costimulatory protein 4 1BBL, which elevated expression of LAG-3, CD30 and TNFR2 and suppressive activity of Tregs. Altogether, we describe mechanisms and transcriptomic/phenotypic changes in different T cell subsets, driven by leukemic EVs. In vivo studies identified EVs as relevant for leukemia development and indicated Rab27a-dependent secretion as a potential therapeutic target in myeloid neoplasms. Supported by grants: National Science Centre 2018/29/N/NZ3/01754 (JS) and Foundation for Polish Science POIR.04.04.00-00-23C2/17-00 (KP).

32

898449

## Preterm Birth (PTB) Detection: A Series of Immuno-Phenotypic Changes That May Serve As A Biomarker For Warning Signs.

Nicolas Loof<sup>1</sup>, Alina Montalbano<sup>2</sup>, Carole Mendelson<sup>2</sup>

<sup>1</sup> BD Biosciences, <sup>2</sup> UT Southwestern

PTB affects ~15 million babies annually and remains the leading cause of death in newborns and children under 5 years worldwide. This is due to our incomplete understanding of the integrated immunoendocrine mechanisms that maintain uterine quiescence throughout pregnancy and those that trigger its transition to an inflammatory state leading to labor. While chorioamnionitis likely incites the inflammatory cascade leading to PTB, a growing body of evidence suggests that the signals for labor at term emanate from both mother and fetus. Herein we describe a series of phenotypic changes that may serve as a biomarker for warning signs of PTB issues. Previously we reported that surfactant protein A (SP-A) and platelet activating factor (PAF), secreted by the maturing fetal lungs beginning at 17.5 days post-coitum (dpc) (term=19 dpc) into amniotic fluid (AF), serve as fetal hormonal signals for labor in mice. Based on these data, we propose that SP-A and PAF regulate the polarization of the AF macrophage (Mf) population to a proinflammatory state that promotes their migration into the maternal uterine compartment where an increase in proinflammatory cytokines is temporally associated with NF- $\kappa$ B activation and parturition. To better understand the regulatory mechanisms involved in AF Mf polarization to an inflammatory state, and the transmission of the pulmonary signal for labor, we characterized AF Mf phenotypic changes associated with SP-A/PAF secretion near term. Polychromatic flow analysis of the CD45+ AF population not only revealed an increase in the total leukocyte population between 15.5 and 18.5 dpc, it also revealed a significant increase in the proportion of F4/80+CD11b+ Mf within the compartment prior to labor (~1.8 x 10<sup>6</sup> at 15.5 dpc, to ~3.1 x 10<sup>6</sup> by 18.5 dpc). Microarray-based transcriptome profiling of F4/80+ AF Mf isolated at 15.5, 17.5 and 18.5 dpc demonstrated a tandem significant increase in both M1 and M2 activation marker expression; a phenotype reminiscent of tumor associated macrophage (TAM). Additionally, a significant increase in the expression of Car4, a lung Mf-specific marker, was noted. These observations were confirmed by flow cytometry and RT-qPCR and are temporally associated with the enhanced expression pulmonary SP-A and

# CYTO 2022 ABSTRACTS

PAF. Ingenuity Pathway Analysis of the AF Mf transcriptome identified IL-8 signaling as the top common canonical pathway in F4/80+ AF Mf at 17.5 and 18.5 dpc, compared to 15.5 dpc. Together, these data suggest that SP-A/PAF induce the polarization of F4/80+ AF Mf to a TAM-like state that may be mediated by IL-8 signaling. In conclusion these studies provide the first comprehensive analysis of the dynamic phenotypic changes in the AF Mf population from myometrial quiescence to contractility and reveal the major molecular pathways by which this unique immune cell population may transmit the signal for labor. Such insights may elucidate novel therapeutic targets for the prevention and intervention of PTB.

**33**  
898497

## **Deep phenotyping of T cells in autoimmune Addison's disease by mass cytometry (Cytof)**

Shahinul Islam<sup>1</sup>, Eystein S. Husebye<sup>1</sup>, Anette Susanne Bøe Wolff<sup>1</sup>

<sup>1</sup> University of Bergen

Autoimmune attack towards steroid producing adrenal cortex results adrenal insufficiency in autoimmune addisons disease (AAD). Organ specific autoimmunity progression is therefore observed by cortisol level in blood, saliva and urine for AAD and often replaced by relevant hormone. Near all AAD patients shows autoantibody against the most vital enzyme 21-hydroxylase but the underlie mechanism is poorly understood. Interestingly, tissue resident autoreactive T cell is still observed in the AAD patients with the complete destruction of the adrenal cortex. Here, we aimed to use mass cytometry (CyTOF) in suspension (blood and saliva) of AAD patients to scrutinize the direct/indirect role of T lymphocytes. The project is in progress and we have recently established a routine CyTOF panel (37 parameter) to characterize immune cells in Addisons patients in compare to healthy donor. A piece of our very preliminary CyTOF data shows a minor impairment of the regulatory T cell (Tregs) compartment in patients with AAD compared to healthy, which we will need to confirm in a larger patient cohort to dig more into this. Tregs dysfunction or unavailability can result in insufficient suppression of inflammation and could be considered critical for the initiation and perpetuation of autoimmune disease. Interestingly, imbalanced Tregs proliferation can lead to Treg conversion into hazardous effector T cells and increase the risk of autoimmune disease development in acute infections. Also, findings of deficient Tregs in many autoimmune disorders, including autoimmune polyendocrine syndrome where Addison's

is one of the disease entities, give hope that we could cure autoimmunity be increasing their function or number. However, Tregs mechanisms and how they function in AAD is an unsolved area. We are now in the position to overcome these obstacles by employing our deeply phenotyped patient cohorts with Treg dysfunction (AAD/APS-I/APS-II) and our optimized novel single cell technologies (mass cytometry and flow-cytometry using both intracellular & extra-cellular marker). Thus, we can extend our knowledge on Treg dysfunction in organ-specific AAD, taking a significant step to understand this relevant immune suppressive immune mediator, which might also be directly used as vehicle or targets in next generation immune therapy with the potential to reverse the existing autoimmune milieus. We will also search to design MHC tetramers to add to the CyTOF and flow cytometry panels to fingerprint autoreactive T cells against 21OH. This could be an initiating point to develop T cell-based assays for AAD and other organ specific disorders.

**34**  
892978

## **Cartography of The Human And Murine Immune System On A 30 Parameter Cytometer: Implementation Of Optimized, 'Ready-To-Use' And Shared Antibody Panels**

Anne-Laure Iscache<sup>1</sup>, Hugo Garnier<sup>1</sup>, Valérie Duplan<sup>1</sup>, Fatima-Ezzahra L'Faqihi<sup>1</sup>

<sup>1</sup> Inserm

Our flow cytometry core facility has acquired a 30 parameter Symphony as part of OCTOPUS, a project supported by the Occitanie region. Our aim is to characterize the networks formed by the cells of the immune system in several conditions: at the extreme stages of life, in pathological contexts before and after treatment and in response to vaccine and infectious stimuli. This should allow to identify predictive biomarkers as therapeutic targets to prevent or correct age related abnormalities. To address these questions, cytometry appears to be the reference technique to determine the phenotype of diverse populations, collect detailed data on the immune response, study rare cell populations and isolate populations of interest by cell sorting. Our main challenge was to set up a collective approach to the development of panels of multicolor conjugated antibodies at the benefice of all users of our core facility. We have therefore implemented a structuring and mutualized approach to design, test and validate the panels by creating within our institute a « Sympony working

# CYTO 2022 ABSTRACTS

group » composed of representative of our private partner BD Biosciences and some of our users. This ‘Symphony working group’ relied on a collaborative approach with shared expertise from the different participants where each one brought its scientific, technical and technological expertise throughout the project. This approach was crucial to develop a structured and standardized approach for the different steps from the panel design to panel validation. We thus set up a workflow with 7 different steps : 1) instrument validation 2) panel design 3) fluorescent cell barcoding and titration 4) panel Test 5) panel validation 6) cytometry store 7) multidimensional analysis. According to this strategy, we were able to create standardized “ready to use” panels allowing the characterization of lymphoid and myeloid cell populations in human and mice. These panels are each composed of a CORE panel and can be implemented with several options (for example regulatory T cell phenotyping, innate lymphoid cell subdivision, etc.), representing in total more than 150 antibodies. Our ultimate goal was to make the developed panels easily accessible to users of our core facility both for routine or occasional use. In order to do so, we set up a « Flow Cytometry panel Store », allowing the management of antibody stocks, orders, and the invoicing of delivered antibodies. Overall, this collaborative approach allowed the development of several 30 color panels not only for our Institute but also for the whole biohealth scientific community of Toulouse.

35

893901

## Practical Cell Counting Method Selection To Increase The Quality Of Cell Counting Results

Jordan Bell<sup>1</sup>, Yongyang Huang<sup>2</sup>, Leo Chan<sup>1</sup>

<sup>1</sup> Nexcelom Bioscience, <sup>2</sup> Kinetic River

The importance of cell counting has increased significantly in the last decade due to the major advances in the fields of cell and gene therapy, biologics production, and regenerative medicine. This has necessitated the development of a standardized approach to cell counting assays. In the recent years, the U.S. Food and Drug Administration (FDA), in collaboration with the National Institute of Standards and Technology (NIST) and the International Organization for Standardization (ISO), has launched an effort to standardize cell counting methods to improve the confidence in cell counting measurements. There is a wide range of biological sample types, various formulations, and bioprocessing steps for cell and gene therapy products. Furthermore, there are no ground truth reference materials for live cells makes determining the accuracy of cell counting difficult defined in the ICH Q2 (R1). Therefore, in order to increase the confidence of cell counting results, it is critical to follow the two recently published ISO cell counting standards to ensure cell counting methods are tailored to the specific sample and purpose. In this work, we will provide insights and guidance for the ISO standards for method selection. The important aspects of the ISO cell counting standards have been distilled to six key factors for selecting the cell counting methods. Attention to these details will allow researchers to more easily adhere to the ISO recommendations to ensure high quality cell counting measurements, and in doing so, sites can meticulously document their rationale, process, and data results.

# CYTO 2022 ABSTRACTS

36

893672

## Building an Industry Standard: Semantic Information Model For Flow Cytometry Discovery Biomarkers

Goce Bogdanoski<sup>1</sup>, Murali Kala<sup>1</sup>, Sowmya Kala<sup>1</sup>, Becky Penhallow<sup>1</sup>

<sup>1</sup>Bristol Myers Squibb

To create business value from data, we need to ensure that our data is findable, accessible, interoperable and reusable. Doing so, large organizations need to find a balance between how easily data can be accessed while maintaining information security. Identifying the sources of information, and the processes used to create and or consume data will enable IT to build digital ecosystems that are integrated and can be orchestrated to extract insights. Business information modeling provides a technology-agnostic view of information that will be used for information management and planning. There are few specialized approaches that our team applied for developing the flow cytometry models. The first step is business blueprinting, which provided a visual representation of business capabilities by triangulating people, processes and technology around critical business information entities – 360 degree view of cytometry information. The second step is classification and standardization of business data to enable collaboration and interoperability. As an example, the day-to-day workflows in discovery space can be very different than workflows in the clinical or CAR-T space, all of which are heavily relying on cytometry data to accelerate drug development. The final step is semantic modeling which provides context and meaning to data, which then makes it human and machine-readable data thus enabling discovery of facts & relationships through inferencing. Our team developed a comprehensive, industry-driven Information model for flow cytometry that spans across the drug development continuum, from discovery to translational and clinical research. We identified the need for granularity, and developed sub-models that focused on biological assays, biospecimen, antibody panels, instruments, results, and analysis methods, which in turn gave us in-depth insights into the patient-centric laboratory workflows. Extending our information-centric approach, we aim to create a flow cytometry-specific data fabric that connects disparate sources of data by leveraging contextual metadata. Additionally, by building relationships between siloed information, our goal is to inform business decisions through scientific insights from semantic cytometry information ecosystem.

37

894955

## The Ecology Of Microbial Communities – How They Can Be Synchronized And Stabilized

Susann Müller<sup>1</sup>, Shuang Li<sup>2</sup>, Zishu Liu<sup>3</sup>

<sup>1</sup> Helmholtz Center for Environmental Research, <sup>2</sup> Helmholtz Centre for Environmental Research – UFZ, <sup>3</sup> Zhejiang University

Microbiomes are found in every corner of the earth and are also an essential part of human life in many ways. Current comprehensive microbiome analyses that assess the composition and functions of the microbiome are mainly based on sequencing technologies that are still far from becoming routine analyses. With the growing demand for rapid assessment of microbiome assembly and monitoring of its dynamic behavior at high resolution, alternative high-throughput methods such as flow cytometry are coming into focus (Molecular Aspects of Medicine (2018), 59, 123-134) to characterize single-cell attributes with high acuity over time (Nature Protocols, 2020, 15, 2788-2812). The workflow's immanent ability to support high temporal sample densities below bacterial generation times provides new insight into the ecology of microbiomes and may also provide access to community control for microbiome based health management (Microbiomes (2020) 8/13). Currently, the control of microbiomes in artificial and natural environments aims to create a niche defined by boundaries to strengthen and maintain a microbiome. However, in isolated environments when microbiomes are not influenced by immigration of new community members, unlike in natural ecosystems, a high degree of variability in community structures has been observed, both between parallel microbiomes and within each microbiome over time (Environmental Microbiology (2019), 21/1, 164-181). Macroecology, which offers a variety of concepts to study population dynamics, such as the concept of metacommunity, has been used to follow up on these findings. We are now able to synchronize and stabilize microbiomes over long periods of time to overcome the known stochastic structural fluctuations in the microbiome.



39

894940

## High-Throughput Image-Activated Cell Sorting by Mitochondrial Relocation

Maik Herbig<sup>1</sup>, Jeffrey Harmon<sup>1</sup>, Justin Findinier<sup>1</sup>, Natsumi Tiffany Ishii<sup>1</sup>, Akihiro Isozaki<sup>1</sup>, Arthur R. Grossman<sup>1</sup>, Keisuke Goda<sup>1</sup>

<sup>1</sup> The University of Tokyo

Various metabolic functions and signaling in unicellular organisms are associated with organelle positioning. The microalga *Chlamydomonas reinhardtii* is no exception as it repositions its mitochondria depending on the availability of inorganic carbon (Ci). Typically, the mitochondria are positioned randomly in the cytoplasm, but will relocate towards the cell periphery when Ci becomes scarce. The repositioning of the mitochondria has been associated with the carbon-concentrating mechanism (CCM), an essential mechanism for the uptake of carbon against a concentration gradient, but the relationship between the CCM and mitochondrial positioning is still not well understood. A better understanding of this relationship could be achieved by examining rare mutant cells that do not redistribute their mitochondria in carbon scarce conditions. However, a method to identify such rare mutants and isolate them in sufficient numbers is currently missing. Here, we report sorting of *C. reinhardtii* cells based on the distribution of mitochondria using an intelligent image-activated cell sorting system. We found that a mutation to the *CIA5* gene reliably prevents the relocation of mitochondria and used this mutant to simulate the phenotype of the rare mutant cells. We imaged both wild type (WT) cells and *cia5* mutants using our imaging flow cytometer and trained a convolutional neural net (CNN) to distinguish the two mitochondrial distributions. Next, we employed the CNN for image-activated sorting to isolate *cia5* mutants. For proof-of-principle, we mixed WT cells and *cia5* mutants in a 1:1 and 1: 19 ratio (WT: *cia5*) and sorted for the *cia5* mutants at a throughput of 180 events per second, which is 1-2 orders of magnitude faster than robotic pipetting combined with optical microscopy. We achieved an enrichment of the *cia5* mutant population from 50% to 80% and from 5% to 57% for the 1:1 and 1:19 experiments respectively. These results show the potential of intelligent image-activated cell sorting to study genotype-phenotype relations of rare mutants existing in large cell populations.

40

894941

## Resolution-Enhanced Imaging Flow Cytometry by Deep Learning

Maik Herbig<sup>1</sup>, Kangrui Huang<sup>1</sup>, Hiroki Matsumura<sup>1</sup>, Yaqi Zhao<sup>1</sup>, Dan Yuan<sup>1</sup>, Yohei Mineharu<sup>1</sup>, Jeffrey Harmon<sup>1</sup>, Justin Findinier<sup>1</sup>, Mai Yamagishi<sup>1</sup>, Shinsuke Ohnuki<sup>1</sup>, Nao Nitta<sup>1</sup>, Arthur R. Grossman<sup>1</sup>, Yoshikazu Ohya<sup>1</sup>, Hideharu Mikami<sup>1</sup>, Akihiro Isozaki<sup>1</sup>, Keisuke Goda<sup>1</sup>

<sup>1</sup>The University of Tokyo

Imaging flow cytometry is a promising tool for diverse biomedical applications by virtue of its high-throughput imaging capability. Unfortunately, there remains a challenge posed by the fundamental trade-off between throughput, sensitivity, and spatial resolution. In this presentation, we report deep-learning-enhanced imaging flow cytometry (dIFC) that circumvents this trade-off by employing an image restoration algorithm on a high-throughput imaging flow cytometry platform. Specifically, we used a virtual-freezing fluorescence imaging (VFFI) flow cytometer as a platform. VFFI flow cytometry enables higher throughput without sacrificing sensitivity and spatial resolution. The key component of dIFC is a high-resolution (HR) image generator, that synthesizes “virtual” high-resolution images from the corresponding low-resolution images obtained by a low-magnification lens (10×/0.4-NA). A low-magnification lens is advantageous for imaging flow cytometers over a high-magnification lens as it allows for capturing blur-free images of cells flowing at higher speed, which permits higher-throughput. The HR image generator was developed using an architecture consisting of two generative adversarial networks (GANs). By combining the trained generator and imaging flow cytometry, dIFC was developed as a method. We experimentally demonstrated dIFC using three types of cells: microalgal cells, microbial cells, and mammalian cells. Specifically, we showed high similarities of images synthesized by the HR image generator to the corresponding images obtained with a high-magnification lens (40×/0.95-NA) using *Chlamydomonas reinhardtii* cell images, *Saccharomyces cerevisiae* (budding yeast) cell images, and fluorescence in situ hybridization (FISH) images of Jurkat cells. Furthermore, we used dIFC to show improvements in the accuracy of FISH-spot counting and the neck-width measurement of budding yeast cells. These results allow statistical analysis of cells with high-dimensional spatial information.

41

898119

## The Use of Deep Learning to Score the Imaging Flow Cytometry-Based In Vitro Micronucleus Assay

Matthew Rodrigues<sup>1</sup>, Yang Li<sup>1</sup>, Vidya Venkatachalam<sup>1</sup>

<sup>1</sup> Luminex Corporation,

The in vitro micronucleus (MN) assay is a well-established method for the quantification of DNA damage, and is essential to numerous fields of study, including genetic toxicology and radiation biodosimetry. The MN assay is typically scored by manual microscopy, but results obtained from manual scoring can lack accuracy and precision due to scorer fatigue and variability. To overcome these limitations, we previously applied imaging flow cytometry (IFC) to develop a rapid and automated MN assay based on high-throughput image capture and feature-based image analysis. However, the analysis strategy relied on the use of morphological features, and required rigorous optimization and a high level of user expertise, limiting widespread adoption of this technique. Recently, we developed a deep-learning method based on convolutional neural networks to identify and score all key events in the MN assay using imagery acquired by IFC. In this study, we show how this deep learning approach can be used to obtain results that are comparable to manual microscopy, and outperforms other image analysis techniques, facilitating full automation of the MN assay.

42

897017

## Uncovering the Pathogenesis Of Microvascular Thrombosis In COVID-19 Via High-Throughput Microscopy On A Chip

Keisuke Goda, Yuqi Zhou<sup>1</sup>, Masako Nishikawa<sup>1</sup>, Hiroshi Kanno<sup>1</sup>

<sup>1</sup> The University of Tokyo

Global case reports of the COVID-19 pandemic have shown that thrombosis is one of the primary factors for the severity and mortality of COVID-19. In fact, COVID-19 autopsy reports have identified widespread thrombotic microangiopathy characterized by extensive diffuse microthrombi within peripheral capillaries and arterioles of different organs. However, the underlying process of COVID-19-associated microvascular thrombosis remains elusive due to the lack of tools to statistically examine the initiation of microthrombus formation in a quantitative

manner. For example, clinical laboratory tests such as D-dimer and fibrinogen tests do not fully reflect microvascular thrombotic events. Also, flow cytometry does not provide spatial resolution to fully differentiate single platelets and various types of platelet aggregates. For this reason, statistical morphometric understanding of platelet aggregates has been inaccessible and hence overlooked to date. Here we study the pathogenesis of microvascular thrombosis in COVID-19 by high-throughput on-chip microscopy of circulating platelet aggregates in the blood of COVID-19 patients (n = 110). This study consists of four steps: (i) blood draw from COVID-19 patients; (ii) sample preparation by isolating platelets and platelet aggregates using a density-gradient method; (iii) acquiring bright-field images of a large population (n = 25,000) of single platelets and platelet aggregates in blood samples; (iv) digital image processing and statistical analysis. In addition to the acquisition and analysis of the images, we also acquired clinical laboratory test results from the patients and investigated potential correlations between the statistical morphometric results and the severity, mortality, and platelet functional assessment. Furthermore, we measured platelet aggregates in the blood of non-COVID-19 thrombosis patients and performed image-based classification of them for revealing the unique features of microvascular thrombosis in COVID-19. Surprisingly, our analysis of the image data shows that nearly 90% of all COVID-19 patients had abnormally high levels of platelet aggregates. Specifically, it shows a strong positive correlation between the platelet aggregation concentration and COVID-19 severity and mortality. In addition, the positive correlation between platelet aggregation concentration and the degree of vascular endothelial dysfunction indicators is consistent with the currently accepted theory of the pathophysiological mechanisms of COVID-19. The image-based classification between COVID-19 and thrombosis patients reached an average testing accuracy of 70.3%, in which the most important feature was found to be the width of the distribution of the objective area. Our findings suggest that measuring the concentration of circulating platelet aggregates is a potentially effective approach to evaluating the risk of microvascular thrombosis.

# CYTO 2022 ABSTRACTS

43

898422

## Comprehensive Flow Cytometry Based Assessment of Anti-SARS-CoV-2 Antibody Isotypes in Vaccinated Control and Cancer Samples

Kamala Tyagarajan<sup>1</sup>, Ashikun Nabi<sup>1</sup>, Tate Sessler<sup>1</sup>, Fabrizio Bonelli<sup>2</sup>, Bianca Oresta<sup>1</sup>, Nicola Corriglio<sup>1</sup>

<sup>1</sup> Luminex Corporation, <sup>2</sup> DiaSorin SpA

The long-lived duration and severity of the COVID-19 pandemic has resulted in intense and continued research in methods to study immune response mechanisms at both antibody and cellular levels. A deeper level of understanding of the role of antibody isotypes to severe acute respiratory syndrome coronavirus 2 (SARS-CoV-2) is playing a critical role in development of new vaccines and their ability to boost immune response in vulnerable subpopulations. However, few methods allow for the assessment of multiple antibody isotypes on the same detection platform. Here we present a comprehensive study of antibody isotypes in samples from naturally infected and SARS-CoV-2 naive normal health care workers (HCWs) and individuals with cancer using flow cytometry. Samples were analyzed with a sensitive flow cytometry based multiplexed bead assay, Guava<sup>®</sup> SARS-CoV-2 Multi-Antigen Antibody Kit assessing IgG, IgM, and IgA antibody isotypes against multiple SARS-CoV-2 antigens, namely nucleocapsid protein, S1 subunit of spike protein and the receptor-binding domain (RBD) of the spike protein in parallel. Serum from 50 health care workers and 22 individuals who had cancer were assessed at time points before and after vaccination with mRNA vaccines. The sample set included individuals who previously had natural infection as well as those that were COVID-19 infection naïve. Results demonstrate development of strong antibody responses in normal HCWs with or without previous infection and most cancer patients who had previous COVID-19 infection with the detection of all three antibody isotypes, IgG, IgM, and IgA against the three antigens tested. Individuals who had previous infection showed a clear presence of antibodies against the nucleocapsid antigen with response absent in COVID-19 naive samples. Results also show significant boosting of predominantly IgG and IgA isotypic response against RBD and S1 proteins with vaccination in these individuals. Samples from infection naïve individuals with cancer, several of whom were on anti-CD20 or B cell directed therapy, showed little or no response to vaccines. The comprehensive screening showed absence of any IgG, IgM,

or IgA antibody isotypes tested for these samples. The results demonstrate the importance of comprehensive antibody isotype profiling in SARS-CoV-2 serology for the development of new vaccination and booster strategies, especially as we evaluate immunocompromised and immunosuppressed individuals and time from treatment for best response to vaccines. For Research Use Only. Not for use in diagnostic procedures.

44

898474

## Spike-Specific Cellular and Humoral Immunity After BNT162b2 Mrna Vaccination In Older Adults: Benefits And Constrains Of “Booster” Vaccinations

Axel Ronald Schulz<sup>1\*</sup>, Addi J. Romero-Olmedo<sup>2\*</sup>, Svenja Hochstätter<sup>3</sup>, Sebastian Ferrara<sup>1</sup>, Dennis Das Gupta<sup>2</sup>, Iiris Virta<sup>1</sup>, Heike Hirseland<sup>1</sup>, Daniel Staudenraus<sup>2</sup>, Bärbel Camara<sup>2</sup>, Carina Münch<sup>3</sup>, Véronique Hefter<sup>3</sup>, Siddhesh Sapre<sup>3</sup>, Christian Keller<sup>3#</sup>, Michael Lohoff<sup>2#</sup> and Henrik E. Mei<sup>1#</sup>

<sup>1</sup> German Rheumatism Research Center, Berlin, Germany

<sup>2</sup> Institute of Medical Microbiology and Hospital Hygiene, Philipps-University Marburg, Marburg, Germany

<sup>3</sup> Institute of Virology, Philipps-University, Marburg, Germany

\*,# equal contribution of first and senior authors

Vaccination of older adults against SARS-CoV-2 significantly reduces the risk of severe courses of COVID-19. Here, we used single-cell flow and mass cytometry to analyze spike-specific CD4 T cells, which were detected and characterized by the co-expression of CD40L and IFN $\gamma$  (and/or other cytokines) after overnight stimulation with SARS-CoV-2 spike peptide pool. Longitudinal analyses were conducted in aged (>80 years) and younger adults (20–53 years) after receiving two or more doses of BNT162b2 mRNA vaccine; unvaccinated senior adults who had recovered from SARS-CoV-2 infection were included for comparison. Our results show the coordinated establishment of SARS-CoV-2-spike-specific humoral and CD4 T-cell immunity in the course of primary and secondary vaccination in the bulk of young and older vaccinees as well as in the recovered participants. However, 10% (n=5) of the older, but none of the young vaccinees, failed to establish significant T-cell and humoral immunity after two doses of BNT162b2. Importantly, a third “booster” vaccination with BNT162b2 induced antibody and T-cell responses in these low-/non-responders similar to those of responders after two vaccinations, suggesting that unresponsiveness in older adults is not fixed, and can

# CYTO 2022 ABSTRACTS

be overcome by repeated vaccination. Moreover, older adults who previously responded to two doses of BNT162b2, also responded to a 3rd vaccination, which temporarily restored declining humoral and cellular immunity. Interestingly, while spike-specific CD4 T cells showed similar rates of decline after the 3rd vaccination compared to the 2nd vaccination, specific antibody levels showed a slower decline, likely reflecting the establishment of longer-term humoral immunity. In sum, waning especially of specific T-cell immunity is not only observed after the 2nd but also after the 3rd vaccination with potential implications regarding the T-cell-mediated protection against the Omicron variant. Finally, an in-depth analysis of spike-specific CD4 T cells in recovered and vaccinated individuals by mass cytometry revealed combinatorial expression profiles of 14 cytokines. Boolean analysis in recovered patients identified a predominant Th1 response characterized by cells expressing combinations of TNF, IFN $\gamma$ , GM-CSF and/or IL-21. Notably, a BNT162b2 vaccination 7 months after recovery induced additional Th2 cells and hybrid Th1/2 cells, expressing combinations of IL-4, IL-5, and IL-13, along with a combination of Th1 cytokines, respectively. This indicates a multifaceted T-cell response with a broadened effector range after BNT162b2 vaccination in a previously recovered individual. Altogether, we here combined sensitive antigen-specific T-cell detection with high dimensional cytometry and provide insight in the specifics of immune responsiveness to SARS-CoV-2 vaccination and infection in senior adults, which may contribute to adjust vaccination schemes and designs for this vulnerable group in the current pandemic.

**45**  
898542

## **An Optimized Flow Cytometry Protocol for Simultaneous Detection of T Cell Activation Induced Markers and Intracellular Cytokines: Application To SARS-CoV2 Vaccinated Individuals**

Scott Bornheimer<sup>1</sup>, Gianluca Rotta<sup>1</sup>, Tiziana Altosole<sup>2</sup>, Daniela Fenoglio<sup>2</sup>

<sup>1</sup> BD Biosciences, <sup>2</sup> University of Genoa

Antigen (Ag)-specific T cell analysis is an important step for investigation of cellular immunity in many settings, such as infectious diseases, cancer and vaccines. In this context, multiparameter flow cytometry has advantages in studying

both the rarity and heterogeneity of these elements, and the expression of activation-induced markers (AIM) following antigen exposure facilitated the study of MHC unrestricted antigen specific T cells. In parallel, assessing the cytokine profile of these cells supports a more comprehensive description of the ongoing immune response. Here, a method and flow cytometry panel were optimized to combine the detection of activated CD4+ and CD8+ T cells in a TCR-dependent manner with the evaluation of cytokine production by intracellular staining, without affecting the positivity of activation markers. In particular, the expression of CD134 (OX40) and CD69 have been tested in conjunction with intracellular (ic) CD137 (4-1BB) to detect SARS-CoV2 Spike protein-specific activated T cells from vaccinated donors. In our setting, following antigen stimulation with Spike peptide pool, with anti-CD28 antibody used as co-stimulus, a clear CD137bright CD3dim/positive population was augmented in PBMCs from healthy vaccinated donors, reaching up to 0.23% of total CD4+ cells and up to 1.3% of total CD8+ cells (data were normalized by subtracting background from unstimulated samples treated with anti-CD28 only). We verified that surface or intracellular CD134 staining did not correlate with the CD137bright expression induced by antigen stimulation. Conversely, a correlation was observed for intracellular CD69 which was co-expressed with ic-CD137bright in both CD4+ and CD8+ activated lymphocytes. Following Spike stimulation, 80% of activated CD4+ and 62% of activated CD8+ cells were secreting Th1 cytokines (any of IFN $\gamma$  or TNF $\alpha$  or IL-2). Notably, these cytokine-producing T cells were positive for intracellular CD69 staining, further confirming the capacity of this marker to identify functionally responsive antigen-specific T cells, whereas these cells were largely negative or poorly positive for CD134 expression. In parallel with method optimization, a comprehensive 12-color flow cytometry panel was developed to detect live, activated CD4+ and CD8+ T cells expressing ic-CD137bright and ic-CD69, their cytokine producing subset cells secreting IFN $\gamma$  or TNF $\alpha$  or IL-2, the T cell maturation curve by means of CD45RA and CCR7 markers, in addition to the follicular helper T cell subpopulation defined as CD4+ CXCR5+ CD45RA- events. In conclusion, we optimized a method and flow cytometry panel combining assessment of activation induced markers and intracellular cytokines, demonstrated in the case of SARS-CoV2 reactive T-cells, that will be useful for measuring of TCR stimulation-dependent activation of CD4+ and CD8+ T cells.

46

## High-parameter flow cytometric analysis of immune responses to SARS-CoV-2 mRNA vaccines in human lymph nodes

Michela Locci, Ph.D. - Assistant Professor of Microbiology, Department of Microbiology, Perelman School of Medicine, University of Pennsylvania

Vaccine-mediated immunity often relies on the generation of protective antibodies and memory B cells, which commonly stem from germinal center (GC) reactions. An in-depth comparison of the GC responses elicited by SARS-CoV-2 mRNA vaccines in healthy and immunocompromised individuals has not yet been performed due to the challenge of directly probing human lymph nodes. In this study, through a fine-needle-aspiration-based approach, we profiled the immune responses to SARS-CoV-2 mRNA vaccines in lymph nodes of healthy individuals and kidney transplant (KTX) recipients. We found that, unlike healthy subjects, KTX recipients presented deeply blunted SARS-CoV-2-specific GC B cell responses coupled with severely hindered T follicular helper cells, SARS-CoV-2 receptor-binding-domain-specific memory B cells and neutralizing antibodies. KTX recipients also displayed reduced SARS-CoV-2-specific CD4 and CD8 T cell frequencies. Broadly, these data indicate impaired GC-derived immunity in immunocompromised individuals, and suggest a GC-origin for certain humoral and memory B cell responses following mRNA vaccination.

47

## Evaluating Correlates and Mechanisms of Protection against Tuberculosis following Intravenous BCG Immunization in Nonhuman Primates

Patricia Darrah<sup>1</sup>

<sup>1</sup>National Institutes of Health

*Mycobacterium tuberculosis* (Mtb) is a leading cause of death from infection worldwide. The only available vaccine, BCG, is given intradermally (ID) and has variable efficacy against pulmonary tuberculosis (TB), the major cause of mortality and disease transmission. We recently showed that IV BCG vaccination in nonhuman primates (NHP) elicited greater antigen specific Th1 CD4 and CD8 T cell responses in blood, spleen, bronchoalveolar lavage (BAL), lung lymph nodes and lung tissue than BCG administered by ID or aerosol routes. When animals were

challenged six months after BCG immunization, 9 of 10 NHP that received IV BCG were highly protected (<50 Mtb CFU), with 6 animals showing no detectable infection as determined by PET CT imaging, Mtb growth, pathology, granuloma formation or induction of primary T cell responses to Mtb-specific antigens. Based on this high level of protection, we were not able to identify immune correlates of protection. To address this, we performed a dose-ranging study in which 34 NHP were immunized with 105-107.5 CFU IV BCG to elicit a range of immune responses and protection. After TB challenge, 17 of 34 animals across a range of doses had no evidence of Mtb infection (i.e., sterile protection). Immune responses were measured longitudinally in the bronchoalveolar lavage (BAL) and blood. The dose of IV BCG immunization itself was strongly correlated with immune responses (cellular and humoral) and protection; thus, either innate or adaptive responses that correlate with the administered dose were potential correlates. We undertook a multi-variate computational analysis, controlling for IV BCG dose, that incorporated all immune and outcome parameters measured in blood or BAL. These analyses revealed multiple T cell and NK cell features that in combination predicted protection. Of note, features were more easily detectable in BAL compared to blood. These data highlight the importance of assessing immune responses at the site of infection for correlates and provide insight into potential mechanisms of protection. To investigate whether IV BCG-induced CD4 and CD8 T cells are mechanistic correlates of protection, we undertook two NHP studies in which IV BCG-immunized animals were depleted of CD4 or CD8 T cells 1 month prior to Mtb challenge. At 8 weeks post-challenge, IV BCG immunized animals that received anti-CD4 antibodies had significantly worse TB disease compared to un-depleted animals, demonstrating that CD4 T cells are required for protection. Preliminary results also suggest a contribution of CD8a-expressing cells in IV BCG-mediated protection against TB. Together, these results have implications for vaccine delivery, dose, and formulation, as well as clinical development for vaccines against TB.

Funding: NIH Intramural Research Program and BMGF

# CYTO 2022 ABSTRACTS

48

## Flow Cytometry Enabling Immunotherapy and Vaccine Clinical Trials

### Flow cytometry enabling vaccine development for major global pathogens

Steven De Rosa<sup>1</sup>

<sup>1</sup>University of Washington

Highly effective vaccines for several infectious diseases of global impact, including HIV, tuberculosis and malaria, have not yet been developed. Because of the unique challenges posed by each of these pathogens, novel vaccine approaches that induce a broad immunogenicity profile including both cellular and humoral immunity are likely needed. Therefore, as compared to most traditional licensed vaccines, sophisticated methods to measure and characterize the induced responses are critical to the clinical developmental pathway as candidates progress through the incremental stages of clinical testing and ultimately to identify immune correlates of vaccine-induced protection. Flow cytometry is used for measurement of both antigen-specific T and B cells induced by vaccination. With the emergence of COVID-19 and the urgency for rapid development and testing of novel vaccines, the experience gained from prior research on other global pathogens enabled quick development and validation of flow cytometric assays for SARS-CoV-2 vaccine assessment. Of particular importance was the documentation of the Th1/Th2 balance, since a Th2 bias was considered a safety concern. Our laboratory validated a 27-color intracellular cytokine staining assay with guidance from the FDA for potential use in Phase 3 clinical trials. The validation process highlights the special considerations for a complex flow cytometric-based functional assay as compared to more typical analytical assays submitted for FDA evaluation. Although our assay has not yet been used to inform the licensure of new vaccines, there are situations where such an assay may provide critical supporting information, such as by bridging immunogenicity data between different population groups (e.g., pediatric, pregnant women, immunocompromised) to reduce the need for large efficacy trials. We have also used this assay to characterize the cellular immunogenicity in early phase studies for several of the SARS-CoV-2 vaccine candidates, as well as in pathogenesis studies. The parameters of interest include several pre-specified cytokines and cytokine combinations that are validated and exploratory unbiased clustering results

across all the functional and phenotyping markers in the assay. This presentation will focus on insights regarding the experimental approach to validation and use of flow cytometry in the context of Phase 1 to 3 vaccine clinical trials.

49

893673

## Considerations for A Smooth Flow from Cell Sorting Into Genomics

Claudia Bispo Gelo de la Cruz<sup>1</sup>, Lola Martinez<sup>2</sup>, Matthew Cochran<sup>3</sup>

<sup>1</sup> UCSF <sup>2</sup> Spanish National Cancer Research Center

<sup>3</sup> University of Rochester

Intended Audience: SRL personnel, especially those working in an environment developing a relationship with a local Genomics resource; researchers considering using both cell sorting and genomic techniques. (25-50 attendees) Problem Focus: Genomic techniques, including single-cell omics, have become significantly more prevalent and sought after as the technologies develop, options expand and costs drop. As such, the need for cell sorting and the generation of purified and/or highly specific populations, to feed into these genomic technologies is increasing. This rapidly changing landscape has created the need for improved processes and collaboration between those of us on the flow cytometry side and our colleagues on the genomic research side. With no existing consensus on how best to tackle these new challenges this workshop will focus on gathering information towards establishing best practices in the future. Key Questions: What key information does the cell sorting facility need from the user, and the genomics resource for a successful sort? What are the key "receipts" the genomics team needs from us? Are there key aspects of the sort that can be standardized and monitored for this work, and are there aspects that have to be optimized independently? Are there established methods/procedures currently in use that can be shared? Description: This workshop will be a highly interactive session designed to collect experiences and knowledge around this developing field.

# CYTO 2022 ABSTRACTS

50

893601

## Can and If So How, Automation And Machine Learning Assist Timely Diagnosis And Prognosis In Everyday Clinical Routine?

Attila Tarnok<sup>1</sup>, Kamila Czechowska<sup>2</sup>, Ryan Brinkman<sup>3</sup>, Wolfgang Kern<sup>4</sup>

<sup>1</sup> University of Leipzig, <sup>2</sup> Metafora Biosystems, <sup>3</sup> University of British Columbia, <sup>4</sup> Munich Leukemia Laboratory (MLL)

There is quite a number of tools allowing for mining of complex flow cytometric data alone or in combination with patient's meta-data to describe retrospectively which parameter combinations are predictive. However, we cannot use these sets so far prospectively and implement it into everyday clinical use. The main reasons are lack of harmonized approaches towards samples testing, analysis and results interpretation. Moreover, there is a limited access to diseased sample databases and that disables development of powerful and robust diagnostic AI based tools. Despite the fact there is an increasing number of available algorithms that attempt to solve multi-dimensional data complexity problem, diagnostic assays data are not infrequently analyzed manually by laboratory analysts bringing significant bias in final results that can neither be controlled nor corrected. For many flow cytometrists it is not always clear which algorithms should be used for given data set as some degree of coding skills or advanced biostatistical knowledge is required. Despite the fact that more and more flow cytometric software developers implement automated data processing algorithms (clustering, cleaning, automated gating or annotations), these features are not commonly used as the solutions are not comprehensive, not intuitive or has user unfriendly interface. The consequence is that the analysts cannot take the full advantage of these software or even make bad choices and that impact the final result quality. 1. What are current pain points in the manual data analysis workflow for clinical flow cytometry data? (Time for manual analysis? Inter-operator variability? Lack of trust of automated results?) 2. What tools exist to address these and what are the challenges in their application individually and in aggregate and how could these be addressed? (Too high cost to research, evaluate and implement an automated approach?) 3. What additional advantages could automate approaches provide that cannot be addressed through manual analysis? Could we use as a start routine diagnostic test results along with augmented intelligence in the meantime to build a robust tool that would allow us to predict the course of the disease?

Workshop participants are especially those whose day-to-day professional activities would profit from availability of tools for automated data analysis: translational as well as CROs, Pharma scientists; haematopathologists, and laboratory technicians. Data scientists and software developers/manufacturers would provide great perspective and bring the know-how to the discussion. We plan to post a series of questions on the social media (Facebook and LinkedIn) every week prior as well as during congress to attract more participants and lead more focused live session at the workshop.

51

893614

## Establishing a Biosafety Plan in an SRL

Avrill Aspland<sup>1</sup>, Jessica Back<sup>2</sup>, Lauren Nettenstrom<sup>3</sup>, Lola Martinez<sup>4</sup>, Kristen M. Reifel

<sup>1</sup> University of Sydney and Centenary Institute, <sup>2</sup> Beth Israel Deaconess Medical Center, <sup>3</sup> Fluidigm Canada Inc., <sup>4</sup> Spanish National Cancer Research Center

Intended Audience - SRL managers and staff (25-50 attendees)  
Problem Focus/Key Questions: A biosafety plan is essential for establishing appropriate laboratory safety practices in a shared resource laboratory (SRL); however, writing a biosafety plan can be a daunting task for SRL staff as the variety of pathogens that come through these facilities may be highly diverse and change over time. Having a plan that can adapt to this variety provides a framework for addressing safety concerns and educating both personnel and users on appropriate practices. A good biosafety plan will contain the essential information for the use of biological samples on specific instrumentation, their associated risks, and the steps that should be taken to mitigate these risks. This workshop will focus on the basic structure of a biosafety plan, identifying readily available resources for essential information to be included, developing a robust relationship with health and safety personnel at your institution and will provide guidance for establishing a dynamic, living biosafety plan. We will also discuss some of the shortfalls and sticking points attendees have experienced in writing their own Biosafety Plans. Key discussion points may include: How did you start your biosafety plan? How do you keep your biosafety plan up to date? What was/is the most difficult part of putting together a biosafety plan? Format/ Agenda - The format will include slides with general guidelines and resources, interactive participation, and live polling. A pre-conference survey will be distributed asking CYTO attendees to describe issues they have encountered with writing a biosafety

# CYTO 2022 ABSTRACTS

plan and identify areas where ISAC could provide additional support. Any common shortfalls or sticking points identified in the survey will be incorporated into the workshop discussion by the facilitators. 15-20 minute guided discussion with audience participation on the basic structure of a biosafety plan, including information gathered from the pre-conference survey. 20-25 minute small-group breakout to discuss sticking points attendees may be dealing with and input from peers on methods for resolving these issues. 10-15 minute presentation of available resources for assisting with this process and polling on future needs for ISAC educational content identified by attendees.

**52**  
892268

## **Consensus Best Practices for User Consultations in an SRL**

Amy Graham<sup>1</sup>, Kewal Asosingh<sup>1</sup>, Michael Gregory<sup>2</sup>

<sup>1</sup> Cleveland Clinic, <sup>2</sup> Cleveland Clinic Florida

The goal of this workshop is to help determine the ISAC SRL community consensus for the Best Practices in User Consultation. We will build off the 2021 publication in Cytometry Part A (<https://onlinelibrary.wiley.com/doi/10.1002/cyto.a.24519>) and receive comments and input from a diverse, global membership. We will identify topics to discuss further and then break into smaller groups to do so. Moderators of each smaller group will then present the discussion findings to the larger group for comment and incorporation into the eventual best practices. This workshop will form the basis for a Best Practices publication and will help the author group recruit more members to cover as many perspectives as possible. It will also become a proof-of-concept, providing a learning experience for how ISAC can facilitate best practice development on other topics going forward. Problem Focus/Key Questions What are the best practices for SRLs when consulting with users? What must be discussed/communicated with the users, and what is the optimal way to do this? Are there differences in these Best Practices across geographic and institutional ranges? If so, what are they? How can we reach a consensus among the ISAC SRL community regarding a final Best Practices for SRL User Consideration? Format/Agenda Quick Introduction - what are Best Practices and why are they important? (5 min) Short presentation - Consideration for User Consultations paper published in Cytometry Part A (<https://onlinelibrary.wiley.com/doi/10.1002/cyto.a.24519>). This presentation will provide the context and structure for the subsequent debate. (10-15

min) Group Discussion - Identification of subgroup topics that need to be addressed in order to expand the above paper into an ISAC-community consensus document that covers a broader range of SRL types and locations. (5-10 min) Subgroup Discussion - Break into small groups to address specific areas identified above. Each subgroup will be governed by a facilitator/moderator. (20 min) Conclusion and Summary - summarize/share subgroup discussions and identify future actions. (10 min) Desired Outcome Identification of the differences in the way geographically and institutionally diverse SRLs handle user consultations. Formulation of a consensus on User Consultation Best Practices (beginnings of one, at least). Future directions to establish these User Consultation Best Practices. Identify members for inclusion in the author group and advertisement of (future) Best Practices development. Other facilitators will include: Alice Baiyana, Uganda Utara Chakraborty, India Karen Hogg, UK Charlotte Christie Petersen, Denmark

**53**  
893665

## **Extracellular vesicle measurement by flow cytometry: Practical examples of MIFlowCyt-EV**

Edwin van der Pol<sup>1</sup>, Estefanía Lozano-Andrés<sup>2</sup>, John Nolan<sup>3</sup>, Vera Tang

<sup>1</sup> Amsterdam University Medical Centers, <sup>2</sup> Utrecht University, <sup>3</sup> Cellarcus Biosciences

Organizer(s)/Facilitator(s): Edwin van der Pol, Vera Tang, John Tigges, Estefania Lozano Andres, John Nolan Intended Audience: SRL members, members of the scientific community, flow cytometry vendors Problem Focus/Key Questions: There is a growing interest in the characterization of extracellular vesicles (EVs) and other submicrometer particles. To improve the standardization of EV measurements by flow cytometry, scientists from three societies, namely the International Society for Extracellular Vesicles (ISEV), the International Society for Advancement of Cytometry (ISAC), and the International Society on Thrombosis and Haemostasis (ISTH), joined forces and initiated the EV flow cytometry working group. Two years ago, the working group published a standard framework (MIFlowCyt-EV) for conducting and reporting EV analyses by flow cytometry. Meanwhile, scientists started using the MIFlowCyt-EV framework, which resulted in the first publications with standardized flow cytometry data of EVs. The goal of this workshop is to give a brief introduction about EV flow



# CYTO 2022 ABSTRACTS

cytometry, followed by practical examples, with discussion, of calibrations and assay controls by interested Parallel and Poster session presenters. Presenters are encouraged to share a set of “what’s wrong with this data” slides, and let the audience solve the puzzle. Key questions involve: 1. What is the impact of calibrating to EV data and research? 2. Which issues can you encounter when calibrating and how can these issues be solved? 3. How can you confirm whether the measured signals are originating from EVs? 4. Which issues can you encounter when performing assay controls and how can these issues be solved? Format/Agenda: 10 min – Introduction to EV flow cytometry, the importance of calibration and assay controls, and available resources 40 min – Short presentations by abstract presenters (Parallel and Poster) highlighting calibration and control elements of their study, MIFlowCyt-EV reporting, and erroneous results 10 min – Wrap-up, announcements, and future activities Desired Outcome:

- Understanding key problems in the standardization of flow cytometry measurements of EVs and submicrometer particles
- Developing experience with calibrations and assay controls to standardize flow cytometry measurements of EVs and submicrometer particles
- Practical, real-world examples of MIFlowCyt-EV framework in planning, carrying out, and reporting future small particle experiments.
- Understanding the need for standard reporting for EV and submicrometer particle research

---

**55**

**CYTO Women**

## **Stress Management for Scientists**

Heather Hersh<sup>1</sup>

<sup>1</sup>Thrive Well-being

Developing a successful career as a scientist in fields like cytometry can be stressful. In recent years, normal work-related stress has been exacerbated due to the changes, losses, and uncertainty brought by the COVID-19 pandemic. Indeed, levels of depression, anxiety, and stress were quite high and rising before the pandemic, and they are currently at all-time heights.

This presentation will help you better understand how you experience stress and how you personally know when you are stressed. My talk will teach you how stress impacts your body. We will focus on how stress engages your Sympathetic Nervous System (or flight-flight-freeze response) and how you can counter this by learning how to better engage your Parasympathetic Nervous System to be calmer and more grounded in your everyday life. Although stress is not something we can avoid, I will provide powerful coping strategies and tools to manage it so that your functioning, productivity, and health (physical and emotional) are minimally impacted.

---

**56**

## **Understanding the dimension of Biasness**

Mónica Guzmán, Ph.D.<sup>1</sup>

<sup>1</sup>Weill Cornell Medical College

There are everyday barriers that women and minoritized populations face in the fields of science, technology, engineering, and mathematics (STEM). To be able to overcome such barriers we need to understand them. We will discuss key definitions in diversity, equity, and inclusion, and discuss the different types of biases that often affect our perspectives even without our complete awareness. In addition, we will examine steps to reduce bias.

# Combining flow cytometry and real time cell analysis for better CAR-T potency evaluation

Commercial Tutorial  
Tuesday, June 7 from 12:00 - 1:00 PM  
Room 120C

Presented by Garret Guenther, Ph.D.  
Agilent Technologies

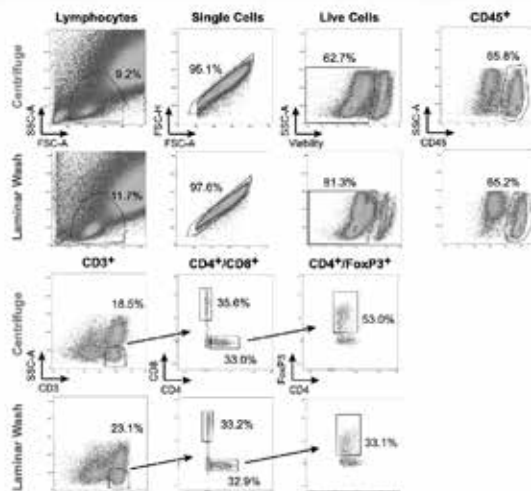


**Agilent**

Trusted Answers

## Centrifuge-free Sample Prep

A next generation solution for alleviating centrifuge-based challenges



### Debris removal

Cleaner data improves data acquisition

### Enhanced cell washing

More appreciable resolution of distinct subpopulations

### Improved cell retention viability

Improve retention and viability of cells while preserving cellular morphology



Visit our website to learn more



# CYTO 2022 ABSTRACTS

SUNDAY, JUNE 5

58

894749

## **A Novel Cytometry Analysis Framework in Python: Application To Real-World Immunophenotyping Of Patients With Severe Sepsis**

Ross Burton<sup>1</sup>, Simone Cuff<sup>1</sup>, Andreas Artemiou<sup>1</sup>, Matthias Eberl Schiemann<sup>2</sup>

<sup>1</sup> Cardiff University, <sup>2</sup> Technical University of Munich

Cytometry has seen a considerable expansion in recent years in the number of parameters that can be acquired in a single experiment. In response to this technological advance there has been an increased demand for new computational solutions for handling high-dimensional data acquired by flow or mass cytometry. Despite the relative success of published packages to replicate and outperform traditional manual analysis, widespread adoption of these techniques has yet to be realised in the field of immunology. Here we present CytoPy, a Python framework for automated analysis of cytometry data. CytoPy provides a platform for open-source cytometry bioinformatics with powerful data structures coupled to a document-based database. This design choice makes CytoPy well placed for integrating cytometry data with experimental meta-data and other related datasets (e.g. proteomics, RNAseq, lipidomics etc). The programming interface of CytoPy is data-centric, focusing on a 'low-code' experience, and is ideal for an iterative analytical environment common-place in modern data science work-streams. This framework is algorithm-agnostic, facilitating all existing and future developments in the cytometry ecosystem. Current tools within this framework include methods for correcting batch effect, autonomous gating algorithms, supervised classification of cytometry data, and high-dimensional clustering. CytoPy provides easy access to popular clustering algorithms such as FlowSOM, Phenograph, and SPADE and introduces ensemble clustering tools to integrate the clustering solutions of multiple algorithms for improved clustering informed by multiple views. In this presentation, the power and versatility of CytoPy is demonstrated on complex real-world data derived from patients with acute severe sepsis. We have utilised CytoPy to characterise the immune response in 77 patients from the largest intensive care unit in Wales, UK. Multiple challenges are discussed, such as correcting batch effect, cleaning data with autonomous gates, and clustering

with multiple algorithms integrated with an ensemble clustering technique. Finally, our findings are combined with data from lipidomic assays, multiplex proteomics, and clinical information systems to generate Logistic Regression models of patient outcome and underlying infection. CytoPy is open-source and licensed under the MIT license. CytoPy is available at <https://github.com/burtonrj/CytoPy>, with accompanying notebooks and software documentation at <https://cytopy.readthedocs.io/>.

59

898478

## **How To Build An Explainable Computational Pipeline To Diagnose And Subtype Patients With Lymphoid Primary Immunodeficiencies**

Annelies Emmaneel<sup>1</sup>, Jana Neirinck<sup>2</sup>, Mattias Hofmans Sofie Van Gassen Filomeen Haerynck Tessa Kerre<sup>3</sup>, Jan Philippé Carolien Bonroy, Yvan Saeys

<sup>1</sup> VIB-UGent Center for Inflammation Research, <sup>2</sup> Palacky University Olomouc, <sup>3</sup> Ghent University Hospital

The usage of computational pipelines to research and classify diseases keeps on increasing, however interpreting the models built for those pipelines remains a difficult task. To resolve this, we have developed a pipeline to classify patients with primary immunodeficiencies (PID) where SHAP values help interpret the model by indicating which cell populations are necessary in the classification and where trajectory inference explains the dynamics of some PID subtypes. Primary immunodeficiencies are a heterogeneous group of rare disorders with impairment in one or more intrinsic elements of the immune system and are characterized by a wide spectrum of clinical manifestations. Fast and accurate diagnosis of the PID subtypes is of utmost importance for timely treatment and prevention of potential life-threatening complications. Multiparameter flow cytometry is an important tool in the diagnostic and prognostic work-up of PID. This technique has the advantage of providing rapid, widely accessible and relatively low-cost analysis. However, data analysis is often complicated. To be able to immunophenotypically diagnose and distinguish PID subtypes, we are analyzing the immune profile in a pediatric and adult cohort of 509 patients with various PID subtypes (n=318), non-PID diseased controls (n=116) and healthy controls (n=75). The cohort was diagnosed according to the IUIS and ESID criteria and the samples were immunophenotypically characterized using the 8-color/12-marker PID Orientation Tube (PIDOT), developed by the EuroFlow consortium. The usage of standardized EuroFlow protocols for

# CYTO 2022 ABSTRACTS

sample pre-processing, stainings and instrument set-up will allow for a pipeline which can be extended across institutions. Currently, our computational pipeline consists of four steps. First, pre-processing is performed by removing low quality cells, debris and doublets using the PeacoQC package and by normalizing for a batch effect with CytoNorm. After selection of the B- and T-cells, their subpopulations are identified using a FlowSOM model built with healthy controls of different ages. Subsequently, individual cell percentages are extracted by mapping the samples onto this model to enable comparison between patients. Finally, we built a preliminary classification model with extreme gradient boosting that is 72% accurate in predicting lymphoid PID patients from diseased controls and patients with other primary antibody disorders. To increase interpretability towards the clinic, we include a SHAP analysis, a theoretical approach from game theory, which allows selecting those cell populations that contribute most in classifying the different subtypes. To get a deeper view into the dynamics of the different disorders, we also applied trajectory inference using Slingshot on top of our FlowSOM model. By building this pipeline, we want to provide an additional tool to help classify the different PID subtypes in a fast, accurate and interpretable way.

60

898471

## **A Flow Cytometry–Based Computational Pipeline To Predict Outcome In Acute Myeloid Leukemia**

Sarah Bonte<sup>1</sup>, Artuur Couckuyt<sup>1</sup>, Sofie Van Gassen<sup>1</sup>, Jan Philippé Tessa Kerre<sup>2</sup>, Yvan Saeys<sup>1</sup>

<sup>1</sup> VIB-UGent Center for Inflammation Research, <sup>2</sup> Ghent University Hospital

Introduction: Acute myeloid leukemia (AML) has a dismal outcome, as demonstrated by a 5-year overall survival rate of less than 30%. Although a complete remission can be achieved in approximately half of the patients, the chances of relapse are high. To prevent relapse, high-risk patients should be accurately identified at diagnosis and treated accordingly. The generally accepted risk stratification, as described in the 2017 ELN risk stratification criteria, classifies patients into favorable, intermediate and adverse risk categories, based on molecular and genetic tests. However, a proportion of favorable risk patients still relapse, indicating a need for improvement. We aim to do this by incorporating flow cytometric analysis. Whereas the current manual analysis of flow cytometry data is mainly subjective and time-consuming, we use a computational pipeline to analyze flow data in an objective way. With this pipeline, we aim to identify novel prognostic markers which could improve risk stratification at diagnosis and aid in determining the optimal treatment strategy for each individual AML patient. Methods: Flow cytometry data (stained according to the standardized EuroFlow panel, which consists of 7 tubes) and clinical data were collected from 197 patients diagnosed with AML. Flow data was preprocessed using a computational pipeline including FlowSOM-based removal of debris and PeacoQC quality control. Batch effects were identified and corrected using CytoNorm. Next, FlowSOM was used to identify cell populations in the preprocessed patient samples. From this clustering, features (e.g. the cluster and metacluster percentages, with the latter corresponding to cell population abundances) were extracted. To prevent overfitting, we analyzed various feature selection methods and four different classification models (random forest, support vector machines, elastic net and naive Bayes) in a cross-validation set-up. Results: Statistical analysis of preliminary results revealed cell populations which were more abundantly present at diagnosis in patients who relapsed after therapy. Some of these cell populations have been previously described, whereas others are yet to be discovered. We trained

# CYTO 2022 ABSTRACTS

machine learning models to predict the outcome of AML patients based on flow cytometry data obtained at diagnosis. Next to relapse, we also analyzed other outcomes, e.g. presence of measurable residual disease (MRD) after chemotherapy, and survival. Our results were validated in an external validation cohort (146 patients) obtained from Erasmus MC Rotterdam, where the standardized EuroFlow workflow is also implemented. Conclusion: By computationally linking flow data to clinical outcome data of patients, we aim to identify novel prognostic markers in AML. In addition, markers expressed on cell populations linked to a poor prognosis, or markers expressed on leukemic stem cells, can be of use as novel therapeutic targets for immunotherapy of AML.

**61**  
893738

## **Large-Batch Evaluation of Cell Counter Instrument-To-Instrument Consistency for Cell Therapy Applications**

Jordan Bell<sup>1</sup>, Yongyang Huang<sup>1</sup>, Leo Chan<sup>1</sup>

<sup>1</sup> Nexcelom Bioscience

Cell therapy has been hailed as a medical revolution, and its rise has only increased the importance of accuracy and precision in cell counting. Ensuring the identity, purity, and viability of cell therapy products is critical for increasing efficacy and avoiding potential harmful side effects. A significant portion of this burden now rests on sample analysis by automated cell counters. As cell therapies move from experimentation to production, the need is growing for higher consistency in cell counting instrumentation. Confidence in a particular cell counting method is reduced if several “identical” instruments disagree on the cell concentration and viability for a given sample. Such comparison among several instruments is rarely done, however, largely due to logistical challenges. Instead, measurements are usually collected with a single instrument and taken at face value, running the risk of discrepancy if a process is moved to a new instrument – transferred from R&D to production, for example. In this work we compare two distinct cell counting instruments. Both instruments are capable of brightfield and fluorescence imaging and are growing in their adoption within the cell therapy community. The first is a well-established single-sample counter utilizing disposable slides (Cellometer K2). The second instrument is a relatively new high-throughput cell counter designed for integration into automated workflows (Cellaca MX). We selected these two instruments for comparison in order to

investigate consistency between a counter that may be used in an R&D setting, and a high-throughput cell counter that may be used in manufacturing. In order to compare large pools of instruments, we use fluorescent beads that are locked in a cured polymer. These samples were observed to be stable and resistant to photobleaching, making them ideal for a longitudinal study. We analyzed these samples using identical instrument settings over a span of more than a year. These samples allow us to investigate agreement among 58 Cellometer K2 instruments and 40 Cellaca MX instruments, what we believe is the largest group of cell counting instruments to be involved in a single comparison study. Our work illustrates experimental methods suitable for the comparison of multiple cell counting methods. We measure consistency among the cell counters, both within groups of similar instruments and between instrument types. This consistency encourages optimism for “future-proof” assays that can survive the transition from R&D to production with minimal adjustment.

**62**  
898429

## **Applications of Machine Vision-Based Cell Sorting For Clinical Diagnosis And Cell Therapy**

Kazuki Teranishi<sup>1</sup>

<sup>1</sup>THINKCYTE INC

Single-cell analysis and sorting have become essential research tools in life sciences and medicine. Conventionally, flow cytometry utilizing fluorochrome-conjugated antibodies or fluorescent dyes has been widely used to characterize and isolate cells from heterogeneous mixtures. However, immunophenotyping using such molecular stains has several disadvantages. Staining can be labor and resource intensive, and emission spectral overlaps limit fluorochrome availability for multiplexing. Furthermore, many molecules used for staining may exhibit cell toxicity or perturb the system, complicating the interpretation of results and are undesirable for cell therapy, especially under GMP requirements. Recent advancements in imaging flow cytometry and microscopy image classification of unstained cells using machine vision have aimed to overcome these limitations, however, cell selection based on these analyses has been limited in speed. We have developed a machine vision-based cell analysis and sorting technology based on label-free ghost cytometry (LF-GC) that addresses these unmet needs. LF-GC exploits compressive acquisition of high-content morphological features of single cells combined with

# CYTO 2022 ABSTRACTS

supervised machine learning without image reconstruction to enable the identification and sorting of cells at high throughput in label-free mode. Here we report the application of LF-GC for clinical diagnostics and cell therapy. First, we evaluated LF-GC's classification of blood cells based on image information. Using CD markers (CD45, CD123, CD14, CD16, CD34, and CD41) as the ground truth for supervised training of convolutional neural networks and macro average F1-score (F1 macro) as a metric for classification ability, LF-GC was able to discern WBCs subtypes and hematopoietic stem cells (F1 macro = 0.908), RBCs and platelets (F1 macro = 0.997), and RBCs from WBCs (F1 macro = 0.996). Secondly, we tested LF-GC's capacity to isolate chondrocytes with high proliferative potential as a surrogate marker of their therapeutic potential. Using CSFE as the ground truth for training a support-vector machine, LF-GC was able to discern cells with high and low proliferative potential (ROC-AUC = 0.86) and sort the live cells without observing any labels. The highly proliferative chondrocytes that LF-GC sorted maintained viability and produced a higher GAG level in the ECM than control, suggesting higher therapeutic potential for tissue regeneration. Overall, these two examples demonstrate LF-GC's capability to (1) multiplex without compensation, (2) sort live cells where molecular labeling is unavailable, and (3) process a wide variety of cell types.

**63**  
901601

## **A 24-Color CAR T Cell Phenotyping Panel to Discern Effects Of Tumor Microenvironment**

Martin Gomez<sup>1</sup>, Nikki Khoshnoodi<sup>1</sup>, Saikat Banerjee<sup>1</sup>, Bhargavi Rajan<sup>1</sup>

<sup>1</sup> Kite Pharma a Gilead Company

We have developed a 24-color flow cytometry panel that characterizes Chimeric Antigen Receptor T cells (CAR T), including assessment of CD4+ T cell subsets and memory populations. Recently adoptive cell therapies, particularly CAR T therapies, have achieved therapeutic efficacy in treating hematological malignancies. However, adoptive cell therapies are less efficacious when targeting solid tumors due to the suppressive effects of the tumor microenvironment (TME) on immune cells. Transforming growth factor beta (TGF- $\beta$ ) is a multifunctional cytokine that fosters an immunosuppressive TME. In T cells, TGF- $\beta$  suppresses the cytotoxic function of CD8+ cells through transcriptional downregulation of perforins, granzymes, and cytotoxins (1). The suppressive effects of

TGF- $\beta$  can be counteracted by arming CAR T cells with TGF- $\beta$  negative receptor. We hypothesize that armored anti-CD19 CAR T cells will have reduced T-regulatory (Treg) subset conversion and maintain functional cells under prolonged exposure to TGF- $\beta$ . The panel was optimized to assess the efficacy, and phenotype differences of armored CAR T vs. non-armored CAR T cells under in vitro antigen stimulation and different TME burdens. The panel is composed of surface markers, cytokines, and transcription factors to distinguish CD4+ cell subsets, Th1 (IL-2, IFN $\gamma$ , CXCR3, T-bet), Th2 (IL-4, CCR4, GATA3), Th17 (CCR6, ROR $\gamma$ t, IL-17), Treg (CD25, FOXP3, CD127, IL-10) and T cell memory populations (CD45RA, CCR7, CD62L). In addition, killing via Luciferase and detection of cytokines via mesoscale discovery (MSD) platform confirmed the data from the flow cytometry panel. In conclusion, the panel detected a reduced Treg cell population in the armored CAR T cells than the non-armored CAR T cells. Data suggests that the TGF- $\beta$  negative receptor is a successful alternate molecular modification of CAR T cells when treating tumors with a high immunosuppressive TME burden.

**64**  
901954

## **Exhausting T Cell Exhaustion: Characterization of CD8 T Cells Chronically Stimulated In Vitro**

Florence Perrin Patel<sup>1</sup>, Katherine Vowell<sup>1</sup>, Shilpa Gandre-Babbe<sup>1</sup>, Thaddeus Carlson<sup>1</sup>

<sup>1</sup> GlaxoSmithKline

The association between T cell exhaustion and cancer/chronic infection has been known for many years now. Therapies blocking T cell exhaustion are efficacious in a variety of tumors, and there is great interest in additional therapeutic mechanisms for blocking exhaustion in this context. More recently a connection between T cell exhaustion and autoimmune disease has been identified. Patients with better long-term prognosis and fewer relapses in a variety of autoimmune diseases were found to have the transcriptional signature of T cell exhaustion in their CD8+ T cells, suggesting potential therapeutic benefit of inducing an exhaustion phenotype in patients with autoimmune disease. In the context of a genome wide pooled CRISPR screen to identify gene edits that either enhance or prevent T cell exhaustion, chronic T cell activation was recreated using repetitive stimulation with anti-CD3/CD28 beads (Balkhi et al., 2018). This protocol upregulated checkpoint inhibitors (PD-1, LAG-3 and TIM-3) while downregulating the secretion of type I cytokines associated with robust cytotoxic response, such as

# CYTO 2022 ABSTRACTS

interleukin-2 (IL-2) and interferon gamma (IFN- $\gamma$ ). However, based on experimental data, it induced a mixed population of T cells including both activated and exhausted phenotypes and a sorting paradigm using PD1, TIM3 and TIGIT expression was not successful at separating functionally exhausted from non-exhausted cells. A prerequisite for a successful genome wide pooled CRISPR screen is to separate exhausted cells from non-exhausted cells in order to sequence guide RNAs and identify the gene edits that are enriched in each population. We developed a 36-parameter CyTOF panel adapted from Bengsch et al. for deep phenotyping and identification of markers associated with exhaustion and loss of function for efficient sorting of the exhausted T cell generated. While we identified dysfunctional cell populations with TIGIT+CD39+ with a feasibly sortable cell number, most cells in these populations overlapped with PD-1 expression, which proved to be an unsuccessful sorting marker in previous studies. Overall, we identified cell surface markers to enrich for a phenotypically exhausted subset but could not identify markers to sufficiently enrich for a subset that remained convincingly functional. Note: The human biological samples were sourced ethically and their research use was in accord with the terms of the informed consents under an IRB/EC approved protocol.

**65**  
894086

## Ensuring Full Spectrum Flow Cytometry Data Quality for High-Dimensional Analysis

Kylie Price<sup>1</sup>, Laura Ferrer Font<sup>1</sup>, Geoff Kraker<sup>1</sup>

<sup>1</sup> Cytek Biosciences

Full spectrum flow cytometry allows the analysis of more than 40 parameters at the single-cell level. High-dimensional data analysis can be used to fully explore single-cell datasets and to obtain additional information reducing analysis time compared to the common practice of manual gating. However, as panel size and complexity increase, so too does the detail involved in validating and optimizing the panel, as well as preparing the resulting data to be used for downstream high-dimensional data analysis. Indeed, excellent data quality is required for high dimensional analysis. To ensure clustering or dimensionality reduction algorithms can be used efficiently, some important steps should be considered, such as proper unmixing/compensation of data, correcting for batch effects, ensuring correct scale transformation and the use of data cleaning gates or algorithms (signal change over time, cell doublets,

aggregates, etc.). A workflow to properly prepare full spectrum flow cytometry data for high-dimensional data analysis will be presented, with a focus on visualizing the impact and importance of each step of data preparation using dimensionality reduction algorithms. Application of our workflow will aid full spectrum flow cytometry users to quality control their panels or datasets to be used in high-dimensional analysis, helping users to obtain valid and reproducible results.

**66**  
894436

## Synthetic Cell Mimics for Next-Generation Flow Cytometry-Based Assays

Ling Zhang<sup>1</sup>, Jason Deng<sup>1</sup>, Tyler Shovah<sup>1</sup>

<sup>1</sup> Slingshot Biosciences

We have developed a new class of engineered polymer reagents for flow cytometry that matches the spectral and physical characteristics of cells. Our scalable platform designs particles that are independently tuned along optical, fluorescent, genomic and biochemical parameters, generating a highly-flexible synthetic cell for a wide range of applications. Existing polystyrene bead reagents have fundamentally different properties when compared to cellular material. This causes difficulties when trying to work with certain classes of dyes (e.g. tandem dyes) and in key fluorescence channels. Here, we show how our spectrally-tuned polymer formulation yields high-performance compensation controls for standard and spectral cytometers. We also demonstrate a new compensation bead technology for cell viability assays that have multi-modal reactivity, for both intercalating and amine-reactive dyes. Finally, we show an advanced cell mimic that allows for streamlined and automated immune cell profiling. Our first-in-class, synthetic cell printing technology promises to improve measurement and assay accuracy for next-generation flow cytometers by decreasing set up costs, reducing time to experimentation, and saving precious sample material, while improving detection limits.

67

894939

## A Standardized Metric for Throughput For Cytometry

Maik Herbig<sup>1</sup>, Akihiro Isozaki<sup>1</sup>, Dino Di Carlo<sup>2</sup>, Jochen Guck<sup>3</sup>, Nao Nitta<sup>1</sup>, Robert Damoiseaux<sup>1</sup>, Shogo Kamikawaji<sup>1</sup>, Eigo Suyama<sup>1</sup>, Hirofumi Shintaku<sup>1</sup>, Angela Ruohao<sup>1</sup>, Wu Itoshi Nikaido, Keisuke Goda

<sup>1</sup> The University of Tokyo, <sup>2</sup> University of California Los Angeles, <sup>3</sup> Max Planck Institut für die Physik des Lichts & Max-Planck-Zentrum für Physik und Medizin

The technological advances of last decades have drastically increased the rates of data acquisition and processing in biology and medicine. Parallelization and robotics were exploited to develop high-throughput techniques for imaging, screening, sequencing, manipulation, or sorting of biomedical samples such as molecules, compounds, genes, cells, or organoids. While the phrase “high-throughput” is abundantly used, the underlying definition of the metric “throughput” is inconsistent across biomedical domains. In contrast, throughput is rigorously defined in electrical engineering, where it describes the rate of data transmission or processing. However, in a biomedical setting, data acquisition is also limited by non-electrical factors such as sample delivery speed, resulting in a difference between theoretically and practically achievable throughput, e.g., in flow cytometry, high-throughput screening, and high-throughput sequencing. Moreover, flow cytometry, high-throughput screening, and high-throughput sequencing currently employ different units for throughput, resulting in ambiguities, which hinders comparison and interdisciplinary collaboration. While this is especially problematic for end users who want to select the ideal method for their specific problem, the significance of the issue is often neglected. In this presentation, we address concerns regarding throughput by defining a set of rules and exploiting a general equation, which allows standardizing throughput claims.

68

898442

## Cell Spike-ins Add Assurance to Flow Cytometry Measurements of Complex Microbial Communities

Kirsten Parratt,<sup>1</sup> Nancy Lin<sup>1</sup>

<sup>1</sup> National Institute of Standards and Technology

Microbial therapeutic products could potentially solve many currently intractable gut-related afflictions, e.g. Clostridioides difficile infection, and usher in next-generation microbiome treatments. However, microbiomes are challenging to measure, especially clinical materials such as stool samples. Flow cytometry has been used to characterize the stool samples, but the lack of reference materials prohibits comparison across laboratories and timepoints. Reference materials added to real samples (“spike-ins”) can account for tube-to-tube variability and potential effects of sample matrix, estimate batch effects, and guide gating thresholds. We demonstrate how analysis of cell spike-ins can increase measurement assurance without significant changes to existing analysis workflows. A combination viability and Gram status assay represented a model workflow. Escherichia coli and Lactobacillus rhamnosus cells were fluorescently tagged (CellBrightFix640) for identification and used as spike-ins. Stool candidate reference material aliquots were defrosted and filtered immediately prior to analysis. A staining cocktail targeting DNA (Hoechst 33342), peptidoglycans (WheatGermAgglutinin-AlexaFluor555), and cell membrane potential (DiBAC4(3)) was prepared. Stool aliquots were mixed with staining cocktail, and spike-ins were added to constitute  $\approx 7\%$  of the total cell population. Controls included unstained and single color samples, fully stained spike-ins without stool (“enumeration controls”), and reference beads. Samples were analyzed on a flow cytometer (Beckman Coulter, CytoFLEX LX) under the same acquisition conditions at 10  $\mu\text{L}/\text{min}$ . Spike-ins were analyzed within stool samples with only small modifications to the existing workflow. Compensation controls demonstrated minimal fluorescence spillover between channels. Enumeration controls and spike-ins within stool samples were compared across replicate tubes (5) and timepoints (3) to evaluate consistency in cell count and intensities. Inter-tube variability was low within a timepoint, however, more L. rhamnosus cells were counted in stool than enumeration controls ( $\approx 15\%$  increase). Staining profiles of the controls were consistent across tested conditions. The spike-in fluorescent tag was sufficient to gate out the spike-



# CYTO 2022 ABSTRACTS

in cells, leaving the remaining data ready for the normal stool analysis workflow. In conclusion, spike-in cells can easily be incorporated into a stool flow cytometry protocol and analyzed to add measurement assurance without compromising the original analysis. On-going work includes evaluating batch effects across timepoints and comparing stool samples from different donors. Disclaimer: Certain commercial materials and equipment are identified to specify the experimental procedure. In no instance does such identification imply recommendation or endorsement by NIST or that the material or equipment identified is necessarily the best available for the purpose.

69  
894802

## High-Dimensional Immune Cell Profiling to Understand How the Immune System Changes Throughout Life: Implications for Human Disease

Sedi Jalali<sup>1</sup>, Daniel Pellicci<sup>1</sup>, Igor Konstantinov<sup>2</sup>, Thomas Ashhurst<sup>3</sup>

<sup>1</sup> Murdoch Children's Research Institute, <sup>2</sup> Royal Children's Hospital, <sup>3</sup> Sydney Cytometry Core Research Facility

Protection against disease requires cells from both the innate and adaptive arms of the human immune system. The impact of disease is often significantly influenced by age. In humans, newborns have immature immune system, thus make them more susceptible to some infectious diseases such as respiratory syncytial virus and diphtheria. In contrast, the immature immune system in infants <14 months provides an advantage for recipients of heart transplants, as they are less likely to reject, even if the transplanted heart is from an ABO mismatched donor. Later on in life, the immune system wanes and this renders elderly people more susceptible to infections and cancers. This has recently been exemplified during the COVID-19 pandemic, which is more fatal in older age groups, particularly in individuals with other co-morbidities. Strikingly, children are less affected by SARS-CoV-2 virus and are often asymptomatic, presumably due to a reduced pro-inflammatory immune response. Therefore, understanding the composition of human immune system throughout life is crucial if we desire to manipulate the immune response for treating human diseases. We used high-dimensional flow cytometric analysis to generate blood immune cell atlas encompassing >50 populations of immune cells from infants <1 month of age to adults >75 years of age. We found that the immune landscape undergoes major

changes early on in life and that this likely influences how the body responds to certain diseases. Our results showed that naïve T and B cells are replaced with different proportions of memory cell subsets. Moreover, the proportion of MAIT cells and gd T cells were low during the first few years after birth, increased in older children, and then decreased in the elderly. This work provides the first comprehensive study of the immune system throughout ontogeny and provides a foundation for understanding how the immune system changes in the context of human disease.

70  
898477

## Unraveling Immunotherapy Response in Lung Cancer by Computational Cytometry

Katrien Quintelier<sup>1</sup>, Sofie Van Gassen<sup>1</sup>, Marcella Willemsen<sup>1</sup>, Mandy van Brakel<sup>1</sup>, Reno Debets<sup>1</sup>, Cor Lamers<sup>1</sup>, Ron Mathijssen<sup>1</sup>, Joachim Aerts<sup>1</sup>, Yvan Saeys<sup>1</sup>

<sup>1</sup> VIB-UGent Center for Inflammation Research

Background and aims: Immunotherapy has revolutionized the treatment of non-small-cell lung carcinomas (NSCLC). Immune checkpoint inhibitors (ICI) are now part of the standard treatment of NSCLC, resulting in longer progression-free survival times and a longer overall survival. However, ICI are not effective in all patients; varying from complete response to no response at all. Additionally, some patients experience severe adverse effects. Predicting which patients will benefit from expensive ICI treatment or for which patients the risk of adverse effects is too high, is not yet possible. Here, we perform a fully automated computational analysis to identify differences in the immune profile of the different response groups, in order to get more insights into the mechanism of action of ICI and eventually build a predictive model to identify responders and patients at risk for severe toxicities based on flow cytometry data.

Methods: An extensive flow cytometry analysis with 6 panels (1 general 13-marker panel and 5 T cell-specific panels) at 3 time points (TPs; at baseline, i.e. before receiving the first dose of nivolumab, a type of ICI, and prior to receiving the subsequent 2 doses) was performed on blood of 71 NSCLC patients (14 partial response, 25 stable disease and 32 progressive disease). We applied an automated analysis pipeline consisting of a preprocessing step including FlowSOM-based removal of debris and PeacoQC quality control and a CytoNorm normalization step to control our batch effect. Next, a FlowSOM clustering to retrieve the cell subset abundances and finally a statistical

# CYTO 2022 ABSTRACTS

analysis. Later, we obtained a second cohort of 174 NSCLC patients (1-9 TPs during the course of treatment) and stained with the general panel, which was used as a validation cohort. For this, we ran the same preprocessing pipeline, recycled the CytoNorm model and mapped our data on the FlowSOM model of the first cohort. Results: We applied the pipeline on the first cohort, performed Kruskal-Wallis and paired Wilcoxon tests to compare the response groups per TP and identified significant differences in FlowSOM metacluster abundances. In the general panel, we found higher percentages of CD8+ T cells in the partial responders at TP2 and 3 versus the other response groups. We also observed that these percentages were higher at TP2 and 3 versus baseline, which was previously described in literature. These findings were confirmed in the validation cohort. The specific T cell panels revealed significant differences in abundances of T cell subsets, e.g. CD4+ and double negative T cells. Moreover, these significantly different cell subsets appeared to have predictive power. Starting from all the metacluster abundances at TP1, we used a feature selection method and built classifiers to predict response and toxicity. These will allow us to obtain deeper insights in the working mechanism of ICI and the immunological changes in lung cancer patients that respond to ICI

71  
898500

## **Methods Used to Validate Cluster and Multidimensional Reduction Programs using data from a SARS-CoV-2 NHP challenge study and NHP BAL samples infected with SARS-CoV-2**

Stephen Perfetto<sup>1</sup>, David Ambrozak<sup>1</sup>, Richard Nguyen<sup>1</sup>, Esther Thang<sup>2</sup>

<sup>1</sup> NIAID, <sup>2</sup>NIH

Panels in flow cytometry are expanding in complexity necessitating more advanced analysis tools to better understand complex phenotypes, which may not be revealed by traditional standard linear gating due in part to the gating structure or previously undiscovered populations. Assessing all relevant measured parameters in multidimensional space is key to the discovery of relevant cell populations and relevant to how linear gating might be used. Using dimensionality reduction (tSNE, UMAP, TriMap, etc.) and cluster (FlowSOM, XShift, Phenograph, etc.) algorithms can lead to these discoveries but are prone

to artefacts and misinterpretation. Thus, understanding the limitation and methods for validation of these programs is of critical importance. Here, we applied these tools to two non-human primate SARS-CoV2 studies with the goal to discuss best practices, how to best validate their output and avoid pitfalls. Method: This work examines two research studies (SARS-CoV-2 NHP challenge study using 13 fluorescent markers and a study of NHP BAL samples infected with SARS-CoV-2 using 21 fluorescent markers) to show the value of using these advanced analysis tools but also the impact of data pre-processing and the importance of validation methods to avoid data misinterpretation. These critical data preprocessing and validation steps include a) the evaluation of compensation controls and the use of biexponential transformation (e.g., use of autospill/autospread and other spillover spread reduction programs or instrument procedures), b) the analysis of data quality processed through FlowAI or similar programs, c) the evaluation of the gating hierarchy to the level of relevant cell populations, d) the formulation of a hypothesis and the use of keywords to answer questions and e) the use of linear gating to determine if cluster populations are real and finally, f) the use of advanced gating to sort (e.g., HyperFinder) to sort out and genetically verify cluster populations in the hypothesis. Results and conclusions: First and foremost, is the formulation of a hypothesis is critical to best structure questions when using these advanced tools, these can best be answered by keywords or relevant gated population gates (e.g., NK cells, CD3+ T cells or CD20+ B cells). Review of the compensation matrix used on the actual test samples provides the robust data for advanced programming tools. Spillover which hasn't been corrected or is incorrectly compensated can lead to artificial populations and data misinterpretation. Quality control tools to detect data anomalies, such as FlowAI provide a routine evaluation for either fluorescent median shifts or data not meeting the dynamic range of a given detector (e.g., aggregates or incorrect titers or high cellular autofluorescence). Using only acceptable data showed better separation of clusters and excluded potential artifacts.

# CYTO 2022 ABSTRACTS

72

898538

## Using Full Spectrum Cytometry to Expand and Enhance High Parameter Immune Fingerprints in Health and Disease

Derek Jones<sup>1</sup>, Jonni S. Moore<sup>1</sup>, Richard Schretzenmair<sup>1</sup>, Robert Balderas<sup>2</sup>

<sup>1</sup> University of Pennsylvania, <sup>2</sup> BD Biosciences

**BACKGROUND:** High parameter cytometry has contributed greatly to advances in immunophenotyping and the understanding of human immune health and disease by providing insight into signature fingerprints that can be sensitive biomarkers for diagnosis and prognosis. The advent of full spectrum cytometry allows the detection of even more detail of these fingerprints, making them truly targetable hallmarks that can be translated to clinical use. By taking advantage of full spectrum capabilities on a BD FACSymphony A5.2, we translated a 28-color T cell panel previously demonstrated to provide actionable biomarkers for pancreatic cancer, to a 37-parameter multilineage immune profiling panel with increased breadth and resolution. **METHODS:** Using an extensively qualified 30-parameter Symphony A5, we validated a 28-color panel to identify multiple T cell populations in a clinical trial to identify signature responses to immune therapies. In order to extend the number of parameters, increase the resolution, and expand the scope of the panel, we sought to transfer this panel to the full spectrum BD Symphony A5.2. A primary goal was to establish critical processes that would allow us to reduce the impact of spectral spreading on the existing backbone, and to facilitate the addition of fingerprint refining markers, resulting in a 37-color panel. To this end, we expanded the original panel and assigned fluorochromes based on expression level of the target and SSM values. Additional methods were developed to minimize the use of FMO controls, including the use of internal controls and the utilization of SSM tables to rationally develop Fluorescence Minus Many (FMM) controls. As a guide, we utilized a variety of original and standard computational approaches to control for batch effects and assure data quality. Finally, to demonstrate the utility of this approach, we tested the panel on human pancreatic cancer patient blood samples and apparently normal human blood samples. **RESULTS AND CONCLUSIONS:** Computational analysis of patient samples readily identified most major immune subsets, including naïve and effector T cells, regulatory T cells, memory B cells, NK cells, and classical and non-classical monocytes, providing the opportunity to further expand the

fingerprints previously identified with the T cell panel alone. This study demonstrated that with attention to detail, translating a well-established clinically validated conventional high parameter panel to a full spectrum panel can be easily accomplished. The process described here also allows for workflow efficiencies to move the use of full spectrum cytometry closer to the bedside.

74

896516

## Uncovering the Pathogenesis and Treatment Of Atherosclerosis By High-Throughput Microscopy

Yunjie Deng<sup>1</sup>, Jaime Duque<sup>1</sup>, Chengxun Su<sup>1</sup>, Yuqi Zhou<sup>1</sup>, Masako Nishikawa<sup>1</sup>, Ting-Hui Xiao<sup>1</sup>, Yutaka Yatomi<sup>1</sup>, HanWei Hou<sup>1</sup>, Keisuke Goda<sup>1</sup>

<sup>1</sup> University of Tokyo

Atherosclerosis, the major cause of cardiovascular disorders such as stroke and myocardial infarction, has a pathological characteristic of vascular stenosis. Extensive research has been undertaken using in vivo and in vitro vascular models to elucidate the stenosis-induced thrombus development. Unfortunately, due to a lack of analytical tools with both high spatial and temporal resolution, the transient and dynamic process of platelet aggregation under stenosis remains elusive. Here we used an in vitro microfluidic stenosis model and high-throughput imaging flow cytometry to observe shear-induced platelet aggregation in a spatiotemporally resolved manner. Specifically, we investigated the size, shape, and population of platelet aggregates at single-cell resolution in the presence of four types of agonists [adenosine diphosphate (ADP), collagen, thrombin receptor activator peptide 6 (TRAP-6), U46619 (thromboxane A2 agonist)] in a three-dimensional stenosis model. When both stenosis and an agonist were present, platelet aggregation increased significantly, implying a synergistic effect of atherogenic blood flow disturbance and circulating factors on platelet activation. In particular, platelets activated by TRAP-6 form massive platelet aggregates with a wide size distribution, followed by ADP and collagen, with U46619 showing a surprise fall in aggregate size at longer chip run periods. These findings are expected to provide further insights into the underlying mechanism of stenosis-induced platelet aggregation and open the way for the development of more effective antithrombotic therapies.

75

896622

## Detection And Characterization Of Circulating Tumor Cell Clusters By High-Throughput Optomechanical Imaging Flow Cytometry

Akihiro Isozaki<sup>1</sup>, Hiroki Matsumura<sup>1</sup>, Larina Shen<sup>1</sup>, Hideharu Mikami<sup>1</sup>, Dan Yuan<sup>1</sup>, Maik Herbig<sup>1</sup>, Yuto Kondo<sup>1</sup>, Tomoko Mori<sup>1</sup>, Yoshika Kusumoto<sup>1</sup>, Masako Nishikawa<sup>1</sup>, Yutaka Yatomi<sup>1</sup>, Satoshi Matsusaka<sup>1</sup>, Keisuke Goda<sup>1</sup>

<sup>1</sup> The University of Tokyo

Circulating tumor cells (CTCs) take up different forms of clusters and associations correlated with unique physiological characteristics, rendering the heterogeneity of CTCs an essential subject of study. Specifically, a recent study has found that a patient has a worse prognosis when CTC clusters associated with leukocytes are present [Szczerba et al., *Nature* 566, 553 (2019)]. Unfortunately, conventional methods are limited in detecting and analyzing various forms of CTCs accurately. Here we demonstrate an efficient method that enables the detection and characterization of heterogeneous CTCs in a blood specimen. To realize this method, we used virtual-freezing fluorescence imaging (VIFFI) flow cytometry [Mikami et al., *Nature Communications* 11, 1162 (2020)] on a blood specimen with malignant-cell-specific stimulation of autofluorescence with 5-aminolevulinic acid (5-ALA) [Matsusaka et al., *Cancer Letters* 355, 113 (2014)] and immunofluorescence labeling. VIFFI is a fluorescence imaging method equipped with a rotating polygon scanner and an excitation beam scanner that virtually freezes the motion of cells flowing at high speeds (>1 m/s), making it possible to image CTC clusters with autofluorescence stimulated by 5-ALA sensitively. In this work, we used peripheral blood mononuclear cell (PBMC) fraction, which includes CTCs, obtained with density gradient centrifugation from a blood specimen of a breast cancer patient. Anti-EpCAM antibody and anti-CD45 antibody were used to stain the membranes of CTCs and leukocytes, respectively. Overall, we imaged cells at a high throughput of 1734 events/s, which was high enough to detect 155 CTCs/clusters out of the massive background of 3467233 leukocytes. Furthermore, our method was able to classify various CTC events into single-cell CTCs, CTC clusters, and leukocyte-associated CTC clusters. This classification is a distinguishing capability of our method unavailable with conventional techniques, which cannot obtain clear images to observe

morphologies of cells at a throughput high enough to detect rare CTCs. We anticipate that our method will aid in understanding the mechanisms of metastasis, determining prognosis, and designing treatment strategies for cancer patients.

76

898552

## To PCR Or Not To PCR: Early Flow Cytometry-Based Measures of HIV infection for Clinical Studies

Veronica Obregon-Perko<sup>1</sup>, Ferzan Uddin<sup>2</sup>, Genevieve G Fouda<sup>3</sup>, Sallie R Permar<sup>3</sup>, Ann Chahroudi

<sup>1</sup> BD Biosciences, <sup>2</sup> Emory University, <sup>3</sup> Duke Human Vaccine Institute

Nearly two million children living with HIV-1 worldwide face a lifetime of daily antiretroviral therapy (ART) to prevent viral rebound. Rare cases of sustained ART-free viral remission have been reported in children where ART was initiated very early after infection, raising the possibility that complements to ART-based measures could further delay or prevent viral rebound without daily medication. Studies in animal models, like simian/human immunodeficiency virus (SIV/SHIV)-infected macaques, could inform progress in this area. However, study designs with early ART initiation face the problem of needing to confirm infection and start ART within 4 days of challenge, a window when plasma viral loads (PVL) are typically undetectable. While SIV/SHIV DNA has been found in lymph nodes as early as 2 days post-challenge (dpc), sampling is invasive and the PCR-based assays time-consuming. Herein, we present a minimally invasive flow cytometry-based approach to test for SHIV infection within the critical early post-infection period. Our collaboration used immune activation at 4 dpc as a systemic measure of infection, based on the findings of a previous study in adult SIV-infected macaques. The cohort was composed of 4-week-old infant macaques (n=9) orally challenged with SHIV.C.CH505. Blood was collected at 0, 4 and 7 dpc for flow cytometry and PVL quantification. Whole blood was stained with a 14-color panel containing lineage markers for T cells, DC, NK cells and monocytes as well as various activation markers (CCR7, CD69, CD80, CD86, CD169, HLA-DR). Samples were acquired on a BD FACSymphony™ A5 Cell Analyzer and analyzed in FlowJo™ Software. PVL was detectable in 4/9 (>60 copies/mL) macaques, but this increased to 8/9 macaques at 7 dpc, with one animal remaining uninfected after 14 d. The frequency of CD169+ cells within non-classical monocytes (CD14lo CD16hi) increased by

# CYTO 2022 ABSTRACTS

approximately 4 fold (med 1.5% to 5%) from 0 to 4 dpc in 7/8 infant macaques that were infected by 7 dpc, although four of these seven macaques had undetectable PVL at the time of staining. Similarly, CCR7+ cells within pDC (CD123+) increased by about 3 fold (med 3.5% to 17%) at 4 dpc in 6/8 macaques, three of which had undetectable PVL. While only five of the eight infected macaques showed elevations in both cell types at 4 dpc, all eight had either increased CD169+ non-classical monocytes or CCR7+ pDC. Thus, evaluating both phenotypes provided the most accurate measure of infection following challenge. Importantly, the animal that remained uninfected at 14 dpc, showed no significant increase in either cell type at 4 dpc (fold change <1.5). While these findings should be confirmed in a larger cohort of animals, they point to intriguing biomarkers to target in future studies and highlight the feasibility of a flow cytometric approach to confirm SHIV infection in infant macaques prior to placing them on ART as part of a long-term pre-clinical study.

77  
896956

## **Selective Nanovial Capture and Single-Cell Sorting of Live Antigen-Specific T Cells Based on Cytokine Secretion**

Doyeon Koo<sup>1</sup>, Zhiyuan Mao<sup>1</sup>, Sohyung Lee<sup>1</sup>, Dino Di Carlo<sup>1</sup>  
Owen Witte<sup>1</sup>

<sup>1</sup> University of California Los Angeles

Despite tremendous successes of engineered cell-based therapies in treating hematologic malignancies and continued efforts to expand treatment to other chronic diseases, the connection between structure, e.g. genetic modification, and therapeutic function is still not strongly linked for cells, suggesting the need for functional based screening. One key function of cells used for therapies, including engineered T cells, is their ability to secrete one or more cytokines simultaneously (i.e. polyfunctionality). However, current phenotyping approaches focus on affinity-based screening of differentially expressed surface receptors which fail to describe their functional potency or mimic the immune synapse for an antigen presenting cell. Therefore, there is a need to develop new platforms to screen and select cells based on their secretory function to identify gene signatures associated with functional responses, uncover novel engineered T cell receptor (TCR) constructs for therapeutic use, or directly select functional base cells for genetic modification. We report a workflow for high-throughput

sorting of individual antigen-specific T cells based on secreted cytokines that are accumulated on 3D structured microparticles using a fluorescence activated cell sorter (FACS). Our cavity-containing hydrogel microparticles (nanovials) are functionalized with cytokine capture antibodies and cell binding motifs, including peptide-major histocompatibility complex (pMHC) or anti-CD45. T cells are loaded and selectively adhere in the cavities of nanovials based on presence of a cognate TCR to the pMHC. Antigen-specific T cells are activated by the pMHC on nanovial and secrete cytokines which are also captured in the cavity, with minimal crosstalk. Captured cytokines are labeled with a fluorescent detection antibody while cells are labeled with live/dead dyes or additional markers. The corresponding cells are sorted based on the secretion level using a commercial FACS. We demonstrated single-cell assays targeting three secreted cytokines (TNF- $\alpha$ , IFN- $\gamma$ , IL-2) and sorted populations of cells with higher cytokine secretion levels based on a combination of fluorescence area and height signals. We also performed multiplexed (TNF- $\alpha$ , IFN- $\gamma$ ) secretion-based sorting of >1 million cells to assess polyfunctional T cells, and cells also maintained viability after sorting for further analysis. Antigen-specific T cells bound to pMHC labeled nanovials, even with low TCR affinity, and secreted cytokines, further increasing specificity in identification of functional TCRs. Our technology can quantitatively screen and sort millions of viable cells based on cytokine secretion, which will aid in discovery of TCRs, chimeric antigen receptors, and surface markers responsible for functional responses. We can further investigate the transcriptome of sorted polyfunctional T cells to uncover drivers of this phenotype, potentially improving upon the current paradigm of cell therapies.

78

896936

## Practical Procedure To Prevent Swarm Detection Of Extracellular Vesicles By Flow Cytometry

Edwin van der Pol<sup>1</sup>, Naomi Buntsma<sup>1</sup>, Chi Hau Rienk Nieuwland<sup>1</sup>

<sup>1</sup> Amsterdam University Medical Centers

Introduction Flow cytometry is widely used to characterize single extracellular vesicles (EVs) in biological fluids. Without appropriate dilution, a single event may be caused by multiple particles that are continuously, simultaneously illuminated. This artefact is called swarm detection and results in incorrect concentration estimates. To find the optimal dilution factor to prevent swarm detection while maximizing EV counts, it is recommended. However, dilution series are laborious and incompatible with clinical routine. Here, we developed a new practical procedure to minimize sample dilution while preventing swarm detection. Methods Five human blood plasma samples (AFFECT EV study) were selected, of which the total concentration of particles as measured by an Apogee A60-Micro flow cytometer (lower EV detection limit ~160 nm) ranges from 3E9 to 1E11/mL. To systematically investigate the relation between the count rate and swarm detection, dilution series of each sample were prepared. Samples were labelled with CD61-APC and measured by FCM using either fluorescence triggering (corresponding to 120 MESF APC) or side scatter triggering (corresponding to a side scatter cross section of 10 nm<sup>2</sup>). Swarm detection was confirmed by a decrease in the measured concentration or an increase in median side scatter cross section with increasing dilution. Results For samples triggered on fluorescence, swarm detection is absent at  $\geq 100$ -fold dilution, although this results in 10-fold overdilution of 2 out of 5 samples. The count rate does not scale linearly with dilution. For all samples triggered by scatter, swarm detection is absent at  $\geq 1,000$ -fold dilution or for count rates  $\leq 2,000$  events/s. However, a fixed dilution of 1,000-fold results in 10-fold overdilution of samples with a relatively low particle concentration, whereas a fixed count rate of 2,000 events/s results in 5-fold overdilution of samples with a relatively high particle concentration. Conclusions For plasma samples measured with our flow cytometer while triggering on fluorescence, a fixed dilution causes overdilution whereas the count rate does not provide a reliable indicator of swarm detection, probably due to dilution-dependent background fluorescence. Hence, for fluorescence triggering dilution series

are required to avoid swarm detection. For scatter triggering, a fixed dilution ( $\geq 1,000$ -fold) or fixed count rate ( $\leq 2,000$  events/s) causes overdilution of some samples. However, when combining a minimum dilution factor of 100-fold with a maximum count rate of 10,000 events/s, swarm can be prevented while maximizing EV counts. Based on a single measurement of the count rate of an overdiluted (e.g., 2,000-fold) sample, the optimal dilution factor can be calculated to achieve a count rate just below 10,000 events/s, while requiring a minimum dilution of 100-fold. Further research is needed to validate and extend the new procedure to other flow cytometers and clinical research studies

79

897384

## An Imaging Flow Cytometry-based Methodology for the Analysis of Single Extracellular Vesicles in Unprocessed Human Plasma

Edwin van der Pol<sup>1</sup>, Wouter Would<sup>2</sup>, Karin Boer<sup>2</sup>, Ana Merino<sup>2</sup>

<sup>1</sup>Amsterdam University Medical Centers, <sup>2</sup>Erasmus MC Transplant Institute

Introduction Extracellular vesicles (EVs) are tissue-specific particles released by cells containing valuable diagnostic information. However, quantification and characterization of EVs are hampered by physical characteristics such as their small size and low epitope copy number, as well as the use of different isolation methods, which may potentially modify EVs. Furthermore, EV analysis in human plasma is complicated due to the molecular complexity of plasma (e.g. lipoproteins and soluble factors). Here, we present a standardized imaging flow cytometry (IFCM)-based methodology to determine the concentration and phenotype of human plasma-derived EV without prior isolation of EVs. Methods All experiments were performed on an ImageStreamx (MkII) IFCM. Sub-micron polystyrene beads with different sizes and fluorescent intensities were used to convert arbitrary SSC signals into standardized units by application of Mie theory (to relate the scatter intensity of events to their size based on their refractive index). Fluorescence signals were calibrated using Equivalent Molecules of Reference (ERF) beads. Platelet-Poor Plasma (PPP) from 5 healthy individuals was diluted ~13-fold in 0.20  $\mu$ m filtered PBS, and directly stained with the tetraspanin EV markers CD9, CD63 or CD81 (all conjugated with APC), or a mix of the three markers in combination with CFDA-SE. No prior

# CYTO 2022 ABSTRACTS

isolation of EVs or washing steps were performed. Acquisition time of samples was standardized at 180 seconds, and assay controls as recommended by the MIFlowCyt-EV framework were used in all experiments. Results An assay was developed to analyze single fluorescent particles  $\leq 400$  nm in unprocessed PPP was developed, and, following detergent treatment (to discriminate vesicular signals from artefacts),  $\sim 94\%$  of double-positive fluorescent events (CFSE+Tetraspanin+) were identified to represent EV ( $5.61E7 \pm 3.36E7$  objects/mL, mean  $\pm$  sd ). Concentrations of double-positive events were linearly proportional to the dilution factor ( $R^2 = 0.93$ ) while the ERF of both fluorescent signals remained stable: mean 119.57 (range 99.6-156) for CFSE and mean 65.33 (range 61.3-69.8). Conclusion We successfully developed a standardized (both size and fluorescence) IFCM-based methodology to discriminate, identify and determine the concentration of single EVs  $\leq 400$  nm in complex mixtures such as human plasma without prior purification or isolation of EVs. Additionally, we demonstrate all relevant assay controls as recommended in the MIFlow-Cyt-EV framework. In summary, we provide a framework that will allow researchers to study the full spectrum of plasma-derived EVs, expanding on the usage of EVs as non-invasive biomarkers in the clinic. We expect that this methodology, after validation of markers of interest, will be useful for EV analysis in many different sample types and in a plethora of clinical settings.

**80**  
898803

## Quantitative Analysis of Molecular Cargo Transfer From Cells To EVs

John Nolan<sup>1</sup>, Erika Duggan<sup>2</sup>

<sup>1</sup> Stanford University School of Medicine, <sup>2</sup> Scintillon Institute

**Introduction.** EVs carry molecular cargo from their cell of origin, but the mechanisms of cargo selection and loading into EVs are not well understood. We used quantitative single cell and vesicle flow cytometry to measure membrane protein expression on cells and EVs. **Methods.** PC3 cells were cultured, media collected, and EVs concentrated using ultrafiltration (100K MWCO). Cell surface markers were measured by flow cytometry (FC). EV concentration, size, and cargo were measured by single vesicle flow cytometry (vFC). Instruments were calibrated and intensity reported in units of antibodies per cell or EV. **Results.** PC3 cells express surface markers at high ( $>250K$  median copies/cell: CD71, CD29, CD44, CD54), medium (50K-250K copies: CD9, CD63, CD49f) and low ( $<50K$

copies: CD81, EPCAM, EGFR, STEAP-1) abundances. Cell permeabilization reduced staining for CD9 and CD81 (due to disruption of the plasma membrane), and increased staining for CD63 and STEAP1 (due to accessibility of internal antigen). EVs expressed detectable ( $>\sim 10$  PE MESF) CD9, CD63, CD81 and CD29, with a fraction ( $\sim 50\%$ ) also staining with AnnV. Expression was proportional to EV surface area, with surface densities ranging from a background of  $\sim 10$  molecules/ $\mu m^2$  to  $>1000$  molecules/ $\mu m^2$  for high abundance targets. Several high abundance markers (CD71, CD44, CD54) were not detectable on EVs, suggesting differential packaging of cell surface cargo into released EVs. CD63 was expressed at low abundance overall, but a subset of smaller EVs ( $<100$  nm) expressed CD63 at high surface density ( $\sim 1000$   $\mu m^2$ ). **Conclusions.** We find that the abundance and surface density of cargo on vesicles can be higher or lower than on the cell of origin. Some abundant cell surface molecules (CD71, ICAM, CD44) were undetectable on EVs, while others (CD9, CD81, CD29) were present at surface density similar to cells. CD63 was present at high density on smaller EVs, consistent with enrichment of CD63 on small exosomes formed inside the cell.

**82**

## Performance Enhancement of Immunity: Pushing the Design and Engineering Envelope in T Cell Manufacturing

Bruce Levine Ph.D.<sup>1</sup>

<sup>1</sup> University of Philadelphia

Since the 1990's, we have conducted clinical trials of gene modified T cells. Gene editing has created T cells resistant to HIV infection. Chimeric antigen receptor (CAR) T cells targeting CD19 on B cells leukemias and lymphomas have induced durable complete responses in patients who are relapsed or refractory to all other available treatments. New designs for genetically modified T cells include switches and potency enhancements that will be required for targeting solid tumors. In one such approach, multiplex gene editing was accompanied by lentiviral transduction of a T Cell Receptor against the cancer antigen NY-ESO-1. The first use of CRISPR in the US in humans demonstrated that multiplex human genome engineering is safe and feasible. Translation of these technologies from research bench to clinical application requires knowledge of the critical quality attributes of the engineered cell product and acceptable limits. Determining dose, potency,

# CYTO 2022 ABSTRACTS

and anticipating pharmacokinetics of a living, dividing drug presents unique challenges. The road forward for wide patient access to engineered cellular therapies depends not only on scientific progress in targeting, gene modification and cellular manipulation methods, but also on meeting automation, engineering, clinical site onboarding, and health policy challenges.

---

## 83 Understanding Multiple Myeloma Resistance to CAR T cell Therapy through Single Cell Analysis

Michael Milone, MD, PhD<sup>1</sup>

<sup>1</sup> University of Philadelphia

Over the past decade, the survival of patients with multiple myeloma (MM), the most frequent hematologic malignancy, has significantly improved due to the advent of several new therapeutic options. Chimeric antigen receptor (CAR) T cells targeting B cell maturation antigen (BCMA) are one of the newest therapies to reach regulatory approval for multiple myeloma (MM). Despite marked anti-tumor activity of BCMA-targeted CAR T cells in MM, nearly all patients eventually progress, even those achieving MRD-negative complete responses. Application of single cell profiling of cells including single cell transcriptomic analysis to explore the mechanisms of CAR T cell therapeutic resistance observed in two phase I clinical trials of a BCMA-targeted CAR T cells will be discussed.

---

## 84 Mechanisms behind CAR T cells

Marcela Maus, VMD, PhD<sup>1</sup>

<sup>1</sup>Massachusetts General Hospital

ABSTRACT MISSING

---

## 85 Unleashing Immune Cells to Cure Multiple Myeloma

Krina Patel, MD

Multiple myeloma is an incurable hematologic malignancy that affects over 160,000 people in the US today. Chemotherapy has been the mainstay for treatment until 2014, when the first monoclonal CD38 antibody was approved. In the past 8 years, immunotherapy approaches to improve outcomes for MM patients have exploded. With the discovery of B cell maturation antigen (BCMA), antibody drug conjugates, bispecific T cell engagers and CAR T cells have been successfully armed to demonstrate the greatest response rates and progression free survival data ever seen for relapsed refractory MM patients. The majority of patients are still not

cured; however, survival has increased significantly. The discovery of additional antigens such as SLAMF7 or CS1, FCRH5, and GPRC5D have advanced knowledge and treatment approaches further. With these novel mechanisms of action and diverse antigens, physicians have learned how to manage unique toxicities. Exciting translational, clinical and outcomes data will be shared to demonstrate the significant improvements made thus far as well as reveal the gaps needed to be closed to finally find a cure for MM.



# CYTO 2022 ABSTRACTS

86

893667

## Engaging the un-Engaged and How to Keep Them

Gelo de la Cruz<sup>1</sup>, Alfonso Blanco<sup>1</sup>, Lourdes Arriaga-Pizano<sup>2</sup>

<sup>1</sup> Novo Nordisk Foundation Center for Stem Cell Medicine (reNEW), <sup>2</sup> IMSS Mexican Institute of Social Security

Organizer(s)/Facilitator(s): Gelo dela Cruz, Flow Cytometry Platform Manager, reNEW (NNF Center for Stem Cell Medicine, Denmark) Lourdes A. Arriaga Pizano, Senior Researcher, IMSS-Mexico Alfonso Blanco, Director of Flow, Flow Cytometry Core Technology (UCD Conway Institute), Ireland Associated Societies Subcommittee, ISAC Intended Audience: SRL personnel, society leadership, individuals in cytometry user groups, individuals in cytometry user/interest groups/societies who are interested in recruiting and retaining new members. Problem Focus/Abstract: Starting a cytometry user/interest group/society, be it at an institutional level or the national level, is not an easy task. There are different ways of creating these groups and these can vary from locality to locality and from country to country. However, what may be as important and probably more difficult, is both recruiting and retaining members. This workshop will focus on activities/initiatives that organizers of these groups have done and can do to recruit and retain members in our ever changing virtual and physical world. The workshop will not touch on how to start or establish a group as local conditions can vary by setting. Key Questions: 1. What activities did you do/can we do to increase membership in your society/group? 2. What activities did you do/can we do to keep your members engaged? 3. With the pandemic, what special activities did you do/can we do to recruit and retain members? 4. What should we NOT do to retain members? Format/Agenda: The format will be an open forum where audience-engagement tools (Slido/Poll Everywhere/ etc) will be used to gather information from the audience and encourage discussion.

87

89360<sup>1</sup>

## Can and If So How, Automation And Machine Learning Assist Timely Diagnosis And Prognosis In Everyday Clinical Routine?

Attila Tarnok<sup>1</sup>, Kamila Czechowska<sup>2</sup>, Ryan Brinkman<sup>3</sup>, Wolfgang Kern<sup>4</sup>

<sup>1</sup> University of Leipzig, <sup>2</sup> Metafora Biosystems, <sup>3</sup> University of British Columbia, <sup>4</sup> Munich Leukemia Laboratory (MLL)

There is quite a number of tools allowing for mining of complex flow cytometric data alone or in combination with patient's meta-data to describe retrospectively which parameter combinations are predictive. However, we cannot use these sets so far prospectively and implement it into everyday clinical use. The main reasons are lack of harmonized approaches towards samples testing, analysis and results interpretation. Moreover, there is a limited access to diseased sample databases and that disables development of powerful and robust diagnostic AI based tools. Despite the fact there is an increasing number of available algorithms that attempt to solve multi-dimensional data complexity problem, diagnostic assays data are not infrequently analyzed manually by laboratory analysts bringing significant bias in final results that can neither be controlled nor corrected. For many flow cytometrists it is not always clear which algorithms should be used for given data set as some degree of coding skills or advanced biostatistical knowledge is required. Despite the fact that more and more flow cytometric software developers implement automated data processing algorithms (clustering, cleaning, automated gating or annotations), these features are not commonly used as the solutions are not comprehensive, not intuitive or has user unfriendly interface. The consequence is that the analysts cannot take the full advantage of these software or even make bad choices and that impact the final result quality. 1. What are current pain points in the manual data analysis workflow for clinical flow cytometry data? (Time for manual analysis? Inter-operator variability? Lack of trust of automated results?) 2. What tools exist to address these and what are the challenges in their application individually and in aggregate and how could these be addressed? (Too high cost to research, evaluate and implement an automated approach?) 3. What additional advantages could automate approaches provide that cannot be addressed through manual analysis? Could we use as a start routine diagnostic test results along with augmented intelligence in the meantime to build a robust tool that would allow us to predict the course of the disease?

# CYTO 2022 ABSTRACTS

Workshop participants are especially those whose day-to-day professional activities would profit from availability of tools for automated data analysis: translational as well as CROs, Pharma scientists; haematopathologists, and laboratory technicians. Data scientists and software developers/manufacturers would provide great perspective and bring the know-how to the discussion. We plan to post a series of questions on the social media (Facebook and LinkedIn) every week prior as well as during congress to attract more participants and lead more focused live session at the workshop. Agenda: 1. Session starts introduction - 10 min 2. Case study presentation - 5 min 3. Work on case study - 30 min 4. Results summary - 15 min

**88**  
892952

## How Can SRLs Best Support High-Dimensional Data Analysis?

Laura Ferrer Font<sup>1</sup>, David Gravano<sup>2</sup>, Lauren Nettenstrom<sup>3</sup>

<sup>1</sup> Cytek Biosciences, <sup>2</sup> University of California Merced, <sup>3</sup> Fluidigm Canada Inc.

With the increase in the number of parameters that can be detected at the single-cell level, there has been a paradigm shift when handling and analysing high-dimensional data sets. SRLs already take on the responsibility of ensuring users have resources and training in experimental design and operation of instruments and to ensure instruments meet quality control standards. However, the role of SRLs downstream during data handling and analysis is less clear cut and uniform. SRLs are in a pivotal position to support research in this context, but key questions need to be addressed first. -What is the role/responsibility of SRLs when it comes to supporting data analysis? -What data analysis services are most beneficial to SRL customers? -Do SRLs have sufficient staffing, resources, and expertise to play this role? In the absence of these things, how can SRLs still succeed in this context? The workshop will further aim to address practical considerations such as: How can data transparency be promoted and make these big datasets available? How to validate that the data has enough quality? Which platforms can be used for High-Dimensional data analysis and which skills are required? As input to the workshop we are planning to perform the following surveys: -Survey to SRL customers at various institutions asking their wishes for SRL support in data handling and analysis. -Survey to SRLs via Purdue list inquiring about their current support and plans to support data handling and analysis. As output of workshop

we will provide a summary of: -Recommendations for data handling and analysis support provided by SRLs. This will include examples of diverse SRLs and provide recommended solutions for each.

**89**  
892170

## Tools for Implementing Measurement Assurance in Every Laboratory Setting: Recent Advances

John Nolan<sup>1</sup>, Lili Wang<sup>2</sup>, Virginia Litwin<sup>3</sup>

<sup>1</sup> Cellarcus Biosciences, <sup>2</sup> NIST, <sup>3</sup> Charles River Laboratories

### Audience

- Research scientists, clinicians, advanced cell manufacturers, innovators, and manufacturers focused on generating comparable and quantitative flow cytometry for basic research, disease diagnosis, immunotherapies, or drug/vaccine development.
- ISAC Members wanting to contribute to best practices related to obtaining reproducible reliable data. Focus Flow cytometry and related technologies are used in a wide variety of laboratory settings—research (immunology, cell biology, cancer), clinical testing and diagnosis, veterinary, drug discovery and development, botany, microbial testing for food safety, environmental and marine biology. No matter the application or laboratory testing environment, every laboratory generating flow cytometry data should be focused on generating robust, reproducible and comparable data. But how to accomplish this objective is not straight forward. Thus, several international initiatives have been created in order to provide cytometrists tools to reach this goal. ISAC has had a large focus on generating robust, reproducible and comparable data since its inception. There has been substantial engagement from ISAC in the NIST, CLSI and EV FC WG projects. The National Institute of Standards and Technology (NIST) Flow Cytometry Standards Consortium, launched Feb, 21. The Consortium is part of the broader advanced therapy program at NIST whose purpose is to provide a neutral forum for stakeholders in the biotechnology/ healthcare sectors, government; to identify and address common measurement challenges; exchange ideas; accelerate the development of standards and reference materials for quantitative flow cytometry. The consortium expects to develop measurement solutions, standards and best practices that will enable more accurate measurements, improved reproducibility and comparability of measurement results. The Clinical and

# CYTO 2022 ABSTRACTS

Laboratory Standards Institute (CLSI) published H62 - validation of assays performed by flow cytometry Oct 21. CLSI H62 is a comprehensive document addressing all aspects of conducting flow cytometry measurement in regulated or non-regulated settings. It brings together information regarding best laboratory practices ranging from uncrating the instrument to reporting final results. ISEV-ISAC-ISTH EV Flow Cytometry Working Group published the MIFlowCyt-EV guidelines for single EV flow cytometry in 2020 and is completing a compendium of procedures and considerations for single EV flow cytometry for publication in 2022. MIFlowCyt-EV is a guideline for single EV flow cytometry covering pre-analytical steps, instrumentation and assays. It complements existing guidelines. Format Background: Brief presentations regarding the three key initiatives Discussion: Extended and interactive discussions

- Historical and current practices for rigorous and reproducible flow cytometry
- Strategies to implement processes for measurement assurance
- Identify unsolved problems in for future initiatives

**90**  
**893221**

## How Will Technical Innovations Shape the Future Of Cytometry?

Betsy Ohlsson-Wilhem<sup>1</sup>

<sup>1</sup> SciGro

FOCUS will be on two major technical areas: Microfluidics/non-fluidic lab-on-a-chip forms and super resolution imaging. Key questions include but are not limited to: 1) What distinguishes microfluidic chips from other lab-on-a chip formats? 2) What are the main characteristics and advantages of super resolution microscopes? 3) Which devices are currently on the market or under development? 4) What are the major challenges in developing assays using these formats? 5) What are the software challenges (digital cytometry?) in analyzing data from these devices? 6) What are the market barriers to commercialization of such devices? 7) How could commercialization of such devices advance both basic and clinical research? FORMAT/AGENDA (2 groups of 5-15 people/table; chairs can be added as needed to form a second circle around a given table) 5 minutes: Introduce the focus areas, the coordinators for each table, and the key questions to be discussed. 30 minutes: Participants will move into two groups (microfluidics/lab-on-a-chip; and super resolution microscopy)

with at least one CYTO Innovation committee member at each table. 20 minutes: Presentation of 5 minute summaries of discussions at each table and 10 minutes of questions/comments/discussion from all participants 5 minutes: Summary of the conclusions reached during the workshop DESIRED OUTCOMES

- Overall goal is to initiate and encourage on-going, potentially asynchronous discussions of novel technologies and the biological questions they may aid in addressing. . Table coordinators summarize each of the discussions at their table.
- Summaries of the discussions to be submitted to Cytometry Part A
- Individuals identify new potential collaborators
- Discussions and collaborations continue following CYTO 2022.

**91**  
**892909**

## Online Tools for Panel Design! Useful Resources or A Waste Of Time?

Marcus Eich<sup>1</sup>, and Steffen Schmitt<sup>2</sup>

<sup>1</sup> HI-STEM gGmbH, <sup>2</sup> German Cancer Research Center (DKFZ)

Intended Audience The workshop is directed to all scientists working with multiparameter panels to answer complex biological questions. That includes bench workers, but also principle investigators supervising projects as well as shared resource laboratory staff, who advises panel design to their users. We expect a group size of 20 to 40 participants to create an atmosphere for a lively discussion and exchange. Problem Focus/Key questions Panel design is getting more difficult since the biological questions, which come in focus, are also getting constantly more complex. Multiparameter analysis no longer contains 5 to 10 parameters, but rather up to 40. Therefore, an efficient selection of the fluorochromes spread over up to 7 lasers and their adequate combination with the marker of interest is crucial. In the meantime, many companies offer online tools to support that challenge, whereby the variety of these tools also increased enormously from simple spectrum viewer up to complex panel builder with many functions. Even if there are general accepted rules facilitating the planning of multicolor stainings, there is so far no consensus about the implementation of such newly available applications in the process of panel design. In that workshop we will discuss the role of the different online tools supporting panel design. We will figure out the following key questions:

# CYTO 2022 ABSTRACTS

- Overview of the available online tools
  - Advantages and disadvantages
  - Identification of most useful and accepted functions but also missing options
  - Reliability of online tools
  - Need of online tools
- Format/Agenda
1. Welcome & Aim of the workshop (5 min by Steffen Schmitt)
  2. Theory Introduction: Summary and comparison of spectrum viewer and panel builder (15 min by Marcus Eich)
  3. (Online) demonstration of the panel design workflow with an own 16-parameter panel (published as OMIP-059) using one of the available tools as an example. (10 min Steffen Schmitt)
  4. Discussion about the community's experiences
- The following questions will be discussed:
- Which spectrum viewer does the community use? Is there a favorite one and why?
  - For which purposes are they used?
  - Do they reflect the truth and are they reliable across different fluorochrome types?
  - Which panel builder does the community use? Is there a favorite one and why?
  - Which are the experiences about them?
  - Are functions (e.g. for spectral application or microscopy) missing? How well can those applications be combined?

(25 min by Marcus Eich and Steffen Schmitt)

5. Concluding remarks (5 min by Steffen Schmitt)

In the workshop we will use the service by [mentimeter.com](https://www.mentimeter.com) or comparable tools for short questionnaires to get an impression of the participants (level of experience, average of panel size, number of designed panels, used cytometers, usage of online tools, ...), to share them with the audience and to foster discussion.

# COPAS *Infinity*



## Increased sensitivity in a smaller footprint



- Gentle analysis and sorting of objects which are too large/too fragile for traditional flow cytometers
- Four instrument models cover the 2-1500  $\mu\text{m}$  range of sample particle sizes
- Up to three lasers
- Six optical detectors measure more than 31 different fundamental parameters for each object in a sample
- PIN diode detectors measure size, optical density and forward scattered light
- Four PMT detectors measure side scatter and fluorescence emissions
- Sorting chamber enclosed for aerosol containment
- UV sterilization enhances biosafety and sterility
- Fits conveniently in a biosafety cabinet



**BioSorter** – four **swappable FOCA** (flow cells) allow one core instrument to cover the entire 2-1500  $\mu\text{m}$  range of large particles.



**COPAS VISION** – Large Particle Flow Cytometer with real time **brightfield image capture**.

Visit us at **CYTO booth # 119**

Union Biometrica, Inc. • 84 October Hill Rd, Holliston, MA 01746 USA • +1-508-893-3115  
European Support Center • Ninovesteenweg 198/16, B-9320 Aalst, BELGIUM • +32 53.51.0246  
[www.unionbio.com](http://www.unionbio.com) • Email: [sales@unionbio.com](mailto:sales@unionbio.com)

# CYTO 2022 ABSTRACTS

MONDAY, JUNE 6

92

898217

## Distinct Intestinal Microbiota Phenotypes Identify Chronic Inflammatory Diseases

Lisa Budzinski<sup>1</sup>, Gi-Ung Kang<sup>1</sup>, Toni Sempert<sup>1,6</sup>, René Riedel<sup>1</sup>, René Maier<sup>1</sup>, Anne E. Benken<sup>2</sup>, Tobias Alexander<sup>2</sup>, Maria Roth<sup>2</sup>, Robert Biesen<sup>2</sup>, Tilman Kallinich<sup>5</sup>, Benjamin Moser<sup>3</sup>, Janine Büttner<sup>3</sup>, Anja Schirbel<sup>3</sup>, Carl Weidinger<sup>4</sup>, Britta Siegmund<sup>4</sup>, Bettina Bochow<sup>3</sup>, Stefanie Bartsch<sup>5</sup>, Kathleen Necke<sup>5</sup>, Leonie Lietz<sup>1,6</sup>, Jannike L. Krause<sup>1</sup>, James Cameron<sup>1</sup>, Katrin Lehman<sup>1</sup>, Gitta A. Heinz<sup>1</sup>, Ute Hoffmann<sup>1</sup>, Mir-Farzin Mashreghi<sup>1</sup>, Andreas Radbruch<sup>1</sup>, Hyun-Dong Chang<sup>1,6</sup>

<sup>1</sup> German Rheumatism Research Centre – A Leibniz Institute, Berlin, Germany, <sup>2</sup> Department of Rheumatology and Clinical Immunology, Charité Universitätsmedizin Berlin, Germany, <sup>3</sup> Department of Hepatology and Gastroenterology, Charité Universitätsmedizin Berlin, Germany, <sup>4</sup> Medical Department of Gastroenterology, Infectious Diseases and Rheumatology, Charité Universitätsmedizin Berlin, Germany, <sup>5</sup> Department of Pediatric Respiratory Medicine, Immunology and Critical Care Medicine, Charité Universitätsmedizin Berlin, Germany, <sup>6</sup> Department for Cytometry, Institute of Biotechnology, Technical University Berlin, Berlin

A hallmark of chronic inflammatory diseases (CID) is an alteration of the intestinal microbiota, titled dysbiosis. Experimental animal models strongly suggest that dysbiosis contributes to the disease. In clinical studies microbial 16S rRNA gene profiling by next generation sequencing has greatly contributed to our understanding of taxonomic alterations of the microbiome in disease, but has failed so far to identify bacteria or bacterial communities contributing to disease pathogenesis conclusively. We are using multi-parametric flow cytometry to analyze the human intestinal microbiota from stool samples on the single cell level and assess phenotypic properties of the bacteria, which may be important for the microbe-host interaction and reflect the intestinal communities' condition. We analyze the coating of patient's intestinal microbiota by isotype-specific staining of host immunoglobulins to capture the immunological context of their recognition by the host. In addition, we characterize microbial surface sugars with specific lectins, which may indicate metabolic conditions, adhesive ability and bacteria-host-crosstalk. Using our method, we discriminate distinct microbial community phenotypes in patients with different chronic inflammatory diseases (Crohn's

disease, ulcerative colitis, IgG4-related disease, juvenile idiopathic arthritis, rheumatoid arthritis). Using machine-learning approaches, we can delineate phenotypic clusters that allow robust classification of disease entities. This approach suggests that we can use multi-parametric microbiota flow cytometry of stool samples for diagnosis and disease-monitoring but also to identify intestinal microbial communities specific for certain diseases and potentially playing a role in disease pathogenesis.

93

898440

## Trust the Process: Bringing High-Dimensional Data Analysis Tools To A Modern CLL Diagnostic Workflow

John Quinn<sup>1</sup>, Wojciech Gorcyca<sup>2</sup>, Maria Pawlik<sup>3</sup>

<sup>1</sup> BD Biosciences, <sup>2</sup> BioReference Laboratory, <sup>3</sup> Bioreference Laboratories

Chronic lymphocytic leukemia (CLL) is the most common leukemia in adults. It is a low-grade lymphoproliferative disorder of mature B cells characterized by lymphocytosis and involvement of blood, bone marrow, spleen, and lymph nodes. Immunophenotyping by flow cytometry plays a crucial role in CLL diagnosis. Traditional workflows for CLL diagnosis involve multiple panels of reagents and a plethora of plots produced on manually created gates for pathologists to render a diagnosis. Herein, we describe a collaborative effort to create a new type of workflow that includes algorithmic gating to complement traditional manual gates and a dramatically reduced set of visualizations produced by dimensionality reduction. CLL is characterized by co-expression of B cell markers (CD19, CD20, CD79a) with strong expression of CD5, CD23 and often CD43. A host of other markers can be used for corroboration, and many additional markers have been shown to be associated with aberrant phenotypes. The assay we have been tasked with analyzing contains 32 markers spread across an array of phenotypes. Pathologists use the Matutes score (MS) to separate CLL from other B cell disorders. The system involves assigning point values to expression levels of a set of markers. Several of the authors are testing an expanded MS system that, in work beyond the scope of this abstract, is being evaluated to improve diagnostic accuracy. The expanded scale adds complexity, making it imperative to reduce the convolution of the data presented to pathologists to effectively test the new system. Toward that end, we have created an analysis pipeline that uses algorithmically derived parameters and visualizations,

# CYTO 2022 ABSTRACTS

with template-based manual gates for cross reference. Color-matched overlays, tSNE plots and multiparametric heat maps are included to allow pathologists to observe the expression of expected populations while simultaneously examining the data holistically for aberrant populations revealed by marker combinations traditional approaches are unlikely to detect. MS scores can be produced by looking at a concise set of plots and validated versus a compendium of pairwise plots. We have used FlowSOM for auto-gating, as the mapping it produces can be forward-propagated and have created an association of specific FlowSOM clusters with manually gated populations so familiar statistics can be evaluated. Additional clusters will be monitored over time for discriminatory power. In conclusion, we have created a workflow to help test a new CLL diagnostic system by providing pathologists with a vastly reduced output that provides holistic visualization using familiar color coding and terminology. We have mapped expected populations to FlowSOM produced clusters that can be forward-propagated. We have done this work with careful consideration of aesthetics, positing that the adoption of more automated technologies is highly dependent on the user experience.

**94**  
895403

## **Changes In The Ovarian Cancer Microenvironment Associated With Tumor Progression And Chemoresistance**

Alexander Xu<sup>1</sup>, Marcela Haro<sup>1</sup>, Sandra Orsulic<sup>2</sup>, Akil Merchant<sup>1</sup>

<sup>1</sup> Cedars Sinai Medical Center, <sup>2</sup> UCLA

Imaging mass cytometry (IMC) is revealing novel insights on tumor architecture, showing that the infiltration and interaction of immune cells, tumor cells, and stromal cells informs the functional activity of those cells and the whole tumor. Imaging analysis has long been used to study cancer and predict patient outcomes via H&E pathology and immunohistochemical (IHC) staining, and IMC is bringing a high-multiplexity revolution to that spatial analysis. Metastatic Ovarian Cancer responds poorly to standard platinum-based chemotherapy for yet unknown reasons. Studying stroma, tumor, and immune subsets such as T cells, B cells, and macrophages alone with standard imaging methods like H&E has revealed limited insights, but without highly multiplexed imaging a unified picture of how these cells interact has not emerged. Here we used IMC to analyze a cohort of 42 patients with paired primary tumor, concurrent tumor, and recurrent tumor after chemotherapy, where the recurrent tumor

emerged between 1 month and 5 years after treatment. While recurrence is extremely common after treatment, we sought to determine functional protein and spatial factors predictive of delayed recurrence and positive outcomes. We analyzed 260 patient samples in total and over 1.5 million cells using cell segmentation and single cell analysis pipelines to identify tumor cells and major immune and stromal cell types, and performed single cell spatial analysis to explore cellular interactions between these cells. First, we analyzed the same tissue using IHC and a machine learning classifier for H&E, showing that IMC reproduced the established imaging findings. Next, we used the multiplexing capability of IMC and found statistically significant differences in spatial architecture by early recurrence, with more stroma-tumor interaction and tumor clustering predicting poor outcomes. In contrast, immune infiltration and the formation of tertiary lymphoid structures was associated with delayed recurrence. This is the largest highly multiplexed ovarian cancer study to date, describing the phenotypes and structure of ovarian cancer in deep detail. We were able to match the architecture to tumors collected from the same patients over time, to show how spatial protein features were associated with early and late recurrence of the tumor.

**96**  
898258

## **Assessment Of Live-Cell Imaging And Flow Cytometry Methods For SARS-CoV-2 Pseudovirus Neutralization Assays Compared To A Surrogate Bead-Based Neutralization Assay**

Lili Wang<sup>1</sup>, Jerilyn Izac<sup>1</sup>, Edward Kwee<sup>1</sup>, Elzafir Elsheikh<sup>1</sup>

<sup>1</sup> NIST

Severe acute respiratory syndrome coronavirus 2 (SARS-CoV-2) virus, the cause of coronavirus disease 2019 (COVID-19), emerged in 2019 and has resulted in a global pandemic. Global efforts to dampen the effects of SARS-CoV-2 infection include mass vaccination, contact tracing, and therapeutic development. Developing broadly protective vaccines and determining titers of neutralizing antibodies (nAbs) against new variants are vital for combating the pandemic. Several methods to quantify nAb titer in patient serum have been established including live virus, pseudovirus, and ELISA-based neutralization assays. While the use of live pathogenic SARS-CoV-2 requires BSL-3 containment, surrogate neutralization assays offer better safety

# CYTO 2022 ABSTRACTS

and improve ease-of-use when implemented as an alternative. In this study, we developed pseudovirus neutralization assays that measure neutralization by both live cell imaging and flow cytometry. Briefly, nine serial dilutions of serum samples are incubated with VSV- $\Delta$ G pseudotype particles expressing the original SARS-CoV-2 spike protein with a GFP reporter for one hour at 37°C. The mixture then incubates with HEK293-hACE2-TMPRSS2 -mCherry target cells for 16 hours. Live cell imaging is performed using GFP fluorescence to monitor infection, enabling quantification of infection and neutralization dynamics. After imaging, cells are further processed and analyzed via flow cytometry, enabling rapid and high-throughput assessment of neutralization. To evaluate these methods, patient serum samples were processed through the cell-based neutralization assay and compared to a surrogate bead-based assay also developed by NIST. Comparing the neutralization (NT50) determined for all three assays, advantages and disadvantages of each assay will be discussed. Based on the data generated, the pseudovirus neutralization assays showed reliable performance for detecting varying degrees of neutralization against SARS-CoV-2 in patient serum samples.

**97**  
898430

## Measuring Apoptosis In Intact Multicellular Spheroids Using The Velocyt™ Large Particle, Multi-Stream Flow Cytometer

Matthew Saunders<sup>1</sup>, Valerie Sanchez<sup>2</sup>, John O'Rourke<sup>3</sup>

<sup>1</sup> BenuBio Inc, <sup>2</sup> Inserm, <sup>3</sup> BenuBio Inc

The use of 3D culture models for drug discovery and cancer biology has increased in recent years due to the unique advantages over traditional 2D cell culture techniques. Multicellular spheroid models can mimic the tumor microenvironment and are more representative of tumor specific signaling and gene expression pathways and more accurately predict the effectiveness of therapeutic agents including small molecule drugs and antibody-based biologics. A key application for 3D models is assessing apoptosis and cell death after drug treatment. Traditional methods use fluorescence microscopy to measure apoptosis which limits the number of spheroids analyzed and a protracted data analysis workflow. Alternatively, flow cytometry can be used for analysis after spheroid dissociation into single cells which is a labor-intensive workflow and results in losing spheroid spatial data. To address these challenges, we used the Velocyt<sup>®</sup> large particle, multi-stream flow

cytometer from BenuBio Inc. to perform a multiplex apoptosis assay on intact spheroids. In this assay, we treated spheroids with various drugs and measured apoptosis and cell viability on hundreds to thousands of intact, multicellular spheroids at each drug concentration. This workflow was greatly simplified compared to traditional flow cytometry and provided statistical power often lacking in microscopy methods. These studies illustrate how the Velocyt large particle flow cytometer can simplify the 3D cell model workflow leading to the rapid analysis of thousands of spheroids with increased biological insight

**98**  
898462

## Flow Cytometry Analysis Of Protein Expression Using Antibody-Oligonucleotide Conjugates Followed By Single-Cell CITE-Seq

Xiaoshan Shi<sup>1</sup>, Majid Mehrpouyan<sup>1</sup>, Stephanie Widmann<sup>1</sup>, Aaron Tyznik<sup>1</sup>

<sup>1</sup> BD Biosciences

Cellular Indexing of Transcriptomes and Epitopes by Sequencing (CITE-Seq) is a single-cell phenotyping method that utilizes antibody oligonucleotide conjugates (AOCs) to quantitatively detect proteins using sequencing. Despite increasing awareness and adoption of this advanced technique to study cellular heterogeneity and dynamics, detailed instructions on how to design an AOC panel and ensure reagent performance in biological relevant systems prior to sequencing is not fully available. A non-optimal AOC panel may increase the cost of single-cell CITE-seq experiment and reduce the quality of the results. In this work, we describe a novel and easy-to-use multiplex flow proxy assay in which multiple protein markers can be measured simultaneously using a combination of AOC reagents and dye-oligo conjugates by flow cytometry. By using the dye-oligo conjugates with complementary sequence to AOC reagents, we can achieve specific binding and evaluate protein marker expression in a multiplex way. This quality control assay is useful for guiding AOC panel design and confirming protein expression prior to sequencing. Importantly, the labeled cells can be directly isolated based on the specific fluorescence from dye-oligo conjugates using a flow cytometry cell sorter and processed for downstream single-cell multiomics. Using this streamlined workflow, we sorted natural killer cells efficiently using only AOC and dye-oligo reagents, avoiding the possibility of decreased marker resolution from co-staining cells with AOC and fluorescent antibody. This novel workflow provides a viable



# CYTO 2022 ABSTRACTS

option for improving AOC panel design and cell sorting efficiency, followed by single-cell CITE-Seq. For Research Use Only. Not for use in diagnostic or therapeutic procedures. BD is trademark of Becton, Dickinson and Company. © 2022 BD. All rights reserved. 0222

99

898524

## Identification Of Human Mesenchymal Stem Cell Biomarkers By Aptamer Cytometry

Henning Ulrich<sup>1</sup>, Ana Paula Santos<sup>1</sup>, Matthias Schiemann<sup>2</sup>

<sup>1</sup> University of Sao Paulo, <sup>2</sup> Cardiff University

Stem cells are capable of self-renewal and to differentiate into cell types with specified functions. Mesenchymal stem cells (MSC) are adult stem cells that can be obtained from different sources, including adipose tissue, bone marrow, dental pulp, and umbilical cord. They can either replicate, originating new identical cells, or differentiate into cells of mesodermal origin and from other germ layers, with promising applications in regenerative therapy. Although encouraging results have been demonstrated, MSC-based therapies still face a great barrier: the difficulty of isolating these cells from heterogeneous tissue environments. MSC are currently characterized by immunolabelling through a set of multiple surface membrane markers, including CD29, CD73, CD90 and CD105, which are also expressed by other cell types. Hence, here we identified new specific biomarkers for the characterization of human MSC using DNA aptamers produced by the SELEX (Systematic Evolution of Ligands by EXponential Enrichment) technique by flow and image cytometry. Our results showed that MSC of different origins bound to FITC- or FAM-labeled DNA candidate aptamers. Aptamer-bound MSC could be isolated by fluorescence-activated cell sorting (FACS) procedures, enhancing the induction of differentiation into specific phenotypes (chondrocytes, osteocytes, and adipocytes) when compared to the whole MSC population. Flow cytometry analyses revealed that candidate aptamers bound to 50% of the MSC population from dental pulp and did not present significant binding rates to human fibroblasts or lymphocytes, both used as negative control. Moreover, immunofluorescence, confocal imaging and image cytometry analyses revealed staining of MSC by aptamers localized in the surface membrane of these cells. To identify aptamer binding targets, we performed a pull-down assay using immobilized aptamers followed by mass spectrometry analysis. Overall, the proteins here identified as targets of MSC-selective

aptamers (proteases) and proteins related to vesicle formation may be cell surface MSC biomarkers, with importance for MSC-based cell and immune therapies. Acknowledgments: This work was supported by the Brazilian funding agencies FAPESP, CNP and CAPES.

100

893151

## Multiplexed Analysis Of Living Cells With SAFE Bioorthogonal Cycling

Jina Ko<sup>1</sup>

<sup>1</sup> University of Pennsylvania

Cells in complex organisms undergo frequent functional changes as they differentiate and respond to their environment, but methods to achieve longitudinal readouts combined with deep profiling are limited. Here, we introduce a bioorthogonal toolkit for multiplexed temporospatial profiling of living cells, applying scission-accelerated fluorophore exchange (SAFE) to first quench and then completely and durably remove immunofluorescent signals from labeled cells. We show that the chemistry is fast, achieving cycling in seconds at nanomolar concentrations, accordingly nontoxic, and functional in both dispersed cells and intact living tissues. The highly efficient scission machinery enables multiparameter ( $n \geq 14$ ), nondisruptive characterization of murine peripheral blood mononuclear cells and bone marrow, allowing serial profiling of cellular differentiation. We demonstrate longitudinal multiplexed immunofluorescence imaging of bone marrow progenitor cells as they develop into neutrophils over 6 days, piloting an approach that we anticipate will find broad utility for investigating physiologic dynamics in living systems.

101

898399

## Multiplex Flow Cytometry With Raman Tags

Ryo Nishiyama<sup>1</sup>, Shintaro Kawamura<sup>1</sup>, Kotaro Hiramatsu<sup>1</sup>, Mikiko Sodeoka<sup>1</sup>, Keisuke Goda<sup>1</sup>, Kosuke Dodo<sup>1</sup>, Kei Furuya<sup>1</sup>, Julia Gala de Pablo<sup>1</sup>, Shigekazu Takizawa<sup>1</sup>, Wei Min<sup>1</sup>

<sup>1</sup> The University of Tokyo

Studying multiple biological functions at a single-cell level is essential for understanding and controlling complicated biological systems. To this end, fluorescence probes are widely used in flow cytometry by virtue of their high chemical

# CYTO 2022 ABSTRACTS

specificity. However, the number of fluorescence probes that can simultaneously be distinguished is typically limited to less than ten in live cell measurements because of the overlap between broad fluorescence spectra of different probes. To break this limitation, spectral flow cytometry has recently been proposed and demonstrated to quantify many fluorescence probes by measuring their emission spectrum with an optical spectrometer. However, spectral flow cytometry requires multiple lasers to increase the number of colors, resulting in high complexity and cost. As another approach to break the limitation, mass cytometry has attracted much attention due to its high multiplexing capability (>100 colors). However, the destructive nature of mass cytometry limits its applications for time-course analysis or further downstream analysis such as RNA-seq after cell sorting. Here, we demonstrate multiplex flow cytometry with Raman tags, enabling multi-color, non-destructive, large-scale single-cell analysis. As the Raman spectral linewidth is much narrower than the fluorescence linewidth, >100 different Raman tags can theoretically be distinguished by spectral unmixing (<40 in fluorescence). Our method is based on the broadband (400-1600 cm<sup>-1</sup>) Fourier-transform coherent anti-Stokes Raman scattering (FT-CARS) flow cytometer. For multiplexing, we prepared 20 cyanine-based Raman-tags, which have many resonantly enhanced peaks in the spectral region of 400-1600 cm<sup>-1</sup>. Our strategy to increase the number of colors is adding functional groups at the edge of the conjugated system of the cyanine skeleton. Furthermore, hydrogens in the isoprene units are substituted with deuteriums. As these two methods do not significantly modify the absorption spectrum of the dyes, more than ten different Raman tags can be synthesized from a single cyanine skeleton without losing their resonance enhancement. To further enhance the sensitivity, we enclosed the Raman-tag molecules in polystyrene nanoparticles to generate Raman-active nanoparticles (Rdots). As more than 1000 Raman-tag molecules are enclosed in a single Rdot particle, signal intensity from a Rdot is ~1000x higher than that from a free Raman-tag molecule, enabling the limit of detection of 15 nM. As a proof of concept, we measured single-cell Raman spectra of 11,777 MCF-7 breast cancer cells stained with 12 different Rdots (~2000 cells for each color) at throughputs of 20–50 cells/s with a spectral acquisition time of ~750 μs/cell. With spectral unmixing, 11,544 out of 11,777 spectra were assigned to the true labels (accuracy = 98.0%), which shows the reliability of the present method and the capability of performing multi-color, non-destructive, large-scale cytometry

**102**

**898435**

## **Time-Lapse Flow Cytometry Using Laser Particle Barcoding Of Individual Cells**

Sheldon Kwok<sup>1</sup>

<sup>1</sup> LASE Innovation Inc.

Tracking immune cell responses due to stimulations or drug treatments often requires single-cell resolution due to heterogeneity of cell populations. However, as a one-time measurement, conventional flow cytometry is limited to comparing differences between treated and untreated samples, which can only identify changes in marker expression at the population-level. Such changes can also be difficult to interpret if specific cell types are more susceptible to dying than others, resulting in proportional differences that are not due to changes in marker expression or expansion of certain subtypes. Thus, there is a major need to enable time-lapse measurements with flow cytometry at the single-cell level. Here, we introduce time-lapse flow cytometry, a dramatically different approach that uses novel laser particles (LPs) to label and measure the same cells over time, including before or after treatment. LPs emit narrowband laser light (<0.5 nm) in the infrared wavelengths (1100-1600 nm) and do not interfere with typical fluorophores used in antibody staining. Each cell is tagged with a random combination of LPs to generate an optical barcode that is unique amongst millions of cells. In a typical experiment, LP-barcoded cells are analyzed in a first cycle to capture their baseline marker expression, then collected, treated in vitro and left to incubate. Cells are then measured again in a second cycle for the same markers as well as functional responses (e.g., intracellular cytokines). Matching of LP barcodes enables quantification of changes in marker expression at the single-cell level. In this presentation, we demonstrate time-lapse flow cytometry of human PBMCs. We show that LPs can be used to tag PBMCs without causing changes in viability, marker expression or cell function. We also verify that LP tagging can accurately track individual cells over multiple measurements, multiple days of incubation, and through cell processing steps such as fix/perm. Using time-lapse flow cytometry, we characterized PBMCs before and after stimulation with PMA/ionomycin. We identified downregulation of CD4 in CD3+ cells that was directly correlated with increases in TNFα and IFNγ secretion. We show that time-lapse flow enables unambiguous characterization of cells that were CD4+ cells pre-stimulation, which is not possible with conventional flow cytometry. Time-

# CYTO 2022 ABSTRACTS

lapse flow cytometry with laser particles expands the utility of flow cytometry beyond static profiling to dynamic, time-lapse analysis of cells at high throughput. The ability to track and measure cells over time enables study of single-cell responses to stimulation, drug treatments, or other interventions. The downregulation or upregulation of key biomarkers on individual cells can be quantified, which may be especially useful for confirming drug mechanisms of actions or for precision medicine applications.

**103**  
898505

## **Analysis of a 12-Color Panel Using a Compensation-Free Flow Cytometer with 6 Fluorescence Detectors**

Alan Chin<sup>1</sup>, Kshitija Shevgaonkar<sup>1</sup>, Elijah Kashi<sup>1</sup>, Jinman Huang<sup>1</sup>, Richard McKay<sup>1,2</sup>, William Telford<sup>3</sup>, Giacomo Vacca<sup>1</sup>

<sup>1</sup> R&D, Kinetic River Corp., Mountain View, CA, United States,

<sup>2</sup> Principal, Full Spectrum Scientific, LLC, East Windsor, NJ, United States, <sup>3</sup> Senior Associate Scientist, Center for Cancer Research, National Cancer Institute, Bethesda, MD, United States

**Background.** In flow cytometry, compensation is required to account for and remove the contribution of signal spillover between spectral channels. Although the technique of spectral flow cytometry can resolve some overlapping fluorophores, it requires spectral unmixing (i.e., another form of compensation) and it does not reduce the population spread associated with the spectral overlaps. To solve these problems, we have developed a time-resolved flow cytometry technology that distinguishes completely overlapping fluorophores based on differences in their fluorescence decay lifetimes. Using a clinically relevant 12-color panel we compare the results from our time-resolved instrument to those obtained using a spectral cytometer.

Since our platform uses both not only fluorescent intensity, but also fluorescence decay data, allowing for multiplexing within each physical detection channel, our system has the added advantage of requiring only 2 lasers and 6 detectors to detect all 12 colors. **Methods.** We used our compensation-free cytometer: the 15-parameter Arno platform. The platform uses two spatially separated, modulated excitation sources (Toptica iBeam 405 and 488); one FSC and two SSC channels; and 12 fluorescence detection channels (6 per laser), from violet to infrared. The 12 fiber-coupled fluorescence signals are sensed by only 6 physical detectors (Hamamatsu PMTs). Each detector collects light from two spectrally overlapping fluorophores, and

the contribution from each fluorophore is resolved using our proprietary time-domain multiplexing technology. Ultrastable sheath flow is established with our custom-built Shasta fluidic control system. Data acquisition is performed using 8-channel 1.25-GHz sampling on a National Instrument PXI platform and custom-written LabVIEW code. Signal processing is performed on a dedicated computing platform running custom-written algorithms. A Cytex Aurora spectral cytometer at the National Cancer Institute was used for comparison. **Results.** The populations obtained using our Arno platform are essentially equivalent to the populations obtained using the spectral cytometer. The key difference is that the panel run on the Arno platform required no compensation or spectral unmixing, and achieved its results with only 2 lasers and 6 detectors. **Conclusion.** We successfully demonstrated compensation-free flow cytometry using our Arno platform. The substantially simplified workflow using our compensation-free Arno platform promises to significantly ease the burden of panel design and analysis.

**104**  
894930

## **mRNA Vaccine-Induced T Cells Transition To A Resting Memory State Capable Of Rapid Proliferation And Differentiation To Effector Lineages Upon Antigen Re-Exposure**

Mark M. Painter<sup>1</sup>, Divij Mathew<sup>1</sup>, Rishi R. Goel<sup>1</sup>, Sokratis A. Apostolidis<sup>1</sup>, Kendall A. Lundgreen<sup>1</sup>, Mihir Kakara<sup>1</sup>, Ajinkya Pattekar<sup>1</sup>, Sigrid Gouma<sup>1</sup>, Amanda Hicks<sup>1</sup>, Harsh Sharma<sup>1</sup>, Sarah Herring<sup>1</sup>, Scott Korte<sup>1</sup>, Josephine R. Giles<sup>1</sup>, Oliva Kuthuru<sup>1</sup>, Scott E. Hensley<sup>1</sup>, Paul Bates<sup>1</sup>, Amit Bar-Or<sup>1</sup>, Allison R. Greenplate<sup>1</sup>, E. John Wherry<sup>1</sup>

<sup>1</sup> University of Pennsylvania

SARS-CoV-2 mRNA vaccines have shown remarkable clinical efficacy against infection in the months following vaccination and sustained protection against severe disease. mRNA vaccine-induced antibody responses are well-defined, with high levels associated with protection immediately after vaccination gradually waning over time. The increasing incidence of SARS-CoV-2 infections in previously vaccinated individuals has revived questions about the durability, quality, and functional relevance of vaccine-induced T cell responses, as these may contribute to reducing disease severity. Furthermore, the role of T cell immunity in immunocompromised individuals with difficulty generating effective antibody responses is also poorly understood. To advance

# CYTO 2022 ABSTRACTS

this understanding, we used both combinatorial MHC-I tetramer staining and activation induced marker expression following peptide megapool stimulation to analyze antigen-specific T cell responses from longitudinal samples collected before and after each of 3 doses of mRNA vaccine. Vaccination induced rapid antigen-specific CD4 and CD8 T cell responses in SARS-CoV-2 naive subjects after the first dose. After an initial contraction from peak levels, SARS-CoV-2 Spike-specific CD4 and CD8 T cell responses were durable, with minimal decay observed in a stable pool of antigen-specific memory cells from 3 to 9 months post-vaccination. These memory T cells were able to participate in recall responses upon administration of a third vaccine dose at least six months after completion of the initial two-dose regimen, with both antigen-specific CD4 and CD8 T cells expanding following booster vaccination. CD8 T cells that had transitioned into a stable memory phenotype at 6 months post-vaccination quickly re-acquired an effector phenotype following the third dose, affirming the functionality of mRNA vaccine-induced memory T cells. We compare these responses to those observed in SARS-CoV-2 infections in previously-vaccinated people to understand the potential contributions of vaccine-induced T cell memory in reducing disease severity. Moreover, we assessed T cell immunity in the context of ongoing immunosuppression, comparing the magnitude and phenotype of vaccine-induced CD8 T cell memory in immunosuppressed and healthy vaccinees. Taken together, we demonstrate that mRNA vaccination induces durable and functional antigen-specific memory T cells that can participate in recall responses following booster vaccination or infection.

**105**

898178

## **Validation and FDA Approval Of A High Parameter Intracellular Flow Cytometry Panel for the Detection of Th1 and Th2 Responses for Characterizing Antigen Specific T cell Responses to SARS-CoV-2 Infection and Vaccine Candidates**

Katharine Schwedhelm<sup>1</sup>, Kristen W. Cohen<sup>2</sup>, M. Juliana McElrath<sup>1</sup>, Stephen C. De Rosa<sup>3</sup>

<sup>1</sup> Fred Hutchinson Cancer Research Center, <sup>2</sup> Ozette Technologies, <sup>3</sup> Partillion Bioscience Corporation

In response to efforts to combat the SARS-CoV-2 pandemic through a safe and efficacious vaccine, the HIV Vaccine Trials Network (HVTN)/COVID-19 Prevention Trials Network (CoVPN) developed and validated a 27-color intracellular cytokine staining (ICS) flow cytometry assay to characterize antigen-specific T-cell responses to both SARS-CoV-2 natural infection and vaccine candidates. The panel built upon prior experience creating high-parameter assays for HIV vaccine research that prioritized detecting Th1 cytokines. This new panel was designed to maintain sensitivity for Th1 markers (IFN-g, IL-2, TNF-a, and CD154 (CD40L)), while incorporating additional markers for sensitive detection of Th2 cytokines (IL-4 and IL-5/13). Th2 markers were of particular importance and interest as there was suspicion that severe disease in some COVID-19 cases, and vaccine-enhanced respiratory disease in SARS-CoV and MERS-CoV candidate vaccines, were associated with a Th2-biased inflammatory response. In assessing potential SARS-CoV-2 vaccine candidates, reliable detection of both Th1 and Th2 phenotypes would contribute to alleviating concerns over potential Th2 skewing. The approach to the validation was based on the FDA document (May 2018): Bioanalytical Method Validation Guidance for Industry and the International Conference on Harmonization (ICH) Q2(R1) guidance document (2005), with some modifications as the ICS assay measures functional cellular responses and differs in some important respects from a bioanalytical assay. Four assay parameters were validated for Th1 and Th2 response: accuracy and precision, sensitivity/LLOQ, specificity, and linearity. Guidance from the FDA in preparation for validation provided valuable insights regarding the experimental approach. Samples with SARS-CoV-2-specific responses, from prior infection or vaccination, must be used. Batch controls must also trend these specific responses. These samples did not exist at the beginning of the pandemic, thus

# CYTO 2022 ABSTRACTS

some validation testing that had previously been initiated with HIV vaccine trial samples with HIV-specific responses needed to be repeated when convalescent samples with spike-specific responses became available. For a batch control, ample PBMC from a leukapheresis with a suitable response were obtained. In the validation assays, for the Th1 and CD8+ T cell responses, samples with spike-specific responses were used. Th2 cytokines were assessed using selected HIV-vaccine trial samples with HIV-specific Th2 responses as Th2 responses were rarely observed in previous analyses of COVID-19 vaccine recipient or convalescent samples. This achievement demonstrates the feasibility of a rigorous validation of a functional cellular assay for both Th1 and low-level Th2 responses. While this panel is currently being used in the context of COVID, the approach described here can be applied to other novel functional flow cytometric assays used to assess HIV, tuberculosis, and malaria vaccines.

106  
898506

## Remodeling of T cell Dynamics During Long COVID is Dependent on Severity of SARS-CoV-2 Infection

Katarzyna Piwocka<sup>1\*</sup>, Milena Wiech<sup>1#</sup>, Piotr Chroscicki<sup>1#</sup>, Julian Swatler<sup>1†</sup>, Dawid Stepnik<sup>1†</sup>, Sara de Biasi<sup>2</sup>, Michal Hampel<sup>3</sup>, Marta Brewinska-Olchowik<sup>1</sup>, Anna Maliszewska<sup>3</sup>, Katarzyna Sklinda<sup>4</sup>, Marek Durlak<sup>3,5</sup>, Waldemar Wierzbica<sup>6,7</sup>, Andrea Cossarizza<sup>2</sup>

<sup>1</sup>. Laboratory of Cytometry, Nencki Institute of Experimental Biology, Polish Academy of Science, Warsaw, Poland; <sup>2</sup>. University of Modena and Reggio Emilia School of Medicine, Modena, Italy; <sup>3</sup>. Department of Gastroenterological Surgery and Transplantology, Central Clinical Hospital of the Ministry of Interior, Warsaw, Poland; <sup>4</sup>. Department of Radiology, Centre of Postgraduate Medical Education, Warsaw, Poland; <sup>5</sup>. Department of Gastroenterological Surgery and Transplantology, Centre of Postgraduate Medical Education, Warsaw, Poland; <sup>6</sup>. Central Clinical Hospital of the Ministry of Interior, Warsaw, Poland; <sup>7</sup>. University of Humanities and Economics, Lodz, Poland

# These authors have contributed equally to this work

Several COVID-19 convalescents suffer from the post-COVID-syndrome (long COVID), with symptoms that include fatigue, dyspnea, pulmonary fibrosis, cognitive dysfunctions or even stroke. Given the scale of the worldwide infections, the long-

term recovery and the integrative health-care in the nearest future, it is critical to understand the cellular and molecular mechanisms as well as possible predictors of longitudinal post-COVID-19. The immune system and T cell alterations are proposed as drivers of post-COVID syndrome. Despite the number of studies on COVID-19, many of them addressed only severe convalescents or short-term responses. Here, we performed longitudinal studies of mild, moderate and severe convalescents, at two time points (3 and 6 months from infection), to assess dynamics of T cells immune landscape, integrated with patients-reported symptoms. 59 COVID-19 convalescents (age 27-64) were divided by severity (mild, moderate, severe), based on lung lesions (CT) and type of applied oxygen therapy. Plasma levels of 13 cytokines were quantified by LEGENDplex™ HU Essential Immune Response Panel (BioLegend). CD4+, CD4+ Treg and CD8+ T cell immunophenotype was assessed by 30-color panel. For polyfunctionality of cytokine production, T cells (stimulated anti-CD3/CD28) were stained against CD4, CD8, Foxp3, TGF-β, IL-2, IL-17, TNF-α, IFN-γ or GranzymeB. Cells were analysed using full spectrum CYTEK Aurora cytometer (CYTEK Biosciences). Data were compensated, cleaned (FlowAI), imported into FloJo (BD) and analysed in R. Subsets were identified by unsupervised clustering (FlowSOM) and visualized by UMAP. For statistics the generalized linear mixed models (GLMM) was used. The long-lasting (over 3 months) common symptoms of long COVID were collected at the follow-up interview. T cells exhibit different, severity- and time-dependent dynamics, that in severe convalescents show polarization towards an exhausted/senescent state of CD4+ and CD8+ T cells and perturbances in CD4+ Tregs. In particular, CD8+ T cells exhibit high proportion of CD57+ terminal effector cells, decrease of naïve cells, Granzyme B and IFN-γ production and unresolved inflammation. Mild convalescents show increased naïve and decreased CM and EM CD4+ Treg subsets. Patients from all severity groups can be predisposed to long COVID symptoms, and fatigue and cognitive dysfunctions are not necessarily related to exhausted/senescent state and T cell dysfunctions, as well as unresolved inflammation found only in severe convalescents. Post-COVID-19 remodeling of T cells leads to distinct convalescent immune states at 6 months after infection. Attenuation of the functional polarization together with blocking Granzyme B and IFN-γ in CD8+ cells might influence post-COVID alterations in severe convalescents. Either the search for long COVID predictors or any treatment to prevent the post-COVID syndrome is mandatory in all patients, not only those suffering from severe COVID-19.

107

898555

## Baseline Immune Signatures Determine COVID-19 Severity

Thomas Liechti<sup>1</sup>, Yaser Iftikhar<sup>1</sup>, Massimo Mangino<sup>2,3</sup>, Margaret Beddall<sup>1</sup>, Charles W. Goss<sup>4</sup>, Jane A. O'Halloran<sup>5</sup>, Philip Mudd<sup>6</sup>, Mario Roederer<sup>1</sup>

<sup>1</sup> ImmunoTechnology Section, Vaccine Research Center, NIAID, NIH, USA, <sup>2</sup> Department of Twin Research & Genetic Epidemiology, King's College of London, London, UK, <sup>3</sup> NIHR Biomedical Research Centre at Guy's and St Thomas' Foundation Trust, London SE1 9RT, UK, <sup>4</sup> Division of Biostatistics, Washington University School of Medicine, St. Louis, MO, USA <sup>5</sup> Division of Infectious Diseases, Department of Internal Medicine, Washington University School of Medicine, St. Louis, MO, USA, <sup>6</sup> Department of Emergency Medicine, Washington University School of Medicine, St. Louis, MO, USA

SARS-CoV2 can cause severe or fatal COVID-19. Although mostly in elderly or individuals with co-morbidities, severe disease can also occur in younger and seemingly healthy individuals. Better knowledge of immunological risk factors contributing to severe COVID-19 is needed to improve current treatment options. Genetic analysis revealed that variants in chromosomal regions of genes encoding for chemokine receptor and type I interferon system are associated with severe COVID-19. However, genetic analyses only enable the identification of associations between genes and disease but do not provide mechanistic insights. Here, we used high-dimensional flow cytometry in individuals recovered from non-severe and severe COVID-19 to gain insights into immunological mechanisms which lead to severe disease. Upon pathogen clearance the immune system largely reverts to baseline and reflects the pre-infection immune composition. Therefore, samples from recovered patients provide a valuable resource if cohorts with pre-infection samples are unavailable. However, since COVID-19 can cause long-term immune perturbations, we used linear regressions to distinguish immune traits which changed over time from those that return to baseline. Within these stable traits, we observed several chemokine receptors on NK cells and T cells which are differentially expressed in individuals recovered from non-severe and severe COVID-19. Thus, altered immune trafficking and tissue distribution may pose an increased risk for the development of severe COVID-19. In addition, we observed reduced levels of TIGIT on several T cell subsets in individuals recovered from severe COVID-19. TIGIT limits virus-induced

immunopathology in mice and may play a similar role in humans. Thus, reduced TIGIT expression may lead to increased tissue damage observed in severe COVID-19. Furthermore, we observed reduced abundance of plasmacytoid dendritic cells which are the main source of antiviral type I interferon. In addition, we observed decreased levels of IFNAR2 on monocytes and dendritic cells but not B cells in individuals recovered from severe disease. Thus, both the production of type I interferon and the responsiveness to type I interferon is altered in the innate immune system and may further contribute to the perturbed type I interferon observed in severe COVID-19. Our study reveals immune signatures which cause a potential predisposition for the development of severe COVID-19. These signatures suggest immunological mechanisms which are decisive for the development of severe COVID-19. Overall, our data supports current clinical trials to modulate immune cell trafficking using chemokine receptor inhibitors or the use of type I interferon to treat severe COVID-19 patients.

**108**

894659

## **Functional single-cell Proteomics of Glioblastoma Defines Extensive Drug Response Heterogeneity and Therapy-Induced Cellular Plasticity**

Dena Panovska<sup>1</sup>, Asier Antoranz<sup>2</sup>, Steven De Vleeschouwer Frederik De Smet<sup>1</sup>

<sup>1</sup> KULeuven, <sup>2</sup> CNRS, <sup>3</sup> UZ Leuven

Our inability to treat glioblastoma (GBM) has been attributed to excessive inter- and intra-tumoral heterogeneity in addition to cellular plasticity, which is reflected by the variable presence of multiple cellular states within each tumor. How each of the tumoral subtypes respond to therapy remains largely unknown. In this work, we developed functional diagnostic assays and analysis pipelines to measure therapeutic activity in freshly isolated GBM tumor cells at single-cell resolution using mass cytometry by time-of-flight (CyTOF). To do so, we designed a novel GBM-specific and therapy-tailored 28-plex antibody panel using a cohort of patient-derived GBM models (n=14), through which we observed marked heterogeneity across tumor cells to induce protein responses upon exposure to radiation therapy (RT) or a small-molecule MDM2 inhibitor (AMG232/KRT232). The identified patterns of single cell drug responses were used to create an integrative model to predict subsequent cytotoxic efficacy in freshly resected samples of newly diagnosed or recurrent GBM (n=34) patient or mouse samples which were ex vivo exposed to therapy within hours following surgery. In line with the difficulty to treat GBM, we generally observed only small groups of patients that showed substantial drug responsiveness, highlighting the need for more precise selection criteria of eligible patients in future clinical trials. We also observed therapy-induced cellular plasticity, which was most exacerbated for standard-of-care RT. Finally, even though therapy was aimed at tumor cells, we also recorded bystander drug response heterogeneity across tumor resident myeloid and T-cells, identifying excessive immune cell destruction in intrinsically resistant tumor samples. Fundamentally, this is the first study at scale to map therapy responses in the phenotypically diverse landscape of GBM across millions of live tumor and tumor-associated immune cells. Overall, our work offers a novel and highly cost/time effective functional precision medicine assay to select eligible patients for future clinical trials.

**109**

898424

## **Toward Ultra-High Parameter Spectral Flow: Probing and Overcoming The Limits Of Spread**

Peter Mage<sup>1</sup>, Andrew Konecny<sup>2</sup>, Florian Mair<sup>2</sup>, Martin Prlc<sup>2</sup>

<sup>1</sup> BD Biosciences, <sup>2</sup> Fred Hutchinson Cancer Research Center

Innovations in spectral cytometer design, paired with an expanded palette of commercially available fluorochromes, have brought flow cytometry close to realizing “ultra-high parameter” panels (defined here as 50+ colors) previously only possible using mass cytometry. However, despite the presence of well over 100 fluorochromes on the market and spectral cytometers with over 180 channels, published flow panels to date have not crossed the 50-color threshold. While panel size on conventional instruments was limited only by the number of detectors, panel size on spectral cytometers now appears to be limited by a progressive deterioration of the signal-to-noise ratio of unmixed data that occurs as the degree of spectral overlap in a panel increases. Metrics like dye similarity and panel complexity partially describe this effect, but flow practitioners working near the upper limit of panel size still face unresolved questions: (1) what sets the panel size limit on a spectral cytometer? (2) why does fluorochrome choice affect unmixed data quality? and (3) how can fluorochrome sets for ultra-high parameter panels be selected in practice? Here we present a clear mathematical analysis, with supporting experimental data, that explains how panel size, fluorochrome choice, and unmixed data quality are interrelated. Using statistical estimation theory, we derive an analytical model for how raw measurement noise maps to unmixed data in a spectral cytometry panel, and we show how this mapping depends on the full set of fluorochromes in the panel. This model reveals two key modes by which noise is introduced into unmixed data, both through exacerbated “spillover spreading” between pairs of fluorochromes and through a previously unexplained mode independent of coexpression. As the overall degree of spectral overlap increases in a panel, these two modes combine to eventually produce an unusable degree of variance (i.e., spreading) in unmixed data, effectively defining an upper limit for feasible panel size given a specific instrument and set of available fluorochromes. Building on this model, we next demonstrate a practical and systematic approach for assessing feasible fluorochrome sets for ultra-high parameter panels using single-stain data alone. We show that the effect of fluorochrome choice on unmixed spread can be evaluated by unmixing the same raw single-stain data under

# CYTO 2022 ABSTRACTS

different panel conditions. We built a Python tool that automates this analysis with supporting visualizations and comparison metrics for evaluating panel-dependent spread across different fluorochrome sets. Finally, we designed an automated algorithm that can identify feasible fluorochrome sets for a given panel size, even in the presence of extreme spectral overlap. We used this approach to identify feasible fluorochrome sets for ultra-high parameter panels on multiple instruments across manufacturers. Add authors: Bipulendu Jena, Aaron Middlebrook, Aaron Tyznik (BD Biosciences)

**110**  
898556

## Quantifying Neural Cell Identity With Mass Cytometry in Ex Vivo Cultures Of Primary Human Glioblastoma

Jonathan Irish<sup>1</sup>, Stephanie Medina<sup>1</sup>, Alejandra Rosario-Crespo<sup>2</sup>, , Amanda Kouaho<sup>1</sup>

<sup>1</sup> Vanderbilt University, <sup>2</sup> University of Puerto Rico

Background: Glioblastoma (GBM) is the most common primary brain tumor in adults and remains poorly understood at the cellular level despite being highly aggressive and nearly always fatal. Recent work in the Irish and Ihrle labs identified two GBM cell subtypes with distinct biological phenotypes whose abundance stratifies patient survival. One type, Glioblastoma Negative Prognostic (GNP) cells, was distinguished by elevated cell signaling (phosphorylation of STAT5, AKT, and S6) and abnormal co-expression of proteins normally restricted to neural stem cells or differentiated astrocytes (SOX2 and S100B, respectively). While clinically significant, the GNP cell subset is not well represented in GBM cell lines and it is not known whether GNP cells depend on the observed signaling. Here, a mass cytometry panel focused on neural differentiation and neural stem cells was applied to track the impact of kinase inhibitors in ex vivo cultures of primary human GBM. Methods: Mass cytometry was used to measure 47 features per cell, including neural cell identity proteins and phospho-proteins. Dimensionality reduction with t-SNE, T-REX (Barone et al., eLife 2021), and biaxial gating approaches were used to quantify the abundance of neural cell types and track changes in signaling and cell identity. Cells collected with informed consent from a primary human GBM tumor were treated for 24 hours with kinase inhibitors imatinib, tofacitinib, and rapamycin to target hallmark signaling nodes active in GNP cells. over Ex vivo culture experiments also varied conditions and tracked neural stem

cells and cells with features of differentiated oligodendrocytes (SOX10), neurons (TUJ1), and astrocytes (S100B) after 7 days. Results: Following imatinib treatment, SOX2+/S100B+ GNP cells died via apoptosis (cleaved Caspase 3+). Cells persisting in cultures after treatment were phenotypically consistent with neural stem cells, seen in higher per-cell SOX2 protein and a lack of all differentiation markers. Changes in culture conditions had opposing impacts from kinase inhibition and increased expression of differentiation markers. For example, the removal of supplement B27 and non-essential amino acids (NEAA) caused GBM cells to adopt multiple differentiated phenotypes, including SOX10+ cells, S100B+ cells, and TUJ1+ cells. Conclusions: These results establish a core set of protein features for single-cell tracking of neural cell identity and demonstrate two ways to shift this identity in primary human tumor cells. First, inhibitor treatment killed key GBM cell subsets but resulted in a culture enriched for SOX2++ cells, supporting the idea that inhibiting multiple signaling pathways will be needed in GBM. Second, changing the culture media composition appeared to differentiate GBM cells. These results establish a framework for shifting GBM cell identity that may enable more effective targeting of therapy-resistant cells in human tumors.

**111**  
898409

## Developing an Imaging Mass Cytometry Immunophenotyping Panel for Non-Human Primate Tissues

Paula Niewold<sup>1</sup>, Marieke Ijsselsteijn<sup>1</sup>, Frank Verreck<sup>2</sup>, Simone Joosten<sup>1</sup>

<sup>1</sup> Leiden University Medical Centre, <sup>2</sup> BPRC

Non-human primates (NHP) are a pivotal model for translational research due to the close evolutionary relationship with humans. In addition, NHP are the main model for diseases that cannot be studied (unmodified) in other organisms due to specific pathogen tropism or divergent disease presentation, such as SARS-CoV-2, human immunodeficiency virus and Mycobacterium tuberculosis. NHP studies have generally focused on clinical parameters and peripheral immunological assays, with immunohistochemistry and immunofluorescence analysis providing low-parameter information on cellular organization within tissues. Recently, imaging mass cytometry (IMC) enabled the expansion of the number of parameters that can be analyzed while preserving spatial information. IMC permits the simultaneous analysis



# CYTO 2022 ABSTRACTS

of ~40 metal isotope-labelled antibodies within a tissue. The importance of analyzing spatial organization of cells, as well as their phenotype, to improve understanding of disease has been demonstrated in several contexts including cancer and infectious diseases. Such approaches are particularly relevant in NHP studies, as tissue organization and immune system are highly similar to humans, aiding translation. Archives of formalin-fixed paraffin-embedded (FFPE) tissue from historical NHP studies provide a great source for IMC studies to expand our knowledge of disease processes without requiring new animal experiments. The main challenge for the application of IMC to NHP tissue is limited knowledge on antibody clones suitable for FFPE NHP tissue. Therefore, we developed a pipeline to efficiently test cross-reactivity of anti-human FFPE antibodies in NHP and incorporate these in an IMC panel for NHP tissue. This resulted in an 18-marker backbone panel with space to customize for specific research questions. Functionality of this panel has been demonstrated in several tissues of rhesus and cynomolgus macaques. This first high-dimensional IMC panel for NHP tissues can be used to increase our knowledge of cellular organization within tissues and its effect on outcome of disease.

**112**  
898470

## **A Side-By-Side Comparison of CITE-seq and Flow Cytometry Data of the COVID-19 SARPAC Study**

Artuur Couckuyt<sup>1</sup>, Ruth Seurinck<sup>1</sup>, Annelies Emmaneel<sup>1</sup>, Sofie Van Gassen<sup>1</sup>, Yvan Saeys<sup>1</sup>

<sup>1</sup> VIB-UGent Center for Inflammation Research

The COVID-19 pandemic has led to an acceleration in studies researching therapeutics to improve and restore lung function in patients. The SARPAC [1] study, for example, found that inhaled leukine or sargramostim improved oxygenation levels over a treatment course of 5 days. This study provided interesting data: both Cellular Indexing of Transcriptomes and Epitopes by Sequencing [2] (CITE-seq) data and flow cytometry data are available of 32 patient samples. We focus on building the bridge between the two techniques by comparing pipelines and data distributions which is facilitated by the already available downstream analysis and results of the SARPAC study. The CITE-seq data was already preprocessed and antibodies (Abs) with a high zero-count were filtered out. Eventually, approximately  $4.0 \times 10^3$  cells per patient and 277 Abs were retained. The flow cytometry data was acquired with a 33 marker (27

fluorochrome) panel of which 27 were common with the CITE-seq data. The flow data was preprocessed using FlowJo and PeacoQC [3] and afterwards approximately  $1.0 \times 10^6$  cells per file were retained. We compared both techniques side-by-side by first matching the corresponding files and markers between the two. The next step was trying to make the data distributions more comparable by trying multiple transformations and normalisations, such as the logicle or the hyperbolic arcsine transformations on the CITE-seq antibody derived tag (ADT) counts. Afterwards, we performed an in-depth FlowSOM [4] analysis where we compared the MFIs and/or cell type abundances to investigate (dis)similarities and to understand how CITE-seq expression differs from flow cytometry data and vice versa. In conclusion, we hope to expose both the similarities and dissimilarities between CITE-seq and flow cytometry and clarify which (pre)processing steps can be applied commonly. This will lead to a better and deeper understanding of both techniques. [1] Bosteels, C. et al. Sargramostim to treat patients with acute hypoxic respiratory failure due to COVID-19 (SARPAC): A structured summary of a study protocol for a randomized controlled trial. *Trials* 21, 491 (2020). [2] Stoeckius, M. et al. Simultaneous epitope and transcriptome measurement in single cells. *Nat. Methods* 14, 865–868 (2017). [3] Emmaneel, A. et al. PeacoQC: Peak-Based Selection of High Quality Cytometry Data. *Cytometry A* n/a, (2021). [4] Van Gassen, S. et al. FlowSOM: Using self-organizing maps for visualization and interpretation of cytometry data. *Cytom. Part J. Int. Soc. Anal. Cytol.* 87, 636–645 (2015).

**113**  
898519

## **BACCHUS: Batch Alignment Using Canonical Correlation in a High-dimensional Unsupervised Setting**

Matei Ionita<sup>1</sup>, Wade Rogers<sup>1</sup>, Richard Schretzenmair<sup>1</sup>, Allison Greenplate<sup>1</sup>, Van Truong, Jonni Moore<sup>1</sup>, Derek Jones, Li-San Wang

<sup>1</sup> University of Pennsylvania

Batch effects often occur when biological samples are processed on multiple instruments or across different days. Human experts who manually gate cytometry data can account for batch effects by adjusting the position of gates between samples. But unsupervised computational methods are increasingly deployed, due to increases in throughput and panel size, as well as a need for reproducible analyses. Efficient use

# CYTO 2022 ABSTRACTS

of these methods requires unsupervised algorithms designed to correct batch effects. One can circumvent the problem by analyzing each sample individually, but then it is difficult to integrate results across samples. Another existing approach uses quantile normalization (1), but this processes each marker individually, rather than exploiting the multivariate nature of the data. We propose BACCHUS, a tool for batch alignment based on Canonical Correlation Analysis (CCA), which uses correlations between high-dimensional data points to align similar cells across batches. It is robust to differences in cell type proportions or local distortions among the batches. CCA has already been used (2) to align single cell data in the context of scRNA-seq or scATAC-seq, but not in the high-throughput world of cytometry. We found significant practical hurdles in adapting the existing tools to cytometry: their quadratic time and memory complexity require multiple days and 8TB of RAM to run on a dataset of 1 million cells and 30 markers. In contrast, BACCHUS scales linearly with the number of cells, so processing the same data takes a few seconds and 500MB of RAM. BACCHUS was evaluated in two experiments at Penn Cytomics and the Immune Health Project at the Perelman School of Medicine. First, a biological sample (PBMCs from a healthy donor) was aliquoted, with one aliquot run on a BD Symphony A5 SE (Spectrally Enhanced), and one on a BD Symphony A5 conventional flow cytometer, using the same 28-color panel. Second, a different sample (whole blood from a healthy donor) was aliquoted and run on two different CyTOF instruments using the Maxpar Direct Immune profiling assay. In both experiments, clustering was performed on data pooled from both batches, before and after batch alignment using BACCHUS. Before alignment, clusters reflected both cell type and batch of origin, whereas after alignment, batches were thoroughly mixed and clusters only reflected cell type. We further showed through back-gating that clustering on aligned data agrees with standard biological definitions of cell types. Our experiments demonstrate that BACCHUS can remove batch effects which arise from using different instruments and is easy to integrate in an unsupervised clustering pipeline.

<sup>1</sup> Van Gassen, Sofie, et al. "CytoNorm: a normalization algorithm for cytometry data." *Cytometry Part A* 97.3 (2020): 268-278  
Butler, Andrew, et al. "Integrating single-cell transcriptomic data across different conditions, technologies, and species." *Nature biotechnology* 36.5 (2018)

**114**  
**898537**

## **Reproducibility in Cytometry: Signals Analysis, Uncertainty Quantification, and Implications for Doublet Deconvolution**

Paul Patrone<sup>1</sup>, Matthew DiSalvo<sup>1</sup>, Anthony Kearsley<sup>1</sup>, Gregory Cooksey<sup>1</sup>

<sup>1</sup> NIST

Signals analysis for cytometry remains a challenging task that has a significant impact on uncertainty. Conventional cytometers assume that individual measurements are well characterized by simple properties such as the signal area, width, and height. However, these approaches have difficulty distinguishing inherent biological variability from instrument artifacts and operating conditions. As a result, it is challenging to quantify uncertainty in the properties of individual cells and perform tasks such as doublet deconvolution. We address these problems via signals analysis techniques that use scale transformations to: (I) separate variation in biomarker expression from effects due to flow conditions and particle size; (II) quantify reproducibility associated with a given laser interrogation region; (III) estimate uncertainty in measurement values on a per-event basis; and (IV) extract the singlets that make up a multiplet. The key idea behind this approach is to model how variable operating conditions deform the signal shape and then use constrained optimization to "undo" these deformations for measured signals; residuals to this process characterize reproducibility. Using a recently developed microfluidic cytometer, we demonstrate that these techniques can account for instrument and measurand induced variability with a residual uncertainty of less than 2.5% in the signal shape and less than 1% in integrated area. We also use the resulting UQ to formulate and validate a first-of-its kind ability to identify and deconvolve from fluorescence measurements alone the singlets that comprise a doublet.

# CYTO 2022 ABSTRACTS

**115**

898560

## **Alignment, Segmentation and Neighborhood Analysis in Cyclic Immunohistochemistry Data Using CASSATT**

Todd Bartkowiak<sup>1</sup>, Asa A. Brockman<sup>1</sup>, Rohit Khurana<sup>1</sup>, Rebecca Ihrle<sup>1</sup>

<sup>1</sup> Vanderbilt University

Cyclic immunohistochemistry (cyclHC) uses sequential rounds of colorimetric immunostaining and imaging for quantitative mapping of location and number of cells of interest. In addition, cyclic immunohistochemistry benefits from the speed and simplicity of brightfield microscopy for data collection, making the collection of entire tissue sections and slides possible at a trivial cost compared to other high dimensional imaging modalities. However, large cyclHC datasets (greater than 50 GB) currently require an expert data scientist to concatenate separate open-source tools for each step of image pre-processing, registration, and segmentation, or the use of expensive proprietary software. Here, we present a unified and user-friendly pipeline for processing, aligning, and analyzing cyclHC data - Cyclic Analysis of Single-Cell Subsets and Tissue Territories (CASSATT). CASSATT is a python based workflow that builds on open source packages and image analysis tools. CASSATT registers scanned slide images across all rounds of staining, segments individual nuclei, and measures marker expression on each detected cell. In addition to straightforward single cell data analysis outputs such as dimensionality reduction, clustering, cell population identification and quantification, CASSATT explores the spatial relationships between cell populations. By calculating the logodds of interaction frequencies between cell populations within tissues and tissue regions, this pipeline helps users identify populations of cells that interact - or do not interact - at frequencies that are greater than those occurring by chance. It also identifies specific 'neighborhoods' of cells based on the assortment of neighboring cell types that surround each cell in the sample. The presence and location of these neighborhoods can be compared across slides or within distinct regions within a tissue. CASSATT was first developed using a newly generated cyclHC dataset consisting of six GBM tissue sections processed through eight cycles of AEC based IHC staining. Additionally, it has been tested on a previously published tissue microarray dataset consisting of 107 cores processed through eighteen cycles of staining and imaging. Future planned expansions will

add functionality to process additional multiplex imaging data types such as mxIF, IMC, and spatial transcriptomics. CASSATT is a fully open source workflow tool developed to process cyclHC data and will allow greater utilization of this powerful multiplex staining technique.

**116**

## **Nucleoside-modified mRNA-LNP therapeutics**

Drew Weismann<sup>1</sup>

<sup>1</sup> University of Pennsylvania

Vaccines prevent 4-5 million deaths a year making them the principal tool of medical intervention worldwide. Nucleoside-modified mRNA was developed over 15 years ago and has become the darling of the COVID-19 pandemic with the first 2 FDA approved vaccines based on it. These vaccines show greater than 90% efficacy and outstanding safety in clinical use. The mechanism for the outstanding immune response induction are the prolonged production of antigen leading to continuous loading of germinal centers and the adjuvant effect of the LNPs, which selectively stimulate T follicular helper cells that drive germinal center responses. Vaccine against many pathogens, including HIV, HCV, HSV2, CMV, universal influenza, coronavirus variants, pancoronavirus, nipah, norovirus, malaria, TB, and many others are currently in development. Nucleoside-modified mRNA is also being developed for therapeutic protein delivery. Clinical trials with mRNA encoded monoclonal antibodies are underway and many other therapeutic or genetic deficient proteins are being developed. Finally, nucleoside-modified mRNA-LNPs are being developed and used for gene therapy. Cas9 knockout to treat transthyretin amyloidosis has shown success in phase 1 trials. We have developed the ability to target specific cells and organs, including lung, brain, heart, CD4+ cells, all T cells, and bone marrow stem cells, with LNPs allowing specific delivery of gene editing and insertion systems to treat diseases such as sickle cell anemia, Nucleoside-modified mRNA will have an enormous potential in the development of new medical therapies.

# CYTO 2022 ABSTRACTS

117

## Advancing Novel Therapies Through Cytometry Biomarker-Driven Clinical Trial Design

Cherie Green<sup>1</sup>

<sup>1</sup> Ozette Technologies

Clinical trials play an important role in objectively determining if drugs, vaccines, medical devices, or procedures are safe and effective for treating or preventing diseases and health conditions, thus adding to a growing corpus of medical knowledge. Clinical studies involve research using human volunteer subjects, also known as participants. There are two main types of clinical studies: interventional and observational studies. As more therapies target modulation of the immune system to fight diseases, such as antibody-based drugs and cell therapy; single-cell technologies have become the key tools to drive the advancement of novel biological therapeutics. Cytometry and single-cell genomic techniques are used to confirm target expression and receptor occupancy, demonstrate pharmacodynamic response, investigate resistance mechanisms, and measure depth of response through tumor burden at the site of disease. Cytometry-based biomarkers are also used for patient enrollment criteria and serve as protocol-defined gating criteria to advance clinical development such as moving from phase 1 to phase 2. With increasingly more novel treatment modalities such as bi- and tri-specifics, genetically-engineered cell therapy, and combination drug strategies, clinical trial design has become more complex. Clinical investigators and drug developers rely on biomarkers to understand disease heterogeneity, the status of the baseline immune landscape, and the changes in a patient's immune and disease profile after treatment to show efficacy and safety. Recently, there has been an emphasis on translational science and biomarker discovery to accelerate the drug development process. Through the application of novel computational approaches using machine learning (ML) and artificial intelligence (AI) to integrate biomarkers and clinical responses, we are gaining new insights beyond safety and efficacy. These insights hold the promise to accelerate the discovery of new targets, new combination strategies, and expansion into new disease areas. In this session, we will review the basic principles of clinical trial design with an emphasis on how immuno-oncology differs from non-oncology studies and how cytometry biomarkers and ML/AI approaches are used to advance drug development.

118

## Application of Flow Cytometry in Clinical Development of Vaccines Against Infectious Diseases: Benefits And Challenges

Stéphane Pillet<sup>1</sup>

<sup>1</sup> Medicago

Identification of a clear correlate of protection across all populations is one of the 'Holy Grails' in vaccine development. The protective role of humoral immunity has been repeatedly supported by the presence of high immunoglobulin titers in protected subjects, the protection provided by the placentally-transferred maternal antibodies to the neonate and by passive immunization in both animal models and human trials. Low cost and convenience of serologic assays have contributed to make antibodies the surrogate of choice for the development of vaccines against infectious diseases.

Despite the crucial role that cell-mediated immunity (CMI) provides in protecting against many infectious diseases, T cell response has been under-investigated in vaccine clinical trials, mainly due to logistics, cost considerations and difficulties in establishing widely-accepted standards for data collection and analysis. The situation has evolved in the last decade with a growing number of infectious disease vaccine clinical trials including CMI outcomes with the encouragement of regulatory agencies to better characterize T cell responses. This was particularly true during COVID-19 vaccine development as there were early fears that an inappropriate Th2 response might promote vaccine associated enhanced disease (VAED). Although VAED has not been reported in any animal model or clinical trial during the development of SARS-CoV-2 vaccines, this concern illustrates the importance of characterizing both humoral and cellular responses. Flow cytometry is an essential tool not only to understand the mechanism of action of vaccines and differences in the responses of target populations, it also allows for better risk assessment. With the success of ongoing standardization efforts, detailed studies of vaccine-induced CMI will likely make a steadily greater contribution to the development of more effective and safer vaccines.

# CYTO 2022 ABSTRACTS

**119**

## **Flow Cytometry Is A Powerful Tool For Informing On Dosing Decisions In Early Drug Development**

Michelle Graham<sup>1</sup>

<sup>1</sup>Abbvie

An overview of practices and methods that can be implemented to increase data quality and the overall value and utility of flow cytometry in clinical trials will be presented. Current challenges for CROs and the integration of possible solutions into daily practice will be discussed. An overview of the impact of the changing regulatory environment on daily practice will be included in the presentation.

**120**

## **Single-Cell Multi-Omics Analysis Reveals Novel Inflammatory Associations in Cardiovascular Disease**

Helen McGuire<sup>1</sup>

<sup>1</sup> University of Sydney

The importance of inflammation in the pathogenesis of atherosclerosis is well accepted, but the role of the adaptive immune system is not yet fully understood. To assess this relationship further, we performed genomic and mass cytometry analysis on the circulating peripheral mononuclear blood cells of human participants with and without coronary artery disease, as defined by atherosclerosis on CT coronary angiography. Our results demonstrate that specific T-regulatory subsets were related to increased odds of having coronary artery disease. An immune signature was developed using these cell subtype changes, and this was assessed using lasso modelling to confirm the robustness of the signature. A complementary analysis using imaging mass cytometry provided in situ detailed analysis of T cells in atherosclerotic tissue. These findings characterise the adaptive T-regulatory cell response seen in patients with atherosclerotic coronary artery disease, and may prove useful in future efforts to guide development of novel therapeutic targets.

**121**

## **Unraveling the Immune Involvement of Draining Sentinel Lymph Nodes in Melanoma Metastasis by Multiplexed Imaging**

Idan Milo<sup>1</sup>

<sup>1</sup> Weizmann Institute of Science

Tumors are spatially organized ecosystems that are comprised of distinct cell types, each of which can assume a variety of phenotypes defined by coexpression of multiple proteins. To underscore this complexity, and move beyond single cells to multicellular interactions, it is essential to interrogate cellular expression patterns within their native context in the tissue. We have pioneered MIBI-TOF (Multiplexed Ion Beam Imaging by Time of Flight), a platform that enables simultaneous imaging of forty proteins within intact tissue sections at subcellular resolution. In this talk, I will describe our application of multiplexed imaging to study the tumor immune microenvironment in the draining sentinel lymph nodes of melanoma patients, and how we combine it with additional modalities to guide target-selection and obtain mechanistic insight on tumor-immune interactions. Our work reveals archetypical organizations, linking molecular expression patterns, cell composition and histology, which are predictive of distant metastases and patient survival.

# CYTO 2022 ABSTRACTS

## TUESDAY, JUNE 7

124

### **Towards Quantitative and Standardized Flow Cytometric Assays**

Lili Wang, NIST

Recent advances in cell and gene therapies are revolutionizing health care by providing curative treatments for previously untreatable diseases. Flow cytometry has served as a critical measurement in the development, translation, testing, and release of products such as CAR-T therapy. Flow cytometry-based assays have been used to measure key quality attributes and/or critical quality attributes, including identity, quantity, and potency, of cellular therapeutic products. However, the lack of reproducibility and comparability of results across various flow cytometry platforms remain a major challenge.

Leveraging NIST's long history of collaboration with the World Health Organization (WHO) and other standards organizations in producing critically needed standards and reference materials for key assays such as HIV/AIDS monitoring, stem cell counting, and most recently, the first WHO serological antibody standard, NIST aims to develop standards towards quantitative flow cytometry. To address this need, NIST recently launched the Flow Cytometry Standards Consortium (FCSC) to help develop measurement solutions and standards needed to accelerate the translation, manufacturing, and approval of cell and gene therapies as well as other advanced therapies. The NIST FCSC also serves as a neutral forum for stakeholders from industries, government agencies, academia, and other organizations to identify and address common challenges, share best practices, and accelerate the development of standards and reference materials towards quantitative flow cytometry. As a part of this effort, NIST is providing metrology and standards development expertise to work with the community to accelerate the development of reliable solutions for emerging flow cytometry applications and better understand the capabilities of new instrumentation. The FCSC expects to develop measurement solutions, standards (including reference materials, documentary standards, data), and best practices for flow cytometry that will enable more accurate quantitation and improved reproducibility and comparability of measurement results. This presentation will provide an update on the current consortium activities.

125

### **Deep Geometric and Topological Representations for Extracting Insights from Biomedical Data**

Smita Krishnaswamy<sup>1</sup>

<sup>1</sup>Yale University

High-throughput, high-dimensional data has become ubiquitous in the biomedical sciences because of breakthroughs in measurement technologies. These large datasets, containing millions of observations of cells, molecules, brain voxels, and people, hold great potential for understanding the underlying state space of the data, as well as drivers of differentiation, disease, and progression. However, they pose new challenges in terms of noise, missing data, measurement artifacts, and the "curse of dimensionality." In this talk, I will show how to leverage data geometry and topology, embedded within modern machine learning frameworks, to understand these types of complex scientific data. First, I will use data geometry to obtain representations that enable denoising, dimensionality reduction, and visualization. Next, I will show how to combine diffusion geometry with topology to extract multi-granular features from the data for predictive analysis. Then, I will move up from the local geometry of individual data points to the global geometry of data clouds and graphs, using graph signal processing to derive representations of these entities and optimal transport for distances between them. Finally, I will demonstrate how two neural networks use geometric inductive biases for generation and inference: GRASSY (geometric scattering synthesis network) for generating new molecules and molecular fold trajectories, and TrajectoryNet for performing dynamic optimal transport between time-course samples to understand the dynamics of cell populations. Throughout the talk, I will include examples of how these methods shed light on the inner workings of biomedical and cellular systems including cancer, immunology and neuroscientific systems. I will finish by highlighting future directions of inquiry.

# CYTO 2022 ABSTRACTS

126

## Digital flow cytometry for single-EV analysis

Nicole Meisner-Kober

We have developed a multi-parametric high-throughput flow-based method for the analysis of individual extracellular vesicles (EVs), which are highly heterogeneous and comprise a diverse set of surface protein markers as well as intra-vesicular cargoes. Yet, current approaches to the study of EVs lack the necessary sensitivity and precision to fully characterize and understand the make-up and the distribution of various EV subpopulations that may be present. Digital flow cytometry provides single-fluorophore sensitivity to enable phenotyping single EVs with unprecedented precision and sensitivity. To further enhance the performance of digital flow cytometry, we have also developed a new class of fluorescent reagents with ultrahigh brightness and multiplexing capability.

I summarize our lab's recent progress in this exciting field and highlight the versatility of acoustofluidic tools for biomedical applications through many unique examples, ranging from the development of high-purity, high-yield methods for the separation of circulating biomarkers such as small extracellular vesicles (sEVs) and circulating tumor cells (CTCs), to our newly developed harmonic acoustics for a non-contact, dynamic, selective (HANDS) particle manipulation platform, which enables the reversible assembly and disassembly of cells. These acoustofluidic devices can precisely manipulate objects across 7 orders of magnitude (from a few nanometers to a few centimeters). Thanks to these favorable attributes (e.g., versatility, precision, and biocompatibility), acoustofluidic devices harbor enormous potential in becoming a leading technology for a broad range of applications, playing a critical role for translating innovations in technology into advances in biology and medicine.

127

## Acoustofluidic technologies for the manipulation of cells and extracellular vesicles

Han wei Hou

The use of sound has a long history in medicine. Dating back to 350 BC, the ancient Greek physician Hippocrates, regarded as "the father of medicine", devised a diagnostic method for detecting fluid in the lungs by shaking patients by their shoulders and listening to the resulting sounds emanating from their chest. As acoustic technology has advanced, so too has our ability to "listen" to the body and better understand underlying pathologies. The 18th century invention of the stethoscope allowed doctors to gauge the health of the heart; the 20th century invention of ultrasound imaging revolutionized the field of biomedical imaging and enabled doctors to diagnose a range of conditions in the fields of obstetrics, emergency medicine, cardiology, and pulmonology. In the last decade, a new frontier in biomedical acoustic technologies has emerged, termed acoustofluidics, which joins cutting-edge innovations in acoustics with micro- and nano- scale fluid mechanics. Advances in acoustofluidics have enabled unprecedented abilities in the early detection of cancer, the non-invasive monitoring of prenatal health, the diagnoses of traumatic brain injury and neurodegenerative diseases, and have also been applied to develop improved therapeutic approaches for transfusions and immunotherapies. In this talk,

128

## Title TBD

Daniel Chiu

We have developed a multi-parametric high-throughput flow-based method for the analysis of individual extracellular vesicles (EVs), which are highly heterogeneous and comprise a diverse set of surface protein markers as well as intra-vesicular cargoes. Yet, current approaches to the study of EVs lack the necessary sensitivity and precision to fully characterize and understand the make-up and the distribution of various EV subpopulations that may be present. Digital flow cytometry provides single-fluorophore sensitivity to enable phenotyping single EVs with unprecedented precision and sensitivity. To further enhance the performance of digital flow cytometry, we have also developed a new class of fluorescent reagents with ultrahigh brightness and multiplexing capability.

# CYTO 2022 ABSTRACTS

129

## Tales of life and death in the ocean from automated flow cytometry and imaging

Heidi Sosik<sup>1</sup>

<sup>1</sup> Woods Hole Oceanographic Institution

Our ocean planet depends on intricate natural ecosystems dominated by plankton. These microscopic organisms are stunningly diverse, highly dynamic, and exert major influences on productivity and biogeochemistry across local to global scales. Yet, many aspects of how and why marine plankton communities change through time and space remain poorly understood, in large part because traditional organism-level sampling strategies are not amenable to high frequency, long duration application. The advance of automated sensors is now addressing this gap and accelerating the pace of discovery. FlowCytobot, a submersible flow cytometer, and Imaging FlowCytobot, which includes integrated video imaging, are capable of rapid, unattended analysis of individual cells and colonies. Nearly two decades of high-resolution observations in U.S. coastal waters have provided measurements of 100s of millions of plankton, which in many cases can be classified to genus or species with automated analysis. These taxon-specific, high resolution records are revealing extraordinary detail about the biology and dynamics of these “unseen” ecosystems. This presentation will highlight vignettes that include parasitoid control of diatom blooms, dynamics of harmful algal blooms that threaten human health, sex and death in the plankton, and climate-related impacts on the phenology of picocyanobacteria.

130

## Cytometric dissection of cell functions and development in complex organs and tissues

David Galbraith<sup>1</sup>

<sup>1</sup>University of Arizona

Flow cytometry and sorting was devised for the study of eukaryotic cells that exist as natural single cell suspensions, for example those of blood. Over the last 50 years, developments in flow cytometry and sorting have provided a uniquely flexible platform for studying the coordinated contributions of different cells to the optimal functioning of multicellular organisms over generations. This required development (i) of methods for the separation of three-dimensional tissues into cell suspensions, (ii) of ways to identify different cell types within these suspensions, and (iii) of technologies to characterize these cell types, their roles within the organism, and the mechanisms regulating their cooperative function.

Using examples drawn predominantly from the plant kingdom, I discuss examples of each of these, and illustrate how they have advanced our understanding of plants, of complicated multicellular animals, and of cytometric technologies. A view to the future will also be provided.



# Spatial Biology Without Limits



Introducing

# CellScape™

PRECISE SPATIAL MULTIPLEXING

## The Next Generation of ChipCytometry™ Instrumentation

CellScape™ is an end-to-end solution for highly multiplexed spatial omics. Combining an advanced, purpose-built imaging system with easy-to-use fluidics for walk-away automation, the CellScape™ system accelerates exploration in the rapidly evolving field of spatial biology.



**Highly Multiplexed**

Measure virtually unlimited protein biomarkers on a single sample



**Throughput and Automation**

Analyze four samples at a time with walk-away automation



**Precision Imaging**

Combine high resolution and innovative High Dynamic Range for true single-cell quantification



**Versatile**

Open-source reagents, no proprietary conjugations

To learn more, visit us at  
[CanopyBiosciences.com/CellScape](https://CanopyBiosciences.com/CellScape)

 **canopy**  
BIOSCIENCES A BRUKER COMPANY

# CYTO 2022 ABSTRACTS

## POSTER SESSION 1 SUNDAY, JUNE 5

**897148 P1**

### **Adaptation of Standard Aerosol Containment Evaluation Procedure for use in BD FACSAria™ Fusion**

Paul Hallberg<sup>1</sup>, Shifu Tian<sup>1</sup>, Charles H. Pletcher, Jr.<sup>1</sup>, Jonni S. Moore<sup>1</sup>

<sup>1</sup> University of Pennsylvania

**Background/Introduction:** Flow cytometric cell sorting of biological specimens has become a common practice in biomedical research labs. Since electrostatic droplet cell sorters are known to generate aerosols, sorting specimens that may contain known or unknown pathogenic materials dictates the need for regular testing procedures to validate the adequate containment of aerosols to assure protection for the operator and environment from potential hazards. Benchmark procedures were described by Holmes et al 1 and Reifel et al 2 and have served as standard operating biosafety procedures to assure safe sorting of potentially infectious organisms and human cells. Here we present modifications to this procedure to validate the containment of aerosols on a BD FACSAria™ Fusion that is enclosed in a Baker Biological Safety Cabinet equipped with an integrated aerosol management system (AMS) in comparison to a standard BD FACSAria™ II cell sorter. These changes were necessitated by the design modifications on the BD FACSAria™ to provide an integrated solution to sorting biohazardous samples by the use of an integrated Aerosol Management System (AMS) in the Baker Class II Type A2 Biological Safety Cabinet (BSC) instead of using an external aerosol evacuation system (i.e., Buffalo Filter® Whisper) as published<sup>1</sup>. **Method/Results:** The BD FACSAria™ Fusion is constructed with sliding doors to access the sort block and collection chamber. These sliding doors are an improved design over the hinged doors on the BD FACSTM Aria II using a super magnet as a latch and rubber seals to contain aerosols when the doors are closed making the previous containment SOP not appropriate. In order to adapt the protocol, we had to partially open the lower collection door and mount the Cyclax-d cassette to the inside of the collection chamber. Note that opening the lower collection door does not enable the safety interlock for the lasers as with the upper sort chamber door. We then tested the change in procedure by performing multiple tests to simulate nozzle clogs and generate aerosols. Aerosol containment was

evaluated when the AMS was turned off and when the AMS was turned on. Failure mode was simulated with a positive control when the AMS was turned off. The positive control had excessive fluorescent particles that were too numerous to count and were visible on the coverslip from the Cyclax-d cassettes using an inverted fluorescent microscope. Conversely, aerosol containment was simulated with a negative control (AMS turned on). There were zero fluorescent particles on the coverslip. This result validates that the integrated Aerosol Management System (AMS) was working effectively to safely remove escaping particles through the AMS-HEPA filter system for safe operation of the BD FACSAria™ Fusion and provided a method to document this performance validation. Reference: 1. Kevin Holmes, et al., Cytometry Part A J Int Soc Anal Cytol, 85A: 434453, 2014 2. Kristen M.

**901356 P3**

### **Cognitive symptoms of long COVID after severe SARS-COV-2 infection correlate with prolonged production of IL-2 and TNF-α proinflammatory cytokines by CD8+ T cells**

Katarzyna Piwocka<sup>1</sup>, Milena Wiech<sup>1</sup>, Dawid Stepnik<sup>1</sup>, Piotr Chroscicki<sup>1</sup>

<sup>1</sup> Nenckie Institute of Experimental Biology PAS, Warsaw

The appearance of post-acute COVID syndrome (PACS), also called “long COVID” significantly decreases the quality of patients’ life. These symptoms include fatigue, shortness of breath and dyspnea but also a broad range of cognitive symptoms such as difficulties in concentration and memory (“brain fog”), sleep problems, depression and others. Despite the number of studies on COVID-19, proposing T cell alterations and neuroinflammation as very probable drivers of long COVID, many of them addressed only short-term responses. Therefore we have assessed the cognitive symptoms of PACS in severe convalescent patients at two time points (3 and 6 months from infection), to evaluate dynamics of T cells immune landscape. **Methods:** We have enrolled 20 patients (all male) at the age of 27-64, who have recovered from severe COVID-19 disease. CD4+, CD4+ Treg and CD8+ T cell immunophenotype was assessed by 28-color panel. For polyfunctionality of cytokine production, T cells (stimulated anti-CD3/CD28) were stained against CD4, CD8, Foxp3, TGF-β, IL-2, IL-17, TNF-α, IFN-γ, Granzyme B and CD107a. Cells were analyzed using full spectrum CYTEK Aurora cytometer (CYTEK Biosciences). Data

# CYTO 2022 ABSTRACTS

was compensated, cleaned (FlowAI), imported into FloJo (BD) and analyzed in R. Subsets were identified by unsupervised clustering (FlowSOM) and visualized by UMAP. For statistics the generalized linear mixed models (GLMM) was used. The long-lasting (over 3 months) common symptoms of long COVID were collected at the follow-up interview. Results: 9 out of 20 severe COVID-19 convalescents showed cognitive symptoms of PACS. Early after acute disease, patients with cognitive PACS symptoms were characterized by several elevated populations of CD8+ T cells producing IL-2 and TNF- $\alpha$ . At the same time we observed decreased levels of CD8+ T cells producing degranulation marker CD107a, which were the most frequent in patients without cognitive symptoms of long COVID. Later during convalescence (3 to 6 months post infection), successfully recovered patients showed polarization of CD8+ T cells towards an exhausted/senescent state, represented by a high proportion of CD57+ TE cells. This associated with significant reduction of Tregs, with high representation of naïve/resting cells and reduced frequencies of effector memory Tregs responsible for inflammation resolution. On the other hand, patients with PACS still possessed increased frequencies of activated CM and EM CD8+ cells. Similarly, Tregs producing CCR4 and CD39 remained at the level from 3 months earlier. Conclusions: Remodeling of T cells early after severe infection might influence their differentiation into memory subsets and attenuate effector functions. We suggest that attenuated polarization into the effector state together with chronic inflammation may be a prerequisite to post-acute COVID syndrome with cognitive dysfunctions. Foundation for Polish Science TEAM-TECH Core Facility Plus (POIR.04.04.00-00-23C2/17-00) grant.

**898466 P9**

## **Comprehensive mapping of innate and adaptive immune response dynamics across the blood and respiratory tract in COVID-19**

Thomas Ashhurst<sup>1</sup>, Wuji Zhang<sup>2</sup>, Nicholas King<sup>1</sup>, Katherine Kedzierska<sup>2</sup>

<sup>1</sup> The University of Sydney, <sup>2</sup> The University of Melbourne

Emerging viral diseases such as viral encephalitis or COVID-19 drive a complex immune response where the inflammatory process intended to eliminate an invading pathogen contributes to significant immunopathology, both at the site of infection and more systemically. To understand this response, careful analysis using high-dimensional (HD) cytometry and single-cell technologies are required. As the size and complexity of HD data continue to expand, comprehensive, scalable, and methodical computational analysis approaches are essential. Yet, contemporary clustering and dimensionality reduction tools alone are insufficient to analyze or reproduce analyses across large numbers of samples, batches, or experiments. Moreover, approaches that allow for the integration of data across batches, experiments, and technologies are not well incorporated into computational toolkits to allow for streamlined workflows. Here we utilised our analysis toolkit 'Spectre' to enable comprehensive mapping of the innate and adaptive immune response dynamics across the blood and respiratory tract in COVID-19. Our integrated analysis across the blood and respiratory tract reveal key changes in the myeloid lineage that drive disease severity over time. Using Spectre, we integrated our datasets with open source reference bone marrow datasets, revealing evidence of an inflammatory-derived acceleration of myelopoiesis and release of immature myeloid cells into the blood during severe disease. Additionally, carefully exploration of immune response in the respiratory tract allowed us to define a continuum of cellular infiltration from the blood into the airways, revealing key response patterns associated with disease severity and progression over time.

# CYTO 2022 ABSTRACTS

**899761 P11**

## **Polymer-based synthetic cells for next-generation multi-modal viability staining and analysis**

Martina de Geus<sup>1</sup>, Jason Deng<sup>1</sup>

<sup>1</sup>Slingshot Biosciences

We have developed new multi-modal viability compensation beads to address major shortcomings of current flow cytometry reagents for viability assays. Despite the fact that several DNA binding dyes are used to identify live cell populations, compensation beads for the DNA dyes are rarely available. In addition, existing polystyrene beads used for amine-reactive dyes have fundamentally different properties when compared to cellular material causing difficulties when trying to work with certain major classes of dyes in key fluorescence channels. Here we present data highlighting particles that are independently tuned along optical, fluorescent, genomic and biochemical parameters, generating a highly-flexible synthetic cell for viability characterization, an important measurement for cell therapy manufacturing, in particular. Our beads react with both DNA and amine-reactive dyes to provide clear separation between positive and negative signals for compensation or spectral unmixing. When decorated with other biomarkers, the beads mimic properties of biological cells for flow cytometry applications but in a consistent manner. This first-in-class technology enables a new paradigm for quantitative flow cytometry.

**901291 P13**

## **Expand your dry, multicolor panels with SuperNova Polymer Dyes**

Mehul Jivrajani<sup>1</sup>, Aditya Jarare<sup>1</sup>, Rajesh Venkatesh<sup>1</sup>, Shiva Ranjini Srinivasan<sup>1</sup>, Naina Arora<sup>1</sup>, Sumeet Chawla<sup>1</sup>, Gopinadh Jakka<sup>1</sup>, Teesta Roy Chowdhury<sup>1</sup>

<sup>1</sup> Beckman Coulter

Polymer-based fluorophores are getting much attention, as they provide remarkably bright readouts for better differentiation of cell subpopulations in flow cytometry workflows. However, because of their inherent nature, they tend to interact with each other and form aggregates. Hence, it is difficult to dry down panels containing two or more polymer-based fluorophores, and even liquid cocktails require specialized non-interaction buffer to avoid non-specific interaction. Beckman Coulter, known for its DURA (Dry Unitized Reagents Assay) innovation products, has developed a breakthrough technology enabling the dry down of multiple bright polymer SuperNova dyes in the same tube along with other conventional dyes (FITC, PE, ECD, etc.). The proprietary technology prevents non-specific interactions between the polymer dyes, and does not require addition of any non-interaction buffers. These tubes enable the same workflows as any DURA Innovations product, with lot-to-lot consistency, and have similar stability. These tubes are compatible with a range of lysis buffer such as Versalyse, Optilyse, IO Test lysing solution, etc. The novel technology can also be used to dry down antibodies for intracellular markers, beads and viability dyes. The panel performance shows good results without any non-specific interaction when compared to other competitors' conjugates. This technology allows users to extend the application of multicolor panels with a novel range of polymer dyes.

**901951 P15**

## **Using 3D Printing and Fabrication to Improve Cytometry Instrumentation**

William Schott<sup>1</sup>, Jarek Trapszo<sup>1</sup>, Austin Wilpan<sup>1</sup>

<sup>1</sup> The Jackson Laborator

In our Flow Cytometry SRL we purchase instrumentation which best meets our needs, however, no instrument is perfect. In operating our various cell sorters and analyzers we often find areas where the instrument could be improved for better functionality or enhanced user experience. In collaboration with the fabrication group at our institution we have made several

# CYTO 2022 ABSTRACTS

improvements to the functionality of our instrumentation. The most significant of these are improvements of the tube holders on our FACSymphony S6 cell sorter. We developed an adaptor capable of being moved forward and back as well as rotation adjustment with set screws to fix the alignment. This adaptor has a laser to illuminate side streams above the tubes which can be moved vertically to adjust for different sized tubes and swept in and out to align the laser with the side streams. We found this upgraded adaptor to greatly improve the set up process for 6-way sorting as the alignment of the streams to the tubes was never perfect with the stock apparatus. We created adaptors to hold 1.5ml and 5ml conical tubes in 5ml and 14ml chilled holders. To aid plate sorting set up, we created an ACDU adaptor with camera mount to visualize the plate sorting process. On our FACS Aria II we created an adaptor which allows us to use two of the S6 tube holders. On our LSR II we created a laser cover for the upgraded UV laser and a stand to secure the computer workstation under the instrument. We will continue this innovation in the future whenever we are faced with unmet needs or if replacement parts become unavailable on unsupported instruments.

**901996 P17**

## **Comparison of Immunomagnetic Bead Types: Cell Yield, Losses, And Time Efficiencies For Cell Therapeutics Manufacturing**

Caroline Hoedemaker<sup>1</sup>, Alex Molto<sup>2</sup>, Sandra Saouaf<sup>1</sup>

<sup>1</sup> Raven Biomaterials LLC, <sup>2</sup> Lafayette

Background: Cell Therapeutics are a revolutionary approach to treat disease: the initial, FDA approved products target curative treatments for blood-based cancers. Manufacturing challenges impede wide adoption and contribute to expense (~\$400,000/treatment). Cell therapy manufacturing relies on immunomagnetic beads to separate cells: first to enriching a heterogeneous mixture of patient cell types (leukopak) to have a higher concentration of specific desired cells (ex. CD4+, CD8+, NK, delta gamma, etc. cells). The mix of remaining cells is then genetically modified, to become therapeutic cells. After cell expansion, unwanted, and/or un-modified residual cells are removed from the final product again using immunomagnetic separation technologies. Purpose: We aim to compare the performance of different immunomagnetic beads to enrich a collection of cells. Obtaining a better, more enriched starting cell set from the original harvested cells, and then preventing therapeutic cell loss in the final therapeutic is paramount to

optimize time to therapeutic treatment. Delays and critical cell losses, can add weeks before patient specific treatment is available. Methods: PBMCs were Ficoll purified from 6 different blood lots within 24h of harvest then frozen. After thawing, PBMCs were washed and concentrated to 1M-5M cells/ml and incubated with 200µl RBI-19 beads with mixing for 5 min. Samples were placed on magnet for 2 minutes. Unbound cells were stained with mAbs to CD4, CD8, CD19 according to standard methods and analyzed on a BD FACS Melody. Results: A comparison of immunomagnetic bead types reveal significantly different physical properties which require different processing procedures and times, varying from 10 min to > 1 hour. Bead: Diameter, Density (g/cc), Magnetic susceptibility ( $\chi$ ), % Vol of Magnetic Material Raven -RBI beads: 0.8-3.5 µm, 7-9, 6-8, >95% Miltenyi-MACS: 67-116 nm, 1.4, 0.0011-0.1114, UKN DYNAL MyOne: 1.05 µm, 1.8, 0.3, UKN DYNAL M280: 2.8 µm, 1.4, 0.14, 2.1% DYNAL M270: 2.75 µm, 1.6, 0.17, 5.3% Flow cytometric analysis of PBMC samples depleted of CD19+ cells by using RBI-CD-19 immunomagnetic beads, shows >98% depletion of CD19+ cells and < 3% loss of CD8+ or CD4+ cells as demonstrated in 6 different samples. Conclusion: Immunomagnetic RBI beads, due to their unique physical properties of being highly magnetically susceptible, dense, and having a different antibody binding mechanism, represents a new option for cell therapeutics separation. Importantly, the RBI-bead CD19 depleted PBMC populations contained < 2% CD19+ cells, >97% CD8+ cells, and >97% CD4+ cells. The resulting high levels of target cell depletion and minimal loss of desired cells can significantly improve cell therapeutics manufacturing efficiencies. Future studies to be presented on the poster include head to head comparison with Dynal and Miltenyi beads.

**901483 P19**

## **Optimized cell isolation for mammalian and plant cells using a gentle microfluidic cell sorter**

Dorinda Moellering<sup>1</sup>, Nicole Jagnandan<sup>1</sup>, Donna Munoz<sup>1</sup>

<sup>1</sup> NanoCollect Biomedical

Gentle cell isolation and cloning are needed for numerous biological workflows including antibody production, stem cell therapy, crop improvement and breeding, and gene editing. Sorting mammalian cell lines requires precise single cell dispensing (monoclonality) to circumvent issues which may result in discrepancies in product quality, stability of recombinant

# CYTO 2022 ABSTRACTS

proteins, metabolic profiles, and growth rates. Methods to obtain monoclonal cells must be capable of discriminating single cells from a heterogeneous population and ensure the established cell line originated from a single cell. Using the WOLF with the N1 Single-Cell Dispenser can increase productivity of cell line development while maintaining high cell viability due to its capability of performing gentle sorting. In plant biology, enrichment of protoplast classes via cell sorting (for crop engineering, improved cell line development, and understanding of gene function) or nuclei (for single-cell genomics) needs to be further developed. Sorting plant protoplasts or nuclei is highly challenging with traditional droplet cell sorters due to the high pressures, shear stress and osmotic changes which damage and/or lyse protoplasts and nuclei making them unusable for downstream cell culture and/or genomic applications. Furthermore, traditional cell sorters are also limited in the use of custom sheath buffers which support cell viability and in the cell size they can effectively enrich (mostly < 30  $\mu\text{m}$ ), with larger nozzles and a stable drop delay. Overall, mammalian cells, plant cells and plant organelles share sensitivity and stress induction when enriched via traditional cell sorting instrumentation. The WOLF microfluidics cell sorter offers a solution that efficiently enriches for populations of interest with very low shear stress and supports cell viability using culture medium as sheath. Herein we demonstrate high viability single cell optimized cell sorting of mammalian cells (CHO ES, Expi293F, JURKAT, MCF7, A549, HEK293), isolation of plant protoplasts from diverse plant tissues, and nuclei from the leaves of Roma tomato and green bell pepper plants.

**901547 P21**

## **Imaging second messenger responses of multi-labeled cells using a prototype LED-based excitation-scanning spectral microscope platform**

Craig Browning<sup>1</sup>, Naga Annamdevula<sup>1</sup>, Deepak Deshpande<sup>2</sup>, Thomas Rich<sup>1</sup>

<sup>1</sup>University of South Alabama, <sup>2</sup>Thomas Jefferson University

Introduction: Ca<sup>2+</sup> as a second messenger is involved in a wide range of intracellular processes. Due to numerous molecular interactions and functions, it can be difficult to relate spatially and temporally-localized Ca<sup>2+</sup> responses to downstream physiologic outcomes. If specific interactions or binding relationships could be monitored, then the information gained

from Ca<sup>2+</sup> signals could be applied more rigorously to study underlying cellular functions. One way to observe specific Ca<sup>2+</sup> signals is through fluorescence microscopy. Hyperspectral imaging (HSI) microscopy can be used to increase the specificity of Ca<sup>2+</sup> signal identification, especially for cellular preparations with high autofluorescence or competing background signals. Furthermore, a newer technique, excitation-scanning HSI may allow for increased signal strength when compared to more traditional emission-scanning techniques. However, most HSI applications cannot support real-time fluorescence acquisition at the desired spatial resolution and high spectral sampling. A goal of our current work is to develop improved excitation-scanning hyperspectral imaging technologies for real-time microscopic imaging. Methods: Ca<sup>2+</sup> signaling in human airway smooth muscle cells (HASMCS) was monitored using a novel LED-based spectral illuminator. Cells were treated with NucBlue, MitoTracker and Cal520 to label the nuclei, mitochondria and Ca<sup>2+</sup>, respectively. Cells were stimulated with carbochol to induce high magnitude and frequency Ca<sup>2+</sup> responses. Excitation-scanning spectral image data were linearly unmixed to separate exogenous fluorescent signals and cellular autofluorescence. Results: Results were used to evaluate: 1) practical acquisition speed of the new LED-based spectral imaging platform, 2) ability to discriminate cellular labels and autofluorescence and 3) quality of spectrally-unmixed images, as measured by signal-to-noise (SNR). Carbochol stimulation resulted in a 3X increase in Cal520 fluorescence signal. Linear unmixing was used to separate fluorescent labels from autofluorescence. Image acquisition was set at 500 ms per wavelength channel and the SNR for unmixed Cal520 signal was 4.0, 6.3 and 2.7 for baseline, stimulation and relaxation, respectively. Conclusion: Our results indicate that LED-based hyperspectral imaging can allow for very rapid wavelength switching while still providing sufficient SNR for spectral analysis. Further testing is ongoing to acquire Ca<sup>2+</sup> signals at video-rate speeds using the LED-based spectral illuminator. This includes device optimization for spectral illumination and repeated testing to determine optimal imaging parameters. When fully optimized, this approach should allow for monitoring of several cellular signaling agents in real-time. This work was supported by NASA/Alabama Space Grant Consortium, NASA grant award NNH19ZHA001C, NIH awards P01HL066299 and R01HL137030 and NSF award MRI1725937.

# CYTO 2022 ABSTRACTS

**901580 P23**

## **Automating antibody titration using a CytoFLEX LX flow cytometer integrated with a Biomek i7 Multichannel workstation and Cytobank streamlined data analysis**

Rita Bowers<sup>1</sup>, Giulia Grazia<sup>1</sup>, Bhagya Wijayawardena<sup>1</sup>, Vashti Lacaille<sup>1</sup>

<sup>1</sup>Beckman Coulter, Inc.,

Flow cytometry is an important research tool for rapidly characterizing cell populations in suspension. Advances in instrumentation and fluorescent reagents have made it possible to perform flow cytometry experiments using high-throughput 96-well plate-based format. Determining the correct concentration/titer of antibody to use in each experiment is a critical quality control parameter. Using too little antibody can result in incomplete labeling, whereas using excess antibody can lead to increased background fluorescence and binding of antibody to low-affinity sites. As performing antibody titrations can be laborious, time consuming and prone to human error, we sought to automate this procedure using a Biomek i7 Multichannel workstation integrated with a CytoFLEX LX flow cytometer. The Biomek i7 Multichannel workstation is an automated liquid handler that is capable of efficiently performing the complex liquid handling steps of flow cytometry workflows, including serial dilutions of antibodies for antibody titrations and sample staining and processing steps. With the integrated system, the stained antibody titration samples are automatically loaded into the flow cytometer for acquisition, minimizing the number of required user interactions and increasing walk-away time, freeing the operator to attend to other research tasks. We further streamlined the workflow for antibody titrations using the Cytobank software platform, which can perform both data analysis and Stain Index (SI) calculations with one program. We present here an automated walk-away research workflow for performing antibody titration experiments for flow cytometry with streamlined data analysis using laboratory solutions available from Beckman Coulter Life Sciences.

**901593 P25**

## **Use Dual Wavelength Side Scatter Light for Detecting Nanometer Size Particles and Large Particles in Flow Cytometry**

Nan Li<sup>1</sup>, Yan Wu<sup>1</sup>, Wenqi Liu<sup>1</sup>, Jian Wu<sup>1</sup>

<sup>1</sup>Agilent Technologies

One of the focusing areas for recent design of flow cytometer instrumentation has been on pushing the limit to detect nanometer size particles using side scatter (SSC) signal. Such capability opens up a new era to use flow cytometer to detect biological samples in sub-micron size range, including extracellular vesicles (EVs). EVs are membrane vesicles released by cells including submicron-size microparticles and nanometer-size exosomes. EVs carry RNAs, proteins and lipids from their parent cells and play a very important role in enabling cell to cell communications by delivering signals through their content and surface proteins to nearby or distant cells. Multiple flow cytometers on the market have equipped with the capability of using violet (i.e. 405nm) laser as the excitation light source for SSC detection. Using shorter wavelength is definitely beneficial to resolve smaller biological particles, as Mie scatter has modeled. However, the dynamic range of detection using shorter wavelength light source is also limited to only cover a small range of particle sizes from 0.1  $\mu\text{m}$  to just a few microns. Usually, it is desired to detect a highly heterogenous populations of biological samples with size ranging from submicron size to a few tens of microns, which makes such an option not feasible. Such limitation has been resolved by using dual wavelength light sources, including a violet 405nm laser and a blue 488nm laser, to detect the side scatter light simultaneously (i.e. VSSC and BSSC respectively). The design of the optical system and electronic system is described which allows detecting VSSC and BSSC signals at the same time. A prototype has been built and shows significant improvement of detection dynamic range using forward scatter (FSC) signal and dual SSC signal. NIST certified size standard beads are tested and the system can resolve particle size from 80nm to 50  $\mu\text{m}$  in the same experiment. This innovative design has significantly expanded the current particle detection capability to one magnitude higher dynamic range, which allows detection of highly heterogenous population within one experiment and can generate insightful data which is more biologically relevant.

# CYTO 2022 ABSTRACTS

**901625 P27**

## **Designing spectrally clean fluorescent dyes for high dimensional biological analysis**

Sean Burrows<sup>1</sup>, Anson Blanks<sup>1</sup>, David Daley<sup>1</sup>, Aaron Stroud<sup>1</sup>

<sup>1</sup> Thermo Fisher Scientific

In flow cytometry, there exists a growing demand for spectrally clean dyes to increase the number of biological parameters that can be analyzed simultaneously. Cross-laser excitation and spectral spillover of conventional dyes remain a challenge in meeting this demand. For decades, protein based fluorochromes such as PE and APC, along with their tandems, have enabled countless discoveries in biology. Although bright, these fluorochromes have considerable cross-laser excitation that blocks complete use of other detector channels. Another challenge is the inability to control the tandem dye placement translating to variable FRET efficiencies, leading to unwanted spectral spillover. To address challenges with a dye's spectral properties, we have designed a novel DNA-based platform that enables precise control over dye composition and placement. Control over these properties reduces both the spectral spillover and cross-laser excitation. As part of the design process, we have demonstrated the ability to fine tune the resultant spectral signature through iterative dye design. Dyes with cleaner spectra translate to less compensation or spread because there is less unwanted fluorescence in secondary channels. As a result, additional detector channels are freed up for more labels to be added to the analysis. Furthermore, through our design process, we targeted empty channels that until now have not been filled by any commercially available dyes. The unique attributes of the DNA-based platform for designing spectrally cleaner dyes affords the ability to obtain higher content data and will enable novel discoveries in biology.

**901933 P29**

## **Concurrent and full intensity detection of fluorescent proteins, DNA, and intranuclear markers by cyclic flow cytometry**

Sheldon Kwok<sup>1</sup>, Marissa Fahlberg<sup>1</sup>, Sarah Forward<sup>1</sup>, Maris Handley<sup>2</sup>

<sup>1</sup> LASE Innovation, <sup>2</sup>Mass General Brigham

Over the past few decades, the breadth of flow cytometry applications has expanded significantly, from measurement of surface markers to detection of fluorescent proteins, DNA, and

intranuclear targets. However, the various methods needed to prepare cells for these measurements are often antagonistic and incompatible, leading to suboptimal data quality. For example, cancer and hematopoietic stem cell researchers often study how specific genes, usually transiently inserted, affect cell cycle. Uptake of these genes is confirmed with a fluorescent protein reporter, and ideally, investigators would only measure cell cycle status of cells with successful insertions. However, the fixation and permeabilization methods often required for intranuclear staining result in signal loss and an inability to measure all the cells of interest. Thus, there is a critical need for a method that can measure various biomarkers concurrently without compromise to data quality. Here, we demonstrate and validate an entirely new approach for optimizing all fluorescence signals with zero loss of quality or intensity. Our approach involves barcoding cells with novel laser particles (LPs) that enable repeated cell measurements. Initially, live cells are tagged with unique combinations of LPs that emit light at very narrow infrared wavelengths (<0.5 nm, 1100-1600 nm spectrum). Live barcoded cells are then acquired to capture the optimal fluorescent protein signal. The entire sample is collected after acquisition, processed with a protocol optimized for cell cycle and transcription factor staining, and is re-acquired. Matching of barcoded cells between analysis cycles links the fluorescent protein information from the initial acquisition with the intranuclear and DNA information from the second acquisition. In this presentation, we show detection of a fluorescent protein (GFP), a DNA dye (DAPI), and a transcription factor (Ki67) in combination and with full intensity and quality for markers. Using LPs to barcode MCF7 cells, we first measure GFP on live cells, and then stain and measure DAPI and Ki67 using established protocols. With cyclic flow cytometry, we identified 100% of GFP+ cells at native fluorescent intensity, their Ki67 proliferation status, and the different cell cycle phases of these cells. Cyclic flow cytometry with laser particles enables the unconstrained detection of fluorescent proteins, DNA, and intranuclear targets without signal compromise of any individual component. Using this method, researchers can measure their fluorescent protein-tagged cells of interest and their relation to cell cycle and intranuclear antigen expression. This method is widely applicable to any assay that combines fluorescent protein expression with another incompatible marker by barcoding cells with laser particles and acquiring fluorescent protein data prior to the other desired signals, such as cell proliferation, immune cell regulation, or cell cycle.



# CYTO 2022 ABSTRACTS

**901988 P31**

## **Addressing the need for workflow efficiency in multi-user laboratories – Optimizing the MA900 Cell Sorter to ensure robustness and operational performance.**

Koji Futamura<sup>1</sup>, Toshiyuki Kaimi<sup>1</sup>, Yugo Kishimoto<sup>1</sup>, Deena Soni<sup>1</sup>

<sup>1</sup> Sony Corporation,

As multicolor flow cytometry is used by an increasing number of users across different life science disciplines, the varying application needs have resulted in operational challenges in shared flow facilities who now need to frequently switch sort setup configurations during the day to accommodate sorting of different cell types. The Sony MA900 sorter, anchored on the utility of an exchangeable microfluidics chip, was the first system to bring ease-of-use to multi-user labs, eliminating the need for precision handling of nozzles and o-rings and manual troubleshooting of sample clogs. The next advancement for the MA900 sorter design was to ensure seamless system calibration and reduce downtime of instrument setup when different types of sorting chips - 100, 70 and 130 microns are sequentially exchanged to support user needs. This study focuses on optimizing the system calibration algorithm, so that the MA900 cell sorter can be set up robustly with multiple chip exchanges over the course of the day and adapt to the needs of different users in providing high throughput sorting capability as well as gentle sorting conditions depending on the cell types used for various sorting applications. **Methods and Results** – For this study, the MA900 Cell Sorter (Sony catalog # MA900FP) configured with 4 lasers 488nm, 405nm, 561nm, 638nm was setup with 70um, 100um and 130um chip and calibrated with Autoseup Beads (Sony catalog # LE-B3001). The proprietary CoreFinder™ algorithm automates system setup controlling key steps of chip alignment, laser delay, droplet calibration, sort delay and side stream adjustment. These different steps of automated system setup were assessed to determine which processes could be modified to enhance robustness of setup. Modifications made to the existing algorithm and the new algorithm resulting thereof was used to continue data collection and assess if reliable improvements could be delivered across for a broad array of applications. During the study, the frequency and time required to complete automated setup for each chip was recorded across 5 instruments and 30 total runs. Each chip was successively exchanged with a chip of a different orifice size and the calibration time was measured for each. During each chip exchange, cells of different sizes ranging from 7um to

20um were sorted and the purity and efficiency of sorting each cell type was measured to assess sort performance. The results of the experiments show that the new CoreFinder™ algorithm streamlines setup and reduces overall setup time. Each chip can be setup at precise frequency and the setup is robust and consistent across frequent chip exchanges over time. Overall this new capability when incorporated in the MA900 Cell Sorter will further deliver benefits to multiuser labs enabling high throughput and high performance sorting in a multi user setting.

**902025 P33**

## **Frequency Encoded Multiplexing in Multiple Region Flow Cytometry**

Paul Patrone<sup>1</sup>, Gregory Cooksey<sup>1</sup>, Frederick Esch<sup>1</sup>, Nikita Podobedov<sup>1</sup>

<sup>1</sup> NIST

Recent microfluidic technology developed by our group allows quantification and improvement of measurement uncertainty by replicating cytometry measurements of individual particles along a single flow path. Importantly, the intensity profiles of each particle are measured with high temporal resolution. Combining repetition with high resolution enables the extraction of additional information from particles in flow, but significant challenges in instrument design are introduced by adding more measurement regions. Each additional detection region (i.e., each 1 of n) requires additional detectors (i.e., a quantity c of optical channels). A novel solution to this bulky, hardware-intensive situation is to encode the region from which signals originate. Here, we apply amplitude modulation (AM) to the signal, whereby each laser source is modulated at a different frequency to encode the region being measured. In this configuration, emissions from multiple regions are optically combined and detected on a single high bandwidth detector and analog-to-digital converter. Detected digital signals are demultiplexed using frequency-space analyses to produce region-specific event profiles. With this solution, fewer detectors are required ( $n \times c \rightarrow 1$ ), significantly reducing hardware complexity. In this work we report the integration of AM into a microfluidic cytometer having two measurement zones combined to a single detector. To understand best practices for modulation frequency selection and to estimate components of uncertainty, we simulated measurements by modulating the integrated light incident on a sphere transiting an excitation beam. Further, we simulated the coincident arrival

# CYTO 2022 ABSTRACTS

of two separate beads at different detection regions to verify the ability to separate overlapped signals from distinct regions. The simulation results demonstrate that uncertainty in our approach scales with the root mean squared detection noise, as is expected for a system with shot noise. We experimentally confirmed the simulation and demodulation of single and coincident events at two regions in the microfluidic cytometer. Our approach improves upon previous methods that required hardware such as lock-in amplifiers to isolate each detection channel. Instead of using such specialized equipment, our approach uses software signals analysis, which affords added flexibility in system configuration and signals processing. Overall, our system demonstrates capability for AM to support multi-region cytometry, with significant potential for reducing hardware cost, improving measurement uncertainty, and enabling new types of data extraction from flow, such as studies of particle or cell shape, flow-induced deformation or migration along a flow path.

**902041 P35**

## **Ultra-High Event Rate Detection & Microfluidic Cell Sorting Utilizing Inertial Focusing on the MACSQuant® Tyto® Sorter**

Evelyn Rodriguez-Mesa<sup>1</sup>, Daryl Grummitt<sup>1</sup>, Mehran Hoonejani<sup>1</sup>, Mark Naivar<sup>1</sup>

<sup>1</sup> Miltenyi Biotec

Traditional assumptions regarding microfluidic cytometry and sorting is that it is slow. Compared with well established droplet sorters, microfluidic devices have typical event and sort rates publicized up to 10,000 events/s and 1,000 sorts/s ranges respectively. However, utilizing precision injection molding methods, inertial microfluidic focusing structures have been designed and incorporated into a closed sorting cartridge whereby we have demonstrated > 10x the throughput of historical microfluidic techniques. This development provides improved performance for rare cell applications requiring high event rates and applications requiring large sort counts, such as select therapeutic applications. The advantages of this high speed sorting technology for these (and other) applications include reduced overall cost, reduced processing time, and improved clinical protocols. Precision injection molding methods were used to create microfluidic inertial focusing structures in polycarbonate substrates. The structures are engineered specifically for the cell size and types common for most flow

sorting applications (~2um to 15um). The microfluidic design is such that the cell's own inertia is used to rotate and center them into the flow channel. This microfabricated 'interposer' is then bonded to a closed cartridge system and silicon microfabricated cell sorting chip. As the inertial focusing mechanism provides a more deterministic location for the cells in the microfluidic channel, it facilitates much higher pulse acquisition rates (the transit of the cell through the interrogating lasers) compared to a simple bulk flow of cells through a microfluidic channel. With asynchronous, independently triggered pulse matching algorithms, a high speed FPGA, and a very high concentration of lysed WB CD45+ \CD4+ \CD3+ sample we achieved acquisition rates in excess of 150,000 events/s. Similarly, in the case of sorting at high rates, the inertial focusing structures provide not only improved cell location for collection using a microfluidic valve, but maintain flow characteristics when interrupted by the valve. This reduction in flow disturbance allows high sorting efficiencies, even upwards of 10,000 sorts/s, which allows large volumes of cells to be collected in a closed, micro-fluidic environment; i.e. naïve Tregs, for therapeutic purposes.

**898173 P39**

## **CellMek SPS Instrument Performance: Percent gated populations from automated versus manual sample preparations using a wash/stain/lyse & fix/wash workflow with a 10-color antibody panel in liquid or dry forma**

Kelly Andrews<sup>1</sup>, Gang Xu<sup>1</sup>, Xizi Dai<sup>1</sup>, Ernesto Staroswiecki<sup>1</sup>

<sup>1</sup> Beckman Coulter

Introduction: The CellMek SPS Instrument is an automated sample preparation system intended for in vitro diagnostic use in flow cytometry laboratories designed to process whole blood (WB), bone marrow (BM), and other relevant single-cell specimens for downstream flow cytometry analysis. Workflows for lab-developed tests commonly consist of washing a specimen aliquot, staining with liquid or dry antibodies, lysing red blood cells and fixing stained white blood cells (WBC), washing lysed/fixed prepared sample, and reconstituting in buffer for downstream flow cytometry analysis. A workflow such as this, which utilizes all modules of the CellMek SPS instrument, was chosen to assess system performance compared to manually prepared samples. Modules used include the sample transport module, reaction plate module, the cell wash module, the dry reagent module, the liquid antibody

# CYTO 2022 ABSTRACTS

module, the prep reagent module, and the output module. Methods: WB, BM, and other single-cell suspensions (cerebral spinal fluid [CSF] or other body fluid) were obtained from normal and clinical donors (97 unique donors) and were processed using a representative wash/stain/lyse & fix/wash workflow with a 10-color antibody panel in either dry DURACartridge format or liquid cocktail format. The 10-color panel consisted of Kappa-FITC, Lambda-PE, CD10-ECD, CD5-PC5.5, CD200-PC7, CD34-APC, CD38-AA700, CD20-AA750, CD19-PB, and CD45-KrO. Samples were prepared in duplicate on one of three CellMek SPS instruments, totaling 152 datapoints each for CD45+ WBC and gated sub-populations (liquid and dry pooled). Each sample processed with the CellMek SPS instrument was compared to a manually prepared matched-donor sample using equivalent workflow and reagents. All prepared sample data were acquired on a Navios flow cytometer and analyzed using Kaluza C software. Measurement Procedure Comparison and Bias Estimation was performed by biostatisticians. Conclusion: Total bias from manually prepared reference of percent positive gated sub-populations was within 5 percentage points for populations  $\leq 20\%$  and within 8 percentage points for populations  $> 20\%$ . Sub-component analysis of panel design (typical incubation or throughput optimized), instrument (1, 2, or 3), antibody format (liquid or dry), anticoagulant (EDTA, ACD, Heparin, or none), and specimen type (WB, BM, body fluid, or CSF) was assessed on a pooled marker dataset. All sub-component categories analyzed were within 5 percentage points for populations  $\leq 20\%$  and within 8 percentage points for populations  $> 20\%$ . The Beckman Coulter products and service marks mentioned herein are trademarks or registered trademarks of Beckman Coulter, Inc. in the United States and other countries.

**898432 P41**

## **Are my purified cells performing optimally after sorting using conventional droplet cell sorting?**

Peter Lopez<sup>1</sup>

<sup>1</sup>NYU Grossman School of Medicine

Droplet cell sorting, originally described by Mack J. Fulwyler, has been an empowering technology that has facilitated many important studies and advances in the biological sciences. This amazing technology continues to be vital, providing purified starting material for a multitude of downstream processes and analyses. Users of this technology have been plagued by certain cell types which perform poorly or simply die after the droplet cell sorting process. Other approaches to the cell sorting process, most recently involving microfluidics, have evolved and now provide an alternative cell sorting approach, while still allowing the multiparametric detection of unique cellular subsets for purification. However cell purification by conventional droplet cell sorting remains the most popular technique for cell purification. Our investigation into the conventional cell sorting process was initiated to try to determine and understand components of this process that have the most significant impact on post-sort cellular dysfunction. While it is clear that cell sorting can have a negative effect on some cell types, other cell types seem to be less susceptible to these effects, at least for their intended downstream utilization. Negative post-sort effects can be mitigated by employing minor changes to the process including lower pressure, use of sorting nozzles with a larger-diameter orifice, system temperature maintenance or sample/collection buffer changes. While these techniques offer mitigation, due to the cell-specific nature of each remedial technique it is unclear if there is an underlying mechanism predisposing sorted cells to unrepresentative post-sort function. We describe Sorter Induced Cellular Stress (SICS) as a functional or phenotypical difference of cells before and after cell sorting. Our initial work has identified a SICS metabolomic phenotype, showing a broadly decreased level of cellular metabolites post sorting, and we believe this is a common consequence of the droplet cell sorting process. While we describe a technique to minimize this phenotype, further studies are needed to fully understand the underlying cause of this phenotype, and to potentially deal with the causative mechanism at its source.

# CYTO 2022 ABSTRACTS

**898509 P43**

## **Automated Autofluorescence Removal in Flow Cytometry**

Giacomo Vacca<sup>1</sup>, Kshitija Shevgaonkar<sup>1</sup>, Alan Chin<sup>1</sup>, Elijah Kashi<sup>1</sup>, Richard McKay<sup>1,2</sup>

<sup>1</sup> R&D, Kinetic River Corp., Mountain View, CA, United States,

<sup>2</sup> Principal, Full Spectrum Scientific, LLC, East Windsor, NJ, United States

**Background.** Most assays in flow cytometry rely on detection of signals from exogenously added fluorescent labels. However, cellular autofluorescence often contributes an unwanted background to such signals. This background, primarily from the metabolic cofactors nicotinamide adenine dinucleotide (NADH) and flavin adenine dinucleotide (FAD), is high for commonly used UV and violet laser wavelengths and is present in most detection channels. Kinetic River is leveraging our proprietary time-resolved flow cytometry technology to allow for discrimination between this unwanted autofluorescence and the desired signal from the fluorescent label. By measuring two different parameters of fluorescent molecules—the fluorescence intensity and the fluorescence lifetime decay—we can distinguish between the two sources and automatically eliminate the contribution of cellular autofluorescence, leaving only the desired signal from the fluorescent label. **Methods.** The Colorado time-resolved multiparametric analyzer system uses pulsed laser excitation at 375 nm and detection channels that have significant overlap with the emission spectra of NADH and/or FAD. The system also has separate channels for FSC and SSC. Ultrastable sheath flow is established with our custom-built Shasta fluidic control system. Data acquisition is based on a National Instrument PXI platform and custom-written LabVIEW code combined with signal processing performed on a computing platform running custom algorithms. The system was tested using cells stained with exogenous fluorescent labels emitting in the blue (strong NADH autofluorescence) and green (strong FAD autofluorescence). **Results.** The Colorado's ability to resolve exogenous fluorescence from cellular autofluorescence based on fluorescence lifetime, regardless of spectral overlap of the signals, was demonstrated in cells stained with common fluorophores emitting in the blue and the green channels. Assays were performed using peripheral blood mononuclear cells (with low-to-moderate levels of autofluorescence) and eosinophils (with high levels of autofluorescence). In both cases, we were able to isolate the contribution from cellular autofluorescence and, using our proprietary algorithms, subtract it from the

signal. **Conclusion.** We demonstrated that the Colorado system can distinguish true signal from autofluorescence background. Current follow-on work is aimed at expanding the system's multiplexing capabilities by increasing the number of lasers and detection channels to create a cell analyzer platform that can automatically eliminate unwanted interference from cellular autofluorescence without alterations in the user's experimental workflow or analysis methods.

**897457 P45**

## **Characterization of UKNEQAS B-ALL samples using an RUO one-tube 12-color antibody panel on the RUO 12-color BD FACSLyric™ Flow Cytometer**

Yang Zeng<sup>1</sup>, Farzad Oreizy<sup>1</sup>, Michelle McNamara<sup>1</sup>

<sup>1</sup> BD Biosciences

Classification and analysis of B-cell acute lymphoblastic leukemia (B-ALL) using flow cytometry has been well established as an important laboratory testing method. Biological applications of flow cytometry rely on standardized multicolor antibody reagents and instrument systems to generate reliable and reproducible data that can be compared across laboratories. The RUO 12-color BD FACSLyric™ Flow Cytometer simplifies cytometer standardization by enabling a one-step daily instrument setup and QC with automatic daily optimization of fluorescence compensation. The system demonstrates faster acquisition with measurement of higher number of total cells to identify low concentration aberrant phenotypes and to characterize phenotype profiles for the abnormal cells. The UK National External Quality Assessment (UK NEQAS) trials provide proficiency tests to assess consistency in laboratory results. In this study, the UKNEQAS B-ALL samples in the non-accredited B-ALL trials were characterized through immunophenotyping on the RUO 12-color BD FACSLyric™ Flow Cytometer using a one-tube 12-color RUO antibody cocktail that was selected based on scientific literature. The antibody cocktail included cell lineage markers and characterization markers for B-ALL: cytoplasmic MPO FITC (cyMPO FITC), cyCD79a PE, CD34 PerCP-Cy5.5, CD19 PE-Cy7, CD7 APC, CD38 APC-R700, CD3 APC-H7, cyCD3 V450, CD45 V500C, CD20 BV605, CD10 BV711, CD58 BV786. The distinct aberrant phenotypes in the UK NEQAS B-ALL samples were identified and the B-ALL cell percentages were calculated and compared with the mean values provided by the UK NEQAS proficiency test reports. Relative to peer laboratories, the

# CYTO 2022 ABSTRACTS

absolute Z score of our results ranked from 0.067 to 0.75. We demonstrated that enumeration of abnormal B-ALL cells in the UK NEQAS samples was feasible using one-tube 12-color RUO antibody cocktail to detect multiple biomarkers simultaneously. For Research Use Only. Not for use in diagnostic or therapeutic procedures. BD and BD FACSLyric are trademarks of Becton, Dickinson and Company or its affiliates. © 2022 BD. All rights reserved. 0222

**900929 P47**

## **Interference evaluation of the BD<sup>®</sup> Stem Cell Enumeration Kit on BD FACSLyric<sup>™</sup> Flow Cytometer**

Diem Le<sup>1</sup>

<sup>1</sup>BD Biosciences

The BD<sup>®</sup> Stem Cell Enumeration Kit is a single tube in vitro diagnostic assay, intended for enumeration of viable dual-positive CD45+/CD34+ hematopoietic stem cell populations to determine viable CD34+ absolute counts (cells/μL) and the percentages of viable CD45+/CD34+ hematopoietic stem cells. The BD<sup>®</sup> Stem Cell Enumeration (SCE) Kit was evaluated using fresh cord blood, fresh bone marrow and fresh leukapheresis in the presence of endogenous and exogenous interfering substances on the BD FACSLyric<sup>™</sup> using the BD FACSuite<sup>™</sup> Clinical Application with the BD<sup>®</sup> Stem Cell Enumeration module for acquisition and analysis. The interferents to be evaluated included substances likely to be present in patient specimens and were evaluated according to CLSI EP07 Interference Testing in Clinical Chemistry, 3rd Edition, April 2018. The concentrations tested were based on three times the maximum therapeutic dose observed in patients or the highest expected concentrations per CLSI EP07 Supplement (EP37) Supplemental Tables for Interference Testing in Clinical Chemistry, 1st Edition, April 2018. The substances evaluated in this study included albumin, bilirubin, cyclophosphamide, hemoglobin, doxorubicin, G-CSF, intralipid and paclitaxel. For each of the specimen types, 15 replicates were stained using the BD<sup>®</sup> SCE Kit for each interferent condition. A total of 9 specimens comprising of 3 leukapheresis, 2 bone marrows, and 4 cord bloods were used to complete the evaluation. A paired-difference analysis was used to evaluate the Control (no interferents) versus the Test (with interferents) conditions. Leukapheresis, bone marrow and cord blood exhibited a maximum mean bias of -3.2% (-10.5, 4.0), -4.7% (-11.6, 2.1) and -1.2% (-2.86, 0.46), respectively,

for viable CD34+ absolute count in the presence of the highest concentrations of interferents evaluated. In the presence of interfering factors, the maximum %CV for CD34+ absolute count in leukapheresis, bone marrow and cord blood specimens were 12.2%, 11.4% and 11.6%, respectively. There was no detectable interference to the enumeration of viable CD34+ absolute counts from the interfering substances tested at their highest concentrations. The BD<sup>®</sup> Stem Cell Enumeration Kit is for In Vitro Diagnostic Use with the BD FACSLyric<sup>™</sup> Flow Cytometer. The BD FACSLyric<sup>™</sup> Flow Cytometer is for In Vitro Diagnostic Use with BD FACSuite<sup>™</sup> Clinical Application for up to six colors. The BD FACSLyric<sup>™</sup> Flow Cytometer is for Research Use Only with BD FACSuite<sup>™</sup> Application for up to 12 colors. Not for use in diagnostic or therapeutic procedures. The BD FACSLyric<sup>™</sup> Flow Cytometer is a Class 1 Laser Products.

**900959 P49**

## **Precision Performance of Cytek<sup>®</sup> cFluor<sup>®</sup> 6-Color TBNK-SL Assay on Northern Light<sup>™</sup> (NL) CLC Cytometer Systems**

Jennifer Liu<sup>1</sup>, Jun Deng<sup>1</sup>, Qing Chen<sup>1</sup>, Mingyan Gong<sup>1</sup>

<sup>1</sup> Cytek Biosciences Inc.

Background Cytek's spectral flow cytometry utilizes the full emission spectrum across all channels. It allows fluorochromes with similar, but not identical, signatures to be used together. This greatly extends the numbers of usable fluorochromes per laser. A blue laser only cFluor<sup>®</sup> 6-Color TBNK-SL assay utilizing a reagent cocktail (CD3-cFluor B520, CD4-cFluor BYG781, CD8-cFluor BYG610, CD19-cFluor BYG667, CD16-cFluor BYG575, CD56-cFluor BYG575, & CD45 cFluor B690) was developed to identify and determine the percentage and absolute count of T lymphocytes (CD45+CD3+), helper/inducer T lymphocytes (CD45+CD3+CD4+), suppressor/cytotoxic T lymphocytes (CD45+CD3+CD8+), B lymphocytes (CD45+CD3-CD19+) and natural killer cells (CD45+CD3-CD(16+56)+) in human peripheral blood. The aim of this study was to evaluate the precision performance of cFluor<sup>®</sup> 6-Color TBNK-SL on NL-CLC cytometer systems. The evaluation includes within-run, between-run, between-instruments, between reagent lots and between operator variables. Materials and Methods Streck CD-Chex Plus normal (CDN) and CD-Chex Plus CD4 Low (CDL) were stained in duplicate with the 6-Color TBNK-SL reagent using a Lyse No Wash method. Samples were prepared and ran by one of the two operators per day for 21 days (10 days for operator

# CYTO 2022 ABSTRACTS

A and 11 days for operator B) with 5 days of data collected on each of 3 cytometer configurations (2LBR, 2LBV, 3LVBR) and 6 days on one laser cytometer configuration (1LB), 7 days of samples stained with each lot of the reagents. All variables were in a randomized order. Daily sample data collection was obtained in two runs (separated by at least 3 hours from the start of the 1st run to the start of the 2nd run) over a minimum of 21 testing days. Standard deviation (SD), coefficient of variation (%CV) and 95% confidence interval (CI) of SD and %CV were calculated to evaluate repeatability and precisions between runs, between lots, between operators and between instruments. Source of variation was analyzed using R-package (VCA). Results For both CDN and CDL controls, the SD of the percentage of CD3+, CD4+, CD8+, CD19+, CD(16+56)+ lymphocyte and %CV of The absolute counts CD3+, CD4+, CD8+, CD19+, CD(16+56)+ lymphocyte met the following predefined precision criteria fo, the precision variables: • Absolute counts: o 95% upper CI on the CV  $\leq$  10% for CD3+, CD4+ and CD8+ o 95% upper CI on the CV  $\leq$  20% for CD19+ and CD16+56+ • Percent positives: o 95% upper CI on the SD  $\leq$  2.5 for CD3+, CD4+ and CD8+, CD19+ and CD16+56+ Conclusion In conclusion, the Cytek 6-Color TBNK-SL assay demonstrated satisfied repeatability and precision between runs, between operators, between instruments and between reagent lots. References EP05-A3 Evaluation of Precision of Quantitative Measurement Procedures EP15-A User demonstration of performance for precision and accuracy

## 901561 P53

### Development of a flow cytometric assay for differentiating T Cell Memory Phenotypes in CAR-T process development

Susan Foster<sup>1</sup>

<sup>1</sup>Beam Therapeutics

Developing a CAR-T cell based therapy involves the isolation of T cells to make up the final drug product, but with no distinction for the isolation of certain T cell phenotypes. Memory phenotype of the final T cell product and the changes to memory phenotypes during cell processing is unknown. Here, we designed an assay to identify memory T cell phenotypes by flow cytometry and tested different time points of the CAR-T cell manufacturing process. After implementation of CD45, CD8, CD2, and CAR marking antibodies in the panel to differentiate T cells, CAR T cells, and cytotoxic T

cells, CD45RA and CCR7 were used to distinguish between 4 subtypes of memory phenotypes: Naïve/Scm, Central memory, effector memory, and terminal effector. CD45RA as a naïveté marker, and CCR7 as a naïve/central memory T cell marker allowed for these separations by gating. This was followed by collecting data for future conclusions through the CD62L marker, as CD62L is a marker for L-selectin that can differentiate between Central memory and effector memory. In this poster, we describe the gating strategy developed to classify CAR-T products into different T cell memory phenotypes. When stained and applied, this assay showed a difference in T cell memory phenotypes between pre and post processed T cells, and transduced CAR cells vs untransduced cell conditions.

## 901636 P55

### Assessing viability dyes for use on Full Spectral Flow Cytometers

Rachael Walker<sup>1</sup>, Sam Thompson<sup>1</sup>, Aleksandra Lazowska-Addy<sup>1</sup>, Christopher Hall<sup>1</sup>

<sup>1</sup> Babraham Institute

Flow Cytometry Core Facility, Babraham Institute, Cambridge, UK, CB22 3AT Assessing viability dyes for use on Full Spectral Flow Cytometers There has been a proliferation in flow cytometry instrumentation recently, many moving away from conventional light collection towards collecting and analysing light across a large spectrum. These full spectrum flow cytometers manufactured by Cytek, Becton Dickinson, Sony, and ThermoFisher have differing, and sometimes contrasting, light collection design concepts. To provide a better service to our users and to increase our understanding of the way fluorophores are being analysed using these instruments we have run 17 viability dyes on multiple instruments; the full spectrum Bigfoot, Aurora and the conventional ZE5, Fortessa, Attune, and CellStream. This will serve as a useful educational reference for our users and has allowed us to validate the spectra published on the vendors website about excitation of these dyes for use in conventional cytometry and has shown which of the viability dyes will be suitable for full spectral cytometry panels. Method Mouse splenocytes were processed as normal (for a phenotyping screen on a flow cytometer), resulting in realistic cell death characteristics for analysis. We looked at 17 viabilities dyes from different manufacturers and at multiple concentrations. The viability dyes were incubated individually and then run on 7

# CYTO 2022 ABSTRACTS

instruments. All channels on the conventional cytometers were enabled to see the spectral signature on all instruments. Data was analysed using FlowJo and R (flowSpectrum). Results We have shown that some of the viability dyes need titrating down for full spectral cytometry, especially compared to the manufacturers recommended concentration. This brightness shows the essential nature of dye titration for full spectrum, as changing individual detector gains or voltages is not desirable on these machines. We have found that a number of the dyes give good separation on the full spectral systems with spectral signatures that mean easy insertion into a multicolour panel. The extra lasers offered by the “high end” instruments add complexity to spectra freeing up more space for other fluorophores.

**901821**

**P57**

## **Tracking Novel HLA Design Features in Engineered Cells Using PrimeFlow™ RNA Assay**

Marjorie Ison-Dugenny<sup>1</sup>

<sup>1</sup>Kite Pharma

Background: Flow cytometry is a valuable tool for identifying and validating novel tumor-specific targets. However, for many novel targets, detection reagents that aid in understanding protein expression in vitro are often limited or otherwise non-existent. For example, artificial Antigen Presenting Cells (aAPC) used to promote expansion and stimulation of T cells can be engineered to express novel human leukocyte antigen (HLA) design features that could enhance T cell immune function. Tracking these multiple novel HLA design features can prove challenging due to the shortage of available detection reagents. Custom reagents can be designed and produced, if cost and time are not of primary concern, but this is often not the case. In the absence of detection reagents, PrimeFlow™ RNA Assay (ThermoFisher Scientific) may be implemented to track gene expression in engineered cells via flow cytometry. PrimeFlow RNA Assay detects RNA using sequence-specific oligonucleotide probe sets that bind to its target. In an expression vector, a specific novel HLA design feature is paired with a unique 28-base DNA sequence, henceforth referred to as the barcode. This barcode serves as a reporter for the expression of the specific design feature. In this case, the target is the barcode. Once the probe sets are bound, the signal is amplified by multiple DNA structures in a branch-like formation, and this is followed by fluorescent labeling. The probe sets are small and

contain 20 to 40 oligonucleotides, thus can be used to detect the 28-base barcode sequence. Methods: Several engineered K562 aAPC cell lines were generated via lentiviral transduction, each expressing a particular HLA subtype paired with a unique barcode. Expression of the HLA mRNA, as well as the paired barcode was determined by PrimeFlow RNA Assay. The assay may also confirm protein expression with the incorporation of conventional flow staining methods using fluorochrome conjugated antibodies. The cells were analyzed on BD Symphony A3 flow analyzer. Conclusions: PrimeFlow RNA Assay specifically detected the barcode uniquely paired with its HLA subtype. This was confirmed with the simultaneous detection of HLA mRNA and HLA protein. The specificity of the barcode probes was confirmed by the absence of signal under a mismatched barcode. The ability of the assay to discern differences between barcodes can potentially be extended to other applications, such as verification of any oligonucleotide sequence as short as 28 bases. We therefore conclude that by using PrimeFlow RNA Assay, cell lines can be engineered to express a wide variety of novel HLA design feature. Each cell line expressing a unique HLA can then be identified and distinguished from other cell lines expressing a different HLA design feature based on detection of paired barcodes. This method eliminates the need for costly and time-consuming antibody production campaigns.

**901853**

**P58**

## **Cryopreservation of Live-Cell Barcodes: a time-course study examining the stability of CD45 cadmium barcodes after freezing at -80°C for 1 week to 3 months**

Martha Brainard,<sup>1</sup> Taylor Witte<sup>1</sup>, Noura Srour<sup>1</sup>, Greg Hopkins<sup>1</sup>

<sup>1</sup> 2seventybio

Sample multiplexing is a popular approach to increase experimental throughput and efficiency in the mass cytometry field. Traditional multiplexing methods involve the use of palladium barcodes. Although palladium barcodes are commercially available in kit form, they cannot be used prior to cell fixation, and thus, may be incompatible with markers that do not stain well on fixed cells. Live-cell barcoding with CD45 platinum and cadmium conjugates allows users to include these markers and is more conducive to multiplexing at experiment start. This multiplexing reduces staining variability, decreases the necessary volume of reagents and antibodies, and increases overall time and cost efficiency. Given the plethora of benefits,

# CYTO 2022 ABSTRACTS

it is advantageous for labs to implement a live-cell barcoding strategy; however, because no live-cell barcoding kits are sold commercially, individual users are left to make their own barcodes. While this option provides flexibility in barcoding strategy, the process is time-consuming and potentially error prone. For this reason, bulk preparation of barcodes for long-term cryopreservation is preferential. Although many users follow this practice, few publications delve into the stability of antibodies upon long-term cryopreservation. Here, we examine the barcoding efficiency when healthy donor peripheral blood mononuclear cells (PBMCs) (N=4) are multiplexed together with freshly prepared barcodes and barcodes that have been cryopreserved at -80°C for 1 week, 1 month, and 3 months. We show the mean intensity of the respective barcode channels on concatenated files at all timepoints. A Mahalanobis Distance (MD) of 10 and a minimum separation (MS) of 0.2 were used to debarcode all files. These parameters were chosen after an optimization analysis. This analysis focused on three outcomes: minimal inter-barcode contamination in de-barcoded FCS files, low percentage of false negative events in the unassigned event files, and maximum yield. After 3 months of cryopreservation, we see a drop in CD45 cadmium intensity; however, this drop does not compromise the ability to distinguish barcodes. The yield, and the percentage each sample contributes to the yield, remain relatively constant. Samples multiplexed with freshly prepared barcodes have a barcoding yield of 73.1% and the samples multiplexed with barcodes that had been cryopreserved for 3 months have a barcoding yield of 75.4%.

**901898 P59**

## **High-throughput screening of antigen-specific IgG secreting cells and linked single-cell sequencing using nanovial technology**

Lucie Bosler<sup>1</sup>, Wei-Ying Kuo<sup>1</sup>, Dino di Carlo<sup>1</sup>, Joseph de Rutte<sup>1</sup>

<sup>1</sup> Partillion

We use flow cytometry to sort IgG-secreting cells based on the specificity and affinity of secreted antibodies to an antigen and seamlessly link the IgG-secretion information with downstream transcriptomic data for the same single cell. Monoclonal antibodies have become both an indispensable tool in life science research and a revolutionary treatment in the clinic. However, traditional tools for antibody discovery, such as hybridoma workflows, direct binding of antigen to the B cell receptor followed by single-cell sequencing, and

yeast & phage display technologies have various trade-offs, in particular, the number of time consuming and laborious steps to validate functional high affinity candidates. Microfluidic approaches have emerged to directly screen individual B cells based on secreted IgG properties, reducing screening time by months. Notably, one of the first approved antibody treatments for SARS-CoV-2, Bamlanivimab, was developed using a microfluidic-based screening approach. Despite the power of these approaches, they have not been widely adopted due to the high level of technical expertise and specialized instruments required. To address this gap, we recently introduced a new approach to screen cells based on secreted products that uses cavity-containing hydrogel particles, “Nanovials”, that act as suspendable wells for individual cells. Nanovials can be analyzed and sorted using common fluorescence activated cell sorters (FACS). Cells are loaded into nanovial cavities with simple pipetting steps and bind via antibodies against cell surface proteins. The nanovials are modified with antibodies against secreted molecules of interest, thereby catching and retaining secretions locally from the cells which are then stained with fluorescent secondary labels for flow cytometry. In this work, we demonstrate the use of this platform to screen over 100,000 hybridomas based on relative affinity of the antibodies secreted to a model antigen and perform single-cell sequencing to recover sequence information associated with the secreted antibodies. We simultaneously stain the captured secretions with a fluorescent antigen and fluorescently labeled anti-IgG antibody to normalize the antigen signal to the total IgG produced for each cell. We show that the relative affinity of the secreted antibodies from two different hybridoma clones can be detected and sorted based off this information. We show that transcript information can be recovered directly from cells and linked to IgG secretion on nanovials using the 10X Genomics single-cell sequencing platform and oligo-barcoded antibodies. Nanovials unlock sophisticated single-cell functional assays, linking between function and underlying transcriptome using FACS and single-cell sequencing technologies. Beyond enabling more researchers to accelerate their antibody discovery workflows, this approach can expand the scope of single-cell biology to include a new layer of functional data.



# CYTO 2022 ABSTRACTS

901942 P61

## Accurate Enumeration of Probiotic Bacteria by Flow Cytometry Depends on the Strain and Storage Conditions

Kevin Galles<sup>1</sup>, Anthony Kiefer<sup>1</sup>, Vincenzo Fallico<sup>1</sup>, Natalie Mysak<sup>1</sup>

<sup>1</sup> IFF

Background: The probiotic industry relies on accurate enumeration of live cells to formulate products meeting specific health claims. The “gold standard” for probiotic enumeration is plate counting (PC) to determine the colony forming units (CFU) on growth promoting agar media. This method has several drawbacks including long time to results and high variability. Alternatively, flow cytometry (FC) and droplet digital PCR (ddPCR) methods can determine viability rapidly and with decreased variability via measuring of membrane integrity and cellular activity. In this study, FC and ddPCR methods were compared to PC for their ability to accurately enumerate freeze-dried preparations of 4 probiotic *Bifidobacterium* strains (HN019, B420, BI-04 and Bi-07) over 2 years of storage at commercially relevant temperature and humidity conditions. Methods: Freeze-dried bacteria were packaged in moisture and oxygen-barrier aluminum bags, stored at 4°C, 25°C, 30°C, 25ICH (25°C, 60% RH) and 30ICH (30°C, 65% RH), and analyzed at 0, 0.5, 1, 2, 3, 6, 12 and 24 months. Membrane integrity was measured by FC using Syto™ 24 and Propidium Iodide as viability markers. ddPCR enumeration analyzed both membrane integrity and cellular activity by crosslinking propidium monoazide and ethidium monoazide to nucleic acids to exclude these cells from PCR and mark them as non-viable. Correlation and linear regression analyses were performed to compare the viability data generated by PC and each of the rapid methods. Results: FC and ddPCR viable counts strongly correlated with PC for HN019, BI-04 and B420 when stored at 25°C, 30°C, 25ICH and 30ICH. Linear regression slopes close to 1 further confirmed the ability of FC and ddPCR to accurately enumerate HN019 and B420 under these storage conditions. Correlation coefficients and regression slopes deteriorated when HN019, BI-04 and B420 were stored at 4°C and were poor for Bi-07 under any storage condition. Differences in FC vs. ddPCR slopes could be due to the use of EMA to measure cellular activity via membrane pump/efflux activity which is absent in FC analysis. Surprisingly, Bi-07 at 4°C shows an increase in viability using the rapid methods. Conclusion: FC and ddPCR can accurately enumerate 2 *Bifidobacterium* strains (HN019 and B420) under most storage conditions. Good correlation in BI-04 between PC and rapid

methods suggest that these methods can be improved to more closely reflect PC. These data suggest that membrane integrity and cellular activity may not be good viability markers for Bi-07. Even though membrane integrity is widely used as rapid marker of bacterial viability, this study shows that it is not suitable for strains and storage conditions. Further long-term studies are needed to have a better understanding of cell physiology and the molecular drivers of viability. These studies will facilitate the adaptation of rapid methods to enumerate bacteria and extend these findings to other commercial probiotic strains.

901966 P63

## Development of a novel flow cytometry-based receptor occupancy assay for assessing target engagement of anti-CCR8 antibody in FIH clinical trial

Iviyan Karki<sup>1</sup>

<sup>1</sup> Bristol Myers Squibb

Receptor occupancy (RO) assays are utilized in clinical trials for evaluating target engagement and determining dose selection providing valuable insights on pharmacodynamic and safety evaluation of a biotherapeutic. Here, we developed and qualified a novel peripheral blood CCR8 RO assay using flow cytometry that was transferred to a CRO to support the anti-CCR8 antibody FIH study. Measurement of CCR8 RO is particularly challenging due to limited assay range as a result of low CCR8 expression on peripheral Tregs. By leveraging a non-competitive anti-CCR8 antibody, a specific CCR8+ve Treg subset was selected as the target cell population for the assay as opposed to the total Tregs. This served as an effective strategy for improving the assay dynamic range by 5x. Two independent RO assay formats were developed: 1) direct/total format (measures bound and total receptor) and 2) indirect/total format (measures free and total receptor). This provided a unique opportunity for head to head comparison between the two distinct RO assay formats for a single asset. Both approaches yielded similar RO drug dose-response curves and EC50s (0.022nM vs. 0.023nM, n=4), indicating the reliability of the developed assay. Both RO formats were independently validated for post-collection sample stability up to 72h, and acceptable intra and inter-assay precisions (CVs ≤ 30%). Additionally, consistent RO data was observed across the drug dose range from intra-subject longitudinally (CVs ≤ 25%). In conclusion, the developed CCR8 RO assay is sufficiently robust for clinical trial use capable of providing informative target engagement data for the CCR8 FIH study.

# CYTO 2022 ABSTRACTS

**901992 P65**

## **Assessing cytometers for detection of small particles.**

Sam Thompson<sup>1</sup>, Aleksandra Lazowska-Addy<sup>1</sup>, Diana Guinot<sup>1</sup>, Christopher Hall<sup>1</sup>, Rachael Walker<sup>1</sup>

<sup>1</sup> Babraham Institute, UK

There has been a recent interest in the detection of microparticles (<1µm). Apogee mixed beads were run on all cytometers to determine which of the core instruments would give the best resolution and sensitivity for these experiments. The Apogee bead mix (range of fluorescent and non-fluorescent 80nm -1300nm beads) were run on our analysers: Becton Dickinson (BD) LSRFortessa, Propel Labs YETI, Luminex Cellstream, Cytex Aurora, and Thermo Fisher Attune CytPix; cell sorters: BD FACSJazz, Thermo Bigfoot and BD FACSAriaFusion; and Luminex Imagestream MkII Image cytometer. We show the plots, assess the sensitivity and resolution of each instrument, and we found that the best machine for detecting the green fluorescent 80nm beads was the Luminex Imagestream MkII, the fluorescent images also allowing confirmation of the beads. Out of the analysers the 80nm beads could only be seen on the Luminex Cellstream when in 'small particle mode' and the Cytex Aurora with the 405nm small particle upgrade. We will discuss the benefits and limitations of this method of instrument comparison. This assessment has been incredibly informative about the detection levels of the cytometers within the core and will allow users to determine which instruments to use for their studies.

**902002 P67**

## **Cellular barcoding method using HPMA polymer coupled spectral probes**

Tomáš Kalina<sup>1</sup>, Daniela Kuzilkova<sup>1</sup>, Julia Kudlackova<sup>1</sup>, František Bárta<sup>2</sup>

<sup>1</sup> Charles University, <sup>2</sup> I.T.A. - Intertact s.r.o

**Introduction** Cell barcoding offers efficient, economical and robust method for sample preparation of a series of samples that can be processed by a single protocol and acquired at once. Current conventional and spectral cytometers offer sufficient number of detectors so that it is feasible to dedicate two of them to barcode resolution. Here we use HPMA polymer nanoprobe labelled with particular ratios of two fluorochromes than enables us to generate 6 spectrally distinct barcodes resolved in two channels of a

**conventional cytometer. Materials and methods** The multispectral nanoprobe containing a monoclonal antibody and HPMA polymeric precursor carrying 2 types of fluorescent dyes (DY-396XL and DY-647P1) were prepared by specific thiol-maleimide click reaction after reduction of antibody with dithiothreitol. Each conjugate of antibody containing 2 fluorophores had the unique characteristic spectral profile that was provided by different molar ratio of dyes on a polymer. Spectral uniqueness of each conjugate was tested first on antibody capture beads (UltraCompbeads, Thermofisher) and subsequently anti-CD45 and anti-MHC-Class1 conjugates were tested on human peripheral blood cells. Acquisition was done on Cytex Aurora spectral flow cytometer. **Results and discussion** We succeeded in creating a multispectral nanoprobe with a distinct spectral profiles as evidenced by their absorption curves. Technical control binding the conjugates on the antibody capture beads showed a distinct spectrum of each nanoprobe resolvable in two channels of a conventional or spectral cytometer. Finally, when conjugates were tested on human peripheral blood cells we were able to barcode each individual cell sample and resolve it after common sample preparation and acquisition. HPMA polymers with proved to be a feasible component that makes stable and robust building block with fixed molar concentration of the parental fluorochromes. This barcoding approach allows us to perform cytometry assays with greater robustness. We will further explore the possibility to add more fluorophores to the combinatorial barcodes.

**902016 P69**

## **Cytokine Multiplexing on a Full Spectral Cytometer**

Michael Solga<sup>1</sup>, Alexander Wendling<sup>1</sup>, Taylor Harper

<sup>1</sup> University of Virginia Flow Core

**Introduction:** Over the past few years, the "cytokine storm" response related to SARS-CoV2 has become an increasingly important measurement in the treatment and understanding of Covid-19. The use of multiplex fluorescent bead-based assays allows the quantification of multiple cytokines and other analytes simultaneously providing a cytokine profile. Instrumentation flexibility to acquire these types of multiplex assays has been limited. Spectral Cytometry provides a unique advantage over traditional cytometers by providing the ability to collect the full fluorescent spectrum. Individual fluorescent signatures can be used to identify unique populations and patterns. MagPlex fluorescent beads used in many of these multiplex bead assays have a unique

# CYTO 2022 ABSTRACTS

dye ratio to identify the individual beads within a mixed sample. Using the raw fluorescent dye signatures acquired on a full spectral cytometer we identified up to 48 unique beads within a multiplex bead-based array and quantified analyte binding. Methods: MagPlex microsphere multiplex cytokine assay kits were processed following manufacturer protocols. Assay kits used have a series of different dye ratio fluorescent beads coated with an antibody specific for an analyte. Beads were incubated with various sample types containing protein, washed, and incubated with biotinylated antibodies specific for individual bead analytes, followed by a SA-PE reporter. Multiplex bead arrays were collected on an Aurora Full Spectral Cytometer and a Luminex MAGPIX. Using Milliplex Analyst software standard curves were generated, and sample MFIs collected from each instrument were correlated against curves to generate relative concentrations. Conclusion: Using the raw spectral signals within the long red wavelengths allowed for the identification of up to 48 multiplexed fluorescent beads on an Aurora full spectral cytometer. The spectral bead signatures had minimal impact on the PE reporting channel allowing measurement of the raw PE MFI reporter. The ability to use the spectral signature allowed for the identification of individual fluorescent beads that is difficult to accomplish using traditional analytical cytometers. Standard curve detectable concentration limits for individual analytes were similar on both instruments, with some analytes having a slightly lower detectable concentration on the full spectral cytometer. Using the Aurora full spectral cytometer to collect multiplex bead assays kits is an alternative option, with results comparable to the traditional Luminex MAGPIX instrument.

**902030 P71**

## **Development of a CD137 receptor occupancy assay to support the phase I/II study of BT7480, a Bicycle tumor-targeted immune cell agonist™ (Bicycle TICA™)**

Julie Bick<sup>1</sup>, Chintan Jobaliya<sup>1</sup>, Heather Cohen<sup>2</sup>

<sup>1</sup> FlowMetric, a KCAS company, <sup>2</sup> Bicycle Therapeutics

Bicycles are fully synthetic constrained peptides with antibody-like affinities that target selectively, readily penetrate tumor tissue, have relatively short half-lives, and can be chemically linked together to generate multifunctional molecules. BT7480 is a Bicycle TICA™ being developed as a first-in-class CD137 therapeutic for the treatment of human cancers associated with Nectin-4 expression which is currently being investigated in an ongoing phase I/II clinical trial<sup>1,2</sup>. Monitoring target engagement

for a given therapeutic can be a key factor in recommending the phase II dose. While flow cytometry-based receptor occupancy (RO) assays are commonly used to monitor target engagement in the clinic, a CD137-specific RO assay presents several important challenges that have historically hampered monitoring RO in the clinic including the dynamic expression of CD137 on unstimulated and stimulated T cells, the low frequency of CD137+ cells in human blood and limited reagents to confidently detect CD137+ cells in the presence of CD137-targeting drugs. To address these challenges, a fit-for-purpose 14-plex flow cytometry panel was developed that incorporates a fluorescently labelled CD137-specific binding Bicycle® dimer, thereby enabling simultaneous detection of various CD137+ immune cell types as well as receptor occupancy by BT7480 in a single blood sample.

**904059 P73**

## **Development of a flow cytometry assay to monitor human PBMC engraftment and PD response in humanized NSG mice**

Janina Schwarte<sup>1</sup>, Poojitha Vellore Jaysukumar<sup>1</sup>, Dilanjan Anketell<sup>1</sup>, Mark Stottlemyer<sup>1</sup>, Yu-An Zhang<sup>1</sup>, Jane Cheng<sup>1</sup>, Fangxian Sun<sup>1</sup>, Marie Bernardo<sup>1</sup>, Shannon McGrath<sup>1</sup>

<sup>1</sup> Sanofi

Murine syngeneic tumor models are valuable tools for characterizing the antitumor efficacy and immune stimulatory activity of novel cancer immunotherapies, however, many biologics in preclinical development lack sufficient cross reactivity with their murine targets. Therefore, we developed a human melanoma xenograft in a NOD SCID gamma mouse (NSG) model with human PBMCs to study the activity of immune stimulatory cancer therapies. Here, we (1) describe the development of a 14-color human antibody panel and murine whole blood flow assay to characterize T and NK cells from a PBMC donor used for engraftment, (2) the instrument and biological controls and instrument set up required for valid comparison over the time course of the study, and (3) the application of the workflow to in vivo studies to confirm engraftment and track the expansion of human cells in mouse whole blood. The assay was successfully adapted for dissociated tumor and spleen, and will be used to monitor pharmacodynamic responses to novel cancer immunotherapies. This assay may be used for future in vivo studies involving PBMC humanized NSG mice.,

**904672**     **P75**

## **Barcoding Developed for Cell Cycle Analysis: A rigorous, efficient method of simplifying compound screening**

Laura Prickett<sup>1</sup>, Jessie Hao-Ru Hsu<sup>1</sup>, Jun Fan<sup>1</sup>, Natasha Narang

<sup>1</sup> AstraZeneca

Profiling the effects of small molecules on cell cycle provides key understanding of cellular potency and selectivity, and is essential to lead series selection. Our standard multiparameter cell cycle assay is low throughput and suffers from sample-to-sample staining variability. To remedy this, we adapted fluorescent cell barcoding (Krutzik 2011) to our multiplexed cell cycle panel. After testing and titrating multiple dye combinations, we optimized staining with two barcoding dyes (DyLight 633 and DyLight 800, ThermoFisher) on our tool cell lines (OVCAR3 and MCF7.) cPARP PE-CF594 (BD Biosciences) and EdU AF488 (Click-It Plus, ThermoFisher) were included to remove apoptotic cells and identify cycling cells. Barcoding removed sample-to-sample variability commonly found in treated samples with different resulting numbers of cells, and eliminated any need to chase gates between samples. We compared our results to individually stained samples treated with DMSO, Palbociclib, Nocodazole, or a CDC7 inhibitor. Barcoded samples showed the same trends, further validating our protocol. Our workflow now provides rigorous data, reduced acquisition and analysis time, and reduced reagent costs.

**898428**     **P77**

## **Imaging flow cytometry as a new route for high-throughput characterisation of pattern recognition receptors binding capabilities for point-of-care device development**

Andrew Farthing<sup>1</sup>, William J. Peveler<sup>1</sup>, Carl S. Goodyear<sup>1</sup>, Melanie Jimenez<sup>2</sup>

<sup>1</sup> University of Glasgow, <sup>2</sup> Monash University

Point-of-care (PoC) devices are becoming increasingly common for rapid diagnostics of infectious diseases and have recently revolutionised testing for COVID-19. These devices commonly rely on indirect detection of an antigen or inflammatory marker and most target only one pathogen. Inspired by the immune system, a new class of PoC devices has recently emerged for broader detection whereby Pattern Recognition Receptors

(PRRs) are used to monitor the presence of pathogen-associated molecular patterns and damage-associated molecular patterns. It has been shown that PRRs such as mannose binding lectin or Toll-like receptors (TLRs) can be used to remove/detect a wide variety of pathogens. These approaches provide a new route to diagnostics/treatment for scenarios where the pathogen identity is unknown such as bloodstream infection or food/water contamination. PRRs are however commonly characterised in terms of immune response as opposed to binding capabilities to cells in vitro which is impeding the development of PoC devices. In this work, we propose a new workflow using flow cytometry to map the binding capabilities of PRRs to whole cells. As proof of principle, the binding capabilities of fluorescently-labelled TLRs to GFP-expressing *Staphylococcus aureus* and *Escherichia coli* were investigated using an imaging flow cytometer. A bespoke data processing pipeline was developed whereby intensity profiles of bacteria without TLRs were fitted with a 2D Gaussian distribution and automated gating was performed to encompass the high-density region of the distribution. Outputs from this data processing strategy consisted of an accurate representation of the percentage of single cells with TLR binding at their surface defined hereafter as 'positive cells'. Using the capabilities of flow cytometry, thousands of single bacteria could be analysed per second. Results with TLRs confirmed strong binding between TLR2 and *S.aureus* with over 90% of cells classified as positive ( $61 \pm 18\%$  -  $92 \pm 4\%$  positive cells for TLR2 concentrations ranging from 0.25 to 2.00 ng/ $\mu$ l) – as expected for this PRR and its affinity with pathogen-associated lipopeptides. Interestingly, binding was also observed between *S.aureus* and TLR4, a PRR mostly known for its interaction with Gram-negative bacteria (up to  $29 \pm 7\%$  positive cells). Comparatively, less than 6% of Gram-negative *E.coli* cells were found positive for the same TLR4 concentration range due to the missing proteins required for LPS recognition (myeloid differentiation factor 2). This work provides a steppingstone toward a high throughput method of characterising the binding of PRRs to whole bacteria using flow cytometry. This method overcomes many of the limitations for quantifying cell:protein interactions and will be used to help parameterise engineered PoC devices for rapid pathogen detection.

# CYTO 2022 ABSTRACTS

901658 P81

## Automatic identification of diagnostic biomarkers for rheumatic diseases: lessons learned building an end-to-end machine learning workflow

Pablo López-García<sup>1</sup>, José A. Vera-Ramos<sup>2</sup>, Thomas R. Pieber<sup>1</sup>, Barbara Prietl<sup>1</sup>

<sup>1</sup>CBmed GmbH - Center for Biomarker Research, <sup>2</sup> Medical University of Graz

Multi-channel flow cytometry and machine learning promise great potential for diagnostic biomarker discovery, but fully automated workflows are scarce. To investigate why, we developed an end-to-end completely automated workflow for diagnosing patients with rheumatoid arthritis (RA) and systemic lupus erythematosus (SLE) using state-of-the-art cytometric and machine learning methods and compared results with a classic manual gating approach. We collected samples from 162 subjects (68 healthy, 64 RA, 30 SLE), stained the cells with 10 markers (CD15S, CD127, CD45RA, Ki-67, CD4, FoxP3, CD25, CD161, FVS, CD3) and analyzed them in a BD LSR Fortessa™ SORP flow cytometer, resulting in 268,793 events per sample on average. Our automated workflow consisted of pre-gating with “flowCore” (non-debris, singlets, viable cells, lymphocytes), auto-gating for markers using “CytomeTree”, population filtering to match a set of 12 reference T-cell subpopulations, and normalizing frequencies to lymphocytes. This dataset was then used to train a 3-class (healthy, RA, SLE) support vector machine (SVM) classifier. Performance (AUC, 10-fold cross validation) was 0.58, and the best explanation for classifications of RA and SLE patients was a low level of non-suppressive Tregs, suggesting this could be a potential biomarker for both diseases. As a reference standard for comparison, we manually gated all 162 samples for our set of 12 reference T-cell subpopulations. With this reference dataset, we trained another SVM classifier and obtained an AUC of 0.72. While the increase in performance was expected due to the careful manual gating, we were surprised to observe that model explanations did not match. Our reference model suggested low CD4CD127+ as the strongest biomarker for RA and high FoxP3+ Tregs for SLE. Moreover, it suggested high values of non-suppressive Tregs for both diseases, contradicting our automated results. A closer investigation revealed why: most subpopulations had been severely affected by the automated gating stage despite all our attempts of parameter optimization: only lymphocytes, CD3+CD4+ (in good agreement with “CytomeTree” results in

FlowCAP I), FoxP3 Treg, and CD127 FoxP3+ subpopulations were not statistically different to our reference manual gating results. We revised our original raw files, manually corrected compensation when necessary, and re-ran our automated workflow. Model performance improved slightly to 0.60 but surfaced biomarkers did not change. Our findings suggest that care must be taken when building automated workflows for biomarker discovery that try to replicate sequential manual gating. While these methods are extremely valuable and robust for well-studied markers (e.g., CD3 and CD4 in our case), they can be problematic with others, or in experiments with a high number of markers. In these cases, dimensionality-reduction or clustering-based methods might be better alternatives and explain their popularity.

901908 P83

## How to make your flow cytometry life easier: finding differences in B cell subsets between autoimmune diseases and healthy controls using CITRUS

Barbara Prietl<sup>1</sup>, Laurin Herbsthofner<sup>1</sup>, Verena Pfeifer<sup>1</sup>, Thomas R. Pieber<sup>1</sup>

<sup>1</sup> CBmed

The unsupervised analysis of high-dimensional FACS data is still not widely used in clinical research and can be highly complicated when dealing with high numbers of patients in different clinical cohorts. Still, the flexibility of machine learning algorithms is needed to dive deeper into unknown cell populations and clinical phenotypes and to compliment manual gating. To investigate its added value over manual gating, we performed CITRUS using the browser based Cytobank software (Beckman Coulter Life Sciences) to identify new cell subtypes and analyse differences between patient groups. A FACS analysis for B cell subtypes was performed targeting 12 surface markers (CD19, CD20, CD27, IgD, CD24, IgM, CD38, CD43, CD1d, CD5, CD86, CD131). 80 individual samples were included in the analysis with CITRUS: 24 healthy controls, 17 rheumatoid arthritis (RA), 17 systemic lupus erythematosus (SLE) and 22 type 1 diabetes (T1D) patients. All files were pre-gated to CD19+ B cells and then equally sampled to reach an event number of over 230,000 events to be subjected to hierarchical clustering in CITRUS. The minimal cluster size was set to 3% (6,900 events) and a false discovery rate of 1% was used. CITRUS identified 55 clusters, 32 of them were flagged as significantly different

# CYTO 2022 ABSTRACTS

between our cohorts using Significance Analysis of Microarrays (SAM). A manual reduction of these 32 clusters had to be done to exclude redundant events. The remaining 9 clusters were additionally tested in a multivariate analysis of variance (MANOVA) with Bonferroni correction of post hoc testing and showed a statistically significant difference between subject groups. Eight of the identified clusters are characterized by a high expression of CD86, known as a common activation marker in B cells, which we also found in our manual gating: higher numbers of CD86+ B cells were found in SLE patients compared to all other groups. In T1D patients two different clusters were identified that were significantly increased compared to the other investigated groups. One cluster was found negative for CD86 but positive for the expression of all other markers included in the panel. The second cluster was found to be negative for CD131 but positive for other markers. Our results show that CITRUS analysis worked on our 12-marker panel for B cells combining data from 80 study participants within one single run. Testing all possible workflows confirmed the pre-gating and downsizing steps as mandatory for this kind of analysis. In our study, comparing B cell phenotypes within different cohorts of autoimmune diseases and healthy controls, CITRUS analysis was successfully implemented and allowed the identification of new cell populations of interests. Therefore this machine learning based analysis could be an important addition to manual gating in clinical studies using FACS data.

---

**901912 P84**

## **A Machine Learning Workflow for Automatic Immune Phenotyping of Type 1 Diabetes Samples**

Barbara Prietl<sup>1</sup>, Thomas R. Pieber<sup>1</sup>, José Antonio Vera-Ramos<sup>1</sup>, Martin Helmut Stradner<sup>1</sup>

<sup>1</sup> CBmed

Autoimmune diseases have a high occurrence in the population, causing great morbidity and mortality. Despite presenting considerable clinical heterogeneity, many autoimmune diseases exhibit common mechanisms leading to a self-tolerance breakdown, suggesting the possibility of finding similar patterns on autoimmune diseases that can be helpful to better understand their behavior, and the recovery of patients suffering from them. We, under this premise, aimed to find common patterns inspecting the cell population distributions of samples coming from patients of different autoimmune diseases. We used

machine learning (ML) to perform deep immune phenotyping of type 1 diabetes (T1D) and healthy controls as a preliminary way of identifying common patterns and dissimilarities among different autoimmune diseases. PBMCs were isolated from patients with T1D (n=69) and healthy donors (n=50). A FACS approach was applied, based on five different panels, each one focusing a different set of cell populations. Then, a traditional analysis was compared to a ML method implemented on R. Such pipeline includes unsupervised pre-gating of lymphocytes using the R package flowCore, a data normalization step to improve the performance of the model, and FlowSOM clustering to group cells based on similarities on their marker expression using Self Organizing Maps (SOM). We apply a Generalized Linear Mixed Models (GLMM) test as a final step to find significant differences of cell population abundance among groups. After applying our automated workflow on two of the panels focusing on T cells we could identify 14 cell clusters on the first panel, and 16 clusters on the second one. The GLMM test on panel 1 revealed a trending cluster ( $p=0.059$ ) on the abundance between T1D and controls. This cluster is defined by CD4pos T cells expressing high IL-7 receptor (CD127) levels and median amounts of CD15s but low CD25, CD161 and FoxP3, and its abundance is increased in T1D samples. In conclusion, our ML workflow is able to determine the cell population profile of many samples and identify differences on the cell population abundance of different groups. This unsupervised analysis approach enables the discovery of new biomarkers complementing traditional workflows and streamlines the profiling of large datasets, otherwise too substantial to be tackled in a conventional manner. We plan to apply this workflow on large clinical studies to automatically classify and compare cell populations of not only T1D patients but other autoimmune diseases such as rheumatoid arthritis and systemic lupus erythematosus.

---

**901939 P85**

## **Benefits of an open source Similarity Score for multiparametric flow cytometry controls.**

Sara Garcia<sup>1</sup>, Lola Martinez<sup>1</sup>, Sara Garcia-Garcia<sup>1</sup>, Julia Garcia-Leston<sup>1</sup>

<sup>1</sup> CNIO

In recent years multicolor flow experiments have significantly increase in complexity as instruments have more lasers and number of detectors. It translates into a higher number of control tubes that need to be run in order to analyze the collected

# CYTO 2022 ABSTRACTS

data files been a burden for users as it is time consuming and can become very expensive doing all those controls. Core unit staff commonly face users not bringing appropriated controls for many reasons (brightness, peak resolution, damaged fluorochromes, ...) leading to the need to redo some of these controls and run them again either the same or another day depending on instrument availability. Having beforehand the information related to which fluorochromes on a specific experiment are more prompt to change their spectral properties due to staining conditions (buffer, temperature and others) or the nature of the control itself (cells vs beads) will reduce the time spent on the instruments as well as the number of tubes needed for the experiment. Therefore, new strategies to simplified our fluorescence controls for any multicolor flow experiment are needed. Some online tools can provide a theoretical score between fluorochromes signatures but they are limited to those listed on their library. On the other hand, some manufacturers provide similar scores but it requires data to be collected following a define workflow which for some comparisons could be cumbersome. To overcome these limitations, we developed an analysis strategy based on vectorial calculations of the distance between the normalized values from fcs files that allow us to compare fluorescent controls independently of the instrument or acquisition software used to generate the data. This score value will help understand the similarity between controls acquired on different days or conditions facilitating core users of multicolor flow to determine in a quick manner the stability of their fluorescent reagents as well as identifying which control will fulfil the criteria to be use in their particular experiment without depending on any proprietary software. Information provided by this tool will certainly be an added value that the core facility could provide to their users helping them to reduce the number of tubes needed to be run for their experiments. Furthermore, it will reduce time spent by core staff troubleshooting user's data. Even this similarity score may have other potential applications that still need to be explore we hope it will facilitate the work of cytometry users and core staff.

**902022 P86**

## **MetaFlow: Innovative Cloud Based Topological Analysis Platform for High-Dimensional Flow Cytometry Data**

Kamila Czechowska<sup>1</sup>, Andy Filby<sup>1</sup>, Raif Yuecel<sup>1</sup>, Alan Saluk<sup>1</sup>, Attila Babes<sup>1</sup>

<sup>1</sup> Metafora Biosystems

As the complexity of flow cytometry experimentation increases in terms of parameter space, advanced analytical tools such as dimensionality reduction and clustering have become essential to the exploration and interpretation of the data. While these approaches are powerful and designed to represent the original data structure, they rely on a number of subjective variables that will affect the results and thus the interpretation. It is therefore attractive to utilize approaches that maintain the original data structure as dictated by the values and signal resolution generated at acquisition. The Metaflow platform was used to analyse four different flow cytometry data sets. 1) A “simple”, well-defined 8 marker fluorescent panel acquired on a conventional fluorescence flow cytometer. 2) A 27 marker fluorescent panel acquired on a conventional fluorescence flow cytometer. 3) A 40 marker mass cytometry panel acquired on a Helios CyTOF system. 4) A 15-colour panel acquired on spectral cell sorter. In all cases, data was also analysed via “ground truth” manual gating as well as FLOWSOM clustering with UMAP visualisation using FCS express software (De Novo) for comparison. Unlike the aforementioned approaches, one can go directly with the native data set after compensation. METAflow automatically performs scaling transformation as adapted to the method of data acquisition. This keeps the entire structure of the data and clusters by taking into account all available parameters, including morphology. Additionally, there are inbuilt modules for signal instability removal and identification of debris and doublets which were vetted against manual gating approaches to the same end. Metaflow based analysis was shown to provide high accuracy results and allows for preservation of the original data structure, independent of the raw data origin as well as increasing numbers of dimensions. Debris was readily clustered for majority of tested files and, automated labelling of debris and doublets was demonstrated to significantly shorten analysis time per sample. The seamless, integrated design of the solution made it insensitive to prior gating, increasing robustness and reproducibility of the end-point analyses. Metaflow provides a powerful platform for exploring, analysing and interpreting flow cytometry data sets. Unlike many cluster-based approaches

# CYTO 2022 ABSTRACTS

that require significant hyper-parameter tuning, offers seamless workflow relying on density-based algorithm that maintains the original data structure akin to auto-gating. This can provide detailed insight into data granularity while operating in multiple dimensions. The clustering algorithm further optimizes achieving robust and rapid data presentation by the cleaning of both doublets and debris, expediting computational time to results. The software can be a gateway for valid and reproducible discovery in data sets to any user with no prior knowledge of current overly-complex automated strategies.

**902027 P87**

## **Quantitative digital image analysis of ultra-high plex immunofluorescence imaging**

Bassem Ben Cheikh<sup>1</sup>, Yasmin Kassim<sup>1</sup>, Aditya Pratapa<sup>1</sup>, Oliver Braubach<sup>1</sup>

<sup>1</sup> Akoya Biosciences

Spatial omics technologies like Co-Detection by indEXing (CODEX) have transformed cancer research from discovery to translation. The CODEX chemistry enables the simultaneous detection of more than 100 protein biomarkers at single cell resolution within their native tissue environment and thus combines the advantages of multi-parameter analyte readout with single-cell optical resolution. The PhenoCycler-Fusion, a novel spatial biology platform, accelerates the CODEX workflow to generate ultra-high plex spatial data that map millions of cells on a single tissue section within a matter of hours. Quantitative digital image analysis plays a critical role in gathering meaningful information from such data. Here we demonstrate the utility of combining computer vision and machine learning techniques for unbiased whole tissue analysis with PhenoCycler-Fusion data. Our image analysis consists of fast cell segmentation into nuclear and membrane compartments via a deep learning model trained on millions of cells that were manually annotated. This is followed by calculations of average protein expression from corresponding immunofluorescence images within individual cell compartments where the proteins are expressed. Feature selection and unsupervised clustering algorithms are then used to identify groups of cells with similar protein expression patterns to accomplish cell phenotyping. Lastly, spatial analyses are performed to characterize the spatial organization of the different cell phenotypes in the tissue and to quantify their spatial interactions using a combination of graph theory and statistical methods. Our analysis pipeline

was tested and validated on a novel 100-plex antibody panel comprising markers for cell lineage, tissue structure, immune activation, apoptosis, DNA damage and cellular metabolism markers developed for human FFPE tissues. The relevant results obtained on this comprehensive panel show the important role that digital image analysis plays in studying critical processes in healthy and diseased tissues and understanding the molecular and cellular mechanisms that underlie disease development, differentiation, and responses.

**902042 P88**

## **Automated Data Analysis of a 24-Color Nonhuman Primate Leukocyte Immunophenotyping Pane**

James Thomas<sup>1</sup>, Cathi Pyle<sup>1</sup>, Charles Trubey<sup>1</sup>

<sup>1</sup> Leidos Biomedical Research, Inc.

Advanced, high-parameter (18+ color capable) flow cytometers are becoming commonplace in flow cytometry cores and research laboratories, allowing researchers to expand the size and complexity of their reagent panels and extract more detailed information from their finite samples. However, as reagent panel parameters increase, the dimensionality of the resulting data and time required to manually analyze corresponding datasets significantly increases. Though “expert” manual analysis remains the gold standard for flow cytometry data analysis, manually analyzing large datasets derived from 18+ color complex reagent panels is exceedingly laborious, time consuming, and user biased. Implementing automated data analysis tools to help mitigate these manual analysis issues has become a necessity. However, assessing and adapting automated data analysis programs can be challenging. In this poster we present a comparative study of our manual versus automated flow analysis methods and share our quantitative results and experiences. For this project, we used FCS Express 7 (De Novo Software), for manual, and Astrolabe (Astrolabe Diagnostics) for automated data analysis of a 24-color reagent panel that identifies most major nonhuman primate (NHP) leukocyte populations and subsets. FCS Express 7 is a highly intuitive and multifunctional flow cytometry data analysis program we routinely use for flow cytometry analysis. The Astrolabe Cytometry Platform is a relatively new, comprehensive data analysis software that incorporates data pre-processing, population identification and clustering algorithms (e.g., FlowSOM), as well as statistical and differential analyses, in one highly automated, cloud-based



# CYTO 2022 ABSTRACTS

system. The results of this comparative analysis revealed several strengths and weaknesses of both approaches. One critical, rate-limiting step in the Astrolabe analysis involved developing an NHP-biology-specific, leukocyte phenotyping hierarchy, which the software requires to correctly categorize cell subsets. Though once established, it was just a matter of setting up the automated and differential expression analysis parameters, uploading the data files and waiting a couple of hours for the results. Astrolabe also annotates the uploaded FCS files, essentially embedding its algorithm-identified population gates, allowing end users to easily compare automated versus manually identified cell populations by back gating. The ability to examine these automated-analysis-defined populations using FCS Express, allowed us to rapidly assess whether cell subsets were correctly identified, and when a cell subset was incorrectly identified, we were able to quickly determine its true identity. Overall, we found good correlations between all major leukocyte populations, especially lymphocyte subsets, when comparing automated analysis with manual. We are working with Astrolabe to refine our NHP hierarchy and analysis parameters, to further improve our automated analysis results.

**902312 P89**

## **Implementation and validation of an automated spectral flow cytometry analysis pipeline in large scale human immune profiling.**

Yi-Dong Lin<sup>1</sup>, Pierre-Emmanuel Jouve<sup>2</sup> and Vilma Decman<sup>1</sup>, Vilma Decman, Pierre-Emmanuel JOUVE

<sup>1</sup> Cellular Biomarkers Group, BIB, IVIVT, GlaxoSmithKline Pharma R&D, 1250 S. Collegeville Road, Collegeville, PA 19426, United States, <sup>2</sup> AltraBio, Lyon, France.

**Background:** Advances in flow cytometry (FCM) technology have resulted in development of high-parameter panels with increased complexity in gating and data analysis. This is notably the case with the recent spectral flow cytometry technology. While this may allow great hypothesis testing, this also generates a massive amount of data, which is typically analyzed manually through the gating process. Manual hierarchical gating, which remains the standard of practice, is unfortunately a rate limiting step for complex panels and big datasets. Additionally, use of multiple analysts in longitudinal studies often leads to increased variability due to the subjectivity in manual gating. In contrast, automated analysis can reduce FCM analysis time from hours to minutes while limiting analysis variability.

**Objective:** To develop, validate, and implement an automated gating pipeline that replicates manual gating to analyze large, deep multi-parameter spectral flow cytometry datasets from TCR samples.

**Methods:** 23-color (spectral flow cytometry) panels were developed and validated for clinical use and evaluated. A Random Forest based machine learning approach was applied to develop an automated gating pipeline that mimics manual gating. An initial training dataset was used to learn the expert manual gating process for panel by building machine-learning models for each individual gating step. Afterwards, we have analyzed samples and evaluated the performance of automated gating analysis by comparison to standard manual gating analysis (carried out with FlowJo version 10.8.2).

**Results:** Our primary goal is not to propose new clustering algorithms or novel automated gating algorithms. Instead, we demonstrate that the fast and reproducible automatic gating analysis of multi-parameter flow cytometry data can be reliably accomplished by auto gating. The robustness of automated gating was evaluated by comparing the %CV of manual gating and automated gating of TCR samples.

**Conclusion:** The developed pipeline mimicked correctly the manual gating but with faster turnaround time. It can analyze large scale clinical datasets with comparable precision and accuracy to traditional manual gating. We have established a sustainable and efficient automated gating pipeline that has the advantages of efficiency, high throughput and consistency.

**Acknowledgement:** Anil Kesarwani, Jiangfang Wang, Taryn Mockus and Danille Stewart

**898154 P91**

## **Fully automated large-scale integration of mass cytometry datasets using deep learning reveals insights into the COVID-19 T-cell landscape**

Hajar Saihi<sup>1</sup>

<sup>1</sup>QMUL

**Meta-analysis of mass cytometry studies will transform the way we study the immune system allowing for improved precision of biomedical conclusions, hypothesis-generating research, and the discovery of novel immune cell signatures. However, meta-analysis suffers from the heterogenous nature of mass cytometry panels, the lack of scalable and automated**

# CYTO 2022 ABSTRACTS

cell identification methods, and technical variation unique to each instrument. Here we demonstrate an end-to-end meta-analysis pipeline making possible for the first-time robust, and scalable meta-analysis of immune cells without prior knowledge integration. To demonstrate the efficacy of our approach, we integrated data from six COVID-19 datasets covering 258 samples and confirmed known COVID-19 immune cell signatures. In addition, we discovered the upregulation (two-sided Wilcoxon,  $p < 0.05$ ) of novel CD3+CD4+CD56+ cell populations that were not observed in the original studies. We anticipate our pipeline to leverage statistical power associated with study integration and allow for detailed insight into meta-immune cell signatures.

**898423 P93**

## **PhenoComb: A discovery tool to assess complex phenotypes in high-dimension, single-cell datasets.**

Paulo Burke<sup>1</sup>, Ann Strange<sup>1</sup>, Emily Monk<sup>1</sup>, Brian Thompson<sup>1</sup>, Carol Amato<sup>1</sup>, David Woods<sup>1</sup>,

<sup>1</sup> CU Anschutz

Modern high-dimension cytometry assays can simultaneously measure dozens of markers, enabling the investigation of highly complex phenotypes. However, as manual gating relies on previous biological knowledge, few marker combinations are assessed. This results in millions or billions of complex phenotypes with a potential for biological relevance being overlooked. Here we present PhenoComb, an R package that allows agnostic exploration of phenotypes by assessing all combinations of virtually any number of markers. PhenoComb uses fluorescence intensity thresholds to assign markers to discrete states (e.g. negative, low, high) and then counts the number of cells per sample from all possible marker combinations in a memory-safe manner, with time and disk space being the only constraints on the number of markers evaluated. It also provides several approaches to perform statistical comparisons, evaluate the statistical relevance of phenotypes, and assess the independence of identified phenotypes. PhenoComb allows users to guide analysis by adjusting several function arguments such as identifying parent population(s) of interest, filtering of low-frequency populations, and defining a maximum complexity of phenotypes to evaluate. We have designed PhenoComb to be compatible with local computer or server-based use. PhenoComb's performance was

assessed on synthetic datasets. Computation on 16 markers was completed in a matter of minutes, and up to 26 markers in a matter of hours. We applied it to two large, publicly available datasets: the COVIDome CyTOF dataset (40 markers and 99 samples), and an HIV flow cytometry dataset (14 markers and 600 samples). In the HIV dataset, PhenoComb was able to automatically identify immune phenotypes associated with HIV seroconversion matching those in the original publication of the dataset. In the COVID dataset, we identified immune phenotypes associated with infection, as compared to healthy individuals. Collectively, PhenoComb represents a powerful discovery tool for agnostically assessing high-dimension, single-cell data.

**898517 P95**

## **Robust Identification of biomarkers through a clustering approach guided by patient outcomes: application in B-cell ALL, melanoma and rheumatoid arthritis**

Julien Nourikyan<sup>1</sup>, Pierre-Emmanuel Jouve<sup>1</sup>

<sup>1</sup> AltraBio SAS

Introduction Current cytometry reagents and instrumentation developments open up new possibilities to test biological hypotheses, identify biomarkers and perform diagnosis from the generated data. Several methods, mainly unsupervised, have been proposed to automate the identification of biomarkers. While they may be extremely valuable in exploratory contexts, the reliability of the identified cell populations and their use for diagnostic approaches are still questionable. To improve the discriminative power of these cell populations, we have developed a semi-supervised approach taking into account additional information, such as patient/treatment status, when identifying cell populations (output-guided clustering). Objective We previously assessed our method on a cytometry dataset in the context of residual disease assessment with excellent results : one of the identified cell clusters allowed to perfectly predict the patient status (100% accuracy). The objective of this study was to confirm the performance of our approach on new datasets. Materiel & Methods Unlike other existing approaches, which identify clusters of cells from a pool of observations, our approach clusters each sample separately and then performs meta-clustering to merge them. This makes it possible to be less sensitive to batch effects and to better capture the specificities of each sample. Furthermore, this method can use additional information such as patient status to guide cluster identification

# CYTO 2022 ABSTRACTS

to further increase the reliability of the results. here, we applied this approach to 3 public cytometry datasets (conventional flow cytometry and mass cytometry) related to B-cell Acute Lymphoblastic Leukemia, anti-CTLA-4 and anti-PD-1 immunotherapy in patient with melanoma, and Rheumatoid Arthritis. Comparisons of our results with those of articles linked to these datasets were made to assess the quality of our results. Results The comparisons show remarkable similarities between our results and those of published papers while our approach implies less intensive work. Furthermore, in some cases some potentially highly interesting additional insights are brought by our method. Conclusion The capacity of our algorithm to identify discriminative cell populations from cytometry data has been confirmed as well as its ability to process higher dimensionality data (mass cytometry data). These experiments validate the fact that our approach can be used with success for tasks such as diagnosis, vaccine efficiency evaluation, and more generally biomarkers identification.

**898554 P97**

## **A simple guide for selecting a cytometry data analysis strategy**

Alice Wiedeman<sup>1</sup>, Carolina Acosta-Vega<sup>1</sup>, Hannah DeBerg<sup>1</sup>, Gautam Goel<sup>1</sup>, Bernard Khor<sup>1</sup>, Jane Buckner<sup>1</sup>, Hamid Bolouri<sup>1</sup>, S. Alice Long<sup>1</sup>,

<sup>1</sup>Benaroya Research Institute (all authors)

As the number of parameters in cytometry continues to grow, the complexity of experiments increases. In parallel, more sophisticated analysis strategies and tools are being developed. However, the most appropriate analysis strategy to fully utilize high-parameter cytometry data is not always evident. Here we propose a simple, two-dimensional rubric for selecting an analysis strategy based on (1) the experimental question or goal and (2) the extent of technical variation (batch effects) in the data. We applied the guide for three kinds of scientific questions with a goal to: (1) Assess known cell subsets or features (e.g. Does abatacept treatment in rheumatoid arthritis decrease regulatory T cells?), (2) explore and compare possible subsets/features (e.g. What phenotypes are dominant among autoreactive CD8 T cells in type 1 diabetes?), and (3) discover differing subsets/features (e.g. Which immune cell subsets are altered in Down Syndrome?). To address the scientific question within each category we utilized intentionally selected analysis tools (Astrolabe, DISCOV-R, and IMPACD) based on extent of

technical variation in our datasets. This simple guide enables scientists at any level to adopt appropriate high-dimensional analysis strategies. The two-dimensional rubric is a foundation that can be augmented by additional axes such as ease-of-use and the speed of computation, and it helps reveal where gaps in the field remain.

**906041 P99**

## **Novel 355nm (and Lower) Excitable and Tuneable Emission (Blue through Red) Fluorophores Utilised in Flow Cytometry**

Sunil Claire,<sup>b</sup> Parvez Iqbal,<sup>b</sup> Michael Butlin<sup>a</sup> Owen Jones,<sup>a</sup> Karolis Virzbickasa,<sup>b</sup> and Jon A. Preecea,<sup>ba</sup>

<sup>1</sup> School of Chemistry, University of Birmingham, Edgbaston, Birmingham B<sup>1</sup>5, <sup>2</sup> TtBChromaTwist, Birmingham Research Park, Vincent Drive, Edgbaston, Birmingham B<sup>1</sup>5 <sup>2</sup>SQ

Labelling antibodies with a fluorescent reporter molecule allows for the detection and localisation of antigens situated within a cell, tissue or organ. An array of fluorescent probes can be attached to different antibodies, each conveying its own distinct spectral properties that can be exploited by flow cytometry and multiphoton microscopy. We have, to date, >50 novel dyes that have an excitation profile from ~250nm to ~420 nm. The dyes can be chemically tuned to emit from 400 nm through to 630 nm,<sup>1, 2</sup> and hence have utility to increase multiplexing in both multicolour and spectral flow cytometry. This study focuses on antibody conjugation of one dye via the formation of an active ester on a novel dye (Gen-2-Dye). The reaction uses EDC/sulfo-NHS chemistry to activate the carboxylic acid functionality on the fluorophore which enables conjugation to a CD8 antibody via an amide linkage. Characterisation by UV-Vis absorbance and steady-state emission spectroscopy confirmed the presence of the antibody with the distinct fluorescent signature of the Gen-2-Dye. A commercial antibody conjugation check kit also confirmed successful conjugation and antibody functionality (Figure 1a). The Gen-2-Dye•CD8 conjugate was used to stain compensation beads and displayed a bimodal distribution in the bead population relative to the unstained control (Figure 1b-d). Further optimisation is underway to achieve two distinctly separated populations of negative and positively stained compensation beads.

# CYTO 2022 ABSTRACTS

**897392 P101**

## **From Automated Antibody Mixing to Reliable Analysis**

Gert Van Isterdael<sup>1</sup>, Victor Bosteels<sup>1</sup>, Sophie Janssens<sup>1</sup>

<sup>1</sup>VIB-UGent Center for Inflammation Research

Due to the continuous increase in number of fluorochrome-labeled antibodies in panels for flow cytometry, the manual mixing of antibodies has become very labor-intensive. Furthermore, larger panels need many more controls including all fluorescence minus one (FMO) controls, to allow proper interpretation of the data. This comes with a significant cost in hands on-pipetting time and an increasing risk of making mistakes. Therefore, we evaluated different dispensing robots to automatically make antibody mixes. Considering several criteria such as low dead volume, source capacity, time, flexibility and price, we chose the iDOT (Dispensex) to implement in our work flow for antibody mixes, including single stained controls on cells and beads, all FMOs and full stains of a 20-color panel in less than 30 minutes. Having all these controls available gave us many advantages during panel optimization and validation, visualization and analysis of the data. The FMOs allowed us to easily visualize and evaluate the extend of data spread and helped in identifying compensation issues. Furthermore, when multiplexing markers (using different markers with same fluorochrome), FMO's (or better, marker minus one (MMOs)) allowed us to validate the reliability of combining different markers and to disentangle them based on other markers. When plotting the gating strategy, we could overlay on every FACS plot the FMOs on X and Y axis and as such show the validity of our gating. On top of this, having all FMO's leads to a more reliable automated gating strategy, and we are currently investigating how they can be help in automatic clustering algorithms such as FlowSOM. In conclusion, we believe automated pipetting robots such as iDOT have a strong added value for flow cytometry and should become the standard in all flow cytometry pipelines. Without much extra effort they will encourage researchers to include all possible controls, which - due to the continuous increase in panel complexity - become absolutely vital to obtain high quality flow cytometry data.

**901054 P103**

## **Determination of optimal settings for detector voltages for resolution of a 14-color panel on the Bigfoot cell sorter**

Sherry Thornton<sup>1</sup>, Kenneth Quayle<sup>1</sup>, Celine Silva-Lages<sup>1</sup>

<sup>1</sup> CCHMC

The Bigfoot cell sorter is a jet-in-air sorter capable of sorting with either traditional compensation or spectral unmixing. The vendor recommendation for setting detector voltages in spectral mode involves using unstained control cells and adjusting the voltage to reach a consistent mean fluorescence intensity (MFI) in each detector, which is 25 by default. When unmixing panels of 10 colors or more in spectral mode using this approach to voltage setting, loss of resolution in dimly fluorescent cell populations was consistently observed, even when the panels were well-designed from a theoretical perspective and those dimly fluorescent populations were observable on other instruments. To assess various approaches for setting detector voltages, a 14-color human PBMC panel using was used with 5 different approaches: 1) voltages set manually in non-spectral mode, 2) MFI of unstained PBMC set to 25 in each detector, 3) 2-peak bead separation adjustment set during instrument QC, 4) rSD of unstained PBMC set to 2.5x the rSD of noise, and 5) optimizing separation between unstained PBMC and noise. Results from this assessment indicate that for the majority of the fluors in the 14-color test panel, voltage settings from the 2-peak bead separation generated the best result both qualitatively based on the ease of manually gating the relevant populations and quantitatively based on the staining index. In addition, while attempting to measure the noise in each detector for tests 4 and 5, we observed several detectors for which unstained PBMC were indistinguishable from electronic and/or optical noise at any voltage. In conclusion, our results indicate that unmixing performance on the Bigfoot platform may likely benefit from taking detector noise into consideration when designing panels by avoiding dyes with bright fluorescence in noisy detectors. A ranking of commonly used fluorescent dyes that takes both the spectral signature and the relative noise of each detector into account will be presented for the instrument tested. Characterization of the instrument detectors appears to be paramount for best performance of this instrument, and in the future, it would be advantageous to compare the noise observed in these detectors against those of similar instruments.

# CYTO 2022 ABSTRACTS

**901481 P105**

## **Expanding the Maxpar Direct Immune Profiling Assay to enable comprehensive antigen-specific immune analysis**

Michael Cohen<sup>1</sup>, Christina Loh<sup>1</sup>, Stephen K. H. Li<sup>1</sup>, Huihui Yao<sup>1</sup>

<sup>1</sup> Fluidigm Canada

Monitoring the immune response to disease and assessing clinical recovery are critical steps towards identifying effective targets for therapies. The complex nature of the immune system often requires deep interrogation at the single-cell level. Mass cytometry, which uses CyTOF<sup>®</sup> technology, utilizes antibodies tagged with unique monoisotopic metals, resulting in distinct signals that provide a high-resolution multiparametric landscape of a single cell. CyTOF enables highly multiplexed cellular phenotyping with more than 50 phenotypic or functional markers simultaneously, significantly increasing the ability to comprehensively evaluate immune responses. The Maxpar<sup>®</sup> Direct<sup>™</sup> Immune Profiling Assay<sup>™</sup> is a pre-titrated, dried-down, 30-marker antibody cocktail for immune profiling of human whole blood and PBMC by CyTOF. Using the assay and Maxpar Pathsetter<sup>™</sup> software, stained samples are automatically resolved into 37 immune populations including major lineages and their subsets. The software automatically reports population statistics, stain assessments, and relevant data plots. In this study, we expanded the capabilities of the Maxpar Direct Assay by adding functional surface markers CD69 and CD107a as well as intracellular cytoplasmic markers IFN  $\gamma$ , TNF- $\alpha$ , IL-2, IL-4, IL-10, IL-17a, CTLA-4, perforin, and granzyme B. The addition of these markers enabled the assessment of cellular function in PMA/ionomycin-stimulated human PBMC samples. Cells were also stimulated with common infectious disease antigen peptides as a means of investigating antigen-specific immune responses. Furthermore, we incorporated sample multiplexing with live-cell barcoding into this workflow to improve data quality and enhance acquisition efficiency. Finally, we modified the Maxpar Pathsetter model to automate analysis of the expanded panel and report on new populations and additional functional parameters such as cytokine production that can be resolved with these markers. Taken together, this work demonstrates the flexibility of the Maxpar Direct Immune Profiling Assay to incorporate additional surface and intracellular markers to study antigen-specific immunity in the context of immune profiling and infectious disease. For research use only. Not for use in diagnostic procedures.

**901599 P107**

## **Identifying Relapse Associated Proteins by Human Surfaceome Screening in B-ALL**

Dorra Jedoui<sup>1</sup>, Astraea Jager<sup>1</sup>, Pablo Domizi<sup>1</sup>, Jolanda Sarno<sup>1</sup>, Charles Mullighan<sup>2</sup>, Sean C. Bendall<sup>3</sup>, Yuxuan Liu<sup>1\*</sup>, Kara L. Davis<sup>1\*</sup>

<sup>1</sup>Bass Center for Childhood Cancer and Blood Disorders, Department of Pediatrics, Stanford University, CA; <sup>2</sup> Department of Pathology, St. Jude Children's Research Hospital, Memphis, TN; <sup>3</sup> Department of Pathology, Stanford University, CA

\* co-corresponding author

B cell acute lymphoblastic leukemia (B-ALL) is the most common cancer of childhood. Despite impressive improvements in outcomes, for patients who relapse, finding a cure remains a challenge. Combining single cell analysis and machine learning, we previously identified a subset of pre-B cells, termed "relapse predictive cells" (RPCs), that are present at the time of diagnosis and highly predictive of relapse. RPCs were enriched in relapse samples demonstrating their persistence from diagnosis to relapse, making them an actionable target to prevent relapse. We aimed to identify RPCs through surface proteins alone thus we performed a comprehensive surfaceome screen of diagnosis-relapse paired B-ALL primary samples and PDXs to identify candidate defining surface proteins of RPCs. Samples were stained for CyTOF using a custom core panel of B cell developmental proteins along with 12 overlapping CyTOF panels staining of 350 proteins in total. Samples underwent B cell developmental classification. We focused ProBII-PreBI populations, the known developmental phenotype of RPCs. We filtered expression based on the 99.9th percentile of expression for each molecule. Differential expression analysis was performed between diagnosis and relapse samples to identify candidate proteins expressed on RPCs. Kolmogorov-Smirnov test was used to determine differences in expression distribution. Publicly available RNA-seq data were used to validate the expression of proteins of interest in diagnosis and relapse paired samples as well as in healthy bone marrows. We identified homogeneously enriched cell populations in leukemia samples. Late pro-B and early Pre-B cells were enriched in the diagnosis samples compared to more mature late pre-B and early immature B in the relapse samples. Our filtering step identified 96 potential proteins of interest of which 47 were differentially expressed in Pre-B cells between diagnosis and relapse in at least one paired sample. We confirmed significant

# CYTO 2022 ABSTRACTS

differences comparing ALL samples with healthy BM samples from publicly available RNA-seq data. Single cell representations uncovered co-expression patterns in late pre-B cells in relapse samples. Four out of 47 proteins were differentially expressed in at least 2 paired samples. We observed co-expression of tetraspanin superfamily molecule CD9, IG superfamily protein CD147 (Basigin), MHC class I molecule  $\beta_2$  microglobulin and Leucocyte-associated Ig-like receptor 1, CD305. In line with our findings, CD9 and CD147 are significantly higher expressed in relapse samples compared to diagnosis in public RNA-seq data. In summary, our approach defined the surfaceome of B-ALL cells with unprecedented resolution. Late Pre-B and early immature B cell populations were enriched with distinct surface molecule expression at the time of relapse, Further validation experiments with healthy and B-ALL primary samples are underway.

**901810 P109**

## **Time to meet the moment: High-speed cell sorting using real-time full spectral unmixing**

Lyadh Douagi<sup>1</sup>, Larry Lantz<sup>1</sup>, Thomas Moyer<sup>1</sup>, Dayton Nance<sup>1</sup>

<sup>1</sup> NIH

Recent advances in full spectral flow cytometry technology continue to expand fluorescence-based applications for advanced single-cell analysis and to overcome some limitations inherited by conventional flow cytometry. In a landscape dominated by a growing need to evaluate simultaneously more features in each cell, full spectral flow cytometry has emerged, allowing capture of the entirety of a fluorochrome's emission, rather than isolated slivers of information from well separated channels. For decades, the fascinating technology of cell sorting has allowed for the precise, high-speed isolation of single cells from diverse cell mixtures. Spectral high-speed cell sorting leverages these two powerful technologies simultaneously, allowing for the first time the utilization of highly complex panels for live single cell isolation. In this study we examine the potential of combining high-speed cell sorting and real-time full spectral unmixing using the spectral Cytek Aurora CS. To confirm that setup of the instrument was repeatable and consistent, day to day performance was tested over many iterations. Optical performance was quantified and monitored. Beads and cells were sorted to confirm that sorting purity could be reached under a variety of circumstances. Rmax calculations were used to examine sort recovery. Autofluorescence (AF) subtraction was utilized to improve signal to noise ratio and facilitate the isolation

of subsets with high AF. A 40-parameter immunophenotyping panel was used to examine sort performance of multiple cell populations. Our results highlight the potential of a novel platform for combined cell analysis and high-speed isolation of rare cell subsets based on deep immunophenotyping. As this technology moves forward, the emergence of spectral sorting is a step forward in the path of cytometry that will undoubtedly add to our understanding of the immune system in health and disease conditions. Acknowledgement: This research was supported by the Intramural Research Program of the NIH, National Institute of Allergy and Infectious Diseases.

**901827 P111**

## **Expanding panel size in spectral flow cytometry with StarBright Dyes excitable by the ultraviolet, violet, blue and yellow lasers.**

Michael Blundell<sup>1</sup>, Sharon Sanderson<sup>1</sup>

<sup>1</sup> Bio-Rad

The recently launched fluorescent dyes from Bio-Rad, StarBright Dyes, deliver tunable brightness and spectral properties, greater stability, improved lot-to-lot reproducibility, and spectral consistency. Specifically designed for multicolor flow cytometry with researchers needs in mind, StarBright Dyes address the common pain points in flow such as brightness, broad emission spectra, staining consistency, and ease-of-use, solving issues of signal resolution when constructing complex panels. These bright dyes have the additional benefit of a unique full spectral profile, making them ideal for inclusion in spectral flow cytometry, when creating multicolor panels. Here we present a preview of our newest additions to the StarBright range, the StarBright Blue and StarBright Yellow Dyes on a five-laser spectral cell analyzer. Both dye series are bright and allow expansion across the 488 and 561 lasers giving more dye choice for panel sizes but are particularly useful when large panel design is required. In this study we show, when StarBright Blue and StarBright Yellow Dyes are combined with other members of the StarBright range, polymer dyes and traditional fluorescent dyes, very large immunophenotyping panels can be constructed allowing identification of many peripheral blood subsets. In addition, novel dye combinations can be identified increasing the numbers of dyes and therefore markers identified from one sample. When combined with their ability to be fixed in both PFA based and alcohol-based fixatives, with

# CYTO 2022 ABSTRACTS

minimal spectral changes, and to be pre-mixed for up to 28 days, the flexibility of StarBright Dyes means they are ideal for new and expanding existing panels regardless of the type of flow cytometer being used.

**901909 P113**

## **Seeing More with the 320nm Laser – How the ID7000 Spectral Cell Analyzer can distinguish Fluorochromes with adjacent and overlapping spectra**

Koji Futamura<sup>1</sup>, Takashi Miyata<sup>1</sup>

<sup>1</sup> Sony Corporation

**Keyword** 320 nm laser, Deep UV Laser, Spectral cell analyzer, ID7000, Multicolor analysis, High Parameter Flow Cytometry  
**Background** In the last two years we have seen growth in the number fluorochromes available for multicolor flow cytometry, with most being excited by the red, blue, violet, yellow-green and UV (355nm) lasers. Some of these fluorochromes may have highly adjacent and even overlapping emission spectra that make them challenging to use in the same panel, which is critical when working with 25 or more colors. However, we have noted that several of these fluorochromes may be secondarily excited by the Deep-UV (320nm) laser and generate a discrete secondary emission signature that can be used to help discriminate it from other fluorochromes with similar primary emission characteristics. Using the ID7000 spectral cell analyzer, which can be equipped with a 320nm excitation source, and collects continuous data across the spectrum, we can utilize the secondary emission spectra for spectral unmixing. This leads to improvement of the signal to noise ratio and the ability to resolve overlapping or highly adjacent fluorochromes is improved. **Methods and Results** Multicolor flow cytometry panels were designed to include fluorochromes having overlapping and adjacent emission characteristics using the traditional 5 lasers (red, blue, violet, yellow-green and UV -355nm). Data was collected using ID7000 spectral cell analyzer using two configurations - with and without the 320 nm laser. Following data collection and spectral unmixing of the data, the separation of the fluorochromes with adjacent and overlapping spectra using the 5-laser configuration was compared with the data from the configuration including the 320 nm laser. Experimental results show the ability to distinguish populations when using spectrally similar fluorochromes is markedly improved by using the 320 nm laser as the emission signals from 320 nm

laser excitation contributes additional information to improve spectral unmixing results, thereby adding to panel design flexibility and maximizing the number of commercially available fluorochromes.

**901998 P115**

## **A 50+ color full spectrum panel to assess the immune landscape in finite quantities of human blood and tissue**

Andrew Konecny<sup>1</sup>, Peter Mage<sup>2</sup>, Andrew Konecny<sup>1</sup>, Florian Mair<sup>2</sup>, Aaron Tyznik<sup>1</sup>, Martin Prlic<sup>1</sup>

<sup>1</sup> Fred Hutchinson Cancer Research Center, <sup>2</sup> BD Biosciences

A comprehensive analysis of the immune system from human tissue biopsies and small volume blood draws is limited by current technologies. The reason for this is that human tissue biopsies typically yield less than  $1 \times 10^5$  haematopoietically derived cells and small volume blood draws yield  $1-2 \times 10^6$  leukocytes. Small tissue biopsies are pivotal in the study of cancer, and small volume blood draws are of particular relevance for pediatric studies and remote patient cohorts that cannot otherwise be recruited into studies. Previously defined high parameter cytometric analysis, like mass cytometry and Infinity Flow, are suboptimal in this setting due to significant sample loss or requirement of tens of millions of cells to perform, respectively. Full spectrum flow cytometry, however, is advantageous in this context as it enables a near complete retention of collected cells as a fluidics-based analysis approach and the potential to break the current 50-parameter ceiling in one cytometric assay. Here we present the first optimized 50+ color full spectrum flow cytometry panel which enables the parallel detection of CD4 T cell, CD8 T cell, T regulatory cell,  $\gamma\delta$  T cell, B cell, NK cell, MAIT cell, monocyte, basophil, and dendritic cell subtypes. In addition to markers that define the breadth of the immune landscape, we have included markers to distinguish costimulatory and inhibitory capacity, tissue residency, cytolytic ability, trafficking, maturation, and activation status. We created this panel by employing a computational approach to panel development in tandem with previously described guidelines in conventional cytometry. Data collection was performed on a flow cytometer in a 184 detector and 6-laser configuration: 320 nm, 355 nm, 405 nm, 488 nm, 561 nm, and 637 nm. To illustrate the panel's broad applicability, we show data derived from both cryopreserved peripheral blood mononuclear cells (PBMC) and cryopreserved tissue that had undergone dissociation. We

# CYTO 2022 ABSTRACTS

include both extracellular and intracellular markers with fixation and permeabilization steps to encompass the most generalized features in staining procedure. Together with pushing the bounds of fluorescence-based cytometry, we believe that our findings are highly clinically relevant as we provide the means to assess the entire immune response with just 2-3 drops of blood or finite tissue samples.

**896847 P117**

## **Imaging flow cytometry analysis of climate change scenarios in freshwater aquatic systems: a case of *Microcystis* spp.**

Dmitry Malashenkov<sup>2</sup>, Eric Jeppesen<sup>3</sup>, Ivan A. Vorobjev<sup>1</sup>, Natasha S. Barteneva<sup>1</sup>

<sup>1</sup> Nazarbayev University, <sup>2</sup>Moscow State University, <sup>3</sup> Aarhus University

**Background:** The alarming frequency of occurring blooms of *Microcystis* spp. in freshwater reservoirs around the world is leading to major ecosystem damages on many levels. The high phenotypical plasticity of colonial *Microcystis* raises an intensive debate about a coordinating basis for such successful expansion. The aim of this work was to provide a comprehensive picture of the seasonal progress of *Microcystis* spp. community by using IFC methodology and mesocosm experiment modeling climate change scenarios (LMWE, Denmark) **Methods:** We analysed samples from the mesocosm with three contrasting temperature scenarios and two different nutrient loadings. The samples were collected on a weekly or bi-weekly basis from May to September in 2019 (n = 117) resulting in the classification of 119,135 images of *Microcystis* spp. Fixed samples were analyzed with autoimage mode on FlowCAM (Yokogawa Fluid Imaging Technologies) cytometer and using a molecular biology approach (RT-PCR and Sanger sequencing). Results were processed via Prism 9.0 (GraphPad) software by principal component analysis (PCA) biplots and Spearman correlation analysis. **Results:** Our findings prove that IFC can be effectively used for detailed characterization of *Microcystis* spp. blooms. Moreover, it can clearly detect blooms of different *Microcystis* morphoforms and demonstrate which of them are the dominant players in a bloom-forming event. Because cyanobacteria have a complex interaction system, IFC important in the identification of morphospecies that have responded to a variety of environmental conditions by tracking parameters such as a colonial type, size, intensity, etc. IFC analysis of mesocosm

samples from tanks imitating climate change scenarios showed recurring weekly fluctuations of the abundance of various *Microcystis* morphoforms, including non-colonial structures. We identified non-colonial small clusters of *Microcystis* cells and gas-filled sheaths as important morphological forms, and with help of IFC demonstrated their role in the complex mosaic of a *Microcystis* bloom. Our results from IFC analysis suggest that composition and spatial-temporal distribution of *Microcystis* forms allude to possible coordinative coherence of the morphoforms on a level higher than colonial response. We validate our findings by the PCA analysis coupled with the constructed associative matrices, according to which two hypothetical models of transitional pathways of *Microcystis* morphoforms are presented. **Conclusion:** To our knowledge, it is the first study using imaging flow cytometry to portray the whole period of *Microcystis* spp. blooms. Collectively, the results of this study may add to the knowledge about the mechanisms of how *Microcystis* morphospecies thrive in freshwater systems.

**898669 P119**

## **From image to flow: an example work flow for single cell image analysis from transmitted light confocal images**

Dominic Jenner<sup>1</sup>

<sup>1</sup>Dstl

Confocal microscopy is a powerful technique, but historically has largely been regarded as qualitative rather than quantitative technique. The use of fluorescence probes increases the quantitative nature of the technique, but quantification of morphological features of cells in transmitted light images is still a challenging task. The reason single cell feature extraction is challenging in this situation is due to the similarity of cells to background, and feature extraction relies on segmentation of the cells from the background. Instance segmentation of cells in transmitted light is a challenging task for image analysis software as the difference between background and cell is minor, making thresholding images for segmentation difficult. Utilising the power of machine learning has been an approach used by many. To this purpose, in 2020 Stringer et al created a generalist algorithm for cellular segmentation, called Cellpose. This algorithm opens up a new avenue for instance segmentation of cells in both fluorescent imagery and transmitted light imagery. This poster demonstrates a work flow to gather single cell morphological data from images of



# CYTO 2022 ABSTRACTS

RAW264.7 murine macrophages from confocal transmitted light images using Cellpose and open source image analysis software. We also demonstrate using FlowJo to analyse single cell morphological data. © Crown copyright (2022), Dstl. This material is licensed under the terms of the Open Government Licence except where otherwise stated. To view this licence, visit <http://www.nationalarchives.gov.uk/doc/open-government-licence/version/3> or write to the Information Policy Team, The National Archives, Kew, London TW9 4DU, or email: [psi@nationalarchives.gsi.gov.uk](mailto:psi@nationalarchives.gsi.gov.uk)

**901385 P121**

## **Imaging Mass Cytometry Identifies Structural and Cellular Composition of the Mouse Tissue Microenvironment**

Clinton Hupple<sup>1</sup>

<sup>1</sup>Fluidigm

Imaging Mass Cytometry™ (IMC™) is a vital tool to deeply characterize the complexity and diversity of any tissue without disrupting spatial context. The Hyperion™ Imaging System utilizes IMC, based on CyTOF® technology, to simultaneously assess up to 40 individual structural and functional markers in tissues, providing unprecedented insight into the organization and function of tissue microenvironment. We have previously demonstrated the application of IMC in combination with Maxpar® panel kits to highlight cellular composition of human tissues. Here, we showcase the recently released Maxpar OnDemand Antibodies for IMC application on mouse tissue. We introduced 11 additional biomarkers to our existing mouse antibody catalog, providing the basis for the use of high-multiplex imaging in preclinical investigations. To demonstrate the IMC workflow on mouse tissue, we analyzed a normal mouse tissue microarray using IMC spatial proteomic analysis. Tissues were stained with a 20-marker panel designed to highlight tissue architecture and major immune lineage markers combined with our IMC Cell Segmentation Kit\*. The IMC Cell Segmentation Kit facilitates identification of cellular borders using plasma membrane markers that lead to improved nucleus and plasma membrane demarcation. We generated a detailed spatial map of the heterogeneous tissue architecture and successfully identified immune, epithelial, and stromal cell populations in various mouse tissues. Additionally, we classified the activation state of immune cell populations, adhesion state of epithelial cells, and molecular composition of the extracellular

matrix. Overall, this work demonstrates the capability of IMC to identify subcellular localization of cellular and structural markers in the mouse tissue microenvironment. Information gained from IMC studies will enable in-depth high-throughput phenotypic characterization of the tissue microenvironment in various mouse models of development and disease, and thus accelerate preclinical discoveries. \*The IMC Cell Segmentation Kit is part of the Innovative Solutions menu of custom-made reagents and workflows developed and tested by Fluidigm scientists to give faster access to new cutting-edge solutions for high-multiplex single-cell analysis. Innovative Solutions are not part of the Maxpar catalog. For Research Use Only. Not for use in diagnostic procedures.

**901629 P123**

## **Combining machine learning and imaging flow cytometry to reduce the need for functional staining in monitoring of infection in algal blooms**

Maxim Lippeveld<sup>1</sup>, Flora Vincent<sup>2</sup>, Daniel Peralta<sup>1</sup>, Assaf Vardi<sup>1</sup>, Yvan Saeys<sup>1</sup>,

<sup>1</sup>Ghent University, <sup>2</sup>Weizmann Institute of Science

Motivation: Algal cells can form enormous blooms in the ocean, and play a major role on our planet by being responsible for 50% of annual O<sub>2</sub> production. Viruses can cause bloom collapse, yet quantification of this process remains elusive. Tracking infection in algal blooms is therefore of vital importance to monitoring the marine ecosystem. Problem statement: Currently, monitoring requires time-consuming manual work, including fluorescent staining with DAPI and specific functional stains, and the manual gating of data to characterize infection (Vincent et al., 2021). Additionally, staining is costly and initial cell concentrations must be high due to successive washes, a potential point of failure during acquisition. We hypothesize that by combining machine learning with the spatial resolution and throughput of an ImageStream MK-II imaging flow cytometry system, we can characterize infection using only a DAPI stain, and the stain-free brightfield (BF) and darkfield (DF) images. Approach: We collected samples from an *E. huxleyi* phytoplankton culture, infected by its giant dsDNA virus EhV, at ten different timepoints post infection. The *E. huxleyi* cells were stained with a nuclear DAPI stain, a stain to detect viral mRNA (major capsid protein viral gene mcp), and a stain to detect a host mRNA for metabolic activity (photosynthetic gene psbA). After acquisition, we

# CYTO 2022 ABSTRACTS

manually gated each cell into one of four states based on the viral and metabolic stain: uninfected & metabolically active, infected & metabolically active, infected & metabolically inactive, and dead. A morphological profile was derived from the BF, DF and DAPI images for each cell. After quality control, 28,791 cells remained for further analysis. Four classification models (K-nearest neighbor, linear and RBF support vector machine and eXtreme Gradient Boosting) were validated on the profiles and ground truth. We optimized hyper-parameters for classifiers with cross-validated successive random halving. We retrained classifiers on all training data using the optimal parameters, and tested them on a separate set of *E. huxleyi* cells. Results: Classification performance was satisfactory for all states, except for the dead cells. The linSVM, RBF-SVM, XGB and KNN achieved a balanced accuracy on the test set of 0.71, 0.81, 0.80 and 0.75, respectively. When performing our approach using only BF- and DF-derived profiles, balanced accuracy dropped to 0.65, 0.76, 0.74 and 0.70, respectively, highlighting the importance of the DAPI stain. Conclusion: We demonstrated how morphological profiles derived from BF, DF and DAPI images acquired with imaging flow cytometry can be combined with machine learning models to monitor infection in an *E. huxleyi* algal bloom, reducing the need for specific staining, and therefore washing step. This enables monitoring of viral infection of single cells in lower biomass samples, which is more realistic for direct application in the natural environment.

**901847**      **P125**

## **Improving plant protoplast cell sorting outcomes with high-speed fluorescence image-enabled cell sorting.**

Gert Van Isterdael<sup>1</sup>, Julie Van Duyse<sup>1</sup>

<sup>1</sup> VIB-Ghent University

Recent advancements in single cell transcriptomics have boosted the field of single cell plant research and illustrated its immense potential (Seyfferth et al. 2021, Wendrich et al. 2020). In order to perform single cell experiments, one needs to make sure that the generated plant samples are of good quality before they get loaded on a microfluidic device as impurities such as cell debris and free mRNA will lead to data loss in downstream processing. To date, fluorescence activated cell sorting (FACS) has been the preferred method to clean up the sample and enrich for specific cell types if needed. To be able to perform cell sorting on plant material we first need to get rid of the cell walls. The

process of enzymatic digestion to create protoplasts generates a lot of debris, nearly indistinguishable from the round, healthy protoplasts. In addition, quite a large variety of protoplast sizes are generated. Different downstream single cell applications rely on the inclusion of small and large protoplasts for an unbiased single cell analysis. Discriminating between single protoplasts, doublets, multiplets, or even large debris using traditional flow cytometry scatterplots is nearly impossible. Here we present our work using a BD Biosciences FACS imaging enabled prototype cell sorter that is equipped with an optical module allowing multicolor fluorescence imaging of fast-flowing cells in a stream enabled by BD CellView™ Image Technology based on fluorescence imaging using radiofrequency-tagged emission (FIRE) (Diebold et al. 2012). Blur-free imaging at high flow velocities combined with the well-established droplet cell sorting technology opens up new avenues to the field of FACS. A full description of this technology has recently been published (Schraivogel et al. 2022) and nicely showcases some of the new possibilities and potential applications. Here we demonstrate how we used an imaging-enabled prototype cell sorter to design a new gating strategy for sorting *Arabidopsis* root protoplasts based on traditional flow parameters combined with image-based features. By using these extra imaging parameters, like eccentricity and size, we can now make better and more confident sorting decisions confirmed by real-time images of the gated subpopulations.

**901921**      **P127**

## **Ultrahigh-content imaging helps to identify CAR target candidates against pancreatic adenocarcinoma**

Nathan Brady<sup>1</sup>

<sup>1</sup>Miltenyi Biotec B.V. & Co. KG

Chimeric antigen receptor (CAR) T cells have become a new pillar of cancer therapy. They proved outstanding efficacies in leukemic patients, formerly believed to be beyond treatment. However, their remarkable success in the context of liquid tumors could not yet be translated to the field of solid malignancies. CARs enable T cells to unfold their cytotoxic potency, independent of the natural T-cell receptor. One major issue in CAR therapy remains the restricted availability of safe tumor-associated antigens (TAA) with restricted healthy tissue expression, that can be targeted by CARs. Here, we show how the newly-developed cyclic immunofluorescence microscopy platform MACSima can be integrated in a wholesome and comprehensive workflow to evaluate target expression on

# CYTO 2022 ABSTRACTS

tumor cells, as well as healthy tissue expression, and to support functional studies. The MACSima platform operates by iterative fluorescence staining, imaging, and signal erasure, enabling the operator to identify and compare the expression of dozens of targets on the very same tissue section. Here we introduce a novel comprehensive workflow for target identification in an immunotherapy setting. The novel MACSima platform proved to be a useful tool throughout the whole procedure, resulting in the discovery of novel CAR targets. MACSima facilitates target discovery and evaluation by (1) high-content imaging of tissue samples, enabling analysis of hundreds of markers in a single experiment, (2) allowing for verification of target specificity and helping to understand healthy tissue expression, and (3) helping to understand escape mechanisms during in vivo trials.

**901980 P129**

## **Altering Gating and Analysis through Integration of High Speed, High Resolution Imaging with Flow Cytometry Data**

Heaven Le Roberts<sup>1</sup>, Chris Langsdorf<sup>1</sup>, Erin Taylor<sup>1</sup>, Kate Alford<sup>1</sup>

<sup>1</sup> Thermo Fisher Scientific

Subjectivity in flow cytometry data analysis decision points has long been a challenge for our industry. Instrument and reagent innovations continue to increase the range of information captured at the single cell level, yet fundamental data quality concerns still plague many flow cytometry experiments. Recent advancements in high speed camera capabilities have led to in-line integration of morphological features with traditional flow cytometry. One hurdle of this integration has been the speed and depth of field challenges as events pass through a flow cytometer – overcome here by coupling hydrodynamic and acoustic focusing to maintain steady-state event position for more accurate and precise imaging. With stable event position through the flow core, high resolution images can now be seamlessly integrated with traditional flow cytometry, and the evaluation of unaltered sample preparations can now be accomplished. Using this approach in the Invitrogen™ Attune™ CytPix™ Flow Cytometer, we have shown that aggregate exclusion, cell cycle analysis, live/dead and bright/dim population delineations can be improved by additional information from cell morphological features. We report altered research conclusions related to rare event immunophenotyping, characterization of toxicological sequela and proper identification of target events in highly heterogeneous samples. Evaluation of brightfield images in tandem with traditional flow cytometry

data improves data quality and integrity, leading to more robust outcomes for downstream research conclusions.

**898476 P135**

## **Let's take a Cell-fie: A high-dimensional learning workflow trained on cell morphologies accurately predicts cell subset heterogeneity within imaging cytometry data**

Diana Ordonez<sup>1</sup>, Ioannis Panetas<sup>1</sup>, James Almarode<sup>1</sup>, Hugo Berthelot<sup>2</sup>

<sup>1</sup>BD Biosciences, <sup>2</sup>EMBL

Recent advances in the field of imaging cytometry have increased the complexity of cytometric data by including multiple modalities of information to each single-cell measurement. This new set of dimensions has created a demand for new analysis tools to identify, visualize and classify cell populations. Previous attempts at combining imaging and cytometric dimensions in a unified analysis workflow have yielded crude phenotypes and poor cellular classification. Hence a cytometric data analysis workflow able to visualize cell images, train on cellular morphology and predict their presence in heterogeneous samples would be a valuable tool for deep immunophenotyping, cell discovery, and diagnosis of pathology. Herein we present an alternative approach of visualizing and analyzing imaging cytometry data derived from different phytoplankton groups using BD® Spyglass and FlowJo™ Plugins, respectively. The multiple dimensions of cell imaging and flow parameters were preprocessed in FlowJo™ Software and selected for dimensionality reduction and clustering. Exported fcs files and images were then loaded in the BD® Spyglass Plugin for imaging and flow-guided gating. Following this, a TensorFlow neural net, trained on different phytoplankton cells, generated a model with high training accuracy. Using the adapted training model within heterogeneous sea-collected samples, predictions were made for the manually gated cell populations and derived clusters, with an output of cell subset classification and partition of the parent gates into morphologically distinct subpopulations. Based on our findings, the machine learning method successfully identified and classified different groups of phytoplankton from a model that was trained using image data. Moreover, dimensionality reduction and clustering algorithms were directed to utilize several imaging features in conjunction with fluorescent labels. The outputs were validated in low-dimensional space, and the cellular classifications were comparable to or better

# CYTO 2022 ABSTRACTS

than manual gates. We demonstrated that a high-dimensional workflow, including dimensionality reduction, clustering, and machine learning tools can be applied to imaging cytometry datasets to generate powerful data visualizations and automated classification into distinct cell subsets. For Research Use Only. Not for use in diagnostic or therapeutic procedures. BD and FlowJo are trademarks of Becton, Dickinson and Company or its affiliates. © 2022 BD. All rights reserved. 0222

**898510 P137**

## **Integration and Control of Low-Cost Industrial Cameras in a Home-Built Flow Cytometer**

Martin Hussels<sup>1</sup>, Jonas Gienger<sup>1</sup>, Christian Goerke<sup>1</sup>, Dirk Grosenick<sup>1</sup>

<sup>1</sup>Physikalisch-Technische Bundesanstalt

Note: Additional Authors are Alexander Hoppe and Alexander Putz with the same affiliation as me. Important Note: Please discard the poster abstract submission with same title and authors, I submitted earlier this day because submission of oral abstracts was not possible at this time. Imaging flow cytometry combines the high information content of microscopic images with the high throughput of flow cytometry. Possible applications include the diagnosis of acute myeloid and lymphoid leukemia in immunophenotyping, detection of rare circulating tumor cells in liquid biopsy, or analysis of morphological cell changes like mitosis. In these applications, very small populations of target cells must be identified and quantified within huge numbers of other cells, coincidences, and agglomerates. Minor errors in counting those populations can have a major impact on the diagnosis. As differentiation between single cells, coincidences, and cell agglomerates is challenging for common flow cytometers, we developed a flow cytometer with integrated multi-dimensional imaging. Our instrument combines the high signal detection rates of photomultiplier tubes (PMTs) with the ability to capture images of cells of interest. For this purpose, we operate a continuous wave laser at 488 nm and a gated laser at 406 nm focused into the flow cell with a small vertical offset. Images are captured by two low-cost industrial CMOS cameras. Triggering of cameras and gating of the 406 nm laser emission are controlled by an FPGA. As the same FPGA processes all data of the PMTs, this enables to set camera trigger conditions for each conventional detector channel of the setup. When an object passes the 488 nm laser focus, the data of the detectors is analyzed by the FPGA and compared to the trigger conditions.

In case all conditions are fulfilled, the cameras are triggered instantaneously, and the laser gate is shortly opened when the object will be in the focus of the 406 nm laser. This results in a short laser flash (0.1  $\mu$ s to 1  $\mu$ s) on the object being much shorter than the minimum exposure time (>59  $\mu$ s) of the cameras to prevent motion blur. This way, we can benefit from low-cost industrial cameras to capture sharp images at high flow velocities (~2 m/s). Currently, we can set a trigger window for each PMT detector channel, but more complex trigger conditions are possible.

**898518 P139**

## **Let's take a Cell-fie: A high-dimensional learning workflow trained on cell morphologies accurately predicts cell subset heterogeneity within imaging cytometry data**

Diana Ordonez<sup>1</sup>, Ioannis Panetas<sup>1</sup>, James Almarode<sup>1</sup>, Hugo Berthelot<sup>2</sup>

<sup>1</sup>BD Biosciences, <sup>2</sup>EMBL

Recent advances in the field of imaging cytometry have increased the complexity of cytometric data by including multiple modalities of information to each single-cell measurement. This new set of dimensions has created a demand for new analysis tools to identify, visualize and classify cell populations. Previous attempts at combining imaging and cytometric dimensions in a unified analysis workflow have yielded crude phenotypes and poor cellular classification. Hence a cytometric data analysis workflow able to visualize cell images, train on cellular morphology and predict their presence in heterogeneous samples would be a valuable tool for deep immunophenotyping, cell discovery, and diagnosis of pathology. Herein we present an alternative approach of visualizing and analyzing imaging cytometry data derived from different phytoplankton groups using BD<sup>®</sup> Spyglass and FlowJo<sup>™</sup> Plugins, respectively. The multiple dimensions of cell imaging and flow parameters were preprocessed in FlowJo<sup>™</sup> Software and selected for dimensionality reduction and clustering. Exported fcs files and images were then loaded in the BD<sup>®</sup> Spyglass Plugin for imaging and flow-guided gating. Following this, a TensorFlow neural net, trained on different phytoplankton cells, generated a model with high training accuracy. Using the adapted training model within heterogenous sea-collected samples, predictions were made for the manually gated cell populations and derived clusters, with an output of cell subset classification and partition of the parent

# CYTO 2022 ABSTRACTS

gates into morphologically distinct subpopulations. Based on our findings, the machine learning method successfully identified and classified different groups of phytoplankton from a model that was trained using image data. Moreover, dimensionality reduction and clustering algorithms were directed to utilize several imaging features in conjunction with fluorescent labels. The outputs were validated in low-dimensional space, and the cellular classifications were comparable to or better than manual gates. We demonstrated that a high-dimensional workflow, including dimensionality reduction, clustering, and machine learning tools can be applied to imaging cytometry datasets to generate powerful data visualizations and automated classification into distinct cell subsets. For Research Use Only. Not for use in diagnostic or therapeutic procedures. BD and FlowJo are trademarks of Becton, Dickinson and Company or its affiliates. © 2022 BD. All rights reserved. 0222

**898563 P141**

## **Studying bacterial-environmental effects by Imaging Flow Cytometry**

Ziv Porat<sup>1</sup>,

<sup>1</sup>Weizmann Institute of Science

Imaging Flow Cytometry (IFC) is a powerful technique, combining the high-throughput quantification of flow cytometry with the information rich microscopy. It is especially beneficial for hard-to-image populations as bacteria, where accurate quantification by either flow cytometry or microscopy is challenging. We utilized IFC to examine several environmental aspects of the Gram-positive bacterium *Bacillus subtilis*. Exopolysaccharides prevent *Bacillus subtilis* from co-aggregating with a distantly related bacterium *Bacillus mycoides*, while maintaining their role in promoting self-adhesion and co-adhesion with phylogenetically related bacterium, *Bacillus atrophaeus*. The defensive role of the exopolysaccharides is due to the specific regulation of bacillaene. Single cell analysis of biofilm and free-living bacterial cells using IFC confirmed a specific role for the exopolysaccharides in microbial competition repelling *B. mycoides*. Unlike exopolysaccharides, the matrix protein TasA induced bacillaene but inhibited the expression of the biosynthetic clusters for surfactin, and therefore its overall effect on microbial competition during floating biofilm formation was neutral. Thus, the exopolysaccharides provide a dual fitness advantage for biofilm-forming cells, as it acts to promote co-aggregation of related species, as well as, a secreted

cue for chemical interference with non-compatible partners. These results experimentally demonstrate a general assembly principle of complex communities and provide an appealing explanation for how closely related species are favored during community assembly. Furthermore, the differential regulation of surfactin and bacillaene by the extracellular matrix may explain the spatio-temporal gradients of antibiotic production within biofilms. Another aspect of the important environmental role of *Bacillus subtilis* is protecting plants from various pathogens due to its capacity to produce an extensive repertoire of antibiotics. At the same time, the plant microbiome is a highly competitive niche, with multiple microbial species competing for space and resources, a competition that can be determined by the antagonistic potential of each microbiome member. Therefore, regulating antibiotic production in the rhizosphere is of great importance for the elimination of pathogens and establishing beneficial host-associated communities. We used *B. subtilis* as a model to investigate the role of plant colonization in antibiotic production. Flow Cytometry and IFC analysis supported the notion that *Arabidopsis thaliana* specifically induced the transcription of the biosynthetic clusters for the non-ribosomal peptides surfactin, bacilysin, plipastatin, and the polyketide bacillaene. IFC was more robust in quantifying the inducing effects of *A. thaliana*, considering the overall heterogeneity of the population. Our results highlight IFC as a useful tool to study the effect of association with a plant host on bacterial gene expression.

**897502 P143**

## **Th17 is the main phenotype displayed by CD4+ CD28null cells from patients with rheumatoid arthritis**

Mariana Patlan<sup>1</sup>, Araceli Paez<sup>1</sup>, Felipe Masso<sup>1</sup>, Luis Amezcua<sup>1</sup>

<sup>1</sup>Instituto Nacional de Cardiologia,

Background: Rheumatoid arthritis (RA) is a prototypal immune-mediated inflammatory systemic disease, characterized by an increase in the number of circulating CD4+ T cells that lack CD28 expression. These cells have inflammatory functions and produce high concentrations of cytokines, but their T helper (Th) phenotype remains to be defined. Objective: to identify the predominant phenotype (Th1, Th2 or Th17) of CD4+CD28null T cells in RA, by evaluating the corresponding transcription factors. Methods: Thirty-nine patients with RA (2010 ACR/EULAR criteria) and 5 healthy individuals (controls) were included. Peripheral

# CYTO 2022 ABSTRACTS

blood mononuclear cells were collected by density gradient separation and analyzed by multicolor flow cytometry. Results: The number of CD4+CD28null T cells was higher in RA patients than in controls (2.2±1.7% vs. 0.8±0.8%; P = 0.040). When the different transcription factors were evaluated, it was found that the percentage of CD4+CD28null cells with the presence of RORyt (53.3% vs. 39.5%; P =0.007), and GATA-3 (9.4% vs. 2.4%; P =0.007) was higher in RA patients than in controls. For T-bet (37.3% vs. 58.1%; P= 0.007) was lower in RA patients than in controls. Conclusion: CD28+CD28null cells are increased and preferentially polarized towards Th17 in RA patients, suggesting a pathogenic role for these cells, and opening the possibility of a treatment specifically targeting these cells.

**899335 P145**

## **NIST Measurements of NanoParticle Intensity and Number Concentration for Characterization of Viruses and EVs using Flow Cytometry**

Lili Wang<sup>1</sup>, Paul DeRose<sup>1</sup>, Dean Ripple<sup>1</sup>, Yu-Zhong Zhang<sup>2</sup>

<sup>1</sup> NIST, <sup>2</sup> Thermo Fisher Scientific

Background: Bioparticles with diameters of less than 500 nm, such as viruses and extracellular vesicles (EVs), are of pressing interest for characterization using flow cytometry and microscopy. Polystyrene microsphere suspensions (with diameters  $\geq 2 \mu\text{m}$ ) with known number concentrations are routinely used to characterize flow cytometer and microscope performance and act as counting controls for calibration when cells are measured. Similar nanosphere suspensions need to be characterized using quantitative number concentration determinations. No techniques have presently been established to determine number concentrations of sub-micron particles with high accuracy and with good traceability to the International System of Units (SI). Number concentrations of polystyrene nanosphere suspensions are reported here using seven different techniques, three of which have traceability to the SI. Methods: Seven different techniques were used to determine the number concentration of nanoparticle suspensions, including flow cytometry (FCM), dry mass (DM) gravimetry with tunneling electron microscopy (TEM), fluorescence microscopy (FM) using charged slides, microfluidic resistive pulse sensing (MRPS), particle tracking analysis (PTA), asymmetrical flow field-flow fractionation with multi-angle light scattering detection (AF4-MALS) and a virus counter. The mean diameters of the

nanoparticles were also measured using the five techniques with those capabilities. Results: The measured number concentrations and diameters of calibration beads in suspension with 100 nm, 200 nm and 500 nm diameters were compared across the different techniques. The three techniques that are traceable to the SI, allowed consensus values to be determined for number concentration of bead suspensions. This enabled equivalent reference fluorophore (ERF) fluorescence intensity assignments to be expanded to these smaller diameter calibration beads. Conclusions: The techniques applied here with rigorous traceability to the SI gave number concentration values for nanoparticle suspensions with the highest degree of accuracy and precision compared to the other techniques. By determining consensus values, uncertainty in number concentration was decreased below that of single techniques. The highly accurate particle counting reported here will improve the accuracy of ERF-based fluorescence intensity assignments of reference beads for the calibration of flow cytometers and microscopes. These improvements in sub-micron bead characterization will also enable more accurate and standardized measurement of nanoparticles and nano-bioparticles, and establish measurement traceability in virus and EV application fields.

**901059 P147**

## **Contributions of extracellular vesicles in the pathophysiology of human cutaneous leishmaniasis**

Vanessa Fernandes de Costa<sup>1</sup>,

<sup>1</sup>Fiocruz

INTRODUCTION: Cutaneous leishmaniasis (CL) is a relevant public health problem in Brazil, being endemic in several states and caused, mainly, by *Leishmania (V.) braziliensis*. The clinical features are localized skin lesions that may solve spontaneously or by antimonial treatment and may become chronic leading to severe tissue destruction. The disease outcome is dictated by the parasite destruction performed by T lymphocytes-activated macrophages with a Th1 profile and a cytotoxic cells activity. Extracellular vesicles (EVs) have attracted attention due to their ability to transfer regulatory molecules and genetic information, being important regulators of cellular functions and physiopathogenesis mechanisms. OBJECTIVE: The aim of this work was to investigate the EVs contributions in patient's plasma with different clinical stages of CL. MATERIALS AND METHODS: Standardization of pre-analytic procedures and flow

# CYTO 2022 ABSTRACTS

cytometry analysis protocols was performed to detect, quantify and determine the EVs phenotypes in plasma samples from CL patients. For this, calcein and annexin V were used to EVs identification and a monoclonal antibodies panel was used to identify their phenotypes. FCM analysis were performed through the CytoFlex flow cytometer. RESULTS: During the analysis, low frequencies and concentrations of EVs were observed in plasma samples from before treatment CL patients. This suggest a relationship between the low modulations of EVs frequency with the acute phase of the disease. In addition, it was observed that most EVs had platelet phenotype. CONCLUSION: This work may report that flow cytometry is useful to identify and quantify EVs in ex-vivo plasma samples. Besides, the investigation of EVs function in the pathophysiological contexts of CL is essential for the generation of knowledge and it could define potential biomarkers of different disease phases and therapeutic targets. KEYWORDS: extracellular vesicles; flow cytometry; cutaneous leishmaniasis; Leishmania braziliensis; immune response.

**901280 P149**

**A 26-color panel for comprehensive immunophenotyping of leukocyte subsets across different murine tissues using the Agilent NovoCyte Penteon flow cytometer**  
Ming Lei<sup>1</sup>, Garret Guenther<sup>1</sup>, Peifang Ye<sup>1</sup>, Yan Lu<sup>1</sup>

<sup>1</sup> Agilent

Multicolor flow cytometric analysis is an incredibly powerful technique that allows the phenotypic and functional characterization of individual cells in a high-throughput manner. Here, we designed and optimized a comprehensive 26-color immunophenotyping panel for the Agilent NovoCyte Penteon flow cytometer to identify and characterize various subpopulations of mouse leukocytes across different murine tissues, defined by the expression of cell surface markers: total leukocytes (CD45), T cell (CD3, CD4, CD8a, CD44, CD62L), B cells (CD19), NK (NK1.1, KLRG1, CD27), monocytes (CD11b, Ly6C), DCs (I-A/I-E, CD11c, XCR1, CD172a, CD317, Siglec-H, CD103), basophils (CD11b, FcεR1a, CD49b, CD117), eosinophils (CD11b, Siglec-F), neutrophils (CD11b, Ly6G) and macrophages (CD11b, F4/80) subsets. Murine blood, spleen, bone marrow and lymph gland cells were collected or isolated from C57BL/6 mice, then erythrocytes were lysed and subsequently stained with Live/Dead dye and a total of 25 antibody mixture detecting the surface markers. These data were obtained using an Agilent

NovoCyte Penteon flow cytometer equipped with five lasers (349, 405, 488, 561, and 640 nm). Samples were analyzed using both NovoExpress software and t-stochastic neighbor embedding (t-SNE) in FlowJo for high dimensional analysis. The results show that all cell types can be clearly distinguished by manual gating as well as t-SNE visualization, including T cells, B cells, NK cells, monocytes, DCs, basophils, eosinophils, neutrophils, and macrophages in normal blood, spleen, bone marrow, and lymph gland. With the Agilent NovoCyte Penteon flow cytometer, researchers can generate highly complex panels up to 26 colors in a single tube. Flow cytometry immunotyping with an increased number of markers allows a more comprehensive analysis of the immune system and offers deeper insights into mouse immunology.

**901284 P151**

**Frozen Murine Monocytes Isolated From Bone Marrow Are Not Able To Efficiently Differentiate And Present Exogenous Nanoparticle Bound Hiv-1 P24 Antigen Due To Failure Of Early Endosome Formation**

Katerina Zachova<sup>1</sup>, Milan Raska<sup>1</sup>, Jaroslav Turánek<sup>1</sup>, Josef Mašek<sup>1</sup>

<sup>1</sup>Palacky University Olomouc, Czech Republic

Structurally conserved HIV-1 p24 protein is often studied as an appropriate candidate for development of the HIV-1 vaccine. To elicit strong immune response p24 may be coupled with various nanoparticles. Here, we evaluated the immunostimulatory and immunomodulatory effect of proteoliposome-formulated p24 in vitro model on dendritic cells differentiated from freshly isolated bone marrow monocytes (BMDC)s and from frozen bone marrow monocytes from BALB/c mice. The expression of the surface molecules MHC I, MHC II, CD80 and CD86 in p24-liposome activated BMDCs (CD11+ cells) was analyzed by spectral cytometry. Using a t-distributed stochastic neighbor embedding (t-SNE) analysis enabling reduction of multidimensional data, distinct population patterns were revealed between frozen and fresh bone marrow derived DCs. To analyze the mechanism of antigen engulfing, internalization and processing, the detection of the p24 antigen in early endosome was performed using the confocal microscopy imaging. Our results indicate that only freshly isolated BMDCs were able to enhance the MHC I expression upon p24-proteoliposome stimulation, whereas the BMDCs derived from frozen monocytes response was poor. The

# CYTO 2022 ABSTRACTS

expression of MHCII was comparable between freshly isolated and frozen cells. Similarly, p24-proteoliposome stimulates CD80 activation marker expression predominantly in freshly isolated BMDC sample. The differences in CD86 expression were not significant because of wide scatter between individual analyses. Confocal microscopy showed that murine BMDCs from frozen monocytes fail to form the early endosomes as the crucial step in the antigen processing by antigen presenting cells. In summary, BMDCs derived from freshly isolated bone marrow monocytes contain subpopulation able to process the p24-proteoliposome and undergo activation as confirmed by detection of DC activation markers MHC I, MHC II, CD80, and CD86 which are crucial for activation of CD4+ and CD8+ T cells and induction of a protective and long-lasting immune response. This study highlights the need for usage of fresh bone marrow monocytes in antigen-pulsing in vitro experiments to prevent misleading artificially poor responses. The research was supported by Ministry of School, Youth, and Sport, Czech Republic grant CEREBIT CZ. 02.1.01/0.0/0.0/16\_025/0007397 and Palacky University Olomouc grant IGA\_LF\_2022\_011.

**901299**      **P153**

## **Diversity of intratumoral regulatory T cells in non-Hodgkin lymphoma**

Ivana Spasevska<sup>1</sup>, Kanutte Huse<sup>1</sup>

<sup>1</sup> Oslo University Hospital

Tumor-infiltrating regulatory T cells (Tregs) contribute to an immunosuppressive tumor microenvironment. While high densities of tumor infiltrating Tregs are associated with poor prognosis in patients with various types of solid cancers, their prognostic impact in B-cell non-Hodgkin lymphoma remains unclear. Emerging studies suggest substantial heterogeneity in the phenotype and suppressive capacity of Tregs. Therefore, we aimed to reveal the diversity of Tregs in non-Hodgkin lymphoma. We combined single-cell RNA sequencing (scRNA-seq) with high-dimensional cytometry and identified three distinct transcriptional states of Tregs; naive, activated and LAG3+FOXP3- Tregs. Activated Tregs were enriched in NHL tumors and mass cytometry showed co-expression of several checkpoint receptors in this subsets. scRNA-seq confirmed that activated Tregs had higher expression of checkpoint receptors (TNFRSF4, TNFRSF18, ICOS), and revealed higher expression of phosphatases (DUSP2, DUSP4), NF- $\kappa$ B pathway genes (NFKBIA, TNFAIP3, NFKBIZ, REL), chemokine receptors

(CXCR4) and transcription factors (JUNB, IRF1, STAT3). The immunosuppressive capacity of Tregs was measured by in vitro co-culture of Treg subsets together with autologous CellTrace Violet-labelled T effector cells. Activated Tregs had stronger immunosuppressive activity compared with naive Tregs. Spatial investigation of Tregs by imaging mass cytometry revealed that activated Tregs were distributed in both malignant follicles and T-cell zones in follicular lymphoma, and that they preferentially interacted with other T cells, supporting a key role in immunosuppression of effector T cells. The computational framework of CIBERSORTx was used to generate signature matrices for the three Treg subsets to facilitate validation in separate scRNA-seq cohorts (King, *Sci Immunol* 2021; Roeder, *Nat Cell Biol* 2020; Steen, *Cancer Cell* 2021). Based on the signature matrices, the frequencies of the Treg subsets were imputed in two follicular lymphoma cohorts with bulk RNA-seq data (Steen *Haematologica* 2019, Pastore *Lancet Oncol* 2015). Activated Tregs were the major Treg subset in both cohorts and high abundance of activated Tregs was associated with adverse outcome. Our in-depth characterization of Tregs in non-Hodgkin lymphoma demonstrated that lymphoma-infiltrating Tregs were transcriptionally and functionally diverse, and included a major subset of highly suppressive Tregs co-expressing checkpoint receptors. These activated Tregs may limit clinical responses to checkpoint blockade and selective targeting of them may enhance anti-tumor immune responses, thus improving outcomes in lymphoma.

**901564**      **P155**

## **TNFAIP3 expression in RAG mice drive colitis in TNF $\alpha$ dependent way**

Alvaro Torres Huerta<sup>1</sup>, Antonia Boger-May<sup>1</sup>, Katelyn Ruley-Haase<sup>1</sup>, David Boone<sup>1</sup>

<sup>1</sup>IUSM,

Inflammatory bowel disease (IBD) is characterized by colon inflammation caused by multiple genetic and environmental factors, at the cellular level IBD is characterized by the high secretion of TNF $\alpha$  and exacerbated cell death from the colon epithelium. We developed a chronic model of innate immune-mediated colitis wherein RAG1<sup>-/-</sup> mice are crossed with mice expressing TNFAIP3 in intestinal epithelial cells (villin-TNFAIP3 mice). These villin-TNFAIP3 x RAG1<sup>-/-</sup> (TRAG) mice develop early-onset, 100% penetrant, chronic colitis. TRAG mice are characterized by the inflammation of the colon at four weeks



# CYTO 2022 ABSTRACTS

with no phenotypical abnormalities. In this study, we evaluate the role of TNF $\alpha$  and cell death mechanisms which are driven by innate immunity in the TRAG mice. To do that, we crossed TRAG mice with TNF $\alpha$  KO mice (named as FRAG mice), the FRAG mice are characterized by ameliorating colitis, consistent with this, FRAG mice had significantly lower histological colitis scores, compared to TRAG mice. To characterize the innate immune profile, we compare the colons from RAG1 KO vs TRAG vs FRAG mice. Leukocytes from the lamina propria were purified, activated four hours *ex vivo* for TNF $\alpha$  assessed, and specific myeloid markers such as CD45, CD11b, MHCII, Ly6C, Ly6G, inflammatory as TNF $\alpha$ , iNOS, and noninflammatory such as Arginase1 markers were assessed by flow cytometer. To address the cellular death mechanisms involved in the TRAG mice, TUNEL assays were done for general cell death and cleaved caspase 3 to mark apoptosis. Our results have shown that TRAG mice have four TNF-myeloid producers (inflammatory monocytes, monocytes, neutrophils, and macrophages) and five non-TNF myeloid producers (ILC1/3, ILC2, CD11b medium expression, NK, and DC cells), In addition, the TRAG mice predominately express iNOS, despite RAG and FRAG which both share the predominant expression of Arginase1 profile. In addition, the TRAG mice sustained more apoptosis and other cell death mechanisms (potentially pyroptosis and necroptosis) than the RAG and FRAG counterparts. The TNFAIP3 gene is upregulated during IBD and is well known to be a negative regulator of NF $\kappa$ B and MAPK activation. The present study, indicating that intestinal epithelial cell expression of TNFAIP3 drives innate colitis, which is dependent on TNF $\alpha$  signaling, highlights potential tissue-specific roles for TNFAIP3 that should be considered in the paradigm of TNFAIP3 as a target for prevention of IBD.

**901849 P156**

## **PD-L1 expression in NSCLC MDSCs and its potential use as a biomarker to determine treatment response through dimensionality reduction of flow cytometric data**

Roser Salvia-Cerdà<sup>1</sup>, Laura G. Rico<sup>1</sup>, Jolene A. Bradford<sup>1</sup>, Michael D. Ward<sup>1</sup>, Marc Sorigué<sup>1</sup>, Teresa Morán<sup>1</sup>, Joan Climent<sup>1</sup>, Rafael Rosell<sup>1</sup>, Jordi Petriz<sup>1</sup>

<sup>1</sup>Germans Trias i Pujol Research Institute (IGTP)

Roser Salvia, Laura G. Rico, Jolene A. Bradford, Michael D. Ward, Marc Sorigué, Teresa Morán, Joan Climent, Rafael Rosell, and Jordi Petriz Introduction: Immunotherapy is currently a

major treatment option for cancer. Non-small cell lung cancer (NSCLC) treatment options include 5 approved immunotherapies to target the Programmed Cell Death Protein 1/Programmed Cell Death Protein Ligand 1 (PD-1/PD-L1) with the aim to avoid tumor immune escape. Accurate detection of PD-L1 is crucial to calculate the Tumor Proportion Score and decide the line of treatment. Therefore, we applied a minimal sample perturbation methodology to target PD-L1 (Rico et al., 2021). This protocol allows the identification of conformational changes in circulating Myeloid-Derived Suppressor Cells (MDSCs). In this study, we present prospective evaluation of PD-L1 expression in MDSCs from patients with NSCLC undergoing anti-PD-L1/PD-1 immunotherapy. Methods: Peripheral blood (PB) samples from NSCLC patients (n = 43) were collected in EDTA-anticoagulated tubes prior and during anti-PD-L1/PD-1 immunotherapy. PB samples were immediately processed using our minimal sample perturbation protocol, and acquired on the Attune™ NxT flow cytometer (Thermo Fisher). MDSCs were stimulated with phorbol esters (PMA) and identified according to HLA-DRloCD33+CD11b+ immunophenotype. FCS files analysis was performed using FlowJo™ (v.10). FCS files were concatenated, downsized, and analyzed with tSNE, UMAP and FlowSOM. Patients were classified based on clinical outcome: tumor reduction (1); tumor stabilization (2); tumor progression (3); no evidence of response (4); non-assessable, death with no evidence of disease (5); and early exitus, without starting immunotherapy (6). Results: tSNE and UMAP allowed comprehensive data visualization of PD-L1 expression in lung cancer samples. Unstimulated MDSCs showed no PD-L1 recognition nor conformational changes. After PMA stimulation, PD-L1 underwent drastic conformational changes, clustering separately when compared with unstimulated MDSCs. FlowSOM provided self-organizing maps with a common backbone for patient's comparisons. Stimulated and unstimulated specimens displayed complementary FlowSOM organizing maps, whereas individual patients exhibited particular features. In addition, FlowSOM generated specific maps according to three clinical outcome groups (nonresponders, partial responders and responders). Conclusions: Further analysis will be needed to ascertain how the conformational changes of PD-L1 may help to accurately predict immunotherapy efficacy. Moreover, the feasibility of determining PD-L1 expression in NSCLC MDSCs may have a potential use as a biomarker to determine treatment response through dimensionality reduction. In fact, data analysis can be beneficial to improve diagnosis as well as to predict immunotherapy response early in the course of treatment.

# CYTO 2022 ABSTRACTS

**901926 P157**

## **Studying the immune-profile in patients with paraneoplastic cerebellar degeneration using imaging mass cytometry**

Ida Viktoria Herdlevær<sup>1</sup>, Sonia Gavasso<sup>1</sup>, Mette Haugen<sup>1</sup>, Christian Vedeler<sup>1</sup>

<sup>1</sup>Haukeland Univeristy Hospital

Paraneoplastic cerebellar degeneration (PCD) is a rare immune-mediated, neurodegenerative disease triggered by cancer and characterized by circulating onconeural antibodies. The dominant onconeural antibody detected in serum and cerebrospinal fluid of patients with PCD and ovarian or breast cancer is anti-Yo. Anti-Yo targets two antigens, cerebellar degeneration-related protein 2 (CDR2) and CDR2-like (CDR2L), expressed in Purkinje neurons in the cerebellum. The interaction between anti-Yo and CDR proteins is thought to mediate Purkinje neuron dysfunction and death, leaving the patients in a severely disabled state. The aim of the project is to study the immune profile in brain and ovarian cancer tissue from PCD patients, as the role of immune cells in disease pathogenesis is not well established. We carried out a pilot project using immunohistochemistry to stain PCD brain sections with immune cell markers. Despite promising results providing new and insightful information, several questions were raised due to limitation in the number of targets that we could visualize simultaneously. The advance of Imaging Mass Cytometry enabled us to overcome this challenge by studying up to 40 metal-tagged markers simultaneously. We designed a 40-marker antibody panel to stain formalin-fixed, paraffin-embedded post-mortem and biopsy tissue from patients and controls. Tissue microarrays were prepared to avoid batch effects and reduce antibody costs. Preliminary results show that the antibodies are successfully conjugated with the corresponding metal tags. Furthermore, a complete Purkinje neuron loss was observed in the cerebellum of patients compared to controls. Although imaging mass cytometry enables deep tissue profiling, co-localization studies and characterization of patients' immune profiles, data processing is complex and needs to be further addressed. \*Additional authors: Jonas Bull Haugsøen, Simeon Mayala, Shamundeewari Anandan, Morten Brun.

**901987 P158**

## **CD8+ regulatory T-cell subset distribution in adolescents with primary hypertension is associated with hypertension severity and hypertensive target organ damage**

Lidia Gackowska, , Izabela Kubiszewska<sup>1</sup>, Anna Helmin-Basa<sup>1</sup>, Mieczyslaw Litwin<sup>1</sup>

<sup>1</sup> Nicolaus Copernicus University in Torun, Collegium Medicum in Bydgoszcz,

Arterial hypertension is one of the most common civilization diseases in the XXI-century. In the last 20 years, there has been a marked increase in the incidence of primary hypertension (PH) in children and adolescents. Delayed diagnosis of PH in children and thus, untreated disease leads to serious organ damage and cardiovascular disease risk at an early age. One of the most important etiological factors of PH is a low-grade inflammation that drives blood pressure elevations and subsequent target organ damage (TOD). A chronic inflammation and the development of PH has been linked to the defect of T lymphocytes activities, especially T regulatory cells (Tregs) but the relationship between the distribution of the Treg subpopulations and the severity of the disease is still unknown. The aim of this study was to evaluate the relationship between PH and the different distribution of CD8+ Treg subpopulations in the peripheral blood of PH adolescents compared to controls. We also aimed to find out if TOD in adolescents with PH is related to defects in CD8+ Tregs distribution reflected by their phenotype characteristics. Method: The study constituted 32 nontreated hypertensive adolescents and 34 sex- and age-matched controls. The informed consent were obtained from the Children's Memorial Health Institute. Using multicolor flow cytometry technique, we assessed a distribution of total CD8+ Tregs and their subsets differing in activation potential and suppressive properties. Peripheral blood samples were collected to tubes containing anticoagulant (EDTA) and the cellular surface antigen-stabilizing agent. The samples were stained with monoclonal mouse anti-human direct conjugated antibodies (CD4APC-Cy7, CD8V500, CD25BV421, CD127PE, CD45RA APC, CD28PerCP-Cy5.5 and CCR7FITC) for identification of CD8+ Treg subsets. Results: Patients with PH are characterized by a higher percentage of total CD8+Tregs, in particular subpopulation involved in the anti-inflammatory tissue response (total Treg CCR7+) and subpopulation of central/memory Tregs (CM Tregs CD8+/CD25+/CD127-/CD45RA-/CCR7+). Additionally, a significantly reduced percentage of thymic origin Tregs, with strong suppressive properties (CD8+/CD25+/CD127-/CD28low)

# CYTO 2022 ABSTRACTS

and central/naive Tregs (CN Tregs CD8+/CD25+/CD127-/CD45RA+/CCR7+) was observed. Cells of thymic origin (Tregs CD28-), as well the percentage of CN Tregs negatively correlate with left ventricular mass index (LVMI), carotid intima-media thickness (cIMT) and wall cross sectional area (WCSA). Moreover, a positive correlation between the percentage of CM Tregs and LVMI was observed. Conclusion: The results suggest that subclinical arterial injury in adolescents with PH is associated with declined thymic function and increased pool of central/memory and CCR7+, anti-inflammatory subpopulations of Treg cells. Co-authors: J. Michalkiewicz, M. Wiese-Szadkowska, A. Wierzbicka, L. Obrycki. This work was supported by National Science Center 2013/11/B/NZ4/03832

**901995 P159**

## **T cell subsets correlating with the onset of GvHD**

Petra Hadlová<sup>1</sup>, Petr Říha<sup>1</sup>, Ondrej Hubálek<sup>1</sup>, Tomáš Kalina<sup>1</sup>

<sup>1</sup> Charles University

Graft versus host disease (GvHD) is a life-threatening complication after hematopoietic stem cell transplantation (HSCT). Timely and effective diagnosis and treatment is crucial for the patient's outcome. Therefore, we search for additional prognostic markers with a strong correlation to the clinical manifestations. T cell subpopulation and their effects on the success of HSCT have been long at the center of attention. It has been shown that presence of naïve T cells (CD8+CD62L+CD45RO-) accelerates the reconstitution, however it simultaneously increases the risk of GvHD development. Our approach was therefore to investigate the naïve T cell population alongside the other major T cell populations in more detail. This was done by staining peripheral blood (PB) samples with an 11-color panel covering all major maturing and mature T cell populations in order to identify which developmental stage correlates with GvHD onset, grade and transition of acute to chronic GvHD. We collected samples from a cohort of 53 patients, collection occurred at pre-defined time points: namely 28 (D28), 60 (D60) and 100 (D100) days after the HSCT. The stem cell memory (SCM) T cells defined as CD95+CD127+ turned out to be strongly correlated with a clinical manifestation of severe GvHD when present at D28. A powerful biomarker has a great potential to be included in the routine clinical tests and monitoring after HSCT and allows the treating clinicians to apply effective treatment in time. Supported by grant no. NU20J-07-00028.

**902009 P161**

## **Suppressive Eosinophils in patients with Type 1 Diabetes – what is its role in immunoregulation and autoimmunity?**

Christine Lingblom<sup>1</sup>

<sup>1</sup>Sahlgrenska University Hospital

It is a huge gap of knowledge when it comes to the role of the eosinophil granulocyte in type 1 diabetes (T1D). T1D is an autoimmune disease caused by T-cell mediated destruction of pancreatic beta cells. It has been reported that eosinophils migrate towards the Langerhans islets just before onset of T1D in rats and the eosinophil-recruiting chemokine, eotaxin, and the high-affinity IgE receptor (FcεRI) were up-regulated in the pancreatic lymph nodes, but it was never clarified why the eosinophils are recruited to the pancreas where the activated T cells are attacking the insulin producing beta cells. It has been shown that human eosinophils can suppress T cell proliferation in part via the immunomodulatory protein Galectin-10, which also contributes to the suppressive function of regulatory T cells. In addition, T cell suppressive eosinophils have been identified in the blood of healthy individuals, these eosinophils express CD16. In addition, eosinophils can regulate the function of T cells, either by suppressing T cell proliferation or by selectively promoting/abrogating the function of particular T cell subsets. Eosinophils are part of the type 2 immune response that balances out type 1 and type 17 responses. If the regulatory functions of eosinophils would be impaired an imbalance between Th2, Th1 and Th17 could occur. Th17 cells have previously been reported to be involved in the development of T1D. All together, these reports have led us to hypothesize that eosinophils in patients with T1D could play an important role and is in need of more research. Therefore we choose to analyze blood samples from patients with T1D and healthy controls using mass cytometry which enables us to get a much wider picture of the immune cells in patients with T1D. We designed the antibody panel with focus on eosinophils and it also covers major T cell and B cell populations. We used multivariate methods and cluster analysis to see if we could find important differences between patients with T1D and healthy subjects. Our analysis revealed that patients with T1D had lower levels of suppressive eosinophils and these eosinophils had decreased levels of CD16. It is possible that suppressive CD16+ eosinophils are impaired in individuals with T1D and that these eosinophils although recruited to the pancreas are failing to dampen the activated T cells, which enables the activated T cells to unrestrictedly kill the beta cells.

# CYTO 2022 ABSTRACTS

**902038 P163**

## **Enhanced expansion and effector function assessment of Natural Killer (NK) Cell Activity for Immunotherapy**

Jody Bonnevier<sup>1</sup>, Li Peng<sup>1</sup>, Christine Goetz<sup>1</sup>, Kevin Flynn<sup>1</sup>

<sup>1</sup>Bio-Techne

Natural killer (NK) lymphocytes exhibit potent responses against transformed and pathogen-infected cells and there is an ever-increasing need for NK cell therapies to treat cancer and immune diseases. We sought to develop novel, clinically relevant, and robust methods for human NK cell expansion. In addition, to simplify the processing of cells for characterization, we developed a flow cytometry based killing assay to monitor NK activity. Therefore, within the same experiment, we can analyze NK cell phenotype profiles with specific antibody panels while also assessing NK cell killing activity. Using optimized serum- and xeno-free conditions with minimal cell manipulations, we have expanded highly purified NK cells up to 500-fold in 14 days from human peripheral blood mononuclear cells (PBMCs) using Cloudz™ Human NK Cell Expansion (NK Cloudz™) microspheres or anti-NKp46 antibody. To characterize peripheral blood mononuclear cells (PBMCs) after expansion with optimized cytokines and NK Cloudz™, we used a unique antibody panel to characterize the NK cells by flow cytometry. Within the same experiment, NK killing assays against K562 cells can be performed using a flow cytometry-based killing assay, which has the advantages of using one instrument for analyses, shortened processing times, and reproducibility. In addition, we designed a novel flow cytometry-based killing assay to show that these NK cells exhibit potent natural killing and antibody dependent cellular toxicity (ADCC) against multiple targets. Using this workflow, we can identify different culture conditions that adversely affect NK activity. Together, this data presents a comprehensive and clinically relevant workflow for the expansion of highly purified NK cells and assessing their killing potential. Furthermore, this workflow can be used for screening the activity of chimeric antigen receptor (CAR) expressing immune cells against specific cancer antigens.

**898485 P165**

## **T Cell Subset Analysis in Autoimmune Addison's Disease (AAD) Using Mass Cytometry in Suspension (CyTOF)**

Shahinul Islam, University of Bergen

Autoimmune attack towards steroid producing adrenal cortex results adrenal insufficiency in autoimmune addisons disease (AAD). Organ specific autoimmunity progression is therefore observed by cortisol level in blood, saliva and urine for AAD and often replaced by relevant hormone. Nea, AAD patients shows autoantibody against the most vital enzyme 21-hydroxylase but the underlie mechanism is poorly understood. Interestingly, tissue resident autoreactive T cell is still observed in the AAD patients with the complete destruction of the adrenal cortex. Here, we aimed to use mass cytometry (CyTOF) in suspension (blood and saliva) of AAD patients to scrutinize the direct/indirect role of T lymphocytes. The project is in progress and we have recently established a routine CyTOF panel (37 parameter) to characterize immune cells in Addisons patients in compare to healthy donor. A piece of our very preliminary CyTOF data shows a minor impairment of the regulatory T cell (Tregs) compartment in patients with AAD compared to healthy, which we will need to confirm in a larger patient cohort to dig more into this Tregs dysfunction or unavailability can result in insufficient suppression of inflammation and could be considered critical for the initiation and perpetuation of autoimmune disease. Interestingly, imbalanced Tregs proliferation can lead to Treg conversion into hazardous effector T cells and increase the risk of autoimmune disease development in acute infections. Also, findings of deficient Tregs in many autoimmune disorders, including autoimmune polyendocrine syndrome where Addison's is one of the disease entities, give hope that we could cure autoimmunity be increasing their function or number. However, Tregs mechanisms and how they function in AAD is an unsolved area. We are now in the position to overcome these obstacles by employing our deeply phenotyped patient cohorts with Treg dysfunction (AAD/APS-I/APS-II) and our optimized novel single cell technologies (mass cytometry and flow-cytometry using both intracellular & extra-cellular marker). Thus, we can extend our knowledge on Treg dysfunction in organ-specific AAD, taking a significant step to understand this relevant immune suppressive immune mediator, which might also be directly used as vehicle or targets in next generation immune therapy with the potential to reverse the existing autoimmune milieus. We will also search to design MHC tetramers to add to the CyTOF and

# CYTO 2022 ABSTRACTS

flow cytometry panels to fingerprint autoreactive T cells against 210H. This could be an initiating point to develop T cell-based assays for AAD and other organ specific disorders.

**901505 P167**

## **Optimization of a 24-Color Flow Cytometry Panel for Natural Killer Cell Phenotypic Profiles Analysis**

Matthew Creegan<sup>1</sup>, Kawthar Leggat<sup>1</sup>, Julie Ake<sup>1</sup>, Michael Eller<sup>1</sup>

<sup>1</sup>Henry M Jackson Foundation for the Advancement of Military Medicine

The new generation of flow cytometers have an increased capacity to accommodate a greater number of lasers and detectors resulting in a higher number of simultaneously compatible parameters. Subsequently, this has similarly increased the complexity of panel design. Here, high parameter flow cytometric panel design and optimization was employed to develop a 24-color panel for phenotypic assessment of natural killer (NK) cells using a BD FACSymphony A5 cell analyzer. A 27 marker/24 color panel was developed to describe the phenotype of human NK cells from peripheral blood mononuclear cells (PBMC). The panel characterizes NK cell subset activation, homing potential, maturation, proliferation, and activating and inhibitory receptors expression. Four markers were used to exclude T cells, B cells, myeloid lineages, and dead cells. CD56 and CD16 were used to identify NK cells. NKG2C, FcRg and CD57 were included to identify adaptive and FcRg-deficient memory NK cells. We have used a combination of two antibodies, CD158e1 (KIR3DL1) and CD158a/h/g which recognize KIR2DL1, KIR2DS1, KIR2DS3 and KIR2DS5 to characterize Immunoglobulin-like Receptor (KIRs) expression. NKG2D, CD94, NKp30, NKp80, NKp46, Siglec7, KLRG1, and NKG2a were included to analyze activating and inhibitory NK cell receptors. CD38 and HLA-DR were included as markers of activation; EOMES and T-bet were used to identify transcription factors; Ki67 was included for proliferation; PD-1 was included for exhaustion; and a4b7 was used as a homing marker. This panel was optimized to analyze NK cell phenotypic profiles by using cryopreserved PBMC from people living with and without human immunodeficiency virus. It is also applicable for immune monitoring relevant to other pathogens, vaccine responses, cancers, and autoimmune diseases where NK cells are involved. A spillover spread matrix (SSM), unique to the BD FACSymphony A5 being used, was employed in conjunction with fluorochrome

stain indices to resolve problematic spectrum interactions due to spreading error and spillover. Through iterative testing and optimization, we developed an effective high parameter flow cytometric panel to comprehensively assess NK cells in peripheral blood.

**901532 P169**

## **Leveraging DNA in fluorescent reporter technology to enable higher plex flow cytometry**

Brandon Trent<sup>1</sup>,

<sup>1</sup>ThermoFisher Scientific

Flow cytometry has long been used to identify cellular populations of interest and investigate changes in immune subsets at the cellular level. With the advent of spectral flow cytometry, the ability to expand flow staining panels to 30 or 40 color panels has allowed for investigation into previously unstudied or neglected cell types that play important roles in the immune response. Increasing the number of fluorescent probes used in these panels results in very complex staining panels, with proper compensation needed to account for the considerable fluorescence spillover present in larger panels. Through specific placement of fluorophores within a DNA-based macromolecule, fine-tuning of both excitation and emission was accomplished, resulting in minimal laser cross excitation and spectral spill-over and use of all detectors on our cytometer. To demonstrate the effectiveness of these novel fluorescent reporters, we performed flow cytometric analysis of a panel built with classic dyes and found that we could optimize the panel with a maximum of 12 dyes while reducing cross excitation and spillover. However, by replacing some commonly used fluorescent dyes with DNA/fluorophore-based reporters, two additional targets were addressable while maintaining clear distinction of our cellular sub-populations. The use of DNA/fluorophore-based dyes can aid to optimize flow cytometry panels and add depth to immunological studies previously not possible.

# CYTO 2022 ABSTRACTS

**901917 P171**

## **Development and validation of a 30-colour spectral flow cytometry immunophenotyping panel designed for determination of antigen-specific B cells, T cell subsets, MAIT, and NK cells, plus a variety of activation markers in human cryopreserved PBMC**

Irene del Molino del Barrio<sup>1</sup>, Esther Perez Garcia<sup>1</sup>, Thea Hogan<sup>1</sup>, Ruth Barnard<sup>1</sup>

<sup>1</sup> GlaxoSmithKline

This 30-colour intracellular flow cytometry panel was developed to immunophenotype multiple B, T and NK subsets as well as to determine the frequency of antigen-specific B cells within human cryopreserved PBMC. The panel comprises markers for clean-up, lineage gating, multiple subsets of T cells (including MAIT, Tfh, liver homing), B cells (memory, plasmablasts, liver homing) and NK cells, plus various activation/exhaustion markers (PD-1, CD38, HLA-DR, OX40, TRAIL, FasL), and other miscellaneous markers covering function, transcription factors and proliferation (Granzyme B, Tox, TCF1/7, Ki-67). Four channels were left free for addition of fluorescently labelled antigens of interest, meaning this panel can be tailored to answer a number of different biological questions. This panel was firstly optimised in cryopreserved human PBMC from healthy volunteers then, when investigating binding of the fluorescent antigens, testing moved into previously vaccinated volunteers, recently vaccinated subjects and finally virus infected subjects. All samples were acquired using the Cytek Aurora spectral cytometer. This panel will be used to investigate pharmacodynamic effects of potential anti-viral therapeutics in Phase II clinical trials with the objective of biomarker/immune signature discovery. The agility of the panel also means it can be applied to other disease indications/targets in the future. Additionally, validation of the panel was planned and performed and 150 reportables subjected to both intra and inter-assay precision assessment. Assessment of both inter-operator and inter-instrument precision was also conducted to determine that CVs fall within pre-defined acceptance criteria. The validation demonstrates the robustness of the panel as panel performance is similar regardless of the operator or instrument used, a critical characteristic for multicentre studies. The human biological samples used were sourced ethically and their research use was in accord with the terms of the informed consents under an IRB/EC approved protocol.

**901487 P173**

## **Groundwater-borne microbes affect the distribution of highly auto-fluorescent cyanobacterial populations in coastal seawater**

Ekaterina Kopitman<sup>1</sup>, Keren Yanuka-Golub<sup>2</sup>, Eyal Rahav<sup>1</sup>, Yael Kiro<sup>1</sup>

<sup>1</sup>Weizmann Institute of Science, <sup>2</sup>The Arab National Society for Health Research and Services

Submarine groundwater discharge (SGD) is a globally important process supplying nutrients and trace elements from the land to the sea, thereby affecting different biogeochemical cycles in coastal environments. Not only a source of chemical substances, SGD also transports allochthonous microbes from the terrestrial subsurface into the sea, directly interacting with coastal microbial communities. Currently, the role groundwater (GW)-borne microbes play upon introduction to seawater and their interactions with the ambient microbial populations is nearly unknown. The main objective of this study is to elucidate the response of coastal microbial communities to discharged GW-borne microorganisms, especially ultra-small microbes. Microcosm bioassays were conducted by mixing sequentially filtered groundwater (non-filtered, 0.22 & 0.1  $\mu\text{m}$ ) with SGD-affected seawater at different ratios. Specifically, we tested the effect of groundwater additions on coastal cyanobacterial populations using spectral flow cytometry technology, which allows thorough characterization of autofluorescence of cells. Several cyanobacterial populations with distinct autofluorescence characteristics were identified. Our results show that mixing seawater with groundwater affect the frequency of several highly autofluorescent cyanobacterial populations compared to the non-mixed seawater. Interestingly, mixing seawater with 0.1  $\mu\text{m}$  filtered groundwater led to a significant reduction in the frequency of specific cyanobacterial populations compared to 0.22  $\mu\text{m}$  filtration treatment. This finding suggests that subsurface ultra-small microbes directly interact with coastal phytoplankton populations, thus affecting primary production rates in these environments. Further studies will be dedicated to explicitly understand interaction types between GW ultra-small bacteria and coastal cyanobacteria that are involved in these complex ecological systems.

# CYTO 2022 ABSTRACTS

**901961**      **P175**

## **Per-cell uncertainty estimates in a serial microcytometer.**

Paul Patrone<sup>1</sup>, Matthew DiSalvo<sup>1</sup>, Gregory Cooksey<sup>1</sup>, Megan Catterton<sup>1</sup>

<sup>1</sup>NIST

Flow cytometry is crucial tool for diagnostics and biomedical research because it enables rapid classification of cells based on optical properties and fluorescent biomarker quantification. Classification based on gating can be subjective, however, and further discrimination of individual cells is limited by unknown uncertainties. Even in well-controlled and calibrated conditions, individual measurement uncertainties are influenced by a convolution of population and instrument (e.g. setting dependent) effects. NIST has recently developed a serial microcytometer capable of assigning uncertainty on a per-event basis by repeatedly measuring the cell. Unlike a conventional cytometer, the microcytometer contains multiple interrogation regions using integrated optical waveguides. Each region allows for an independent measurement of the individual particle for comparison, which can be tracked between regions at very low variations of particle velocity. This low velocity variation is achieved by a novel combination of hydrodynamic and inertial focusing. We have recently demonstrated less than 2% measurement variation per particle for calibration microspheres travelling through two measurement regions (DiSalvo et al. in review, Lab on a Chip). Here we demonstrate comparable performance of the microcytometer to a conventional analytical flow cytometer and report uncertainty analysis of cells with multiple fluorophores. We first investigated the linear range of the microcytometer for three different excitation wavelengths using commercially available multi-intensity fluorescent beads. Like a conventional instrument, the microcytometer could separate 9 different fluorescent intensities from excitation wavelengths of 642 nm, 488 nm and 395 nm. Uniquely, measurements from the microcytometer included estimates of uncertainty (CV) for individual beads, which could be studied across the dynamic range of the instrument due to large range in intensities within the sample. To demonstrate uncertainties on single cells, we conducted cell cycle analysis on a population stained with DNA binding dye (Hoechst 33342). For the first time, we demonstrate per-particle uncertainty estimates in cytometry-based cell-cycle analysis, which provide a more rigorous analytical framework for determining and comparing cell states from different conditions. This method can be generalized to other classification problems,

such as rare event detection or expression level changes within groups of cells. Overall, single cell uncertainties can improve classification and assist in other biomedical research and clinical challenges such as cell counting.

**901983**      **P177**

## **Correlating NAD(P)H lifetime shifts to treatment of breast cancer cells: a metabolic screening study with time-resolved flow cytometry**

Jesus Sambrano, <sup>1</sup>, Samantha Valentino<sup>1</sup>, Andrea Perez<sup>1</sup>, Aric Bitton<sup>1</sup>

<sup>1</sup>New Mexico State University,

Autofluorescence excited state lifetimes of NAD(P)H are important photophysical traits that are not only detectable with flow cytometry, but also shown to be reliable metrics for determining the binding state of this metabolite under varying cellular conditions. NAD(P)H facilitates the transport of electrons during energy generation; therefore, its function and binding state to other enzymes (e.g. lactate dehydrogenase) are critical to cellular metabolism. Since the autofluorescence decay kinetics of NAD(P)H are altered upon protein binding, the average fluorescence lifetime is a direct indicator of how, if, and when NAD(P)H is actively facilitating different metabolic pathways (i.e. oxidative phosphorylation or glycolysis). Yet, it is non-trivial to detect the autofluorescence lifetime shifts of NAD(P)H with flow cytometry. Challenges with cytometry include (1) the ability to accurately resolve small lifetimes (100 picoseconds to 1.0 nanosecond); (2) the need to understand if there is a distribution of lifetimes from different binding states within a single cell;(3) how to maintain the throughput of standard cytometry while scanning lifetimes in real time; and (4) the ability to use dim autofluorescence for lifetime analyses at rapid cellular transit times. With a simple time-resolved flow cytometer we are able to analyze cells for their autofluorescence lifetimes to address these challenges. We do so by correlating measured lifetimes with differences across cell populations when the cells are treated to exhibit different metabolic pathways. With MCF-7 and T47D breast cancer cells, we developed different treatment conditions (e.g. serum-free, rotenone) to alter the cellular metabolic state. Under these varied conditions we compared the measured lifetimes to determine resolution limits as well as lifetime variation. Additionally, we correlated our measurements with an Agilent Seahorse HS Mini. In preliminary findings, the

# CYTO 2022 ABSTRACTS

average fluorescence lifetime is shifted in the direction (higher vs lower) that corresponds to the metabolic alteration. The Seahorse measurements also correlate to the metabolic profile expected. Future work will involve measurement of antiestrogen treated breast cancer cells and breast cancer cells that are anti-estrogen resistant. Mapping the metabolic profiles of cancer cells with time-resolved flow cytometry will lead to knowledge on the development of chemotherapeutic resistance and a possible connection of resistance to cellular metabolism.

---

**898804 P179**

## **MIFlowCyt-EV reporting of single vesicle flow cytometry methods and results**

Thomas Maslanik<sup>1</sup>, Erika Duggan<sup>2</sup>, John Nolan<sup>2</sup>

<sup>1</sup>Scintillon Institute, <sup>2</sup> Cellarcus Biosciences

**Introduction.** Rigor and reproducibility are major issues for science in general, and the EV field in particular. It is increasingly appreciated that the key to data interpretation lies in the details of the methods used to produce the data. Recent guidelines aim to progress the EV field towards greater reproducibility and better interpretability by providing prescriptive guidelines on appropriate methods and reporting for EV research. Using these methods, in practice, is sometimes unclear and examples of proper reporting of suitable experiments is necessary. Here we illustrate a flow cytometry-based approach to EV analysis that is compliant the recent MIFlowCyt-EV guidelines. **Methods.** EVs were enriched from culture media and whole blood by pelleting cells and were then diluted or concentrated by ultrafiltration as required. EV concentration, size distribution, and surface cargo was measured by single vesicle flow cytometry (vFC) which incorporates reagents, necessary controls, protocols and data analysis methods into an assay. vFC was run on commercial flow cytometers that were qualified and calibrated using multifluor, multiplex calibration beads (nanoRainbow, Cellarcus) to enable data reporting in standardized units. **Results.** We report size, concentration, and tetraspanin number per EV in standard units on EVs from blood and cell culture. Calculation of these parameters is described within the context of the sample preparation and assay protocols. Example calibration and control data that might be included in supplementary methods as suggested by the MIFlowCyt-EV ISEV position paper is reported. Data analysis protocols with an example of how to report a gating strategy and resulting data are illustrated. A walkthrough of the data repository and best-practices for use are described.

**Conclusion.** Single EV analysis using flow cytometry offers great potential for understanding the diverse origins and functions of EVs, but only if performed in a way that report essential details and assay specificity and sensitivity to be transparently documented. The MIFlowCyt-EV guidelines provide a framework that enables EV FC measurements to be reported in the context of essential experimental details, calibrations, and controls. This example of a well-run experiment reported in accordance with those guidelines should assist in complying with MIFlowCyt-EV. Many of the concepts and procedures developed for EV FC are extensible to other single EV counting, sizing, and cargo analysis methods.

---

**901438 P181**

## **Polymer-based synthetic cells for next-generation compensation and spectral unmixing**

Jason Deng<sup>1</sup>, Anh-Tuan Nguyen<sup>1</sup>, Brandon Miller<sup>1</sup>, Keunho Ahn<sup>1</sup>

<sup>1</sup>Slingshot Biosciences,

We have developed a new class of engineered polymer reagents for flow cytometry that match the spectral characteristics of cells. Our platform designs particles that are independently tuned along optical, fluorescent, genomic and biochemical parameters, generating a highly-flexible synthetic cell for a wide range of applications. One target application addresses a major shortcoming of current flow cytometry reagents, spectral unmixing. Existing polystyrene bead reagents have fundamentally different properties when compared to cellular material, causing difficulties when trying to work with major classes of dyes (e.g. tandem dyes) and in key fluorescence channels (Violet/UV). This problem is exacerbated when using spectral cytometers, a new flow cytometry paradigm that promises to expand panel complexity and assay breadth. Here, we present data comparing our engineered polymer reagents to traditional compensation beads, highlighting key advantages for tandem dyes, and in violet/UV channels. Our spectrally-tuned compensation product highlights a new performance standard for both traditional and spectral cytometers. This first-in-class technology promises to increase measurement and assay accuracy for next-generation flow cytometers by decreasing set up costs, reducing time to experimentation, and saving precious sample material, while improving detection limits.



# CYTO 2022 ABSTRACTS

**901528 P183**

## **Antibody quality – How antibody validation contributes to optimal research conditions**

Stefanie Ginster<sup>1</sup>, Sabina Kaczmarzyk<sup>1</sup>, Margarita Kist<sup>1</sup>, Sabrina Schmitz<sup>1</sup>

<sup>1</sup>Miltenyi Biotec

Reproducibility and therefore lot-to-lot consistency in reagents is crucial for experiments. A researcher needs to be able to identify if the inability to reproduce results is due to biological differences or due to inconsistencies in reagent performance. Antibodies are often the source of irreproducibility due to biological variations in production. The majority of antibodies on the market is derived from hybridomas. They are, however, often contaminated with antibody impurities from two sources: myeloma-derived Ig light chains, and serum-derived IgGs. With the introduction of recombinant antibodies in 2012, Miltenyi Biotec made a significant investment into improving the quality and consistency of our antibody performance. Recombinant antibodies do not display any undesired mixtures of heavy and light immunoglobulin chains, which is often the case with conventional hybridoma-derived antibodies. Furthermore, our REAfinity™ Recombinant Antibodies have a mutated Fc region that abolishes any binding to Fcγ receptors, resulting in a background-free analysis. To even further monitor and ensure superior performance of our antibody conjugates, we introduced our extended validation program. In this program we evaluate antibody sensitivity, meaning the ability of an antibody conjugate to detect markers with low expression levels, antibody specificity, meaning the ability of an antibody conjugate to recognize its target with minimal cross-reactivity, and we compare the performance of Miltenyi Biotec's recombinant antibodies with other antibodies that are available on the market. This way, we ensure to decrease the validation efforts that are required by the researcher. In this poster, we will demonstrate the efforts that we make to validate our antibodies in more detail.

**901546 P184**

## **Monitor Critical Parameters in Advanced Flow Cytometers**

Daniela Ischuu Gutierrez<sup>1</sup>, Erica Smit<sup>1</sup>, Richard Nguyen<sup>1</sup>, Esther Thang<sup>1</sup>, David Ambrozak<sup>1</sup>, Mario Roederer<sup>1</sup>, Stephen Perfetto<sup>1</sup>

<sup>1</sup> NIAID

Flow cytometry is used to detect small biological and synthetic particles. Due to important data that is generated from flow cytometers, it is critical to establish a quality control program, which includes instrument calibration, optimization, and standardization. In doing so, researchers can obtain accurate and reproducible data output. This poster focuses on the importance of flow cytometer standardization for biological reproducibility purposes. To achieve this, the instrument undergoes daily quality control (QC). The standardization process consists of verifying the absence of fluidics issues and tracking specific particles to control laser alignments and laser time delays. Methods: Our performance standards test for an optimal laser delay, area scaling, and verifying an unobstructed and hydrodynamically focused fluidics system. For this we use Supra, Rainbow, and Negative Control Beads. We run positive QC beads to track critical values, e.g.: laser delay, robust coefficient of variation (rCV), median fluorescence intensity (MFI) and detector voltages. After voltages and tolerance ranges have been set, rainbow and supra beads mix must be run. To calibrate intensities and measure instrument performance on a standardized scale, fluorescent calibration marker beads (FC beads), were run in a longitudinal study to demonstrate instrument technical reproducibility. Results and Conclusions: At least 20 continuous data points are collected for the parameters described above. Tolerance ranges are established and captured, and trends are assessed monthly. Daily monitoring parameters are critical as they pick up rCVs deviations, and large changes in voltages due to MFI fluctuations. Additionally, the beads help assess fluidics or other alignment issues. Incongruencies in rCVs, MFIs and voltage values can be identified early. Data reflects an out-of-range rCV point, thus showing the instrument's inability to generate biological reproducibility. Tolerance ranges are compared to relative channel numbers showing the errors when set side-by-side to quantitative units. In some cases, these values can be as high as a 6X difference. Moreover, FC beads were acquired on 2 different flow cytometer analyzers for a longitudinal study over 19 experiments, demonstrating inter- and intra-instrument comparability and performance over time. These findings show that setting and monitoring

# CYTO 2022 ABSTRACTS

tolerance ranges is vital to maintaining the consistency and performance of flow cytometers, eliminating technical variability for correct biological data interpretation. Based on these findings we show that optimizing and standardizing flow cytometers generate biologically reproducible results. If a cytometer has been optimized yet fails to meet defined tolerances, biological reproducibility may be compromised and a service engineer must be consulted. Instruments with large variance ranges should not be used in research or clinical trials and should be evaluated to improve performance.

**901566 P185**

## **PBMC processing conditions to optimize isolation of immune cell subsets**

John Wherry<sup>1</sup>, Ajinkya Pattekar<sup>1</sup>, Michelle McKeague<sup>1</sup>, Allie Greenplate<sup>1</sup>

<sup>1</sup> University of Pennsylvania

Whole blood and peripheral blood mononuclear cells (PBMCs), isolated from whole blood, are an optimal source of white blood cells for longitudinally monitoring immune health in preclinical and clinical studies. Several factors can affect overall sample quality and quality of key immune cell populations, including storage conditions and length of time between blood draw and processing. Immediately isolating PBMCs from whole blood or staining whole blood for flow cytometry after draw is ideal; however, it is often impossible for high-volume, multi-center studies. Using blood drawn from healthy donors, we evaluated how blood storage conditions including temperature, agitation, and time from the blood draw impacted both the immune landscape and individual cell subsets using flow cytometry. Blood was collected in heparin tubes and stored for various times at either room temperature (RT) or 4 degrees C (4C), and with or without agitation on a rocker until PBMC isolation. Timepoints for blood processing were 1, 3, 7, 24, 48 and 72 hours after blood draw. At each time point complete blood count (CBC) readings were taken to ascertain absolute changes in granulocytes and lymphocytes and PBMCs were isolated cryopreserved. Neutrophils persisted better at 4C compared to RT at all timepoints until 48 hours. Cryopreserved PBMCs were thawed 4 weeks later and stained with an 18-color flow cytometry panel to identify T cell subsets, B cells, NK cells, and myeloid cells. The overall lymphocyte landscape and individual cell subsets did not differ when comparing samples that were stored on a rocker or not. Temperature did affect the ratio of T

and B cells, with a specific loss of T cells after 24 hours at 4C. In line with the latter observation, Tregs are better maintained across all time points at RT compared to 4C. Additionally, blood should be processed to PBMCs within 24 hours of draw to best capture T follicular helper cells. Although cryopreservation is not ideal for plasmablast phenotyping, plasmablasts can be captured if the blood is processed within 24 hours. Overall, room temperature storage during the initial hours conserved most lymphocyte subsets whereas 4C preserved neutrophils. Therefore, storage conditions should be tailored to your biological question of interest.

**894956 P186**

## **Bacterial mock communities as standards for reproducible cytometric microbiome analysis**

Susann Müller<sup>1</sup>

<sup>1</sup> Helmholtz Centre for Environmental Research – UFZ

The composition of natural microbial communities rapidly changes due to the short generation times of the microorganisms, interactions with fluctuating environments, and migration. Microbial flow cytometry has recently established itself as a tool to track short-term community dynamics and link with ecological parameters. Here, we developed an artificial microbial Cytometric Mock Community (mCMC) as a reference standard and benchmark to support the generation of dynamic, high quality cytometric microbial community data (Nature Protocols, 2020, 15, 2788-2812). The mCMC comprises up to four different species, two gram negative (*S. rhizophila*, *E. coli*) and two gram positive (*P. polymyxa*, *K. rhizophila*) strains. It supports comprehensive instrument adjustment, specifically for small cells with scatter and fluorescence intensities below the 0.5 µm microspheres. Our approach upholds quantitative assessments and qualified decisions for sorting of subcommunities suitable for subsequent high resolution sequencing or proteomic routines.

# CYTO 2022 ABSTRACTS

**901296 P187**

## **Step by Step Approach for Training and Education of Flow Cytometry Users Including Roadblocks and Cross Platform Considerations: An SRL Perspective**

Kathleen Daniels<sup>1</sup>, Andrea Bedoya-Lopez<sup>1</sup>, Eva Orlowski<sup>2</sup>, Alexis Conway<sup>1</sup>

<sup>1</sup> Sana Biotechnology, <sup>2</sup>Burnet Institute

Education and training of end users is one of the main services provided by shared resource laboratories. While there are a variety of approaches for how this is accomplished, the main components of these educational programs share common ground across SRLs. In this poster we will outline a standard step by step approach for training new users, highlighting common potential roadblocks that may arise in the process. Additionally, we will dedicate a portion of this poster to address the challenges that arise when carrying out cross platform instrument training, such as training a user who has historically used conventional flow cytometer in the use of a full spectrum cytometry technology. In experience, it is convenient at the time of requesting the service, the application of exams to evaluate the level of knowledge or to have training in the basic concepts (equipment, systems, controls, types of data and analysis software). This point allows to have a base to direct the training strategy and its depth.

**901381 P188**

## **Optimizing User-Staff Communication in a Large Multi-Site Shared Resource Laboratory**

Derek Jones<sup>1</sup>, Jonni S. Moore<sup>1</sup>, William Murphy<sup>1</sup>

<sup>1</sup> University of Pennsylvania

Introduction: The Penn Cytomics Shared Resource Lab is one of the largest academic cytometry labs in the world, with over 9 satellites, 37 instruments and serving over 1000 users. Maintaining timely and useful interactions with our users is critical to assuring investigators have the technology access they require to perform successful studies. This can include real-time digital communications (ex. Slack, instant messaging, text messaging), instrument desktop access to troubleshooting, messaging capabilities to staff online, seminars, live meetings). Our goal was to identify the preferred and most effective communication tools for each task and to create a comprehensive communication

plan for Penn Cytomics. The overall aim is to identify processes to support the efficient operation of a large, shared resource lab in a cost-effective manner. This plan will become a cornerstone for, business, technical and scientific processes to best establish and maintain easy and effective communications with our users at close and distant sites, and to integrate this plan with our daily operations. Methods: There are 3 primary steps to implementing a communication plan into our operation: design, develop, apply. Each part has multiple steps. The information reported here focuses on the design aspect. To understand how users best receive information, we conducted a survey, via Survey Monkey, of 431 users who had been logged into our system over the last 60 days. We asked their opinions about how we are communicating with them currently, what works and what doesn't, and some possible new approaches that could be more effective. We will expand this information by doing live interviews with selected responders. Results and Conclusions: Our response rate was 23% (99 out of 431 surveys sent) and preliminary analysis of the survey data indicated that the users who resounded identified as the best way to communicate is through email (89%). Many users would like a Penn Cytomics Slack channel (65%) for communicating with staff about down machines and to assist in troubleshooting. The information that users felt most valuable was cytometer instrument status (60%), including QC pass or fail and instrument status (down or running). Using this data as well as user interviews, our next step is to design and develop a plan and processes that will be easy to implement and test it, integrated into in our daily operations. This user-facility communication plan will serve as the basis for enhancing interactions with our large and disperse client base and to identify processes that not only can support direct communication with users, but also enhance our workflow by identifications of instrument and user issues in a more timely manner.

**901404 P189**

## **Flow Cores in the time of COVID**

Sara Bowen<sup>1</sup>, John Tigges<sup>2</sup>, Kevin Ferro<sup>3</sup>, Kathy Brundage<sup>2</sup>

<sup>1</sup> Diginity Health, <sup>2</sup>Beth Israel Lahey Health, <sup>3</sup>Stowers Institute

Association of Biomolecular Resource Facilities (ABRF) Flow Cytometry Research Group (FCRG) put out a survey to acquire a better understanding of how Flow Cytometry Cores are changing in response to various factors present in today's scientific investigative climate. These include training practices during the current COVID-19 pandemic, ability to recruit qualified core staff,

# CYTO 2022 ABSTRACTS

availability of instrumentation and services, instrument service response times, and cytometry instrumentation placement into individual labs away from Flow Cores. All these factors affect not only the financial stability of a core, but also its sustainability. Survey responses are helping the FCRG create discussion groups around topics that are important to the Flow Community. FCRG projects for the next year include creation of Flow Cytometry course curriculum for community college technical training programs and development of SOPs for: antibody/dye titration and setting of Drop Delay based on particle size. Does this sound interesting to you? Inquire about joining the FCRG!

**901928 P190**

## **SRL Technicians Exchange: How Knowledge Sharing Increases Versatility and Offers Fresh Insight in Facility Operations.**

Rachael Walker<sup>1</sup>, Sam Thompson<sup>1</sup>, Aleksandra Lazowska-Addy<sup>1</sup>, Christopher Hall<sup>1</sup>

<sup>1</sup>Babraham Institute,

This poster will describe the experiences and benefits of a technician exchange programme between the Babraham Institute and Newcastle University, UK. These programmes are of great benefit to both senior and junior SRL staff, especially the latter, and we will highlight these benefits. This will be illustrated through the personal perspectives of the SRL technicians whom took part and we will outline examples of where cross-training and knowledge exchange led to the implementation of new innovations and technical solutions in our facilities which validated the exchange. An exchange opens an unbiased dialogue into standard operating procedures in the lab which, with constructive input and critical thinking, can influence and theoretically stress test the reliability and integrity of practical approaches taken. This supplies the framework for an evolution, growth, and adaptation of methods to form a more consistent and standardised approach to applications across a larger community of cytometrists which can be progressively shared through an open and active repository. Knowledge exchange programmes align with the ethos of the Technicians' Commitment which aims to improve visibility, recognition, career development and sustainability for technicians working in higher education and research by serving as a functional technical education tool. These opportunities are invaluable following two years of limiting virtual and remote learning exercises as physical, practical interactions within a lab environment allow for more thorough and genuine hands-on

experience. SRL staff from the Babraham Institute Flow Cytometry Facility and the Newcastle University Flow Cytometry Core Facility took part in an exchange for three days with staff travelling to attend the alternating facility. During the time spent at the hosting facility, SRL staff are be exposed to a variety of new flow instrumentation, take part in day-to-day practices, network with the respective members of staff, and gain an insight and new perspective in the work ethics of a different facility. Pursuing this concept further and involving other willing, openly collaborative facilities within the community, will build a network of SRL staff and develop mutually beneficial links with other leading external contacts. Staff themselves can strengthen their academic profiles and increase their own employability.

**902028 P191**

## **TROUBLESHOOTERS WANTED: FlowRemedy Diagnostic Chart for Cytometer Users in the Shared Resource Laboratory**

Derek Jones<sup>1</sup>, Jonni S. Moore<sup>1</sup>, Jennifer Jakubowski<sup>1</sup>

<sup>1</sup>University of Pennsylvania

**INTRODUCTION:** Instrument operation and training are the bread and butter for a shared resource laboratory (SRL), where supporting instrument users is paramount. In order to promote a more user-enabled SRL environment, communication between the SRL staff and its large pool of users is key. A considerable portion of SRL staff time is spent on assisting users with analyzer problems over the phone or through email. In our large facility (37+ instruments), many flow cytometers are often at nearby satellite locations, requiring additional staff time for offsite travel support. Overall, most issues are easily avoidable or could be remedied by the user directly with the proper guidance. In an effort to extend our instrument user support services, we have developed and implemented a troubleshooting flowchart (FlowRemedy) to aid SRL users in resolving basic analyzer issues. **METHOD:** Phone calls, emails, and our internal software messaging system were monitored for SRL user analyzer issues over the course of several months to identify the most frequent user issues. Each specific problem was categorized and quantified for analyzers (n=25). Troubleshooting flowcharts addressing the most common analyzer issues were then created and designated as FlowRemedy. FlowRemedy was displayed in all rooms with analyzers, email blasted to users, and posted on our department's web and social media page. All the above measures were monitored again as done previously to determine

# CYTO 2022 ABSTRACTS

the impact of FlowRemedy as a communication method.

**RESULTS/CONCLUSION:** After FlowRemedy implementation, there was a significant decrease in phone calls, emails, and internal software messages regarding analyzer issues. Correspondingly, users were able to run and finish their experiments with minimal interruptions within and between different user sessions. These findings suggest that FlowRemedy implementation served as an effective reference tool for user adoption when encountering basic analyzer issues.

---

**898809 P193**

## **Flow cytometry based single cell isolation and RNA sequencing of primary tumor, rare circulating tumor cells and metastases characterizes the poorly defined metastatic cascade in pancreatic cancer**

Moën Sen<sup>1</sup>,

<sup>1</sup>University of Pennsylvania

**Introduction:** Metastatic disease is the cause of over 90% of all cancer deaths. Metastatic pancreatic ductal adenocarcinoma (PDA) has a 5 year survival rate of 3% vs 39% for local PDA, yet no clinical tests exist to predict or monitor lethal disseminated disease. Circulating tumor cells (CTCs) shed into the blood from solid tumors are thought to mediate the metastatic cascade by extravasating from the blood and seeding distant metastases. Interrogation of CTCs from blood samples allows for non-invasive approaches of diagnosis, disease monitoring and unraveling what drives the selective advantage in this rare subpopulation of primary tumor cells that metastasize. Current PDA CTC detection and isolation techniques are limited by poor sensitivity. **Methods:** The rare cell enrichment approach utilizes magnetic bead-based white blood cell (WBC) depletion followed by acoustic focusing to deplete RBCs resulting in enrichment of tumor cells, CTCs and metastatic cells by FACS on a BD Influx<sup>TM</sup> cell sorter. Samples were incubated with antibodies against known epithelial cell markers (EPCAM and E-Cadherin) as well as WBC marker CD45-PE and anti-PE iMag<sup>TM</sup> beads for magnetic depletion followed by processing on the platform. Sorted cells were analyzed by WTA using a pre-market BD method. We used this workflow to isolate cells from the genetically engineered autochthonous KPCY (Kras;p53;Cre;YFP (yellow fluorescent protein) alleles) mouse model of PDA wherein the YFP lineage label expressed in cells of pancreatic origin facilitates sensitive detection of tumor cells

in blood and metastatic sites. **Results:** The optimized workflow was used to isolate 1,019 single tumor cells, including 417 CTCs, 278 primary tumor cells, 184 micro metastases, 140 metastases, and 99 ten-cell pools of WBCs sorted from 8 mice. Single-cell sequencing and index sorting allowed us to correlate the transcriptional signature of cells with its flow cytometric phenotype including expression of EPCAM and E-Cadherin. t-SNE analysis of gene expression revealed that tumor cells clustered away from WBCs and expressed YFP while WBCs expressed CD45. Index sorting further allowed identification of distinct epithelial, mesenchymal and hybrid sub-populations in CTCs, primary tumor cells and metastases. WTA analysis revealed cells separated into five clusters based on increased expression of epithelial, mesenchymal, platelet, proliferative and extracellular matrix genes. Intra tumor heterogeneity, as observed by the percent distribution of primary tumor cells across the five clusters, was highly conserved in CTCs reflecting that CTCs accurately mimic the molecular composition of tumors and liquid biopsy can accurately describe tumor heterogeneity. Thus, comparative comprehensive single cell RNA analysis of CTCs with matched tumor and metastases will produce an unprecedented understanding of the metastatic process in PDA.

---

**901028 P195**

## **“Single-cell immune profiling of the SARS-CoV-2 immune response**

Kivin Jacobsen<sup>1</sup>, Amir Ameri<sup>1</sup>, Dilek Inekci<sup>1</sup>, Charlotte Halgreen<sup>1</sup> and Liselotte Brix<sup>1</sup>

<sup>1</sup> Immudex, Bredevej 2A, DK-2100 Virum, Kivin Jacobsen, Immudex aps

Understanding T- and B-cell immunity is important in vaccine development. Advanced single-cell genomics technologies have enabled researchers to profile cell heterogeneity by assessing cell surface proteins, the transcriptome and TCR and/or BCR gene rearrangement, at the single cell level. However, understanding antigen-recognition at the immune synapse is key to understand specificity of an immune response. The DNA barcoded dCODE MHC Dextramer<sup>®</sup> technology combine single-cell genomic profiling with antigen-recognition which allows for the deep analysis of antigen-specific T cells at the single cell level adding to unveil specificity and heterogeneity of an induced T-cell response. Here we report deep T cell immune profiling of PBMCs from an individual previously infected with and vaccinated against

# CYTO 2022 ABSTRACTS

SARS-CoV-2. We investigated SARS-CoV-2-specific CD8+ cytotoxic T cells from thousands of captured single cells using dCODE MHC Dextramer (RiO) reagents for profiling of the cognate antigen-specific TCR clonotypes and in-depth phenotyping using the AbSeq® Immune discovery for Immune profiling and gene expression of the SARS-CoV-2-specific T-cells. We created a panel of 28 virus-specific dCODE MHC Dextramer reagents by combining easYmers®, a loadable MHC monomer, with a panel of peptides spanning the SARS-CoV-2 proteome, followed by attachment of these MHC-peptide monomers to U-Load dCODE Dextramer® reagents. This panel together with a set of 30 AbSeq antibodies were used to stain PBMCs, allowing detection of antigen-specific T cells on the single cell level using the BD AbSeq on the BD Rhapsody™ Single-Cell Analysis system. We were able to identify SARS-CoV-2-specific T-cells and characterize the individual clones of spike and non-spike-specific CD8+ T cells, by their phenotypes, and targeted immune-responsive transcription providing molecular description of the antigen-specific CD8+ T cells upon COVID-19 infection and vaccination. Our data provides resource for understanding and studying the immunology of infectious disease and adds to the development of effective therapeutic strategies for COVID-19. In conclusion, we provide a detailed view of the SARS-CoV-2-specific CD8+ T-cell response in a COVID-19 convalescent individual. Immudex®, Dextramer®, dCODE®, Klickmer™ and U Load™ are trademarks owned by Immudex ApS (da Klickmer og U-Load ikke er registreret i USA endnu).

**901251**      **P197**

## **Single cell proteomics complements transcriptomic read outs enabling detailed cell type classification on multiple sample types**

Rea Dabelic<sup>1</sup>, Alaina Puleo<sup>1</sup>, Valeria Giangarra<sup>1</sup>, Sarah E. B. Taylor<sup>1</sup>

<sup>1</sup>10x Genomics,

Cell type characterization in single cell studies relying on transcriptomic data can provide important cellular insights. Pairing gene expression (GEX) based profiling with simultaneous cell surface protein detection can bridge the gap between genomics and flow cytometry studies, thereby making it a more comprehensive and attractive approach for cellular characterization. We used the 10x Genomics Single Cell Immune Profiling Solution with Feature Barcode technology

in conjunction with BioLegend's Human Universal TotalSeq-C Cocktail (137 antibodies) to characterize a healthy human peripheral blood mononuclear cell (PBMC) sample and a human clear cell renal cell (CCRC) carcinoma sample. We generated whole transcriptome and targeted GEX libraries, along with immune repertoire and cell surface protein sequencing libraries from both samples. PBMC subpopulations characterized using either the GEX or the cell surface protein expression profiles showed comparable fractions of different cell types for both methods. For the CCRC sample, finer resolution of kidney and tumor cell types was observed in the GEX data compared to the cell surface protein data, which can be attributed to the antibody panel used for protein detection. Overall, the combined GEX and protein data provided the most valuable insights in this case, enabling the identification and characterization of different cell types. We also performed single cell repertoire profiling of the immune cells in the samples. In the CCRC sample, a T cell clonal expansion that constituted ~9% of all T cells in the tumor was identified. Characterization of these clonally expanded T cells, using both GEX and cell surface protein readouts, identified them as predominantly memory CD8+ T cells. While this can be traditionally done using upregulated memory cell markers, cell surface protein can enable isoform detection, e.g. CD45RA/RO - ensuring correct classification of cells. The memory CD8+ T cell population had upregulated mRNA expression of CTLA4 and LAG3, indicating that the clonally expanded T cells were exhausted. We found elevated cytokine GEX in the infiltrating immune cells, and a high level of IL6 GEX in macula densa cells in both whole transcriptome and targeted libraries. Our study shows that single cell GEX profiling in conjunction with cell surface protein detection using a sample-appropriate antibody panel provides complementary insights for cell characterization. While transcriptomics can be used for the discovery of new cell types and states, carefully curated antibody panels can be used to examine hundreds of cell surface proteins simultaneously for ultra-high parameter multiomic cytometry allowing the identification of isoforms not possible by examining the transcriptome alone. Based on these findings, we envision that this approach can be used widely to characterize many different sample types, including tumors, to enhance our understanding of biology.

# CYTO 2022 ABSTRACTS

**901813 P199**

## **CosTaL: An accurate and scalable graph-based clustering algorithm for high-dimensional single-cell data analysis**

Yijia Li<sup>1</sup>

<sup>1</sup> University Of Minnesota

The single-cell omics analysis has been widely used in many aspects of research work. Nowadays, as the size of the datasets grows bigger and bigger, it becomes more prohibitive to analyze the data by using manual investigations, such as gating strategies. Here, we are reporting the strategy of CosTaL (Cosine-based Tanimoto similarity-pruned graph for community detection by Leiden algorithm) for clustering multidimensional omics data of single cells. Similar to the predecessors like PhenoGraph and PARC, CosTaL transforms the cells with high-dimensional features from omics data into a weighted k-nearest-neighbor (kNN) graph. The cells are converted to the vertices of the graph, while the close relatednesses between similar cells are kept, represented by the weight of the edges between vertices. Specifically, CosTaL builds an exact kNN graph using cosine similarity and uses the Tanimoto coefficient as the pruning strategy to re-weight the edges for the graph to improve the accuracy of clustering. As a result, we demonstrate that CosTaL generally gets higher accuracy scores on 7 benchmark cytometry datasets and 6 benchmark single-cell RNA-sequencing datasets using 6 different evaluation metrics, when comparing against other graph-based clustering methods including PhenoGraph, Scanpy, and PARC. Additionally, CosTaL has the fastest computational time on large datasets, suggesting that CosTaL generally has better scalability over the other methods, which is beneficial for processing large-size datasets.

**901981 P201**

## **An automation-based workflow for gentle dissociation and high-speed nuclei sorting upstream of single nuclei RNA sequencing.**

Evelyn Rodriguez-Mesa<sup>1</sup>, Benjamin Finnin<sup>1</sup>, Reid Nakamoto<sup>1</sup>, Rachel Barhouma<sup>1</sup>

<sup>1</sup> Miltenyi Biotec

Single-cell sequencing is a powerful technique that examines the sequence information from individual cells and combined with next-generation sequencing technologies, provides high resolution of cellular differences and a way to understand the function of an individual cell in the context of its microenvironment. To perform such detailed analysis, individual cells have to be separated from their original environment, minimizing perturbation of the cell's original state is one of the greater challenges for cell separation technologies upstream of this process. One of the alternatives, to overcome such a challenge, is working with nuclei instead of cells, especially when working with frozen material where the cell integrity is compromised after dissociation. Conventional methods involve manual and lengthy protocols to produce single nuclei suspension. Here we present an automated workflow for dissociating and sorting nuclei, for single-cell nuclei sequencing analysis, from different frozen tissue sources, in a benchtop setting. We combined the use of the gentleMACS dissociator and the MACSQuant Tyto cell sorter, and show reproducibility across multiple tissues for yield and integrity of the nuclei upstream of genomics analysis. This robust, automated protocol for nuclei preparation from a range of starting materials could easily be adopted by core facilities for customers unfamiliar with the technique, increasing adoption of single nuclei technologies to scientists not familiar with single cell, suspension based analysis.

# CYTO 2022 ABSTRACTS

**902036 P203**

## **Morphological characterization and sorting of viable and label-free malignant cells from NSCLC tissue using deep learning**

Andreja Jovic<sup>1</sup>, Kiran Saini<sup>1</sup>, Michael Phelan<sup>1</sup>, Jeanette Mei<sup>1</sup>, Stephane Boutet<sup>1</sup>, Kevin Jacobs<sup>1</sup>, Julie Kim<sup>1</sup>, Chassidy Johnson<sup>1</sup>, Nianzhen Li<sup>1</sup>, Mahyar Salek<sup>1</sup>, Maddison (Mahdokht) Masaeli<sup>1</sup>

<sup>1</sup> Deepcell Inc., Menlo Park, CA

Methods to study cancer at the single cell level and capture the heterogeneity are important to better understand tumor biology. However, isolation of tumor cells from tissue typically relies on targeting biomarkers overexpressed in tumor cells, such as EpCAM, resulting in isolation of a subset of the tumor cell population which is used for further molecular and functional analysis. We developed COSMOS, a platform that performs high-dimensional morphology analysis of single cells using deep learning on high resolution bright-field images captured in microfluidic flow to phenotype and enrich target cells in realtime. We applied COSMOS to train a deep convolutional neural network classifier to identify and enrich malignant cells from non-small cell lung cancer (NSCLC) dissociated tumor cell (DTC) samples. The enriched NSCLC cells are label-free, unperturbed and viable, making them amenable to molecular and functional analysis methods. Importantly, the cell images can be used to generate high-dimensional morphological profiles that can be visualized by Uniform Manifold Approximation and Projection (UMAP) to discover morphologically heterogeneous populations of cells. We verified enrichment of malignant cells by performing RNA and DNA analysis on the enriched sample. Single cell RNA-sequencing (scRNA-Seq) analysis showed populations of cells with high levels of EpCAM expression in sorted cells. Copy number variation (CNV) analysis demonstrated increased amplitude of deletion and amplification peaks relative to the pre-sorted DTC sample. Further, mutational analysis shows increased allele frequency of mutations including P53 and KRAS in sorted compared to pre-sorted samples. Multiple clusters of morphologically unique tumor cell populations were detected by UMAP analysis. We further trained the classifier to detect and enrich for each of these subpopulations; CNV, mutation, bulk RNASeq, and scRNA-Seq analysis revealed molecular differences between the morphologically unique subgroups. Additionally scRNAseq identified EpCAM positive and negative

populations. We demonstrate the use of COSMOS to perform high-dimensional morphological profiling of NSCLC tumor cells from DTC, revealing heterogeneous populations of tumor cells that can be further characterized by molecular analysis offering a new dimension to understand tumor heterogeneity. Further work is planned to evaluate the link between the morphological, molecular and functional characteristics of each subpopulation.

**898531 P205**

## **Parallelization of single-cell multi-omics assays by designing smart consumables**

Ricarda Wallinger<sup>1</sup>, Magdalena Schimke<sup>1</sup>

<sup>1</sup>STRATEC Consumables GmbH

Innovative single-cell technologies have drastically changed the way we study biology in the recent decade. From measuring genome-wide gene expressions in a few cells since 2010ish, researchers now are able to investigate multiple modalities in thousands to millions of cells across tissues, individuals, species, time and conditions. Commercialization is a key driver to achieve robustness as it allows a wide availability for researchers from basic labs to clinics. Publications of more than 1000 tools and devices for scRNA-seq alone were published the last 10 years and strongly indicate the need and hence the trends to combine smart micro-structured consumables with high quality of computational and statistical analysis. However, many analyzer systems still struggle to gather the whole complexity of neuronal cells for example – pivotal to understand the biology of neurodegenerative diseases and psychological disorders. Together with STRATEC Consumables, BD developed its BD Rhapsody™ Single-Cell multi-omics platform with its patented Molecular Indexing technology paired with targeted scRNA-seq approach to get a deeper understanding of the biology behind pathologies. We here show the significant contribution of microfluidics and design to this project and discuss trends towards next generations consumables.



# CYTO 2022 ABSTRACTS

**901416 P209**

## **“Optimization and quantification of small particle sensitivity on the Cytex Aurora platform using FCMPASS software.**

Joshua A. Welsh<sup>1</sup>, Vera A. Tang<sup>1</sup>, Claudia Bispo<sup>1</sup>, Jennifer C. Jones<sup>1</sup>, Maria Jaimes<sup>1</sup>, Joanne Lannigan<sup>1</sup>

<sup>1</sup>University of Ottawa

The ability of flow cytometers to measure small particles, such as extracellular vesicles and viruses, has been made widely accessible by the employment of avalanche photodiode (APD) technology. Instrument alignment, maintenance, and quality control procedures employed by most manufacturers cater to cellular signals which are hundreds to thousands fold brighter than the detection requirements required for small particle analysis. Here we demonstrate the utility of small particle optimisation on the Cytex Aurora platforms and their consistency in the field by utilizing FCMPASS software. Each of the cytometer's fluorescence detector gains were optimized to peak sensitivity by performing detector incrementation analysis of QbSure beads. Using the FCMPASS v4 detection optimization module this data was analysis to derive the most sensitive detector gains. Using dim signal optimized gains, cross platform sensitivities for fluorescence were then compared in ERF units. Using FCMPASS light scatter calibration from NIST-traceable bead data, light scatter detector sensitivities were also compared in standard units.

**901850 P211**

## **A rapid method for assessing the accumulation of nanoplastics in human peripheral blood**

Roser Salvia, Laura G. Rico, Jolene A. Bradford, Michael D. Ward, Michael Olszowy, Laura Díaz Cano, Jana Caniego, Ramon Susanna, Cristina Martínez, Álvaro D. Madrid, Joan R. Grífols, Águeda Ancochea, Jordi Petriz

Introduction: Plastic pollution is a global problem. Animals and humans can ingest plastic particles, with uncertain health consequences. Nanoplastics (NPs) result from the erosion or breakage of larger plastic debris and they are therefore highly polydisperse in physical properties and heterogeneous in composition. Given the potential risks of environmental NPs to humans have not yet been extensively studied, we have focused on the study of the presence of NPs in peripheral blood (PB)

using nanocytometry and fluorescence techniques. Material and methods: PB samples were collected from donors with informed consent in EDTA-anticoagulated tubes. Nile Red (NR) fluorescence staining was used to determine the presence of the most common plastics in PB: low density polyethylene, polystyrene, polyethylene terephthalate, and polyamide. NR staining was performed after degradation of the organic matter by incubating 20µL of PB in the presence of 1% KOH (1 ml final volume), at 60°C in a dry block for a minimum of 10 days. 200, 500 and 800 nm calibration microspheres (Bangs Laboratories, Inc.) were used on the Attune™ NxT flow cytometer (Thermo Fisher), with the H-pulse parameter and collecting the violet side scattering. The specific filter set used to analyze submicrometer particles, consisted of the Attune™ NxT Small Particle Side-Scatter, and the Attune™ NxT Violet Side-Scatter Filter Kits. NPs evaluation was always in triplicate and in quadruplicate when one of the results had discrepancy. The IncuCyte® SX5 Live-Cell Analysis Instrument (Sartorius Stedim) was used as a real-time system to capture and analyze images of phagocytic cells for days, while the cells remained in growth condition inside a tissue culture incubator. Results: Our preliminary results on a sample of more than one hundred humans, including healthy blood donors (HD), newborns (NB), and patients with lung cancer (LC), acute myeloid leukemia (AML), acute lymphoblastic leukemia (ALL), multiple myeloma (MM), and idiopathic nephrotic syndrome (INS), already confirm the presence of NPs. Through fluorescence microscopy and long-term in vitro studies, we also confirmed the inability of cells to phagocytose and degrade plastics. In the case of HD (n=29), there was a strong dispersion among specimens. NB (n=21) had similar NP levels when compared with HD and lower dispersion numbers. LC (n=13) and MM (n=25) had the lowest levels detected, whereas ALL (n=19) the highest. Conclusions: Here, for the first time, we provide evidence of the presence of NPs in human blood. This accumulation may be related to inhalation of NPs originated from wheeled traffic and suspended materials in cities. Further analyses will be needed to associate this accumulation with lifestyle, health and pathology.

**901994 P213**

## **Sized Based Separation of Extracellular Vesicles Using an Elasto-Inertial Approach**

Jessica Houston<sup>1</sup>, Hassan Pouraria<sup>1</sup>,

<sup>1</sup>New Mexico State University

High throughput and efficient separation/isolation of extracellular vesicles (EVs) remains a challenge owing to their nanoscale size, biological milieu, and molecular heterogeneity. While cytometric labeling and analysis of EVs has been widely established, sorting and separation techniques remain underdeveloped. Elasto-inertial approaches have a new potential to be leveraged because of the ability to achieve fine control over the forces that act on extremely small particles. That is, the viscoelasticity of fluid that helps carry EVs, cells, and other particles through microfluidic channels can be tailored to optimize how different sized particles move within the chip. In this contribution we demonstrate through computational fluid dynamics (CFD) simulations the ability to separate nano-sized diameter particles from larger spheres with densities and velocities comparable to cells and EVs. Our current design makes use of a flow focusing geometry at the inlet of the device in which two side channels deliver the sample, while the inner channel injects the sheath flow. Such flow configuration results in an initial focusing of all the particles near the sidewalls of the channel at the inlet. Additionally, we show that the initially focused particle adjacent to the wall, will gradually migrate towards the center of channel due to the exerted elastic lift force. This results in larger particles experiencing larger elastic forces, thereby migrating faster towards the center of the channel. By adjusting the size and location of the outlets, EVs within a critical size range (30nm to 150nm) will be effectively separated from other particles. Thus, sorting and isolation is possible by collecting at specific outlet locations. The influence of different parameters such as channel geometry, flow rate and fluid rheology on the separation process are evaluated by CFD. Other results from CFD simulations include a fully resolved flow-field and quantification of the magnitude of different forces exerted on the particles. Furthermore, a Lagrangian particle tracking simulation is carried out to predict the trajectory of particles in different test conditions. The computational analysis is used to precisely tune the exerted forces on the particles so that the highest throughput and separation efficiency can be achieved. In future work we will validate this experimentally with a designed and fabricated microfluidic device. Testing will include preparation of heterogeneous populations of EVs, cells, and other molecular particulates.

**902034 P215**

## **Lectin-based multi-parametric flow cytometry analysis of glycosignatures in prostate cancer patient extracellular vesicles.**

Michelle Gomes<sup>1</sup>, Randall Armstrong<sup>1</sup>, Trevor Enright<sup>1</sup>, Mark Garzotto<sup>1</sup>

<sup>1</sup>OHSU

Aberrancies in glycosylation can enhance cancer cell survival and metastasis, and knowledge of the glycan landscape of cancer-derived extracellular vesicles (EVs) may provide unique markers for disease progression. Lectins are powerful tools to analyze glycosylation patterns, as their binding to discrete glycan structures is well characterized. Prostate cancer (PrCa), the most commonly diagnosed cancer in males, lacks robust minimally-invasive diagnostic and prognostic tools. Therefore, we initiated a study to investigate the value of prostate-derived EV glycosignatures as a triage test prior to prostate biopsies. Towards this goal, we enriched EVs from post-digital rectal examination (DRE) urine of low-risk (Gleason <7; n=25), high-risk (Gleason >7; n=25) PrCa patients and benign controls (n=25) using density gradient ultracentrifugation. The patient EVs were characterized by Nanoparticle Tracking Analysis (NTA) and Transmission Electron Microscopy (TEM), showing typical sizes in the range of 50-150 nm and characteristic cup-shaped morphology, respectively. Next, we analyzed the glycosylation patterns on patient EVs by multi-parametric flow cytometry using a panel of six fluorescently conjugated lectins with specificities for different sugars. In addition, the panel included antibodies against prostate disease and canonical EV markers. Computational analysis of the glycosylation patterns on EVs of PrCa patients and controls may distinguish populations of EVs that have unique glycosignatures. With the integration of patient clinical data, we hope to model risk stratification and prognostic potential to improve patient outcomes.

# CYTO 2022 ABSTRACTS

902047 P216

## The Delaware: A Flow NanoCytometer for Nanoparticle Analysis

Giacomo Vacca<sup>1</sup>, Richard Hanson<sup>1</sup>, Giovanni Contini<sup>2</sup>, Paolo Cappella<sup>2</sup>, Anna Sannino<sup>2</sup>

<sup>1</sup>Kinetic River Corp., <sup>2</sup>Romeo Bernini, IREA, National Research Council, Naples, Italy

**Background.** Detection and characterization of sub-micron biological entities, such as exosomes, extracellular vesicles (ECVs), liposomes, and micelles, represents an important next frontier in both research and clinical applications. The main obstacles to nanoparticle analysis in flow cytometry are (i) the small particle sizes and (ii) the short time available for interrogation, which, combined, result in exceedingly small scattering and fluorescent signals. Commercial hardware either modified or tailored for this problem has so far been underwhelming in terms of both speed of analysis and ease of use. There is unmet demand for flow cytometry systems that deliver nanoparticle analysis without compromising usability and throughput. **Methods.** We have developed a new cell analyzer, the Delaware Flow NanoCytometer, designed for sensitive detection and characterization of sub-micron particles (biological or otherwise). The Delaware is based on the architecture of our Potomac modular flow cytometry platform (CYTO 2017; CYTO 2021), with design modifications specifically intended to enhance nanoparticle sensitivity. The Delaware has four excitation wavelengths (Toptica 120 mW and DTR 800 mW at 405 nm, Coherent 300 mW at 488 nm, Coherent 50 mW at 532 nm, and Coherent 25 mW at 640 nm). The detection module, which—like on the Potomac—has user-selectable Semrock filters, uses a high-NA collection lens and offers two scattering channels and three fluorescence channels; the module is expandable up to eight fluorescence channels. Ultrastable sheath flow for superior core stream control is established with our previously introduced Shasta fluidic control system (CYTO 2021). The analyzer is operated using our Panama flow cytometry software for instrument control and data visualization. **Results.** We will present results from two systems—the newly developed Delaware, as well as the Potomac installed at IREA-CNR in Naples, Italy. Both instruments were tested with nanoparticle characterization kits (50, 100, 140, 200, 500, and 1,000 nm colloidal silica nanoparticles from Alpha Nanotech and 100, 200, 500, and 800 nm polystyrene nano/microparticles from Spherotech). The two analyzers were additionally characterized using 6- and 8-peak broad-spectrum fluorescent microparticles

(Spherotech Rainbow beads) and alignment microparticles for system CVs (Spherotech). **Conclusion.** We have demonstrated the integration of powerful multicolor excitation sources, an optical system designed to maximize light collection, an ultrastable fluidic control module, and a highly flexible yet intuitive graphical user interface. The Delaware Flow NanoCytometer combines ease of use with advanced nanoparticle sensitivity to offer users a powerful new tool for exosome and ECV research. [This work was made possible in part by government support under one or more grants awarded by the NIH.

This work was made possible in part by U.S. government support under one or more grants awarded by the NIH, and by Italian government support under the POR CIRO project.

896787 P217

## Next generation nanoFACS with high resolution imaging and custom 50um nozzle

Terry Morgan<sup>1</sup>, Mayu Morita<sup>1</sup>, Pamela Canaday<sup>1</sup>, Antonio Frias<sup>1</sup>

<sup>1</sup>OHSU

**Background:** Nanoscale flow cytometry is an emerging technology designed to image, count, and isolate cell- and size-specific extracellular vesicles (EVs). More efficient approaches to nanoscale flow sorting (nanoFACS) are required for sufficient EV yield per volume for validation studies of sorting specificity and more precise characterization EV protein and nucleic acid contents. Published studies suggest that nanoFACS yields approximately 1 EV/1 nanoliter droplet using 70um nozzle and 70 PSI at 75 KHz. This yields  $10^6$  sorted EVs/ml in one hour, which would be the same total EV volume/ml as 1 squamous cell contaminating 1ml of sorting buffer. The RNA and protein yields from  $10^6$  EVs are sufficient for targeted ELISA and qRT-PCR, but insufficient for -omics analyses. Concentrating sorted EVs using ultracentrifugation or cellulose-based 10kD filters loses >90% of events into polypropylene tubes and charged filter matrix. Our objective was to test whether a narrower custom nozzle design at lower PSI and higher kHz could decrease nanoFACS droplet size while maintaining specificity and sorting time. **Methods:** Studies were performed using a FACSria Fusion customized with ZenPure PES 0.1um filter, SP-SCC small particle analyzer module (BD Biosciences), and custom made 50um nozzle (BD). For comparison, we also imaged and sorted EVs using the same machine, but with a commercially available 70um nozzle (BD) and standard imaging module available with the FACSria Fusion. Machine settings were standardized

# CYTO 2022 ABSTRACTS

using fluorescently labeled polystyrene beads (Megamix 100nm-900nm, 40nm-F, and 70nm-FITC beads, and MESF standard beads [BD]) and all comparisons were made against the 70um nozzle 70 PSI baseline. We tested the 70um nozzle and the 50um nozzle at 30-, 50-, and 70 PSI at 75 kHz and 85 kHz. Drop delay was optimized using fluorescent sky blue particles (Spherotech). We imaged, counted, and sorted 40nm beads, 200nm beads, 120nm inactive murine leukemia virus +/- surface GFP (ViroFlow), FITC-conjugated 180nm liposomes [BD], and Muc5ac/CD63 positive EVs from pancreatic cancer culture media. Results and Conclusion: The high resolution SP-SCC imaging module provided a 2-fold increase in resolution below 100nm imaging the 40nm bead whereas the standard FACSaria Fusion could only resolve a 70nm bead. Increased resolution is important because differences in target refractive index may impact estimated size by at least 2-fold compared with polystyrene. Baseline nanoFACS of 200nm beads yielded 105/100ul concentration at 85 kHz. We observed at least 5-fold enrichment of sorted nanoparticles when using the 50um nozzle at 50 PSI at 85 kHz. The limitations of this approach were increased sorting time/volume sorted (droplet size ~ 0.3 nl) and challenges visualizing drop delay with the 50um nozzle.

**898467 P218**

## **Small particle flow cytometry using 3D light scatter detection enhances extracellular vesicle analysis in liquid biopsies highlighting the potential to segregate EVs by refractive index.**

Desmond PINK<sup>1</sup>, Arghya Basu<sup>1</sup>, Julianna Valencia<sup>1</sup>, Diana Pham<sup>1</sup>

<sup>1</sup>Nanostics

Extracellular vesicle analysis using “small particle” flow cytometry would be greatly enhanced if data from materials of different refractive index (RI) could be segregated. Likewise, relative sizing of EVs using small particle flow cytometry is confounded by the influence of RI on light scatter. Beads of different composition and refractive index scatter light differently, so that small beads of high RI and large beads of lower RI can have overlapping signals on a two dimension light scatter plot. In this project, we aimed to demonstrate practically and graphically, the enhancement of EV flow data analysis when using an additional angle of light scatter detection. An Apogee A60 Micro-Plus outfitted with a third (medium) angle of light scatter (MALS) detection was used to analyze samples typical

of EV analysis. Events were triggered solely by MALS excited from a 405nm laser. NIST bead (70 -200nm) and silica bead standard mixtures (100-400nm) were analyzed first to define cytometer settings. Next, refractive index (Cargille) oil emulsion standards (R.I. 1.38, 1.42, 1.59) were prepared to generate a continuum of particle sizes; each emulsion was analyzed separately. The multi-angle light scatter data from each R.I. standard was plotted (3D) to yield the distinct pattern of particle size influenced by refractive index. NIST (polystyrene) bead data overlaid against the silica data demonstrated different patterns as expected. NIST bead data overlaid almost perfectly with the 1.59 RI standard emulsion data. Similarly, silica bead standards followed the pattern of the 1.42 RI reference emulsions. Analyzed in the same manner, Verity beads (Exometry) overlaid atop the 1.38 RI reference emulsions. Concluding that the reference beads and emulsions overlapped in the expected manner, a variety of samples including plasma, serum, urine, semen, saliva, tissue culture media, etc were reacted with a variety of antibodies or dyes and the resulting patterns compared to the reference emulsion patterns. Other media such as IntraLipid, reference sera for tryglycerides and aggregated antibodies were likewise compared to the reference emulsions. Practically, the data, when plotted in 2 dimensions, show regions where large particles of low refractive index overlap significantly with smaller particles of higher refractive index, seen with both beads and samples (e.g lipid versus aggregated protein). Collecting and plotting data from a third angle significantly improves the resolution of these overlapping regions. However, as light scatter intensity decreases with either particle size or refractive index, especially in the <200nm biological particle range (70-90nm polystyrene, 100-120nm silica) the effective separation of particles of different R.I. is confounded by the overlap of signals. Addition of a 3rd light scatter collection significantly enhances the analysis of EVs by small particle flow cytometry, but practical thresholds still exist.

# CYTO 2022 ABSTRACTS

**898521**      **P219**

## **Proteomic characterisation of CD81–tdTomato prostate cancer–derived sEVs and their distribution in two–dimensional dynamic cell systems**

Rachel Errington<sup>1</sup>, Timothea Konstantinou<sup>1</sup>, Aled Clayton<sup>1</sup>

<sup>1</sup> Cardiff University

Small extracellular vesicles (sEVs) are nanometre-sized vesicles (<100nm diameter) produced in multivesicular bodies (MVBs), which are released from cells upon fusion of MVBs with the cell membrane. sEVs deliver and exchange cargo as a means of intercellular communication; this cargo includes lipids, nucleic acids and proteins (e.g., members of the tetraspanin protein family like CD9, CD63, and CD81). Through this communication-mode, cancer-derived sEVs disseminate through the tumour microenvironment to promote cancer progression, angiogenesis, metastasis and formation of the pre-metastatic niche. However, the underlying mechanisms and kinetics of sEV uptake and distribution within propagating cell populations are still greatly unexplored. To directly detect sEVs in dynamic cell systems we have developed a prostate cancer cell line that generates fluorescent sEVs by expressing the tdTomato fluorescent protein fused to CD81, an established sEV marker. The phenotype and proteome of these engineered CD81-tdTomato sEVs were extensively characterised across various platforms including Nanoparticle Tracking Analysis, Western blot analysis, ELISA-like assays, Confocal Microscopy, Cryo-Electron Microscopy, Micro-Particle Flow Cytometry and SWATH-MS (Sequential Window Acquisition of all Theoretical Mass Spectra) proteomic analysis. Phenotypic analysis demonstrated significant differences in CD81-tdTomato sEV size, protein cargo and morphology compared to age-matched non-transfected control sEVs. The data-independent acquisition-based SWATH-MS proteomic analysis further revealed a number of dysregulated proteins in CD81-tdTomato sEVs, which were implicated in MVB/sEV-, growth-, cytoskeleton, adhesion-, migration- and survival-associated pathways. After phenotypic and proteomic analysis, CD81-tdTomato sEV uptake and retention in prostate cancer- and bone marrow-derived mesenchymal stem cell-populations was visualised and quantified using Widefield Fluorescence Microscopy with a developed Fiji macro. Analysis of CD81-tdTomato sEV uptake and retention demonstrated differential dynamics between prostate cancer- and mesenchymal stem cell recipients. However, heterogeneous sEV uptake was observed for both cell systems and was found to associate with cell

area. To conclude, overexpression of the tetraspanin CD81 fused to a fluorescent protein caused significant alterations to the phenotype and proteome of secreted sEVs, which appear to be under-appreciated in similar studies. Furthermore, the understanding of uptake and distribution of these sEVs in 2D dynamic cell systems provided a quantifiable benchmark and starting point for further investigations in 3D microenvironments.

**898527**      **P220**

## **Physical association of lipoprotein particles and extracellular vesicles unveiled by single particle flow cytometry**

Estefania Lozano-Andres<sup>1</sup>,

<sup>1</sup>Utrecht University

Introduction: Human plasma is a complex biofluid that contains several submicron entities including extracellular vesicles (EVs) and lipoprotein particles (LPPs). Plasma tumor derived EVs (tdEVs) have a huge potential to be used as minimally invasive biomarkers for diagnosis and prognosis of patients. However, to exploit the potential of tdEVs in plasma we have to deal with the presence of LPPs. We here investigated how the presence of LPPs can influence the analysis of td-EVs at the single particle level. Methods: tdEVs were isolated from conditioned media of the mouse 4T1 mammary carcinoma cell line by density gradient ultracentrifugation and size-exclusion chromatography. For fluorescence-based flow cytometry (FC) of tdEVs and commercially available LPPs, samples were stained with PKH67 and/or CD9-PE and succumbed to density gradient floatation prior FC analysis on an optimized BD Influx. Results: When analysed by FC, we found that PKH67 stains both EVs and various types of LPPs (CM, VLDL and LDL). Although their light scattering and fluorescence signal intensities from the generic membrane staining partially overlap, the peak enrichment of tdEVs or LPPs was found in different density fractions (1.16-1.12 or 1.10-1.06 g/cm<sup>3</sup> respectively). Furthermore, by using spike-in experiments we found that the presence of LPPs not only impacts the generic staining of tdEVs but also the antibody labelling of specific EV-markers. Spiked-in samples showed a distinct results compared to individual tdEVs or LPP samples, thus reflecting that interactions between different types of submicron sized particles present in plasma can affect both quantitative and qualitative analysis. Interestingly, the smaller LDL particles showed a singular staining pattern and revealed a higher signal from EV-markers in LPP-enriched densities. Thus

# CYTO 2022 ABSTRACTS

indicating a more prominent association between tdEVs and LDL compared to CMs or VLDL particles. We confirmed in a label-free setting that the presence of LDL affects the signature of single tdEVs by synchronized Rayleigh and Raman scattering. In addition, by cryo-electron tomography we were able to observe that EVs present in human plasma can be physically bound to LDL particles in a physiological condition. Summary/Conclusion: The interaction between tdEVs and LPPs needs to be considered when plasma tdEVs are being investigated as biomarkers for diseases. Especially since the physical LPP-tdEVs interactions might impact the analysis of EV signatures and specific biomarkers at the single particle level. Funding: European Union's Horizon 2020 research and innovation programme under the Marie Skłodowska-Curie grant agreement No [722148] and STW-Perspectief Cancer-ID grant [14,191].

**898529 P221**

## **“Small particle flow cytometry using 3D light scatter detection enhances extracellular vesicle analysis in liquid biopsies highlighting the potential to segregate EVs by refractive index.**

Desmond PINK<sup>1</sup>, Arghya Basu<sup>1</sup>, Julianna Valencia<sup>1</sup>, Diana Pham<sup>1</sup>, Robert Paproski<sup>1</sup>, John D Lewis<sup>1</sup>

<sup>1</sup>Nanostics

Extracellular vesicle analysis using “small particle” flow cytometry would be greatly enhanced if data from materials of different refractive index (RI) could be segregated. Likewise, relative sizing of EVs using small particle flow cytometry is confounded by the influence of RI on light scatter. Beads of different composition and refractive index scatter light differently, so that small beads of high RI and large beads of lower RI can have overlapping signals on a two dimension light scatter plot. In this project, we aimed to demonstrate practically and graphically, the enhancement of EV flow data analysis when using an additional angle of light scatter detection. An Apogee A60 Micro-Plus outfitted with a third (medium) angle of light scatter (MALS) detection was used to analyze samples typical of EV analysis. Events were triggered solely by MALS excited from a 405nm laser. NIST bead (70 -200nm) and silica bead standard mixtures (100-400nm) were analyzed first to define cytometer settings. Next, refractive index (Cargille) oil emulsion standards (R.I. 1.38, 1.42, 1.59) were prepared to generate a continuum of particle sizes; each emulsion was analyzed

separately. The multi-angle light scatter data from each R.I. standard was plotted (3D) to yield the distinct pattern of particle size influenced by refractive index. NIST (polystyrene) bead data overlaid against the silica data demonstrated different patterns as expected. NIST bead data overlaid almost perfectly with the 1.59 RI standard emulsion data. Similarly, silica bead standards followed the pattern of the 1.42 RI reference emulsions. Analyzed in the same manner, Verity beads (Exometry) overlaid atop the 1.38 RI reference emulsions. Concluding that the reference beads and emulsions overlapped in the expected manner, a variety of samples including plasma, serum, urine, semen, saliva, tissue culture media, etc were reacted with a variety of antibodies or dyes and the resulting patterns compared to the reference emulsion patterns. Other media such as IntraLipid, reference sera for tryglycerides and aggregated antibodies were likewise compared to the reference emulsions. Practically, the data, when plotted in 2 dimensions, show regions where large particles of low refractive index overlap significantly with smaller particles of higher refractive index, seen with both beads and samples (e.g lipid versus aggregated protein). Collecting and plotting data from a third angle significantly improves the resolution of these overlapping regions. However, as light scatter intensity decreases with either particle size or refractive index, especially in the <200nm biological particle range (70-90nm polystyrene, 100-120nm silica) the effective separation of particles of differe

**897407 P222**

## **Design of “smart” nanoparticles for combined in-vivo imaging and advanced drug delivery therapeutics for single-cell nanomedicine**

James Leary<sup>1</sup>,

<sup>1</sup>Aurora Life Technologies LLC

Nanomedicine is massively parallel-processing “single-cell medicine”. It involves the packaging of drugs or genes into “smart” nanoparticles that can perform complex multi-step targeting to diseased cells while sparing damage to normal cells. Many drugs, including already FDA approved drugs, are already being re-packaged into nano-drug delivery systems allowing patent extensions and reducing the harmful effects of some drugs by vastly reducing the dose (10-100 times) exposures to patients. These nano-delivery systems can simultaneously provide imaging contrast agents for a number of non-invasive imaging modalities. Why does nanomedicine represent a huge

# CYTO 2022 ABSTRACTS

promise for our healthcare system? Earlier diagnosis increases chances of survival. By the time some symptoms are evident to either the doctor or the patient, it may be already too late, in terms of irreversible damage to tissues or organs. When this damage occurs, the costs of the treatments rise steeply and the probability of successful patient outcomes declines steeply. It can also reduce or eliminate “side effects”. Nanomedicine will diagnose and treat problems at the molecular level inside single-cells, prior to traditional symptoms and, more importantly, prior to irreversible tissue or organ damage – saving both costs and, more importantly, improving the chances for a successful patient outcome. Smart nanoparticles are drug-device combinations that are revolutionizing drug delivery. Nanomedicine bridges the gulf between diagnostics and therapeutics with a new concept of “theranostics”. Earlier diagnosis increases chances of survival, as well as reducing irreversible damage to tissues or organs. Nanomedicine is the destruction of individual diseased cells (“nanosurgery”) or repair (regenerative medicine, including CRISPR) of tissues and organs, WITHIN individually targeted cells, cell-by-cell. Nanomedicine typically combines use of molecular biosensors to provide for feedback control of treatment and repair. Drug use is targeted and adjusted appropriately for individual cell treatment at the proper dose for each cell (single cell medicine). Nanomedical devices can be targeted to single diseased cells within the human body using a variety of targeting molecules and strategies, including: antibody targeting, peptide targeting, aptamer targeting, ligand-receptor targeting (e.g. folate receptors). Combinational chemistry and high-throughput screening methods can screen over 100 million possible targeting molecules or therapeutic drug molecules in a day, including peptides, aptamers or other molecules. Flow and image cytometry are integral parts of nanomedicine, as well as all of the non-invasive imaging technologies.

**901367**

**P223**

## **Evaluation of dry DURAClone antibody panels for the characterization of human PBMCs, enriched T cell fractions and anti-BCMA CAR-T cells**

Rita Bowers<sup>1</sup>, Giulia Grazia<sup>1</sup>, Michael Kapinsky<sup>1</sup>, Anis Larbi<sup>1</sup>, Vashti Lacaille<sup>1</sup>

<sup>1</sup>Beckman Coulter, Inc.

CAR-T cells are becoming a more common therapeutic approach and are setting forth to targeting of hematological disorders other than CD19+ entities and also solid tumors. However, the immunological determinants of CAR-T efficacy still need comprehensive investigation from starting material to final product, covering different CAR constructs, transfection methods and targets. DURAClone dry antibody panels were designed to overcome standardization issues and operator-dependent impact on accuracy and precision in multicentric flow cytometry studies. The aim of this study was to evaluate the utility of DURAClone dry antibody panels for the characterization of PBMCs, derived T cell-enriched fractions as well as anti-BCMA CAR-T cells (ProMab Inc.), including MOCK-transfected controls. DURAClone dry antibody panels were used as pre-configured or extended with CAR-specific probes and further antibodies. Viable CD45+ leukocyte and CD3+ T cell count, leukocyte composition (CD3/CD19/CD56/CD14/CD16) and the T cell (CD3/CD4/CD8) maturation profile (CD45RA, CD197/CCR7, CD27, CD57) including expression of checkpoint markers (LAG-3, PD-1) were assessed. Regardless of sample type, absolute counts and cellular composition were assessed using streamlined procedures. Typical staining patterns for T cell maturation profile were observed, revealing unchanged proportions for the different stages between PBMCs and enriched T cell fractions and strong skewing toward effector cell phenotypes with elevated expression of a checkpoint markers in case of CAR-T cells. Our experiments demonstrate the flexible utility of DURAClone dry antibody panels for the phenotypic characterization from starting material to final CAR-T cell product.

# CYTO 2022 ABSTRACTS

**901841**      **P224**

**Delivery of oligonucleotides into tumor cells via monoclonal antibodies: targeting of mRNA following release of antisense oligonucleotides through cell surface protease activities using Antibody Substrate Oligonucleotide Conjugates (ASOCs)**

Beverly Packard<sup>1</sup>, Akira Komoriya<sup>1</sup>

<sup>1</sup> Oncolmmunin, Inc.

Antibody Substrate Oligonucleotide Conjugates (ASOCs) are monoclonal antibodies (mAbs) that are covalently modified with protease substrates; the latter are also covalently linked to oligonucleotides bearing H-type excitonic dimers. The substrates can be cleaved by proteolytic enzymes on a tumor cell surface that the cell might use to metastasize. Cleavage of the protease substrates results in localization of oligonucleotides at the tumor cell surface. Oligonucleotides are then able to diffuse into the tumor cell and inhibit translation of targeted mRNAs. The oligonucleotides enter cells via the delivery mechanism we have previously used to block HIV proliferation in CD4+ T cells (Cytometry A 97:945-54 (2020)). Thus, ASOCs differ from the current armed mAb-based therapies, e.g., antibody-drug conjugates (ADCs) or antibody-oligonucleotide conjugates (AOCs), in that delivery of the oligonucleotides into the cytoplasm does not require internalization of the mAb or endosomal processing; additionally, off-target toxicity will be reduced by release at the cell surface of the payload (the oligonucleotide). With this approach, using an MHC-Class I mAb we have delivered an antisense oligonucleotide targeting KRAS into the following tumor cell lines: A549 (NSCLC), COLO205 (colon), MB-MDA231 (breast), and Caki (kidney) as well as using the antiCD20 mAb Rituxan to deliver an antisense oligonucleotide targeting actin mRNA into Raji cells. Proof of delivery of oligonucleotides into cells was confirmed by confocal imaging after binding of mAbs to the cell surface as measured by flow cytometry.



# CYTO 2022 ABSTRACTS

## POSTER SESSION 2 MONDAY, JUNE 6

**901582 P4**

### **Evaluation of absolute and percentage counts of the total, B, NK, T lymphocytes, and TCD4 and TCD8 subpopulations in patients with COVID-19 during the hospitalization and after hospital discharge,**

Gabriela Eburneo<sup>1</sup>, Milena Brunialti<sup>1</sup>, Giuseppe Leite<sup>1</sup>, Reinaldo Salomão<sup>1</sup>

<sup>1</sup>UNIFESP

Patients with COVID-19 present a wide spectrum of clinical manifestations, from asymptomatic infections to severe disease with fatal outcomes. Changes in leukocyte populations, including lymphopenia and neutrophilia, correlate with the clinical manifestations, with persistent lymphopenia observed in patients with clinical deterioration. This study evaluated total lymphocytes and their subpopulations in 48 patients with COVID-19 admitted with the moderate disease to the University Hospital of the Universidade Federal de São Paulo, Brazil. Patients were 58.6 years old (mean), and 62% male. The patient's samples were divided into two groups: critical (C, N=34) and non-critical (NC, N=14), according to the clinical course, including the need for oxygen support, vasoactive drugs, and intensive care support. Four patients from the Critical group died during hospitalization. In addition, 19 healthy volunteers (HV) were included for control, with gender 63% male and age (mean – 55.7 years old) similar to the patient group. Total, B, NK, T lymphocytes counts and TCD4, and TCD8 subpopulations were analyzed in patients on admission (D0), on the seventh day of hospitalization (D7), and on average 31 days after hospital discharge (Convalescent Sample CS-31). Samples were processed in whole blood using the TruCount method and the FACSCalibur flow cytometer. The absolute counting of the total, NK, B, T, TCD4, TCD8, and TCD4CD8 lymphocytes are decreased on D0 samples compared to HV, however, there was no difference in the percentage of these cells or in the CD4/CD8 ratio. Along the follow-up, it was observed that the absolute counts of the total, T, TCD4, TCD8, and NK lymphocytes were lower on D0 and D7 when compared to the CS-31 samples. The percentages of T and B lymphocytes were decreased on D0 when compared to CS-31 samples. The lymphocytes cell counts in CS-31 samples presented even higher for total lymphocytes, T and TCD8 than for the HV.

When patients were grouped according to clinical evolution, those who progressed to critical disease (DOC) showed a lower absolute count of the total, T, TCD4, TCD8, and TCD4CD8 lymphocytes compared to the DONC group. This difference was extended for the percentages of T and TCD8 lymphocytes. A lower percentage of NK cells was observed in the D7C group compared to the D7NC group. In the CS-31 samples, there was no difference between the C and NC groups. COVID-19 patients had profound lymphopenia, affecting the total, T, B, and NK lymphocytes populations, which was most evident in the Critical group of patients. Despite these features, COVID-19 patients, even those who survived the critical illness, demonstrated a capacity to return to homeostasis presenting a lymphocyte count profile similar to that of healthy volunteers after 31 days of convalescence.

**901596 P6**

### **SARS-CoV-2 vaccine Humoral and Cellular responses in B cell immunocompetence and immunodeficiency,**

Berenice Cabrera-Martinez<sup>1</sup>, Ryan Baxter<sup>1</sup>, Ross Kedl<sup>1</sup>, Elena W-Y Hsieh<sup>1</sup>

<sup>1</sup>University of Colorado Anschutz Medical Campus

The Coronavirus disease 2019 (COVID-19) global pandemic has set an unprecedented challenge to develop safe and effective vaccines in record time; however, questions remain about currently deployed vaccines including the durability and quality of the response, and the nature of T cell responses and their immunogenicity in immunocompromised individuals. To address these questions, we evaluated SARS-CoV-2-specific antibody and T cell antigen-specific responses to currently approved vaccines in healthy donors and patients with primary B cell defects at different time points post-vaccination. To assess the durability and quantity of antibody responses we used SARS-CoV-2 Multiplex (Multi-antigen IgG and IgA assay) Microsphere Immunoassay (MMI), a highly sensitive and specific test that facilitates a reliable detection of antibodies (IgG and IgA) to multiple SARS-CoV-2 antigens in plasma/serum and nasal swab samples. To address the nature of T cell responses, an antigen-specific activation induced markers (AIM) T cell assay was applied using peripheral blood mononuclear cells. Our data show that the MMI assay can segregate the immunocompetent healthy donors infection and vaccination status based on SARS-CoV-2 anti-IgG RBD and S1 and S2 antibody profiles. Furthermore,

# CYTO 2022 ABSTRACTS

spike protein receptor binding domain (RBD)-specific CD8 T cell responses defined by expression of CD69+CD137+ (activation induced markers, AIM), and IFN-g production, were increased in individuals who were SARS-CoV-2 infected prior to vaccination. Additionally, vaccinated individuals with B cell defects due to primary immunodeficiencies, displayed increased RBD-specific CD8 T cell responses, despite negligible anti-RBD IgG responses. Together, these data indicate healthy donors who were infected prior to vaccination demonstrated a more robust CD8 T cell activation than uninfected vaccinees, despite similar anti-RBD IgG responses. In addition, patients with primary B cell defects exhibited low RBD-specific IgG levels post-vaccination, yet robust RBD-specific CD8 T cell responses, suggesting a compensatory mechanism related to the lack of B cells.

**896789 P8**

## **Physical phenotype of blood cells is altered in COVID-19 and beyond: causal relation for long-term imprint?**

Martin Kräter<sup>1</sup>, Markéta Kubánková<sup>1</sup>, Bettina Hohberger<sup>2</sup>, Jochen Guck<sup>1</sup>

<sup>1</sup>Max Planck Institute for the Science of Light,

<sup>2</sup> Universitätsklinikum Erlangen

Clinical syndrome coronavirus disease 2019 (COVID-19) induced by severe acute respiratory syndrome coronavirus 2 is characterized by rapid spreading and high mortality worldwide. Although the pathology is not yet fully understood, hyperinflammatory response and coagulation disorders leading to congestions of microvessels are considered to be key drivers of the still-increasing death toll. Until now, physical changes of blood cells have not been considered to play a role in COVID-19 related vascular occlusion and organ damage. Here, we report an evaluation of multiple physical parameters including the mechanical features of five frequent blood cell types, namely erythrocytes, lymphocytes, monocytes, neutrophils, and eosinophils. More than four million blood cells of 17 COVID-19 patients at different levels of severity, 24 volunteers free from infectious or inflammatory diseases, and 14 recovered COVID-19 patients were analyzed. We found significant changes in lymphocyte stiffness, monocyte size, neutrophil size and deformability, and heterogeneity of erythrocyte deformation and size. Although some of these changes recovered to normal values after hospitalization, others persisted for months after hospital discharge, evidencing the long-term imprint of COVID-19 on the body.

**901203 P12**

## **High-density glass-bottom nanowell-in-microwell arrays for cell tracking image cytometry**

Jeonghyun Lee<sup>1</sup>, Hongshen Ma<sup>1</sup>, Samuel Berryman<sup>1</sup>, Jinpyo Jeon<sup>1</sup>

<sup>1</sup>University of British Columbia

A frequent need in image cytometry is to isolate single cells in separated containers, such as nanowells, to enable analysis of cell function or behaviour at the single cell level, as well as to track cell behaviour over hours or days. Previous methods involved fabricating nanowells in PDMS or plastic by molding or embossing. However, these approaches cannot fully utilize the available high throughput infrastructure for microscopy and liquid handling because they provide limited nanowell density, they cannot retain cells in nanowells during reagent exchange, and importantly, they cannot provide a glass-bottom surface for high-quality imaging. Here, we developed a method to fabricate glass-bottom nanowell arrays inside standard microwells. The nanowells are fabricated using laser micropatterning of polyethylene glycol diacrylate (PEGDA) hydrogel on a glass substrate. A standard 384-well square microwell can hold up to 2,100 nanowells with dimensions of 50×50×50 µm. These PEGDA hydrogel nanowells show stable adhesion to the glass substrate, while minimizing swelling or protein absorption. We show this approach can produce high-aspect ratio nanowells that can retain suspension and adhesion cells during reagent exchange, enabling immunoassays of cell behaviour without cell loss. We demonstrated the capabilities of PEGDA nanowell-in-microwells for three different image cytometry applications. First, we assess cell proliferation in nanowells and established that cultured cells could be continuously monitored for cell function, state, and phenotype changes. We then surveyed heterogeneity of cytokine secretion for thousands of single cells. Cells were seeded with protein capture beads into nanowells, which limited cross-contamination and permit quantification of secreted protein by fluorescence staining. Finally, we used this approach to assess the heterogeneity of CAR-T cell cytotoxicity and found distinct populations of serial killers, partial killers, and non-killers. Together, these capabilities suggest that PEGDA nanowell-in-microwells could greatly expand the applications of image cytometry by utilizing high-throughput microwell plate screening platforms.

# CYTO 2022 ABSTRACTS

**901295 P14**

## **A UV-C LED-based reactor for continuous decontamination of the sheath fluid in a flow-cytometric cell sorter**

Toralf Kaiser<sup>1</sup>, Konrad v. Volkman<sup>2</sup>, Jenny Kirsch<sup>1</sup>, Kerstin Heinrich<sup>1</sup>

<sup>1</sup>DRFZ, <sup>2</sup>APE

Flow-cytometric cell sorting is a key technology in modern research laboratories. In many experiments, cells are cultivated after cell sorting requiring aseptic sorting. Contamination of the sheath fluid used for hydrodynamic focusing must therefore be avoided. However, cell sorters typically do not operate in a sterile environment, making contamination with germs very likely, e.g., when sheath fluid reservoir are opened for refilling or through contamination of compressed air required for operation. For this reason, decontamination is usually accomplished by regular flushing the fluidics with sodium hypochlorite or ethanol. However, such cleaning procedures are time consuming and, more importantly, the researcher can never be sure that the cleaning process was successful. Furthermore, residues of cleaning reagents in the fluidics are toxic for the cells of interest. In many cell sorting laboratories, antibiotics are added to the collection medium of the sorted cells to prevent the proliferation of bacteria entered by sheath fluid. This in turn can lead to a change in gene expression and regulatory level of the cultured cells and more importantly, the use of antibiotics allows the development of resistant bacteria. The lethal effect of UV light is well known for inactivating microorganisms without the side effects of chemical treatment. UV light is divided into UV-A (380 – 315 nm), UV-B (315 – 280 nm) and UV-C (280 – 100 nm). The antimicrobial effect of UV-C light is based on the absorption of photons in the wavelength range of 200 – 280 nm by the DNA, resulting in the formation of pyrimidine dimers, which inhibit DNA replication and consequently block transcription of RNA. UV-C light can be generated by mercury-based lamps, pulsed xenon lamps, or more recently by UV-C LEDs. The latter have very small dimensions and require low current to provide UV-C doses sufficient to reduce the quantity of bacteria in water by several log levels. These properties make UV-C LEDs very interesting for the on-the-fly decontamination of sheath fluids in flow-cytometric cell sorters as an alternative to cleaning procedures based on chemical decontamination. Here we present a method based on a UV-C reactor module for flow-through irradiation of sheath fluid used in a BD Influx™ cell sorter. The reactor contains 6 UV-C LEDs with an emission

wavelength of 275 nm providing a maximum UV-C dose of  $4.2 \times 10^4$  mJ/cm<sup>2</sup> and allows also the temperature stabilization of the sheath fluid. In a proof-of-principle, the UV-C reactor enabled a 5.8 log reduction of *Pseudomonas aeruginosa*.

**901985 P16**

## **Novel live-cell and fixable mitochondrial probes for cytometry and imaging.,**

Hannah Maple<sup>1</sup>, Paul Wood<sup>1</sup>, Jody Bonnevier<sup>1</sup>, Li Peng<sup>1</sup>

<sup>1</sup>Bio-Techne

Fluorescent probes that accumulate specifically in cellular organelles are widely used and valuable components of the 'toolkit' for fluorescence imaging and flow cytometry. Functioning mitochondria underpin many critical cellular processes are commonly referred to as the 'powerhouse of the cell', while mitochondrial dysfunction is linked to numerous diseases. The mitochondrial membrane potential ( $\Delta\psi_m$ ) is an indicator of mitochondrial activity and health because it relates directly to the cells' ability to generate ATP. Fluorescent probes that accumulate in the mitochondria specifically as a result of the transmembrane potential can therefore provide insights into mitochondrial and cell health. We report the development of novel fluorescent probes that specifically localize to the mitochondria due to the mitochondrial membrane potential: called MitoBrilliant™ probes. MitoBrilliant™ live; 646 and 549 are far-red and orange probes, respectively, that are suitable for staining healthy mitochondria in live cells in flow cytometry, imaging and high-content screening. MitoBrilliant™ 646 is a corresponding far-red probe suitable for both live and fixed-cell staining. It retains brightness and fidelity to the mitochondria after fixation, and is suitable for use in flow cytometry, imaging, high-content screening and performs well in STED super-resolution microscopy.

# CYTO 2022 ABSTRACTS

**901203 P12**

## **High-density glass-bottom nanowell-in-microwell arrays for cell tracking image cytometry**

Jeonghyun Lee<sup>1</sup>, Hongshen Ma<sup>1</sup>, Samuel Berryman<sup>1</sup>, Jinpyo Jeon<sup>1</sup>

<sup>1</sup>University of British Columbia

A frequent need in image cytometry is to isolate single cells in separated containers, such as nanowells, to enable analysis of cell function or behaviour at the single cell level, as well as to track cell behaviour over hours or days. Previous methods involved fabricating nanowells in PDMS or plastic by molding or embossing. However, these approaches cannot fully utilize the available high throughput infrastructure for microscopy and liquid handling because they provide limited nanowell density, they cannot retain cells in nanowells during reagent exchange, and importantly, they cannot provide a glass-bottom surface for high-quality imaging. Here, we developed a method to fabricate glass-bottom nanowell arrays inside standard microwells. The nanowells are fabricated using laser micropatterning of polyethylene glycol diacrylate (PEGDA) hydrogel on a glass substrate. A standard 384-well square microwell can hold up to 2,100 nanowells with dimensions of 50×50×50 µm. These PEGDA hydrogel nanowells show stable adhesion to the glass substrate, while minimizing swelling or protein absorption. We show this approach can produce high-aspect ratio nanowells that can retain suspension and adhesion cells during reagent exchange, enabling immunoassays of cell behaviour without cell loss. We demonstrated the capabilities of PEGDA nanowell-in-microwells for three different image cytometry applications. First, we assess cell proliferation in nanowells and established that cultured cells could be continuously monitored for cell function, state, and phenotype changes. We then surveyed heterogeneity of cytokine secretion for thousands of single cells. Cells were seeded with protein capture beads into nanowells, which limited cross-contamination and permit quantification of secreted protein by fluorescence staining. Finally, we used this approach to assess the heterogeneity of CAR-T cell cytotoxicity and found distinct populations of serial killers, partial killers, and non-killers. Together, these capabilities suggest that PEGDA nanowell-in-microwells could greatly expand the applications of image cytometry by utilizing high-throughput microwell plate screening platforms.

**901295 P14**

## **A UV-C LED-based reactor for continuous decontamination of the sheath fluid in a flow-cytometric cell sorter,**

Toralf Kaiser<sup>1</sup>, Konrad v. Volkmann<sup>2</sup>, Jenny Kirsch<sup>1</sup>, Kerstin Heinrich<sup>1</sup>

<sup>1</sup>DRFZ, <sup>2</sup>APE

Flow-cytometric cell sorting is a key technology in modern research laboratories. In many experiments, cells are cultivated after cell sorting requiring aseptic sorting. Contamination of the sheath fluid used for hydrodynamic focusing must therefore be avoided. However, cell sorters typically do not operate in a sterile environment, making contamination with germs very likely, e.g., when sheath fluid reservoir are opened for refilling or through contamination of compressed air required for operation. For this reason, decontamination is usually accomplished by regular flushing the fluidics with sodium hypochlorite or ethanol. However, such cleaning procedures are time consuming and, more importantly, the researcher can never be sure that the cleaning process was successful. Furthermore, residues of cleaning reagents in the fluidics are toxic for the cells of interest. In many cell sorting laboratories, antibiotics are added to the collection medium of the sorted cells to prevent the proliferation of bacteria entered by sheath fluid. This in turn can lead to a change in gene expression and regulatory level of the cultured cells and more importantly, the use of antibiotics allows the development of resistant bacteria. The lethal effect of UV light is well known for inactivating microorganisms without the side effects of chemical treatment. UV light is divided into UV-A (380 – 315 nm), UV-B (315 – 280 nm) and UV-C (280 – 100 nm). The antimicrobial effect of UV-C light is based on the absorption of photons in the wavelength range of 200 – 280 nm by the DNA, resulting in the formation of pyrimidine dimers, which inhibit DNA replication and consequently block transcription of RNA. UV-C light can be generated by mercury-based lamps, pulsed xenon lamps, or more recently by UV-C LEDs. The latter have very small dimensions and require low current to provide UV-C doses sufficient to reduce the quantity of bacteria in water by several log levels. These properties make UV-C LEDs very interesting for the on-the-fly decontamination of sheath fluids in flow-cytometric cell sorters as an alternative to cleaning procedures based on chemical decontamination. Here we present a method based on a UV-C reactor module for flow-through irradiation of sheath fluid used in a BD Influx™ cell sorter. The

# CYTO 2022 ABSTRACTS

reactor contains 6 UV-C LEDs with an emission wavelength of 275 nm providing a maximum UV-C dose of  $4.2 \times 10^4$  mJ/cm<sup>2</sup> and allows also the temperature stabilization of the sheath fluid. In a proof-of-principle, the UV-C reactor enabled a 5.8 log reduction of *Pseudomonas aeruginosa*.

**901985 P16**

## **Novel live-cell and fixable mitochondrial probes for cytometry and imaging.**

Hannah Maple<sup>1</sup>, Paul Wood<sup>1</sup>, Jody Bonnevier<sup>1</sup>, Li Peng<sup>1</sup>

<sup>1</sup>Bio-Techne

Fluorescent probes that accumulate specifically in cellular organelles are widely used and valuable components of the 'toolkit' for fluorescence imaging and flow cytometry. Functioning mitochondria underpin many critical cellular processes are commonly referred to as the 'powerhouse of the cell', while mitochondrial dysfunction is linked to numerous diseases. The mitochondrial membrane potential ( $\Delta\psi_m$ ) is an indicator of mitochondrial activity and health because it relates directly to the cells' ability to generate ATP. Fluorescent probes that accumulate in the mitochondria specifically as a result of the transmembrane potential can therefore provide insights into mitochondrial and cell health. We report the development of novel fluorescent probes that specifically localize to the mitochondria due to the mitochondrial membrane potential: called MitoBrilliant™ probes. MitoBrilliant™ live; 646 and 549 are far-red and orange probes, respectively, that are suitable for staining healthy mitochondria in live cells in flow cytometry, imaging and high-content screening. MitoBrilliant™ 646 is a corresponding far-red probe suitable for both live and fixed-cell staining. It retains brightness and fidelity to the mitochondria after fixation, and is suitable for use in flow cytometry, imaging, high-content screening and performs well in STED super-resolution microscopy.

**898418 P18**

## **CellMek SPS Instrument Performance: Cellular and Reagent Carryover when using the Cell Wash Module**

Brittany Kuhl<sup>1</sup>,

<sup>1</sup>Beckman Coulter Inc

Introduction: The CellMek SPS instrument is an automated sample preparation system intended for in vitro diagnostic use in flow cytometry laboratories. It will automatically prepare a variety of specimen types using standard reagents and workflows that wash, stain, lyse, and fix the stained white blood cells, offering fully prepared samples that are ready for analysis. The Cell Wash Module (CWM) is a component of the CellMek SPS instrument that was designed to wash either unprocessed biological specimen or in-process biological sample during preparation. Wash buffer is automatically added to the specimen or sample within the CWM, which undergoes cyclonic centrifugation to separate cells from buffer, followed by aspiration of waste. After washing, the system automatically performs a cleaning cycle on the CWM prior to use with the next specimen/sample. The purpose of this study is to demonstrate the Cellular and Reagent carryover (CO) performance when running the CWM, showing the effectiveness of the CWM cleaning routine. Methods: This study was designed to measure the CO of the CWM, as defined by a percent effect of one sample on the succeeding sample (per CLSI H26-A2 guideline), considering both Cellular and Reagent CO. Cellular CO measured the interference of a preceding washed specimen or sample (stained and lysed) with high cell count on the subsequent washed specimen or sample with low cell count. Staining for CD45, CD235a, and CD41 was used to differentiate WBCs, RBCs, and platelets, respectively. Cellular CO was verified for unprocessed biological specimen and for in-process samples. Reagent CO measured the interference of a preceding washed sample with high level reagent staining on the subsequent washed sample with low reagent staining (unstained). The staining panel incorporated 10 marker/fluorochrome combinations that represented detection in each fluorescent channel (FL1-FL10). Reagent CO was verified for in-process samples only, as native biological specimen presented to the system would not normally contain fluorescent antibodies or dyes. For both Cellular and Reagent CO, two CellMek SPS instruments were used; specimens were prepared in triplicate sets of high-concentration samples followed by low-concentration samples, then data was acquired on a Navios

# CYTO 2022 ABSTRACTS

cytometer. Total percent CO was calculated from the averages of each CellMek SPS instrument. A 95% confidence was used to calculate the upper limits (UL) of both Cellular and Reagent COs by parameter for each module assembly based on their individual runs. Results: The calculated 95% confidence ULs for CWM Cellular CO using specimen and sample wash workflows were below 0.05% for CD45+ WBCs. The calculated 95% confidence UL for CWM Reagent CO was below 0.05% for all markers in the representative 10-Color panel. The Beckman Coulter products and service marks mentioned herein are trademarks or registered trademarks of Beckman Coulter, Inc. in the United States and other countries

---

**901523 P20**

## **Internally stained multiple fluorescent microsphere intensity reference with assigned ERF-values for quantitative flow cytometry analysis,**

Paul DeRose<sup>1</sup>, Yu-Zhong Zhang<sup>2</sup>, Adam W. York<sup>2</sup>, Eric Welch<sup>2</sup>

<sup>1</sup>NIST, <sup>2</sup>Thermo Fisher Scientific

Multicolor flow cytometry assays are routinely used in biomedical and clinical laboratories where instrument calibration is critical. Reliable instrument performance, assay standardization and measurement traceability can be achieved by using fluorescence intensity calibrators. These calibrators are typically micron sized particles that have been internally stained, or surface reacted to small molecule fluorescent dyes. Until recently, it has been recommended for flow cytometry users to use fluorescent particles with assigned Molecules of Equivalent Soluble Fluorophore (MESF) values. However, MESF values are currently measured by individual manufacturers using their own developed methods which leads to lot-to-lot and manufacturer-to-manufacturer variability. To address the inconsistencies of MESF values, the National Institute of Standards and Technology (NIST) has proposed a new fluorescence intensity unit known as the Equivalent number of Reference Fluorophores (ERF). Through collaborative research with NIST, a set of multi-color fluorescent microparticles, the AccuCheck™ ERF Reference Particles, were developed by Thermo Fisher Scientific. These multiple fluorescent, internally dye-stained particles were characterized using NIST developed measurement methods and ERF values were assigned to 26 different commonly used flow cytometry filter sets. One key advantage is that these particles fluoresce across the entire visible spectrum at three varying intensity levels, thus, allowing simultaneous fluorescence intensity

measurements across multiple filter sets. Using a single set of particles is more practical than having to run multiple different single-dye stained particle calibrators, like MESF based products, to achieve calibration of the entire fluorescence intensity scale. Furthermore, calibrators that have dyes internally loaded have excellent shelf-life as the dyes are protected against environmental degradation and experience less photobleaching relative to dyes conjugated to the particle's surface. These ERF reference particles ensure consistency and traceability of the sample's intensity measurements, make intra- and inter-laboratory data comparison possible, and allow the performance characteristics of flow cytometers to be tracked. Perhaps most important of all will be the use of ERF particles in conjunction with a biological standard in order to quantify the expression level of surface and intracellular biomarkers. Herein, we will highlight the use and advantages of these fluorescent calibrators.

---

**901556 P22**

## **Semi and fully automated sample preparation platforms improve washing efficiency, reproducibility, and recovery of live leukocytes in fresh and freeze-thawed specimens,**

Melvin Lye<sup>1</sup>, Geoffrey Feld<sup>1</sup>, Christoph Eberle<sup>1</sup>, Chyan Ying Ke<sup>1</sup>

<sup>1</sup>Curiox Biosystems

Limited innovation in automated cell and organelle sample preparation methodology limits the effectiveness and high-content data generation of modern analytical methods, such as single-cell 'omics, flow and mass cytometry. These techniques traditionally rely on manual and disruptive centrifugation-based protocols for cell washing and suspension preparation, which introduce variability and bias in the resulting data. We have developed a suite of cell suspension preparation systems that enable semi and full automation of cell washing protocols. These Lamina Wash™ technologies robustly, gently, and efficiently remove debris, dead cells, and unbound reagent using laminar flow and liquid handling robotics, rather than turbulent and harsh pelleting-plus-pipetting methods. Adapting standard protocols to Lamina Wash automation removes intervention steps and streamlines the immunostaining workflow, reducing hands-on time and improving inter- and intra-operator precision. We demonstrate the superior live cell retention and reproducibility of Lamina Wash over centrifugation in processing murine and humanized mouse peripheral blood mononuclear cells (PBMCs)

# CYTO 2022 ABSTRACTS

and tumor infiltrating lymphocytes (TILs) for flow cytometry. Furthermore, we show that Laminar Wash maintains relative abundances of immune cell subpopulations in freeze-thawed samples relative to conventional washing, a token of classical sample bio-banking. Overall, these results show how Laminar Wash methodology assists in standardizing sample preparation for cytometric analysis, an important and unmet need in cell-based therapy development and product manufacturing.

**901583 P24**

## **Performance of SiPM for Dim Fluorescence Signal Detection in Flow Cytometry,**

Garret Guenther<sup>1</sup>, Nan Li<sup>1</sup>, Yan Wu<sup>1</sup>, Wenqi Liu<sup>1</sup>

<sup>1</sup>Agilent Technologies,

Solid state silicon photomultiplier (SiPM) has been proved to be a sensitive detector for flow cytometry detection, benefited from its high gain, low dark count, and fast temporal response. With thousands of micron-size avalanche photodiode (pixel) working in parallel in a Geiger mode, SiPM can detect light on single photon level. In this study, the performance of SiPM has been evaluated regarding its capability to detect dim fluorescence signals with qualification beads products and biological samples. The capability of SiPM to resolve dim fluorescence signal is compared to other type of photodetectors including PMT and APD. The Quantum Efficiency (QE) of SiPM is a very important parameter to detect low light signals, and it increases with the pixel size of the SiPM. Therefore, different models of SiPM with different QE are compared, and the same model of SiPM with different pixel sizes are compared using compensation beads conjugated with multiple fluorescent antibodies. In addition, the characteristics of SiPM, including Gain, QE, and dark count, in relationship with the Stain Index (SI) is studied to have a better understanding of the impact on the dim signal detection capability and resolving power for the low expressed biomarkers. The study can serve as a guidance to implement SiPM for any applications in which very low level of light signal needs to be resolved, including flow cytometry.

**901598 P26**

## **Time-resolved measurements of MCF-7 breast cancer cells using CD29-Alexa Fluor 488 and CD29-FITC as discriminants with acoustofluidic flow cytometry,**

Jessica Houston<sup>1</sup>, Jesus Sambrano<sup>1</sup>

<sup>1</sup>New Mexico State University

**BACKGROUND** Time-resolved flow cytometry provides complimentary quantitative analysis to conventional cytometric methods with the fluorescence lifetime parameter. The advent of microfluidics facilitated single-cell analysis by increasing observation time underneath an excitation source, allowing for enhanced exploitation of the biophysical and biochemical attributes of label-free and exogenous cell assays. Further external control is desirable to overcome limitations inherent to conventional cytometry. Herein we present a time-resolved acoustofluidic cytometric platform (TRAFFC) that incorporates ultrasonic focusing in a microfluidic platform in place of traditional hydrodynamics for substantive improvement to temporal resolution using fluorescently labeled fluorospheres and MCF-7 breast cancer cells. **METHODS** TRAFFC is deployed as follows. A 488 nm laser diode is digitally modulated at a radio frequency of 1 MHz. The acoustofluidic device has a piezoceramic transducer driven at 1.51 MHz, allowing for samples to align to a singular pressure node in the microchannel. The DAQ and offline oscilloscope data are calibrated to a fluorophore with a known lifetime value. Two (2) separate populations of MCF-7 breast cancer are fluorescently labeled. One population is labeled with conjugated CD29-Alexa Fluor 488, and the second population is labeled with conjugated CD29-FITC. Conventional methods would produce significant spectral emission overlap. However, time-resolved measurements of each fluorophore will produce a lifetime unique to that fluorophore, negating the need for color compensation. Up to 5,000 events are collected for offline analysis in MATLAB from multiple experiments. **RESULTS** Previous cytometric analysis for multiple trials and ~3,000 MCF-7 cells conjugated CD29-Alexa Fluor 488 yielded mean lifetime values by two acquisition methods; data acquisition system derived at 5.8 +/- 2.4 ns, and offline waveform analysis collected by an oscilloscope at 5.2 +/- 1.6 ns. **CONCLUSION** TRAFFC has demonstrated the ability to provide time-resolved measurements that are complimentary to conventional methods while providing additional raw cytometric data that will allow us to create phasor graphs. These phasor graphs will allow us to

# CYTO 2022 ABSTRACTS

illustrate significant cellular heterogeneity through observation of lifetime distributions on a single cell. The achievable analysis is consequential to quantitative cell sciences.

---

**901896 P28**

## **Optimization and set-up of the BD Spectral Enabled Prototype Analyzer,**

Stephen Perfetto<sup>1</sup>, Richard Nguyen,<sup>1</sup> Erica Smit<sup>1</sup>, David Ambrozak<sup>1</sup>, Esther Thang<sup>1</sup>, Mario Roederer<sup>1</sup>

<sup>1</sup>NIH

Flow cytometry instrumentation is developing at a steady rate. Today, flow cytometers can measure 38+ mAb-conjugates simultaneously and recently the spectral-enhanced capabilities have been configured to the conventional analyzers. These configurations include a variation of the optical bench to include a selection of photon detection devices. This provides the user with a choice between utilizing a wide range of optical filters (spectral detection) or a limited number of optical filters (traditional detection). The resulting analysis will therefore depend on the research question and need. The complexity of these instruments and their filter configuration requires a well-defined calibration procedure, to generate accurate and interpretable biological results. Once an instrument is properly setup, daily monitoring is essential to maintain data quality. Here we describe the set of validation procedures we utilized to calibrate, optimize, and standardize a prototype spectral analyzer. We also describe the measured differences within unmixing algorithms vs. the traditional compensation method due to potential variations in the spillover spreading error matrix. Method: We used the quantiFlash™ LED pulser (method not yet published), CD4-stained compensation beads, followed by cells stained with a standard lineage panel. The calibration step, using the LED pulser, is to establish the set point voltages for each detector (not yet published). Set point voltages were used to measure CD4-stained COMP beads, which defines the optimized (or balanced) voltages for all detector pairs. At the same time each PMT was assessed for technical issues (e.g., fluidics, background, alignment) and were corrected before continuing to the next step. Using these optimized voltages, cells stained with a standard lineage panel was used to validate the voltages based on the biological performance of the markers. Data analysis on COMP tubes using multiple spectral unmixing repeats (SSM), and the comparison to traditional compensation, was performed using the FlowJo version 10.8.1 software.

These outcomes were compared to the same stained sample to determine if differences in the SSM produced notable differences in cell populations. Results & Conclusion: Using the LED pulser to generate set point voltages for all detectors was shown to be a fast and efficient method for setting up a spectral analyzer. Final voltages were confirmed and validated using a well characterized lineage panel showing marker relevance and reproducibility. Few detectors required optimization changes in detection pairs. Multiple spectral unmixing runs with the same COMP tubes showed differences in the spillover spreading errors, compared to traditional COMP analysis. These changes can show differences in stained cell samples as these COMP values are used in the same panel. Hence, potential population errors can be realized in longitudinal studies using the same panel and stained COMP beads.

---

**901955 P30**

## **High Marker T Cell Characterization with Reduced Spillover using Cyclic Flow Cytometry,**

John Tigges<sup>1</sup>, Sean Cosgriff<sup>1</sup>, Jessica Liegel<sup>1</sup>, Giulia Cheloni<sup>1</sup>

<sup>1</sup>LASE Innovation

As the complexity of cancer immunotherapies increases, there is a growing demand to fully characterize these treatments in a simplistic manner. Due to the diversity of T cell subtypes, activation markers, and functional parameters relevant to immune-oncology, researchers often require the measurement of 20 or more markers per cell. Traditionally, flow cytometry has been the platform of choice to characterize the expression of proteomic markers. However, multiplexing of fluorescent based signals is fundamentally limited by spectral spillover. As a result, increasing the number of markers to measure per cell increases the complexity of both the panel design and instrumentation. Here, we present a novel approach to high marker (>20) flow cytometry that significantly reduces spectral spillover. Our technique leverages laser particles (LPs) to barcode cells, enabling repeated measurements of the same cells. This reduces the required number of colors and compensation needed per acquisition: for example, 1/2 the colors are needed if cells are measured twice, 1/3 if cells are measured 3 times. LPs are micron sized particles that emit laser light in the infrared wavelengths and confer a unique barcode for each cell. In a typical experiment, LP barcoded cells are analyzed on a proprietary flow cytometer that detects both fluorescence and LP signal. Cells are



# CYTO 2022 ABSTRACTS

captured, antibody fluorescence is removed, cells are re-stained, and run again. Data from each cycle are then concatenated on each barcoded cell. Using this novel, cyclic approach, we characterized T cells that were incubated ex-vivo with a dendritic-tumor cell fusion-based vaccine. Phenotyping immunotherapy T cell products is critical to quickly ascertain effects of stimulation. Our panel consisted of 20 surface markers, 7 intracellular, 3 intranuclear markers, and a live/dead dye. Cells were barcoded with LPs and measured over 3 cycles. With our in-house photobleacher, fluorochromes could be reduced to 10 per cycle, simplifying panel design, instrumentation requirements, and compensation. Following vaccine stimulation, we identified increased markers of T cell activation such as CD25, CD69, 4-1bb and PD1 which captures vaccine priming of T cells. Lastly, we noted a shift of CD4 and CD8 T cells from naïve to memory following vaccine priming when compared to unstimulated samples, suggesting that vaccine-stimulation may enhance T cell persistence in vivo. Cyclic flow cytometry utilizing LPs to barcode single cells enables high marker flow cytometry while avoiding many of the technical challenges that come with establishing >20 color panels. In simplifying panel construction, it becomes feasible to reduce the number of control samples required, antibody reagents, and amount of time necessary to validate and run a complex panel. We expect the benefits of this technique, including ease-of-use and improved data quality, will greatly help characterize increasingly complex immuno-oncology-based therapies.

**902018 P32**

## **Uniform Light-Sheet Excitation Beam Formed by Integrated Optics for Sensitive Optofluidic Cytometry,**

Matthew DiSalvo<sup>1</sup>, Gregory Cooksey<sup>1</sup>, Megan Catterton<sup>1</sup>, Jalal Sadeghi<sup>1</sup>

<sup>1</sup>National Institute of Standards and Technology

Applications in flow cytometry increasingly involve dim and/or small particles that push the limits of detection and quantification, such as unlabeled cells, bacteria, organelles, or vesicles. The measurement of such particles is strongly influenced by the optical path of the flow cytometer. A particularly notable factor is the spatial profile of the light beam(s) used to illuminate particles. Narrow, high-powered beams with uniform profiles promote high signal-to-noise and lower uncertainty (i.e., from the positional dependence of particle positions as they cross the beam) in cytometry measurements.

We previously achieved a narrow beam by spatially filtering light through a slit opening in an opaque material, but since most of the light was absorbed by the filter, the transmission efficiency (through a microcytometer to a fiber optic-coupled detector) was limited to 4 % and the input power was limited to < 80 mW to prevent damaging the filter. More optical advancements are needed to improve measurement robustness and to facilitate better quantification of particle properties such as size. In this work, we demonstrated an efficient, uniform, and filter-free excitation beam formed by integrated optical lenses within a microfluidic flow cytometer. Laser light from a fiber optic was first collimated to a width of 210  $\mu\text{m}$  by a planar, micromolded, and fiber-coupled waveguide. This beam was then confined and focused by a series of integrated lenses to form a “pseudo light sheet” with a waist of 40  $\mu\text{m}$  at a focal length of 190  $\mu\text{m}$ , which agreed with computational ray-physics modeling. The waist was sufficiently narrow that light obscuration-based particle size calibration was achieved for particles as small as 1.04  $\mu\text{m}$  in diameter with < 5 % error. The beam uniformity was maintained at < 5 % variation in width as it propagated through a 40  $\mu\text{m}$  wide microfluidic channel and < 5 % variation in integrated beam intensity was observed between the bottom and top of the 80  $\mu\text{m}$  tall channel. Significantly, the light sheet allowed for 43 % transmission efficiency of a 200 mW laser through the microcytometer. The enhanced sensitivity of the flow cytometer was evaluated using the dim autofluorescence of unlabeled polystyrene microspheres by the separation index (the difference in intensity from noise relative to the spread of the noise). A separation index > 10 was achieved by the microcytometer with particles with intensities of at least 80 mean equivalent soluble fluorophores (MESF), comparing favorably with an intensity of 550 MESF for the same test on a commercial flow cytometer. These results mark a substantial improvement in the intensity and uniformity of on-chip light beams, and in the sensitivity of optofluidic microcytometers. Future work will explore the impact of beam optimizations on measurement variations in flow cytometry as well as ramifications for particle size analyses.

# CYTO 2022 ABSTRACTS

**902040 P34**

## **Fluorescence and Transmission Intensity-Over-Time Measurement Simulation in an Optofluidic Cytometer,**

Paul Patrone<sup>1</sup>, Matthew DiSalvo<sup>1</sup>, Gregory Cooksey<sup>1</sup>, Nikita Podobedov<sup>1</sup>

<sup>1</sup>National Institute of Standards and Technology

Flow cytometry already is a powerful measurement technique, but there are interesting possibilities to extract untapped information about particles in flow, such as shape and velocity, and to further understand how unexpected changes to these properties might lead to measurement error. While methods like imaging cytometry are promising (and may address this question from a different perspective), full intensity-over-time measurements may contain additional information that is not completely captured by scalar parameters recorded by traditional flow cytometers. Our group is developing a serial optofluidic cytometer, which records each object at high temporal and digital resolution multiple times as it travels past a series of detection regions in the device. To aid in understanding the shape of this fluorescent signal, a simulation was developed to approximate fluorescent peaks of objects passing through a measurement region. The simulation combines fluorescence images of the illuminated flow channel with simulated objects of various physical characteristics (size, shape, streamline position, velocity, fluorophore distribution) to create a modeled emission signal. The simulation was used to facilitate device design and to investigate how the shape of the signal is influenced by particle and device geometry. We demonstrate an additional functionality to model non-fluorescent transmission intensity-over-time traces, which was developed through a similar framework to the original simulation. For both fluorescent and non-fluorescent peaks, we conducted a more thorough comparison of simulated peaks with experimental data. Peaks from a population of ~15  $\mu\text{m}$  diameter polystyrene beads were analyzed alongside a synthetic peak dataset (generated using the same size and velocity distribution) for similarity in average peak shape and distribution characteristics. For example, the fluorescent peak area coefficient of variation (CV) was 9.6% for the experimental population and 10.2% for the simulated beads. Along with such experimental comparisons, we also discuss novel uses for this simulation, which include optimization of encoding signals with amplitude modulation, object size detection, and determination of closest-fit object parameters for a real recorded peak. Due to its ease of set-up and wide utility, simple, virtual laboratory tools such as this one may be of interest for optimizing design and understanding performance of a range of optofluidic systems.

**902044 P36**

## **Sorting large and fragile cells - A model cell line and novel microfluidic device,**

Benjamin Finnin<sup>1</sup>, Mehran Hoonejani<sup>1</sup>, Kevin Shields, John Harley

<sup>1</sup> Miltenyi Biotec

Cytometry and cell sorting are powerful tools used by scientists worldwide, yet there are some applications where existing technologies do not deliver the required performance. Sorting large cells is challenging on the ubiquitous droplet sorters in most flow cores, large cells behave differently in regards to fluidics and sort mechanics. Beyond the challenge of physically being able to sort large cells, some applications require healthy, viable cells, an even more challenging prospect on droplet based instruments. Large cell sorting on droplet sorters requires extra-large nozzles, special set up particles and low drop drive frequencies that result in lower possible sort rates. Microfluidic based cell sorting has become attractive for many applications where conventional sorting has been indicated to negatively impact cell function and viability. Microfluidic sorting, while being widely accepted as more gentle, is usually multiple of orders of magnitude slower than conventional sorters. Moreover, the sort mechanisms used in most microfluidic based devices are extremely sensitive to cell size and have mostly been optimized to work on smaller lymphocyte sized cells. Here we present a novel microfluidic device based around a 50 $\mu\text{m}$  channel and physical sorting valve. To test the efficacy and gentleness of this sorting technology we use the MEG01 cell line as a model line. We demonstrate viability and function across a range of variables. Comparative sorts on a droplet sorter show deficits in viability and function. In this work we have characterized the MEG01 cells line as a model cell line for evaluating large cell sorting technologies. The novel microfluidic chip we have designed is capable of sorting large fragile cells with minimal negative effects, at speeds greater than established technologies.

# CYTO 2022 ABSTRACTS

**894183 P38**

## **Linking Blood Analyzer and Flow Cytometry Capabilities Creates a Powerful Method for Monitoring Tumor Cell Engraftment and Aiding Drug Development Decisions in Mouse Models**

Antony Chadderton<sup>1</sup>, Melody Diamond<sup>1</sup>, Matthew Stubbs<sup>1</sup>

<sup>1</sup>Incyte Research Institute, Wilmington, DE

Flow cytometry analyses are commonly used for assessing hematologic tumor cell engraftment in mouse blood, but unfortunately require large volumes of blood. Processing blood can result in inaccuracy, ultimately forcing a larger cohort in numbers of mice used in a given study. Standard hematology analyzers utilize whole blood without processing, and advanced analyzers, such as the Sysmex XN-V, can create flow cytometry standard (FCS) files, which are then compatible for advanced data analysis of each blood sample with any stand-alone flow cytometry software. Our objective was to assess whether the exportable FCS files from the Sysmex XN-V hematology analyzer contain sufficient information to detect the malignant cells in unprocessed mouse blood directly by using basic flow cytometry software (e.g. FlowJo™). With this data, a more precise study design, including dosing initiation and cohort size, can be determined. Preliminary ex vivo experiments involved spiking a range of tumor cells into normal mouse blood. A correlation between number of spiked-in cells and detection rate was found down to 10 tumor cells, indicating that identifying injected malignant cells from mouse blood was possible. Studies monitoring injected malignant cells in mice via serial bleeds were then performed. NSG mice were injected with 10,000 tumor cells intravenously (IV) and regularly monitored by retro-orbital blood collection (around 100 µl twice a week) which became terminal at day 9. Cohorts were also dosed with targeted therapeutics known to inhibit growth of the injected malignant cells and similarly analyzed. We found that the FCS files allowed a more sensitive way of tracking engraftment than any other specific complete blood count (CBC) parameter. Comparisons were performed of the direct flow cytometry of recipient tumor cells by surface antigen with the tumor cell counts from the hematology analyzer FCS files. Although there was limited correlation between each detection method, the number of tumor cells derived from the FCS files more accurately predicted mouse survival. In summary, we have developed a simple method that is accurate, sensitive and, based on hematology analysis linked to flow cytometry gating, for monitoring tumor cell engraftment in mouse whole blood that will be informative for future in vivo study design.

**898201 P40**

## **CellMek SPS Instrument Performance: Repeatability and reproducibility of a wash/stain/lyse & fix/wash workflow with a 10-color antibody panel in DURACartridge custom dry reagent format,**

Kelly Andrews<sup>1</sup>, Gang Xu<sup>1</sup>, Xizi Dai<sup>1</sup>, Ernesto Staroswiecki<sup>1</sup>

<sup>1</sup>Beckman Coulter

Introduction: The CellMek SPS Sample Preparation System is an automated system intended for in vitro diagnostic use that can be programmed by the user to perform a variety of operations for sample preparation, including those for flow cytometry. It is designed to automate staining, lysing, incubating, and washing of different biological specimen types, which enhances productivity by minimizing resource allocation for repetitive work in the clinical laboratory. The purpose of this study is to examine the repeatability and reproducibility performance of CellMek SPS instrument using a Wash/Stain/Lyse & Fix/Wash sample preparation workflow that is representative of common lab-developed tests, which also utilizes the Cell Wash Module (CWM) and the Dry Reagent Module that supports the DURACartridge format for custom dry reagents. Methods: The test cases in this study utilized a Wash/Stain/Lyse & Fix/Wash workflow with a custom 10-Color (10C) cocktail in DURACartridge dry format and the IOTest 3 +0.25% fixative lysing solution. The 10C cocktail included Kappa-FITC, Lambda-PE, CD10-ECD, CD5-PC5.5, CD200-PC7, CD34-APC, CD38-AA700, CD20-AA750, CD19-PB, and CD45-KrO. Data from samples prepared by the CellMek SPS were acquired on a Navios flow cytometer and analyzed using Kaluza C software. Standard Deviation (SD) and Coefficient of Variation (%CV) were calculated for each marker by each instrument and across all instruments. For repeatability testing, peripheral blood specimens obtained from normal donors were spiked with CD34+ KG1a Cells and processed by three CellMek SPS instruments (1 donor/instrument, 10 replicates/donor) utilizing the custom 10C DURACartridge and Wash/Stain/Lyse & Fix/Wash workflow. A single-output-tube panel was defined to process 100 µL of specimen at a time, which was then run-in replicate, thus eliminating any system variability due to multi-dispense of specimen. For reproducibility testing, one lot of ClearLLab Control Cells, Abnormal was processed on three CellMek SPS instruments utilizing the custom 10C DURACartridge and Wash/Stain/Lyse & Fix/Wash workflow. To ensure even use of both assemblies within the CWM and capture of maximum module variability, a two-output-tube panel

# CYTO 2022 ABSTRACTS

was defined to process 100  $\mu$ L of specimen in duplicate per specimen tube run, which was then assigned to two identical specimen tubes run in parallel (4 output tubes total). Specimen pairs were run in duplicate (8 output tubes) AM and/or PM for at least five days for a total of 80 replicates per instrument. Conclusion: Data of the repeatability and reproducibility samples were analyzed for each marker by each instrument and across all instruments. For each immune subset, the SD was less than 2 when the population was  $\leq$  20%, and the %CV was less than 10 when the population was  $>$  20%.

**898436 P42**

## **Multiphysics innovation for high speed, high recovery, and high viability automated cell separation,**

Liping Yu<sup>1</sup>, Michael Kempnich<sup>1</sup>, Candice (Zixuan) Liu<sup>1</sup>, Silin Sa<sup>1</sup>

<sup>1</sup>Applied Cells, Inc

Tumor biology, immunology, and immune-oncology from multi-omics at single cell level has witnessed unprecedented acceleration in recent years, with a major contribution of such speedup from new technologies and products bursting into market. New technological solutions also contributed deterministically to the promise of cell-based therapy. However, conventional cell separation tools, such as density-gradient based centrifugation, column-based magnetic cell separation and even FACS (fluorescent activated cell sorting) have become limiting factor to broaden the applications of single cell analysis from simple cell suspension to complex tissues samples and large-scale process. In development of cell therapy drugs, robust cell manufacturing platforms that are flexible, adaptable to various processes, and involving minimal human factor, are also widely sought after. MARS<sup>®</sup> Cell Separation Platforms incorporate innovations in multiple cell separation technologies. The active acoustic cell separation does label-free separation at unprecedented flow rate for any microfluidic device. Cell are moved in or out of clean buffers based on their physical parameters and the selection threshold is tunable. MARS<sup>®</sup> platform also offers a column-free in-flow magnetic cell separation technology, which allows specific selection of cells based on their surface markers. The separation process is done in a closed fluidic path in a fully automated version and has no capacity limit. MARS are constructed as modular platforms to support wide range of applications in life science arena, including single cell analysis, precision medicine, as well as cell therapy. In this talk,

we will present to you - 1) Case studies of using MARS<sup>®</sup> high speed tunable acoustic chip technologies to purify single cells and sing cell nuclei from various organ tissue dissociation and demonstrate  $>$ 99% debris removal to achieve cell purity range from 79.8% to 96.9% in an automated workflow. 2) Label-free isolation of neutrophil from whole blood with average 87.7% purity achieved without activating neutrophils 3) Rare Cells Isolation examples using MARS “add-add-run” magnetic cell separation reagents and programs to obtain high purity and high recovery of HSCs (hematopoietic stem cells) and plasma cells from whole blood and bone marrows. 4) large scale T cell separation, with both magnetic cell separation and acoustic cells separation process done in a closed fluidic tubing set, to demonstrate MARS<sup>®</sup> application in cell therapy development. We will show you how automated MARS cell separation platforms married the benefits of acoustic and magnetic cells separations in realizing first-of-its-kind cell separation results, and offering a robust effective, and revolutionary solution to cell separation for downstream applications.

**898545 P44**

## **Utilization of Distinct Autofluorescent Spectra From Different Subsets Provides Best Fluorescent Signal Resolution in High Parameter Spectral Flow Cytometry,**

Kewal Asosingh<sup>1</sup>, Nicholas Wanner<sup>1</sup>, Jerry Barnhart<sup>2</sup>, Violetta Zlojutro<sup>1</sup>

<sup>1</sup>Cleveland Clinic, <sup>2</sup>SONY

Innate to all cells, autofluorescence (AF) is the natural emission of light due to biomolecules present in the cell, such as flavins, porphyrin, NADH, collagen, and elastin. The amount of AF that each cell type emits varies in terms of its spectral pattern and intensity, depending on the type and number of fluorescent molecules that are present in the cell. AF in flow cytometry is useful for visualizing non-expressor cells. However, in some cell types, high AF spreads across several log decades and can mask dim signals from low expressors. Spectral flow cytometry offers unmixing of the AF spectra, allowing reduction of the fluorescence background originating from biomolecules in the cell. AF heterogeneity is common in cell suspensions obtained from complex tissues consisting of multiple cell types. Identification of the AF signals from these different cell types may be helpful to fine tune the spectral unmixing to bring the background signal down to its lowest level. However, screening

# CYTO 2022 ABSTRACTS

for the different AF subsets is a challenge. Here we report the utilization of an AF Finder tool with the Sony ID7000™ Spectral Cell Analyzer to identify subsets of AF cells in a single cell suspension obtained from a complex tissue. Murine lungs were digested into a single cell suspension and stained for markers to detect immune, epithelial, stromal, and endothelial cell subsets using a 20-color panel. The AF Finder Tool was used to screen and identify subsets with a unique spectral signature. Data was analyzed with and without AF unmixing. Without AF unmixing, background signals spread across several log decades masking subtypes of lung resident and immune cells. In total, six distinct subsets of AF cells with four unique spectra were identified in the unstained sample. Unmixing of the unique AF spectra resulted in increased signal resolution. All subsets in the lung were easily identified using this approach, in contrast to gating without AF subtraction. These findings highlight the significance of defining distinct cellular AF subgroups in order to reduce fluorescence noise and improve the signal resolution of markers of interest in a spectral flow cytometry panel.

**898448 P46**

## **Performance evaluation of the BD Leucocount™ Assay on the BD FACSLyric™ and BD FACSCalibur™ Flow Cytometers using UK NEQAS leukoreduced RBC and PLT samples,**

Yang Zeng, Farzad Oreizy<sup>1</sup>, Angela Chen<sup>1</sup>, Harshada Rohamare<sup>1</sup>

<sup>1</sup>BD Biosciences

The presence of white blood cells (WBCs) in transfusion blood products is associated with increased incidence of febrile transfusion reactions, cytomegalovirus transmission and HLA alloimmunization in transfusion recipients. Leukoreduction can minimize transfusion complications, and the determination of residual WBC levels in leukoreduced blood products is an important quality control procedure. Designed to stain nucleated WBCs with propidium iodide, the BD Leucocount™ Kit utilizes BD Trucount™ Tubes to enumerate absolute residual WBC counts in leukoreduced blood products by flow cytometry. The BD Leucocount™ Assay was evaluated on the BD FACSLyric™ and BD FACSCalibur™ Systems using samples provided by the UK NEQAS Low Level Leukocyte Enumeration Program. Each RBC or PLT sample was obtained by UK NEQAS using a sample of filtered blood or platelets, respectively, from an anonymous donor and then stabilized and spiked with stabilized buffy coat. In five UK NEQAS Low Level Leukocyte Enumeration Programs

we participated in, the absolute rWBC counts of fifteen samples (RBC and PLT) were determined. The BD results were compared to the mean absolute rWBC counts of more than 72 laboratories that participated in the UK NEQAS Low Level Leukocyte Enumeration Program. Absolute Z-scores of RBC samples ranged from 0.06 to 1.32 on the BD FACSLyric™ System and 0.01 to 1.53 on the BD FACSCalibur™ System, while absolute Z-scores of PLT samples ranged from 0.04 to 2.12 on the BD FACSLyric™ System and 0.03 to 2.46 on the BD FACSCalibur™ System. By meeting the acceptance criteria (absolute Z-score  $\leq 2.5$ ) in the UK NEQAS Low Level Leukocyte Enumeration Program, both the BD FACSLyric™ and BD FACSCalibur™ Systems demonstrated consistent results with peer laboratories using the BD Leucocount™ Assay. Direct comparisons of absolute rWBC counts of leukoreduced samples between the BD FACSLyric™ and BD FACSCalibur™ Systems were conducted. The absolute rWBC counts of RBCs as well as PLTs demonstrated agreement results between the BD FACSLyric™ and BD FACSCalibur™ Systems as supported by the respective correlation coefficient (0.9834 for RBCs and 0.9969 for PLTs), slope (1.0455 for RBCs and 1.0148 for PLTs), and intercept (0.2919 for RBCs and 0.2128 for PLTs). For Research Use Only. Not for use in diagnostic or therapeutic procedures. Class 1 Laser Product. BD, the BD Logo, BD FACSLyric, BD Leucocount, BD Trucount and FACSCalibur are trademarks of Becton, Dickinson and Company or its affiliates. © 2022 BD. All rights reserved. 0222

**898661 P48**

## **Multi-site evaluation of the BD® Stem Cell Enumeration Kit for CD34 cell enumeration on BD FACSLyric™ and BD FACSCanto™ II Flow Cytometers,**

Yang Zeng<sup>1</sup>, Maurice O’Gorman, Ruba Hsen, Rakesh Nayyar, Anubha Purang,<sup>2</sup> Angela Chen,<sup>3</sup> Denis-Claude Roy,<sup>4</sup> Martin Giroux,<sup>4</sup> Caren Mutschmann,<sup>5</sup> John S. Carabott,<sup>5</sup> Maryam Saleminik,<sup>6</sup> Anna Lin,<sup>6</sup> Yuanyuan Yang,<sup>3</sup> Imelda Omana-Zapata<sup>3</sup>

<sup>2</sup> Cytoquest Corporation, Toronto, Canada. <sup>3</sup> BD Biosciences, San Jose, California, USA. <sup>4</sup> Center of Excellence in Cellular Therapy, Hospital Maisonneuve Rosemont, Montreal, Canada. <sup>5</sup> SGS Analytics Germany GmbH, Berlin, Germany. <sup>6</sup> BD Corporate Clinical Affairs, Franklin Lakes, NJ, USA.

Hematopoietic stem cells are obtained from bone marrow, peripheral blood and cord blood. Flow cytometric enumeration of CD34+ cells plays a critical role in identifying the optimum

# CYTO 2022 ABSTRACTS

product for transplantation and continues to have a major role in evaluating the most suitable product(s) for stem cell transplantation therapies. In this study, the BD<sup>®</sup> Stem Cell Enumeration (SCE) Kit\* was evaluated on the BD FACSLyric<sup>™</sup> and the BD FACSCanto<sup>™</sup> II Flow Cytometry Systems using revised ISHAGE gating strategy for acquisition and analysis. A total of 501 specimens including fresh and freeze-thawed samples (from leukapheresis, bone marrow and cord blood), and fresh normal/mobilized peripheral blood, were analyzed on the two flow cytometry systems. Results from both systems were highly congruent, with an overall R<sup>2</sup>= 0.983 and 0.989 for viable CD34+ absolute count and viable CD45+ absolute counts, respectively; slope values for viable CD34+ of 1.06 (10.4, 1.08) and viable CD45+ of 1.00 (0.99, 1.01); and an almost ideal steepness of the trend line. The mean relative bias of percentages of viable CD34+ cells in viable CD45+ cells also showed high level of agreement between systems. The study results demonstrated agreement and equivalence for enumeration of viable CD34+ absolute count and percentage of viable CD34+ cells in viable CD45+ cells using the BD<sup>®</sup> SCE Kit on BD FACSLyric<sup>™</sup> and BD FACSCanto<sup>™</sup> II Flow Cytometer Systems. This study is sponsored by BD Biosciences. \*BD<sup>®</sup> SCE Kit on BD FACSLyric<sup>™</sup> Flow Cytometer with BD FACSuite<sup>™</sup> Clinical Application is not for sale in the United States.

---

## 901025 P50

### Development of a 10-color flow cytometric assay to assess binding of a monoclonal antibody (VB421) against IGF-1R in Peripheral Blood Mononuclear Cells (PBMCs) from patients with Thyroid Eye Disease.,

Michael Podolsky<sup>1</sup>, Amanda Hays<sup>1</sup>, Timothy Mack<sup>2</sup>, Stephen Thomas<sup>2</sup>, Thomas Schneider<sup>1</sup>, Michael Mullen<sup>1</sup>, Naveen Daryani<sup>2</sup>

<sup>1</sup>BioAgilytix, <sup>2</sup>ValenzaBio

Thyroid Eye Disease (TED), also known as Graves' ophthalmopathy, is a debilitating autoimmune disorder that occurs in patients with Graves' Disease in which inflammation in the muscle and fat tissue behind the eyes results in proptosis, diplopia, redness, pain, and swelling, leading to photosensitivity, blurred vision, and in serious cases, blindness. The mechanistic underpinnings of TED involve a complex interaction between autoantibody-mediated stimulation of Thyroid Stimulating Hormone Receptor (TSHR) and Insulin-like growth factor 1

receptor (IGF-1R) signaling in orbital fibroblasts that cause orbital tissue inflammation and expansion. Current therapies include corticosteroids and teprotumumab, as well as surgical intervention to prevent vision loss. VB421 (lonigutamab) is a high-affinity (K<sub>D</sub> <50 pM) monoclonal antibody directed against IGF-1R that induces rapid and efficient receptor internalization. VB421 is being developed as a potential treatment for TED. To support clinical development of VB421, a multi-color flow cytometric assay was developed to monitor the binding of VB421 to IGF-1R on the surface of human Peripheral Blood Mononuclear Cells (PBMCs). As VB421 induces rapid IGF-1R internalization upon binding, a traditional receptor occupancy assay format is less feasible. Therefore, this assay is designed to detect both total IGF-1R (free IGF-1R and IGF-1R/VB421 complex) as well as free IGF-1R. This assay utilizes two anti-IGF-1R antibodies that bind different IGF-1R epitopes and do not compete with each other. 1H7 competes with VB421 while 33255 does not; together these two antibodies allow the assay to distinguish between unbound and total IGF-1R. This format was qualified using a cell line that constitutively expresses IGF-1R at high levels (A549). This assay will be used to monitor total and free amounts of IGF-1R on live CD3+ Total T Cells, CD4+ T Cells, CD8+ T Cells, CD19+ B Cells, and Myeloid Cells expressing both CD11b and CD16 after administration of VB421. This assay format has the potential to be applied to other situations where target-receptor binding leads to rapid internalization and loss of receptor binding epitopes.

---

## 901545 P52

### Visualization of calcium flux in bone marrow using leukaemia initiating cells transduced with Salsa6f,

Pathik Sen<sup>1</sup>, Alexander Morris<sup>2</sup>, Shu-Chi Allison Yeh<sup>2</sup>, David Sykes<sup>2</sup>

<sup>1</sup>Massachusetts General Hospital, <sup>2</sup>Harvard University

In this study, we wished to develop and validate a novel leukemia model with the incorporation of a dynamic calcium indicator to visualize calcium flux within the bone marrow microenvironment niche. The Salsa6f calcium reporter was delivered into murine leukemia progenitor cell lines (FM1 and FM4) using retroviral transduction. We hoped that this would provide a fluorescent indicator of calcium response that could be used to track the cells in vivo. Using flow cytometry before and after the addition of calcium, we aimed to confirm that

# CYTO 2022 ABSTRACTS

these genetically modified cell lines were indeed responsive to changes in calcium concentration. The Salsa6f reporter was developed by Dong et al (eLife 2017;6:e32417) as a Ca<sup>2+</sup> indicator for cells allowing for real time cytosolic Ca<sup>2+</sup> tracking. Salsa 6f is a fusion of GCaMP6f (green fluorescence) to tdTomato (red fluorescence). The constitutive red signal is useful for tracking cells while the changes in the ratio of the green fluorescence to red allows us to observe changes in cytosolic Ca<sup>2+</sup> levels. Our initial tests found that compared to non-transfected cells, there is low baseline green fluorescence from GCaMP6f. However, the fluorescence intensity sharply rose when exposed to increasing Ca<sup>2+</sup> concentrations. This fluorescent signal could be enhanced by the addition of ionomycin, in concentrations ranging from 2-10 mM. We found that the higher ionomycin concentration resulted in a greater degree of flux. Using two different promoters to drive Salsa6f expression, we found that the RSV transduced cells had less Salsa6f reporter expression and did not exhibit any Ca<sup>2+</sup> sensitivity as compared with the MSCV-based retrovirus transduced cell lines. Furthermore, the FM1 cell line exhibited a higher degree of calcium responsiveness as compared to the FM4 cell line. Once these leukemia cell lines were introduced into mice by intravenous injection, it seems that many of the cells were lost rapidly after injection. We hypothesized that this may be due to immune clearance of cells, as immunocompetent mice were used in our experiments, and the Salsa6f does represent a foreign protein. This led to difficulties in resolving the transplanted cells from the background fluorescence inherent in live tissue. Despite these difficulties, calcium dynamics from the transplanted leukemia cells were still visible in vivo within the bone marrow. Here we have validated an important tool for tracking the calcium sensitivity of leukemia initiating cells in vivo. This tool may prove useful in identifying and ultimately targeting specific signaling relationships between these cells and their environment. The fluorescent signal of these cells may be improved by co-culturing the genetically modified leukemia cells with stromal cells, improving engraftment and resolution. There may be benefits in future studies to incorporating other cell types with this reporter to further improve the resolution within the bone marrow niche.

**901591**

**P54**

**Novel Whole Blood Depletion Assay to Assess Fc Effector Function of Therapeutic Antibodies,**  
Benjamin Ordonia<sup>1</sup>, Peter Tran<sup>1</sup>, Jesse Woodbury<sup>1</sup>, Kate Peng<sup>1</sup>

<sup>1</sup>Genentech, Inc.

It is the ultimate goal for in vitro biological characterization assays to assess the mechanism of action (MOA) of a drug in the setting that most closely mimics the disease state or physiological conditions. One primary MOA of antibody therapeutics is via target cell lysis, which is mediated by a variety of mechanisms, including Fc effector function, receptor-mediated apoptosis, or targeting of immune effector cells through directed bispecific molecules. While there are assays available to measure the target cell lysis of antibody therapeutics, a common strategy for these assays utilizes in vitro mixing of isolated effector and target cells. This approach maximizes the sensitivity of the assay but do not necessarily reflect the in vivo activities due to lack of presence of the relevant biomatrices for effector and target cells. However, for antibody therapeutics that target cells within the blood, it is feasible to develop in vitro assays that can measure target cell lysis mimicking the physiological setting because of the ready availability of blood. Multi-parameter flow cytometry allows for the specific gating of cellular subsets, making it an ideal technology to use for measuring target cell lysis in whole blood. We detail the development of a flow cytometer-based whole blood depletion assay using a panel of anti-CD20 therapeutic monoclonal antibodies to demonstrate B cell lysis measurement directly from blood. Our work demonstrated that B cell depletion is directly correlated with the testing antibody concentrations in a dose-dependent manner. We have observed different patterns of B cell depletion in the tested anti-CD20 antibodies, which could be due to variations in target binding and engagement of the Fc gamma receptors (FcγRs) to induce B cell depletion. Our data suggest that multiple mechanisms of effector function are involved in B cell depletion, as applying various FcγR blocking antibodies has only demonstrated partial responses. Additional work is pending to explore other potential mechanisms causing B cell depletion.

# CYTO 2022 ABSTRACTS

901809 P56

## Effects of fixation and photobleaching on fluorochrome stability revealed by full spectral flow cytometry analysis

Lyadh Douagi<sup>1</sup>, Larry Lantz<sup>1</sup>

<sup>1</sup>NIH

Several factors can severely affect integrity of samples and interfere with data quality during flow cytometry analysis. A common approach employed in flow cytometry is the fixation of samples prior to analysis. Fixation allows to preserve sample integrity and provide flexibility for later analysis, prepare for intracellular antigen staining, and in some cases to inactivate selected pathogens when handling infectious samples. Typical protocols for flow cytometry analysis often involve fixing with buffers containing 0.5-4% formaldehyde after staining, followed by storage of samples for various periods of time prior to analysis on the cytometer. Certain dyes are known to be sensitive to degradation due to fixation, often leading to a weaker signal. Similarly, photochemical alteration of a fluorophore may arise due to prolonged exposure to light. In practice, common causes of photobleaching are excessive exposures of the fluorophore to light during storage, sample manipulation, or incubation. Although there has been limited reports on fluorochrome stability there is a paucity of precise information on the alterations in emission properties of the dyes. In this study we evaluate the effects of formaldehyde fixation and photobleaching on the spectral properties of selected fluorochromes as well as on cell autofluorescence. Commonly used fluorochromes were evaluated for their stability to fixation and photobleaching. Fluorochromes with previously reported levels of sensitivity to fixation and photobleaching were also included. Ultracomp plus beads were stained with the fluorochromes using standard techniques. These samples were treated with varying concentrations of formaldehyde or exposed to bright full spectrum light for 1 hour or ON incubations. To investigate whether fixation contributes to changes in cellular autofluorescence, PBMCs were treated for varying concentrations (0, 0.5, 1, 2, 4 and 8%) of formaldehyde for 30min, 1 hour or ON incubations. Samples were washed and analyzed using the Sony ID7000 spectral analyzer. Formaldehyde fixation and light exposure caused varying degree of alterations in spectral signature and staining index depending on the fluorochrome tested. Interestingly, alterations in cell autofluorescence were also observed at the lowest concentration of formaldehyde tested (0.5%.) These

effects were amplified as the formaldehyde concentration and incubation time increased. The change in fluorescence intensity following staining and fixation varies with the fluorophore being examined. Additionally, fixation produces qualitative alterations in cell autofluorescence. Care must be exercised to consider the effects of fixation and photobleaching on fluorescence as revealed by full spectral cytometry analysis. Acknowledgement: This research was supported by the Intramural Research Program of the NIH, National Institute of Allergy and Infectious Diseases.

901853 P58

## Cryopreservation of Live-Cell Barcodes: a time-course study examining the stability of CD45 cadmium barcodes after freezing at -80°C for 1 week to 3 months,

Martha Brainard<sup>1</sup>, Taylor Witte<sup>1</sup>, Noura Srour<sup>1</sup>, Greg Hopkins<sup>1</sup>

<sup>1</sup>2seventybio

Sample multiplexing is a popular approach to increase experimental throughput and efficiency in the mass cytometry field. Traditional multiplexing methods involve the use of palladium barcodes. Although palladium barcodes are commercially available in kit form, they cannot be used prior to cell fixation, and thus, may be incompatible with markers that do not stain well on fixed cells. Live-cell barcoding with CD45 platinum and cadmium conjugates allows users to include these markers and is more conducive to multiplexing at experiment start. This multiplexing reduces staining variability, decreases the necessary volume of reagents and antibodies, and increases overall time and cost efficiency. Given the plethora of benefits, it is advantageous for labs to implement a live-cell barcoding strategy; however, because no live-cell barcoding kits are sold commercially, individual users are left to make their own barcodes. While this option provides flexibility in barcoding strategy, the process is time-consuming and potentially error prone. For this reason, bulk preparation of barcodes for long-term cryopreservation is preferential. Although many users follow this practice, few publications delve into the stability of antibodies upon long-term cryopreservation. Here, we examine the barcoding efficiency when healthy donor peripheral blood mononuclear cells (PBMCs) (N=4) are multiplexed together with freshly prepared barcodes and barcodes that have been cryopreserved at -80°C for 1 week, 1 month, and 3 months. We show the mean intensity of the respective barcode channels on concatenated files at all timepoints. A Mahalanobis Distance (MD) of 10 and a minimum separation



# CYTO 2022 ABSTRACTS

(MS) of 0.2 were used to debarcode all files. These parameters were chosen after an optimization analysis. This analysis focused on three outcomes: minimal inter-barcode contamination in debarcoded FCS files, low percentage of false negative events in the unassigned event files, and maximum yield. After 3 months of cryopreservation, we see a drop in CD45 cadmium intensity; however, this drop does not compromise the ability to distinguish barcodes. The yield, and the percentage each sample contributes to the yield, remain relatively constant. Samples multiplexed with freshly prepared barcodes have a barcoding yield of 73.1% and the samples multiplexed with barcodes that had been cryopreserved for 3 months have a barcoding yield of 75.4%.

---

## 901911 P60

### **A quantitative, lyse no-wash blood flow cytometric assay to monitor immune subpopulation changes in inflammatory disease mouse models.,**

Alexander Fleming<sup>1</sup>, Sofia Grammenoudi<sup>1</sup>, Aikaterini Nanou<sup>1</sup>, Kleopatra Dagla<sup>1</sup>, George Kollias<sup>1</sup>

<sup>1</sup>Bsrc

A multi-color assay of two panels was designed and optimized to identify mouse blood myeloid and lymphoid leukocyte subpopulations. The assay was designed for use in a two-laser (488nm, 633nm) flow cytometry analyzer, with each panel utilizing 7 markers to detect natural killer cells (CD45+ NK1.1+), neutrophils (CD45+ Ly6G+), dendritic cells (CD45+ CD11c+ MHCII+), eosinophils (CD45+ NK1.1- Ly6G- MHCII- CD11b+ SSC<sub>high</sub>), monocytes (CD45+ NK1.1- Ly6G- MHCII- CD11b+ SSC<sub>low</sub>), B cells (CD45+ CD19+), T helper cells (CD45+ CD8- CD4+) and cytotoxic T cells (CD45+ CD4- CD8+). Monocytes are further subdivided to inflammatory (Ly6C<sub>high</sub>) and resident (Ly6C<sub>low</sub>), whereas T cell activation and memory/effector status is also determined using CD25 (activation) and CD62L and CD44 to distinguish between naïve (CD62L+ CD44-), memory (CD62L+ CD44+) and effector (CD62L- CD44+) T cells. The assay was established to meet the challenges of quantitative and qualitative monitoring of immune subpopulation changes in inflammatory disease mouse models. By following an optimized lyse no-wash protocol, with the use of only 40µl of heparinized whole blood for both panels, the assay allows for multiple, in-life, facial vein-derived blood withdrawals to detect and monitor inflammation during disease progression. Additionally, the incorporation of counting beads allows quantitation of the identified populations

which was validated with parallel complete blood count analysis. The assay was applied to blood derived from mice after induction of Experimental Autoimmune Encephalomyelitis (EAE), a model of neuroinflammation where in-life monitoring of inflammation is not feasible through conventional methods. The assay presented here allows the quantification and monitoring of the changes in the peripheral blood myeloid and lymphoid compartments prior to EAE induction and during the pre-symptomatic, peak and remission disease phases.

---

## 901958 P62

### **Flow Cytometric Analysis of mTORC1 and mTORC2 Signaling Pathway Markers in Human Smart Tube Samples,**

Heather Evans-Marin<sup>1</sup>, Stefan Hailey<sup>1</sup>, Julie Bick<sup>1</sup>, Arumugam Palanichamy<sup>2</sup>

<sup>1</sup>FlowMetric, <sup>2</sup>Avalo Therapeutics, Inc.

The Mammalian target of Rapamycin (mTOR) pathway plays a key role in metabolism and physiology by regulating gene transcription and protein synthesis involved in immune cell proliferation and tumor metabolism. A novel, four-tube flow cytometry assay was developed to detect surface and intracellular phosphoprotein markers in the mTORC1 and mTORC2 pathway in human total CD45+, B cell, and T cell populations. One of the major challenges in performing Phosflow™ assays is the transient nature of signaling protein modifications. Therefore, Smart Tubes were selected as the assay matrix to preserve protein phosphorylation states during the time between sample collection and flow cytometry analysis. Upon thaw, samples were stained with antibodies to the surface markers CD45, CD3, and CD19. They were subsequently permeabilized with a methanol-based buffer, followed by intracellular staining. The mTORC2 full panel was stained with fluorescently conjugated anti-pAKT, with the appropriate control antibody used for the isotype well. The mTORC1 full panel was stained with unconjugated anti-pPRAS40 and fluorescently conjugated anti-Caspase 3, anti-Ki67, anti-p4EBP1, and anti-pS6. The mTORC1 isotype control tube was stained with appropriate isotypes for all markers except anti-Caspase 3, which used an FMO control. Both mTORC1 tubes were then stained with a secondary antibody to detect pPRAS40. After staining, cells were fixed and acquired on an LSRII Fortessa. Quantum Simply Cellular beads were used to quantify the number of antibodies bound per cell for all intracellular markers

# CYTO 2022 ABSTRACTS

except pPRAS40. This assay supports monitoring abnormalities in human mTOR signaling and evaluating mechanistic changes during therapeutic intervention of the pathway.

**901974 P64**

## **Detecting Human Eosinophils in Peripheral Blood by Adding a Heterogeneous Auto-Fluorescent Parameter as a Fluorescent Tag in Cytek Aurora,**

Yi-Dong Lin<sup>1</sup>, Esther Perez Garcia<sup>1</sup>, Ruth Barnard<sup>1</sup>, Jiangfang Wang<sup>1</sup>,

<sup>1</sup>GlaxoSmithKline

Eosinophils make-up about 1-3% of leukocytes in normal individuals. They are known to provide host protection against parasitic infection; however, aberrant activation of eosinophils can also cause inflammation leading to the tissue damage observed in some diseases such as asthma. Here, we describe the development of a simple 7-color flow cytometry panel to phenotype eosinophils in the peripheral blood of patients with hypereosinophilic syndromes. The Cytek Aurora is a spectral flow cytometer that has the capacity to detect more than 40 markers simultaneously, but more importantly for this panel can also generate better resolution data due to its auto-fluorescent extraction feature. It is well known that eosinophils are highly auto-fluorescent and this heterogeneous auto-fluorescence was observed in most of the detection channels. This usually causes difficulties to do unmixing, however, the problems were solved in this report after the eosinophils were gated and used as a fluorescent tag which we defined as AF-Eos (Auto-Fluorescent Eosinophils). The addition of this AF parameter as a fluorescent tag improved unmixing results for eosinophils. In addition, we showed that FITC (fluorescein isothiocyanate) non-specifically binds to eosinophils, and this is not related to any unmixing error. FC block treatment did not reverse this non-specific binding. Thus, we suggest not to use FITC dye for eosinophils panel design to avoid false positive results. We believe that this work will help improve design of panels that include eosinophil markers and highlights the usefulness of the AF extraction ability of the Cytek Aurora. This panel will be used in an upcoming clinical trial to develop a better understanding of eosinophil-related diseases such as hypereosinophilic syndromes. Acknowledgements: we thank Irene del Molino del Barrio<sup>2</sup> for helpful discussions and Danielle Stewart<sup>1</sup> for helping to stain samples in some experiments. The human biological

samples were sourced ethically and their research use was in accord with the terms of the informed consents under an IRB/EC approved protocol.

**901997 P66**

## **Fast and simple assay of cell cycle analysis via direct labeling of newly synthesized DNA.,**

Erika Kuzmova<sup>1</sup>, Zbigniew Zawada<sup>1</sup>, Jana Gunterova<sup>1</sup>, Tomas Kraus<sup>1</sup>

<sup>1</sup>Institute of Organic Chemistry and Biochemistry of the Czech Academy of Sciences

The cell cycle is one of the most important processes in the growth, maintenance, and repair of an organism and its tissues. It is a fundamental process by which the cell increases its size (G1 phase), replicates its DNA (S phase), prepares to divide (G2 phase), and divides (M phase). Most cancers are a result of aberrations in normal cell cycle regulation. Analysis of cell cycle is an essential tool employed in many scientific fields from cell and stem cell biology, cancer research to clinical medicine and drug development. Labeling of newly replicated DNA is one of the most powerful and robust approaches used for monitoring of the cell cycle progression in eukaryotic cells. Traditionally BrdU and EdU methods are used which are quite laborious. We decided to work up a faster and easier method by exploiting the synthetic nucleoside triphosphate transporter SNTT1 we developed recently. This transporter allows for direct transport of any nucleoside triphosphates (NTPs) into live cells. Practically it means, that fluorescently labeled nucleotides, deoxyuridine triphosphate derivative bearing Cy3 fluorophore (Cy3-dUTP) in our case, can be directly transported into the cell and immediately incorporated into DNA. We significantly improved the cell cycle protocol by removing all washing and centrifugation steps. All steps consist only of additions of treating solutions and incubations but not removing of any material from the sample. This was allowed by our new fixation technique with a solution of a cyclodextrin derivative in DMF as a fixative, and replacement of trypsin by TrypLE. These lead to significant reduction of cell loss, time and labor. Such a protocol could be completed within 1 h with an excellent reproducibility. We demonstrated the robustness of our method on several adherent (U-2 OS, HeLa S3, RAW 264.7, J774 A.1, Chem-1, U-87 MG) and suspension (CCRF-CEM, MOLT-4, THP-1, HL-60, JURKAT) cell lines, including those affected by a DNA polymerase inhibitor (aphidicolin). The results were compared to standard

# CYTO 2022 ABSTRACTS

EdU method. We anticipate that the method can be used for a multiple DNA labeling using dNTPs with different fluorophores at various time points under the same downstream procedure. We show that the reduced number of procedural steps and mild conditions of the assay for adherent cells allow that the assay can be down-scaled and performed with approximately 10,000–20,000 cells available from a single well of a 96-well plate. Thus, we suggest that this protocol could be adapted to high-throughput automated assays. Recently we performed a structure activity relationship (SAR) study and prepared a series of diverse SNTTs with broad scope of chemical modification. Some of the transporters (SNTTs) showed better performance in transporting NTPs in full media or improved signal and slightly outperformed SNTT1, however unlike SNTT1, they were more toxic for the cells.

---

**902015 P68**

## **Steric Hindrance of HIV Envelope for Binding to Streptavidin Results in Reduced Valency of B Cell Tetramers,**

Evan Trudeau<sup>1</sup>, Robert J. Edwards<sup>1</sup>, Aria Arus-Altuz<sup>1</sup>, Derek W. Cain<sup>1</sup>

<sup>1</sup>Duke Human Vaccine Institute

T cell and B cell tetramers are mainstays for the flow cytometric identification and antigen-specific sorting of T and B cell subsets. The basis for this technology is that streptavidin contains four biotin-binding sites that facilitate the generation of tetrameric multimers when biotinylated proteins and streptavidin are mixed at a 4:1 molar ratio. A T cell tetramer typically comprises biotinylated complexes of a conserved MHC I or II protein displaying a short peptide, that are bound to a fluorochrome-conjugated streptavidin molecule. B cell tetramers, however, display B cell epitopes that often require proper tertiary and quaternary structure of an antigenic protein, and therefore, may reflect a much wider range of protein sizes and structures. In our HIV vaccine studies, we noted variability in the capacity of different envelope (Env)-based B cell tetramers to label Ramos B cells expressing defined Env-specific B cell receptors (BCRs). These differences were not easily explained by affinity of the BCR-Env interaction, so we sought to understand the basis for this variability in staining intensity. Using negative stain electron microscopy (NSEM), we analyzed a variety of biotinylated HIV-1 Env proteins for their ability to form streptavidin multimers. We observed that smaller Env-based proteins, such as eODGT8

(~22.5kD), primarily formed tetramers when conjugated to streptavidin. However, when we prepared biotin/streptavidin multimers using larger, well-folded, stabilized Envs (~215kD “SOSIP” trimers), the dominant multimer species was a dimer, even in the presence of excess biotinylated SOSIP protein (i.e., 8:1 SOSIP:streptavidin). Structural modeling suggested that steric hindrance between SOSIP trimers prevents full occupation of the four biotin binding sites on streptavidin. Notably, when SOSIP multimers were prepared at a 4:1 molar ratio of SOSIP:streptavidin, there was a considerable amount of unbound SOSIP in addition to SOSIP-streptavidin dimers. We found that fluorochrome-containing multimers prepared at a 2:1 molar ratio of SOSIP:streptavidin exhibited enhanced labeling of Ramos B cells compared to multimers prepared at a 4:1 molar ratio of SOSIP:streptavidin. We hypothesize that the presence of free SOSIP protein in the 4:1 multimer competed with fluorochrome-containing SOSIP dimers for binding to BCRs. These studies provided important insights into B cell “tetramer” technology which led to modifications in our protocol for their preparation. By changing the molar ratio of SOSIP to streptavidin during multimer preparation from 4:1 to 2:1, we enhance labeling of antigen-specific B cells and reduce consumption of SOSIP protein during preparation. Our finding that some biotinylated proteins fail to form tetramers on streptavidin also has implications for functional studies of B cell receptor signaling that rely on multimers to increase antigen valency for ex vivo stimulation of B cells.

---

**902026 P70**

## **Cell Sorting, FLIM and Imaging Analysis of Plasmodium falciparum Exposed to Artemisinin,**

Ludmila Krymskaya<sup>1</sup>, Sean V. Connelly<sup>2</sup>, Javier Manzella-Lapeira<sup>1</sup>, Joe Brzostowski, Juliana M. Sá<sup>2</sup>, Thomas E. Wellems<sup>2</sup>

<sup>1</sup> Laboratory of Immunogenetics (LIG), National Institute of Allergy and Infectious Diseases (NIAID), National Institutes of Health (NIH), Bethesda, MD, <sup>2</sup> Laboratory of Malaria and Vector Research (LMVR), National Institute of Allergy and Infectious Diseases (NIAID), National Institutes of Health (NIH), Bethesda, MD

Malaria remains a major cause of morbidity and mortality worldwide. Emerging mechanisms of resistance against antimalarial drugs require improved knowledge about Plasmodium's blood stage. Plasmodium falciparum

# CYTO 2022 ABSTRACTS

recrudescence after 3-7 days artemisinin monotherapy is well known. Recrudescence is also observed in vitro when early ring stage parasites are exposed to the drug. Parasites after recrudescence are just as sensitive to artemisinin as before the initial drug treatment, indicating no change of drug response phenotype. Microscopic observation of a delay in the intraerythrocytic cycle with arrested development of the ring-stage parasites suggested cell dormancy may provide a means to escape artemisinin toxicity. For the analysis of blood stages of Plasmodium, the isolation of ring stages is essential. Here, we apply cell sorting, Fluorescence Lifetime Imaging (FLIM), and super-resolution AiryScan microscopy to compare ring-stage parasites exposed to dihydroartemisinin (DHA) or to control medium with dimethylsulfoxide (DMSO, DHA vehicle). Cell populations were isolated by FACS in each sample through staining with a DNA dye, SYBR Green, and a mitochondrial potential marker, MitoTracker Deep Red FM. The putative dormant parasite fraction was verified by re-culturing experiments. FLIM of intrinsic reduced nicotinamide adenine dinucleotide (NADH) was used to quantify the metabolic state and AiryScan microscopy was used to visualize parasite structure. DHA-treated parasites showed a collapse of the nucleus and mitochondria as well as a lower mean lifetime, whereas parasites in control medium showed these two organelles apart from one other. After standardizing this method, other antimalarials will be tested to see if these changes are uniquely associated with DHA exposure. Further characterization of this phenomenon may provide insights on prevention of clinical recrudescence.

**902032 P72**

## **New fixable viability dyes and applications for flow cytometry,**

Chris Langsdorf,<sup>1</sup> Brandon Trent<sup>1</sup>

<sup>1</sup>ThermoFisher Scientific

Flow cytometry provides many advantages including single-cell quantitative analysis, high sample throughput, and multiplex cell characterization. Accurate discrimination of live and dead cells is a fundamental component of most flow cytometry experiments, but many viability dyes were optimized using legacy instruments and outdated model systems. Here we provide an updated overview of methods and reagents to assess cell viability with flow cytometry. Results and discussion are based on our recent efforts to expand the color palette of fixable viability dyes. We

introduce six new dyes, each with narrow and unique emission spectra ideal for expanding high-parameter conventional and spectral cytometry experiments. Additionally, we will present new data to demonstrate updated workflow recommendations for modern cytometers, improving stability, efficiency, and sample throughput. Novel insights and methods presented here will streamline complex experiments and provide deeper insight into cell behavior.

**904062 P74**

## **Identifying Unconventional T Cell Populations in Non-Human Primates in Mycobacterium tuberculosis Vaccines Studies using Flow Cytometry,**

Samantha Provost

Tuberculosis (TB) is a debilitating disease with a global impact. There is not yet a highly effective vaccine to protect against primary or latent infection from the Mycobacterium tuberculosis bacteria in adults. Therefore, the development of superior TB vaccine continues to be a priority in vaccine research. While memory T cells are typically correlated with protection after vaccination, populations of unconventional T cells and innate cells are also associated with control of TB due to their pattern recognition abilities and rapid responses. The use of flow cytometry to identify, quantify, and characterize these T cell and innate populations in unvaccinated nonhuman primates prior to challenge with M. tuberculosis allows for the delineation of the role of these populations in control of TB infection.

This is a multi-center study utilizing PBMCs of rhesus and cynomolgus macaques from control groups in TB vaccination studies that were later challenged with M. tuberculosis. A 21-color flow cytometry surface panel was developed to identify key unconventional T cell populations of interest. These populations include mucosal associated invariant T (MAIT) cells identified with an MR1 tetramer, invariant natural killer T (iNKT) cells using a CD1d tetramer, and V $\gamma$ 9 T cells using  $\gamma\delta$ -T cell receptor and V $\gamma$ 9 antibodies. Innate populations of interest include monocyte populations defined by CD14 and CD16 and natural killer (NK) cells. Other markers include trafficking and activation markers associated with control of TB infection like CCR5, CCR7 and CXCR3, as well as HLA-DR.

Preliminary analysis of the flow cytometry data indicates differences in frequencies of populations of interest between samples. Of 10 animals studied so far, only 1 shows a CD1d+

# CYTO 2022 ABSTRACTS

population, 2 show distinct MR1+ populations, and 1 animal has a very low frequency of NK cells. Other differences of note include CD14+ monocyte populations varying from 5-55 percent of their parent populations and Vy9 frequencies ranging from 7-50 percent of all  $\gamma\delta$  T cells. Variance in these populations between animals will give us the ability to elucidate their role in protection.

In conclusion, the panel is successfully able to identify populations of interest and demonstrates substantial differences in population frequencies between animals. Once the data from all PBMC are collected, a correlates analysis will be performed between the frequencies of the immune populations of interest and protection results after Mtb challenge. This data set will also allow for the use of advanced analysis tools like clustering plots such as tSNE, to further characterize differences in cell populations between animals.

---

**898406 P76**

## **Quantitative Expression Profiling of Surface Antigens on Peripheral Blood Leukocyte subsets and Childhood T-cell Acute Lymphoblastic Leukemia (T-ALL) [MvZ1] Cells using a Standardized Flow Cytometry Workflow: A HCDM CDMaps Initiative,**

Tomáš Kalina<sup>1</sup>, Daniela Kuzilkova<sup>1</sup>, Pablo Engel<sup>1</sup>, Menno van Zelm<sup>1</sup>, Joan Punet Ortiz<sup>1</sup>, Pei Mun<sup>1</sup>, Javier Fernández<sup>1</sup>, Karel Fiser

<sup>1</sup>Charles University, 2nd Faculty of Medicine

Background: Human Leukocyte Differentiation Antigen (HLDA) workshops are organized by the Human Cell Differentiation Molecules (HCDM) consortium to test and validate the reactivity of particular antibody clones to specific targets. We aimed to develop a flow cytometric procedure allowing CD marker expression profiling in a standardized way in time and place. The panels enable identification of 27 innate and adaptive leukocyte cell populations present in peripheral blood. The panels were custom dried in 96-well plates, and the Quantibrite™ PE Beads were used for quantification of the PE signal. Subsequently, we developed a high content framework to evaluate the titration of PE conjugated monoclonal antibodies using fluorescently barcoded cell lines and peripheral blood cells. The selected titer and critical antibody information (such as clone, catalogue number, vendor, gene and CDname etc.) were centrally stored

in an inventory table, which was expanded into an experiment master table (EMT) following inclusion of experimental details (e.g. the position of individual mAbs in 96-well plate, experiment name, operator etc.). Post acquisition, the fcs files were annotated using all relevant experimental information from the EMT table. To validate our approach, we quantified protein expression of four selected CD markers (CD11b, CD31, CD38 and CD40) with well-known expression pattern on peripheral blood leukocytes that showed high reproducibility across centers. We also performed benchmarking of four anti-CD3 clones, of which the titration curves revealed variable performance. Our pilot results on childhood T-ALL patient samples (n=7) revealed potential targets for minimal residual disease monitoring. In summary, we optimized a procedure for quantitative expression profiling of surface antigens on subsets of blood leukocyte and proved its feasibility with inter-laboratory comparison in three different laboratories. The presented workflow enables (i) to map the expression patterns of HLDA-approved antibody clones to CD markers, (ii) to benchmark new antibody clones to established CD markers, (iii) to define new clusters of differentiation in future HLDA workshops and (iv) mapping of childhood T-ALL cells. Acknowledgement: The reagents were kindly provided by Exbio and BioLegend. The work was financially supported by project NU20-05-00282 of the Czech Republic Ministry of Health

---

**902029 P78**

## **Expanding Practical Education in a Core Facility with the Attune CytPix Brightfield Imaging Capable Flow Cytometer,**

Cora Chadick<sup>1</sup>, Tanja Konijn<sup>1</sup>, Carolien Zeelan<sup>1</sup>, Priscilla Heijnen<sup>1</sup>

<sup>1</sup>Amsterdam UMC

One of the many roles core facilities and shared resource laboratories often inhabit is that of educator and trainer to assure that researchers of all levels can quickly comprehend basic principles of the flow cytometry method. Those who are new to the world of conventional flow cytometry (FC) often do not find the interpretation of FC data from a dot plot or histogram to be intuitive. It is simple enough to take cells in suspension and load them onto a hemacytometer or mount them on a microscope slide to assess viability, quality, and quantity of cells intended for FC analysis but coupling that information to morphological homogeneity and diversity based on light scatter properties at a flow cytometer

# CYTO 2022 ABSTRACTS

takes a lot of experience. Often, new users in FC will accidentally set their side scatter (SSC) and forward scatter (FSC) voltages or gains too high or, in the case of a FC analyzer, the threshold too low leading to events of interest that cannot be analyzed or .fcs files that are unnecessarily large. That addition of the Attune CytPix from Thermo Fisher to the Microscopy and Cytometry Core Facility (MCCF) at Amsterdam UMC has provided quick feedback for the assessment of sample quality and setting scatter parameter sensitivity. This is entirely because of the capability of the CytPix which couples brightfield images to fcs data which allows for the display of captured images corresponding to regions on dot plots and histograms. The reverse can also be done in that images can be selected and displayed on a dot plot to visualize their fluorescence and light scatter intensity. In addition to the possibilities of image analysis, this commercialized capability coupled to an acoustic focusing flow cytometer has proved to be a great educational tool in the core facility due to its ease of use for instantly and directly correlating images to .fcs data without the time-consuming process of cell sorting or not capturing the conventional FSC and SSC information as is the case in most imaging flow cytometers. We have designed an introductory practical workshop that allows users to quickly and intuitively set detector sensitivity and event thresholding and more easily assess variability in sample preparation. Overall, brightfield images couple with FC data is a perfect learning tool for any lab environment and particularly in a core facility with many students and trainees who need to quickly have a firm grasp of core FC concepts to make the most of their time in the lab. The Attune CytPix make this possible in a simple and user-friendly way.

**901495**      **P80**

## **Automated Analysis of 14-Color Immunophenotyping Data,**

Benjamin Hunsberger<sup>1</sup>, Maria Jaimes<sup>2</sup>, Mark Herberger<sup>2</sup>, Beth Hill<sup>1</sup>

<sup>1</sup>Verity Software House, <sup>2</sup>Cytek Bio

The cFluor 14-Color Immunoprofiling Kit (Cytek Biosciences) allows for the identification of helper T cells, cytotoxic T cells, B cells, NK cells and monocytes in human peripheral blood mononuclear cells and in whole blood. The reagents in this kit help to distinguish subsets of T, B, NK, and monocytic cells. We developed an automated analysis approach to fully characterize seven cell types and fifteen subsets using GemStone (Verity Software House), with no user intervention required. The

approach uses Probability State Models to track intensity shifts from sample to sample and automatically adjusts for changes in variability in the population distributions. A clean-up step removes debris, aggregates, and dead cells prior to the immunophenotyping analysis. A full report is generated for each sample, including a summary table, key plots and overlays for each cell type, a Cen-se' plot, and staining assessment for each measurement. In this study, we describe how the automated analysis is constructed, the training dataset used, and how the results compare with expert gating analysis.

**901823**      **P82**

## **Identification of immunologic similarities between autoimmune diseases using flow cytometry and disease sub-clustering,**

Pablo López-García, Thomas R. Pieber<sup>1</sup>, Barbara Prietl, Laurin Herbsthof<sup>1</sup>,

<sup>1</sup>CBmed GmbH

Autoimmune disease, including type 1 diabetes (T1D), rheumatoid arthritis (RA), and systemic lupus erythematosus (SLE), have been studied in great detail, but many research efforts focused only on comparison between one disease and healthy controls. Despite attempts to characterize disease differences, the immunological similarities between disease are not fully understood yet. However, a joint analysis of autoimmune disease could shed light on potential targets for drug repurposing, but the identification of meaningful similarities in a multi-parameter experiment can be difficult. To investigate similarities between T1D, RA, and SLE we used flow cytometry to characterize the immune system of 179 patients and established a data analysis methodology to assess cross-disease similarity. We therefore stained PBMC samples of patients with five marker panels targeting T and B cell subtypes and regulatory immune cells. We manually gated flow cytometry measurements for 61 cell populations and used phenotype abundances for downstream data analysis. We performed L1-regularized logistic regression to identify 26 relevant populations that were responsible for disease separation. We used these populations to cluster patients of each disease individually into three disease sub-clusters (DSC). For RA patients, we found that RA clusters 0 and 1 (characterized by high % CD279+CD45RA- Tregs) were associated with prior treatment of immune-suppressant Methotrexate, indicating that it leads to distinguishable immunological subtypes. DSC were then

# CYTO 2022 ABSTRACTS

again subjected to L1-regularized logistic regression showing that T1D, RA, and SLE had 9, 5, and 1 populations, respectively, that were responsible for sub-disease clustering. Only two populations (Tregs and CD147 positive effector T cells) appeared as relevant to both T1D and RA sub-clustering. Finally, we calculated inverse centroid distances between all nine DSC. For every disease pair, we found at least one above-average, cross-disease similarity. Notably, the highest similarity was found between a diabetes cluster (T1D cluster 0, high % effector Tregs) and the Methotrexate-associated RA cluster 1. We subsequently identified seven populations that are responsible for this similarity, including effector Tregs, proliferative effector Tregs, and CD307c positive Tregs. These findings suggest that subtypes of Tregs are one of the main drivers behind the T1D and RA sub-cluster similarity. These populations are active Tregs with highly suppressive potential and have been previously described to play a role in Methotrexate unresponsiveness in RA patients. Although preliminary, these insights into the similarity of the immunological states of some T1D and RA patients could hint at potential immunological targets that may enable repurposing immune modulating drugs in the future.

**901912 P84**

## **A Machine Learning Workflow for Automatic Immune Phenotyping of Type 1 Diabetes Samples,**

Barbara Prieti<sup>1</sup>, Thomas R. Pieber<sup>1,2</sup>, José Antonio Vera-Ramos<sup>1</sup>, Martin Helmut Stradner

<sup>1</sup>CBmed GmbH, <sup>2</sup>Med Uni Graz

Autoimmune diseases have a high occurrence in the population, causing great morbidity and mortality. Despite presenting considerable clinical heterogeneity, many autoimmune diseases exhibit common mechanisms leading to a self-tolerance breakdown, suggesting the possibility of finding similar patterns on autoimmune diseases that can be helpful to better understand their behavior, and the recovery of patients suffering from them. We, under this premise, aimed to find common patterns inspecting the cell population distributions of samples coming from patients of different autoimmune diseases. We used machine learning (ML) to perform deep immune phenotyping of type 1 diabetes (T1D) and healthy controls as a preliminary way of identifying common patterns and dissimilarities among different autoimmune diseases. PBMCs were isolated from patients with T1D (n=69) and healthy donors (n=50). A FACS

approach was applied, based on five different panels, each one focusing a different set of cell populations. Then, a traditional analysis was compared to a ML method implemented on R. Such pipeline includes unsupervised pre-gating of lymphocytes using the R package flowCore, a data normalization step to improve the performance of the model, and FlowSOM clustering to group cells based on similarities on their marker expression using Self Organizing Maps (SOM). We apply a Generalized Linear Mixed Models (GLMM) test as a final step to find significant differences of cell population abundance among groups. After applying our automated workflow on two of the panels focusing on T cells we could identify 14 cell clusters on the first panel, and 16 clusters on the second one. The GLMM test on panel 1 revealed a trending cluster ( $p=0.059$ ) on the abundance between T1D and controls. This cluster is defined by CD4pos T cells expressing high IL-7 receptor (CD127) levels and median amounts of CD15s but low CD25, CD161 and FoxP3, and its abundance is increased in T1D samples. In conclusion, our ML workflow is able to determine the cell population profile of many samples and identify differences on the cell population abundance of different groups. This unsupervised analysis approach enables the discovery of new biomarkers complementing traditional workflows and streamlines the profiling of large datasets, otherwise too substantial to be tackled in a conventional manner. We plan to apply this workflow on large clinical studies to automatically classify and compare cell populations of not only T1D patients but other autoimmune diseases such as rheumatoid arthritis and systemic lupus erythematosus.

**902022 P86**

## **MetaFlow: Innovative Cloud Based Topological Analysis Platform for High-Dimensional Flow Cytometry Data,**

Andy Filby<sup>1</sup>, Raif Yuceel<sup>2</sup>, Alan Saluk<sup>3</sup>, Attila Babes<sup>2</sup>

<sup>1</sup>Newcastle University, <sup>2</sup>University of Exeter, <sup>3</sup>Scripps Research

As the complexity of flow cytometry experimentation increases in terms of parameter space, advanced analytical tools such as dimensionality reduction and clustering have become essential to the exploration and interpretation of the data. While these approaches are powerful and designed to represent the original data structure, they rely on a number of subjective variables that will affect the results and thus the interpretation. It is therefore attractive to utilize approaches that maintain the original data structure as dictated by the values and signal

# CYTO 2022 ABSTRACTS

resolution generated at acquisition. The Metaflow platform was used to analyse four different flow cytometry data sets. 1) A “simple”, well-defined 8 marker fluorescent panel acquired on a conventional fluorescence flow cytometer. 2) A 27 marker fluorescent panel acquired on a conventional fluorescence flow cytometer. 3) A 40 marker mass cytometry panel acquired on a Helios CyTOF system. 4) A 15-colour panel acquired on spectral cell sorter. In all cases, data was also analysed via “ground truth” manual gating as well as FLOWSOM clustering with UMAP visualisation using FCS express software (De Novo) for comparison. Unlike the aforementioned approaches, one can go directly with the native data set after compensation. METAflow automatically performs scaling transformation as adapted to the method of data acquisition. This keeps the entire structure of the data and clusters by taking into account all available parameters, including morphology. Additionally, there are inbuilt modules for signal instability removal and identification of debris and doublets which were vetted against manual gating approaches to the same end. Metaflow based analysis was shown to provide high accuracy results and allows for preservation of the original data structure, independent of the raw data origin as well as increasing numbers of dimensions. Debris was readily clustered for majority of tested files and, automated labelling of debris and doublets was demonstrated to significantly shorten analysis time per sample. The seamless, integrated design of the solution made it insensitive to prior gating, increasing robustness and reproducibility of the end-point analyses. Metaflow provides a powerful platform for exploring, analysing and interpreting flow cytometry data sets. Unlike many cluster-based approaches that require significant hyper-parameter tuning, offers seamless workflow relying on density-based algorithm that maintains the original data structure akin to auto-gating. This can provide detailed insight into data granularity while operating in multiple dimensions. The clustering algorithm further optimizes achieving robust and rapid data presentation by the cleaning of both doublets and debris, expediting computational time to results. The software can be a gateway for valid and reproducible discovery in data sets to any user with no prior knowledge of current overly-complex automated strategies.

**902042 P88**

## **Automated Data Analysis of a 24-Color Nonhuman Primate Leukocyte Immunophenotyping Panel,**

James Thomas<sup>1</sup>, Cathi Pyle<sup>1</sup>, Charles Trubey<sup>1</sup>

<sup>1</sup>Leidos Biomedical Research, Inc.

Advanced, high-parameter (18+ color capable) flow cytometers are becoming commonplace in flow cytometry cores and research laboratories, allowing researchers to expand the size and complexity of their reagent panels and extract more detailed information from their finite samples. However, as reagent panel parameters increase, the dimensionality of the resulting data and time required to manually analyze corresponding datasets significantly increases. Though “expert” manual analysis remains the gold standard for flow cytometry data analysis, manually analyzing large datasets derived from 18+ color complex reagent panels is exceedingly laborious, time consuming, and user biased. Implementing automated data analysis tools to help mitigate these manual analysis issues has become a necessity. However, assessing and adapting automated data analysis programs can be challenging. In this poster we present a comparative study of our manual versus automated flow analysis methods and share our quantitative results and experiences. For this project, we used FCS Express 7 (De Novo Software), for manual, and Astrolabe (Astrolabe Diagnostics) for automated data analysis of a 24-color reagent panel that identifies most major nonhuman primate (NHP) leukocyte populations and subsets. FCS Express 7 is a highly intuitive and multifunctional flow cytometry data analysis program we routinely use for flow cytometry analysis. The Astrolabe Cytometry Platform is a relatively new, comprehensive data analysis software that incorporates data pre-processing, population identification and clustering algorithms (e.g., FlowSOM), as well as statistical and differential analyses, in one highly automated, cloud-based system. The results of this comparative analysis revealed several strengths and weaknesses of both approaches. One critical, rate-limiting step in the Astrolabe analysis involved developing an NHP-biology-specific, leukocyte phenotyping hierarchy, which the software requires to correctly categorize cell subsets. Though once established, it was just a matter of setting up the automated and differential expression analysis parameters, uploading the data files and waiting a couple of hours for the results. Astrolabe also annotates the uploaded FCS files, essentially embedding its algorithm-identified population gates, allowing end users to easily compare automated versus



# CYTO 2022 ABSTRACTS

manually identified cell populations by back gating. The ability to examine these automated-analysis-defined populations using FCS Express, allowed us to rapidly assess whether cell subsets were correctly identified, and when a cell subset was incorrectly identified, we were able to quickly determine its true identity. Overall, we found good correlations between all major leukocyte populations, especially lymphocyte subsets, when comparing automated analysis with manual. We are working with Astrolabe to refine our NHP hierarchy and analysis parameters, to further improve our automated analysis results.

**904674 P90**

## **Separating Flow Cytometry Populations Based on Probabilistic Analysis,**

Danielle Middlebrooks<sup>1</sup>

<sup>1</sup>NIST

Modern day flow cytometry experiments can measure on the order of one million events, each comprising scalar measurements that correspond to a particle's relative size, complexity and biomarker expression levels. These experiments also contain background populations including leftover particles from previous experiments and cells in the sample that have broken apart into smaller pieces. Data analysis (e.g. via gating) is critical for interpreting FC measurements, but traditional techniques are often time-consuming and subjective to the user. One method known as the Histogram Subtraction method can identify populations by detecting those regions where a test sample has statistically significantly more events than a control sample. While the simplicity of this method makes it practical, histograms suffer from subjectivity and difficult-to-quantify uncertainties. We developed a methodology that identifies a population by constructing probability density functions (PDFs) from the histograms of specific biomarker expression levels in a sample. To generate the PDFs, we use a Spectral Monte Carlo method which consist of constructing the PDFs using a set of smooth orthogonal basis functions. Our method combines prior knowledge about the support of the PDFs with constrained optimization to subtract off one population from another within a given experiment. Once we estimate the unknown distribution, we compute the relative fraction of the population in the mixture and estimates of the uncertainty. We apply our algorithm to testing data obtained from stained cells to differentiate populations. Our preliminary results suggest our method can efficiently separate populations comparable to that of traditional gating methods while removing initial subjectivity in the data analysis.

**898212 P92**

## **flowSim: improving the quality of training sets and machine learning models applied to FCM data analysis,**

Sebastiano Montante<sup>1</sup>, Yixuan Chen<sup>1</sup>, Ryan Brinkman<sup>1</sup>

<sup>1</sup>BC Cancer Research Center

The analysis of big flow cytometry (FCM) data is important for the development of machine learning (ML) models that aim to overcome the performance issues of automated data analysis approaches. flowSim is a tool designed to visualize, detect and remove highly redundant information in large FCM training sets, increasing the performance of ML algorithms by reducing overfitting while at the same time decreasing the computational time. The tool performs the near duplicate image detection (NDD) task by combining community detection algorithms with a density analysis of the marker expression values. In order to evaluate its efficiency, flowSim was tested on two datasets composed by 1,537,846 images selected from 20 studies, and 160 curated images of bivariate FCM data. It generated two final datasets composed respectively by 719,615 and 85 significant examples, identifying and removing 818,231 and 75 redundant examples as verified by manual inspection of the removed data. Finer detailed evaluation was conducted on a dataset constructed by co-mixing the curated dataset. To the best of our knowledge, flowSim is the first tool designed to perform the NDD task on FCM data.

**898475 P94**

## **Projection of high-dimensional cytometry data using regularised autoencoders,**

Sofie Van Gassen<sup>1</sup>, Yvan Saeys<sup>1</sup>, David Novak<sup>1</sup>,

<sup>1</sup>IRC-VIB UGent

Cytometry data can be projected to lower-dimensional (LD) space via dimension-reduction methods such as t-SNE or UMAP. Recently, variational autoencoders (VAEs), a type of neural nets, have been used for visualisation (ivis, scvis) and clustering (SAUCIE, MoE-Sim-VAE, VAE-SNE). Conveniently, VAEs can use combinations of objectives to preserve relationships between points at different scales, can be made robust to noise and are generative models, allowing for sampling new data from learned distributions. These properties make VAEs promising for generating latent representations of cytometry data. We present cyen, a parametric model for learning LD embeddings.

# CYTO 2022 ABSTRACTS

We combine features from published methods and a novel implementation of quartet loss [1], preserving global structures. Moreover, we use smoothing, an iterative algorithm based on nearest-neighbour relations, to reduce noise. This achieves clearer visualisation and better clustering. For benchmarking, we adapted the Area Under RNX Curve metric [2] to assess preservation of neighbourhood structures in LD, both on a local and global scale. With the 39-dimensional Samusik\_01 CyTOF dataset [3], a cyen VAE model with target dimensionality of 2 yields a local score of 0.236 and global score of 0.488 after 40 training epochs. During this training, global score generally decreases and local score increases. However, a VAE model with a quartet loss term (VAE-quad), scores 0.265 locally and 0.607 globally, with no local-global trade-off during training, and after smoothing we score 0.271 locally and 0.600 globally, showing a local-score boost due to less noise. In contrast, t-SNE gets a local score of 0.284 but a subpar global score of 0.411, while UMAP scores 0.267 locally and 0.497 globally. For the 32-dimensional Levine32 CyTOF dataset [3], the local score of cyen VAE-quad (versus VAE) is boosted from 0.206 to 0.232, and the global score increases from 0.404 to 0.558. A smoothed VAE-quad projection scores 0.271 locally and 0.546 globally. Other models and combinations of objectives are explored, to obtain faithful embeddings of original data. Furthermore, we build on previous work [4] to provide supervised quality-assessment metrics, using expert labelling of cells. Additionally, we measure performance and speed of pre-training strategies, which involve training with different loss functions sequentially. We also explore the amenability of latent representations to clustering via a mixture-of-experts decoder module. This work constitutes a step toward designing useful embeddings for interpretation and further analysis of high-dimensional biological data that reduce noise and preserve important local and global relationships between cells. [1] Lambert, P. et al. (2021). DOI: 10.1101/273862v2 [2] de Bodt, C. et al. (2020). DOI: 10.1109/TNNLS.2020.3042807 [3] Weber, L. and Robinson, M. (2016). DOI: 10.1002/cyto.a.23030 [4] Konstorum, A. et al. (2018). DOI: 10.1101/273862v2

**898548**    **P96**

## **Analysis Paralysis: How to choose the optimal algorithm for compensation when highly autofluorescent cells are present,**

Jack Panopoulos<sup>1</sup> Jay Almarode<sup>1</sup> Richard Halpert<sup>1</sup> Bridget McGlaughlin<sup>2</sup>

<sup>1</sup>BD Biosciences    <sup>2</sup>University of California, Davis

Recent advances in cytometric hardware, reagents and software have given scientists more information about the cells they are interrogating. Larger spectral footprints, narrower excitation or emission spectra, autofluorescence correction and different compensation algorithms ostensibly contribute to refined observations of cellular phenotypes and functional states. Software applications have evolved to incorporate this new information to facilitate use of these methodologies. However, it is rapidly becoming apparent that these novel algorithms, and the decision to correct for autofluorescence, do not result in a single solution for all experiments. Moreover, these options provide a myriad of permutations, making it difficult to decide which combination works best for the current data set. Herein we compare the interplay of gate based versus robust linear regression based (Autospill) population identification, and traditional versus spectral methods of compensation, with or without the subtraction and/or removal of various autofluorescent populations across four data sets with panels ranging from 8 to 40 colors. Each panel stained peripheral blood mononuclear cells for the more highly autofluorescent myeloid lineages or both myeloid and lymphoid lineages. We evaluate the impact of these methods on well-defined populations spanning a range of low to high autofluorescence and in a variety of staining conditions. Finally, we have assessed the outcomes using a variety of compensation goodness metrics and produced a series of recommendations for working with compensation of autofluorescent cells. Our results indicate that no single approach was best for all conditions, but AutoSpill produced outcomes at least on par with traditional gate-based methods with significantly less effort when attempting to correct for highly autofluorescent cells. Further, we find that the Total Spread Matrix (TSM) and/or Spillover Spread Matrix (SSM) are useful metrics for evaluating the quality of compensation even with high autofluorescence, and the channel used for autofluorescence removal and the proximity of other detectors to the autofluorescence channel provide good hints about which algorithm to use for specific panel designs.

# CYTO 2022 ABSTRACTS

**901376 P98**

## **MACSima imaging cyclic staining (MICS) technology reveals combinatorial target pairs for CAR T cell treatment of solid tumors,**

Travis Jennings<sup>1</sup>, Ali Kinkhabwala, <sup>1</sup>, Dmytro Yushchenko<sup>1</sup>

<sup>1</sup>Miltenyi Biotec

Many critical advances in research utilize techniques that combine high-resolution with high-content characterization at the single cell level. We introduce the MICS (MACSima Imaging Cyclic Staining) technology, which enables the immunofluorescent imaging of hundreds of protein targets across a single specimen at subcellular resolution. MICS is based on cycles of staining, imaging, and erasure, using photobleaching of fluorescent labels of recombinant antibodies (REAffinity Antibodies), or release of antibodies (REAlase Antibodies) or their labels (REAdye\_lease Antibodies). Multimarker analysis can identify potential targets for immune therapy against solid tumors. With MICS we analysed human glioblastoma, ovarian and pancreatic carcinoma, and 16 healthy tissues, identifying the pair EPCAM/THY1 as a potential target for chimeric antigen receptor (CAR) T cell therapy for ovarian carcinoma. Using an Adapter CAR T cell approach, we show selective killing of cells only if both markers are expressed. MICS represents a new high-content microscopy methodology widely applicable for personalized medicine.

**902007 P100**

## **Evaluation of a complex antigen to stimulate cellular responses to Coccidioides and advance diagnostics.,**

Mrinalini Kala<sup>1</sup>, Garrett Grischo<sup>1</sup>, Chiung-Yu Hung<sup>2</sup>, Kenneth Knox<sup>1</sup>, Althea Campuzano<sup>2</sup>, Eric Holbrook<sup>1</sup>

<sup>1</sup>University of Arizona, <sup>2</sup> University of Texas at San Antonio

**BACKGROUND:** Coccidioidomycosis (CM), also known as Valley Fever (VF) is caused by the endemic fungus *Coccidioides*. An increasing number of individuals are at risk for infection given climate change and our growing elderly and vulnerable populations. The morbidity associated with CM is substantial with a median time to return to normal activity at 47 days. The financial impact associated with CM is estimated at over \$200 million to the healthcare system. Even during COVID, a time when many were masking, the incidence of VF has

continued to increase. Currently available diagnostic tests rely on an individual's ability to generate a measurable antibody immune response and are prone to false positives and false negatives, causing frustration and delays in care. Many patients have mild infections resembling bronchitis and were never formally diagnosed with VF. Some of these patients have lung scarring and nodules resembling lung cancer, which leads to unnecessary scans and biopsies. We are interested in developing more accurate diagnostic tests for these scenarios by studying the cellular immune response to *Coccidioides*. We plan to use flow cytometry as the methodology to further characterize the cellular immune response to VF. **METHODS:** IRB approved subjects underwent informed consent for a one-time blood draw. Frozen PBMCs from healthy and valley fever subjects were used for the study. The VF antigen used in this study is T27k antigen, synthesized using *Coccidioides posadasii* C735 isolate and is a validated, complex extract. PBMCs were used at 1x10<sup>6</sup> cells/well in 96 well plate and stimulated with- PMA/iono (positive control), T27k (VF test antigen, 10, 25 and 50 ug/ml) and unstimulated control. Stimulation was done for 6 hr with last 5 hr with Golgi stop. PBMCs were stained with viability dye, followed by surface staining markers (CD3, CD4 and CD8), fixing/permeabilization and staining for intracellular cytokines (IFN-g, IL-2 and TNF-a). FMO and compensation was performed for the fluorochrome sets. Data was acquired with a 3 laser Canto II analyzer and analyzed by flowjo. To optimize, some conditions included CD28/49 addition in order to augment the response. **RESULTS:** Stimulation of VF subjects with T27K antigen lead to increased secretion of IL-2 and TNF-a compared to healthy controls. IL-2 and TNF-a secretion levels were very similar when stimulated with different doses (10, 25 and 50 ug/ml) of T27K antigen. The INF-a secretion was not measurable above baseline controls. C28/49 stimulation showed above baseline response for INF-g after 18 hr stimulation. The elevated cytokine responses were preferentially higher in the CD8 T cell population. **CONCLUSIONS:** A complex valley fever antigen extract, T27K, is able to stimulate cellular responses measurable by intracellular flow cytometric techniques. These preliminary studies provide the rationale for testing specific antigens and epitopes with a goal of improving options for VF testing.

# CYTO 2022 ABSTRACTS

**901032 P102**

## **Advancements in single cell multiomic profiling of antigen-specific T cells with dCODE Dextramer® (RiO) and BD® AbSeq Reagents on the BD Rhapsody™ Single-Cell Analysis System,**

Kivin Jacobsen<sup>2</sup>, Cynthia Sakofsky<sup>1</sup>, Vadir Lopez-Salmeron<sup>3</sup>, Margaret Nakamoto<sup>4</sup>, Aruna Ayer<sup>1</sup>, Liselotte Brix<sup>2</sup>

<sup>1</sup>BD Biosciences, <sup>2</sup>Immudex, <sup>3</sup>BD Biosciences, Germany, <sup>4</sup>BD Biosciences, United States

The advancement of immunotherapies and drug development relies on the characterization of antigen-specific T cells. However, due to their low frequency among T cells and their inherent weak affinity to bind known MHC-peptide complexes, detection of these cells has been difficult. Furthermore, pairing this information with the corresponding variable (V), diversity (D), and joining (J) [V(D)J] sequences of the antigen-specific T cell receptors has also been challenging due to hurdles in sequencing these large regions, particularly at the single-cell level. Here, we have expanded our previous work of combining two powerful technologies, Immudex dCODE Dextramer® (RiO) Reagents and the BD Rhapsody™ Single-Cell Analysis System, to detect and characterize low-frequency antigen-specific T cells, including the full sequences of the V(D)J gene segments of the T cell receptors, as well as profile transcriptome and protein expression. Specifically, thousands of sorted PBMCs were multiplexed to provide high-throughput detection of individual antigen-specific CD8+ T cells in combination with the corresponding full V(D)J sequences of the T cell receptors. In addition, we simultaneously obtained gene expression data for over 400 immune-related mRNAs as well as cell phenotypes using a panel of 30 cell surface BD® AbSeq Protein Markers. Together these data can be used to define T cell phenotypes associated with T cell activation states, alongside antigen specificity of enriched CD8+ dextramer+ cells from PBMC populations. This study showcases the importance of multiomic analysis for high-resolution T cell profiling that has broader implications and utility in immuno-oncology, infectious diseases, and autoimmunity. For Research Use Only. Not for use in therapeutic or diagnostic procedures BD, the BD Logo and Rhapsody are trademarks of Becton, Dickinson and Company or its affiliates. All other trademarks are the property of their respective owners. © 2021 BD. All rights reserved. 1221 Immudex®, Dextramer®, dCODE®, Klickmer™ and U Load™ are trademarks owned by ImmudexApS

**901397 P104**

## **CyTOF XT allows for automated and streamlined high-plex cytometric immunophenotyping,**

Christina Loh<sup>1</sup>, Lauren Tracey<sup>1</sup>, Stephen K. H. Li<sup>1</sup>, Nick Zabinyakov<sup>1</sup>

<sup>1</sup>Fluidigm

High-parameter immune profiling is a cornerstone in translational and clinical research to quantify changes in immune cell populations over time. CyTOF® mass cytometry is a single-cell analysis platform that uses isotope-tagged antibodies to resolve 50 or more markers in a single tube without signal compensation. Therefore, it is ideal for routine immunophenotyping. CyTOF XT™, the latest CyTOF system, features automated sample acquisition. Following staining, tubes of pelleted samples are placed into the Autosampler carousel, and the Autosampler resuspends the samples with EQ™ Calibration Beads for acquisition. User input is only required during instrument startup, tuning, and batch setup. The added automation of CyTOF XT provides a streamlined workflow for suspension mass cytometry. To assess performance of the CyTOF automated acquisition system, human PBMC samples were stained and acquired in parallel using the automated CyTOF XT system and manually using the Helios™ system. Suspension mass cytometry staining workflows that were evaluated included sample barcoding with the Cell-ID™ 20-Plex Pd Barcoding Kit, phosphostaining, and surface, cytoplasmic, and nuclear staining. Population frequencies and resolution indices for markers were assessed by manual gating. There was no significant difference between population frequencies analyzed between the two CyTOF systems. On average, samples acquired on CyTOF XT resulted in greater resolution between positive and negative populations compared to Helios. The Maxpar Direct Immune Profiling System, which comprises the Maxpar® Direct™ Immune Profiling Assay™ and Maxpar Pathsetter™ software, was also used to compare the CyTOF XT and Helios systems. The Maxpar Direct Immune Profiling Assay includes a 30-marker panel in a dry, single-tube format for staining human whole blood or PBMC. Maxpar Pathsetter automates reporting of population statistics and stain assessments for the panel. Stained samples acquired on CyTOF XT and Helios were compared based on their staining assessment in Maxpar Pathsetter. Comparable population frequencies were obtained between the two acquisition systems, and improved staining assessment was observed on CyTOF XT. Overall, these studies

# CYTO 2022 ABSTRACTS

find that the CyTOF XT system generates better signal resolution than the Helios system. Automated acquisition by CyTOF XT enables researchers to accurately and reproducibly streamline human immunophenotyping. For Research Use Only. Not for use in diagnostic procedures.

**901590 P106**

## **Extending the capabilities of a high-parameter immunophenotyping assay with cytoplasmic staining applications for mass cytometry,**

Michael Cohen<sup>1</sup>, Christina Loh<sup>1</sup>, Huihui Yao<sup>1</sup>,

<sup>1</sup>Fluidigm Canada Inc

Mass cytometry, powered by CyTOF<sup>®</sup> technology, utilizes monoisotopic metal-tagged antibodies and a high-sensitivity mass cytometer to enable high-dimensional single-cell analysis in complex biological samples. Using the 30-marker Maxpar<sup>®</sup> Direct<sup>™</sup> Immune Profiling Assay<sup>™</sup> for suspension mass cytometry provides an unprecedented sample-to-answer solution for detecting and analyzing 30 surface markers in a single experiment. With 18 open mass channels for additional biological markers, the Maxpar Direct Assay facilitates panel expansion and enables flexibility for higher multiplexity and applications. Among the potential complementary applications with the Maxpar Direct Assay, intracellular cytokine staining (ICS) is of particular interest, as it may be used to assess antigen-specific immune responses in the context of infectious disease and cancer. However, for the purpose of assessing cell viability in this workflow, the effectiveness of the Cell-ID<sup>™</sup> Intercalator-Rh that is included in the Maxpar Direct Assay is in question, since cell permeabilization during ICS can potentially damage the DNA-intercalator bond. In this study, we investigated the compatibility of the Cell-ID Intercalator-Rh (103Rh) with intracellular staining. To do this, we stained either human PBMC or whole blood samples with the Maxpar Direct Assay followed by intracellular staining for the detection of expressed cytokines. The intercalator was evaluated for its ability to discriminate live and dead cells when the sample undergoes surface antibody staining. The monoisotopic Cell-ID Cisplatin-194Pt was used as the control to provide benchmark measurement of cell viability of the samples. For both sample types, known percentages of heat-killed PBMC were spiked into the samples in order to evaluate the influence of dead cells. We demonstrate that 103Rh provides equivalent functionality as a cell viability indicator during

intracellular staining for cytoplasmic proteins compared to Cell-ID Cisplatin-194Pt. This work was designed to support the use of the Maxpar Direct Immune Profiling Assay in combination with additional intracellular markers. Overall, these findings expand the applicability of Cell-ID Intercalator-Rh (103Rh) to processes that involve cytoplasmic staining. For Research Use Only. Not for use in diagnostic procedures.

**901796 P108**

## **DNA-Based Dye Nanostructures Enable New Directions in Spectral Flow Cytometry,**

Anson Blanks<sup>1</sup>, Nicholas Pinkin<sup>1</sup>, Seddon Thomas<sup>1</sup>, , Craig LaBoda<sup>1</sup>

<sup>1</sup>Thermo Fisher Scientific

To increase the complexity of flow cytometry panels and allow scientists to dig deeper into the biology made accessible by these experiments, more antibody conjugates are needed with spectrally unique dyes that can be easily differentiated on spectral cytometers. Using DNA-based macromolecules, dyes can be attached at defined positions, enabling the design of highly efficient FRET networks with tunable fluorescence properties that minimize cross-excitation and spectral spillover. Unlike PE or APC tandem dyes, which can display significant lot-to-lot variability due to differences in the degree of labeling or FRET efficiency, our approach allows for high lot-to-lot consistency (<5% spectral difference between lots) due to the highly specific attachment of the dyes at defined positions on the DNA nanostructure. Combined with the controlled 1:1 labelling of antibodies that our chemistry affords, we were able to demonstrate a relative similarity  $\geq 0.99$  for each of these novel dyes when comparing the spectral signatures on cells to those on compensation beads. In addition, our testing shows that individual antibody-dye conjugates are stable for at least three years when stored at 4C and that different antibody-dye conjugates are compatible when stored mixed together in solution for up to 14 days. Furthermore, the DNA nanostructures are compatible with methanol as well as 2% formaldehyde fixation and the antibody-conjugates exhibit high stability on cells after fixation, displaying no appreciable change in signal for up to 14 days when stored in fixation buffer.

# CYTO 2022 ABSTRACTS

**901826 P110**

## **Build bigger better panels with superior dyes excitable by the ultraviolet, violet, blue and yellow lasers.,**

Michael Blundell<sup>1</sup>

<sup>1</sup>Bio-Rad

The recently launched fluorescent dyes from Bio-Rad, StarBright Dyes, deliver tunable brightness and spectral properties, greater stability, improved lot-to-lot reproducibility, and spectral consistency. Specifically designed for multicolor flow cytometry with researchers needs in mind, StarBright Dyes address the common pain points in flow such as brightness, broad emission spectra, staining consistency, and ease-of-use, solving issues of signal resolution when constructing complex panels. Here we present a preview of our newest additions to the StarBright range, the StarBright Blue and StarBright Yellow Dyes on the five laser ZE5 Cell Analyzer. StarBright Blue Dyes are bright and allow an expansion of dyes to be used using the 488 laser, whereas StarBright Yellow Dyes are optimally excited by the 561 laser with reduced excitation from the 488 laser making large panel design using both the 488 and 561 laser easier. In this study we show, when StarBright Blue and StarBright Yellow Dyes are combined with other members of the StarBright range and traditional fluorescent dyes, large immunophenotyping panels can be easily constructed allowing identification of many peripheral blood subsets, without the requirement of special staining buffers. When combined with their ability to be fixed in both PFA based and alcohol-based fixatives, and to be pre-mixed, the flexibility of StarBright Dyes means they are ideal for new and expanding existing panels.

**901859 P112**

## **22-color Spectral Flow Cytometry Panel Development for Exploring Circulating Gut-homing T cells in CeD Patients after Dietary Gluten Challenges,**

Taryn Mockus<sup>1</sup>, Katherine Nevin<sup>1</sup>, Yi-Dong Lin<sup>1</sup>, Vilma Decman<sup>1</sup>

<sup>1</sup>GSK

Celiac Disease (CeD) is an autoimmune disease of the intestine in response to dietary gluten. Although the prevalence of CeD is between 0.7% and 1.4% worldwide, the only treatment available is for patients to follow a gluten-free diet. Additionally, diagnosis

of CeD is burdensome with biopsy following gluten challenge as the gold standard. Current work has indicated that exposure to gluten correlates with mobilization of gut-homing CD4+ and CD8+ T cells in the peripheral blood, providing a minimally invasive biomarker assay for diagnosis of CeD. High-dimensional biomarker profiling of these populations would increase our understanding and, potentially, lead to novel diagnosis methods and/or treatment. Here, we developed a 22-color spectral flow cytometry panel for use on a Cytex Aurora to assay the phenotype of CD45+CD19-CD14-CD11c-TCR $\gamma\delta$ - effector memory (TEM) CD4+ and CD8+ T cells in healthy donors as well as CeD patients following gluten challenge. This high parameter flow cytometry panel was rigorously developed through titration of antibodies and testing of fluorescence minus one (FMO) and fluorescence minus many (FMX) experiments to ensure assay robustness on these rare populations. We identified a small population of CD8+ TEM cells that are  $\beta 7$ brightCD38bright following gluten challenge, but CD4+ TEM cells did not have this population. This population began to appear one day post gluten challenge and peaked 6 days post gluten challenge. This panel also includes a few activation markers of interest, such as ICOS, PD-1, CD25, CD39, CD161, and CXCR3. Acknowledgement: Jiangfang Wang (cell preparation), Esther Pérez García and Ruth Barnard (cell shipping and management). The human biological samples used were sourced ethically and their research use was in accord with the terms of the informed consents under an IRB/ERC approved protocol.

**901925 P114**

## **Characterization of Autologous Hematopoietic Stem Cell Transplantation in Multiple Sclerosis,**

Jonas Haugsøen<sup>1,2</sup>, Shamundeeswari Anandan<sup>2</sup>, Ida Viktoria Herdlevær<sup>2</sup>, Gerd Haga Bringeland<sup>2</sup>, Simeon Mayala<sup>3</sup>, Morten Brun<sup>3</sup>, Nello Blaser<sup>4</sup>, Christian Alexander Vedeler<sup>1,2</sup>, Kjell-Morten Myhr<sup>1,2</sup>, Anne Kristine Lehmann<sup>5</sup>, Øivind Torkildsen<sup>1,2</sup>, Lars Bø<sup>1,2</sup>, Sonia Gavasso<sup>1,2</sup>

<sup>1</sup> Department of Clinical Medicine, Neuro-SysMed, University of Bergen, Bergen, Norway, <sup>2</sup> Department of Neurology, Neuro-SysMed, Haukeland University Hospital, Bergen, Norway, <sup>3</sup> Department of Mathematics, University of Bergen, Bergen, Norway, <sup>4</sup> Department of Informatics, University of Bergen, Bergen, Norway <sup>5</sup> Department of Internal Medicine, Haukeland University Hospital, Bergen, Norway

# CYTO 2022 ABSTRACTS

Multiple Sclerosis (MS) is an autoimmune neurological disease where the myelin-producing oligodendrocytes of the central nervous system are targeted. This causes neurodegeneration and subsequent loss of neurological function. The most common MS subtype, relapsing-remitting MS (RRMS), is characterized by relapses with increasing neurological disability, followed by complete or partial remission. Current RRMS treatments successfully reduce disease activity in most patients. Nevertheless, RRMS eventually progresses into the treatment-resistant progressive variant for most patients. Over the last few decades, autologous hematopoietic stem-cell transplantation (aHSCT) has shown great potential as a lasting cure for RRMS. In aHSCT, the patient's stem cells are mobilized from the bone marrow to peripheral blood by a combination of growth factors and low-dose chemotherapy. Stem cells are then harvested by apheresis and cryopreserved before the patient undergoes a chemotherapy conditioning regimen. Then, the stem cell product is thawed and reinfused. aHSCT is thought to "reset" the immune system by replacing its pathological self-reactive cells with healthy self-tolerant ones. We aim to improve our understanding of the immunological mechanisms in aHSCT by using mass cytometry to investigate the immune system's reaction to mobilization, chemotherapy, and stem-cell reinfusion. RAM-MS is a clinical trial at Haukeland University Hospital where 100 patients will be randomized 50–50 to compare established highly efficient treatments with aHSCT. We are using apheresis products and blood samples from several time-points to model the mechanisms of aHSCT. We also hope to find biomarkers that can predict clinical outcomes before starting treatment. We have designed and validated a 42-marker mass cytometry panel allowing detailed characterization of immune cells, focusing on hematopoietic stem- and progenitor subsets. We are currently collecting data, which we will analyze using an analysis pipeline developed with collaborators at the Department of Mathematics which allows us to perform deep characterization of rare stem cell populations.

**896542 P116**

## **Hyperspectral imaging, region analysis, and filtering to identify second messenger signals in signal-limited images**

Silas Leavesley<sup>1</sup>, Naga Annamdevula<sup>1</sup>, Marina Parker<sup>1</sup>, , Andrea Britain<sup>1</sup>

<sup>1</sup>University of South Alabama

Background: Second messenger signals, such as calcium (Ca<sup>2+</sup>) and cyclic nucleotides, coordinate a wide range of cellular functions. Recent studies have indicated that signal specificity may be encoded within certain aspects of second messenger signals, such as frequency or spatial encoding. Hence, it is important to be able to detect the complex frequency and spatial components of signals. Unfortunately, in fluorescence microscopy there is typically a trade-off between signal-to-noise ratio, spatial resolution, temporal resolution, and wavelength sampling. Our previous studies suggest that spectral imaging approaches may provide opportunities to overcome specificity limitations of fluorescence microscopy. Here, we present results from spectral imaging of Ca<sup>2+</sup> signals and intensity filtering to distinguish meaningful regions of Ca<sup>2+</sup> signals from background or autofluorescence. Methods: Human airway smooth muscle cells (HASMCS) were grown to confluency on laminin-coated round glass coverslips. Cells were loaded with 50  $\mu$ M Cal 520-AM and NucBlue. Imaging was performed an excitation-scanning hyperspectral imaging microscope consisting of an inverted microscope base (TE-2000, Nikon Instruments), 300 W Xe arc lamp (SunOptic Technologies), thin-film tunable filters (VersaChrome, Semrock) mounted in a tuning system (VF-5, Sutter Instruments), and sCMOS camera (Prime 95B, Photometrics). Time-lapse, excitation-scanning spectral image data were acquired from 360–480 nm, in 5 nm increments. After 5 minutes baseline acquisition, cells were treated with Ca<sup>2+</sup> agonist (histamine or carbochol) or vehicle control. Spectral images were analyzed to separate Cal 520, NucBlue, and autofluorescence. Results: Unmixed Cal 520 images were processed to identify whole field and single-cell regions and quantify Ca<sup>2+</sup> kinetics. Images were also processed to remove pixels with low signal-to-noise using Otsu thresholding as well as a theoretical sensitivity analysis. The theoretical sensitivity analysis simulated signal-to-noise properties of a characteristic Cal 520 image, to identify optimal thresholding conditions for separating Cal 520 from autofluorescence after linear unmixing. Results indicate that pixel filtering can separate the true cell Ca<sup>2+</sup> signal measurements from

# CYTO 2022 ABSTRACTS

background or autofluorescence. Differences in filtered vs. unfiltered signal trends were most pronounced for whole field measurements. Subtle differences were also found in cells with lower intracellular Cal 520 labeling levels. Conclusions: Spectral imaging capabilities allow simultaneous detection of second messenger signals and additional labels, as well as autofluorescence separation. However, for weakly-labeled cells, it may be advantageous to further select which pixels to extract quantitative information from. A theoretical sensitivity analysis may aid in identifying well-labeled pixels. This work was supported by NIH awards P01HL066299, R01HL58506, and R01HL137030, and NSF award MRI172

---

## 901041 P120

### **A rapid and fully automated in vitro micronucleus assay using imaging flow cytometry and convolutional neural network analysis,**

Matthew Rodrigues<sup>1</sup>, Raymond Kong<sup>1</sup>, Maria Gracia<sup>1</sup> Garcia Mendoza<sup>1</sup>, Alexandra Sutton<sup>1</sup>

<sup>1</sup>Luminex Corporation

Micronuclei (MN) originate from whole chromosomes or chromosome fragments that lag behind during cell division and fail to be incorporated into one of the two main nuclei. As a result, scoring MN using the well-established in vitro micronucleus assay enables the assessment of the ability of chemicals or other agents to induce DNA damage. This technique is typically performed by manual microscopy, which can be time-consuming and prone to variability. Additionally, automated methods lack cytoplasmic visualization when using slide-scanning microscopy, and conventional flow cytometry doesn't provide visual confirmation of MN. The ImageStream<sup>®</sup>X Mk II (ISX) imaging flow cytometer combines the high-resolution imagery of microscopy with conventional flow cytometry's speed and statistical robustness in a single system. Previously, we developed a rapid and automated MN assay based on high-throughput image capture and feature-based image analysis using IDEAS<sup>®</sup> Software. However, the feature-based analysis was not readily applicable to multiple cell lines and chemicals, so we developed a deep learning method based on convolutional neural networks to score imaging flow cytometry data in both the cytokinesis-blocked and unblocked versions of the MN assay using Amnis<sup>®</sup> AI Software. Our current study validates our previously established assay and analyses using three different

chemicals (clastogens, Mitomycin C and Cyclophosphamide, and a negative control [Eugenol]) and three different cell lines (TK6, L5178Y, CHO-K1). Here, we demonstrate how using Amnis AI to score imagery acquired on the ISX provides a rapid and fully automated in vitro MN assay with improved accuracy, reproducibility, and time-to-results in toxicity and biodosimetry applications across multiple cell lines.,

---

## 901488 P122

### **Multi-Dimensional Imaging Flow Cytometer for Improved Cell Counting Accuracy,**

Christian Goerke<sup>1</sup>, Martin Hussels<sup>1</sup>, Jonas Gienger<sup>1</sup>, Alexander Putz<sup>1</sup>, Alexander Hoppe<sup>1</sup>, Dirk Grosenick<sup>1</sup>,

<sup>1</sup>Physikalisch-Technische Bundesanstalt

Conventional laser-flow cytometers measure directional intensities from laser-light scattering and fluorescence from immunostaining. However, this gives limited information on the objects passing the laser as cells show a wide variety in properties like size, shape, and expression levels of antigens. Consequently, different cell populations overlap in the measured data, hindering the correct identification of cell types. This reduces the counting accuracy significantly, especially for rare events like circulating tumor cells with rates as low as 0.01%. To overcome these limitations, we built a multi-dimensional imaging laser-flow cytometer to acquire high-content information from cells of interest. It incorporates photomultiplier tubes (PMTs) to obtain high signal detection rates and an FPGA gating mechanism to capture objects at flow velocities of 2 m/s. When cells of interest pass the focus of a 488 nm CW laser, a gating signal is generated for a vertically shifted 406 nm imaging laser. The gate induces an imaging laser flash of 0.1–1  $\mu$ s. Its pulse width is much shorter than the minimum exposure time of 59  $\mu$ s of two lost-cost industrial CMOS cameras. This way, we prevent motion blur and take sharp images from cells from the forward and sideward directions. The user sets the window trigger conditions while the FPGA evaluates their validity. Since the FPGA also acquires the data of the PMTs, we can trigger on any PMT channel. We provide data on variously shaped polystyrene and silica particles and preliminary results on cells. By comparing the imaging data with the conventional flow cytometry information acquired by the PMTs, we demonstrate the value of multi-dimensional imaging for accurate cell counting.



# CYTO 2022 ABSTRACTS

**901918 P126**

## **Bright fluorescent conjugates for imaging applications with erasable signal via dual-release mechanism**

Thorge Reiber<sup>1</sup>, Dmytro Yushchenko<sup>1</sup>

<sup>1</sup> Miltenyi Biotec

Cell analysis techniques like flow cytometry and fluorescence microscopy are widely used to explore cell biology and provide important insights into a variety of physiological and pathological processes. These techniques require bright and specific staining reagents to enable reliable read-out, making the choice of fluorescent labels a key aspect of experimental design. Conventional labels, however, usually do not permit the high multiplexing and multiparameter analysis that is often required for samples with high diversity. This is mainly due to the limitations of the spectrum detection range used in fluorescence-based applications, which in turn limits the depth of phenotypic analysis to a small number of expression markers. In order to address this limitation, several approaches of releasable labels have been developed. In particular, REAlease<sup>®</sup> and REAdyelease<sup>®</sup> conjugates were designed for this purpose, thus enabling subsequent staining and imaging. Ultimately, it was demonstrated on the MACSima<sup>™</sup> Cyclic Imaging Platform that these reagents permit cell analysis with a potentially unlimited number of parameters, allowing the identification of potential targets for immune therapy against solid tumors. However, a challenge exists when fluorescent conjugates are not completely released from the tissue section, resulting in carryover signal from previous imaging cycles and ultimately a lower depth of analysis. Here it becomes evident that the number of imaging cycles is not only determined by the number of available conjugates but also by their release efficiency. In this work, we present a promising approach for the design of the aforementioned conjugates with the aim to further increase the efficiency of dye release without compromising their brightness. This approach relies on conjugates decorated with fluorophores via two spacers (polymer backbones) that can orthogonally be digested by two different enzymes, thus permitting efficient release of the dyes from the binder. In addition, such design allows high multimerization of the fluorophores leading to the increased brightness of the probes that is especially helpful for reliable signal detection, e.g. in the analysis of rare epitopes.

**901952 P128**

## **Exploring Imaging Flow Cytometry and Morphometrics for Characterization of Leukemic Stem Cells in Acute Myeloid Leukemia,**

Trine Engelbrecht Hybel<sup>1</sup>, Carina Agerbo Rosenberg<sup>1</sup>, Marie Bill<sup>1</sup>, Maja Ludvigsen<sup>1</sup>

<sup>1</sup>Aarhus University

**Introduction & Hypothesis** Acute myeloid leukemia (AML) is a rapidly progressing malignant blood cancer characterized by accumulation of immature myeloid cells in the bone marrow (BM). The relapse rate is high, and the median overall survival is approximately 50% for younger patients (<60 years). Relapse is believed to emanate from a small population of chemo-resistant leukemic stem cells (LSCs) enriched in the immature CD34+CD38- stem cell compartment of the BM. Leukemic stem cells are heterogeneous and may differ from healthy hematopoietic stem cells (HSCs) by genetic abnormalities and/or aberrant antigen expression. Importantly, no unique marker is aberrantly expressed across all AML samples and in many cases, immunophenotypic abnormalities are not sufficient to separate LSCs from HSCs, complicating LSC monitoring. Of note, studies have observed altered scatter properties on immunophenotypically defined LSCs, indicating morphological differences between LSC and HSC subsets. We hypothesize that an imaging flow cytometry (IFC) based LSC/HSC-tube, in combination with artificial intelligence (AI), can distinguish LSCs from HSCs based on deviating morphometric parameters, e.g., cell and nuclear size, texture, and shape, and that this approach could be a powerful tool for monitoring measurable residual disease at the stem cell level. **Methods** Thawed BM mononuclear cells from AML patients were stained with the following pre-titrated monoclonal antibodies: CLEC12A PE, CD14 PE-Texas Red, CD7 BB700, CD45 KrO, CD38 StarBright Violet 610, and CD34 AF647. In addition, Vybrant DyeCycle Violet and Zombie Green were included as DNA stain and viability marker, respectively. The panel was optimized for use on an Amnis ImageStreamX MK II Imaging Flow Cytometer (Luminex). **Results** We designed an eight-color IFC panel for morphometric characterization of LSC subsets in BM samples from AML patients. The panel includes the surface markers CLEC12A and CD7, described as aberrantly expressed on LSCs. The applicability of the panel has been evaluated on BM samples from AML patients. Initially, immature HSCs and LSCs were identified as CD45<sup>low</sup>CD14-CD34+CD38- among live,

# CYTO 2022 ABSTRACTS

nucleated, single cells in focus. Next, LSCs were phenotyped for aberrant CLEC12A and/or CD7 expression. To leverage the high-content information contained in the vast amount of image data, we will train an AI algorithm to discriminate between aberrant marker positive LSCs in AML BM and HSCs from healthy individuals and explore AI for label-free LSC identification in AML BM samples. **Conclusion & Perspectives** In conclusion, we have demonstrated the feasibility of an eight-color LSC/HSC-tube to phenotypically distinguish aberrant marker positive LSC subsets from HSCs in AML BM samples. Certainly, the applicability of AI-assisted IFC for MRD monitoring at the stem cell level during treatment and follow-up requires exploration in a large cohort of AML patients.

**893902 P130**

## **High-throughput chemotherapeutic drug screening of tumor spheroids with individual spheroid results using image cytometry,**

Jordan Bell<sup>1</sup>, Leo Chan<sup>1</sup>, Shilpa Mukundan<sup>1</sup>, Biju Parekkadan<sup>2</sup>

<sup>1</sup>Nexcelom Bioscience, <sup>2</sup>Rutgers

Three-dimensional cancer models have gained popularity for in vitro studies of chemotherapeutic compounds by providing a more physiologically relevant analog of gas, nutrient, and drug diffusion throughout the tumor microenvironment. Some 3D assays are performed to study individual spheroids over time, where a majority of these assays rely on maintaining a single spheroid in each well of a 96-well round-bottom ultra-low attachment plate, limiting the number of spheroids in a study. Other assays may gather population-level data from large ensembles of spheroids grown together, but the information about individual differences amongst the spheroids is lost. Important kinetic information may also be lost for destructive endpoint assays such as MTS or MTT. Here, we describe the development of a 3D image cytometry assay that is capable of generating kinetic data for thousands of breast cancer spheroids at the individual level. T47D spheroids are grown and maintained in a 24-well AggreWell™400 plate and imaged using the Celigo image cytometer. Each well contains more than 1000 subwells that both aid in spheroid formation and constrain each spheroid to a specific location. Using the spheroid location data, we are able to track and monitor the growth of each spheroid over 7 days. Furthermore, we investigate the dose-dependent effects on spheroid viability of 6 anti-cancer drugs (Doxorubicin, Everolimus, Gemcitabine, Metformin, Paclitaxel and Tamoxifen) using calcein AM and propidium iodide (PI). To validate

the viability measurement results, we utilize the CellTiter96® MTS assay as an orthogonal method to compare the dose-dependent trends using both the calcein AM and PI fluorescence intensities as well as the spheroid sizes. This work may lay a foundation for the investigation of other spheroids, organoids, or tissue samples, significantly increasing the number of spheroids analyzed per condition, improving the statistical analysis, and adding more parameters to further analyze the spheroids. These improvements may be especially helpful for spheroids grown from patient-derived or otherwise heterogeneous cell populations

**896493 P132**

## **Imaging flow cytometer based on linear array spot illumination generated by diffractive optical elements**

Yong Han<sup>1</sup>, Jingjing Zhao<sup>2</sup>, Zixi Chao<sup>1</sup>, Zheng You<sup>1</sup>

<sup>1</sup>Tsinghua University, <sup>2</sup>Stanford University

Imaging flow cytometer (IFCM) is a technique for high-throughput imaging of a large number of fast-moving cells. However, due to the weak fluorescence emission of cells and the trade-off between imaging speed and sensitivity, it is a challenge to image the cells moving at a speed of several meters per second. In this work, we developed a new method for high throughput imaging flow cytometry, using diffractive optics elements to generate linear laser spot array for illumination, and single-pixel detectors (PMT) for detection. The illumination spots are arranged in a line at equal intervals and form a small angle with the direction of the cell movement. In the direction of the cell moving, the distance between two adjacent laser spots is greater than the size of common human cells, which ensures that there is only one spot illuminates the cell. When the cell passes through the illumination area, the two-dimensional information of the cell's fluorescence and scattered intensity profile is encoded into the signals detected by the PMTs. Then the image of the cell can be obtained from the PMT signal by segmenting, recombining, and deconvolution. In this work, fluorescence and scattering imaging were experimentally demonstrated for beads and cells traveling at a velocity of 4.7 m/s in a microfluidic chip, with a resolution of 1 μm and a maximum throughput of 5000 cell/s. Based on this method, an IFCM with multi-color fluorescence channels and multi-lasers could be achieved by only replacing the illumination optics in conventional flow cytometers. This makes it possible for IFCMs to have the same number of detection channels as conventional

# CYTO 2022 ABSTRACTS

flow cytometers, which greatly enriches the detection information for single cell analysis.

**898251 P134**

## **High dimensional imaging of human cutaneous squamous cell carcinoma reveals a specific signature associated with relapse,**

Aïda Meghraoui<sup>1</sup>, Roxane Elaldi<sup>1</sup>, Veronique Braud<sup>1</sup>, Fabienne Anjuere<sup>1</sup>

<sup>1</sup>AMKbiotech

Background: Cutaneous squamous cell carcinomas (cSCC) are the second deadliest skin cancer. They are currently treated by excisional surgery but can reach, for some patients, a non-operable stage associated with rapid local and nodal relapses and a very poor prognosis. However, no consensus has been reached on the clinical or molecular factors predicting these recurrences. It is therefore crucial to improve the identification of patients that would relapse by the characterization of prognostic biomarkers. An integrative spatial characterization of cSCC immune microenvironment and the interactions of their components are required to identify such biomarkers. The objective of our study is to obtain an exhaustive characterization of the immune microenvironment (TiME) of recurrent and non-recurrent cSCC, including the interaction maps between the main actors described to be associated to tumor progression. The comparison of the specific signature of these two cSCC groups will allow the identification of prognostic biomarker candidates that could help predict relapses. Methods: A cohort of cSCC with different prognosis comprising one group of non-relapsing tumors (n=10) and one group of primary tumors having a local relapse at 2 years (n=10) were used. An imaging mass cytometry (IMC) panel of 39 antibodies targeting components of the cSCC TiME (tumor cells, immune subtypes, fibroblasts, blood and lymphatic vessels, extracellular matrix and nerves fibers) was designed (Elaldi et al, Front Immunol 2021) and used to stain a section of each formalin fixed and paraffin-embedded (FFPE) tumor of the cohort. Each section was analyzed by IMC and the 40-dimensional images obtained were processed using an in-house developed analysis pipeline. All specimens were obtained in accordance with the Declaration of Helsinki following protocols approved by Nice Hospital Ethical Comity (DRCI). Results: IMC image preprocessing and computational analysis of the single cell phenotypes extracted from the images allowed (1) the identification of each targeted

TiME component subset, from tumor cells and activated fibroblasts to both myeloid and lymphoid immune cells, (2) in addition to their functional status (proliferation, apoptosis, exhaustion) and (3) their localization within tumor structures. This analysis also led to the identification of specific spatial features characterizing the TiME of each tumor group. The comparison of these specific signatures uncovered a predictive signature associated with relapse risk after surgical excision of cSCC tumors that will be confirmed in an independent validation cohort. Highlights: We developed a 39-marker Imaging Mass Cytometry panel that allowed the spatial characterization of the TiME of a human cSCC cohort. With this panel, we identified a predictive signature associated with tumor relapse.

**898504 P136**

## **Imaging flow cytometry-based analysis of Leishmania's cell cycle**

Melanie Jimenez<sup>2</sup>, Jessie Howell<sup>1</sup>, Tansy Hammarton<sup>1</sup>,

<sup>1</sup>University of Glasgow, <sup>2</sup> University of Strathclyde, Glasgow

Leishmania parasites cause a variety of debilitating diseases, affecting millions of humans and animals throughout 90 countries. Despite their prevalence, there are no anti-Leishmania vaccines currently approved for human use, and treatment methods are often insufficient and toxic. Understanding how the molecular control of Leishmania's cell cycle differs from mammalian cells may provide new therapeutic targets. Studying the cell cycle of Leishmania, requires being able to determine the specific cell cycle stage of individual cells. Typically, analysis is carried out on fixed cells stained with a DNA dye, with microscopy analysing key morphological changes, and flow cytometry quantifying DNA content (Wheeler et al. 2011 Mol. Microbiol.79: 647-662). However, these methods have limitations, with cell fixation potentially introducing artefacts and affecting morphology, and microscopy often being labour intensive and low throughput. Here, we have developed a new high throughput workflow to analyse live Leishmania using imaging flow cytometry (IFC). While IFC has previously been applied to study host-pathogen interactions (Haridas et al. (2017) Methods, 112, 91-104; Terrazas et al. (2015) J Immunol Methods, 423, 93-98), its application for molecular analysis in parasites remains largely unexplored (Wiedeman et al. (2018) PLOS ONE, 13, e0197541-e0197541). We demonstrate for the first time that cell cycle analysis is possible in live *L. mexicana* stained with the DNA dye Vybrant™ DyeCycle™ Orange (DCO)

# CYTO 2022 ABSTRACTS

through analysis of simultaneously acquired IFC brightfield images (morphology) and fluorescence spectra (DNA content). To optimise DNA quantification in live *Leishmania*, several dyes were trialled. However, a requirement for cell fixation (e.g. propidium iodide (PI), which is often used for DNA quantification in *Leishmania*) or disproportional binding to DNA (e.g. Hoechst) prevented their use in live cells. DCO was the only dye to accurately quantify DNA in live *L. mexicana*. This was validated against PI staining in equivalent, but fixed cells. Distributions of cells in G1, S-phase and G2/M phase were calculated using a model fitting algorithm, which were highly similar between the two staining methods. Morphological analysis of the IFC images allowed all cell cycle stages to be identified. Further, preliminary data indicates that automatic calculation of cell dimensions correlates well with microscopy-based measurements. Thus, we demonstrate a new high throughput method for analysing live *L. mexicana* that combines morphological and DNA content analysis. To our knowledge, this is the first time IFC has been applied to study the molecular processes of an extracellular parasite. More broadly, our novel application of IFC technology should facilitate a range of molecular analyses, including tracking the localisation of fluorescently tagged proteins and detection of morphological changes across the cell cycle in a wide range of important pathogens.

**898516 P138**

## **Exploring cell-cell interactions through simultaneous imaging cytometry and multi-color immunophenotyping**

Aaron J Middlebrook<sup>1</sup>, Peter Mage<sup>1</sup>, Keegan Owsley<sup>1</sup>, Tri Le<sup>1</sup>, Patricia Lovelace and Eric Diebold<sup>1</sup>

<sup>1</sup> BD Biosciences

Cells communicate with one another in a variety of ways in the context of normal function and as a consequence of a disease state. Communication can be long range as in the case of hormones, short range as in the case of chemokines or direct as in the case of cell-to-cell engagement. Direct cell-cell interactions have been widely studied in immune cells and are often referred to as the immune synapse, wherein an antigen presenting cell engages with a T cell. These engagements have been shown to be more frequent during infection or after immunization, demonstrating their importance as a function of the immune system. Due to the complex phenotypes of the cells involved and the low frequency of these interactions

(less than 1–5% of events in healthy donor peripheral blood mononuclear cell preps), the robust throughput and multichannel phenotyping capabilities of flow cytometry coupled with the ability to sort cells for downstream analyses make this an ideal platform to decipher these interactions. However, conventional flow cytometry, which is restricted to fluorescence intensity measurements, does not provide the spatial information required to distinguish engaged cell doublets from two random cells processed as one event (coincident doublets) nor can it resolve what part of a cell a signal is coming from. Imaging cytometry has emerged as an ideal platform to study cell-cell interactions as it couples some basic immunophenotyping capabilities with the spatial discrimination to interrogate these interactions at a detailed level, enabling the identification of true engagements and quantifying receptor accumulation at the cell-to-cell synapse. However, researchers are limited by the relatively low number of fluorescence channels available for immunophenotyping and the inability of current imaging cytometry systems to support sort functionality for downstream analyses. Building on the work we presented using an image-based cell sorter (ref. Schraivogel et al., Science 2022), we describe a detailed interrogation of these cell-cell interactions. The panel design approach for this work was to enable detailed T cell and B cell immunophenotyping of the cells involved in these interactions while preserving the image-based analyses of the spatial distribution of fluorescence and cell orientation. The use of sort compatible, image-based metrics is leveraged to characterize the nature of the cell-cell interaction and to quantify receptor accumulation at the site of the interface. The technical limitations of multi-parameter cytometry within the context of image-based analysis are explored and some basic guidelines for designing experiments of this nature are presented. For Research Use Only. Not for use in diagnostic or therapeutic procedures. BD is a trademark of Becton, Dickinson and Company. © 2022 BD. All rights reserved. 0222

# CYTO 2022 ABSTRACTS

**898534 P140**

## **Using integrated multidimensional mass cytometry and multiplex immunohistochemistry to infer spatial relationships between phenotypically distinct glioblastoma infiltrating immune cells.,**

Todd Bartkowiak<sup>1</sup>, Asa A. Brockman<sup>1</sup>, Sierra M. Lima<sup>1</sup>, Madeline J. Hayes<sup>1</sup>

<sup>1</sup>Vanderbilt University

Glioblastomas (GBM) account for 60% of adult primary brain tumors. With few advances in therapeutics, median overall survival remains 15-months post-diagnosis. Immunotherapies may provide therapeutic benefit in GBM patients; however, no predictive immune features currently inform therapeutic stratification in GBM. We have shown that, independently of known prognosticators, radiographic tumor contact with the lateral ventricle (C-GBM) correlates with 7-months worse survival compared to patients with ventricle non-contacting GBM (NC-GBM). This study sought to characterize the GBM immune microenvironment to identify targetable mechanisms of immunosuppression correlating with worse outcomes in C-GBM. Primary glioblastoma tissue was provided for research purposes with written informed consent in accordance with the Declaration of Helsinki and with approval of the Vanderbilt Institutional Review Board (IRB #131870). Twelve patients presented with primary, IDH wildtype C-GBM and 13 with NC-GBM. High dimensional mass cytometry and matched multiplex immunohistochemistry (mxIHC) performed on formalin-fixed paraffin embedded (FFPE) tissue for each patient interrogated the phenotype and matched spatial position of GBM infiltrating immune cells. Machine learning tools characterized tumor-infiltrating immune populations and identified biomarkers correlating with C-GBM and patient survival. Mass cytometric profiling was integrated into mxIHC images to infer broader immune phenotypes from spatial positions within the tissue. K-means clustering identified immunological neighborhoods within the tissue and a log odds ratio quantified the likelihood of cell-cell interactions in the tissue. C-GBM tumors were enriched in CD32+CD44+HLA-DR+ monocyte-derived macrophages (MDM) compared to NC-GBM ( $19 \pm 8\%$  vs.  $6 \pm 2\%$ ;  $p < 0.001$ ) and depleted in lymphocytes ( $2.9 \pm 1\%$  vs.  $7.6 \pm 2\%$ ;  $p < 0.001$ ) and tissue-resident microglia ( $1.8 \pm 0.3\%$  vs.  $7 \pm 3\%$ ;  $p < 0.001$ ). Further, T cells in C-GBM co-expressed the checkpoint receptors PD-1 and TIGIT, suggesting greater T cell exhaustion in the C-GBM tumor microenvironment. K-means

clustering identified 10 common immunological niches prevalent in GBM tissue. Macrophage-tumor niches were most common, accounting for 17.93% of all niches, followed by T cell-microglia-tumor niches (17.72%). Conversely, tumor-tumor niches were the least prevalent, accounting for only 2.51% of niches. Within niches, T cell-T cell interactions were more prevalent (log odds ratio = 0.90) whereas T cell-macrophage interactions were less prevalent (log odds ratio = -1.61). These findings suggest that factors within the periventricular space may influence the immune microenvironment within tumors, and identify clinically targetable immune biomarkers in glioblastoma. Notably, radiologic assessment of lateral ventricle contact by standard-of-care MRI may guide clinical trial design for immunotherapies in neuro-oncology based on tumor proximity to the lateral ventricle.

**898564 P142**

## **Imaging Flow Cytometry as a tool to study distribution dynamics of extra-cellular vesicles RNA cargo within immune cells,**

Ziv Porat<sup>1</sup>

<sup>1</sup>Weizmann Institute of Science

Extracellular vesicles (EVs) are produced by across almost all the living kingdoms and play a crucial role in cell-cell communication processes. EVs are especially important for pathogens, as *Plasmodium falciparum* (Pf) parasite, the leading causing species in human malaria. Malaria parasites are able to modulate the host immune response from a distance via delivering diverse cargo components inside the EVs, such as proteins and nucleic acids. We have previously shown that imaging flow cytometry (IFC) can be effectively used to monitor the uptake of different cargo components of malaria derived EVs by host human monocytes. Here, we take this approach one step further and demonstrate that we can directly investigate the dynamics of the cargo distribution pattern over time by monitoring its distribution within two different recipient cells of the immune system, monocytes vs macrophages. By staining the RNA cargo of the vesicles and monitor the signal we were able to evaluate the kinetics of its delivery and measure different parameters of the cargo's distribution post internalization. Interestingly, we found that while the level of the EV uptake is similar, the pattern of the signal for RNA cargo distribution is significantly different between these two recipient immune cells. Our results demonstrate that this method can be applied

# CYTO 2022 ABSTRACTS

to study the distribution dynamics of the vesicle cargo post uptake to different types of cells. This can benefit significantly to our understanding of the fate of cargo components post vesicle internalization in the complex interface between pathogen-derived vesicles and their host recipient cells.

**898433 P144**

## **The Critical Role of IL-23 Receptor Positive T cells in the Pathogenesis of Anterior Uveitis Associated with Spondyloarthropathy,**

Robert Hedley<sup>1</sup>

<sup>1</sup>University of Oxford

The spondyloarthropathies (SpAs) are a group of chronic inflammatory diseases which predominantly affect the joints of the axial skeleton. However, many patients with SpA may have extra-articular manifestations within the skin and gut. Pathology of SpA in all of these tissues has been shown in recent studies to be driven by local resident populations of interleukin (IL)-23 responsive cells. The eye is also involved in these diseases, with uveitis occurring in up to 40% of patients with SpA. Therefore, it is feasible that a resident population of IL-23 responsive cells could also exist within the eye. Recently, systemic overexpression of IL-23 in mice has shown the accumulation of a small number of  $\gamma\delta$  T cells proximal to the anterior uvea. However, although work has been done to characterize resident leukocyte populations within the anterior compartment of the eye there has been no documentation of resident lymphoid cells in these tissues and there is no evidence suggesting the presence of a sentinel cell capable of responding to IL-23. In this study we document for the first time that a diverse population of T cells (CD4+, CD8+, and CD4-CD8-) occupies the extravascular tissues of the anterior compartment (iris, ciliary body, trabecular meshwork, and limbal sclera) of the eye in both mice and humans. We identify the presence of a resident IL-23R+CD3+CD4-CD8-  $\gamma\delta$  T cells in the anterior compartment of the eye, providing a potential explanation for why IL-23 is capable of affecting this tissue. We next stimulated T cells of the anterior compartment to demonstrate functional IL-23R activity and that IL-23 is sufficient to drive uveitis in the absence of any pro-inflammatory mediator. We achieve this in vivo in mice through a novel mechanism enabling the sustained localized overexpression of IL-23 in the inner eye by adeno-associated virus gene transfer. Since this could not be replicated in human disease, we stimulated human eye tissue digests with PMA/ionomycin in vitro. We demonstrated in both

mouse and humans that a small fraction of anterior compartment T cells are capable of producing the IL-23R downstream pro-inflammatory cytokine Interleukin-17A (IL-17A). Furthermore, we show that in mice IL-17A production is upregulated after in vivo exposure to IL-23. Consistent with the concept of IL-23 being a unifying factor in SpA, we propose that like the gut, skin, and joints, IL-23 can also act locally on a resident IL-23 responsive cells to drive ocular pathology.

**899722 P146**

## **High-risk neuroblastoma survivors show signs of immunosenescence early after therapy and retain increased myeloid cell activation status,**

Petra Laznickova<sup>1</sup>

<sup>1</sup>FNUSA-ICRC

Introduction Deterioration of adaptive and innate immune responses described as immunosenescence has been reported in older adults. Furthermore, frailty, condition linked to chronic inflammation and accelerated aging, has already been described in young adult childhood cancer survivors (CCS). The therapy of neuroblastoma, the most frequent extra-cranial solid tumor in early childhood, is targeting important functions of tumor cells. We hypothesize that intensive therapy and/or inflammatory burden caused by acquired comorbidities serve as inducers of accelerated aging of immune system. Materials and methods Multiple cohorts were established for the evaluation of immunosenescent phenotype – two follow up groups of high-risk neuroblastoma CCS (nCCS) - Survivors 1-4years after diagnosis, Survivors 5+years after diagnosis, and two control groups - Child controls, Elderly. Flow cytometric analysis of immunosenescent phenotype of CD4 and CD8 T cells was performed via evaluation of naive, memory, CD57+ memory and terminal effector memory T cells re-expressing CD45RA with concomitant expression of CD57 (TEMRA) subsets. Alongside the T cells phenotyping, frequency of three monocyte subsets based on CD14 and CD16 surface expression and their activation/maturation status via HLA-DR were analyzed. Evaluation of myeloid cells functionality was performed via determination of phagocyte frequency and phagocytosis efficiency in whole blood. Results We were able to recruit 14 participants of Survivors 1-4y with median age 5 (range 2-8) and 22 participants in Survivors 5+y with median age 12 (range 5-27) for this study. These nCCS groups were statistically different in age, while the

# CYTO 2022 ABSTRACTS

group of Child controls with median age 14 (range 1-23) was not statistically different from either of the nCCS groups. The Elderly groups were statistically older than both nCCS groups and Child controls. The proportion of males and females was not statistically different between the nCCS groups or in comparison with the Child controls and Elderly groups. All the survivors in this study were treated with chemotherapy and autologous hematopoietic stem cell transplantation and only 1 survivor in the Survivor 1-4y group did not have radiotherapy included in the treatment regimen. **Conclusions** We detected a transient immunosenescence-like phenotype in CD8 naive and CD57+ memory subsets and confirmed the age-independent increase of CD57+ memory CD8 T cells in Survivors 1-4y. The distribution of HLA-DR+ monocytes and their expression of HLA-DR remains unchanged within nCCS groups. However, we detected increased efficiency of phagocytosis in Survivors 5+y. Even though, we detected only transient immunosenescence-like phenotype in CD8 T cells, the functionality of myeloid compartment through heightened phagocytosis suggests ongoing late effects of treatment and/or their development and more detailed studies on immune cell responses in nCCS are required.

**901279 P148**

## **Phenotypic analysis of mouse hematopoietic stem and progenitor cells using a 14-color panel with the Agilent NovoCyte Penton flow cytometer,**

Ming Lei<sup>1</sup>, Garret Guenther<sup>1</sup>, Peifang Ye<sup>1</sup>, Yan Lu<sup>1</sup>

<sup>1</sup>Agilent

Hematopoietic stem/progenitor cells (HSPCs) isolated from bone marrow have been successfully employed for many years in hematological transplantations. These cells can be identified using flow cytometry by a set of cell surface markers. Here, we developed and optimized a 14-color panel for the in-depth analysis of the mouse bone marrow HSCs, five multipotent progenitors (MPPs), the common lymphoid progenitor (CLP) and eight myeloid-committed progenitors along with CD45.1 and CD45.2. In this panel, each population was delineated by specific expression of surface markers with high resolution and cells expressing lineage markers (CD3, CD11b, B220, Gr-1, Ter119) are excluded from the analysis using a dump channel. HSCs and MPPs can be identified by analyzing the cell surface proteins Sca-1, c-Kit, CD150, CD48, CD34, and CD135. They are defined as indicated: HSCs (LSK, CD150+, CD48-, CD34-,

CD135-), MPP1 (LSK, CD150+, CD48-, CD34+, CD135-), MPP2 (LSK, CD150+, CD48+, CD135-), MPP3 (LSK, CD150-, CD48+, CD135-), MPP4 (LSK, CD150-, CD48+, CD135+, and MPP5 (LSK, CD150-, CD48-, CD135-). Additionally, the myeloid-committed progenitors (common myeloid progenitor, CMP; granulocyte macrophage progenitor, GMP; megakaryocyte erythrocyte progenitor, MEP; megakaryocytic progenitor, MkP; pre-granulocyte-macrophage progenitor, Pre GM; pre-common MegE progenitor, Pre MegE; colony-forming unit-erythroid, CFU-E; and Pre CFU-E) are defined by specific expression patterns of Sca-1 and c-Kit plus CD16/32, CD34, CD41, CD105, and CD150: CMP (LK, CD34+, CD16/32-), GMP (LK, CD34+, CD16/32+), MEP (LK, CD34-, CD16/32-), MkP (LK, CD150+, CD41+), Pre GM (LK, CD150-CD105-CD41-CD16/32-), Pre MegE (LK, CD150+CD105-CD41-CD16/32-), CFU-E (LK, CD150-CD105+CD41-CD16/32-) and Pre CFU-E (LK, CD150+CD105+CD41-CD16/32-). Furthermore, the resulting cell population expressing Sca-1 and c-Kit at a low level is then analyzed for CD135 and CD127 to determine the CLP population (LSlowKlow, CD135+CD127+). This 14-color panel can be used for deeper phenotypic characterization of the mouse hematopoietic compartment and greatly improve our understanding of the relationships between HSCs, MPPs, and mature blood cells.

**901281 P150**

## **What Is Responsible For Abnormal Galactose-Deficient IgA Production In Iga Nephropathy? Looking For The Source,**

Petr Kosztyu<sup>1</sup>, Katerina Zachova<sup>1</sup>, Jana Jemelkova<sup>1</sup>, Milan Raska<sup>1</sup>

<sup>1</sup>Palacky University in Olomou

IgA nephropathy is characterized by the deposition of IgA1 immune complexes in glomerular mesangium. The IgA1 immunoglobulin in immune complexes of IgA nephropathy (IgAN) patients shows aberrant O-glycosylation, consisting in galactose deficiency of hinge region of IgA1 (gd-IgA1). Increased gd-IgA1 was detected in the serum of IgAN patients together with immune complexes formed by gd-IgA1 and anti-gd-IgA1 autoantibodies, that are of IgG or IgA isotype. The origin nor the molecular mechanism of the gd-IgA1 or anti-gd-IgA1 production is mostly unknown. Here, we use the 35A12 antibody specifically detecting the gd-IgA1 in serum or on the cells expressing surface gd-IgA1. By this method we characterized B cells responsible for the production of gd-IgA1 in systemic or mucosal compartments. Using a panel of antibodies characterizing

# CYTO 2022 ABSTRACTS

B cells subsets positive for CD19, CD20, CD38, CD138, IgA, gd-IgA1 we were able to explore the possible sites of Gd-IgA1 production. From our results we could summarize that umbilical cord blood, as a representative of systemic compartment of immune system, contains surface gd-IgA1+ B cells in very low levels (about 0.14% of all IgA+ cells) similarly to peripheral blood (1% of IgA+ cells) according to recent publication. On the other hand, the breast milk contains higher levels of gd-IgA1+ B cells and the breast milk from IgAN mothers contains significantly lower levels of gd-IgA1+ B cells (20% of IgA+ B cells) compared to healthy controls (85% IgA+ B cells). Also the cell surface density of gd-IgA1+ on B cells, as measured by MFI, is 7-times higher in healthy controls than in IgAN patients. Analysis of tonsils from IgAN patient did not reveal the deposition of gd-IgA1+ B cells, as the source of gd-IgA1 production, neither in mantle zone nor in germinal centers of B cells. Our study characterizes, for the first time, several possible sites of gd-IgA1 production and reveals that systemic immune sites of human body such as peripheral blood, umbilical cord blood, or tonsils do not contain considerable population of gd-IgA1+ B cells in contrast to breast milk. The research was supported by Ministry of School, Youth, and Sport, Czech Republic grant CEREBIT CZ. 02.1.01/0.0/0.0/16\_025/0007397 and Palacky University Olomouc grant IGA\_LF\_2022\_011.

## 901285 P152

### **Influence of IL-6 on B regulatory lymphocytes and $\lambda$ light chain expression in IgA nephropathy,**

Katerina Zachova<sup>1</sup>, Jana Jemelková<sup>1</sup>, Milan Raska<sup>1</sup>,

<sup>1</sup>Palacky University

An autoimmune disease IgA nephropathy (IgAN) is characterized by the deposition of IgA containing immune complexes in the kidney mesangium. IgA1 in the serum and kidney deposits of IgAN patients is enriched with aberrantly glycosylated form – the galactose deficient IgA1 (Gd-IgA1) which serves as an epitope for anti-glycan autoantibodies. Gd-IgA1 positive cells in peripheral blood of IgAN patients express predominantly  $\lambda$  light chain. Interleukin 6 (IL-6) is supposed to be involved in the pathogenesis of IgAN. First, IgAN patients have increased levels of IL-6 concentration in serum and IL-6 enhances Gd-IgA1 production of IgA secreting cells in vitro. Therefore, we analyzed the effect of IL-6 stimulation on  $\lambda$  light chain expression. Regulatory B cells (Bregs) attenuate inflammation and

contribute to the maintenance of immune tolerance. Breg cell population is reduced or dysfunctional in several autoimmune diseases, however, it has not been thoroughly examined in IgAN yet. We used spectral flow cytometry to analyze the frequency of CD19+, IgA+ and Gd-IgA1+ populations with Breg phenotype (CD24<sup>high</sup>, CD38<sup>high</sup>) in peripheral blood of IgAN patients and healthy controls. We stimulated peripheral blood mononuclear cells (PBMC) with IL-6 and analyzed the effect on Bregs subpopulations. Finally, we studied the  $\lambda$  light chain expression in IL-6 stimulated cells. In our study, we confirmed reduced numbers of Breg cells in the peripheral blood of IgAN patients including the IgA+ and Gd-IgA1+ subpopulations. IL-6 stimulation did not affect Bregs in CD19+ populations and IgA+ populations but decreased the frequency of Bregs in the Gd-IgA1+ populations. We also showed that the IL-6 stimulation of PBMCs preferentially stimulated  $\lambda$  light chain positive IgA+ and Gd-IgA1+ cells in both IgAN patients and healthy controls. Our data indicate that the dominance of  $\lambda$  light chain positivity in Gd-IgA1+ cells might be associated with elevated levels of IL-6 in IgAN patients' serum. Reduced numbers of Bregs in IgAN patients might contribute to the disease pathogenesis. The research was supported by Ministry of School, Youth, and Sport, Czech Republic grant CEREBIT CZ. 02.1.01/0.0/0.0/16\_025/0007397 and Palacky University Olomouc grant IGA\_LF\_2022\_011.

## 901502 P154

### **Exploring the Association of Preexisting Mycobacterial T Cell Responses With Mtb Challenge Outcome in Unvaccinated and Vaccinated NHP**

Evan Lamb<sup>1</sup>, Samantha Provost<sup>1</sup>, Mitzi Donaldson<sup>1</sup>, Patricia A. Darrah<sup>1</sup>, Kathryn Foulds<sup>1</sup>, Mario Roederer<sup>1</sup>

<sup>1</sup> Vaccine Research Center<sup>1</sup>, NIAID<sup>1</sup>, NIH<sup>1</sup>, Bethesda<sup>1</sup>, MD

An estimated 10 million people worldwide develop TB disease every year. A more versatile vaccine than the current BCG vaccine is vital in reducing the negative impacts of Mtb infection. Previous research shows both unconventional and conventional T cells can contribute to primary and vaccine-mediated protection against TB. The non-human primate (NHP) model accurately reflects human TB disease and can be used to understand how a variety of cell populations respond to vaccination and Mtb infection. Both NHPs and humans can have preexisting T cell responses to mycobacterial antigens, likely



# CYTO 2022 ABSTRACTS

caused by exposure to nonpathogenic mycobacterium species in the environment. In what way such pre-existing responses impact the efficacy of TB vaccination or the outcome of TB infection is unclear. A greater understanding of pre-existing immunity and whether it contributes to variability between animals is important both for novel vaccine design, and for interpreting the protective efficacy of vaccine candidates. In a collaborative effort to investigate NHP samples from diverse geographical regions, we collected approximately 200 PBMC samples from Mauritian, cynomolgus, and rhesus macaques which were enrolled in TB vaccination and/or challenge studies in six different labs across the US and Europe. We characterized the phenotype and functional responses of conventional CD4 and CD8 T cells, as well as donor-unrestricted T cells (including gamma delta T cells and MAIT cells) in the PBMC of macaques before TB vaccination or Mtb challenge. Using a 20-color intracellular cytokine staining assay, we measured mycobacterial whole cell lysate induced IFN-g, IL-2, TNF, IL-17, CD40L and 4-1BB as well as the expression of activation/homing markers including HLA-DR, CCR7, CCR6, and CXCR3. Preliminary results from 10 macaques indicate varying levels of preexisting cytokine production after stimulation with mycobacterial whole cell lysate. Compared to unstimulated control samples, we detected low-level IFN-g responses from MAIT cells in 3 animals and IFN-g and TNF responses from gamma delta cells in 5 animals. From conventional T cells, there were moderately elevated preexisting IFN-g and TNF responses, and slightly elevated IL-17 responses. Once the preexisting cytokine specific responses and phenotypic data from all samples are collected, they will be compared to protective outcome measures after Mtb challenge (for example, MTb bacterial burden) to understand if any of the pre-existing immune parameters correlate with the extent of disease after TB infection.

**901849 P156**

## **PD-L1 expression in NSCLC MDSCs and its potential use as a biomarker to determine treatment response through dimensionality reduction of flow cytometric data,**

Roser Salvia-Cerdà<sup>1</sup>, Germans Trias<sup>1</sup>, Laura G. Rico<sup>1</sup>, Jolene A. Bradford<sup>1</sup>, Michael D. Ward<sup>1</sup>, Marc Sorigué<sup>1</sup>, Teresa Morán<sup>1</sup>, Joan Climent<sup>1</sup>, Rafael Rosell<sup>1</sup>, Jordi Petriz<sup>1</sup>

<sup>1</sup> Pujol Research Institute (IGTP)

Introduction: Immunotherapy is currently a major treatment option for cancer. Non-small cell lung cancer (NSCLC) treatment options include 5 approved immunotherapies to target the Programmed Cell Death Protein 1/Programmed Cell Death Protein Ligand 1 (PD-1/PD-L1) with the aim to avoid tumor immune escape. Accurate detection of PD-L1 is crucial to calculate the Tumor Proportion Score and decide the line of treatment. Therefore, we applied a minimal sample perturbation methodology to target PD-L1 (Rico et al., 2021). This protocol allows the identification of conformational changes in circulating Myeloid-Derived Suppressor Cells (MDSCs). In this study, we present prospective evaluation of PD-L1 expression in MDSCs from patients with NSCLC undergoing anti-PD-L1/PD-1 immunotherapy. Methods: Peripheral blood (PB) samples from NSCLC patients (n = 43) were collected in EDTA-anticoagulated tubes prior and during anti-PD-L1/PD-1 immunotherapy. PB samples were immediately processed using our minimal sample perturbation protocol, and acquired on the Attune™ NxT flow cytometer (Thermo Fisher). MDSCs were stimulated with phorbol esters (PMA) and identified according to HLA-DRloCD33+CD11b+ immunophenotype. FCS files analysis was performed using FlowJo™ (v.10). FCS files were concatenated, downsized, and analyzed with tSNE, UMAP and FlowSOM. Patients were classified based on clinical outcome: tumor reduction (1); tumor stabilization (2); tumor progression (3); no evidence of response (4); non-assessable, death with no evidence of disease (5); and early exitus, without starting immunotherapy (6). Results: tSNE and UMAP allowed comprehensive data visualization of PD-L1 expression in lung cancer samples. Unstimulated MDSCs showed no PD-L1 recognition nor conformational changes. After PMA stimulation, PD-L1 underwent drastic conformational changes, clustering separately when compared with unstimulated MDSCs. FlowSOM provided self-organizing maps with a common backbone for patient's comparisons. Stimulated and unstimulated specimens displayed complementary FlowSOM organizing maps, whereas

# CYTO 2022 ABSTRACTS

individual patients exhibited particular features. In addition, FlowSOM generated specific maps according to three clinical outcome groups (nonresponders, partial responders and responders). Conclusions: Further analysis will be needed to ascertain how the conformational changes of PD-L1 may help to accurately predict immunotherapy efficacy. Moreover, the feasibility of determining PD-L1 expression in NSCLC MDSCs may have a potential use as a biomarker to determine treatment response through dimensionality reduction. In fact, data analysis can be beneficial to improve diagnosis as well as to predict immunotherapy response early in the course of treatment.

**901987 P158**

## **CD8+ regulatory T-cell subset distribution in adolescents with primary hypertension is associated with hypertension severity and hypertensive target organ damage,**

Lidia Gackowska<sup>1</sup>, Izabela Kubiszewska<sup>1</sup>, Anna Helmin-Basa<sup>1</sup>, J.Michalkiewicz<sup>1</sup>, M.Wiese-Szadkowska<sup>1</sup>, A.Wierzbicka-Rucinska<sup>2</sup>, L.Obrycki<sup>2</sup>, Mieczyslaw Litwin<sup>2</sup>

<sup>1</sup>Nicolaus Copernicus University in Torun, Collegium Medicum in Bydgoszcz, Poland <sup>2</sup>The Children's Memorial Health Institute, Warsaw, Poland

Arterial hypertension is one of the most common civilization diseases in the XXI-century. In the last 20 years, there has been a marked increase in the incidence of primary hypertension (PH) in children and adolescents. Delayed diagnosis of PH in children and thus, untreated disease leads to serious organ damage and cardiovascular disease risk at an early age. One of the most important etiological factors of PH is a low-grade inflammation that drives blood pressure elevations and subsequent target organ damage (TOD). A chronic inflammation and the development of PH has been linked to the defect of T lymphocytes activities, especially T regulatory cells (Tregs) but the relationship between the distribution of the Treg subpopulations and the severity of the disease is still unknown. The aim of this study was to evaluate the relationship between PH and the different distribution of CD8+ Treg subpopulations in the peripheral blood of PH adolescents compared to controls. We also aimed to find out if TOD in adolescents with PH is related to defects in CD8+ Tregs distribution reflected by their phenotype characteristics. Method: The study constituted 32 nontreated hypertensive adolescents and 34 sex- and age-matched controls. The informed consent were obtained from

the Children's Memorial Health Institute. Using multicolor flow cytometry technique, we assessed a distribution of total CD8+ Tregs and their subsets differing in activation potential and suppressive properties. Peripheral blood samples were collected to tubes containing anticoagulant (EDTA) and the cellular surface antigen-stabilizing agent. The samples were stained with monoclonal mouse anti-human direct conjugated antibodies (CD4APC-Cy7, CD8V500, CD25BV421, CD127PE, CD45RA APC, CD28PerCP-Cy5.5 and CCR7FITC) for identification of CD8+ Treg subsets. Results: Patients with PH are characterized by a higher percentage of total CD8+Tregs, in particular subpopulation involved in the anti-inflammatory tissue response (total Treg CCR7+) and subpopulation of central/memory Tregs (CM Tregs CD8+/CD25+/CD127-/CD45RA-/CCR7+). Additionally, a significantly reduced percentage of thymic origin Tregs, with strong suppressive properties (CD8+/CD25+/CD127-/CD28low) and central/naive Tregs (CN Tregs CD8+/CD25+/CD127-/CD45RA+/CCR7+) was observed. Cells of thymic origin (Tregs CD28-), as well the percentage of CN Tregs negatively correlate with left ventricular mass index (LVMI), carotid intima-media thickness (cIMT) and wall cross sectional area (WCSA). Moreover, a positive correlation between the percentage of CM Tregs and LVMI was observed. Conclusion: The results suggest that subclinical arterial injury in adolescents with PH is associated with declined thymic function and increased pool of central/memory and CCR7+, anti-inflammatory subpopulations of Treg cells. Co-authors: J.Michalkiewicz, M.Wiese-Szadkowska, A.Wierzbicka, L.Obrycki. This work was supported by National Science Center 2013/11/B/NZ4/03832

# CYTO 2022 ABSTRACTS

902003 P160

## The distribution of CD4+ T cell subpopulations in adolescents with non-alcoholic fatty liver disease.,

Izabela Kubiszewska<sup>1</sup>, Lidia Gackowska<sup>1</sup>, Anna Helmin-Basa<sup>1</sup>, Jacek Michalkiewicz<sup>1</sup>, Malgorzata Wiese-Szadkowska<sup>1</sup>, Sara Balcerowska<sup>1</sup>, Aleksandra Wasilow<sup>2</sup>, Aldona Wierzbicka-Rucinska<sup>3</sup>, Wojciech Janczyk<sup>4</sup>, Piotr Socha<sup>4</sup>.

<sup>1</sup>Department of Immunology, Faculty of Pharmacy, Nicolaus Copernicus University in Torun, Collegium Medicum in Bydgoszcz, Poland, <sup>2</sup>Department of Clinical Biochemistry, Faculty of Pharmacy, Nicolaus Copernicus University in Torun, Collegium Medicum in Bydgoszcz, Poland, <sup>3</sup>Department of Biochemistry, Radioimmunology and Experimental Medicine, The Children's Memorial Health Institute, Warsaw, Poland, <sup>4</sup>Department Gastroenterology, Hepatology, Nutritional Disorders and Pediatric, The Children's Memorial Health Institute, Warsaw, Poland

**Introduction:** Non-alcoholic fatty liver disease (NAFLD) is characterized by chronic, systemic low-grade inflammatory response often associated with metabolic syndrome. The clinical profile of pediatric NAFLD patients is very similar to the group of patients with primary hypertension (PH). The latest research indicates a potential similarity in the pathomechanism of both diseases. Our previous results confirmed impact of CD4+ T cells in the development of hypertension and target organ damage. Because the immune mechanism in NAFLD is still unknown the main aim of our study was evaluation of CD4+ T cells populations in NAFLD adolescents. **Material and Methods:** The study included 26 patients with NAFLD (diagnosed based on CAP fibroscan assessment and increased ALT) and 13 age-matched controls: 6 overweight (BMI-matched to NAFLD) and 7 normal weight adolescents. The informed consent were obtained from the Children's Memorial Health Institute. Peripheral blood samples were collected into tubes containing tripotassium EDTA and the cellular surface antigen-stabilizing agent. Phenotypic analysis of T cell receptors was performed by direct nine-color flow cytometry with the use of monoclonal mouse anti-human antibodies (CD4 APC-AF700, CD8-BV650, CD45-KRO, CCR7-PE, CD45RA-APC, CD45RO-ECD, CD39-PC5.5, PD1-PC7, CD161-APC-AF750). **Results:** Despite the lack of differences in the total percentage of CD4+ T cells between the study groups, NAFLD patients showed a reduced percentage of CD4+ T naive cells (TN CD4+/CD8-/CD45RO-/CD45RA+/CCR7+) and CD4+ central/memory T cells (TCM CD4+/CD8-/CD45RO+/CD45RA-/CCR7+)

while increasing the percentage of CD4+ effector/memory T cells (TEM CD4+/CD8-/CD45RO+/CD45RA-/CCR7-). Additionally, an increased percentage of cells with a suppressive potential (CD39+) in terminally differentiated EM CD4+ T cells (TEMRA CD4+/CD8-/CD45RO-/CD45RA+/CCR7-) and EM CD4+ T cells was demonstrated in overweight control group. There was no difference in the percentage of cells with PD1 expression (apoptotic potential) and cells with expression of CD161 receptor (cells promoting the production of IL-17) between investigated groups. **Conclusions:** We showed changes in the distribution of CD4+ T cell subpopulations in NAFLD adolescents compared to controls. Preliminary results showed that patients with NAFLD are characterized by the increased % of memory T cells, mainly involved in immediate but unstable defense against pathogens (EM CD4+ T cells), decreased % of naive T cells and cells supporting a long-term immune response (CM CD4+ T cells). In further studies we will perform a comparative analysis with the group of PH patients and investigate the correlation between analysed CD4+ T cells and selected anthropometric, biochemical, and clinical parameters. The study was supported by the Polish National Science Center (2018/31/B/NZ5/02735).

902014 P162

## Regulatory B cells in the development and control of nonalcoholic fatty liver disease in adolescents.,

Anna Helmin-Basa<sup>1</sup>, Lidia Gackowska<sup>1</sup>, Izabela Kubiszewska<sup>1</sup>, Wojciech Janczyk<sup>1</sup>, J. Michalkiewicz<sup>1</sup>, M. Wiese-Szadkowska<sup>1</sup>, A. Wasilow<sup>1</sup>, Aldona Wierzbicka-Rucinska<sup>1</sup>, Ł. Obrycki, M. Litwin<sup>1</sup>, J. Ostrowski<sup>1</sup>, M. Szalecki<sup>1</sup>, Piotr Socha<sup>1</sup>

<sup>1</sup>Nicolaus Copernicus University

**Introduction:** Despite the increasing importance of the regulatory function of B cells in many infection diseases, their immunosuppressive role remains elusive in pediatric nonalcoholic fatty liver disease (NAFLD). Here we studied the proportion of different peripheral B cell subsets, inclusive regulatory B cells (Bregs) from obese adolescents with or without (obese control) NAFLD confirmed by increased ALT and CAP assessment by fibroscan. We also examined whether changes in the frequency or phenotypic distribution of B cells are associated with fibrosis measured by fibroscan, and circulating markers of hepatocellular damage, ALT and AST. **Methods:** Thirty-eight obese adolescents: thirty-two of them with NAFLD and 6 adolescents with no-metabolic disease. The study was

# CYTO 2022 ABSTRACTS

approved by the Bioethics Committee of the Children's Memorial Health Institute. In addition, clinical characteristics including serum triglyceride, ALT and AST levels were obtained. The frequencies of the circulating total B cells, naïve (CD19+CD27-IgD+CD38-) and memory (CD19+CD27+IgD-CD38-) B cells, CD5-positive B-1 B cells (CD19+CD5+), immature transitional B cells (CD19+CD27-IgD+CD38+CD24+) and plasmocytes (CD19+CD27+IgD-CD38+CD24-) were examined by flow cytometry. Results: We showed an expansion of total B cells, CD5-positive B-1 B cells and transitional B cell subsets while the decreasing plasmocyte frequency in the obese adolescents with NAFLD. In further studies we will investigate the correlation between analysed B cell subsets and selected clinical parameters. Conclusions: Our research demonstrate that CD5-positive B-1 B cells and transitional B cells are greatly expanded in obese adolescents with NAFLD. These findings provide insight into the phenotypic distribution of Bregs in NAFLD patients, an important step towards novel therapeutic strategies for NAFLD. This study was supported by the Polish National Science Center (2018/31/B/NZ5/02735).

**898434 P164**

## **The Critical Role of IL-23 Receptor Positive T cells in the Pathogenesis of Anterior Uveitis Associated with Spondyloarthritis**

Robert Hedley<sup>1</sup>

<sup>1</sup>University of Oxford

The spondyloarthropathies (SpAs) are a group of chronic inflammatory diseases which predominantly affect the joints of the axial skeleton. However, many patients with SpA may have extra-articular manifestations within the skin and gut. Pathology of SpA in all of these tissues has been shown in recent studies to be driven by local resident populations of interleukin (IL)-23 responsive cells. The eye is also involved in these diseases, with uveitis occurring in up to 40% of patients with SpA. Therefore, it is feasible that a resident population of IL-23 responsive cells could also exist within the eye. Recently, systemic overexpression of IL-23 in mice has shown the accumulation of a small number of  $\gamma\delta$  T cells proximal to the anterior uvea. However, although work has been done to characterize resident leukocyte populations within the anterior compartment of the eye there has been no documentation of resident lymphoid cells in these tissues and there is no evidence suggesting the presence of a sentinel cell capable of responding to IL-23. In this study we document for the first time that a diverse

population of T cells (CD4+, CD8+, and CD4-CD8-) occupies the extravascular tissues of the anterior compartment (iris, ciliary body, trabecular meshwork, and limbal sclera) of the eye in both mice and humans. We identify the presence of a resident IL-23R+CD3+CD4-CD8-  $\gamma\delta$  T cells in the anterior compartment of the eye, providing a potential explanation for why IL-23 is capable of affecting this tissue. We next stimulated T cells of the anterior compartment to demonstrate functional IL-23R activity and that IL-23 is sufficient to drive uveitis in the absence of any pro-inflammatory mediator. We achieve this in vivo in mice through a novel mechanism enabling the sustained localized overexpression of IL-23 in the inner eye by adeno-associated virus gene transfer. Since this could not be replicated in human disease, we stimulated human eye tissue digests with PMA/ionomycin in vitro. We demonstrated in both mouse and humans that a small fraction of anterior compartment T cells are capable of producing the IL-23R downstream pro-inflammatory cytokine Interleukin-17A (IL-17A). Furthermore, we show that in mice IL-17A production is upregulated after in vivo exposure to IL-23. Consistent with the concept of IL-23 being a unifying factor in SpA, we propose that like the gut, skin, and joints, IL-23 can also act locally on a resident IL-23 responsive cells to drive ocular pathology.

**901366 P166**

## **Use of Vio® and Vio® Bright Dyes with REAfinity™ Recombinant Antibodies for Phenotypic Characterization of human $\gamma\delta$ T-cells by Multicolor Flow Cytometry,**

Dirk Meineke, Miltenyi Biotec B.V. & Co. KG, Stefanie Wilhelm, Susanne Krauthäuser, Travis Jennings

Increasingly complex biological questions require the investigation of dim cellular markers and rare events, thus necessitating the need for new tools capable of probing such questions in an efficient manner. New generations of dyes combined with recombinant antibody technologies are necessary to realize this future of multiparameter flow cytometry as panel sizes and complexity grow. Vio® and Vio® Bright Dyes represent a family of fluorochromes for flow cytometry and fluorescence microscopy. They are characterized by high fluorescence intensities and low spillover, making them an ideal choice for multicolor flow applications. Combined with traditional fluorochromes, such as FITC, PE, PerCP, and APC, the Vio and Vio Bright family of Dyes expand available dye options, giving more flexibility in setting up multiparameter cell analyses. When used in combination with REAfinity™ Recombinant

# CYTO 2022 ABSTRACTS

Antibodies, Vio and Vio Bright Dye conjugates show superior lot-to-lot consistency compared to conventional monoclonal and polyclonal antibodies. The use of REAfinity technology also saves precious sample because these antibodies are engineered in such a way that only one isotype control is required. Additionally, researchers save valuable time because there is no need for FcR blocking. The OMIP-020 panel was designed to investigate the differentiation stages of human  $\gamma\delta$  T-cells in peripheral blood mononuclear cells (PBMC) by flow cytometry. The original OMIP-020 panel includes a live/dead marker and CD3, CD4 and CD8 markers to distinguish CD4-CD8- cells from CD8 expressing cells. To identify all  $\gamma\delta$  T-cells, an indirect staining with a pan- $\gamma\delta$  TCR antibody is used with a secondary antibody conjugate.  $\gamma\delta$  T-cell subpopulations were analyzed using CD16, CD27, CD28, CD45RA, TCR- $V\delta 1$  and  $-V\delta 2$  markers. In this study, we increase the robustness of the OMIP-020 panel with the replacement of REAfinity Recombinant antibody conjugates in an 11-color flow cytometry panel. Most markers were replaced by conjugates with a similar excitation/emission profile, but changing specific conjugates with Vio Bright alternatives on a MACSQuant<sup>®</sup> Analyzer 16 yielded improved brightness and better separation of the respective cell subsets. The modified panel is an example of the benefits of combining the power of REAfinity and VioDye technologies toward high lot-to-lot consistency, high brightness and low background. These improvements result in an easier workflow for the researcher, while still allowing to use increasingly complex multicolor panels in the future.

**901506 P168**

## **Comprehensive Immunomonitoring Of Patients After Hematopoietic Stem Cell Transplantation Using Omip-080,**

Sarka Vanikova<sup>1</sup>, Abhishek Koladiya<sup>1</sup>, Jan Musil<sup>1</sup>

<sup>1</sup>Institute of Hematology and Blood Transfusion

Hematopoietic stem cell transplantation (HSCT) represents the standard curative treatment for a variety of haematological malignancies, i.e. AML and MDS. However, it is still associated with high treatment-related mortality, caused mainly by a relapse of the original disease and infectious complications. All these complications are caused by improper immune system function. To further deepen the understanding of the underlying post-HSCT immune dysfunction we developed an optimized 29-colour immunophenotyping panel allowing us to monitor the reconstitution of NK cell and T cell subpopulations as these

represent major drivers of anti-leukaemia and anti-pathogen responses. Our project aims to determine immune signatures of high-risk patients, that could in the future be used for the identification of individuals requiring more intensive post-HSCT care or would be suitable for immunotherapeutic interventions. Our highly optimized panel, published as OMIP-080, includes markers for all major NK cell and T cell subsets and for analysis of their quantitative and qualitative properties. In the NK cell compartment, we focus mainly on CD57+NKG2C+ cells and the expression of activating (NKG2D, DNAM-1) and inhibitory receptors (NKG2A, TIGIT). Regarding T cells, we analyse the emergence and properties of major T cell populations with a particular interest in CD8, Th1, ThCTL and Treg subsets. Besides that, we use the detection of CD4+ recent thymic emigrants based on CD45RA, CD62L, CD95 and CD31 as a marker of thymus function. In conclusion, we have established a comprehensive immune system monitoring project intending to identify predictive risk factors on transplant outcomes that would allow us to suggest potential immunotherapeutic interventions.

**901915 P170**

## **Development and validation of a 23-colour spectral flow cytometry immunophenotyping panel designed for determination of activated dendritic cell, monocyte and B cell populations in human cryopreserved PBMC.,**

Irene del Molino del Barrio<sup>1</sup>, Esther Perez Garcia<sup>1</sup>, Thea Hogan<sup>1</sup>, Ruth Barnard<sup>1</sup>

<sup>1</sup>GSK

Whilst historically the main immunophenotyping focus has centred around T cells as the primary defence against infectious diseases and cancer, myeloid cells are now emerging as a key compartment in determining whether this response is, crucially, tolerogenic or pro-inflammatory. Furthermore, much of what we know is still extrapolated from mice, and studies in human blood often suffer from poor cleanup of contaminating populations. Spectral flow cytometry offers us a unique opportunity to glean more information from these subsets whilst including a wide breadth of exclusion markers and maintaining high resolution on the makers of interest. Combined with the advent of high-dimensional algorithms, the presence of multiple markers in one well can lead to the discovery of novel, disease-linked phenotypes. This 23-colour flow cytometry panel was developed to immunophenotype the myeloid compartment in both resting

# CYTO 2022 ABSTRACTS

and CD3/CD28 stimulated human cryopreserved PBMC using the Cytex Aurora. The optimised panel allows for the detection of canonical dendritic cell (DC) subsets including MDSCs, with parallel identification of monocyte subsets and B cell populations. A set of 8 surface molecules was compiled to evaluate various activation/exhaustion and co-stimulatory/inhibitory markers that have been reported in literature to be a relevant readout in the context of chronic infection or anti-tumour response, as well as 5 lineage markers for pre-gating and 10 markers for subset characterisation. This panel was optimised in healthy adult volunteers but will ultimately be used to investigate pharmacodynamic effects of potential therapeutics in the context of clinical trials. The human biological samples were sourced ethically and their research use was in accord with the terms of the informed consents under an IRB/EC approved protocol. Additionally, validation was performed and 190 reportables subjected to both intra and inter-assay precision assessment, as well as ascertaining inter-operator and inter-instrument CVs fall within acceptance criteria. This demonstrates the robustness of the panel performance is similar regardless of the operator or instrument used, a critical characteristic for multicentre studies.

**898256 P172**

## **CellMek SPS Instrument Performance: WBC and subpopulation recoveries using Specimen Wash and Sample Wash workflows,**

Kelly Andrews<sup>1</sup>, Casey Roberts<sup>1</sup>,

<sup>1</sup>Beckman Coulter

**Introduction:** The CellMek SPS Instrument is an automated sample preparation system intended for in vitro diagnostic use in flow cytometry laboratories that will aliquot specimen, add antibodies, lyse or other reagents, mix and time incubations, and wash samples as needed. The Cell Wash Module (CWM) within the CellMek SPS instrument is composed of two sub-assemblies designed to wash unprocessed biological specimen volumes between 300µL and 475µL as well as in-process samples ≤ 2.3mL. For native specimen washes, the system automatically over-aspirates and dispenses to counteract cell loss inherent to washing, keeping subsequent stain reactions at appropriate cell-to-antibody ratios. This study was conducted to assess population recovery performance of workflows that utilize the CWM for native specimen wash and for in-process sample wash. **Methods:** Peripheral blood or bone marrow specimen from normal and clinical donors (n=42) were prepared using 3

CellMek SPS instruments with workflows that included either native specimen wash, post-lyse sample wash, or no wash steps as reference. The specimen wash workflow included: wash of native specimen, stain, lyse, then transfer to output tubes. The sample wash included: stain, lyse, wash sample, then resuspend to normalize volume and transfer to output tubes. The no wash reference workflow included: stain, lyse, then transfer to output tubes. All samples were stained with CD45-KRO, CD3-PB, CD19-APC, CD10-ECD, CD14-PC7; specimen wash samples also included Kappa-FITC and Lambda-PE. As Kappa and Lambda require a specimen wash step for appropriate staining, an additional reference sample was prepared manually to assess these markers. Prior to acquisition on Navios flow cytometer, Flow-Count Fluorospheres were manually added to all samples enabling population enumeration. White blood cell (WBC) recovery was calculated as a percentage of the no wash reference using counts/µL. The % gated populations were also compared to the no wash references for WBCs and subsets. Manually prepared specimen wash references were used for Kappa and Lambda % gated comparisons for the specimen wash workflow. A 95% confidence was used to calculate WBC recovery for both specimen and sample wash workflows. **Conclusions:** For specimen wash recovery of the CWM on the CellMek SPS instrument, the lower 95% confidence interval was 101% for WBC counts/µL across 3 instruments; % gated subpopulations (monocytes, granulocytes, lymphocytes, CD19+ B cells, CD3+ T cells, Lambda and Kappa) were within 5% of the no wash or manual wash reference. For sample wash recovery, the lower 95% confidence interval was 81% for WBC counts/µL across 3 instruments; WBC subpopulations (monocytes, granulocytes, lymphocytes, CD19+ B cells, CD3+ T cells) were within 5% of the no wash reference. The Beckman Coulter products and service marks mentioned herein are trademarks or registered trademarks of Beckman Coulter, Inc. in the United States and other countries.

# CYTO 2022 ABSTRACTS

**901489 P174**

## **Method for low cell number sample preparation – automated up-concentration, washing and staining using acoustic trapping,**

Jessica Congiu<sup>1</sup>, Erik Karlsson<sup>1</sup>, Anke Urbansky<sup>1</sup>, Maria Agemark<sup>1</sup>

<sup>1</sup>AcouSort AB

Background Conventional techniques are ill-suited for handling of precious cell samples. Manual pipetting and centrifugation-based washing can dramatically decrease cell recovery and viability, further lowering the cell number in already scarce samples. Therefore, sample preparation involving these conventional techniques in protocols for e.g. staining and washing of cells can be challenging. The AcouTrap core technology uses non-contact acoustic trapping to capture cells in a microfluidic flow-through format, and acoustic-induced mixing to enhance binding kinetics, thus decreasing incubation times. AcouSort has developed novel methods for its AcouTrap system to enable handling of scarce cell samples and low sample volumes with high recovery. This allows for automated up-concentration, specific staining, and efficient washing of precious cell samples. Study design and methods Cell washing and staining using the AcouTrap was performed on cultured Jurkat cells. In the cell washing protocol, samples of 45 000 cells in ranging concentrations of 0.25-1M cells/mL were aspirated and captured in the AcouTrap. While trapped, the cells were washed with PBS and subsequently released in 30  $\mu$ L. To perform in-trap cell staining, fluorescent antibody dyes were aspirated over the cluster of trapped cells, followed by a wash. Cell samples were released and analyzed in a flow cytometer. Results We demonstrate automated washing of low cell number samples, achieving over 90% recovery. The system can collect cells from dilute samples and release the cells in a volume as low as 30  $\mu$ L with no decrease in viability. Furthermore, we demonstrate rapid automated staining and washing of trapped cell samples, achieving over 90% staining efficiency within minutes. The acoustic trapping chip can process cell samples at a flow rate of 50  $\mu$ L/min, with a maximum capacity of 50 000 cells per sample run. With customized acoustic trapping chips, the throughput and capacity can be increased. Conclusion The current study demonstrates the utility of acoustic trapping as a unique tool for automated processing of low cell number samples, enabling up-concentration, staining and washing, combined or as individual protocols, of precious cells with high recovery.

**901979 P176**

## **Hot Flow: Attune Plumbing for Radioactive Samples,**

Kathryn Fox<sup>1</sup>, Kathryn Dagna Sheerar Kyle Christie Alex Henkel Lauren Nettenstrom Ofelia Lapacek Zach Stenerson Ashley Weichmann Justin Jeffrey Jamey Weichert Manish Patankar

<sup>1</sup> UW-Madison

Flow cytometry with radio-labeled samples generates waste that is both a biological and radiological hazard. While samples can be cryopreserved until radiolabels have decayed (Carlson et al, PMC8313010), simple modifications can be made to the waste output(s) of the cytometer to reduce risks and allow for more timely analysis. Here we illustrate the modifications we made to a ThermoFisher Attune NxT cytometer and CytKick autosampler to route liquid waste to a shielded carboy, and provide a link to the full parts list and instructions for the modifications. Before making the cytometer available for researchers, we worked with our institution's Office of Radiation Safety to test residual radiation levels in the instrument and the liquid waste. Through this testing we determined that a Sanitize SIP function followed by a Quick Deep Clean brought radiation levels in the waste output down to background levels and also greatly reduced the residual radiation reading of the Sample Injection Port. For permit purposes, the cytometer is housed in the Small Animal Imaging and Radiotherapy Facility where experienced staff can oversee periodic radiation testing and waste disposal. Fresh waste carboys are pre-loaded with concentrated bleach and placed within a shielded container. The waste station sits on a scale and is labeled with a "full" weight so the fill level can be assessed without removing shielding or putting unnecessary strain on connection points during repeated checks. Once full, carboys are sealed with a solid cap and moved to a separate shielded storage location. When practical, carboys are stored for at least 10.5 half-lives, surveyed to confirm emissions have reached background, and liquid is rinsed down the drain. For longer-lived isotopes, full carboys are picked up by the Office of Radiation Safety. Future work will involve finding a bleach substitute to use if any researchers need to run samples labeled with radioiodine isotopes; bleach is not appropriate because oxidation could volatilize the radioiodine. This new ability to do "hot flow" opens up the opportunity for Carbone Cancer Center researchers to do experiments that would otherwise not be allowed at UW.

# CYTO 2022 ABSTRACTS

**902004 P178**

## **Innate Immune Response In Alzheimer`s Disease Mediated By Bradykinin,**

Micheli Pillat<sup>1</sup>, Henning Ulrich<sup>1</sup>, Fernanda Viero<sup>1</sup>, Leonardo Martins<sup>1</sup>

<sup>1</sup>Federal University of Santa Maria

Recent data show that the kinin system is stimulated by the pathologic amyloid- $\beta$  ( $A\beta$ ) in AD patients. The effects of this system are primarily mediated by bradykinin (BK) and its kinin-B2 receptor (B2R), and the role of BK/B2R in AD is not completely understood. Thus, the aims of this study were to determine effects of B2R blockage in different AD models: transgenic triple mouse as a model of the familial AD without B2R expression (APP<sup>swe</sup>/PS1<sup>dE9</sup>/B2R<sup>-/-</sup>) or injection of oligomeric  $A\beta$ -peptide mouse model. Our work is the first to show that  $A\beta$  oligomers increased blood-brain barrier (BBB) permeability and genetic and pharmacological blockade of B2R provided BBB protection in AD mice. Moreover, HOE-140, a B2R antagonist, prevented the increase of reactive oxygen species (ROS) in hippocampus of  $A\beta$ -treated mice, as evidenced by a decrease of DCFH-DA-positive cells. Interestingly, besides the neuroinflammation observed by an increase of microglia cells (Iba+ cells), the peripheral immune system also presented some alterations, which were modulated by BK/B2R signaling. HOE-140 counteracted the increase of IL-6 serum levels of  $A\beta$ -treated mice and prevented granulocyte death (7AAD+ cells), suggesting that NET formation in peripheral blood of AD mice depended on bradykinin signaling. Both HOE-140 and B2R<sup>-/-</sup> knockout prevented long memory loss in different AD models, observed in new object recognition task experiments. Moreover, 100nM, 500nM and 1 $\mu$ M  $A\beta$  oligomers progressively reduced neurosphere diameter in vitro, and 1 $\mu$ M HOE-140 prevented this effect. Moreover, differentiated APP<sup>swe</sup>/PS1<sup>dE9</sup> cells in vitro expressed up to 100-times levels of CCL12, CCL5 (RANTES), CCL3, CX3CR1 chemokine and C3, TLR2, and TNF inflammatory mediator levels as shown by real time PCR. The expression of the microglial marker Iba-1 was also 20-fold upregulated in APP<sup>swe</sup>/PS1<sup>dE9</sup>  $\rightarrow$ cells. Interestingly, HOE significantly decreased CCL12, CCL5 and C3 levels, while BK increased CCL12, CCL3 and TLR2 levels in APP<sup>swe</sup>/PS1<sup>dE9</sup>  $\rightarrow$ cells, suggesting that the B2R signaling triggers chemoattraction of inflammatory cells. Taken together, these data suggest that the B2R presents a key role in neuroinflammation observed in AD, from disruption of the BBB and peripheral immune system alterations to memory loss.

**901427 P180**

## **Impact of Fixation on Autofluorescence, Fluorescence, Spectral signature, and Data Quality,**

Giri Buruzula<sup>1</sup>, Yi Ren<sup>1</sup>, Felisha Lopez<sup>1</sup>, Pu Zhang<sup>1</sup>, Connie Gee<sup>1</sup>

<sup>1</sup>Novartis Institutes for Biomed

The current spectral flow cytometers have the capability to detect the entire emission spectra for fluorochromes depending on their laser configuration and number of detectors (5L Aurora detection range is 365-829nm). Signals from individual laser detector modules are stitched together to generate spectral signatures of the fluorochromes. The differences in spectral signatures across all lasers can be used to resolve challenging combinations of fluorochromes in the same panel with high spectral overlap (similar peak channel) otherwise unusable in a conventional cytometer. It is critical to preserve the integrity of spectral signatures during sample preparation. One factor that can impact spectral signatures is fixation used in sample processing. Very often, fixation is used in sample preparation, either to analyze intracellular targets or to preserve samples post immunostaining to allow for flexibility in data acquisition. Fixation time and fixatives used vary depending on the protocols. It has been reported that fixation can induce autofluorescence as well as influence fluorescence stability of FITC and PE when conjugated to different antibodies (Stewart et al. 2007; Lal et al. 1988). However, the impact of fixation on most fluorochromes remains unclear. In this study, we investigated the effects of fixation with 1.6% PFA on human PBMCs stained with 18 different fluorochromes and stored for up to 6 days. We assessed their fluorescence intensity, spectral signature integrity, stability of tandem dyes used, and cellular autofluorescence. The data were acquired on a 5L Aurora. To further examine the effects of fixation and sample storage on data quality, we used a 14-color panel (all of which are in the 18 fluorochromes assessed) to evaluate unmixing and ability to resolve populations. Our data indicate that fixation affects autofluorescence as reported previously, fluorescence intensity decreased with time on some of the fluorochromes, and changes spectral signature slightly on several fluorochromes. These changes also impact unmixing quality of certain fluorochromes. Further studies are planned with other fixation methods, especially for intracellular and intranuclear staining to evaluate selected fluorochromes and fluorescent proteins.



# CYTO 2022 ABSTRACTS

**P901468 P182**

## **Flow Cytometry Optimization Protocol Improves Detection of Fluorescent EV Populations,**

Sean M. Cook , Dove-Anna Johnson<sup>1</sup>, Nooshin Mirza Nasiri<sup>1</sup> , Jason Savage<sup>1</sup> , Joshua A. Welsh<sup>1</sup> Jennifer C. Jones<sup>1</sup>

<sup>1</sup>NIH

Introduction Flow Cytometry (FCM) is a useful tool for the analysis of cells and may be adapted as a method for analyzing smaller particles such as extracellular vesicles (EV). However, configurations for best achievable EV detection and resolution are not the same as are commonly used for cells, and therefore EV FCM assays require further instrument optimization to resolve EV populations. FCM Post Acquisition Software Suite (FCMPASS) software was developed to enable calibrated scaling of EV FCM data for both fluorescence and scatter intensities, and we present here a major update to the software, which enables optimization of fluorescent detector settings and reports calibrated per-channel limits of detection. Methods 8-peak rainbow calibration beads (Spherotech) were acquired on Aurora and CytoFLEX cytometers across monotonically increasing fluorescent gains (10000 bead events/acquisition). Two side scatter channels were used to collect the rainbow bead events and sample the instrument optical noise separately. FCMPASS code (MATLAB, <https://nano.ccr.cancer.gov>) was updated to include a setting optimization module using acquired data rainbow bead data. Validation for EV phenotyping studies was performed with PSMA-positive PC3-PIP EVs, derived from conditioned serum free OptiMEM media (Lonza) cultures, JumboSep Omega 100K (PALL) ultrafiltration, qEV10 (Izon) size exclusion chromatography, and PE anti-PSMA (BioLegend). Results Data analysis was completed with FCMPASS. Following manual gating of the noise peak and rainbow bead events, the software gated individual rainbow bead populations on each fluorescent channel, normalized the bead populations and noise, and determined the gain for which the noise was most separated from the bead populations for each fluorescent channel. We compared this optimal gain with manufacturer-recommended settings using PC3-PIP extracellular vesicles overexpressing PSMA stained with a PSMA-PE conjugated antibody confirmed improved resolution of fluorescent extracellular vesicle population, relative to resolution with manufacturer-recommended settings. Conclusions Improved resolution of fluorescent EV populations will allow for greater probing into the supposed heterogenous nature of

EV populations and allow for phenotyping of EV populations previously undetectable. We have expanded FCMPASS to support a routine voltration protocol as a simple way to optimize flow cytometer fluorescent settings for avalanche photodiode (APD) cytometers. This current implementation of FCMPASS has only been verified on APD instruments. While the algorithm is readily applicable to PMT instruments, computational efficiency must be improved for adoption by PMT instruments, and future work will center upon extending the protocol to photomultiplier tube (PMT)-based and other optical FCM instruments.

**901546 P184**

## **Monitor Critical Parameters in Advanced Flow Cytometers,**

Daniela Ischiu Gutierrez<sup>1</sup>, Erica Smit<sup>1</sup>, Richard Nguyen<sup>1</sup>, Esther Thang<sup>1</sup>, David Ambrozak<sup>1</sup>, Mario Roederer<sup>1</sup>, Stephen Perfetto<sup>1</sup>

<sup>1</sup>NIAID

Flow cytometry is used to detect small biological and synthetic particles. Due to important data that is generated from flow cytometers, it is critical to establish a quality control program, which includes instrument calibration, optimization, and standardization. In doing so, researchers can obtain accurate and reproducible data output. This poster focuses on the importance of flow cytometer standardization for biological reproducibility purposes. To achieve this, the instrument undergoes daily quality control (QC). The standardization process consists of verifying the absence of fluidics issues and tracking specific particles to control laser alignments and laser time delays. Methods: Our performance standards test for an optimal laser delay, area scaling, and verifying an unobstructed and hydrodynamically focused fluidics system. For this we use Supra, Rainbow, and Negative Control Beads. We run positive QC beads to track critical values, e.g.: laser delay, robust coefficient of variation (rCV), median fluorescence intensity (MFI) and detector voltages. After voltages and tolerance ranges have been set, rainbow and supra beads mix must be run. To calibrate intensities and measure instrument performance on a standardized scale, fluorescent calibration marker beads (FC beads), were run in a longitudinal study to demonstrate instrument technical reproducibility. Results and Conclusions: At least 20 continuous data points are collected for the parameters described above. Tolerance ranges are established and captured, and trends are assessed monthly. Daily monitoring parameters are critical as they pick up rCVs deviations, and large changes

# CYTO 2022 ABSTRACTS

in voltages due to MFI fluctuations. Additionally, the beads help assess fluidics or other alignment issues. Incongruencies in rCVs, MFIs and voltage values can be identified early. Data reflects an out-of-range rCV point, thus showing the instrument's inability to generate biological reproducibility. Tolerance ranges are compared to relative channel numbers showing the errors when set side-by-side to quantitative units. In some cases, these values can be as high as a 6X difference. Moreover, FC beads were acquired on 2 different flow cytometer analyzers for a longitudinal study over 19 experiments, demonstrating inter- and intra-instrument comparability and performance over time. These findings show that setting and monitoring tolerance ranges is vital to maintaining the consistency and performance of flow cytometers, eliminating technical variability for correct biological data interpretation. Based on these findings we show that optimizing and standardizing flow cytometers generate biologically reproducible results. If a cytometer has been optimized yet fails to meet defined tolerances, biological reproducibility may be compromised and a service engineer must be consulted. Instruments with large variance ranges should not be used in research or clinical trials and should be evaluated to improve performance

**894956 P186**

## **Bacterial mock communities as standards for reproducible cytometric microbiome analysis,**

Susann Müller<sup>1</sup>

<sup>1</sup> Helmholtz Centre for Environmental Research – UFZ

The composition of natural microbial communities rapidly changes due to the short generation times of the microorganisms, interactions with fluctuating environments, and migration. Microbial flow cytometry has recently established itself as a tool to track short-term community dynamics and link with ecological parameters. Here, we developed an artificial microbial Cytometric Mock Community (mCMC) as a reference standard and benchmark to support the generation of dynamic, high quality cytometric microbial community data (Nature Protocols, 2020, 15, 2788-2812). The mCMC comprises up to four different species, two gram negative (*S. rhizophila*, *E. coli*) and two gram positive (*P. polymyxa*, *K. rhizophila*) strains. It supports comprehensive instrument adjustment, specifically for small cells with scatter and fluorescence intensities below the 0.5 µm microspheres. Our approach upholds

quantitative assessments and qualified decisions for sorting of subcommunities suitable for subsequent high resolution sequencing or proteomic routines.

**901381 P188**

## **Optimizing User-Staff Communication in a Large Multi-Site Shared Resource Laboratory,**

Derek Jones<sup>1</sup>, Jonni S. Moore<sup>1</sup>, William Murphy<sup>1</sup>,

<sup>1</sup> University of Pennsylvania

Introduction: The Penn Cytomics Shared Resource Lab is one of the largest academic cytometry labs in the world, with over 9 satellites, 37 instruments and serving over 1000 users. Maintaining timely and useful interactions with our users is critical to assuring investigators have the technology access they require to perform successful studies. This can include real-time digital communications (ex. Slack, instant messaging, text messaging), instrument desktop access to troubleshooting, messaging capabilities to staff online, seminars, live meetings). Our goal was to identify the preferred and most effective communication tools for each task and to create a comprehensive communication plan for Penn Cytomics. The overall aim is to identify processes to support the efficient operation of a large, shared resource lab in a cost-effective manner. This plan will become a cornerstone for all business, technical and scientific processes to best establish and maintain easy and effective communications with our users at close and distant sites, and to integrate this plan with our daily operations. Methods: There are 3 primary steps to implementing a communication plan into our operation: design, develop, apply. Each part has multiple steps. The information reported here focuses on the design aspect. To understand how users best receive information, we conducted a survey, via Survey Monkey, of 431 users who had been logged into our system over the last 60 days. We asked their opinions about how we are communicating with them currently, what works and what doesn't, and some possible new approaches that could be more effective. We will expand this information by doing live interviews with selected responders. Results and Conclusions: Our response rate was 23% (99 out of 431 surveys sent) and preliminary analysis of the survey data indicated that the users who resounded identified as the best way to communicate is through email (89%). Many users would like a Penn Cytomics Slack channel (65%) for communicating with staff about down machines and to assist in troubleshooting. The information that users felt most valuable was cytometer instrument status (60%), including QC pass or fail and

# CYTO 2022 ABSTRACTS

instrument status (down or running). Using this data as well as user interviews, our next step is to design and develop a plan and processes that will be easy to implement and test it, integrated into in our daily operations. This user-facility communication plan will serve as the basis for enhancing interactions with our large and disperse client base and to identify processes that not only can support direct communication with users, but also enhance our workflow by identifications of instrument and user issues in a more timely manner.

---

**901928 P190**

## **SRL Technicians Exchange: How Knowledge Sharing Increases Versatility and Offers Fresh Insight in Facility Operations.,**

Rachael Walker<sup>1</sup>, Sam Thompson<sup>1</sup>, Aleksandra Lazowska-Addy<sup>1</sup>, Christopher Hall<sup>1</sup>

<sup>1</sup>Babraham Institute

This poster will describe the experiences and benefits of a technician exchange programme between the Babraham Institute and Newcastle University, UK. These programmes are of great benefit to both senior and junior SRL staff, especially the latter, and we will highlight these benefits. This will be illustrated through the personal perspectives of the SRL technicians whom took part and we will outline examples of where cross-training and knowledge exchange led to the implementation of new innovations and technical solutions in our facilities which validated the exchange. An exchange opens an unbiased dialogue into standard operating procedures in the lab which, with constructive input and critical thinking, can influence and theoretically stress test the reliability and integrity of practical approaches taken. This supplies the framework for an evolution, growth, and adaptation of methods to form a more consistent and standardised approach to applications across a larger community of cytometrists which can be progressively shared through an open and active repository. Knowledge exchange programmes align with the ethos of the Technicians' Commitment which aims to improve visibility, recognition, career development and sustainability for technicians working in higher education and research by serving as a functional technical education tool. These opportunities are invaluable following two years of limiting virtual and remote learning exercises as physical, practical interactions within a lab environment allow for more thorough and genuine hands-on experience. SRL staff from the Babraham Institute Flow Cytometry Facility and the

Newcastle University Flow Cytometry Core Facility took part in an exchange for three days with staff travelling to attend the alternating facility. During the time spent at the hosting facility, SRL staff are be exposed to a variety of new flow instrumentation, take part in day-to-day practices, network with the respective members of staff, and gain an insight and new perspective in the work ethics of a different facility. Pursuing this concept further and involving other willing, openly collaborative facilities within the community, will build a network of SRL staff and develop mutually beneficial links with other leading external contacts. Staff themselves can strengthen their academic profiles and increase their own employability.

---

**902031 P192**

## **Quality Control Testing of Biobank Cryopreserved PBMCs,**

Karen Millerchip<sup>1</sup>, Carlos Ramos<sup>2</sup>, Heather Otte<sup>2</sup>, Cara Haymaker<sup>2</sup>

<sup>1</sup>MD Anderson Cancer Center

One of the challenges for biobanks is developing and maintaining a consistent process for cryopreserving peripheral blood mononuclear cells (PBMCs). PBMCs are banked, along with serum and plasma, for later clinical trial translational research correlates such as flow cytometry, single-cell sequencing, and live-cell assays such as ELISPOT. Many factors can influence the quality of these blood products including the cell isolation procedure, time between blood draw and processing, time to freeze down the cells, and staff turnover. To address this challenge, the CCSG ORION Core developed a quality control testing procedure that provides participating biobanks a pass/fail report on percent cell recovery, percent cell viability, and an assessment of the percent of T cells, B cells and NK cells by flow cytometry after cryogenic storage. The main focus of the QC test is on cellularity and viability post cryopreservation. To provide comparative data, ORION processes and banks their own PBMCs from normal donor buffy coats procured from the Gulf Coast Regional Blood Center. These buffy coats are processed via a Ficoll gradient and are frozen using 10% DMSO in fetal bovine serum at a rate of -1°C/minute and stored in a vapor phase liquid nitrogen freezer. Each normal donor is then quality tested, and passing donor aliquots are then used as a QC control for biobank samples. Additional parameters for QC testing, such as a reference range of T cell/B cell/NK cell percentages, are explored here from retrospective flow cytometry analysis.

# CYTO 2022 ABSTRACTS

**900938 P194**

## **An integrated single-cell multiomics approach to characterize mRNA, intracellular, and surface proteins using intracellular AbSeq and BD® AbSeq Immune Discovery Panel,**

Adam Wright<sup>1</sup>, Hye-Won Song<sup>1</sup>, Jody Martin<sup>1</sup>, Eileen Snowden

<sup>1</sup>BD Biosciences

DNA-barcoded antibodies enable single-cell multiomics approaches that examine protein alongside mRNA in a single cell. Although it is a powerful approach, leading methods are currently limited to surface proteins, which limits understanding of signal-transduction and transcriptional pathways that are often governed by expression changes and posttranslational modifications of intracellular proteins. The ability to analyze intracellular proteins alongside the transcriptome is complicated by the fix and perm processes necessary to access intracellular epitopes, which can negatively impact RNA assay sensitivity. Furthermore, nonspecific binding of antibody-oligos to nucleic acids can generate high background signals. To address these issues, we generated a protocol that can recover high-quality RNA alongside specific intracellular and surface protein information. Using this protocol in conjunction with the BD Rhapsody™ Single-Cell Analysis System, we simultaneously profiled over 50 protein markers including 14 intracellular proteins with the whole transcriptome. We identified predicted patterns, including increased phosphorylation of AKT protein correlated with the proliferation marker Ki67 upon immune stimulation, and transcription factor (T-bet) expression in a specific cell subset. Together these preliminary results suggest that analysis of intracellular proteins together with the transcriptome may be possible using single-cell sequencing technologies and can enable a deeper understanding of cellular states.

**901130 P196**

## **High-parameter protein profiling on the BD Rhapsody™ Single-Cell Analysis System,**

Manish Thakran,<sup>1</sup> Amie Radenbaugh<sup>1</sup>, Devon Jensen<sup>1</sup>, Aruna Ayer<sup>1</sup>

<sup>1</sup>Texas A&M University

High-parameter protein profiling on the BD Rhapsody™ Single-Cell Analysis System Manish Thakran,<sup>1</sup> Amie Radenbaugh,<sup>1</sup> Devon Jensen,<sup>1</sup> Aruna Ayer,<sup>1</sup> Hye-Won Song<sup>2</sup> 1BD Biosciences, 2350 Qume Drive, San Jose, CA 95131 2BD Biosciences, 10975 Torreyana Rd, San Diego, CA 92121 Recent technology using DNA-barcoded antibodies alongside single-cell (sc) RNAseq has emerged as a powerful multiomic approach for sensitively profiling complex and diverse cell populations. This approach requires both protein and gene expression analysis to identify and characterize putative cells; however, there are many applications that require only protein profiling without the need for gene expression data. For protein-only profiling applications, sequencing mRNA is not needed and can be burdensome as it adds unnecessary library generation and sequencing costs to a user; yet many single-cell analysis tools still require these data for analysis. Additionally, samples with compromised RNA stability would not be analyzed by tools relying on gene expression data, therefore a protein profiling-only approach provides a powerful alternative solution that can generate meaningful information about cells that would otherwise not be considered in an analysis. Therefore, we developed a bioinformatic pipeline for the BD Rhapsody™ System that can identify and profile putative cells solely from protein data. Here, we evaluate the accuracy and utility of this bioinformatic pipeline by comparing its data output with the standard BD bioinformatic pipeline that utilizes both protein and gene expression data. We found that the new protein-only pipeline can comparably call cells without RNA information. Furthermore, we identified additional cells with low RNA abundance that were missed from the standard pipeline. Finally, we developed a protocol to generate a protein-only library and tested various sequencing strategies. Altogether, this methodology, in association with our new bioinformatic pipeline, reduces cost and enables users to profile over hundreds of protein markers simultaneously in individual cells. For Research Use Only. Not for use in diagnostic or therapeutic procedures. BD, the BD Logo and BD Rhapsody are trademarks of Becton, Dickinson and Company or its affiliates. © 2022 BD. All rights reserved. 0322

# CYTO 2022 ABSTRACTS

**901539 P198**

## **Single-cell interactive cytometry using made-to-order droplet ensembles.**

Russell Cole<sup>1</sup>, Ian Walton<sup>1</sup>, William Hyun<sup>2</sup>, Justin Madrigal<sup>1</sup>

<sup>1</sup>Scribe Biosciences, Inc., <sup>2</sup>Genoa Ventures

Cell-cell interactions are important to numerous biological systems, including tissue microenvironments, the immune system, and cancer. However, current methods for the precise study of single-cell combinations and interactions are limited in scalability, allowing just hundreds to thousands of multi-cell assays per experiment; this limited throughput makes it difficult to characterize interactions at biologically relevant scales. Here, we describe a new paradigm in cell interaction profiling, Microenvironment on Demand (MOD), that allows for the construction of precision cell ratio assays and characterization of their interactions for tens to hundreds of thousands of combinations. MOD leverages high throughput droplet microfluidics to construct multicellular combinations in a deterministic process that allows inclusion of programmed reagent mixtures and beads. The combination droplets are compatible with common manipulation and measurement techniques, including imaging, barcode-based genomics, and sorting. We demonstrate the efficacy of MOD by building assays with a variety of cell types (PBMCs, NKs, CAR-T) and measuring single cell functional readouts such as cytokine secretion, granzyme, and cytotoxicity, enabling single-cell library screening at scale. The compatibility of MOD assays with 3rd party flow cytometry and scRNA-seq instruments is also demonstrated.

**901902 P200**

## **Accelerating generation of single cell clones by using CellRaft™ AIR system coupled with Fluorescence Activated Cell Sorting,**

Sobha Thamminana<sup>1</sup>

<sup>1</sup> Kite Pharma

Accelerating generation of single cell clones by using CellRaft™ AIR system coupled with Fluorescence Activated Cell Sorting  
Sobha Thamminana<sup>1</sup>, Aronpreet Atwell<sup>1</sup>, Jessica Hartman<sup>2</sup>, Richard Smith<sup>1</sup>, and Bhargavi Rajan<sup>1</sup> <sup>1</sup>Flow Cytometry and Cell Engineering Core; Cell Biology, Kite Pharma, a Gilead Company, Emeryville, CA 94402 <sup>2</sup>Cell Microsystems Durham NC 27713  
CRISPR genome engineering of target cell lines enables target discovery and serves to provide exceptional disease model

for preclinical research, including in the field of CAR T therapy. The bottleneck for engineering cells continues to be single cell clone generation. Current processes vary from manual limiting dilution (preferred for adherent lines), to using a variety of high-speed cell sorters to a combination of both (bulk sort and plate them into single cells). In order to increase the frequency of single cell clone generation, we looked at various technologies available at disposal including several varieties of cell sorters, and an image-based cell isolation system, CellRaft AIR™ by Cell Microsystems™. Here we evaluate these technologies for isolating single cell clones based on their colony forming efficiency, ease of use and out-growth of cells. All the platforms we analyzed, show comparable results in terms of their single-cell growth efficiencies. We have observed less than 30% out-growth from each 96 well plate from BDFACS Aria fusion™, Sony SH800™, and Thermo Fisher Bigfoot™ sorters based on the cell type. Adherent lines show much lower growth efficiency (3%). However, with CellRaft™ AIR system, we isolated almost 400 single-cell rafts (more than 4X96 well plates) from each array. From those, more than 50% have out-growth. Additionally, this system allows us to image and monitor the cell growth from single cell to at least 32 cell stage before isolating them into 96 well plate. Moreover, the instrument does not require start up and shut down time, as with cell sorters, that take several hours of preparation time based on the nozzle used and stability of the fluidics as well as operator's experience. In comparison, CellRaft™ AIR system needs array preparation time 24hrs prior to seeding cells and after isolation the clones take 5-10 days to reach multi-cell stage. CellRaft™ systems needs optimization in determining seeding density, array type, and array coating for each suspension cell type needs to be optimized. Overall, CellRaft™ air system in combination with BDFACS Aria fusion™ or used as a stand-alone system shortened our timelines considerably compared to other FACS platforms alone.

# CYTO 2022 ABSTRACTS

902035 P202

## Realtime enrichment and high-dimensional morphology analysis of malignant cells from effusion samples using deep learning,

Chassidy Johnson<sup>1</sup>, Anastasia Mavropoulos<sup>1</sup>, Janifer Cruz<sup>1</sup>, Jordan Nieto<sup>1</sup>, Kiran Saini<sup>1</sup>, Jeanette Mei<sup>1</sup>, Weibo Yu<sup>2</sup>, Stephane Boutet<sup>1</sup>, Thomas Lee<sup>2</sup>, Nianzhen Li<sup>1</sup>, Jianyu Rao<sup>2</sup>, Mahyar Salek<sup>1</sup>, Maddison (Mahdokht) Masaeli<sup>1</sup>

<sup>1</sup>Deepcell Inc., Menlo Park, CA, <sup>2</sup>University of California, Los Angeles (UCLA), Los Angeles, CA

Malignant ascites and pleural effusion samples represent a non-invasive (compared to tissue biopsy) and valuable source of tumor cells with great potential for diagnostic, precision medicine and biomarker discovery work. Thus, development of tumor cell isolation methods capable of capturing the phenotypically heterogeneous populations of malignant cells that are often in low abundance, yet remaining amenable to diverse downstream analysis methods including molecular and functional assays, would be of great value. We developed COSMOS, a novel platform that combines microfluidics and brightfield imaging with artificial intelligence for high-dimensional morphology analysis to profile cells based on morphology in real-time resulting in a population of unlabeled, viable and unperturbed single cells which can be used for molecular and functional analysis. In addition to enrichment, the cell images can be used to generate high-dimensional morphological profiles that can be visualized by Uniform Manifold Approximation and Projection (UMAP) to discover morphologically heterogeneous populations of cells. We applied COSMOS to the challenges in malignant effusion samples by training a deep convolutional neural network classifier using >3 million training cell images from malignant body fluid samples. In silico analysis was used to validate the model (AUC=0.96). Sorting performance was demonstrated by SNP analysis on contrived clinical samples. We then verified enrichment of malignant cells from clinical samples. Cytology analysis of sorted samples yielded intact malignant cells with comparable morphological characteristics and higher purities compared to pre-sorted samples. Copy number variation analysis demonstrated increased amplitude of deletion and amplification peaks, and targeted sequencing showed increased allele frequency of somatic mutations of TP53 in sorted compared to pre-sorted samples. Furthermore, single cell RNAseq showed an enrichment of cells with gene expression profiles indicative of carcinoma cells. Using UMAP analysis of embeddings, we found

multiple distinct clusters of cells with morphologic features indicative of cancer cells that were present in the malignant and absent in the benign ascites sample. Together these results demonstrate that COSMOS can yield enriched populations of malignant cells from effusion samples that are compatible with common downstream analysis methods used in cytology, precision medicine and discovery studies. Additionally, high-dimensional morphology analysis can reveal heterogeneous populations of tumor cells that can offer a new dimension to understand tumor cell diversity within the fluids. Further work is planned to evaluate the link between the morphological, molecular and functional characteristics of identified subpopulations.

898319 P204

## See-N-Seq: RNA Sequencing of Target Single Cells Identified by Microscopy,

Jeonghyun Lee<sup>1</sup>, Emily Park<sup>1</sup>, Kerryn Matthews<sup>1</sup>, Hongshen Ma<sup>1</sup>

<sup>1</sup>University of British Columbia

Single cell RNA sequencing has the potential to elucidate transcriptional programs underlying key cellular phenotypes and behaviors. However, there are many phenotypes that are incompatible with indiscriminate single cell sequencing because they are rare, transient, or can only be identified by imaging. Existing methods for isolating cells based on i, g for single cell sequencing are technically challenging and prone to cell loss because of the need to physically extract single cells. To address this challenge, we developed See-N-Seq, a simple strategy to selective sequence RNA from single cells identified by microscopy without needing to physically extract each cell. The See-N-Seq process involves (1) dividing cells among microwells, (2) fixing cell position by encapsulation in porous hydrogel thin-film, (3) imaging to select one target cell from each microwell, (4) target cell isolation by embedding non-target cells in non-porous hydrogel, and (5) selective lysis and mRNA extraction for sequencing preparation. We first investigated laser micropatterning of hydrogel porosity by polymerizing a non-porous hydrogel inside a porous hydrogel. Using a laser scanning system integrated inverted microscope, we achieved a minimum spatial resolution of 12 μm using 20X objectives. To confirm micropatterning of hydrogel porosity, we stained the hydrogel using 10 kDa FITC-dextran, which only stained the central circular region of the porous hydrogel. Micropatterning the non-porous hydrogel to selectively expose target cells and

# CYTO 2022 ABSTRACTS

embed non-target cells enabled selective lysis of a single target cell, which is demonstrated by the loss of fluorescence after adding the lysis buffer. RNA isolation from target single cells were test by qPCR, which were confirmed by the presence of the mCherry or EGFP transgenes in the appropriate target cells. To demonstrate See-N-Seq transcriptome sequencing of complex image-defined cell phenotypes, we generated an immunological synapse using model T-cells (Jurkat), antigen presenting cells (Raji), and SEE super-antigen. Synapses cell pairs were selected based on the localization of CD3 after 0, 4, and 24 hours of incubation (S0sc, S4sc, S24sc). Controls included single Jurkat (Jsc), single Raji (Rsc), and non-synapsing cell pairs (N0Ssc, NS4sc, NS24sc). Differential gene expression analysis revealed distinct transcriptomes between Jsc and Rsc, but highly consistent transcriptomes between S0sc and NS0sc, as well as between NS0sc and merged Jsc+Rsc data sets. Transcriptomes of immunological synapses at 4 hr (S4sc) begins to diverge from synapses at 0 hr (S0sc). After 24 hr incubation, the S24sc transcriptomes diverged into two distinct groups, corresponding with Th1 (S24scG1) and Th2 (S24scG2) lineages. See-N-Seq addresses a key challenge in single cell sequencing to associate single cell transcriptome data directly with observed cell phenotypes to elucidate transcriptional programs that drive specific cellular processes.

**898549 P206**

## **A virus, a stim and a control enter a room: Novel phenotypic differences discovered from sort to sequence experiments,**

Aaron Tyznik<sup>1</sup>, Robert Balderas<sup>1</sup>, Jack Panopoulos<sup>1</sup>, Jay Almarode<sup>1</sup>

<sup>1</sup>BD Biosciences

The single-cell sequencing revolution has vastly increased the pool of phenotypes and functional states of cells throughout the body. Hundreds of cell surface or intracellular markers can be monitored on cells and existing RNAs can be identified on a per cell basis, thus multiplying the number of phenotypes discoverable in a single experiment. Compared to flow cytometry, the number of dimensions that can be analyzed on any given cell are between 2- and 25-fold more. However, the comparison of samples from single-cell sequencing experiments is hampered by a plethora of technical effects including the identification and removal of doublets, dead cells and debris, batch effects, discordance between RNA and protein expression,

read-loss due to antigen skewing, and the relatively high cost of sequencing. These detrimental technical effects contaminate the data, ultimately leading to false positives and an agonizing amount of time re-analyzing these data to mitigate these effects. Sorting of target populations prior to sequencing greatly reduces the false-positive error rate, reduces the occurrence of dead cells, doublets and debris, and diminishes antibody read-loss. It is also much less expensive to sort and enrich a broad target population than to run multiple sequencing panels to accumulate enough cells to achieve statistical relevance. Herein we analyze AbSeq data from pre-sorted mouse NK and CD8 T effector memory cells from mice infected with the single-stranded RNA virus MCMV, stimulated with Poly I:C or left untreated. Importantly, the Poly I:C-stimulated mice served as a solid internal control to validate phenotypes discovered in the MCMV cohort. The cells were fluorescently labeled for sorting, barcoded and pooled prior to staining with 54 sequence-tagged antibodies, reducing many of the technical effects common to single-cell sequencing experiments. Cells were then sorted, sequenced and analyzed, producing a myriad of novel phenotypes from the NK and CD8 T effector memory populations. We find that maximizing the sorting potential and barcoding samples prior to the addition of sequence-tagged antibodies greatly enhances the yield of high-quality data, in terms of the purity of single-cell isolation and reduction of technical batch effects.

**899721 P207**

## **Conjugated Oligoelectrolytes (COE): A Novel Class of Fluorogenic Membrane Dyes That Do Not Form Micelles of the Same Size as Extracellular Vesicles**

Wan Ni Geraldine Chia<sup>1</sup>, Sarah Cox-Vazquez<sup>1</sup>, Vera Tang<sup>2</sup>, Andria Doty<sup>3</sup>, Betsy Ohlsson-Wilhem<sup>4</sup>

<sup>1</sup>National University of Singapore, <sup>2</sup>University of Ottawa, <sup>3</sup>University of Florida, <sup>4</sup>SciGro, Inc.

The detection of extracellular vesicles (EVs) on flow cytometers usually works in tandem with fluorescent membrane dyes, traditionally relying on the carbocyanine family of dyes. The challenge in working with these dyes is that they form aggregates with similar dimensions to EVs when diluted into aqueous media, thereby confounding accurate assignments. Carbocyanine dyes are characterized by two long aliphatic chains and a hydrophilic headgroup. This amphiphilic framework promotes aggregation, even at low concentrations. To address the challenge, a fundamental change in dye chemistry is required. In response, we designed a new class of amphiphiles,

# CYTO 2022 ABSTRACTS

known as conjugated oligoelectrolytes (COE). COEs are characterized by a hydrophobic conjugated core that is flanked by side chains carrying positively charged ionic pendants. Their molecular framework deviates from that of carbocyanines and mimics the hydrophobic/hydrophilic profile of the lipid bilayer, thereby allowing COEs to intercalate spontaneously into lipid bilayers. The structural features of COE confer excellent solubility in aqueous media. We have demonstrated that COEs labelled PC3 EVs with high efficiency, >70% dye-positive events detected on the conventional flow cytometer and the nano flow cytometer. In the absence of EVs, no particles were detected in the aqueous solution of pure COEs, in contrast to the positive events detected with pure PKH26 dye solution. The low background signal of COE is also related to its “light up” mechanism, where the fluorescence emission increases only when the COE is bound to the target. Moreover, there is minimum exchange of dyes between two populations of 130 nm vesicles labeled with COE, suggesting the stability of COE after being inserted into the lipid bilayer. Membrane dyes are positioned to be useful for EV detection because (1) all EV have a lipid bilayer and (2) the labelling efficiency of membrane dyes is typically high. As such, they will be useful for labeling the entire EV population, that can then be used for normalization in multiplexing for sub-population analysis. The design and development of the COE dye herein therefore provides new opportunities for EV research, in which COEs fulfil the functions of a membrane dye whilst circumventing the challenges lipid-specific dyes are traditionally associated with.

**901042 P208**

## **Enrichment of microRNA and Virus-Like Particles using a novel avalanche photodiode-based benchtop cell sorter,**

John Tigges<sup>1</sup>, Brandy Pinckney<sup>1</sup>, Ionita Ghiran<sup>1</sup>

<sup>1</sup>Beth Israel Lahey Health

In recent years extracellular vesicles (EVs) have become one of the most studied entities due to their ability to regulate gene expression and alter the function of various cell types. There has been significant interest in the cargo and the cells of origin due to this effect. Nano-flow cytometry is one of the techniques employed in these characterization efforts. With hardware advancements and the increase in the use of flow cytometry to analyze EV populations, there have been efforts to standardize nano-flow data for ease of comparison and collaboration. While

these efforts have made progress for nano-flow analysis, nano-sorting is still a complex technique that is not commonly used. It has been previously demonstrated on a MoFlo Astrios (Beckman Coulter, Brea, CA) that nanoscale vesicles could be sorted with efficiencies ranging from 25 to 45%. In an effort to increase this efficiency, we employed the use of the CytoFLEX SRT (Beckman Coulter, Brea, CA) and miRNA detection via molecular beacons. Due to the complimentary nature of the CytoFLEX SRT and the CytoFLEX S, both use APD detectors, WDM, and VSSC detection, it was deemed as a suitable instrument for sorting of nanometer sized particles. In addition, the automated sort setup and minimal instrument modifications necessary to perform nano-flow cytometry made the instrument an attractive option for standardized and reproducible experiments. Previously, Pereira et al described successful analysis of the miRNA content of red blood cell derived EVs (RBCEVs) using MBs and nano-flow cytometry. Therefore, in order to validate the plausibility of the CytoFLEX SRT as a small particle sorter, miR451a and miR495 specific molecular beacons (MBs) were used. Red blood cell derived EVs (RBCEVs) and platelet derived EVs (PEVs) were generated via calcium ionophore treatment and incubated with MB451-AF488 and MB 495-AF594, respectively, after size exclusion chromatography. The RBCEV MB451-AF488 sample was analyzed under FITC channel fluorescent triggering. The sample was sorted into positive and negative after which fluorescent microscopy was used to verify increased target miRs in the positive as compared to the negative. After the SRT's ability to sort was verified PEVs and RBCEVs were combined. The AF488 and AF594 positives were sorted out and verified via fluorescent microscopy. These results show the CytoFLEX SRT to be a viable instrument for sorting of nanoscale particles and the potential of molecular beacons to be multiplexed.

**901685 P210**

## **Fluorescent nanoparticle flow cytometry calibrators with NIST-assigned ERF and concentration values for Viral and EV analysis,**

Lili Wang<sup>2</sup>, Paul DeRose<sup>2</sup>, Yu-Zhong Zhang, <sup>1</sup>, Adam York<sup>1</sup>

<sup>1</sup>Thermo Fisher Scientific <sup>2</sup>NIST

The analyses of viruses and extracellular vesicles (EVs) by flow cytometry is a rapidly growing area of interest, even more so since the onset of the COVID-19 pandemic. Instrument hardware has and continues to be adapted for detection of nanoparticle-based samples. Currently, most nanoparticle detection problems



# CYTO 2022 ABSTRACTS

by flow cytometry arise from poor instrument particle size resolution, inaccurate concentration measurements and or inconsistent fluorescence intensity values due to improper instrument settings. To help address these detection issues, we have collaborated with the National Institute of Standards and Technology (NIST) to develop the first ever fluorescence intensity and concentration nanoparticle standard kit to aid in the analyses of viruses and EVs by flow cytometry. This first of its kind fluorescent nanoparticle kit (ViroCheck NanoParticle Reference Kit) is comprised of 5 fluorescent components with particle diameters ranging from 100 to 500nm. This includes FITC-like (100nm), PE-like (100nm), APC-like (100nm) and Multicolor (200 & 500nm) fluorescent nanoparticles with NIST-assigned equivalent number of reference fluorophore (ERF) values for UV to red laser excitation. In addition, both the 200 and 500nm components are supplied with NIST-confirmed particle/mL concentration values. This kit will provide users with several nanoparticle calibrators that will help determine the appropriate instrument settings for detection of viruses and EVs, allow standardization of the fluorescence intensity scale for accurate data comparisons, and known nanoparticle concentration values for help in determining viral or EV sample concentrations. Herein, we will discuss and highlight the features of these new nanoparticle calibrators for flow cytometry

**901984 P212**

## **Detection of extracellular vesicles using the BD FACSymphony™ A1 Cell Analyzer,**

Estefanía Lozano-Andrés<sup>1</sup>, Tina Van Den Broeck<sup>1</sup>, Mark Delsing, Annette Meyer, Estefanía Lozano-Andrés<sup>#</sup>, Tim Schenkel, Marca Wauben<sup>2, #</sup>,

<sup>1</sup> Becton Dickinson, BD Biosciences, Europe, <sup>2</sup> Department of Biomolecular Health Sciences, Faculty of Veterinary Medicine, Utrecht University, Utrecht, The Netherlands, <sup>3</sup> Becton Dickinson, BD Biosciences, CA, United States, <sup>#</sup> TRAIN-EV Marie Skłodowska-Curie Action-Innovative Training Network, train-ev.eu

Extracellular vesicles (EVs) are small lipid-based vesicles secreted from cells. Present in all bodily fluids, EVs carry various biomolecules such as proteins, lipids, DNA and RNA. Accurate characterization of EVs is critical to further explore their biological function and potential diagnostic and therapeutic applications. Flow cytometry provides an attractive analytical approach as the heterogeneous EV populations can be studied with high-throughput, single-vesicle, multiparameter analysis.

Conventional flow cytometry instruments and methods optimized for cell analysis are not well suited for the measurement of EVs as the small size and low refractive index of EVs make it challenging to resolve them from noise. Improvement in instrument performance, method robustness, experiment design, data analysis and cross-measurement standardization are necessary to support analysis of EVs using flow cytometry. In this study, we evaluated the BD FACSymphony™ A1 Cell Analyzer with Small Particle Detector Option for analysis of small particles including EVs and sub-micron beads. Following the MIFlowCyt-EV framework for publication, we stained and examined EVs purified from the MCF7 breast cancer cell line, along with necessary controls, using a novel small particle side scatter channel (SP-SSC, the BD® Small Particle Detector Option). We also explored the value of “OR” thresholding (SP-SSC “OR” fluorescence) over fluorescence only. Using the FACSymphony A1 Cell Analyzer, we evaluated the sensitivity, size resolution, noise levels and dynamic range using various sub-micron beads and/or compared to the regular side scatter channel, which can be run in parallel to the SP-SSC. We also tested performance and setup robustness by evaluating data from instrument to instrument and day to day tests. Class 1 Laser Product. For Research Use Only. Not for use in diagnostic or therapeutic procedures. BD and BD FACSymphony are trademarks of Becton, Dickinson and Company or its affiliates. © 2022 BD. All rights reserved. 0322 Funding: European Union’s Horizon 2020 research and innovation programme under the Marie Skłodowska-Curie grant agreement No [722148] BD Biosciences is a partner organization in TRAIN-EV and offered training and secondment to a PhD student within the consortium.

# CYTO 2022 ABSTRACTS

**902008 P214**

## **Good practice for analyzing extracellular vesicles using the BD FACSymphony™ A1 Cell Analyzer,**

Ludovic Monheim<sup>1</sup>, Andrew Bantly<sup>1</sup>, , Tina Van Den Broeck<sup>1</sup>, Mark Dessing<sup>1</sup>

<sup>1</sup> BD Biosciences

Biophysical and immunochemical characterization of extracellular vesicles (EVs) has attracted intense interest due to their emerging diagnostic and therapeutic applications. EV characterization using high-resolution multicolor flow cytometry holds great promise; however, the small size, low marker expression and heterogeneous nature of EVs present unique challenges for instrument setup and sensitivity, reference standards, experimental design, and data analysis.

The BD FACSymphony™ A1 Cell Analyzer with BD® Small Particle Detector Option enables small particle analysis using a novel small particle side scatter channel (SP-SSC) within a sensitive 4-laser flow cytometer. Here, we describe operational guidelines for experimental design, instrument calibration to instrument set up and data analysis, including “OR” thresholding (SP-SSC “OR” fluorescence). These general guidelines are critical to achieving a high signal-to-noise ratio that allows sensitive and accurate detection of EVs on the BD FACSymphony™ A1 Cell Analyzer. Furthermore, these guidelines can improve comparability of EV data among research groups.

Class 1 Laser Product., For Research Use Only. Not for use in diagnostic or therapeutic procedures.,

BD and BD FACSymphony are trademarks of Becton, Dickinson and Company or its affiliates. © 2022 BD. All rights reserved. 0322

Funding: European Union’s Horizon 2020 research and innovation programme under the Marie Skłodowska-Curie grant agreement No [722148]

BD Biosciences is a partner organization in TRAIN-EV and offered training and secondment to a PhD student within the consortium.

**902047 P216**

## **The Delaware: A Flow NanoCytometer for Nanoparticle Analysis,**

Giacomo Vacca<sup>1</sup>, Richard Hanson<sup>1</sup>, Giovanni Contini<sup>2</sup>, Paolo Cappella<sup>2</sup>, Anna Sannino Romeo Bernini<sup>2</sup>

<sup>1</sup>Kinetic River Corp., <sup>2</sup> IREA, National Research Council, Italy

**Background.** Detection and characterization of sub-micron biological entities, such as exosomes, extracellular vesicles (ECVs), liposomes, and micelles, represents an important next frontier in both research and clinical applications. The main obstacles to nanoparticle analysis in flow cytometry are (i) the small particle sizes and (ii) the short time available for interrogation, which, combined, result in exceedingly small scattering and fluorescent signals. Commercial hardware either modified or tailored for this problem has so far been underwhelming in terms of both speed of analysis and ease of use. There is unmet demand for flow cytometry systems that deliver nanoparticle analysis without compromising usability and throughput. **Methods.** We have developed a new cell analyzer, the Delaware Flow NanoCytometer, designed for sensitive detection and characterization of sub-micron particles (biological or otherwise). The Delaware is based on the architecture of our Potomac modular flow cytometry platform (CYTO 2017; CYTO 2021), with design modifications specifically intended to enhance nanoparticle sensitivity. The Delaware has four excitation wavelengths (Toptica 120 mW and DTR 800 mW at 405 nm, Coherent 300 mW at 488 nm, Coherent 50 mW at 532 nm, and Coherent 25 mW at 640 nm). The detection module, which—like on the Potomac—has user-selectable Semrock filters, uses a high-NA collection lens and offers two scattering channels and three fluorescence channels; the module is expandable up to eight fluorescence channels. Ultrastable sheath flow for superior core stream control is established with our previously introduced Shasta fluidic control system (CYTO 2021). The analyzer is operated using our Panama flow cytometry software for instrument control and data visualization. **Results.** We will present results from two systems—the newly developed Delaware, as well as the Potomac installed at IREA-CNR in Naples, Italy. Both instruments were tested with nanoparticle characterization kits (50, 100, 140, 200, 500, and 1,000 nm colloidal silica nanoparticles from Alpha Nanotech and 100, 200, 500, and 800 nm polystyrene nano/microparticles from Spherotech). The two analyzers were additionally characterized using 6- and 8-peak broad-spectrum fluorescent microparticles (Spherotech Rainbow beads) and alignment microparticles for

# CYTO 2022 ABSTRACTS

system CVs (Spherotech). Conclusion. We have demonstrated the integration of powerful multicolor excitation sources, an optical system designed to maximize light collection, an ultrastable fluidic control module, and a highly flexible yet intuitive graphical user interface. The Delaware Flow NanoCytometer combines ease of use with advanced nanoparticle sensitivity to offer users a powerful new tool for exosome and ECV research. [This work was made possible in part by government support under one or more grants awarded by the NIH.

This work was made possible in part by U.S. government support under one or more grants awarded by the NIH, and by Italian government support under the POR CIRO project.

---

**898467 P218**

## **Small particle flow cytometry using 3D light scatter detection enhances extracellular vesicle analysis in liquid biopsies highlighting the potential to segregate EVs by refractive index.,**

Desmond PINK<sup>1</sup>, Arghya Basu<sup>1</sup>, Julianna Valencia<sup>1</sup>, Diana Pham<sup>1</sup>

<sup>1</sup>Nanostics

Extracellular vesicle analysis using “small particle” flow cytometry would be greatly enhanced if data from materials of different refractive index (RI) could be segregated. Likewise, relative sizing of EVs using small particle flow cytometry is confounded by the influence of RI on light scatter. Beads of different composition and refractive index scatter light differently, so that small beads of high RI and large beads of lower RI can have overlapping signals on a two dimension light scatter plot. In this project, we aimed to demonstrate practically and graphically, the enhancement of EV flow data analysis when using an additional angle of light scatter detection. An Apogee A60 Micro-Plus outfitted with a third (medium) angle of light scatter (MALS) detection was used to analyze samples typical of EV analysis. Events were triggered solely by MALS excited from a 405nm laser. NIST bead (70 -200nm) and silica bead standard mixtures (100-400nm) were analyzed first to define cytometer settings. Next, refractive index (Cargille) oil emulsion standards (R.I. 1.38, 1.42, 1.59) were prepared to generate a continuum of particle sizes; each emulsion was analyzed separately. The multi-angle light scatter data from each R.I. standard was plotted (3D) to yield the distinct pattern of particle size influenced by refractive index. NIST (polystyrene) bead data overlaid against the silica data demonstrated different patterns

as expected. NIST bead data overlaid almost perfectly with the 1.59 RI standard emulsion data. Similarly, silica bead standards followed the pattern of the 1.42 RI reference emulsions. Analyzed in the same manner, Verity beads (Exometry) overlaid atop the 1.38 RI reference emulsions. Concluding that the reference beads and emulsions overlapped in the expected manner, a variety of samples including plasma, serum, urine, semen, saliva, tissue culture media, etc were reacted with a variety of antibodies or dyes and the resulting patterns compared to the reference emulsion patterns. Other media such as IntraLipid, reference sera for tryglycerides and aggregated antibodies were likewise compared to the reference emulsions. Practically, the data, when plotted in 2 dimensions, show regions where large particles of low refractive index overlap significantly with smaller particles of higher refractive index, seen with both beads and samples (e.g lipid versus aggregated protein). Collecting and plotting data from a third angle significantly improves the resolution of these overlapping regions. However, as light scatter intensity decreases with either particle size or refractive index, especially in the <200nm biological particle range (70-90nm polystyrene, 100-120nm silica) the effective separation of particles of different R.I. is confounded by the overlap of signals. Addition of a 3rd light scatter collection significantly enhances the analysis of EVs by small particle flow cytometry, but practical thresholds still exist.

---

**898527 P220**

## **Physical association of lipoprotein particles and extracellular vesicles unveiled by single particle flow cytometry,**

Estefania Lozano-Andres<sup>1</sup>

<sup>1</sup> Utrecht University

Introduction: Human plasma is a complex biofluid that contains several submicron entities including extracellular vesicles (EVs) and lipoprotein particles (LPPs). Plasma tumor derived EVs (tdEVs) have a huge potential to be used as minimally invasive biomarkers for diagnosis and prognosis of patients. However, to exploit the potential of tdEVs in plasma we have to deal with the presence of LPPs. We here investigated how the presence of LPPs can influence the analysis of td-EVs at the single particle level. Methods: tdEVs were isolated from conditioned media of the mouse 4T1 mammary carcinoma cell line by density gradient ultracentrifugation and size-exclusion chromatography. For fluorescence-based flow cytometry (FC) of

# CYTO 2022 ABSTRACTS

tdEVs and commercially available LPPs, samples were stained with PKH67 and/or CD9-PE and succumbed to density gradient floatation prior FC analysis on an optimized BD Influx. Results: When analysed by FC, we found that PKH67 stains both EVs and various types of LPPs (CM, VLDL and LDL). Although their light scattering and fluorescence signal intensities from the generic membrane staining partially overlap, the peak enrichment of tdEVs or LPPs was found in different density fractions (1.16-1.12 or 1.10-1.06 g/cm<sup>3</sup> respectively). Furthermore, by using spike-in experiments we found that the presence of LPPs not only impacts the generic staining of tdEVs but also the antibody labelling of specific EV-markers. Spiked-in samples showed a distinct results compared to individual tdEVs or LPP samples, thus reflecting that interactions between different types of submicron sized particles present in plasma can affect both quantitative and qualitative analysis. Interestingly, the smaller LDL particles showed a singular staining pattern and revealed a higher signal from EV-markers in LPP-enriched densities. Thus indicating a more prominent association between tdEVs and LDL compared to CMs or VLDL particles. We confirmed in a label-free setting that the presence of LDL affects the signature of single tdEVs by synchronized Rayleigh and Raman scattering. In addition, by cryo-electron tomography we were able to observe that EVs present in human plasma can be physically bound to LDL particles in a physiological condition. Summary/Conclusion: The interaction between tdEVs and LPPs needs to be considered when plasma tdEVs are being investigated as biomarkers for diseases. Especially since the physical LPP-tdEVs interactions might impact the analysis of EV signatures and specific biomarkers at the single particle level. Funding: European Union's Horizon 2020 research and innovation programme under the Marie Skłodowska-Curie grant agreement No [722148] and STW-Perspectief Cancer-ID grant [14,191].

**897407 P222**

## **Design of “smart” nanoparticles for combined in-vivo imaging and advanced drug delivery therapeutics for single-cell nanomedicine,**

James Leary<sup>1</sup>

<sup>1</sup> Aurora Life Technologies LLC

Nanomedicine is massively parallel-processing “single-cell medicine”. It involves the packaging of drugs or genes into “smart” nanoparticles that can perform complex multi-step targeting to diseased cells while sparing damage to normal cells. Many drugs, including already FDA approved drugs, are already being re-packaged into nano-drug delivery systems allowing patent extensions and reducing the harmful effects of some drugs by vastly reducing the dose (10-100 times) exposures to patients. These nano-delivery systems can simultaneously provide imaging contrast agents for a number of non-invasive imaging modalities. Why does nanomedicine represent a huge promise for our healthcare system? Earlier diagnosis increases chances of survival. By the time some symptoms are evident to either the doctor or the patient, it may be already too late, in terms of irreversible damage to tissues or organs. When this damage occurs, the costs of the treatments rise steeply and the probability of successful patient outcomes declines steeply. It can also reduce or eliminate “side effects”. Nanomedicine will diagnose and treat problems at the molecular level inside single-cells, prior to traditional symptoms and, more importantly, prior to irreversible tissue or organ damage – saving both costs and, more importantly, improving the chances for a successful patient outcome. Smart nanoparticles are drug-device combinations that are revolutionizing drug delivery. Nanomedicine bridges the gulf between diagnostics and therapeutics with a new concept of “theranostics”. Earlier diagnosis increases chances of survival, as well as reducing irreversible damage to tissues or organs. Nanomedicine is the destruction of individual diseased cells (“nanosurgery”) or repair (regenerative medicine, including CRISPR) of tissues and organs, WITHIN individually targeted cells, cell-by-cell. Nanomedicine typically combines use of molecular biosensors to provide for feedback control of treatment and repair. Drug use is targeted and adjusted appropriately for individual cell treatment at the proper dose for each cell (single cell medicine). Nanomedical devices can be targeted to single diseased cells within the human body using a variety of targeting molecules and strategies, including: antibody targeting, peptide targeting, aptamer targeting, ligand-receptor targeting (e.g. folate receptors). Combinational chemistry and

# CYTO 2022 ABSTRACTS

high-throughput screening methods can screen over 100 million possible targeting molecules or therapeutic drug molecules in a day, including peptides, aptamers or other molecules. Flow and image cytometry are integral parts of nanomedicine, as well as all of the non-invasive imaging technologies.

---

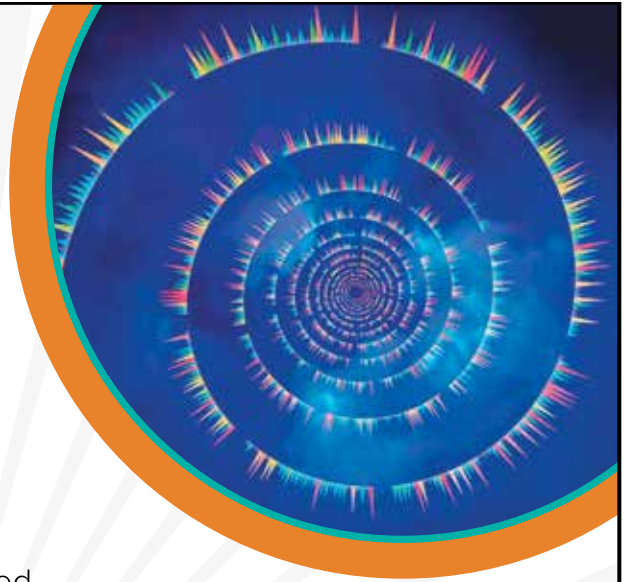
**901841**      **P224**

**Delivery of oligonucleotides into tumor cells via monoclonal antibodies: targeting of mRNA following release of antisense oligonucleotides through cell surface protease activities using Antibody Substrate Oligonucleotide Conjugates (ASOCs),**

Beverly Packard,<sup>1</sup>, Akira Komoriya<sup>1</sup>

<sup>1</sup>Oncolmmunin, Inc.

Antibody Substrate Oligonucleotide Conjugates (ASOCs) are monoclonal antibodies (mAbs) that are covalently modified with protease substrates; the latter are also covalently linked to oligonucleotides bearing H-type excitonic dimers. The substrates can be cleaved by proteolytic enzymes on a tumor cell surface that the cell might use to metastasize. Cleavage of the protease substrates results in localization of oligonucleotides at the tumor cell surface. Oligonucleotides are then able to diffuse into the tumor cell and inhibit translation of targeted mRNAs. The oligonucleotides enter cells via the delivery mechanism we have previously used to block HIV proliferation in CD4+ T cells (Cytometry A 97:945-54 (2020)). Thus, ASOCs differ from the current armed mAb-based therapies, e.g., antibody-drug conjugates (ADCs) or antibody-oligonucleotide conjugates (AOCs), in that delivery of the oligonucleotides into the cytoplasm does not require internalization of the mAb or endosomal processing; additionally, off-target toxicity will be reduced by release at the cell surface of the payload (the oligonucleotide). With this approach, using an MHC-Class I mAb we have delivered an antisense oligonucleotide targeting KRAS into the following tumor cell lines: A549 (NSCLC), COLO205 (colon), MB-MDA231 (breast), and Caki (kidney) as well as using the antiCD20 mAb Rituxan to deliver an antisense oligonucleotide targeting actin mRNA into Raji cells. Proof of delivery of oligonucleotides into cells was confirmed by confocal imaging after binding of mAbs to the cell surface as measured by flow cytometry.



## Reimagine flow cytometry

No unmixing or compensation controls required  
Hundreds of 30- and 40-plus-marker panels published  
The broadest range of panel applications

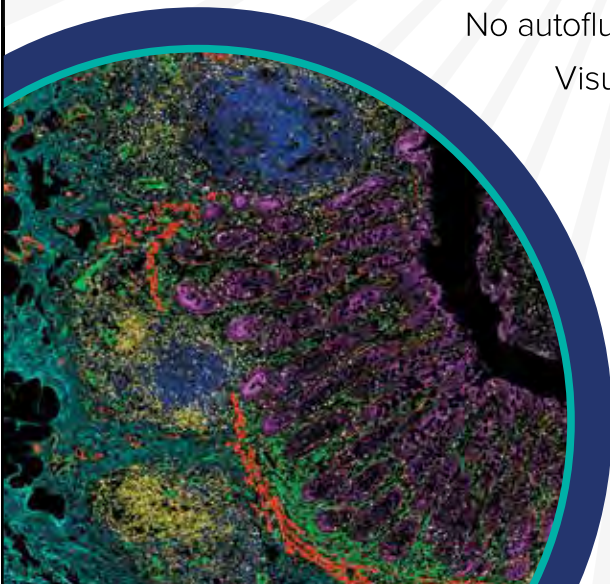
---

Why not get your high-plex panel right on the first try?  
**Use the power of CyTOF<sup>®</sup> technology.**

---

## Uncover spatial biology

Quantifiable single-cell analysis  
No autofluorescence, no time-consuming cyclic protocols  
Visualize 40-plus markers at subcellular resolution



**For Research Use Only. Not for use in diagnostic procedures.**

**Limited Use Label License:** [www.fluidigm.com/legal/salesterms](http://www.fluidigm.com/legal/salesterms); **Patents:** [www.fluidigm.com/legal/notices](http://www.fluidigm.com/legal/notices). **Trademarks:** Standard BioTools, the Standard BioTools logo and CyTOF are trademarks and/or registered trademarks of Standard BioTools Inc. (f.k.a. Fluidigm Corporation) or its affiliates in the United States and/or other countries. © 2022 Standard BioTools Inc. 05/2022

**Visit Booth 113**

# AUTHOR INDEX

|                              |                    |                          |                      |
|------------------------------|--------------------|--------------------------|----------------------|
| Carolina Acosta-Vega.....    | 163                | Robert Balderas.....     | 107, 255             |
| Joachim Aerts.....           | 105                | Saikat Banerjee.....     | 102                  |
| Maria Agemark.....           | 247                | Andrew Bantly.....       | 258                  |
| Carina Agerbo Rosenberg..... | 233                | Rachel Barhouma.....     | 191                  |
| Keunho Ahn.....              | 184                | Ruth Barnard.....        | 182, 218, 230, 245   |
| Julie Ake.....               | 181                | Jerry Barnhart.....      | 212                  |
| Kate Alford.....             | 171                | František Bárta.....     | 154                  |
| James Almarode.....          | 171, 172           | Natalie Barteneva.....   | 168                  |
| Jay Almarode.....            | 226, 255           | Todd Bartkowiak.....     | 53, 131, 237         |
| Tiziana Altosole.....        | 92                 | Arghya Basu.....         | 196, 198, 259        |
| David Ambrozak.....          | 106, 185, 208, 249 | Ryan Baxter.....         | 201                  |
| Amir Ameri.....              | 46, 189            | Andrea Bedoya-Lopez..... | 187                  |
| Luis Amezcua.....            | 173                | Jordan Bell.....         | 28, 31, 101, 234     |
| Shamundeeswari Anandan.....  | 178, 230           | Samuel Berryman.....     | 202, 204             |
| Kelly Andrews.....           | 40, 146, 211, 246  | Hugo Berthelot.....      | 171, 172             |
| Fabienne Anjuere.....        | 235                | Julie Bick.....          | 155, 217             |
| Naga Annamdevula.....        | 142, 231           | Marie Bill.....          | 233                  |
| Asier Antoranz.....          | 127                | Claudia Bispo.....       | 30, 46, 193          |
| Randall Armstrong.....       | 194                | Aric Bitton.....         | 183                  |
| Lourdes Arriaga-Pizano.....  | 33, 113            | Alfonso Blanco.....      | 33, 113              |
| Andreas Artemiou.....        | 99                 | Anson Blanks.....        | 144, 229             |
| Aria Arus-Altuz.....         | 219                | Michael Blundell.....    | 42, 52, 166, 230     |
| Thomas Ashhurst.....         | 39, 48, 139        | Anette Susanne.....      | Bøe Wolff<br>86..... |
| Kewal Asosingh.....          | 30, 212            | Karin Boer.....          | 110                  |
| Avrill Aspland.....          | 30, 95             | Goce Bogdanoski.....     | 28, 88               |
| Aruna Ayer.....              | 228, 252           | Antonia Boger-May.....   | 176                  |
| Ania Baaziz.....             | 82                 | Fabrizio Bonelli.....    | 91                   |
| Attila Babes.....            | 159, 223           | Jody Bonnevier.....      | 44, 180, 203, 205    |
| Jessica Back.....            | 27, 30             |                          |                      |

# AUTHOR INDEX

|                                |                  |                        |                         |
|--------------------------------|------------------|------------------------|-------------------------|
| Sarah Bonte.....               | 31, 100          | Paolo Cappella.....    | 195, 258                |
| David Boone.....               | 176              | Thaddeus Carlson.....  | 102                     |
| Scott Bornheimer.....          | 92               | Megan Catterton.....   | 45, 84, 183, 209        |
| Lucienne Bosler.....           | 41, 152          | Tony Chadderton.....   | 49, 211                 |
| Victor Bosteels.....           | 42, 164          | Cora Chadick.....      | 51, 221                 |
| Sara Bowen.....                | 187              | Leo Chan.....          | 27, 52, 101, 234        |
| Rita Bowers.....               | 39, 47, 143, 199 | Hyun-Dong Chang.....   | 118                     |
| Nathan Brady.....              | 43, 170          | Zixi Chao.....         | 234                     |
| Martha Brainard.....           | 41, 50, 151, 216 | Bassem Ben Cheikh..... | 42, 160                 |
| Oliver Braubach.....           | 160              | Giulia Cheloni.....    | 208                     |
| Veronique Braud.....           | 235              | Angela Chen.....       | 49, 213                 |
| Emma Brentjens.....            | 81               | Qing Chen.....         | 149                     |
| Marta Brewinska-Olchowik.....  | 125              | Yixuan Chen.....       | 225                     |
| Ryan Brinkman.....             | 30, 33, 113, 225 | Alan Chin.....         | 35, 40, 123, 148        |
| Andrea Britain.....            | 231              | Piotr Chroscicki.....  | 125, 138                |
| Asa A Brockman.....            | 237              | Aled Clayton.....      | 197                     |
| Craig Browning.....            | 39, 142          | Matthew Cochran.....   | 30                      |
| Kathy Brundage.....            | 187              | Heather Cohen.....     | 155                     |
| Milena Brunialti.....          | 201              | Kristen Cohen.....     | 124                     |
| Lisa Budzinski.....            | 34, 118          | Michael Cohen.....     | 42, 165, 229            |
| Jonas Bull Haugsøen.....       | 52, 178          | Russell Cole.....      | 55, 253                 |
| Naomi Buntsma.....             | 32, 110          | Jessica Congiu.....    | 54, 247                 |
| Paulo Burke.....               | 162              | Giovanni Contini.....  | 195, 258                |
| Sean Burrows.....              | 40, 144          | Alexis Conway.....     | 187                     |
| Ross Burton.....               | 31, 99           | Sean Cook.....         | 249                     |
| Giri Buruzula.....             | 54, 248          | Gregory Cooksey.....   | 130, 145, 183, 209, 210 |
| Berenice Cabrera-Martinez..... | 48, 201          | Sean Cosgriff.....     | 49, 208                 |
| Derek W Cain.....              | 219              | Artuur Couckuyt.....   | 36, 100, 129            |
| Pamela Canaday.....            | 195              | Sarah Cox-Vazquez..... | 255                     |



# AUTHOR INDEX

|                                  |                          |                                  |                  |
|----------------------------------|--------------------------|----------------------------------|------------------|
| Matthew Creegan .....            | 45, 181                  | Iyadh Douagi .....               | 26, 42, 50       |
| Janifer Cruz .....               | 254                      | Oleksii Dubrovskiy .....         | 81               |
| Simone Cuff .....                | 99                       | Steven Dudek .....               | 81               |
| Kamila Czechowska.....           | 30, 33, 42, 51, 113, 159 | Erika Duggan .....               | 111, 184         |
| Rea Dabelic .....                | 46, 190                  | Valérie Duplan .....             | 86               |
| Kleopatra Dagla .....            | 217                      | Jaime Duque .....                | 107              |
| Xizi Dai .....                   | 49, 146, 211             | Sarah E B Taylor.....            | 190              |
| David Daley .....                | 144                      | Matthias Eberl .....             | 99               |
| Kathleen Daniels.....            | 25, 46, 187              | Christoph Eberle .....           | 206              |
| Kara Davis .....                 | 165                      | Gabriela Eburneo .....           | 201              |
| Sara De Biasi .....              | 125                      | Robert Edwards .....             | 219              |
| Martina de Geus .....            | 39, 140                  | Marcus Eich.....                 | 34, 115          |
| Gelo de la Cruz .....            | 30, 33, 113              | Roxane Elaldi .....              | 235              |
| Stephen De Rosa .....            | 30, 124                  | Michael Eller .....              | 181              |
| Joseph de Rutte.....             | 152                      | Elzafir Elsheikh .....           | 119              |
| Frederik De Smet.....            | 127                      | Annelies Emmaneel .....          | 31, 99, 129      |
| Steven De Vleeschouwer.....      | 127                      | Pablo Engel .....                | 221              |
| Hannah DeBerg .....              | 163                      | Trine Engelbrecht Hybel .....    | 52, 233          |
| Vilma Decman .....               | 161, 230                 | Trevor Enright .....             | 194              |
| Irene del Molino del Barrio..... | 54, 182, 218, 245        | Rachel Errington .....           | 47, 197          |
| Jason Deng .....                 | 103, 140, 184            | Frederick Esch.....              | 40, 145          |
| Jun Deng.....                    | 149                      | Heather Evans-Marin .....        | 50, 217          |
| Yunjie Deng .....                | 107                      | Marissa Fahlberg .....           | 40, 144          |
| Paul DeRose .....                | 44, 174, 206, 256        | Vincenzo Fallico .....           | 153              |
| Deepak Deshpande.....            | 142                      | Andrew Farthing .....            | 41, 156          |
| Mark Dessing .....               | 257, 258                 | Geoffrey Feld .....              | 48, 206          |
| Dino Di Carlo .....              | 104, 109, 152            | Daniela Fenoglio .....           | 92               |
| Eric Diebold .....               | 28, 52, 236              | Vanessa Fernandes de Costa ..... | 174              |
| Matthew DiSalvo.....             | 49, 130, 183, 209, 210   | Laura Ferrer Font.....           | 31, 33, 103, 114 |

# AUTHOR INDEX

|                            |                        |                          |               |
|----------------------------|------------------------|--------------------------|---------------|
| Kevin Ferro .....          | 187                    | Michelle Gomes .....     | 47, 194       |
| Andy Filby.....            | 25, 27, 159, 223       | Martin Gomez .....       | 31, 102       |
| Benjamin Fynn .....        | 49, 191, 210           | Mingyan Gong .....       | 149           |
| Kevin Flynn.....           | 180                    | Carl Goodyear.....       | 156           |
| Sarah Forward.....         | 144                    | Wojciech Gorcyca .....   | 118           |
| Susan Foster.....          | 150                    | Amy Graham.....          | 30            |
| Genevieve G Fouda .....    | 108                    | Sofia Grammenoudi .....  | 50, 217       |
| Kathryn Fox .....          | 54, 247                | David Gravano .....      | 33, 114       |
| Antonio Frias.....         | 195                    | Giulia Grazia .....      | 143, 199      |
| Koji Futamura .....        | 43, 145, 167           | Allison Greenplate ..... | 123, 129, 186 |
| Lidia Gackowska.....       | 44, 53, 178, 242, 243  | Michael Gregory .....    | 25, 30        |
| Julia Gala de Pablo .....  | 121                    | Garrett Grischo .....    | 227           |
| Kevin Galles.....          | 41, 153                | Dirk Grosenick.....      | 172, 232      |
| Ekambaram Ganapathy.....   | 42                     | Daryl Grummitt.....      | 40, 146       |
| Shilpa Gandre-Babbe.....   | 102                    | Jochen Guck.....         | 104, 202      |
| Maria Garcia Mendoza ..... | 232                    | Garret Guenther .....    | 175, 207, 239 |
| Sara Garcia-Garcia .....   | 42, 158                | Diana Guinot.....        | 154           |
| Julia Garcia-Leston.....   | 158                    | Jana Gunterova .....     | 218           |
| Hugo Garnier .....         | 86                     | Petra Hadlová .....      | 44, 179       |
| Mark Garzotto.....         | 194                    | Stefan Hailey .....      | 217           |
| Sonia Gavasso .....        | 178, 230               | Christopher Hall.....    | 154           |
| Ionita Ghiran .....        | 256                    | Paul Hallberg .....      | 39, 138       |
| Valeria Giangarra .....    | 190                    | Richard Halpert.....     | 226           |
| Jonas Gienger .....        | 28, 172, 232           | Tansy Hammarton.....     | 235           |
| Julien Gigan.....          | 82                     | Yong Han .....           | 52, 101, 234  |
| Stefanie Ginster .....     | 45, 185                | Maris Handley.....       | 144           |
| Keisuke Goda .....         | 37, 104, 107, 108, 121 | Richard Hanson .....     | 195, 258      |
| Christian Goerke .....     | 52, 172, 232           | John Harley .....        | 210           |
| Christine Goetz .....      | 180                    | Jeffrey Harmon.....      | 89            |

# AUTHOR INDEX

|                             |                       |                                |              |
|-----------------------------|-----------------------|--------------------------------|--------------|
| Marcela Haro .....          | 119                   | Jinman Huang .....             | 123          |
| Taylor Harper .....         | 154                   | Kangrui Huang.....             | 89           |
| Erica Hasten .....          | 81                    | Yongyang Huang.....            | 87, 101      |
| Chi Hau.....                | 110                   | Ondrej Hubálek.....            | 179          |
| Mette Haugen .....          | 178                   | Chiung-Yu Hung.....            | 227          |
| Madeline J Hayes .....      | 237                   | Benjamin Hunsberger .....      | 51,223       |
| Cara Haymaker.....          | 251                   | Clinton Hupple .....           | 169          |
| Amanda Hays .....           | 214                   | Kanutte Huse.....              | 176          |
| Robert Hedley.....          | 58, 238, 266          | Eystein S Husebye .....        | 86           |
| Priscilla Heijnen.....      | 221                   | Martin Hussels.....            | 172 232      |
| Kerstin Heinrich .....      | 28                    | William Hyun .....             | 252          |
| Anna Helmin-Basa.....       | 44, 53, 178, 242, 243 | Yaser Iftikhar.....            | 126          |
| Martin Helmut Stradner..... | 158, 223              | Rebecca Ihrle.....             | 131          |
| Mark Herberger .....        | 222                   | Marieke Ijsselsteijn.....      | 128          |
| Maik Herbig .....           | 29, 31, 104, 108      | Matei Ionita.....              | 36 129       |
| Laurin Herbsthofer.....     | 51, 157, 222          | Jonathan Irish.....            | 25 128       |
| Ida Herdlevær .....         | 44, 178, 230          | Anne-Laure Iscache .....       | 28 86        |
| Beth Hill.....              | 217                   | Daniela IschIU Gutierrez ..... | 54, 184, 249 |
| Kotaro Hiramatsu .....      | 83, 121               | Shahinul Islam.....            | 86, 180      |
| Svenja Hochstätter.....     | 91                    | Marjorie Ison-Dugenny .....    | 151          |
| Caroline Hoedemaker .....   | 39, 141               | Akihiro Isozaki .....          | 83, 89, 104  |
| Thea Hogan .....            | 82, 245               | Jerilyn Izac .....             | 119          |
| Bettina Hohberger .....     | 202                   | Kivin Jacobsen .....           | 51, 189, 228 |
| Mehran Hoonejani.....       | 146, 210              | Astraea Jager .....            | 165          |
| Greg Hopkins .....          | 151, 216              | Nicole Jagnandan .....         | 141          |
| Jessica Houston .....       | 194, 207              | Maria Jaimes.....              | 192, 222     |
| Jessie Howell .....         | 52, 235               | Jennifer Jakubowski.....       | 188          |
| Ruba Hsen .....             | 213                   | Sedi Jalali.....               | 105          |
| Elena W-Y Hsieh .....       | 201                   | Wojciech Janczyk .....         | 53, 243      |

# AUTHOR INDEX

|                            |                         |                             |              |
|----------------------------|-------------------------|-----------------------------|--------------|
| Sophie Janssens.....       | 164                     | Iviyan Karki.....           | 153          |
| Aditya Jarare .....        | 140                     | Erik Karlsson .....         | 247          |
| Dorra Jedoui.....          | 42, 165                 | Elijah Kashi.....           | 123, 148     |
| Jana Jemelkova.....        | 239                     | Yasmin Kassim .....         | 160          |
| Dominic Jenner .....       | 79, 169                 | Anthony Kearsley.....       | 130          |
| Travis Jennings.....       | 227, 244                | Ross Kedl .....             | 201          |
| Devon Jensen.....          | 252                     | Katherine Kedzierska .....  | 139          |
| Jinpyo Jeon .....          | 202, 204                | Michael Kempnich .....      | 212          |
| Melanie Jimenez.....       | 74, 157, 235            | Wolfgang Kern.....          | 95, 113      |
| Mehul Jivrajani .....      | 140                     | Tessa Kerre.....            | 99, 100      |
| Chintan Jobaliya .....     | 155                     | Nikki Khoshnoodi.....       | 102          |
| Chassidy Johnson.....      | 192, 254                | Rohit Khurana.....          | 131          |
| Dove-Anna Johnson.....     | 249                     | Anthony Kiefer .....        | 153          |
| Derek Jones .....          | 107, 129, 187, 188, 250 | Nicholas King.....          | 139          |
| Simone Joosten.....        | 128                     | Ali Kinkhabwala.....        | 227          |
| Pierre-Emmanuel Jouve..... | 160, 162                | Yael Kiro .....             | 183          |
| Andreja Jovic.....         | 192                     | Jenny Kirsch.....           | 203, 204     |
| Sabina Kaczmarzyk .....    | 185                     | Yugo Kishimoto .....        | 145          |
| Daniel Kage .....          | 29, 75, 83              | Margarita Kist.....         | 185          |
| Toshiyuki Kaimi.....       | 40, 145                 | Kenneth Knox .....          | 227          |
| Toralf Kaiser .....        | 48, 203, 204            | Jina Ko .....               | 121          |
| Mrinalini Kala.....        | 227                     | Abhishek Koladiya.....      | 245          |
| Murali Kala .....          | 88                      | Abhishek Koladiya.....      | 245          |
| Sowmya Kala.....           | 88                      | George Kollias.....         | 217          |
| Tomas Kalina .....         | 13                      | Akira Komoriya .....        | 200, 261     |
| Tomáš Kalina .....         | 154, 179, 221           | Andrew Konecny.....         | 43, 127, 167 |
| Gi-Ung Kang .....          | 118                     | Raymond Kong .....          | 52, 232      |
| Hiroshi Kanno .....        | 90                      | Tanja Konijn .....          | 221          |
| Michael Kapinsky.....      | 199                     | Timothea Konstantinou ..... | 197          |

# AUTHOR INDEX

|                               |               |                               |               |
|-------------------------------|---------------|-------------------------------|---------------|
| Igor Konstantinov .....       | 105           | Heaven Le Roberts.....        | 171           |
| Doyeon Koo .....              | 109           | James Leary.....              | 56, 198, 260  |
| Petr Kosztyu.....             | 239           | Silas Leavesley .....         | 53, 231       |
| Amanda Kouaho .....           | 129           | Jeonghyun Lee .....           | 202, 204, 254 |
| Geoff Kraker .....            | 103           | Sohyung Lee.....              | 109           |
| Martin Kräter .....           | 202           | Kawthar Leggat .....          | 181           |
| Tomas Kraus.....              | 218           | Ming Lei .....                | 175, 239      |
| Susanne Krauthäuser.....      | 244           | Giuseppe Leite.....           | 201           |
| Ludmila Krymskaya .....       | 219           | Fatima-Ezzahra L'Faqihi ..... | 86            |
| Markéta Kubánková.....        | 202           | Nan Li.....                   | 143, 207      |
| Izabela Kubiszewska.....      | 178, 242, 243 | Shuang Li .....               | 88            |
| Julia Kudlackova.....         | 154           | Stephen K H Li.....           | 165, 228      |
| brittany kuhl .....           | 205           | Yang Li.....                  | 90            |
| Wei-Ying Kuo .....            | 152           | Thomas Liechti .....          | 126           |
| Daniela Kuzilkova .....       | 154, 221      | Jessica Liegel.....           | 208           |
| Erika Kuzmova.....            | 218           | Sierra M Lima.....            | 237           |
| Edward Kwee .....             | 119           | Nancy Lin .....               | 105           |
| Sheldon Kwok.....             | 122, 144      | Yi-Dong Lin.....              | 161, 218, 230 |
| Craig LaBoda .....            | 74, 229       | Matthew Lindley .....         | 12            |
| Vashti Lacaille.....          | 143, 199      | Christine Lingblom.....       | 178           |
| Evan Lamb.....                | 53, 240       | Maxim Lippeveld .....         | 43, 169       |
| Chris Langsdorf .....         | 171, 220      | Mieczyslaw Litwin .....       | 179, 242      |
| Joanne Lannigan .....         | 193           | Virginia Litwin.....          | 78, 114       |
| Larry Lantz .....             | 166, 216      | Candice Liu.....              | 212           |
| Anis Larbi .....              | 199           | Jennifer Liu .....            | 149           |
| Petra LAZNICKOVA .....        | 238           | Wenqi Liu .....               | 143, 207      |
| Aleksandra Lazowska-Addy..... | 154, 188, 251 | Yuxuan Liu .....              | 165           |
| Diem Le.....                  | 149           | Zishu Liu.....                | 88            |
| Tri Le .....                  | 52, 236       | Christina Loh .....           | 165, 228, 229 |

# AUTHOR INDEX

|                              |               |                            |          |
|------------------------------|---------------|----------------------------|----------|
| S Alice Long.....            | 163           | Michelle Mckeague.....     | 186      |
| Nicolas Loof.....            | 85            | Michelle McNamara.....     | 148      |
| Felisha Lopez.....           | 248           | Stephanie Medina.....      | 128      |
| Peter Lopez.....             | 78, 147       | Aida Meghraoui.....        | 235      |
| Pablo López-García.....      | 157, 222      | Majid Mehrpouyan.....      | 120      |
| Estefanía Lozano-Andrés..... | 96, 257       | Henrik Mei.....            | 91       |
| Yan Lu.....                  | 175, 239      | Dirk Meineke.....          | 244      |
| Fabienne Lucas.....          | 69            | Carole Mendelson.....      | 85       |
| Maja Ludvigsen.....          | 233           | Akil Merchant.....         | 119      |
| Melvin Lye.....              | 206           | Ana Merino.....            | 110      |
| Hongshen Ma.....             | 202, 204, 254 | Annette Meyer.....         | 257      |
| Timothy Mack.....            | 214           | Aaron Middlebrook.....     | 128      |
| Justin Madrigal.....         | 253           | Danielle Middlebrooks..... | 225      |
| Peter Mage.....              | 127, 167, 236 | Hideharu Mikami.....       | 89, 108  |
| Florian Mair.....            | 127, 167      | Brandon Miller.....        | 184      |
| Massimo Mangino.....         | 126           | Karen Millerchip.....      | 251      |
| Zhiyuan Mao.....             | 109           | Takashi Miyata.....        | 167      |
| Hannah Maple.....            | 203, 205      | Taryn Mockus.....          | 161, 230 |
| Jody Martin.....             | 252           | Dorinda Moellering.....    | 39, 141  |
| Lola Martinez.....           | 94, 95, 158   | Alex Molto.....            | 141      |
| Leonardo Martins.....        | 248           | Ludovic Monheim.....       | 258      |
| Josef Mašek.....             | 175           | Alina Montalbano.....      | 85       |
| Thomas Maslanik.....         | 184           | Sebastiano Montante.....   | 51, 225  |
| Felipe Masso.....            | 173           | Jonni Moore.....           | 129      |
| Hiroki Matsumura.....        | 89, 108       | Terry Morgan.....          | 195      |
| Kerryn Matthews.....         | 254           | Mayu Morita.....           | 195      |
| Anastasia Mavropoulos.....   | 254           | Alexander Morris.....      | 214      |
| M Juliana McElrath.....      | 124           | Thomas Moyer.....          | 166      |
| Bridget McGlaughlin.....     | 226           | Shilpaa Mukundan.....      | 234      |

# AUTHOR INDEX

|                              |                    |                            |                        |
|------------------------------|--------------------|----------------------------|------------------------|
| Susann Müller .....          | 88, 186, 250       | Farzad Oreizy .....        | 148, 213               |
| Donna Munoz .....            | 141                | Eva Orłowski .....         | 187                    |
| William Murphy .....         | 187, 250           | John O'Rourke .....        | 120                    |
| Jan Musil .....              | 245                | Sandra Orsulic .....       | 119                    |
| Natalie Mysak .....          | 153                | Heather Otte .....         | 251                    |
| Ashikun Nabi .....           | 91                 | Keegan Owsley .....        | 236                    |
| Mark Naivar .....            | 146                | Beverly Packard .....      | 200, 261               |
| Reid Nakamoto .....          | 191                | Araceli Paez .....         | 173                    |
| Dayton Nance .....           | 166                | Mark Painter .....         | 35, 123                |
| Aikaterini Nanou .....       | 217                | Arumugam Palanichamy ..... | 217                    |
| Rakesh Nayyar .....          | 213                | Ioannis Panetas .....      | 43, 171, 172           |
| Jana Neirinck .....          | 99                 | Ioannis Panetas .....      | 171, 173               |
| Lauren Nettenstrom .....     | 114, 247           | Jack Panopoulos .....      | 226, 255               |
| Katherine Nevin .....        | 230                | Dena Panovska .....        | 127                    |
| Anh-Tuan Nguyen .....        | 184                | Biju Parekkadan .....      | 234                    |
| Richard Nguyen .....         | 106, 185, 208, 248 | Emily Park .....           | 254                    |
| Wan Ni Geraldine Chia .....  | 255                | Marina Parker .....        | 231                    |
| Rienk Nieuwland .....        | 110                | Kirsten Parratt .....      | 104                    |
| Paula Niewold .....          | 69, 128            | Manish Patankar .....      | 247                    |
| Masako Nishikawa .....       | 90, 107, 108       | Mariana Patlan .....       | 173                    |
| Ryo Nishiyama .....          | 121                | Paul Patrone .....         | 84, 130, 144, 182, 210 |
| John Nolan .....             | 96, 111, 114, 184  | Ajinkya Pattekar .....     | 123, 186               |
| Julien Nourikyan .....       | 162                | Maria Pawlik .....         | 118                    |
| David Novak .....            | 225                | Daniel Pellicci .....      | 105                    |
| Maurice O'Gorman .....       | 213                | Kate Peng .....            | 215                    |
| Veronica Obregon-Perko ..... | 108                | Li Peng .....              | 180, 203, 205          |
| Betsy Ohlsson-Wilhem .....   | 145, 255           | Becky Penhallow .....      | 88                     |
| Diana Ordonez .....          | 73, 171, 172       | Daniel Peralta .....       | 43, 169                |
| Benjamin Ordonia .....       | 215                | Andrea Perez .....         | 183                    |

# AUTHOR INDEX

|                                   |                        |                               |                        |
|-----------------------------------|------------------------|-------------------------------|------------------------|
| Esther Perez Garcia.....          | 182, 218, 245          | Alaina Puleo.....             | 190                    |
| Stephen Perfetto.....             | 79, 106, 185, 208, 249 | Cathi Pyle.....               | 160, 224               |
| Sallie R Permar.....              | 108                    | Kenneth Quayle.....           | 164                    |
| Florence Perrin Patel.....        | 102                    | John Quinn.....               | 118                    |
| Ekaterina Petrovich-Kopitman..... | 45, 182                | Katrien Quintelier.....       | 105                    |
| William Peveler.....              | 156                    | Amie Radenbaugh.....          | 252                    |
| Verena Pfeifer.....               | 157                    | Eyal Rahav.....               | 182                    |
| Diana Pham.....                   | 196, 198, 259          | Bhargavi Rajan.....           | 102, 253               |
| Michael Phelan.....               | 192                    | Carlos Ramos.....             | 251                    |
| Thomas Pieber.....                | 157, 158, 222, 223     | Milan Raska.....              | 175, 239, 240          |
| Thomas R Pieber.....              | 157, 158, 222, 223     | Yi Ren.....                   | 248                    |
| Micheli Pillat.....               | 248                    | Thomas Rich.....              | 142                    |
| Micheli Pillat.....               | 248                    | Aja Rieger.....               | 72                     |
| Brandy Pinckney.....              | 256                    | Petr Říha.....                | 179                    |
| Desmond PINK.....                 | 196, 198, 259          | Dean Ripple.....              | 174                    |
| Nicholas Pinkin.....              | 229                    | Casey Roberts.....            | 246                    |
| Katarzyna Piwocka.....            | 84, 125, 138           | Matthew Rodrigues.....        | 90, 232                |
| Charles Pletcher, Jr.....         | 138                    | Evelyn Rodriguez-Mesa.....    | 146, 191               |
| Nikita Podobedov.....             | 84, 145, 210           | Caroline Roe.....             | 71                     |
| Nikita Podobedov.....             | 84, 145, 210           | Wade Rogers.....              | 129                    |
| Michael Podolsky.....             | 214                    | Harshada Rohamare.....        | 213                    |
| Ziv Porat.....                    | 173, 237               | Addi J Romero-Olmedo.....     | 91                     |
| Hassan Pouraria.....              | 194                    | Alejandra Rosario-Crespo..... | 128                    |
| Aditya Pratapa.....               | 160                    | Gianluca Rotta.....           | 92                     |
| Kylie Price.....                  | 103                    | Katelyn Ruley-Haase.....      | 176                    |
| Laura Prickett.....               | 156                    | Silin Sa.....                 | 212                    |
| Barbara Prietl.....               | 157, 158, 222, 223     | Jalal Sadeghi.....            | 84, 209                |
| Martin Prlic.....                 | 127, 167               | Yvan Saeys.....               | 99, 100, 105, 129, 169 |
| Samantha Provost.....             | 220, 240               | Hajar Saihi.....              | 161                    |



# AUTHOR INDEX

|                             |                    |                                |               |
|-----------------------------|--------------------|--------------------------------|---------------|
| Kiran Saini .....           | 192, 254           | Kshitija Shevgaonkar .....     | 123, 148      |
| Cynthia Sakofsky .....      | 228                | Xiaoshan Shi .....             | 120           |
| Reinaldo Salomão .....      | 201                | Kevin Shields .....            | 210           |
| Alan Saluk .....            | 159, 223           | Tyler Shovah .....             | 103           |
| Roser Salvia .....          | 177, 193, 241, 273 | Celine Silva-Lages .....       | 164           |
| Jesus Sambrano .....        | 182, 207           | Erica Smit .....               | 185, 208, 248 |
| Valerie Sanchez .....       | 120                | Eileen Snowden .....           | 252           |
| Sharon Sanderson .....      | 166                | Mikiko Sodeoka .....           | 121           |
| Ana Paula Santos .....      | 121                | Michael Solga .....            | 154           |
| Sandra Saouaf .....         | 141                | Hye-Won Song .....             | 252           |
| Matthew Saunders .....      | 120                | Deena Soni .....               | 145           |
| Tim Schenkel .....          | 257                | Ivana Spasevska .....          | 176           |
| Matthias Schiemann .....    | 121                | Benjamin Spurgeon .....        | 68            |
| Magdalena Schimke .....     | 192                | Shiva Ranjini SRINIVASAN ..... | 140           |
| Steffen Schmitt .....       | 115, 116           | Noura Srour .....              | 151, 216      |
| Sabrina Schmitz .....       | 185                | Ernesto Staroswiecki .....     | 146, 211      |
| William Schott .....        | 140                | Dawid Stepnik .....            | 125, 138      |
| Richard Schretzenmair ..... | 107, 129           | Ann Strange .....              | 162           |
| Axel Ronald Schulz .....    | 29                 | Aaron Stroud .....             | 144           |
| Janina Schwarte .....       | 155                | Chengxun Su .....              | 107           |
| Katharine Schwedhelm .....  | 124                | Sareena Sund .....             | 42            |
| Toni Sempert .....          | 118                | Alexandra Sutton .....         | 232           |
| Moen Sen .....              | 189                | Julian Swatler .....           | 84, 125       |
| Pathik Sen .....            | 214                | David Sykes .....              | 214           |
| Tate Sessler .....          | 91                 | Attila Tarnok .....            | 77, 95, 113   |
| Ruth Seurinck .....         | 129                | Erin Taylor .....              | 171           |
| Dagna Sheerar .....         | 247                | Kazuki Teranishi .....         | 101           |
| Larina Shen .....           | 108                | Manish Thakran .....           | 252           |
| Rachael Sheridan .....      | 26, 80             | Sobha Thamminana .....         | 253           |

# AUTHOR INDEX

|                            |                        |                                  |                         |
|----------------------------|------------------------|----------------------------------|-------------------------|
| Esther Thang .....         | 106, 185, 208, 249     | Sofie Van Gassen .....           | 99, 100, 105, 128, 225  |
| James Thomas .....         | 160, 224               | Gert Van Isterdael .....         | 164, 170                |
| Seddon Thomas .....        | 229                    | Menno van Zelm .....             | 221                     |
| Stephen Thomas .....       | 214                    | Sarka Vanikova .....             | 245                     |
| Sam Thompson .....         | 150, 154, 180, 250     | Christian Vedeler .....          | 178                     |
| Sherry Thornton .....      | 164                    | Vidya Venkatachalam .....        | 90                      |
| Shifu Tian .....           | 138                    | Rajesh Venkatesh .....           | 140                     |
| John Tigges .....          | 96, 87, 208, 256       | José A Vera-Ramos .....          | 157                     |
| Alvaro Torres Huerta ..... | 176                    | Frank Verreck .....              | 128                     |
| Lauren J Tracey .....      | 51, 228                | Fernanda Viero .....             | 248                     |
| Peter Tran .....           | 215                    | Flora Vincent .....              | 169                     |
| Jarek Trapszo .....        | 140                    | Konrad Volkmann .....            | 28, 203, 204            |
| Brandon Trent .....        | 181, 220               | Katherine Vowell .....           | 102                     |
| Brandon Trent .....        | 181, 220               | Rachael Walker .....             | 150, 154, 188, 250      |
| Charles Trubey .....       | 160, 224               | Ian Walton .....                 | 253                     |
| Evan Trudeau .....         | 219                    | Jiangfang Wang .....             | 161, 218, 230           |
| Jaroslav Turánek .....     | 175                    | Lili Wang .....                  | 114, 119, 134, 174, 256 |
| Laura Turos-Korgul .....   | 84                     | Nicholas Wanner .....            | 212                     |
| Kamala Tyagarajan .....    | 91                     | Jamey Weichert .....             | 247                     |
| Aaron Tyznik .....         | 70, 120, 128, 167, 225 | Eric Welch .....                 | 206                     |
| Ferzan Uddin .....         | 108                    | Joshua A Welsh .....             | 46, 193, 249            |
| Henning Ulrich .....       | 77, 121, 248           | Alexander Wendling .....         | 154                     |
| Anke Urbansky .....        | 247                    | John Wherry .....                | 123, 186                |
| Giacomo Vacca .....        | 123, 148, 194, 258     | Stephanie Widmann .....          | 120                     |
| Julianna Valencia .....    | 196, 198, 259          | Milena Wiech .....               | 138                     |
| Samantha Valentino .....   | 183                    | Alice Wiedeman .....             | 163                     |
| Tina Van Den Broeck .....  | 257, 258               | Aldona Wierzbicka-Rucinska ..... | 243                     |
| Edwin van der Pol .....    | 96, 110                | Bhagya Wijayawarden .....        | 143                     |
| Julie Van Duyse .....      | 170                    | Stefanie Wilhelm .....           | 244                     |

# AUTHOR INDEX

|                           |               |                          |               |
|---------------------------|---------------|--------------------------|---------------|
| Austin Wilpan.....        | 140           | Pu Zhang .....           | 248           |
| Owen Witte .....          | 109           | Wuji Zhang .....         | 139           |
| Taylor Witte.....         | 151, 216      | Yu-Zhong Zhang .....     | 174, 206, 256 |
| Paul Wood.....            | 203, 205      | Jingjing Zhao .....      | 234           |
| Jesse Woodbury .....      | 215           | Yuqi Zhou.....           | 90, 107       |
| David Woods.....          | 162           | Adina Zhumakhanova ..... | 43            |
| Wouter Woud .....         | 110           | Violetta Zlojutro.....   | 212           |
| Adam Wright.....          | 252           | Robert Zucker .....      | 81            |
| Jian Wu .....             | 143           |                          |               |
| Yan Wu .....              | 143           |                          |               |
| Alexander Xu .....        | 119           |                          |               |
| Gang Xu.....              | 147, 211      |                          |               |
| Keren Yanuka-Golub .....  | 182           |                          |               |
| Huihui Yao.....           | 165, 229      |                          |               |
| Peifang Ye.....           | 175, 239      |                          |               |
| Shu-Chi Allison Yeh ..... | 214           |                          |               |
| Li Yijia.....             | 46, 191       |                          |               |
| Chyan Ying Ke.....        | 206           |                          |               |
| Adam W York .....         | 206           |                          |               |
| Zheng You.....            | 234           |                          |               |
| Liping Yu.....            | 212           |                          |               |
| Raif Yuecel.....          | 159, 223      |                          |               |
| Dmytro Yushchenko .....   | 227, 233      |                          |               |
| Nick Zabinyakov .....     | 228           |                          |               |
| Katerina Zachova .....    | 175, 239, 240 |                          |               |
| Zbigniew Zawada .....     | 218           |                          |               |
| Carolien Zeelan.....      | 221           |                          |               |
| Yang Zeng.....            | 148, 213      |                          |               |
| Ling Zhang .....          | 103           |                          |               |



# SONY

## Is your lab prepared for what's next?

**Find your competitive advantage, accelerate discovery.**

Explore the advantages of innovative spectral cell analysis from Sony Biotechnology that supports a wide variety of applications, designed for ease of adoption and reliable operation – which are critical for today's multi-user environments.

### ID7000™ Spectral Cell Analyzer

- **Advanced design for your high parameter experiments** — Up to 7 lasers, 186 detectors to detect signal between 360–920 nm
- **Ready for future fluorochrome development** — The ability to expand your multi-color panels, so you can lead today and be prepared for tomorrow
- **Industry-leading AutoSampler and intuitive software workflows** — Enhance your laboratory's operations, efficiency, and productivity




**Power your performance. Empower your team. Accelerate discovery.**

Contact us to further explore the features of the ID7000 that will help you stay ahead of today and outpace tomorrow. **Schedule your Virtual Product Tour** to learn more about the ID7000 system.



[go.sonybiotechnology.com/id7000-virtual-demo-request](https://go.sonybiotechnology.com/id7000-virtual-demo-request)



©2022 Sony Biotechnology Inc. All rights reserved. Sony, the Sony logo, and ID7000 are trademarks of Sony Corporation. For Research Use Only. Not for use in diagnostic or therapeutic procedures. The ID7000 spectral cell analyzer is classified as a Class 1 laser product.

10.15.041422.0





# Catch the live flow

Amplify your flow cytometry data with spatial and morphological insights.

Do you have the right parameters to identify populations of interest? When you select target cells without using imaging parameters, you could miss targets or undiscovered populations. Real-time image analysis provides data plots of size, shape and fluorescence localization. With BD CellView™ Image Technology, you can create an image of each cell in real time, which enables novel image-based gating and cell sorting. Plus, gain confidence in your data through live visual confirmation of cell morphology, doublets, clumps and debris. Our latest breakthrough could lead to your next breakthrough.

Visualize the difference at [bdbiosciences.com/CellView](https://bdbiosciences.com/CellView)

For Research Use Only. Not for use in diagnostic or therapeutic procedures.

BD, the BD Logo and CellView are trademarks of Becton, Dickinson and Company or its affiliates. © 2022 BD. All rights reserved. BD-46645 (v1.0)0122

